UNIVERSITÀ DEGLI STUDI DI TRIESTE

XXX CICLO DEL DOTTORATO DI RICERCA IN

INGEGNERIA E ARCHITETTURA

CURRICULUM INGEGNERIA MECCANICA, NAVALE, DELL'ENERGIA E DELLA PRODUZIONE

WASTE HEAT RECOVERY WITH ORGANIC RANKINE CYCLE (ORC) IN MARINE AND COMMERCIAL VEHICLES DIESEL ENGINE APPLICATIONS

Settore scientifico-disciplinare: ING-IND/09

DOTTORANDO
SIMONE LION

COORDINATORE
PROF. DIEGO MICHELI

SUPERVISORE DI TESI
PROF. RODOLFO TACCANI

CO-SUPERVISORE DI TESI
DR. IOANNIS VLASKOS

ANNO ACCADEMICO 2016/2017

UNIVERSITÀ DEGLI STUDI DI TRIESTE

XXX CICLO DEL DOTTORATO DI RICERCA IN

INGEGNERIA E ARCHITETTURA

CURRICULUM INGEGNERIA MECCANICA, NAVALE, DELL'ENERGIA E DELLA PRODUZIONE

WASTE HEAT RECOVERY WITH ORGANIC RANKINE CYCLE (ORC) IN MARINE AND COMMERCIAL VEHICLES DIESEL ENGINE APPLICATIONS

Settore scientifico-disciplinare: ING-IND/09

DOTTORANDO
SIMONE LION

COORDINATORE
PROF. DIEGO MICHELI

SUPERVISORE DI TESI
PROF. RODOLFO TACCANI

CO-SUPERVISORE DI TESI
DR. IOANNIS VLASKOS

ANNO ACCADEMICO 2016/2017

Author's Information

Simone Lion

Ph.D. Candidate at Università degli Studi di Trieste

Development Engineer at Ricardo Deutschland GmbH

Early Stage Researcher (ESR) in the Marie Curie FP7 ECCO-MATE Project

Author's e-mail:

- Academic: *simone.lion@phd.units.it*
- Industrial: *simone.lion@ricardo.com*
- Personal: *simone_lion@hotmail.com*

Author's address:

- *Academic:* Dipartimento di Ingegneria e Architettura, Università degli Studi di Trieste, Piazzale Europa, 1, 34127, Trieste, Italy
- *Industrial:* Ricardo Deutschland GmbH, Güglingstraße, 66, 73525, Schwäbisch Gmünd, Germany

Project website:

- *ECCO-MATE Project:* www.ecco-mate.eu

Official acknowledgments:

The research leading to these results has received funding from the People Programme (Marie Curie Actions) of the European Union's Seventh Framework Programme FP7/2007-2013/ under REA grant agreement n°607214.

Abstract

Heavy and medium duty Diesel engines, for marine and commercial vehicles applications, reject more than 50-60% of the fuel energy in the form of heat, which does not contribute in terms of useful propulsion effect. Moreover, the increased attention towards the reduction of polluting emissions and fuel consumption is pushing engine manufacturers and fleet owners in the direction of increasing the overall powertrain efficiency, still considering acceptable investment and operational costs.
For these reasons, waste heat recovery systems, such as the Organic Rankine Cycles (ORC), are undergoing a period of intense research and development.
However, in most of engine waste heat recovery studies in literature, the engine side analysis is not considered in a detailed way, even though the engine architecture and the operational behaviour strongly influence the availability of heat sources, and their characteristics, to be recovered using waste heat recovery systems. As an example, the use of emission reduction strategies, such as Exhaust Gas Recirculation (EGR), can introduce an additional heat source and modify the temperatures in the engine gas lines, thus leading to new possible scenarios for the exploitation of the engine wasted heat.
The scope of this work, carried out in collaboration with Ricardo, an international engineering consulting company, is to introduce an innovative combined engine-waste heat recovery system analysis and design methodology, which could go beyond the traditional development approach, considering both the engine and the ORC system as a synergic and integrated powertrain. For this reason, industry-standard engine gas dynamics simulation software and thermodynamic process simulation techniques have been used and further developed in order to study the combined effects and performance of engine-ORC systems in the commercial vehicle and marine sectors, addressing at the same time several development issues, such as: working fluid and layout choice, powertrain thermal management, energy utilization, turbocharging and emission reduction strategies, in the direction of a co-simulation approach, which is one of the industry's main interests, to reduce development time and costs.
After a detailed literature review and modelling approach explanation, four different case studies have been proposed, to demonstrate an increasing level of integration between engine and ORC system analysis, addressing also applications which are not commonly considered in literature, such as off-highway vehicles and two-stroke ships propulsion units.
The first case study is focused on an agricultural tractor Diesel engine application, using engine data obtained from Ricardo's testing activities. These data are the starting point for the investigation of the performance of different ORC architectures and working fluids, as well as for the exploitation of EGR wasted heat and the integration of the system with a preliminary study of the vehicle thermal management and cooling system. The results obtained show how the recovery of EGR heat can be beneficial both in terms of ORC system's performance increase and decreased impact on the vehicle cooling system. A parallel exhaust gas and EGR ORC architecture is able, in principle, to allow around 10% maximum fuel saving, still considering a good trade-off with cooling radiator dimensions and parasitic fan consumption increase, when using water-steam, toluene or ethanol as possible working fluids.
The second case study refers to a 1.5 MW, four-stroke, Diesel engine power generator, generally used for auxiliary power production on board ships. A detailed thermodynamic model of the engine has been developed in the commercial software Ricardo WAVE and the performance have been calculated at varying exhaust backpressure levels, in order to represent different possible designs for an ORC boiler fitted on the exhaust side of the engine. Three turbocharging systems have been assessed: a fixed geometry turbocharger, a turbocharger with Waste-Gate (WG) and a Variable Geometry Turbocharger (VGT). An ORC thermodynamic model has been then implemented, considering simple or recuperated architectures and different suitable working fluids, in order to assess the potential for exhaust gas heat recovery. From the simulations' results, on the engine side, the VGT system allows to better withstand

the adverse effect of the ORC boiler backpressure, while at the same time fulfilling the requirements for combustion air-fuel ratio and maximum turbocharger exhaust temperature. Additionally, a recuperated ORC, running with acetone, allows a fuel consumption reduction between 9.1 and 10.2%, depending on the boiler design backpressure. Flammability and health hazards could however still be a problem, when installing the system onboard ships, even though an intermediate oil loop can mitigate the issues, separating the hot engine exhaust gas from the ORC working fluid.
The third case study is focused on a 13.6 MW, low-speed, two-stroke, Diesel engine propulsion unit, typically installed in bulk carriers, oil tankers and container ships. A thermodynamic model of the engine, in typical IMO Tier II configuration, has been developed and validated, in Ricardo WAVE, based on the experimental data supplied by the project partner Winterthur Gas & Diesel (WinGD). Starting from the validated baseline model, a Low Pressure (LP) EGR circuit has been implemented for IMO Tier III operations, and the engine thermodynamic performance and characteristics evaluated in order to understand the impact of the emission reduction strategy on the engine fuel consumption and possible waste heat sources exploitable through the use of ORCs. A general increase of the heat available to be recovered can be evinced when using EGR, especially for the Scavenge Air Cooler (SAC) and the exhaust gas economizer. Four different ORC architectures, and two different working fluids (water-steam and R1233zd(E)) have been assessed, with the scope of obtaining the highest power production from the recovery of the waste heat. When combining the different ORC architectures, in order to try to fully exploit the engine waste heat available, a combined system with a water-steam Rankine cycle on the exhaust gas side and a refrigerant-based ORC recovering jacket cooling water and SAC heat, in an innovative two-stage SAC configuration, has been estimated to bring 5.4% fuel economy benefit in Tier II operation, and 5.9% in Tier III (at full load). The results achieved show the possibility of mitigating the increased fuel consumption effect of EGR operations using waste heat recovery systems. A preliminary economic feasibility analysis shows how a fuel cost savings of about 4% to 5.7% can be expected.
The second and third case studies show how engine simulation tools can be used to assess the engine performance under different operational strategies, while at the same time, supplying the right boundary conditions for the evaluation of the performance of the waste heat recovery system, saving time and expensive test campaigns. However, a more synergic approach should be considered, when evaluating the combined engine-ORC systems. For this reason, the last case study aims to set the basics, and open the path, to a new methodology which can be helpful to understand the overall system and optimize its combined performance. In particular, a model of a four-stroke, 200 kW, Diesel engine, for on-highway trucks applications, has been developed in Ricardo WAVE. Innovative post-processing routines, developed in MATLAB, have been used to calculate a detailed First and Second Law analysis, for every engine operating point which can be simulated. The ORC models, for different architectures and working fluids, have also been adapted in order to calculate a complete energy and exergy balance. The calculation of the exergy destruction terms, for every sub-system of the overall engine-ORC powertrain, allows also to highlight where the main inefficiencies concentrate, thus helping to propose improvement strategies.
Once energy and exergy streams are known, it has been possible to implement a techno and thermo-economic analysis, allowing not only to understand the performance of the powertrain, but also its Specific Investment Cost (SIC) and its operational costs, addressing if the costs invested in the development of the system are really used for effective power production, or wasted in system's inefficiencies or un-useful streams. Additionally, as an example, an exhaust gas manifolds insulation strategy has been proposed, on the engine side, demonstrating the capability of reducing the SIC from 268 to 246 $/kW at C100 operating point, and from 1219 to 941 $/kW at B50 operating point. The results demonstrate how this strategy can help to improve the trade-off between performance and costs, especially at partial load and speed points, in which exhaust gas temperatures are expected to be lower, decreasing the ORC performance. The proposed insulation strategy is, however, just an example of

the different scenarios which can be evaluated with a fully-developed and combined simulation platform.
Indeed, the combination of energy, exergy and economic analysis allows the developer to deeply understand the thermodynamics of the combined engine-ORC systems, addressing all the energy and exergy streams available for heat recovery, highlighting the main sources of inefficiencies in the powertrain, and proposing improvements to increase the overall system efficiency at acceptable investment and operational costs. The methodology can be, in principle and with further developments, applied to any type of engine-waste heat recovery system powertrain.
Moreover, the combined use of emission reduction strategies and new technologies, such as EGR and ORC, can allow to develop clean, but at the same time efficient, propulsion units. However, while for commercial vehicles the recovery of high temperature exhaust gas and EGR heat is more beneficial in terms of compromise between performance, system costs and packaging issues, in the case of large ship propulsion units, the recovery of lower temperature heat sources, such as coolant and scavenge air, could become very interesting for future developments, because of the high amount of heat available, even if at lower temperature levels, but for this reason suitable for the use of an ORC technology.
The results of the proposed case studies show a fuel consumption reduction up to around 5-10% when adopting ORC systems, depending on the application, type of engine, overall system architecture, working fluid and design point chosen, showing the potential of the technology in the two considered sectors, and demonstrating the need to further develop combined simulation platforms able to predict and optimize the overall system performance, operations and costs.

Sommario

Nei motori Diesel per impieghi pesanti, quali ad esempio la propulsione di navi o veicoli commerciali, più del 50-60% dell'energia fornita con il carburante viene dissipata in forma di calore, senza fornire effetto propulsivo. Inoltre, la crescente attenzione verso la riduzione delle emissioni e del consumo di carburante, sta spingendo i produttori di motori a sviluppare sistemi per il miglioramento dell'efficienza, continuando però a considerare investimenti e costi operativi accettabili.
Per tali motivi, i sistemi di recupero di calore, quali i cicli ORC (cicli di Rankine a fluido vapore organico), stanno attraversando un periodo di intensa attività di ricerca e sviluppo.
Tuttavia, nella maggior parte degli studi disponibili in letteratura, l'analisi dei processi termodinamici della parte motore non è considerata in modo dettagliato, nonostante l'architettura del motore e il suo comportamento operativo influenzino fortemente la disponibilità di fonti di calore da recuperare. Ad esempio, l'utilizzo di strategie di riduzione delle emissioni, come il ricircolo dei gas di scarico (EGR), può introdurre una fonte di calore aggiuntiva e modificare le temperature all'interno del motore, aprendo così nuovi possibili scenari per lo sfruttamento del calore di scarto.
Lo scopo di questo lavoro, sviluppato in collaborazione con Ricardo, azienda di ingegneria internazionale leader nei settori automotive e marino, è quello di introdurre una metodologia innovativa di analisi combinata per sistemi di recupero di calore per motori industriali, che vada oltre il tradizionale approccio, considerando motore e ORC come un unico sistema sinergico e integrato.
Per questo motivo, software per lo studio delle prestazioni di motori e tecniche di simulazione di processo termodinamico sono stati utilizzati e ulteriormente sviluppati al fine di studiare gli effetti combinati motore-ORC, affrontando allo stesso tempo diverse tematiche critiche nello sviluppo di tali sistemi in ambito marino e veicolare quali: scelta del fluido di lavoro e dell'architettura, gestione termica del sistema, utilizzo dell'energia prodotta, uso di tecniche di sovralimentazione e di riduzione delle emissioni, il tutto nell'ottica di un approccio di co-simulazione, su cui l'industria sta puntando molto per ridurre tempi e costi dello sviluppo.
Dopo una revisione dettagliata della letteratura e la descrizione dei modelli sviluppati, quattro casi-studio sono stati proposti, al fine di dimostrare un livello crescente di integrazione tra l'analisi del motore e del sistema ORC, affrontando anche applicazioni non comunemente considerate in letteratura, come i trattori agricoli e le grosse unità di propulsione navale a due tempi.
Il primo caso studio riguarda un trattore agricolo con motore Diesel da 300 kW, i cui dati sperimentali sono stati ottenuti da test condotti al banco motore presso Ricardo. Tali dati sono stati utilizzati come punto di partenza per lo studio delle prestazioni di differenti architetture e fluidi di lavoro per cicli ORC, nonché per il possibile sfruttamento del calore del ricircolo dei gas di scarico (EGR) e l'integrazione del sistema nel veicolo, con lo studio preliminare del circuito di raffreddamento e della gestione del calore di scarto. I risultati ottenuti dimostrano come il recupero del calore dell'EGR possa essere vantaggioso sia in termini di aumento delle prestazioni del sistema ORC che di riduzione dell'impatto sul circuito di raffreddamento del veicolo. Un'architettura ORC con recupero in parallelo del calore dell'EGR e dei gas di scarico è in grado, in linea di principio, di ridurre di circa il 10% il consumo di carburante, considerando comunque un buon compromesso con l'aumento delle dimensioni del radiatore di raffreddamento e del consumo di potenza della ventola, quando si utilizzino come possibili fluidi di lavoro per l'ORC vapore acqueo, toluene o etanolo.
Il secondo caso studio si riferisce ad un generatore di potenza ausiliaria, Diesel, a quattro tempi, da circa 1.5 MW di potenza, per applicazioni navali. Un modello termodinamico dettagliato del motore è stato sviluppato usando il codice commerciale Ricardo WAVE e le prestazioni calcolate al variare del livello di contropressione allo scarico del motore stesso, allo scopo di rappresentare possibili design differenti di un evaporatore ORC installato sulla linea dei gas di scarico. Tre sistemi di sovralimentazione sono stati valutati: un turbocompressore a geometria fissa, un turbocompressore con valvola Waste-Gate (WG), e un turbocompressore a geometria variabile (VGT). È stato quindi implementato un modello termodinamico per cicli ORC, considerando architetture semplici o con

recuperatore interno, e diversi fluidi di lavoro, al fine di valutare il potenziale di recupero del calore dei gas allo scarico del motore. Dai risultati delle simulazioni, per quanto riguarda la parte motore, si evince come il turbocompressore VGT consenta di contrastare in maniera più adeguata gli effetti negativi della contropressione creata dall'evaporatore ORC, rispettando allo stesso tempo i requisiti per il rapporto aria-combustibile per un'adeguata combustione, nonché la temperatura massima dei gas allo scarico, per questioni di resistenza del turbocompressore stesso. Inoltre, un ORC con recuperatore interno, funzionante con acetone, consente una riduzione del consumo di carburante tra il 9.1 e 10.2%, a seconda della contropressione dovuta al design dell'evaporatore. L'infiammabilità e i rischi per la salute potrebbero tuttavia essere ancora un problema quando si installi il sistema a bordo di una nave, anche se il circuito ad olio diatermico intermedio può mitigare tali problemi, separando i gas di scarico del motore dal fluido di lavoro dell'ORC, aumentando il livello di sicurezza.
Il terzo caso studio riguarda una unità propulsiva lenta a due tempi, Diesel, da circa 13.6 MW, tipicamente installata in navi petroliere, portacontainer e mercantili. Un modello termodinamico del motore, in tipica configurazione IMO Tier II, è stato sviluppato e validato, in Ricardo WAVE, sulla base dei dati sperimentali forniti dal partner di progetto Winterthur Gas & Diesel. A partire dal modello di base validato, un circuito EGR di ricircolo dei gas di scarico a bassa pressione (LP) è stato implementato per simulare operazioni di tipo IMO Tier III, e le prestazioni termodinamiche del motore calcolate al fine di comprendere l'impatto della strategia di riduzione delle emissioni sul consumo di carburante del motore e sulle possibili fonti di calore di scarto recuperabili tramite l'uso di ORC. Un aumento del calore disponibile per essere recuperato si può notare, quando si utilizzi l'EGR, in particolare per lo scambiatore di calore dell'aria di lavaggio (SAC) e per l'economizzatore montato sulla linea dei gas di scarico. Quattro diverse architetture ORC e due fluidi di lavoro (vapore acqueo e R1233zd(E)) sono stati valutati, allo scopo di ottenere la massima produzione di energia utile dal recupero del calore di scarto. Combinando le diverse architetture ORC, per sfruttare appieno il calore di scarto disponibile dal motore, un sistema combinato con ciclo Rankine a vapore acqueo sul lato gas di scarico e uno a refrigerante ORC, che recuperi calore dal circuito di raffreddamento di alta temperatura (HT) e dal SAC, in una configurazione innovativa a doppio stadio di raffreddamento dell'aria di lavaggio, è stato stimato in grado di portare 5.4% di risparmio di carburante in operazioni IMO Tier II, e 5.9% in IMO Tier III (a pieno carico). I risultati ottenuti mostrano la possibilità di mitigare l'aumento del consumo di carburante, dovuto all'uso dell'EGR, utilizzando sistemi di recupero del calore quali l'ORC. Un'analisi di fattibilità economica preliminare mostra inoltre come, per un caratteristico profilo operativo annuale, ci si possa aspettare un risparmio, in termine di costi operativi dovuti al carburante, nell'ordine del 4-5.7%.
Il secondo e il terzo caso studio mostrano come gli strumenti di simulazione per la parte motore, come Ricardo WAVE, possano essere utilizzati per valutare le prestazioni del motore in base a diverse strategie operative e architetture, fornendo allo stesso tempo le condizioni al contorno per il calcolo dei sistemi di recupero di calore, risparmiando tempo e costose campagne di test. Tuttavia, nel valutare i sistemi combinati motore-ORC, un approccio più sinergico dovrebbero essere considerato. Per tal motivo, l'ultimo caso studio proposto mira a stabilire le basi e ad aprire la via verso una nuova metodologia che possa essere utile per studiare il sistema nel suo totale, e ottimizzarne le prestazioni combinate. In particolare, un modello di motore Diesel a quattro tempi da 200 kW, per applicazioni su camion stradali, è stato sviluppato in Ricardo WAVE. Alcune routine innovative per l'elaborazione dei dati, sviluppate su piattaforma MATLAB, sono state utilizzate per calcolare un bilancio dettagliato di Primo e Secondo Principio della Termodinamica, per ogni punto di funzionamento del motore che può essere simulato. I modelli ORC, per diverse architetture e fluidi di lavoro, sono stati adattati per calcolare un bilancio energetico ed exergetico completo. Il calcolo dei termini di distruzione di exergia, per ogni sottosistema dell'intero sistema propulsivo motore-ORC, consente inoltre di evidenziare dove si concentrano le principali inefficienze, contribuendo così a proporre strategie di miglioramento delle prestazioni.

Una volta calcolati i flussi di energia ed exergia, è stato possibile implementare un'analisi di tipo tecno e termo-economico, che consente non solo di comprendere le prestazioni del sistema, ma anche il suo costo specifico di investimento (SIC) e i suoi costi operativi, aiutando a capire se i costi investiti nello sviluppo del sistema stesso vengano realmente utilizzati per produrre energia utile, o sprecati in inefficienze o flussi energetici (o exergetici) non utilizzati. Inoltre, a titolo di esempio, è stata proposta una strategia di isolamento dei collettori dei gas di scarico, sul lato motore, che dimostra la capacità di ridurre il SIC da 268 a 246 $/kW al punto operativo C100 (pieno carico) e da 1219 a 941 $/kW al punto operativo B50 (carichi parziali). I risultati dimostrano come questa strategia possa aiutare a migliorare il compromesso tra prestazioni e costi, specialmente ai carichi parziali, in cui ci si aspetta che le temperature dei gas di scarico siano inferiori, riducendo così le prestazioni dell'ORC. La strategia di isolamento proposta è, tuttavia, solo un esempio dei diversi scenari che possono essere esplorati con una piattaforma combinata di simulazione completamente sviluppata.
Infatti, l'uso combinato di un'analisi energetica, exergetica ed economica, può consentire all'ingegnere sviluppatore di comprendere a fondo il funzionamento dei sistemi combinati motore-ORC, individuando tutti i flussi energetici ed exergetici, evidenziando le principali fonti di inefficienze del sistema e proponendo miglioramenti al fine di aumentare l'efficienza complessiva, a costi operativi e di investimento competitivi.
Inoltre, l'uso combinato di strategie di riduzione delle emissioni, come l'EGR, e sistemi ORC, può consentire di sviluppare unità propulsive a emissioni ridotte, ma allo stesso tempo efficienti. Tuttavia, mentre per i veicoli commerciali il recupero dei gas di scarico e del calore dell'EGR può essere più vantaggioso in termini di compromesso tra prestazioni, costi e ingombri dei componenti, nel caso di grandi unità propulsive navali, il recupero di fonti di calore a bassa temperatura, come l'aria di lavaggio e il fluido di raffreddamento del motore, potrebbe diventare molto interessante, a causa dell'elevata quantità di calore disponibile, seppure a temperature inferiori, tuttavia, proprio per tal motivo, adatte per l'uso di sistemi ORC.
I risultati ottenuti mostrano una possibile riduzione del consumo di carburante fino al 5-10% adottando sistemi ORC, a seconda dell'applicazione, del tipo di motore, dell'architettura del sistema, del fluido operativo e del punto di progetto scelto, dimostrando il potenziale della tecnologia nei due settori considerati in questo lavoro, e determinando la necessità di sviluppare ulteriormente piattaforme di simulazione combinata in grado di predire e ottimizzare le prestazioni, le strategie operative e i costi di sistemi combinati sempre più complessi.

Acknowledgments

In this section of my Ph.D. thesis I would like to acknowledge some of the people, and institutions, who helped me in the preparation of this work, both directly and indirectly, with their priceless support and commitment.
First of all, I would like to thank all my academic, and industrial, supervisors and advisors. In particular, Prof. Rodolfo Taccani, from University of Trieste, who supported me during the whole period of my doctoral studies, understanding the challenging requirements of an industrial Ph.D., and promoting a fruitful collaboration between the University of Trieste and the industrial sector.
Special thanks go also to Dr. Ioannis Vlaskos, my industrial supervisor from Ricardo Deutschland GmbH, who followed me during the entire ECCO-MATE project, being not only my bureaucratical reference in the company, but also a professional engineer a student can learn a lot from.
A particular acknowledgement goes also to Dr. Cedric Rouaud, who, even if not officially my supervisor, contributed with his experience and guiding support to the positive outcome of the research project, very often being a help for me when internal company issues had to be solved.
Finally, from the company point of view, I would like to thank also Dr. Simon Edwards, who advised me many times, both technically and personally, and supported me also in my professional and personal development.
From the institutional point of view, for sure the European Union, the ECCO-MATE project consortium (in particular Prof. Maria Founti and Tasia Gkika) and Ricardo must be acknowledged, because, without their financial support, I could not have had the opportunities I had, in particular regarding the very interesting seminars and conferences I attended, and the competent researchers and people I had the chance to meet.
Besides my supervisors and advisors, I would like to thank also the reviewers and the committee for their support in the preparation and review of the overall work, as well as Pietro Scrocco, from Winterthur Gas and Diesel, and Prof. Lambros Kaiktsis, from NTUA Athens, for their insightful comments, their commitment and their guidance during our project collaborations.
I am also very grateful to all the nice colleagues and friends I met in Ricardo during my stay, who helped me during my challenging work, stealing time to their families or to their job, when I asked them for support. They also contributed to my integration in the company and in the new country. Sincere thanks go to: Dr. Andrea Marchi, Dr. Contantine Michos, Markus Borrmann, Ekrem Burma, Harshal Desai, Mayur Patwari, Shyam Sasidharan, Hari Markapuram, Srinivasan Kannan, Roland Bremer, Christian Hoerter, Sandra Breuning, Daniel Deurer, Christina Kramer, Dr. Franz Berndt, Peter Giess, David Weissert, Georg Deutschle, Marie Durampard, Praveen Pothumahanty, Joshua Dalby, James Baxter, Nicholas Brown, Amy Walker, Pavel Gonda, Christian Antoniutti, Stefano Granvillano, Stefano Di Palma, Giovanni Costa, George Robson and Luigi Fileppi. I apologize if I forgot someone: you have been really a big bunch of friendly people, I will never forget you guys!
Special thanks go also to my student Marco Giovanni Momesso, who supported me during our six months collaboration in the frame of the project, as well as to all the ECCO-MATE fellows, and the Enesys Lab researchers, professors and friends, I had the chance to share the fruitful experience with.
I am also immeasurably grateful to my girlfriend, Svetlana Samarova, for all the support, love and understanding during these last challenging years. We grew up together!
Last, but not least, I would like to acknowledge my family: my mother Anna, my father Lucio and my brother Jacopo. Without your support, your understanding, your incitement and your love, during all these years, I would for sure not be where I am now. Simply…I owe you everything!

The author,

Simone Lion

Contents

Index of Figures

Index of Tables

Nomenclature

a	specific availability (exergy), *J/kg*
A	area, m^2, or availability (exergy), *J*
$\dot{A}$	availability (exergy) rate, *W*
b	specific flow availability (exergy), *J/kg*
c	speed of sound, *m/s*, or average cost per unit exergy, *$/J*
C	cost, *$*
$\dot{C}$	cost rate, *$/h*
C_D	discharge coefficient
c_p	specific heat at constant pressure, *J/kgK*
D	cylinder bore, *m*, or depth (dimension), *m*
E	energy, *J*
g	Specific free Gibbs enthalpy, *J/kg*
G	free Gibbs enthalpy, *J*
h_c	convective heat transfer coefficient, W/m^2K
h	specific enthalpy, *J/kg*
H	enthalpy, *J,* or height (dimension), *m*
i	interest rate
I	irreversibilities, *J*
$\dot{I}$	irreversibilities rate, *W*
k	thermal conductivity, *W/mK*
L	length, *m*
m	mass, *kg*
$\dot{m}$	mass flow, *kg/s*
mf	maintenance factor
MW	Molar Weight, *g/mol*
n_r	number of revolutions per cycle
n_h	annual number of hours, *h/year*
N	rotational speed, *rev/s or rpm*
Nu	Nusselt number
p	pressure, *Pa or bar*
PR	Pressure Ratio
q	heat per unit mass, *J/kg*
Q	heat, *J*
$\dot{Q}$	thermal power (heat transfer rate), *W*
R	specific gas constant of the mixture, *J/molK or J/kgK*
$\bar{R}$	universal gas constant, *J/molK or J/kgK*
Re	Reynolds number
$r_{p,opt}$	built-in expansion ratio
s	specific entropy, *J/kgK*
S	engine stroke, m or entropy, *J/K*
t	time, *s or h*
T	temperature, *°C or K*
U	internal energy, *J*, or Overall Heat Transfer Coefficient, W/m^2K
UA	conductance, *W/K*
v	specific volume, m^3/kg
V	volume, m^3

V_d	engine displacement, *m^3 or l*
w	characteristic velocity, *m/s*, or specific work, *J/kg*
W	work, *J*, or width (dimension), *m*
$\dot{W}$	power, *W*
x	mass fraction or vapour quality
$\dot{x}$	mass fraction time derivative, *1/CAD*
y	molar fraction
$\dot{Z}$	levelized cost, *$/h*

Acronyms

AC	Air Conditioning
AFR	Air-Fuel-Ratio
AT	After-Treatment
BDC	Bottom Dead Centre
$BMEP$ (or $bmep$)	Brake Mean Effective Pressure, *bar*
$BSFC$ (or $bsfc$)	Break Specific Fuel Consumption, *g/kWh*
C	Compressor
CAC	Charge Air Cooler
CAD	Crank-Angle-Degree, °
CAE	Computer Aided Engineering
$CAPEX$	Capital Expenditure
$CEPCI$	Chemical Engineering Plant Cost Index
CFC	Chloro-Fluoro-Carbon
CFD	Computational Fluid Dynamics
CFR	Capital Recovery Factor
CI	Capital Investment
CHP	Combined Heat and Power
CV	Control Volume
DC	Direct Condensation
DI	Direct Injection
DOC	Diesel Oxidation Catalyst
DPF	Diesel Particulate Filter
ECA	Emission Controlled Area
$EEDI$	Energy Efficiency Design Index
$EGHX$	Exhaust Gas Heat Exchanger
EGR	Exhaust Gas Recirculation
ENG	Engine
EPA	Environmental Protection Agency (United States)
ESC	European Stationary Cycle
EVC	Exhaust Valve Closing, CAD
EVO	Exhaust Valve Opening, CAD
EXP	Expander
FC	Fuel Consumption
$FMEP$	Friction Mean Effective Pressure, *bar*
GA	Genetic Algorithm
GHG	Green House Gas
GWP	Global Warming Potential

HC	Hydro-Carbon
$HCFC$	Hydro-Chloro-Fluoro-Carbon
$HDDE$	Heavy Duty Diesel Engine
HFC	Hydro-Fluoro-Carbon
HFE	Hydro-Fluoro-Ether
HFO	Heavy Fuel Oil
HiL	Hardware in the Loop
HP	High Pressure
HT	High Temperature (or Heat Transfer)
$HVAC$	Heating, Ventilation and Air Conditioning
IC	Indirect Condensation
$ICCT$	International Council on Clean Transportation
IG	Ideal Gas
$IMEP$	Indicated Mean Effective Pressure, *bar*
IMO	International Maritime Organization
IRR	Irreversibilities
IVC	Inlet Valve Closure, CAD
IVO	Inlet Valve Opening, CAD
LHR	Low Heat Rejection
LHV	Lower Heating Values, *MJ/kg or kJ/kg*
$LMTD$	Log-Mean-Temperature-Difference
LNG	Liquefied Natural Gas
LP	Low Pressure
LPG	Liquefied Petroleum Gas
LT	Low Temperature or Life-Time, *years*
MCR	Maximum Continuous Rating
MDO	Marine Diesel Oil
MFR	Mass Flow Ratio
$NEDC$	New European Driving Cycle
$NFPA$	National Fire Protection Agency (United States)
NG	Natural Gas
NTU	Number of Transfer Units
ODP	Ozone Depletion Potential
OEM	Original Equipment Manufacturer
OM	Operation and Maintenance
$OPEX$	Operating Expenditure
ORC	Organic Rankine Cycle
P	Pump or Product
PC	Parallel Cycle
PEC	Purchased Equipment Cost, *$*
PID	Proportional Integrative Derivative
PM	Particulate Matter
$PMEP$	Pumping Mean Effective Pressure, *bar*
PP	Pinch Point
PT	Power Turbine
PTO	Power Take Off
RC	Rankine Cycle
RS	Rejected Streams
RT	Real Time

SAC	Scavenge Air Cooler
SC	Simple Cycle
SCR	Selective Catalytic Reduction
$SEEMP$	Ship Energy Efficiency Management Plan
$S\&T$	Shell & Tube
$SFOC$	Specific Fuel Oil Consumption, *g/kWh*
SPP	Steam Produced Power
SI	Surface Index, *kJ/kg°C*
SIC	Specific Investment Cost, *$/kW*
SiL	Software in the Loop
SOC	Start of Combustion, CAD
SOI	Start of Injection, CAD
ST	Steam Turbine
T	Turbine
TC	Turbocharger
TCR	Thermo-Chemical Recuperation
TDC	Top Dead Centre
TEG	Thermo-Electric-Generator
TO	Thermal Oil
$UDDS$	Urban Dynamometer Driving Schedule
UPS	Useful Power Streams
VER	Volumetric Expansion Ratio
VGT	Variable Geometry Turbocharger
VTA	Variable Turbine Area
VVT	Variable Valve Timing
WG	Waste Gate
$WHTS$	World harmonized Transient Cycle
WTS	Water Treatment System

Subscripts and Superscripts

0	reference state (T=298.15 K, p=1 atm), dead state
abs	absorbed
air	air
avg	average
$boil$	boiling
$brake$	brake (power)
$burned$	burned
c	critical (or characteristic)
cf	cooling fluid
ch	chemical
$cold$	cold (stream)
$cool$	coolant
$cond$	condensation or condenser
$conv$	conversion
cyl	cylinder
$desuph$	de-superheating
$ducts$	ducts
el	electrical

$econ$	economizer
$evap$	evaporation or evaporator
exh	exhaust
f	freezing (or frontal)
fan	fan
$frict$	friction
$fuel$	fuel
gas	gas
$gross$	gross
$head$	head (cylinder)
hot	hot (stream)
hs	heat source
$impr$	improvement
$incr$	increase
ind	indicated
in	inlet
inj	injected
int	intake
inv	investment
irr	irreversibilities
is	isentropic
I	First Law
II	Second Law
kin	kinetic
$junctions$	junctions
$liner$	liner (cylinder)
liq	liquid
$manifolds$	manifolds
max	max
$mech$	mechanical
mix	mixture
net	net
$norm$	normal
oil	oil
out	outlet
$pipes$	pipes
$piston$	piston
$ports$	ports
pot	potential
$power$	power
$preh$	pre-heating
$pump$	pumping
rad	radiator (or radiation)
rec	recovery
$recp$	recuperator
$released$	released
$residuals$	residuals
$scav$	scavenging
$sens$	sensible

$shaft$	shaft (crankshaft or propeller shaft)
$sub-cool$	sub-cooling
$suph$	superheating
th	thermal
$total$	total
$trapped$	trapped
unb	unburned
vap	vaporized
$wall$	wall
wf	working fluid
$work$	work

Greek symbols

ε	error (or effectiveness)
η	efficiency
θ	crank-angle, °
λ	air-fuel equivalence ratio
μ	chemical potential, *J/kg*
ν	kinematic viscosity, m^2/s
π	pi
ρ	density, kg/m^3
τ	torque, *Nm*
φ	equivalence ratio

List of Publications and Conferences

Peer-Reviewed Journal Articles

1. C. N. Michos, S. Lion, I. Vlaskos, R. Taccani. Analysis of the backpressure effect of an Organic Rankine Cycle (ORC) evaporator on the exhaust line of a turbocharged heavy duty diesel power generator for marine applications. *Energy Conversion and Management, 132, 347-360, 2017*. doi: 10.1016/j.enconman.2016.11.025.

2. S. Lion, C. N. Michos, I. Vlaskos, R. Taccani. A thermodynamic feasibility study or an Organic Rankine Cycle (ORC) for heavy-duty diesel engine waste heat recovery in off-highway applications. *International Journal of Energy and Environmental Engineering, 1-18, 2017*. doi: 10.1007/s40095-017-0234-8.

3. S. Lion, C. N. Michos, I. Vlaskos, C. Rouaud, R. Taccani. A review of waste heat recovery and Organic Rankine Cycles (ORC) in on-off highway vehicle Heavy Duty Diesel Engine applications. *Renewable and Sustainable Energy Reviews, 79, 691-708, 2017*. doi: 10.1016/j.rser.2017.05.082.

Conference Proceedings and Abstracts

1. S. Lion, C. N. Michos, I. Vlaskos, R. Taccani. A thermodynamic feasibility study of an Organic Rankine Cycle (ORC) for Heavy Duty Diesel Engine (HDDE) waste heat in off-highway applications. *Proceedings of 29th International Conference on Efficiency, Cost, Optimisation, Simulation and Environmental Impact of Energy Systems (ECOS 2016). Portorož, Slovenia, June 19-23, 2016*.

2. S. Lion, I. Vlaskos, C. Rouaud, R. Taccani. First and Second Law Analysis Approach for the Study of Internal Combustion Engine Waste Heat Recovery with Organic Rankine Cycles (ORC). *Book of Abstracts of the 3rd Annual Engine ORC Consortium Workshop for The Automotive and Stationary Engine Industries. Belfast, United Kingdom, September 14-16, 2016*.

3. S. Lion, M. G. Momesso, I. Vlaskos, C. Rouaud, R. Taccani. Combined Engine-ORC Thermodynamic Analysis Based on a Second Law and Thermo-Economic Approach. *IMechE Vehicle Thermal Management Systems Conference and Exhibition – VTMS 13. London, United Kingdom, May 17-18, 2017.*

4. S. Lion, I. Vlaskos, R. Taccani. Preliminary thermodynamic analysis of waste heat recovery in marine diesel engines using Organic Rankine Cycle. *Proceedings of 30th International Conference on Efficiency, Cost, Optimisation, Simulation and Environmental Impact of Energy Systems (ECOS 2017). San Diego, California, United States, June 2-6, 2017.*

5. S. Lion, I. Vlaskos, C. Rouaud, R. Taccani. Overview of the activities on heavy duty diesel engines waste heat recovery with Organic Rankine Cycles (ORC) in the frame of the ECCO-MATE EU FP7 project. *ORC 2017, International Seminar on ORC Power Systems. Energy Procedia, September 13-15, 2017.*

6. S. Lion, I. Vlaskos, C. Rouaud, W. Thelen, R. Taccani. Optimisation of internal combustion engine coupled with Organic Rankine Cycle with exergo-economic approach. *Book of Abstracts of the 4th Annual Engine ORC Consortium Workshop for The Automotive and Stationary Engine Industries. Detroit, USA, November 15-17, 2017*.

7. S. Lion, R. Taccani, I. Vlaskos, P. Scrocco, X. Vouvakos, L. Kaiktsis. Thermodynamic analysis of waste heat recovery using Organic Rankine Cycle (ORC) for a two-stroke low speed marine Diesel engine in IMO Tier II and Tier III operation. *Proceedings of 31st International Conference on Efficiency, Cost, Optimisation, Simulation and Environmental Impact of Energy Systems (ECOS 2018). Guimaraes, Portugal, June 17-22, 2018. Under final review at the time in which this thesis has been submitted.*

ECCO-MATE Events, Seminars and Conferences

1. S. Lion, I. Vlaskos, C. Rouaud, R. Taccani. First and Second Law Analysis of Internal Combustion Engines and Waste Heat Recovery with Organic Rankine Cycles (ORC). *1st ECCO-MATE LOGE Conference, Combustion Processes in Marine and Automotive Engines. Lund, Sweden, June 7-8, 2016.*

2. S. Lion. Introduction to Ricardo WAVE 1-D Engine Performance Simulation. *Seminar at ICISS / ECCO-MATE Summer School, Advanced Combustion Engine Technologies. Chania, Greece, June 19-23, 2016.*

3. S. Lion. Overview of Turbocharging and ORC Analysis Activities in the ECCO-MATE project. *Ricardo / ECCO-MATE Turbocharging and ORC Summer School and Conference. Ricardo plc Headquarter (STC), Shoreham-by-Sea, United Kingdom, September 29-30, 2016. Event co-organized by the author.*

4. S. Lion, I. Vlaskos, P. Scrocco, S. Hensel, X. Vouvakos, L. Kaiktsis, R. Taccani. Thermodynamic analysis of waste heat recovery using Organic Rankine Cycles (ORC) for a 2-stroke low speed marine diesel engine in IMO Tier II and IMO Tier III operations. *ECCO-MATE / SMARTCATS Final Conference, Recent Outcomes on Marine and Automotive Combustion Research. Sounion, Greece, June 8, 2017.*

1 Introduction

The work reported in this thesis has been carried out in the frame of the EU ECCO-MATE project, in which Ricardo and the University of Trieste have been involved as leaders of the Work Package 1, focusing on engine, steam Rankine and ORC waste heat recovery systems thermodynamic analysis for marine and commercial vehicles medium and heavy duty Diesel engines applications.
ECCO-MATE is an European Union FP7 (Framework Package 7) project, funded under a Marie Curie ITN (Initial Training Network) scheme, which connects 16 leading international partners between academy and industry, with the scope of training young researchers and exchange knowledge between the two sectors. As mentioned, between the partners are University of Trieste and Ricardo, whose results, during the collaboration, in particular, with Winterthur Gas & Diesel (WinGD) and National Technical University of Athens (NTUA), have been reported in this work.
ECCO-MATE stands for "Experimental and Computational Tools for Combustion Optimization in Marine and Automotive Engines", and aims to create a reseach platform for the analysis, development and implementation of new technologies in order to improve the efficiency of Diesel internal combustion engines used in marine and automotive applications, creating a bridge between the two sectors, which share essentially the same challenges, in terms of energy efficiency measures and efficient combustion technlogies, in order to meet stringent new emissions standards and decrease fuel consumption.
Heavy Duty Diesel Engines (HDDE) are between the engine research targets of the ECCO-MATE project, and are also widely used in several applications, such as vehicle and ship propulsion, as well as, together with reciprocating gas engines, for small-medium size distributed stationary power generation. However, they are also among the main contributors to CO_2, Green House Gases (GHG) and several other pollutants emissions. The US EPA [1] reports that the road goods transport sector, mostly powered by HDDE, has been estimated to contribute for 14% to the world global Green House Gases (GHG) emissions in 2014, while the global carbon emissions footprint from fossil fuels have significantly increased since 1900, with a 1.5 factor in the years between 1990 and 2008.

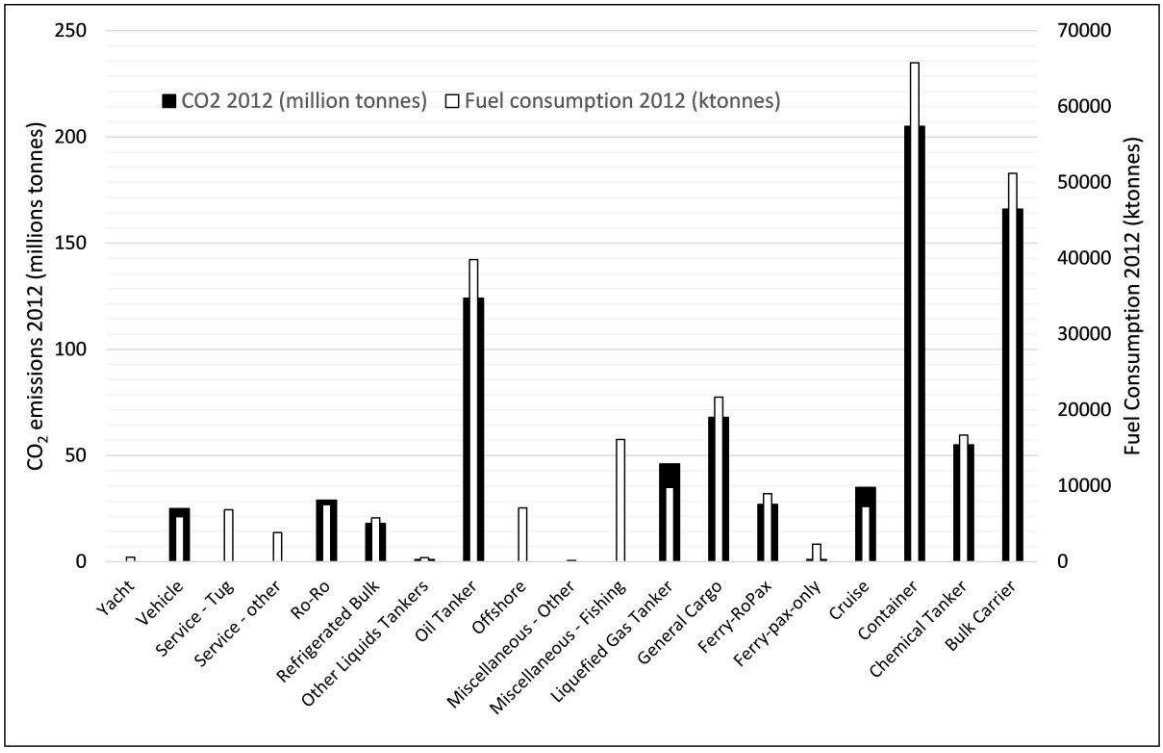

Fig. 1. CO_2 emissions and fuel consumption for different types of ships in 2012. Elaborated from [2]

In the case of the marine sector, the Third IMO GHG study [2] reports the fuel consumption and CO_2 emissions estimated for different types of ships used in the marine shipping sector in 2012. The data have been presented, after elaboration, in Fig. 1. From the analysis of the data reported, it is possible to infer that the ships which emit more CO_2 and use more fuel are: container ships, bulk carriers, oil tankers, general cargo ships and chemical tankers. These types of ships are typically powered by low speed two-stroke propulsion units, one of the main HDDE applications considered in this work and in the ECCO-MATE project, which are not broadly analysed in literature.
For these reasons, the emission reduction challenge, in order to fulfil new stringent legislations, is pushing engine manufactures and developers in the direction of further increasing the engine efficiency. Furthermore, due to the recent scandal related to polluting Diesel emissions even more measures and investments are required in order to produce a cleaner and more efficient technology, but at the same time, at accessible costs. However, no matter if the international governments are considering of banning diesel passenger cars in the next future, heavy duty Diesel engines will still remain the prime movers for commercial vehicles and ships, due to the difficulty of finding a new propulsion system which could be, at the same time, efficient and at a low cost.

2 Research Question

As already stated, large ships and commercial vehicles, powered by heavy and medium-duty Diesel engines, basically face similar challenges in terms of emissions reduction and efficiency improvement, as can be observed in the schemes proposed in Fig. 2 and Fig. 3, based on Ricardo's analysis.

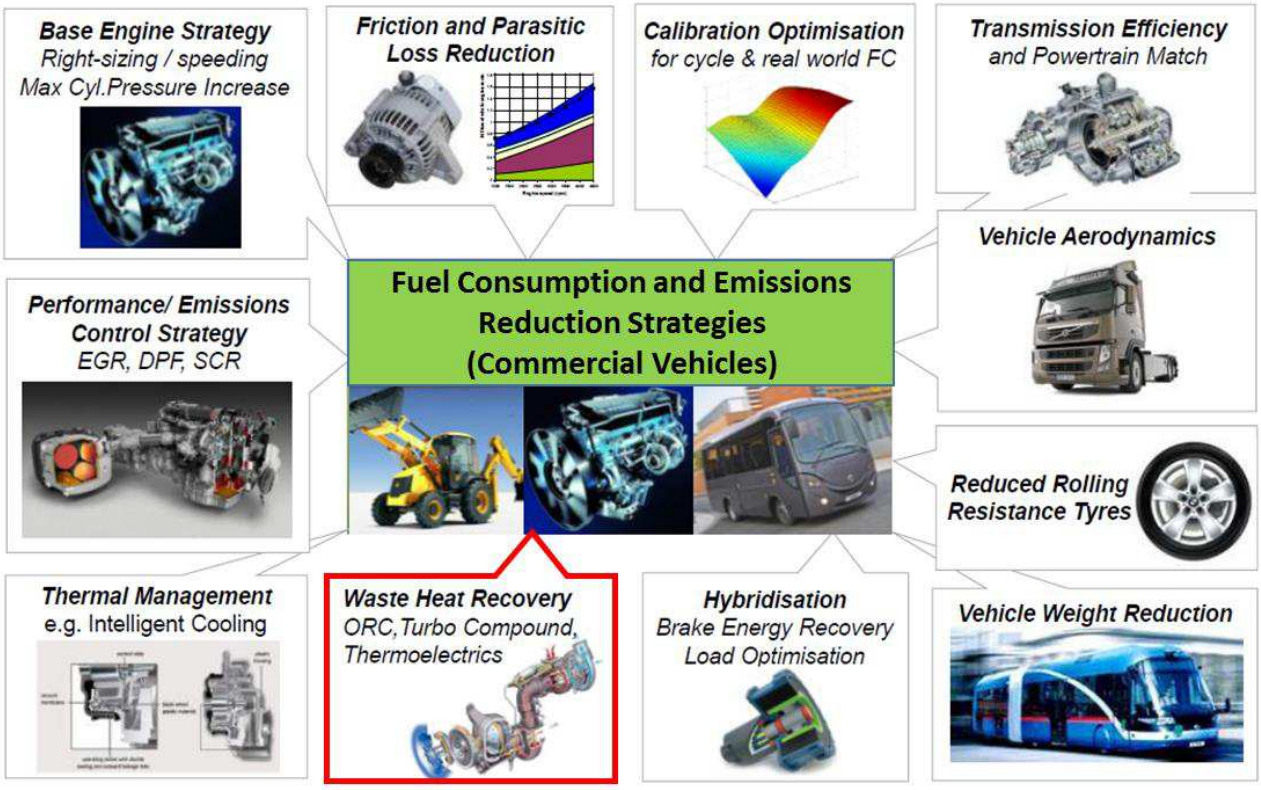

Fig. 2. Strategies to reduce fuel consumption and emissions in the commercial vehicles sector (courtesy of Ricardo)

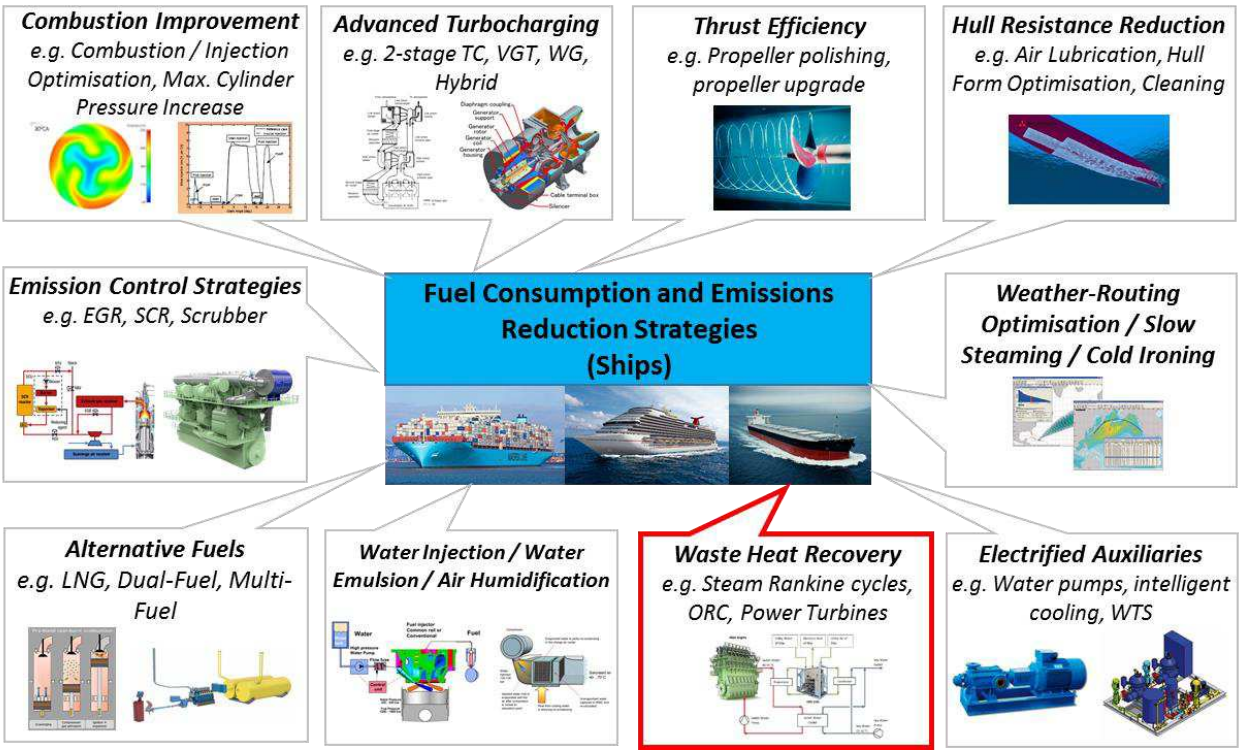

Fig. 3. Strategies to reduce fuel consumption and emissions in the marine sector

The proposed range of solutions for emissions reduction and fuel efficiency improvement, adopted or under development, encompasses, for example, combustion strategies, advanced turbocharging techniques, emission control technologies (e.g. Exhaust Gas Recirculation, EGR), alternative fuels, aerodynamics or hydrodynamics improvements, hybridization and operational strategies.
Between all solutions, waste heat recovery systems and the Organic Rankine Cycle (ORC) technology, seem to be expected to enter the market in the next decade, promising high fuel economy, and thus emissions reduction benefits.
Narrowing the field of interest of the work carried out, the research question of the proposed Ph.D. work can be explained as follows:

- ***can marine and commercial vehicles' Diesel engines emissions be reduced ensuring the same, or improved, level of powertrain efficiency, recovering the engine wasted heat by means of waste heat recovery systems, such as ORC?***

The answer to this research question has been investigated using and developing thermodynamic process simulation approaches for the combined evaluation of the overall engine-waste heat recovery system powertrain, as introduced in the next "methodology" section.

3 Methodology

In this section, a general overview of the contents of the thesis and the methodology applied has been proposed.
The first part of the work is a detailed review of Diesel engine technologies and architectures used for commercial vehicles and ship propulsion, with an overview of the most common emission reduction technologies developed in these sectors, as well as typical engine configurations statistical market data obtained, and elaborated, from Ricardo's internal resources.

Several engine heat balances have been also estimated and reported in order to obtain a clear overview of the possible energy streams characterizing the engines thermodynamic processes, and thus the use of waste heat recovery systems.
Additionally, different commercial vehicles and marine applications engine operational data have been analysed and reviewed, in order to assess the best design point for the waste heat recovery system.
A detailed overview of waste heat recovery in commercial vehicles and ships applications has been also reported, focusing the attention on the ORC technology, and in particular the working fluids used, the most common architectures proposed and the main components of the system. When considering water-steam as working fluid, the system can be thought as a traditional steam Rankine cycle.
A thermodynamic analysis of engine and waste heat recovery systems is a necessary step for the design and optimization of an efficient powertrain. For this reason, the actual industry standard powertrain development approach makes extensive use of Computer Aided Engineering (CAE) simulation software in every phase of a project, from the blank sheet, to the upgrade of existing systems, allowing to save testing and prototyping time and costs.
In this research work, the 1-D engine gas dynamic simulation software Ricardo WAVE has been used to simulate different types of engines, both for marine and commercial vehicles applications. However, Ricardo WAVE is not programmed to provide a complete overview of the energy and, in particular exergy, streams characterizing the system and its operations. For these reason, detailed post-processing routines have been developed in MATLAB, based on the principles of First and Second Law of Thermodynamics and ideal gas properties formulations. This can be seen as an extension of the capabilities of the software itself, in order to reach a higher level of detail and knowledge of the thermodynamic processes involved in engine operations.
ORC systems process simulation tools have been implemented in Engineering Equation Solver (EES) and MATLAB, in order to calculate the ORC expected performance, at different heat sources boundary conditions, and for several architectures and working fluids at the chosen design point.
In particular in the last case study proposed in this work, a First and Second Law analysis has been implemented also for the ORC system, in order to evaluate the combined engine-ORC powertrain as a whole system. Finally, a techno and thermo-economic analysis has been carried out, in order to assess the technology investment costs and the expected operational costs associated to every energy (and exergy) stream produced by the system, since costs are always the biggest driving factor for the technology acceptance and market penetration.
Following a holistic approach and the guidelines proposed in the Working Package 1 of the ECCO-MATE project, the research has been carried out at system level, rather than focusing on the single sub-system or component, considering the engine and ORC not as separated systems, but rather as a unique combined powertrain, which architecture, fluids and operational behaviour influences the overall performance, emissions and costs.
The aim of the research is to introduce and develop an approach, based on the synergic use of industry-standard engine simulation software and thermodynamic process simulation techniques, capable to assess the combined powertrain performance in the first stage of a development project. Indeed, a complete feasibility study is needed, in order to understand which configuration and technology is expected to have the best compromise between performance and costs.
The case studies proposed in this thesis have been reported in the order so to show an increased level of synergy between the engine and ORC sides analysis, with the last case study introducing a more complete methodology which could be, in principle and with further developments, applied to any kind of engine-waste heat recovery system combined powertrain.
The main issues of the use of waste heat recovery systems in marine and commercial vehicles applications have been also analysed, considering the challenges and constraints of different applications in these sectors, which are sometimes, however, not completely analysed in literature.

4 Technology Background

This section aims to introduce medium and heavy-duty Diesel internal combustion engine technologies developed in the marine and on-off highway sectors. In particular, an overview of the related emission legislations has been carried out, since strengthening of the pollutants emissions limits it is for sure, nowadays, one of the drivers of the challenge related to engine efficiency improvement.
A short overview of typical Diesel cycle engines has also been reported, considering engine architectures and emission reduction strategies and technologies, both for commercial vehicles and ships applications, as those analysed in this work.
The typical applications operating profiles have also been analysed, with the scope of giving some hints for the design of engine waste heat recovery systems. Indeed, the design point must be carefully chosen based on the typical applications' duty cycle, in order to maximize the overall system efficiency during the whole operation.
Finally, an overview of possible waste heat recovery systems has been proposed, both in the commercial vehicle and marine sector, with particular interest on the Organic Rankine Cycle (ORC) and steam Rankine cycle technology, considering technical aspects, issues and challenges for the applications investigated in this work. Some other considerations have been then drawn from the results of the four case studies proposed in this work.

4.1 Heavy Duty Diesel Engines (HDDE)

Heavy duty Diesel engines have been developed for decades to achieve the best possible fuel consumption consistently with other constraints such as legislations on exhaust emissions and noise, cost, durability and reliability. They are the most used sources of power for commercial vehicles, ships and power generation applications. An overview of their main characteristics has been reported in the next sections.

4.1.1 Emission Legislations in On-Off Highway and Marine Sectors

4.1.1.1 On-off highway commercial vehicles sector

As already stated, one of the drivers in the challenge of internal combustion engines efficiency improvement, is the introduction of new, more stringent, emission limits and legislations, which are pushing engine developers and manufacturers in the direction of introducing more advanced powertrain technologies, such as also, for example, waste heat recovery systems.
In this work, for brevity of discussion, just some of the emissions standards have been reported, concerning on-highway, off-highway and marine sectors, with particular interest on the engine types considered in the case studies proposed.
In Tab. 1, the most recent emissions legislations for HDDE on-highway vehicles have been reported, considering in particular the US Federal EPA'10 and the European standards Euro V and Euro VI. The emission limits for NO_x, PM (Particulate Matter), CO and PN (Particle Number, introduced with Euro VI) have been presented, together with the typical test cycles used for certification purpose and the date of introduction. The data have been obtained and elaborated from Ricardo EMLEG database [3].
In Tab. 2, the most recent emissions legislations for off-highway (non-road) HDDE vehicles have been reported, divided for engine brake power category (data have been presented only for engines with more than 50-60 kW brake power and divided by power range). The US Federal Tier 4 interim and Tier 4 final, as well as the European Stage IV and future Stage V have been considered.

	EPA '10	EU V	EU VI
NOx (mg/kWh)	270	2000	400 (WHSC) 460 (WHTC)
PM (mg/kWh)	13	20	10
CO (mg/kWh)	20786	1500	1500 (WHSC) 4000 (WHTC)
PN (#/kWh)	/	/	8.0×10^{11} (WHSC) 6.0×10^{11} (WHTC)
Test Cycles	FTP & SET	ESC & ETC	ESC & ETC (Future WHSC & WHTC)
Introduction	1/1/2010	10/2008	31/12/2013

Tab. 1. HDDE emission legislation for on-highway applications

	Tier 4i	Tier 4f	Stage IV	Stage V
NOx (mg/kWh)	3500 (kW>900, all others) 670 (kW>900, gensets) 3500 (560-900 kW) 400 (56-560 kW)	400 (56-560 kW)	400 (56-560 kW)	3500 (kW>560) 400 (56-560 kW)
PM (mg/kWh)	100 (kW>560) 20 (56-560 kW)	40 (kW>560, all others) 30 (kW>560, gensets) 20 (56-560 kW) 30 (19-56 kW)	25 (56-560 kW)	45 (kW>560) 15 (56-560 kW)
PN (#/kWh)	-	-	-	1×10^{12} (56-560 kW)
CO (mg/kWh)	3500 (kW>130) 5000 (37-130 kW)	3500 (kW>130) 5000 (19-130 kW)	3500 (130-560 kW) 5000 (56-130 kW)	3500 (130-560 kW) 5000 (56-130 kW)
Test Cycles	NRSC & NRTC	NRSC & NRTC	NRSC & NRTC	NRSC & NRTC
Introduction (approval)	2011 (kW>130) 2012 (56-130 kW)	1/1/2014 (130-560 kW) 1/1/2015 (56-130 kW)	31/12/2012 (130-560 kW) 30/09/2013 (56-130 kW)	Proposed 09/2014 Planned 2018/2019

Tab. 2. HDDE emission legislation for off-highway (Non-Road) applications

4.1.1.2 Marine sector

In the marine sector and, in particular, considering large size Diesel engines such as those analysed in this work, the International Maritime Organization (IMO) adopted the MARPOL Annex VI first in 1997 [4], in order to limit the main air pollutants contained in ships' exhaust gas (and in particular SO_x, NO_x and PM). Following the introduction of MARPOL Annex VI in 2005, the Marine Environmental Protection Committee (MEPC), decided to revise the MARPOL Annex VI in order to strengthen the emission limits, considering future technological improvements. In 2008, the revised MARPOL Annex VI entered into force. ECAs (Emission Control Areas) and IMO Tier II and Tier III emission limits have been proposed [3,5].
Emission Control Areas are currently established in the Baltic Sea (SO_x), North Sea (SO_x), North America (NO_x and SO_x), US Caribbean Sea, Puerto Rico and US Virgin Islands (NO_x and SO_x), but other are planned to be established in the next future, with particular interest to Mexican Caribbean Sea, Mediterranean Sea and Japan.
In the SO_x ECAs, the legislation introduced special fuel quality requirements, in particular the sulphur compounds amount in the fuel must be below 0.1% in mass. For this reason, cleaner fuel must be used, unless efficient scrubbing and cleaning technologies are used when employing Heavy Fuel Oils (HFO) for propulsion, in order to respect sulphur limits.

With respect to NO_x emissions, the limits imposed by the IMO Tier regulations depend on the maximum engine rotational speed (*N, rpm*) as shown in Tab. 3. The Tier I and II thresholds are global, while the Tier III standards apply only in NO_x ECAs.

IMO Tier	Date	NO_x Limit, g/kWh		
		N < 130	**130 ≤ N < 2000**	**N ≥ 2000**
Tier I	2000	17.0	$45 \cdot n^{-0.2}$	9.8
Tier II	2011	14.4	$44 \cdot n^{-0.23}$	7.7
Tier III	2016	3.4	$9 \cdot n^{-0.2}$	1.96

Tab. 3. IMO Tier NO_x regulation limits

Tier II standards are expected to be met by combustion processes optimization and engine operations improvements, with particular focus, for example, on fuel injection timing, injection pressure, injector and spray developments, intake and exhaust valve timing (e.g. Miller timing) and cylinder compression ratio. These topics have also been considered in the ECCO-MATE project by some project partners.
However, Tier III standards are expected to require dedicated NO_x emission control strategies or technologies, such as water injection, Exhaust Gas Recirculation (EGR) or Selective Catalytic Reduction (SCR).
Tier III regulation imposes up to 80% NO_x reduction compared to IMO Tier I, in particular for low speed, large bore, Diesel engines, as those evaluated in this work.
Moreover, with the MARPOL Annex VI introduction, the Energy Efficiency Design Index (EEDI) [6] was made mandatory for new ships, and it aims at promoting the use for more energy efficient and less polluting engines and ships' equipment, thus including also waste heat recovery systems, in order to reduce CO_2 emissions, which are directly related to fuel consumption. The Ship Energy Efficiency Management Plan (SEEMP) also established a mechanism for operators in order to improve energy efficiency of all ships.

4.1.2 Engine Performance Introduction

The internal combustion engine is a device, based on an open thermodynamic cycle, whose scope is to convert the chemical energy of a fuel (e.g. diesel) into mechanical energy for different uses, such as vehicles or ships propulsion, or power generation.
It is out of the scope of this work to report a detailed overview of the working principles of an internal combustion engine, which can be deepened in very well-known references in the field, such as [7–9]. However, in this work, some of the main performance parameters connected to the engine operations have been shortly considered because often reported in engine and waste heat recovery research. Some other performance information has been reported in section 5.1, when considering engine modelling topics.
Traditionally, two operating cycles can be possible for reciprocating combustion engines: two-stroke and four-stroke. The two-stroke cycle accomplishes all events in one revolution (two piston strokes), while the four-stroke cycle accomplishes all events in two revolutions (four piston strokes).
The Diesel cycle is an ideal cycle which, however, does not represents the real processes happening in a compression ignition engine. It is composed by four reversible transformations:

- 1 – 2: isentropic compression;
- 2 – 3: constant pressure heat addiction;
- 3 – 4: isentropic expansion;

- 4 – 1: constant volume heat rejection;

The volume changes during operations from the one at the Top Dead Centre (TDC) and the one at the Bottom Dead Centre (BDC), while the ideal pressure vs volume trend has been reported in Fig. 4.

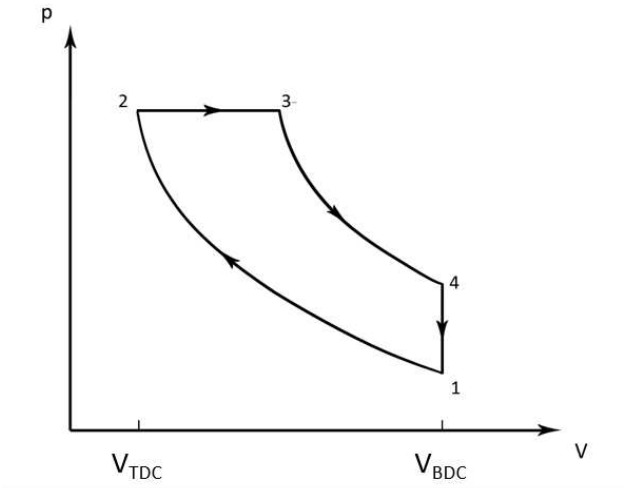

Fig. 4. Diesel ideal cycle pressure-volume diagram

The ideal cycle is not representative of reality mostly because of gas exchange processes and valves interactions.

As already stated, the objective of an engine is to provide work to the shaft. For this reason, generally, engines are rated by their power output, which is the time rate of the work developed. For an engine cycle, the work (often called indicated work, [J or kJ]) is calculated as the area within the curve of a pressure-volume diagram [7]:

$$W_{ind} = \oint p \cdot dV \qquad (1)$$

An example of pressure-volume diagram has been reported in Fig. 5, for the four-stroke engine considered in the case study in section 6.4. The curve has been calculated from a detailed 1-D gas dynamic model considering all gas exchange processes, thus showing the differences compared to the ideal cycle example reported in Fig. 4.

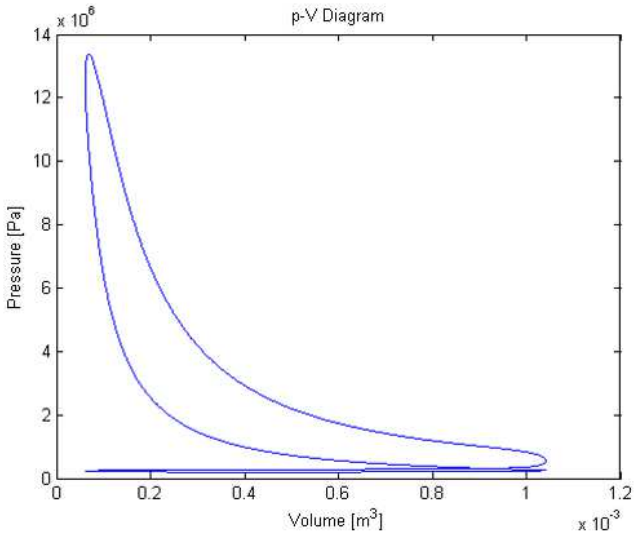

Fig. 5. Diesel pressure-volume diagram obtained from a detailed 1-D gas dynamic model

When considering the two-stroke cycle, the interpretation of eq. (1) is straightforward, while, with the addition of the intake and the exhaust strokes, in case of the four-stroke cycle, usually two different cases can be observed:

- Gross indicated work per cycle ($W_{ind,gross}$): it considers only the work delivered to the piston during compression and expansion strokes;
- Net indicated work per cycle ($W_{ind,net}$): it considers the work delivered to the piston over the entire cycle;

The two terms differ for a four-stroke cycle, in which the pumping work (W_{pump}, [J or kJ]) term can be observed, due to the work done by the piston during the gas exchange processes during the intake and exhaust strokes. This work can be either negative (usually naturally aspirated engines) or positive (usually supercharged or turbocharged engines).

$$W_{ind,net} = W_{ind,gross} - W_{pump} \quad (2)$$

Usually, the work considered in the engine rating is the one obtained at the shaft, measured by a dynamometer on the test bench (shaft power, or brake power, [J or kJ]), thus considering also the engine mechanical efficiency, through the friction losses (W_{frict}) [10]:

$$W_{brake} = W_{ind,net} - W_{frict} \quad (3)$$

The power obtained at the shaft [kW] can then be calculated as:

$$\dot{W}_{brake} = \frac{W_{brake} \cdot N}{n_r} \quad (4)$$

in which N is the rotational speed is [rev/s] and n_r are the number of revolutions per cycle (2 for the four-stroke cycle and 1 for the two-stroke). In the same way, the power can be calculated also for the net indicated and gross indicated cases.
Another useful parameter to evaluate engine performance is also the brake torque [Nm], which can be obtained from the dynamometer tests, or from the brake power as [10]:

$$\tau_{brake} = \frac{\dot{W}_{brake}}{2\pi N} \quad (5)$$

Very often used in engine performance studies is also the parameter mean effective pressure (MEP), which is the average cylinder pressure which provides the equivalent work of the engine cycle [10]. For the brake mean effective pressure (BMEP):

$$BMEP = \frac{\dot{W}_{brake} \cdot n_r}{V_d \cdot N} \quad (6)$$

with V_d the engine displacement [m^3]. The BMEP can be considered as a measure of the load of the engine and is usually reported in [bar]. Generally, a high BMEP indicates an engine design which produces high power compared to its size. Highly boosted engines have usually high BMEP compared to naturally aspirated.
In the same way, the mean effective pressure can refer to the indicated power (IMEP, gross or net), to the pumping power (PMEP) or to the friction dissipated power (FMEP), with the same relationships reported previously for the work terms.

The thermal efficiency (or brake thermal efficiency, $\eta_{th,eng}$) is another parameter which is used to quantify engine performance during the design phase and, in particular, it correlates the amount of work produced per amount of fuel energy introduced into the system. Generally, the fuel energy is quantified through the Lower Heating Value (LHV), which for diesel is around 44.8 MJ/kg [7,11]. The brake thermal efficiency can be written as [7,10]:

$$\eta_{th,eng} = \frac{\dot{W}_{brake}}{\dot{m}_{fuel,inj} \cdot LHV} \quad (7)$$

with $\dot{m}_{fuel,inj}$ the mass flow of fuel injected per engine cycle [kg/s].
One of the main parameters considered during engine development phases is for sure the brake specific fuel consumption (BSFC, [g/kWh]), which is a measure of the fuel efficiency of any engine, despite of its size. It is generally used to compare the performance of different engines architectures, types and sizes. This performance parameter is largely considered throughout the entire work of this thesis.

$$BSFC = \frac{\dot{m}_{fuel,inj}}{\dot{W}_{brake}} \quad (8)$$

For a scope of comparison, a chart with different BSFC data for several different engines has been reported in Fig. 6, obtained from a Ricardo internal data analysis. Every point reported in the chart represents a commercial engine, with name, brake power output [kW] and BSFC reported in the associated label. The typical application segment has been also reported above the horizontal axis. The coloured circles have been proposed just in order to give a qualitative idea of the increased size of the engine.

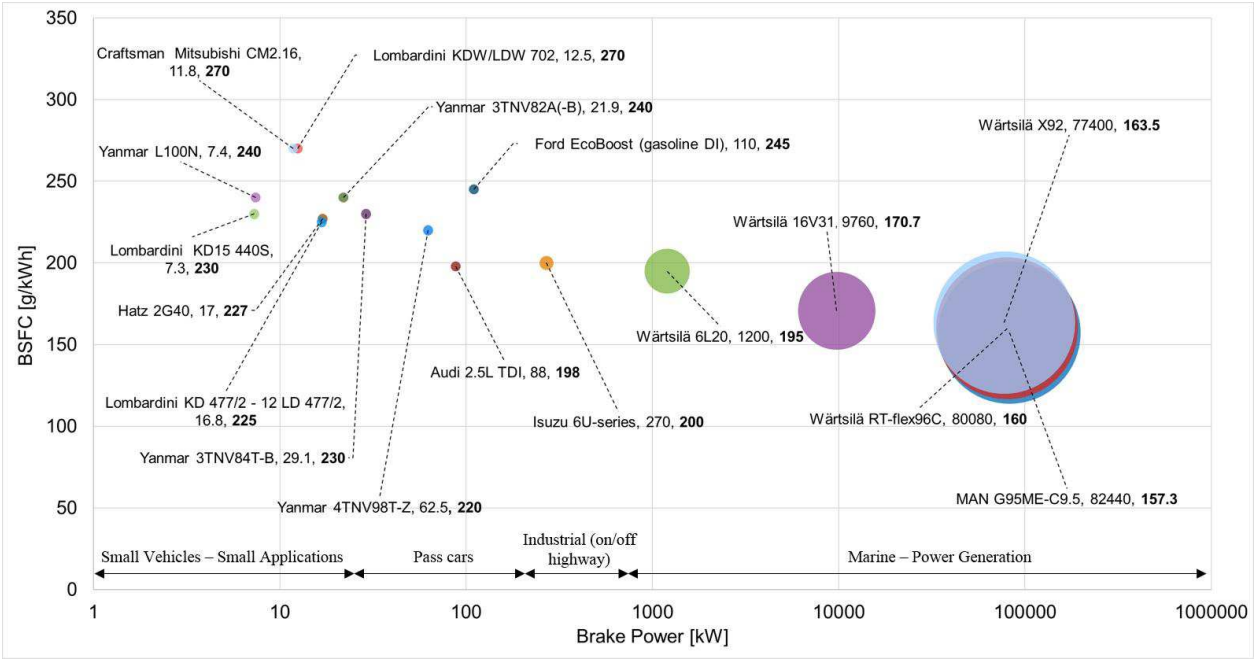

Fig. 6. BSFC vs brake power chart for different engines available on the market (courtesy of Ricardo)

The data reported in Fig. 6 clearly show how larger engines have a lower BSFC, thus being much more efficient than smaller ones. In particular, large two-stroke low speed marine Diesel engines, such as those considered in the case study in section 6.3 are the most efficient combustion engines commercialized, with around 155 – 170 g/kWh BSFC levels.

4.1.3 HDDE Architectures and Energy Balances

In this section, a short overview has been proposed regarding the most common architectures and technologies used in commercial vehicles and marine Heavy-Duty Diesel Engines (HDDE). In particular, the technological solutions proposed are usually the result of the need of meeting BSFC and emissions reduction targets, in order to improve overall powertrain efficiency and reduce fuel consumption.
Some data, coming from a detailed analysis of engine production databases, have been reported for the two sectors considered in this work, in order to highlight which technologies are currently considered by engine manufacturers and developers.
The different engine configurations are then also impacting the system energy balance, introducing, for example, new possible heat sources to be recovered through the means of thermodynamic bottoming cycles such as Organic Rankine Cycles (ORC), as it happens in the case of exhaust gas recirculation (EGR).

4.1.3.1 On-off Highway Commercial Vehicles Engines

Most of nowadays commercial vehicles are powered by Heavy Duty Diesel Engines (HDDE) with a brake power output usually up to 600 kW for on-highway applications, and even more for off-highway (e.g. heavy haul mining trucks). The last generation engines are commonly high pressure common rail, direct injection (DI), Diesel engines, with in-line or V configurations and 4 to 12 cylinders, with displacements up to around 12 litres. Some statistics, regarding air management strategies, fuel and emissions reduction technologies used, have been reported in Fig. 7. The data have been elaborated from the database EnginLink [12], which contains, as declared, global engine production, forecast and specification data for 92% of the world's engine produced from 1958 until February 2016.

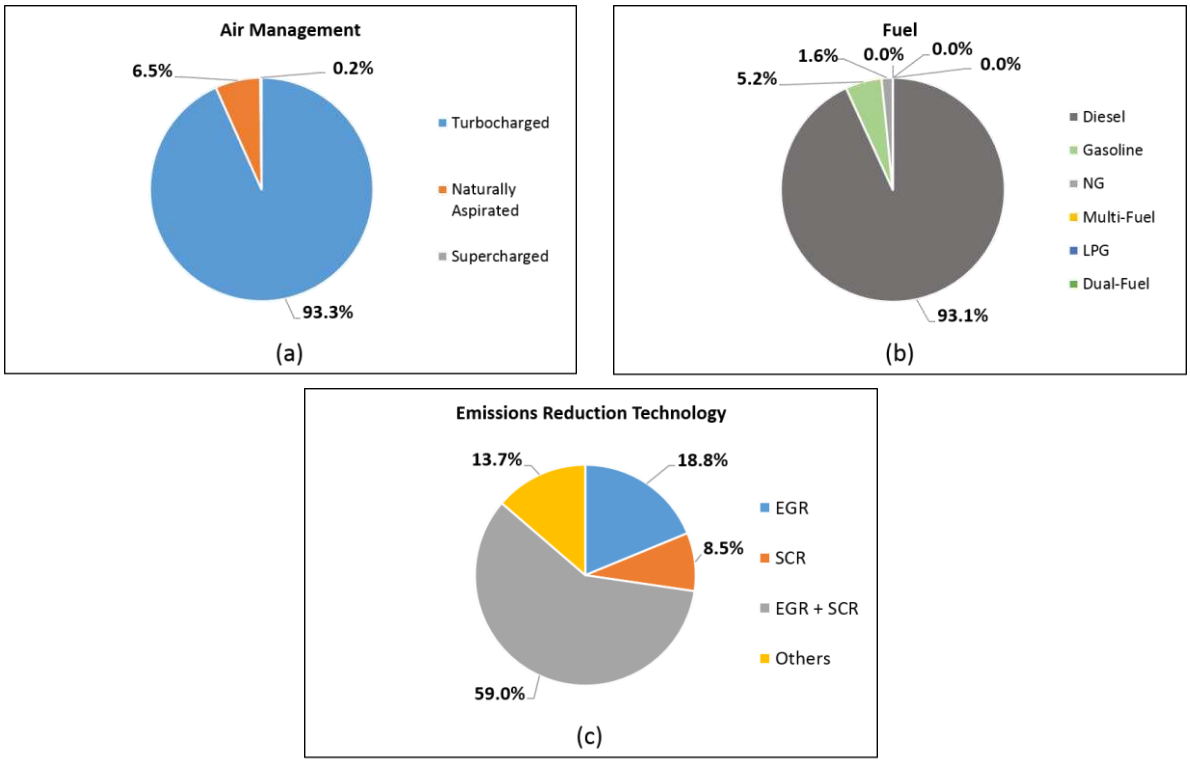

Fig. 7. Analysis of produced engines statistics in the on-off highway commercial vehicles sector: (a) air management strategy, (b) fuel used and (c) emissions reduction technology applied

The data reported in this work are for engines in the brake power category between 200 kW and 1 MW brake power, for on and off highway applications. The categories reported in the emissions reduction technology charts have been reduced to four main macro-categories: Exhaust Gas Recirculation (EGR) only, Selective Catalytic Reduction (SCR) only, EGR and SCR used together (EGR+SCR) and an "others", which mainly includes catalysts, Diesel Oxidation Catalyst (DOC) only and combustion optimization systems.
As can be observed from the data previously reported, most of the engines in the on-off highway sectors, for the search criteria considered, are turbocharged engines (93.3%), running on diesel fuel (93.1%), using mostly a combination of EGR and SCR (59%) to meet emissions legislations pollutants limits. Some configurations, depending on the manufacturer, are available also with EGR (18.8%) or SCR (8.5%) only.
EGR recirculates exhaust gas before (high pressure, HP) or after (low pressure, LP) the turbocharger in order to decrease combustion temperatures and NO_x emissions. On the other hand, SCR uses injection of a urea-based mixture, inside a reactor with a catalyst, in order to directly reduce NO_x on the exhaust line of the engine.
Generally, engine manufacturers choose the most suitable emission reduction technology based on a combination of cost, reliability, fuel economy and customers' acceptance. Some possible benefits and concerns regarding the most common emission tackling approaches have been reported in Tab. 4.

	EGR	**Cooled EGR + SCR**	**Uncooled EGR + SCR**	**High Efficiency SCR**
Typical EGR Rates (%)	~45% - 55%	~20% - 30%	~15% - 25%	none
SCR Conversion Efficiency (%)	none	~90% - 92%	~94% - 96%	~94% - 99%
Urea Consumption (% of fuel)	none	~2% - 3%	~5% - 7%	~6% - 8%
Benefits	No problems of SCR warm-up (light-off) and thermal management Lower engine backpressure issues Compact system	Evolution of known technology NO_x reduction from cold start NO_x reduction with low exhaust temperature	Costly EGR cooler deleted (no fouling problems) NO_x reduction from cold start NO_x reduction with low exhaust temperature Faster catalyst warm-up (light-off)	More efficient combustion if SCR backpressure optimized No EGR system (saves weight and cooling demand) Potential for fuel consumption improvement compared to cases with EGR use
Concerns	Less efficient combustion due to EGR use High increase in cooling demand Oil change interval shortened Not enough to meet new emissions targets unless combustion is heavily optimized	Less efficient combustion due to EGR use Cost of EGR + DPF + SCR Additional weight due to urea storage tank Increased cooling demand Oil change interval shortened	Less efficient combustion due to EGR use Relatively high urea consumption and need of storage Additional weight for the vehicle In-service compliance with aged catalysts	Decreased NO_x reduction under cold start. Thermal management is critical Sophisticated control strategies with additional sensors (NH_3) High urea consumption and need of storage Additional weight for the vehicle In-service compliance due to deterioration of catalysts

Tab. 4. Most common NO_x emissions reduction strategies for commercial vehicles: benefits and concerns

Many manufacturers push in the direction of improving SCR efficiency and use lower EGR rates, uncooled EGR or no EGR, to reduce heat rejection to the engine cooling system and the need of advanced boosting strategies (Variable Geometry Turbines, VGT, or two-stage turbocharging), as well as for better combustion efficiency.
However, the tendency could be inversed when designing efficient waste heat recovery systems recovering heat from EGR circuit, leading to the possibility to obtain additional net power output and to reduce the cooling system impact, transforming into useful energy the heat that, otherwise, should be rejected to ambient through the vehicle cooling package.
An advanced HDDE, two-stage turbocharged, configuration has been reported in Fig. 8, with cooled Exhaust Gas Recirculation (EGR), Diesel Oxidation Catalyst (DOC), Diesel Particulate Filter (DPF) and Selective Catalytic Reactor (SCR) after treatment, as well as aftercooler (HP CAC, High Pressure Charge Air Cooler), intercooler (LP CAC, Low Pressure Charge Air Cooler), HP turbine-compressor (HPT, HPC), LP turbine-compressor (LPT, LPC). The scheme is representative of the engine considered in the case study in section 6.1, and is one of the most used architectures for commercial vehicles HDDE emissions compliancy.

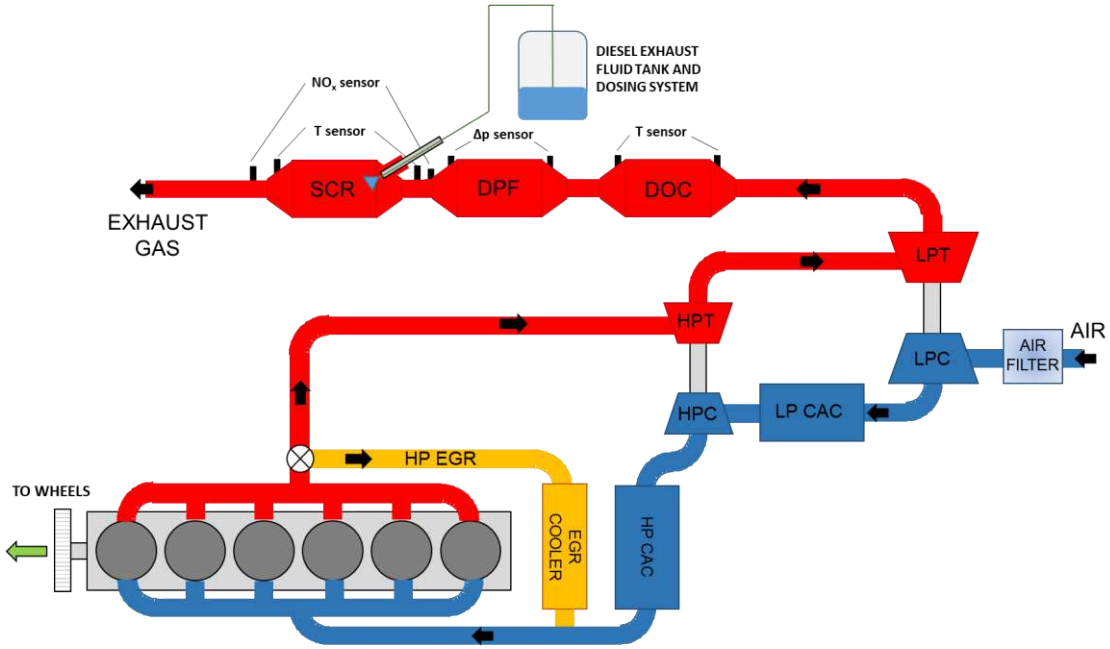

Fig. 8. Advanced Tier 4 final compliant commercial vehicle HDDE scheme with two-stage turbocharging, cooled EGR, DOC, DPF and SCR

As can be partially observed from the engine scheme and the previously reported statistics, several strategies are currently adopted and developed, in the on-off highway commercial vehicles sector, in order to meet emissions legislations' target and improve engine fuel consumption, and can be divided basically in two categories: engine-powertrain-applied or engine-bottoming technologies, depending if they are directly applied or retrofitted to the engine-powertrain system, or if they recover wasted engine energy.
Examples of first category technologies are engine downsizing, using advanced turbocharging or boosting technologies (e.g. waste gate, variable geometry turbines, e-boost, two-stage and series turbocharging) [13,14], coupled with exhaust gas recirculation (EGR) for NO_x reduction [15], Variable Valve Timing (VVT) and advanced Miller timing strategies [16]. Other possibilities are related to combustion improvement using particularly shaped combustion chambers (optimized using Computational Fluid Dynamics and improved chemical kinetics combustion modelling as proposed in ECCO-MATE) together with high pressure injection (up to more than 2500 bar) and advanced

injection strategies [17]. Moreover, engine friction reduction is also under study [18], using improved coatings for the cylinder liners, better surfaces finish, new piston rings and bearings designs, lubricants and seals as well as variable speed electrically driven lubricating oil and coolant water pumps and cooling fans.
Furthermore, engine-tailpipe or bottoming technologies are under development, such as advanced aftertreatment strategies using Diesel Oxidation Catalysts (DOC), Diesel Particulate Filters (DPF) and Selective Catalytic Reduction (SCR) with urea injection for emissions reduction (e.g. DEF, Diesel Exhaust Fluid, or the commercial AdBlue®) [19], or waste heat recovery technologies such as Organic Rankine Cycles (ORC) and steam Rankine cycles (RC) [20,21], turbo-compounding [22] and Thermo-Electric Generators (TEG) [23,24].
In the last years, great importance has been given also to the study of alternative powertrain concepts, such as, for example, hybrid-electric [25,26] and fuel cell powered vehicles [27] architectures.
New fuels, previously not considered for engine or vehicle applications, such as LNG (Liquefied Natural Gas) [28,29], biofuels and biodiesel (or diesel additives) [30–35] are also currently investigated and developed in order to reduce engine emissions. In particular, as reported by Chauhan *et al.* [30] and Shahir *et al.* [34], the use of biodiesel blends in traditional compression ignition engines tends to reduce particular matter (PM), unburned hydrocarbons (HC) and carbon monoxide (CO) emissions, at the price of a slight increase in fuel consumption and nitric oxide (NO_x) emissions.
Kinetic energy recovery systems are also under development such as brake energy recovery or flywheels [36].
As already presented in the reported charts and tables, some main technologies, which are mostly affecting the architecture of the engine itself, and thus also the possibility of waste heat recovery, can be considered: turbocharging strategies (series turbocharging in particular), Exhaust Gas Recirculation (EGR) circuits and Selective Catalytic Reactor (SCR), usually on the tailpipe of the engine.
As a matter of comparison, some heat balances, for different engines configurations, have been reported below, with the scope of demonstrating how the chemical energy, supplied with the diesel fuel, is divided into the various heat balance contributions. In particular, this kind of analysis is very important when considering waste heat recovery studies or combined engine-waste heat recovery powertrain developments, as those proposed in this work. The charts reported come from different engine data available in Ricardo.

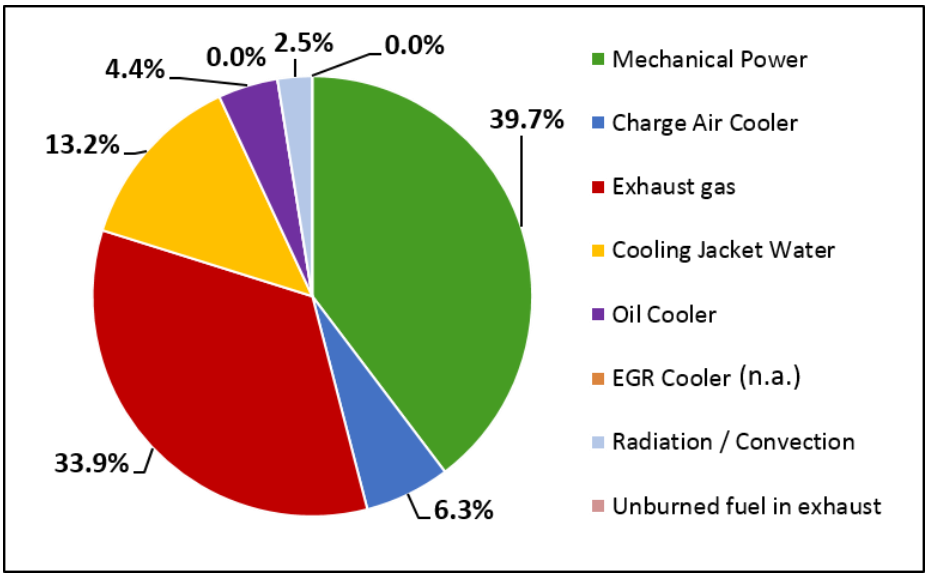

(a)

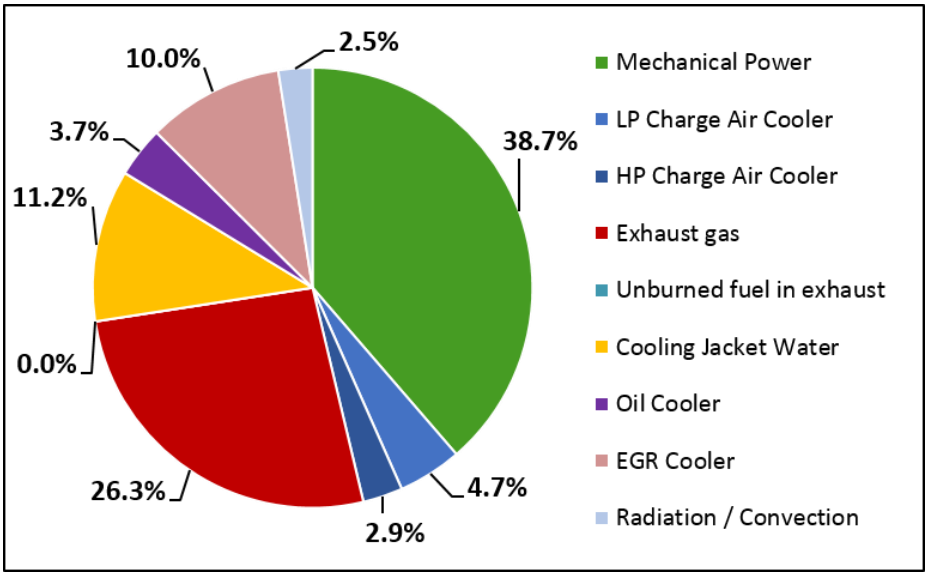

(b)

Fig. 9. Heat balances. (a) 300 kW brake power @ 2000 rpm (full load) engine with charge air cooler, single-stage turbocharger and no EGR. (b) 300 kW brake power @ 2000 rpm (full load) engine with two-stage charge air cooler, two-stage turbocharger and HP EGR

The heat balances reported in the proposed charts have been estimated from real test data, imposing a 2.5% radiation term and a coolant/oil heat distribution based on typical values for commercial vehicles HDDE, from Ricardo's experience.

As can be observed from the charts in Fig. 9 (a-b), exhaust gas, engine coolant, charge air cooling and EGR (when available) are between the most important contributions in terms of energy streams. In particular, when available, EGR has a big impact on the engine heat balance. For this reason, the recovery of EGR heat through the mean of possible bottoming cycles, such as an ORC or RC systems, can be beneficial both in term of powertrain performance and vehicle thermal management. Moreover, lower temperature contributions, such as charge air cooling and coolant heat, can also, in principle, be recovered through the means of a power cycle, in order to decrease the impact on the vehicle cooling system and, at the same time, improve overall powertrain efficiency. In this case, low temperature suitable cycles, such as ORC, can become very interesting.

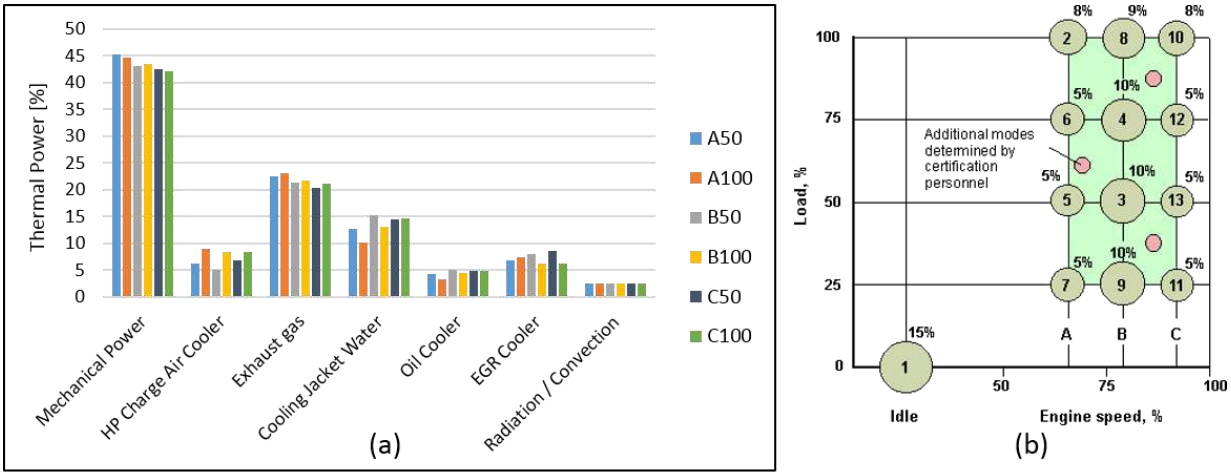

Fig. 10. (a) Thermal power (energy) distribution for different ESC cycle operating points for a 390 kW brake power @ 1800 rpm engine with two-stage turbocharger and high pressure EGR. (b) ESC cycle speed-load points scheme [37]

Also in Fig. 10, the energy distribution of a typical two-stage turbocharged heavy duty Diesel engine for commercial vehicles applications (on-highway, truck) has been reported. The engine has a configuration with high pressure EGR. Also in this case, it is possible to observe the important energy contributions, at different engine speed-load points, of the several heat balance entries, showing once again the importance of recovering heat streams which otherwise would be lost or just an additional load for the vehicle cooling package.
In this case the data have been reported for different operating points which are usually tested during a European Stationary State (ESC) cycle, whose characteristics can be explored in references [3,37].
Once again, the data have been estimated with the same assumptions proposed for the charts reported in Fig. 9.
Similar considerations as reported for the commercial vehicles engines have been proposed for the marine engines considered in this study. An overview has been reported in the next section, while more detailed information about waste heat recovery have been collected in section 4.2.

4.1.3.2 Marine Engines

Most of nowadays HDDE used for auxiliary power generation and main propulsion are either four-stroke medium speed or two-stroke low speed engines, as those considered in this work.
As already done for the on-off highway commercial vehicles case, some statistics regarding air management, fuel and emissions reduction technologies used have been also reported for marine auxiliary and propulsion engines, both four-stroke and two-stroke in the brake power range higher than 1 MW, representative of the engines considered in the case studies reported in section 6.2 and section 6.3. The data have been elaborated again from the EnginLink database [12] and reported in Fig. 11, for a time frame between 1975 and February 2016.

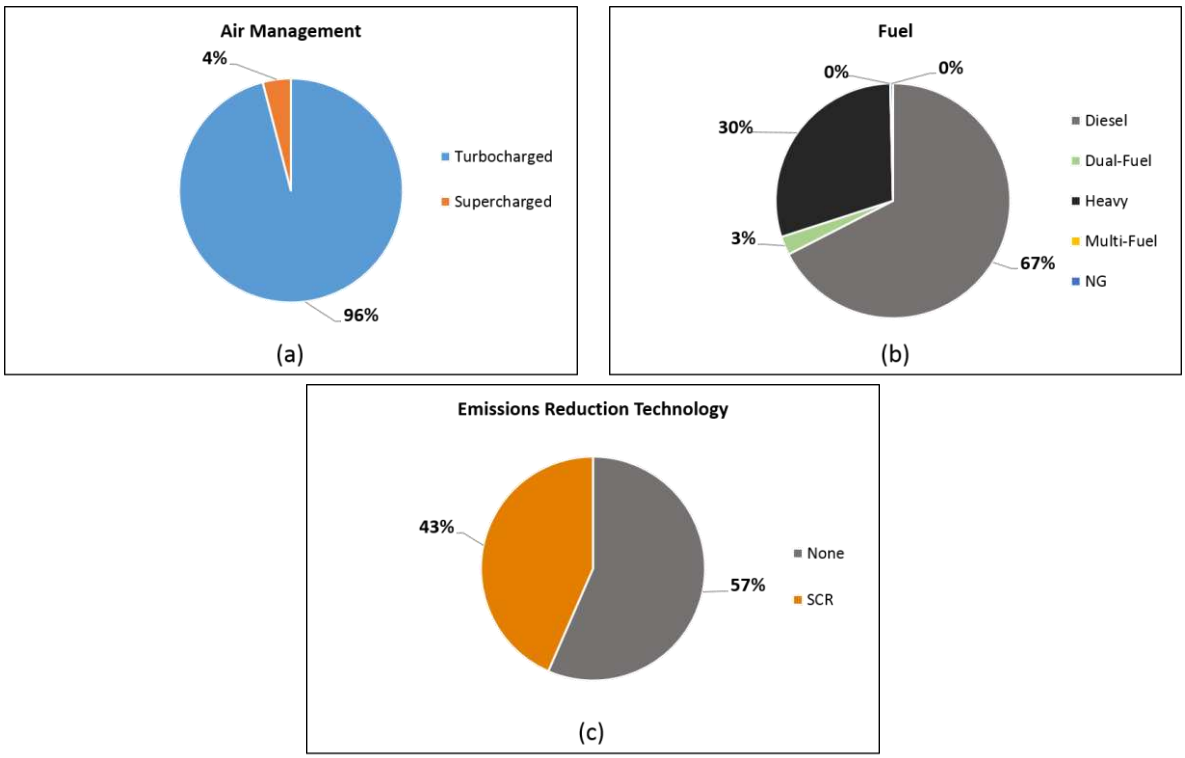

Fig. 11. Analysis of produced engines statistics in the marine sector: (a) air management strategy, (b) fuel used and (c) emissions reduction technology applied

As can be evinced from the proposed charts, most of the engines produced for marine auxiliary power generation or for ship propulsion are turbocharged (96%), running on Marine Diesel Oil (MDO, "Diesel", 67%), Heavy Fuel Oil (HFO, "Heavy", 30%) or, in small percentage, dual-fuel (3%, typically methane or natural gas plus diesel for pilot injection). It is also possible to observe how, due also to the presence in the data of old engines built even before the year 2000, most of the engines produced have no emissions reduction technologies (57%), while the other percentage uses SCR (43%). Some engines, produced recently, uses however also EGR, even if in case of four-stroke engines or two-stroke propulsion units, however, both SCR and EGR systems are still under development due to stringent emissions limitations.
Generally, in the marine sector, several emissions reduction technologies are available or currently developed in order to meet IMO Tier III standards.
MAN ([38–43]) presented a series of reports investigating the performance and technical feasibility of some different strategies, focusing in particular on EGR and SCR for the reduction of NO_x and SO_x, also through the use of scrubbing technologies, but also considering engine combustion tuning strategies, water injection, waste heat recovery and natural gas utilization.
Also several Wärtsilä and Winterthur Gas & Diesel (e.g. [44–47]) presentations and reports are available in literature concerning the possible emission reduction strategies for low and medium speed marine engines.
The US EPA (Environmental Protection Agency) presented some reports ([48,49]) regarding NO_x emissions reduction technologies as well as considering the economic impact of several strategies which can be applied to marine Diesel engines to meet IMO Tier III standards. The ICCT (International Council on Clean Transportation) reported a white paper [50] evaluating the techno-economic feasibility of different possibilities to reduce greenhouse gases emissions from ships, not only considering engine related solutions, but other actions such as, for example, hull coatings, water flow optimization, weather routing and efficient route optimization, air hull lubrication, wind and solar powered propulsion.
Also, several researchers considered emissions reduction topics in marine applications. For example, Geist *et al.*_[51] presented an overview of NO_x reduction techniques to be applied to marine Diesel engines, developed and studied at the New Sulzer Diesel Ltd (later Wärtsilä and now WinGD). They declared, at that time, that IMO Tier I emission standards could be met with well-chosen engine primary methods only, such as combustion tuning, fuel injection tuning, compression ratio, Miller supercharging, excess air ratio, scavenging air temperature. wet technologies and EGR. Secondary methods, such as SCR, are declared to be more efficient but also more expensive, thus being suitable for future emission legislations (actual IMO Tier III).
Other overviews of emissions reduction technologies and strategies developed and used in the marine sector can be found in references such as [52–55]. A detailed description is avoided in this work, but it is going to be proposed in a review paper, which investigates the influence of different emissions reduction technologies on the possible use of waste heat recovery systems for marine engines. In this work, only a more detailed description of the advanced turbocharging strategies and EGR systems has been proposed, because considered in the case studies in section 6.2 and section 6.3.
Emission reduction technologies can be basically divided in primary methods (engine related) and secondary methods (engine retrofitting). In the first category, technologies as advanced turbocharging strategies coupled with Miller timing, combustion tuning, wet methods, alternative fuels usage, EGR can be classified. In the second category, technologies such as scrubbers, SCR and waste heat recovery can be considered. Other strategies can also be applied and can be more related to ships operations or ships design, such as slow steaming, route and weather routing optimization, hull fluid dynamic optimization and coating. A conceptual scheme of the possible engine-related emission reduction technologies and strategies for four-stroke and two-stroke engines has been reported in Fig. 12.

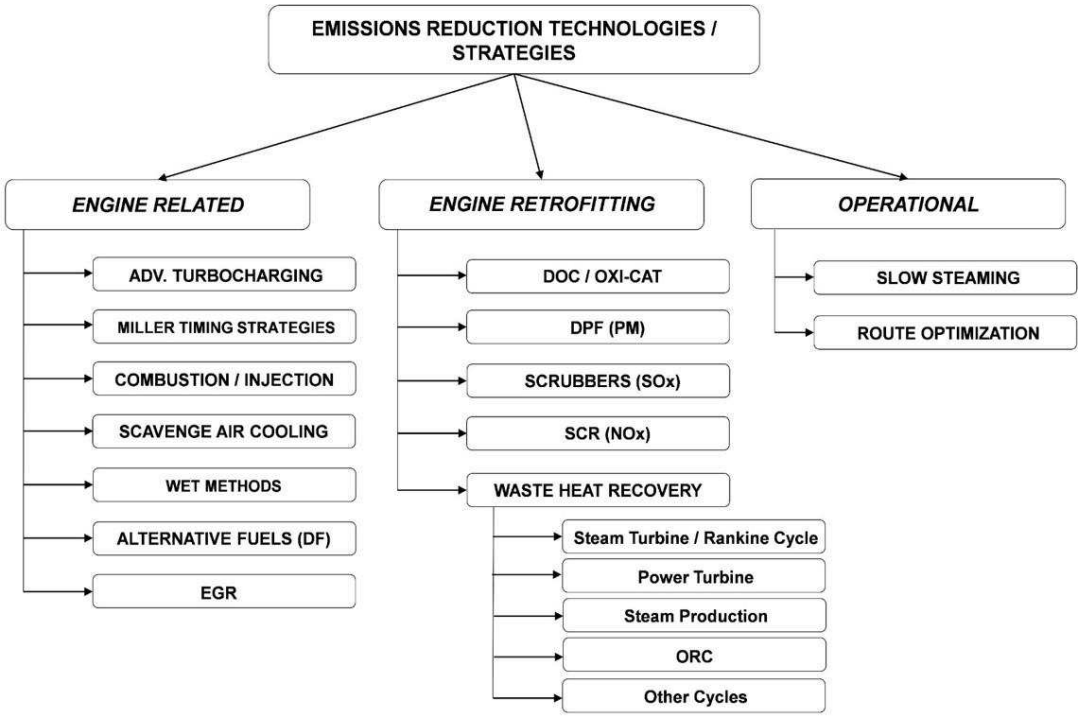

Fig. 12. Emission reduction technologies / strategies conceptual scheme (marine engines)

Emission Reduction Technology / Strategy	**NO_x reduction potential (%)**	**SO_x reduction potential (%)**	**Technology Maturity**	**Fuel Efficiency Impact (%)**	**Initial Cost (CAPEX)**	**Operational Cost (OPEX)**	**WHR Impact**
Optimization Engine Internal Parameters	20 - 30	/	Conventional	+0 to 3	Low	Low	Neutral
Miller Timing + 1 ST TC	40 - 50	/	Conventional	+2 to 3	Low	Low	Negative
Miller Timing + 2 ST TC	40 - 50	/	Conventional / Not very spread	+1 to 2	Medium	Medium	Negative
Water-in-Fuel-Emulsion (WFE)	15 - 50	/	Developed / limited long-term experience	+2 to 3	Medium	Medium	Neutral
Direct Water Injection (DWI)	40 - 50	/	Developed and used (especially in medium speed 4 stroke engines)	+7 to 10	Medium	Medium	Neutral
Humid Air Motor (HAM)	10 - 40	/	Developed / Limited long-term experience	+2 to 3	Medium	Medium	Negative
Dual / Multi-Fuel (LNG) - Diesel / Otto	25 - 85	92 - 99	Developed / trial phase, first commercialization	/	High	High	Positive
HP EGR + Scrubbing	80 - 93	90 - 99	Developed / first commercialization	+1 to 3	High	Medium	Positive
LP EGR + Scrubbing	80 - 85	90 - 99	In development / testing phase	+0 to 2	High	Medium / High	Neutral / Positive
SCR (LP & HP)	80 - 95	/	Developed / first commercialization	+0 to 2	High	High	Negative
Slow Steaming	To be calc	To be calc	In use	-2 to 0	Low	Low	Negative

Tab. 5. Comparison between emissions reduction technologies and strategies

From a general overview of literature references reported in this work [45,53,56–59], and from some qualitative considerations, Tab. 5 has been proposed as a comparison between the most used and developed emissions technologies and strategies, focusing the attention on the NO_x and SO_x emissions reduction potential, the technology maturity, the fuel efficiency, costs and waste heat recovery impact.

As already proposed in the section about commercial vehicles engines, also for the marine engines, some heat balances have been reported from data elaborated from the GTD software (WinGD, [60]) and from the open literature (Wärtsilä, [61]) for typical marine two-stroke propulsion units and four-stroke auxiliary generators, similar to those considered in this work.

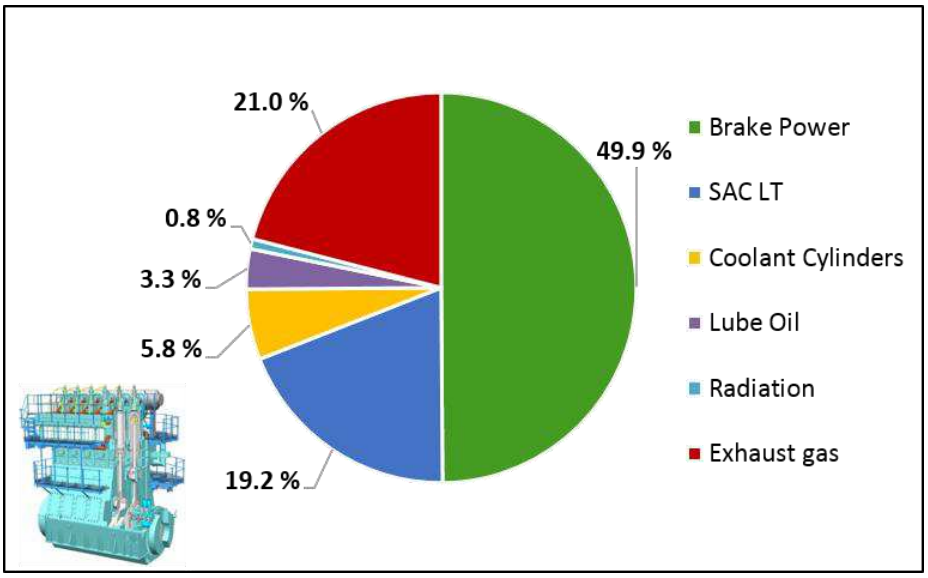

(a)

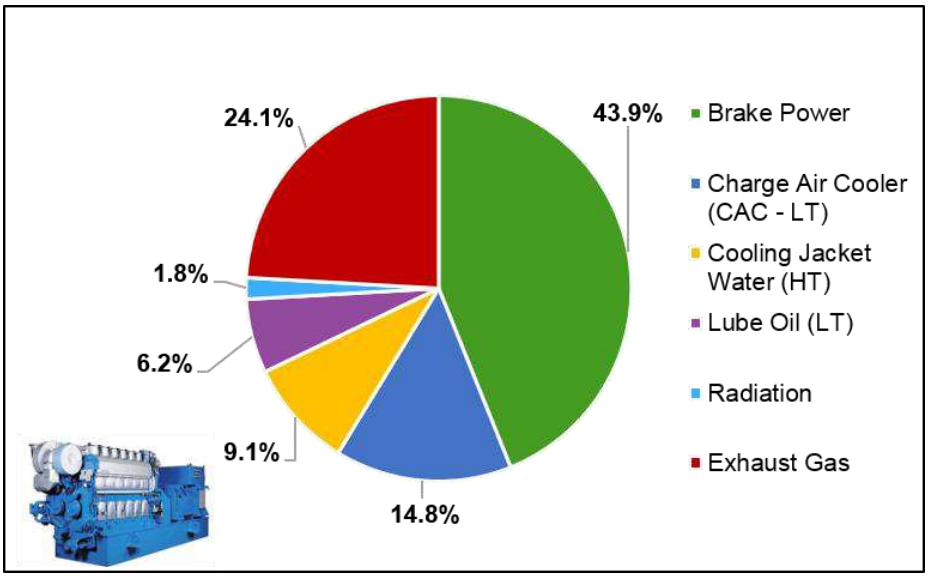

(b)

Fig. 13. Heat balances. (a) 13.6 MW Two-stroke ship main propulsion unit and (b) 1.2 MW auxiliary power generator for marine applications

In Fig. 13 (a), the heat balance for a 13.6 MW, low speed, two-stroke ship main propulsion unit with single-stage turbocharging and Scavenge Air Cooling (SAC LT, Low Temperature cooling water circuit), for IMO Tier II operations has been reported [60], while in Fig. 13 (b), a 1.2 MW, four-stroke auxiliary power generator, with single-stage turbocharging and charge air cooling can be observed [61]. The engines considered are similar to those analysed in sections 6.3 and 6.2 respectively.
As can be observed from the reported charts, MW size two-stroke engines for ship propulsion can reach a brake thermal efficiency up to even more than 50%, while four-stroke units are typically in the range between 40 to 50%. For these types of engines, due to the high gas flows involved in the thermodynamic processes, a high potential for waste heat recovery can be expected, considering heat sources as exhaust gas, EGR when used, Charge Air Cooling (CAC, four-stroke), Scavenge Air Cooling (SAC, two-stroke), cooling jacket water and lubrication oil ("lube oil" in the figures). In particular, a higher potential regarding exhaust gas heat recovery is expected for four-stroke units, due to the higher temperature of the exhaust gas after the turbine (300 – 500°C). However, the large amount of gas mass flows available in two-stroke engines could also lead to possible advantages when considering heat recovery systems, even though, often, exhaust gas economizers are already installed on the engine tailpipe in order to recover heat for the production of on-board steam or electricity with common Rankine cycles. However, heat sources such as high temperature (HT) jacket coolant, or lower temperature (LT) scavenge air or charge air circuits sources could be exploited due to the high availability of wasted heat, even if at lower temperature. In this case, the ORC technology could become interesting in order to recover this otherwise lost energy, as proposed in the case study in section 6.3.
In the next sections, just engine architectures regarding turbocharging and EGR strategies have been explained more in the details, because considered in the case studies in section 6.2 and 6.3.

Advanced Turbocharging Strategies

As already introduced, a short description of turbocharging strategies used and developed in marine applications has been proposed because different turbocharging technologies have been considered in the case study in section 6.2, investigating the engine increased backpressure effect of fitting an ORC evaporator on the exhaust line of a marine power generator. In this case, indeed, the best turbocharging strategy has been proposed in order to counterbalance the effect and keep the system efficiency at adequate levels.
Turbocharging is the oldest developed method to increase engine efficiency. Turbochargers use the enthalpy of the exhaust gas to rotate a turbine which is connected to a compressor, in order to rise the boost pressure, increase engine volumetric efficiency and thus engine performance, reducing fuel consumption [62].
Turbochargers are essential for the scavenging process in a two-stroke low speed Diesel engines, which can be equipped with up to 4 units, serving each between 3 and 5 cylinders [62].
Due to the higher exhaust gas temperatures, advanced turbocharging strategies, as for example two stage turbochargers (combined with Miller timing), are mostly used and developed for medium speed four-stroke engines. Indeed, exhaust gas temperature at the outlet of the first turbine stage, especially in case of low speed two-stroke engines, is quite low (250-300°C). For this reason, two-stage configurations are less spread in the low speed marine propulsion engine sector but could become interesting in the very next future.
It has also been proven that, two-stage strategies, for low speed two-stroke Diesel engines, are less effective than EGR and SCR in reducing NO_x emissions. Anyway, two-stage configurations can be used in order to improve engine power output and decrease Brake Specific Fuel Consumption, BSFC (or Specific Fuel Oil Consumption, SFOC, as usually reported for the marine sector).

Two-stroke turbocharging can be basically of two types: constant pressure (used by almost all two-stroke low speed marine Diesel engines) and pulse [62].
In the constant pressure type, all cylinders' exhaust in the common exhaust receiver, which dampens out the gas pulses, thus maintaining almost a constant pressure, eliminating multiple complex exhaust manifolds systems and leading to higher turbine efficiency and lower BSFC. Higher flexibility in the positioning of the turbocharger is also possible. This configuration has low performance at part load and during transition periods due to the slow response of the turbocharger, but this could be not a very big drawback during constant speed and load operations typical of a ship engine.
Charge Air Cooling (or Scavenge Air Cooling) is used to decrease temperature and increase air density after the compressor in order to improve engine volumetric efficiency and performance.
The most common type of CAC (or SAC) is a water-cooled design with finned tubes in a casing carrying seawater or fresh water, over which the engine intake air passes [62]. A mist-catcher is also placed in order to collect condensed water from the gas flow, expected at the cooler outlet.
Large turbochargers for low-medium speed ships Diesel engines can be manufactured based on radial or axial turbines, usually connected to radial compressors.
Single stage turbocharging architectures are able at the moment to supply boost pressures up to 4 – 6 bars, with compression ratios up to 5.8:1 [63]. Due to the improvement of turbochargers efficiency in the last decades, up to 70% and more, considerable BSFC reduction has been achieved, and some other concepts and modifications have been applied to two-stroke low speed engines.
Waste Gate (WG) controlled turbochargers are not very commonly used in low speed two-stroke engines, due to the fact that the operational profile of a ship usually does not show many transitional periods, leading mostly to steady state operating points [64]. Exhaust WG could be even a disadvantage because the loss of exhaust gas reduces the turbocharger efficiency, thus leading to higher thermal load of the combustion chamber components and lower boost for the scavenging process.
At part-load conditions (especially lower than 30% load) auxiliary blowers are used to support turbochargers operations.
Variable Geometry Turbines (VGT) can also be used in order to improve engine performance at part-load conditions (e.g. slow steaming operations), allowing optimisation of the performance for the considered operating point, with a smooth continuous control over speed and load points. MAN supplies a VTA (Variable Turbine Area) turbocharger, with a nozzle ring with adjustable vanes [65]. This allows to increase boost pressure in the low and medium speed/load range, thus increasing engine efficiency. MAN declares up to 8.5% fuel efficiency improvement at loads between 25 and 70%.
Heim [64] reported that VGT turbochargers are not very practical for two-stroke low speed engines running on HFO, due to fooling problems due to unburned and lubricating oil in the gas stream. Increased cost is another drawback.
Some other technologies variants have been considered in recent developments. For example, a hybrid turbocharger [66] comprises an electrical generator embedded in the turbocharger body (Mitsubishi Heavy Industries, MHI). In this way, the turbocharger can be used as a generator and, also, as a motor through the application of bidirectional frequency converters (AC-DC). The power produced by the hybrid system is AC. It must be converted to DC to be used in ships utilities. The hybrid turbocharger can be used in order to reduce the required electric power needed for the auxiliary blower at part load conditions and is declared to operate with useful power output for engine loads higher than 75%. However, MHI declares the hybrid option more efficient than using an auxiliary blower, leading to a benefit in terms of both improved fuel efficiency and decreased blower configuration power consumption [67].
Two-stage turbocharging systems are more commonly developed for four-stroke medium speed engines, due to the higher exhaust gas temperature and enthalpy available to run a second stage turbine (Low Pressure Turbine, LPT) after the High-Pressure Turbine (HPT) stage.

Two-stage turbocharging architectures are commonly considered in four-stroke engines also in combination with Miller timing strategies [68] in order to profit of the higher boosting pressure capabilities during the longer intake valve closure period used to reduce NO_x emissions.
Some of the benefits of two-stage turbocharging are: intercooling (in order to decrease second stage compression work needed), respected strength limits of the materials, optimization of turbocharger operations over a wider range of speeds and loads, due to the operational flexibility of this configuration.
Some of the drawbacks are: low-load efficiency worse than single-stage configurations, more complex architectures with lower reliability, increased space required for installation, lower heat available for steam production and waste heat recovery purpose.
Two stage turbocharging efficiencies are expected in the range between 70 and 80% [69].
In case of Miller timing strategies, often used in combination with two-stage turbocharging or efficient turbochargers, the idea is to compress the scavenge air to a pressure higher than that needed for the engine operation, but the cylinder filling is reduced, as well as the effective compression ratio, using a suitable timing of the inlet valve (Inlet Valve Closure, IVC). For example, an opportunity is using early IVC before the BDC, for internal sub-cooling. This, of course, is valid for four-stroke medium speed engines, in which, a maximum NO_x reduction of around 40 to 50%, compared to Tier I levels, can be expected [55,68,70].
In two-stroke low speed engines, characterized by just one exhaust valve on the top of the cylinder head, Miller timing strategies can be implemented retarding Exhaust Valve Closure (EVC) and increasing scavenging boost pressure [71].
Because of late EVC, a part of the scavenging charge is pushed out from the cylinder. For this reason, in order to maintain similar Air-Fuel Ratio (AFR) for combustion efficiency reasons, Miller timing strategies need a higher intake pressure than commonly supplied with single-stage turbochargers architectures. For this reason, Miller strategies are commonly used in combination with highly efficient turbochargers or two-stage turbocharging architectures to supply enough boost for operations.
If the maximum achievable boost pressure supplied by the compressor is too low, Miller timing strategies result in worse engine performance and increased fuel consumption.
As reported by Feng *et al.* [56], in their simulation analysis about a 2 stroke low speed 3.6 MW brake power marine engine, Miller timing in combination with single-stage turbocharging has the potential of around 45% NO_x reduction at full load, but with a penalization in power and SFOC.
Again Feng *et al.* [56], proposed to implement Miller timing and two-stage turbocharging, obtaining from their 1D-3D performance and combustion coupled analysis results, better results than with single-stage turbocharging architecture (higher NO_x decrease but lower SFOC and power penalty).
Two-stage turbocharging architectures are usually not beneficial for combined use with waste heat recovery systems such as steam Rankine (RC) or Organic Rankine Cycles (ORC), since the two-stage expansion results in a decreased amount of energy that can be recovered from the exhaust gas at the turbine outlet, due to the lower gas enthalpy at the low-pressure turbocharger outlet. Possible waste heat recovery systems, such as Power Turbines (PT), steam Rankine or ORC could be used when considering Waste-Gate systems in operations, eventually considering recovering by-passed exhaust gas heat, which would be in this case not utilized.

EGR Systems for Low Speed Two-Stroke Marine Engines

A short description of Exhaust Gas Recirculation (EGR) systems, with particular focus on low speed two-stroke marine engines, has also been proposed because evaluated in the case study reported in section 6.3. In particular, a Low Pressure (LP) EGR configuration has been analysed, using detailed 1-D gas dynamic simulations, in order to evaluate the detrimental effect of the gas recirculation on the engine performance. At the same time, a thermodynamic analysis has been proposed to assess the potential of waste heat recovery when considering different Organic Rankine Cycle (ORC) systems, as those proposed in this work.

Exhaust Gas Recirculation (EGR) is commonly applied in EURO VI four-stroke HDDE in the vehicle transportation sector. EGR, together with SCR (Selective Catalytic Reduction), is gaining also more interest for two-stroke ship propulsion engines, as one the most effective technologies to reduce NO_x emissions for IMO Tier III legislation compliancy. EGR could also lead to benefits regarding waste heat recovery systems applications, as already considered for smaller HDDE applications in literature [72–75] and in the case study in section 6.1, but not yet well spread in the marine sector.

Usually, EGR could be internal or external, depending if it is accomplished through particular valve timing or scavenging port height sizing, for the first, or through the use of an external circuit to recirculate the gas to the intake side of the engine [55], for the second.

As stated by Raptotasios *et al.* [59], one of the main effects of EGR on Diesel engine combustion and, in particular, NO_x emissions reduction, is due, to the increase of the charge mixture specific heat capacity (higher when recirculating CO_2 and H_2O) which leads to a reduction of the in-cylinder gas temperature, thus reducing nitric oxides emissions. Another important effect is due to the decreased oxygen concentration in the intake due to the recirculated exhaust gas containing CO_2 and H_2O, which leads to a decrease of combustion rate and temperature.

Despite the EGR benefits considering NO_x reduction, the recirculation of exhaust gas leads to a general increase in fuel consumption and soot emissions. Moreover, when using HFO, the high sulphur content of the fuel can lead to corrosion and wear issues in the engine components, and in particular for the EGR cooler, particularly used in the HP (High Pressure) EGR configuration, and for the EGR blower, used to push the recirculated gas from the exhaust to the intake side, both in HP and LP (Low Pressure) configurations.

To try to overcome these issues, usually, a scrubbing system is used in order to clean the recirculated exhaust gas. The system could be either a dry or wet system, with the second usually preferred in marine applications. The water used for scrubbing the exhaust gas could be fresh water, usually used in ECAs, recycled and cleaned on-board, or sea water, used outsides ECAs and discharged back into the see after cleaning. The EGR scrubber is usually more compact compared to the main exhaust scrubber, and this in particular for the HP configuration, in which gas pressure is higher compared to the LP case, which is recirculating gas after the turbine, so almost at ambient pressure [76,77].

The scrubbing system needs a Water Treatment System (WTS) because compliancy of IMO criteria for washed water discharge must be considered [42]. The contaminated scrubber water needs to be cleaned for soot particles to avoid clogging up the system, and, as well, the water generated during combustion, condensed in the EGR cooler, needs to be discharged to the sea, in clean conditions. Simple and compact installation for the WTS unit is essential for on-board installation.

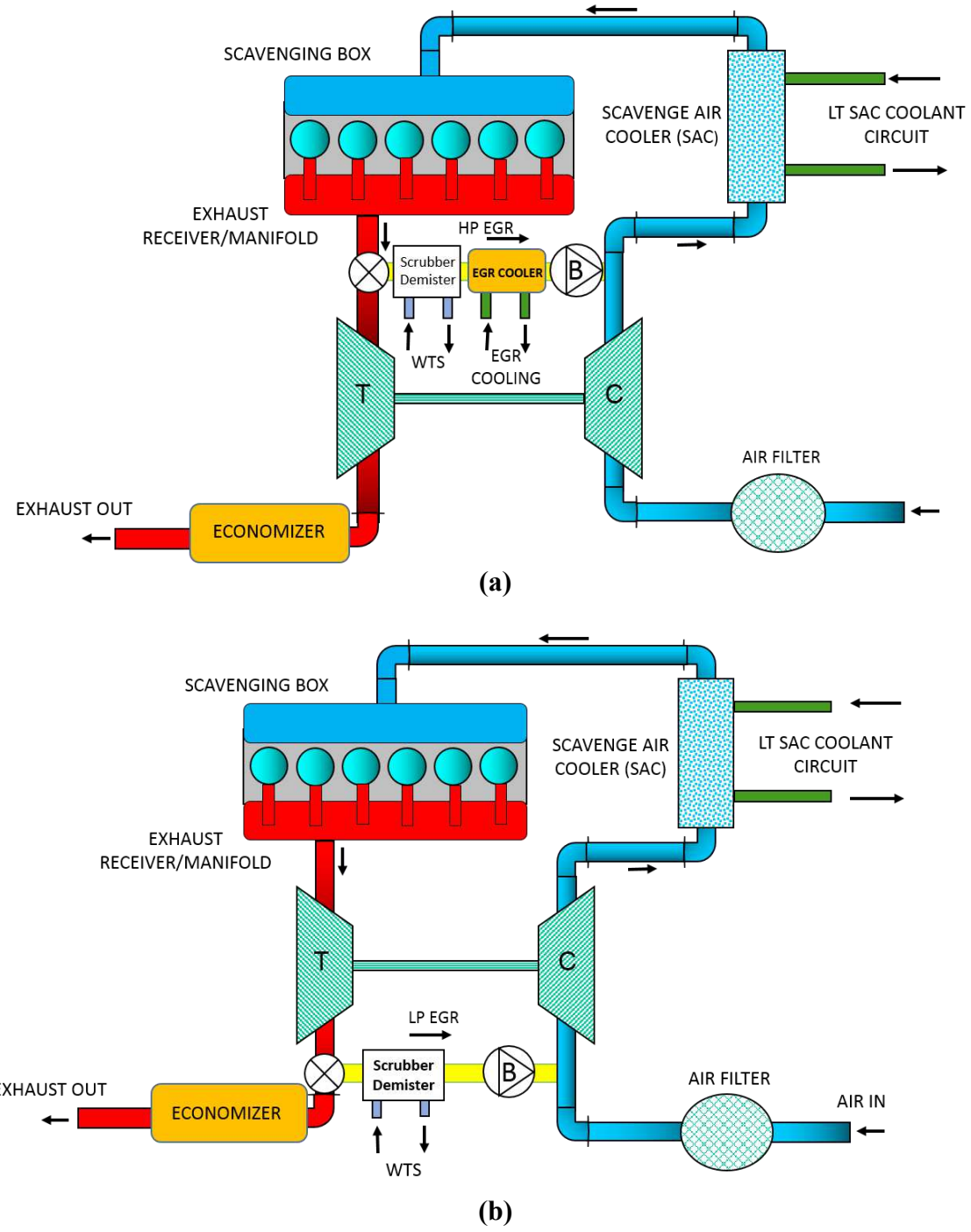

Fig. 14. Simplified schemes of two-stroke, low-speed, HP (a) and LP (b) EGR configurations

As already introduced, the EGR system could be either a High Pressure (HP) or Low Pressure (LP) configuration. The HP system recirculates the gas from the turbine inlet to the SAC inlet, while the LP system recirculates the exhaust gas from the turbine outlet to the compressor inlet. The HP system is used and developed, for example, by MAN [40], while the LP system is under development, and in particular by Mitsubishi Heavy Industries (MHI, [58]). Some simplified schemes have reported in Fig. 14. HP EGR has been reported in Fig. 14(a), while LP EGR in Fig. 14(b).

In case of HP EGR, usually an EGR cooler is used in order to cool the recirculated gas to a temperature compatible to the temperature of the intake air (150-250°C) before the Scavenge Air Cooler (SAC), from a temperature before the turbine of around 300-450°C, depending on the engine operating point

[60]. For this reason, a high amount of heat is rejected to the engine cooling circuit, being this an energy loss for the overall system, and an additional thermal load to be rejected into the coolant. In this case, a waste heat recovery system such as a steam Rankine cycle or an ORC could be beneficial in order to recover the wasted heat and produce additional useful energy, in the form of mechanical or electrical power (or producing steam for ships usage), thus counterbalancing the typical EGR fuel consumption increase drawback.
The EGR cooler is usually made of stainless steel and can be subjected to highly corrosive environment, especially when HFO is used, even though, in ECAs, a low sulphur fuel should be used, thus limiting the issue. Also, the position of the scrubber and the demister (used to catch condensed water and eject it from the gas line) should be carefully considered before or after the EGR cooler, depending on deposition and fouling problems, and considering system packaging constraints.
Additionally, when recirculating exhaust gas to the intake before the SAC, depending on the degree of cooling of the gas in the EGR cooler, the temperature of the mixed gas in the intake could slightly increase, which, together with the high amount of mass flow of gas available in large low speed two-stroke Diesel engines, can lead to a large increase in heat rejection in the SAC, thus also allowing to consider waste heat recovery systems, such as ORC, to recover additional available heat from the SAC, that otherwise would just be a load for the cooling circuit. A similar approach has been proposed in the case study in section 6.3.

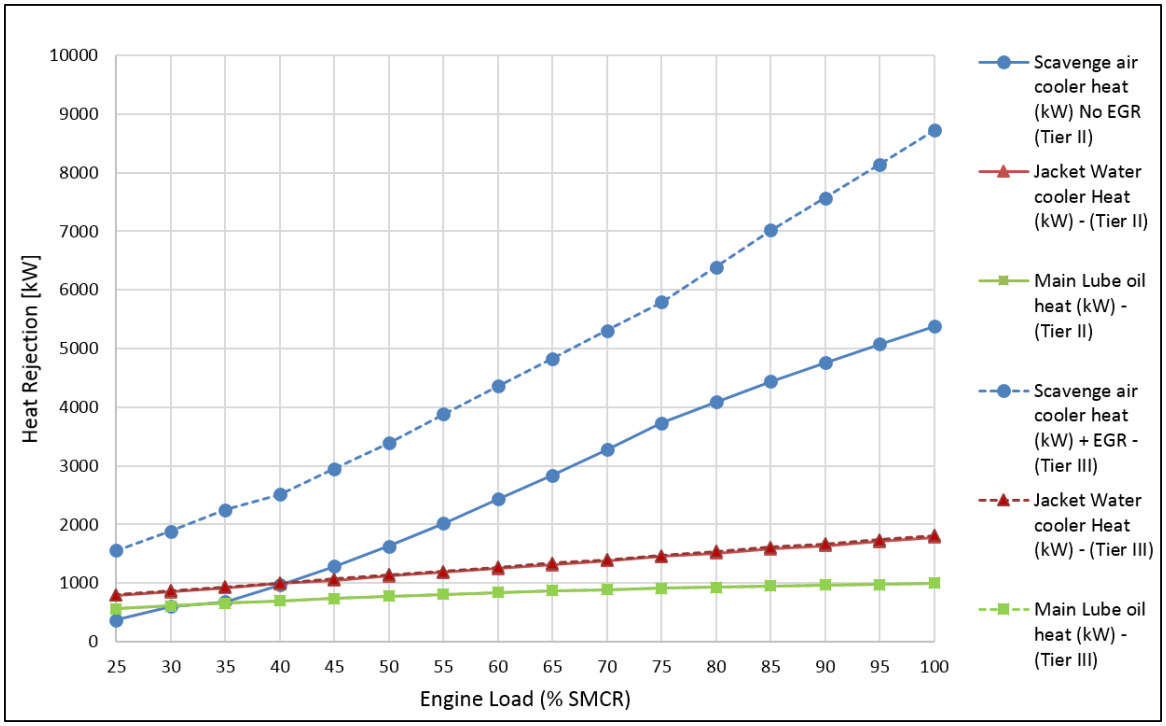

Fig. 15. Comparison between heat rejection in Tier II and Tier III (EGR by-pass configuration) modes for a MAN 6S60ME-C8.5 14.3 MW, two-stroke, low speed Diesel engine. Data extracted and post-processed from MAN CEAS software [78]

An example of what reported above can be observed in Fig. 15. The data have been obtained from MAN CEAS online software [78] and refer to a comparison between Tier II and Tier III (with HP EGR) operations for an MAN 6S60ME-C8.5 engine (14.3 MW brake power at full load, 105 rpm, with EGR by-pass configuration).
From the analysis of the data reported in Fig. 15, it is possible to observe how SAC and EGR heat rejection are reported together, showing an increased heat rejected of about 62% at full load conditions, 108% at 50% load and even up to 322% at 25% load conditions, when considering Tier III HP EGR

operations in comparison to Tier II operations without EGR. No significant heat rejection increase is observed concerning coolant and lube oil circuits. The reported data clearly show how recovering heat from the EGR cooler and/or the SAC, by means of a bottoming cycle such an ORC, could be a benefit regarding overall system performance. This observation leaves space to the evaluation of several different bottoming cycle layouts and working fluid variants, with the scope of maximizing the power output that could be expected from the waste heat recovery system.
Both in HP and LP EGR configurations, an EGR blower is needed to push the recirculated gas through the EGR circuit and equilibrate the pressure between the exhaust and the scavenging receivers (in Fig. 14 the blower has been reported as B). MAN is involved in the development of an efficient EGR blower, based on a high-speed radial turbo-compressor wheel [42], capable of withstanding the challenging conditions of the EGR circuit. As reported by MAN, the blower must be highly efficient over a wide flow range (0 – 40% EGR rate usually considered for IMO Tier III operations), should have a fast-dynamic response, should be corrosion resistant, reliable, compact, leakage proof. In some configurations the blower could become part of a turbo configurations, as reported by Codan *et al.* [71], or could be just electrically driven, thus allowing an higher controllability.
Another consideration can also be drawn from the data obtained from CEAS calculations for the previously considered MAN 6S60ME-C8.5 engine. In particular, during Tier III operations with HP EGR, further power consumption can be evinced when operating the blower and the WTS system [78]. For the considered engine, for example, an EGR blower electric power consumption of around 108 kW can be expected at full load, while around 88 kW at 50% load and 51 kW at 25% load. Moreover, the WTS system also requires power to be consumed, e.g. 57 kW at full load, 41 kW at 50% load and 33 kW at 25% load. The sum of the reported consumed power leads to an overall power need of 165 kW at full load, 129 kW at 50% load and 84 kW at 25% load, which must be summed to the increased fuel consumption expected during EGR operations. For this reason, waste heat recovery systems can become even more attractive in order to counterbalance also this increased power consumption required (around 1.1% of the produced engine brake power at full load for the proposed example).
Compared to LP EGR, HP EGR recirculates exhaust gas before the turbine, on the high-pressure side, with the drawback of reducing the exhaust gas mass flow which rotates the turbine, thus leading to a boost and engine performance decrease. A more efficient turbocharger is then required, or cylinder by-pass strategies must be adopted. Two stage turbocharging architectures can also be considered in synergy with EGR strategies in order to improve the boosting capabilities of the engine, as reported in the study by Feng *et al.* [56].
As reported before, the EGR tends to increase engine fuel consumption. Some data have been reported in Tab. 6, as an example, for a 4 cylinders MAN 4T50ME-X test engine, with HP EGR, 7 MW brake power and 123 rpm at 75% load, not considering EGR blower and auxiliaries power consumption [42]. As observed from the data, EGR rates up to more than 40% are usually required for two-stroke large low speed marine Diesel engines; an higher amount compared to commercial vehicles smaller HDDE, as also reported by Codan *et al.* [71].

	NO_x [g/kWh]	$\Delta SFOC$ [g/kWh]	EGR [%]
Without EGR	17.8	0	0
With HP EGR (max without modifications)	2.3	+4.9	39
EGR Reference Point	3.7	+3.0	36
Tier III Setup (cylinder by-pass)	3.4	+0.6	41

Tab. 6. MAN 4T50ME-X: HP EGR NOx reduction and Specific Fuel Oil Consumption (SFOC) data

Low Pressure (LP) EGR is another concept, which currently is less spread in marine applications and still facing development and testing stages, as reported by MHI [58,79,80], but promising a very good

compromise between NO_x reduction capabilities, fuel consumption and easiness of construction. From author's knowledge, not many information is available in literature regarding LP EGR in large marine two-stroke applications.
In the LP EGR concept, the exhaust gas is extracted from the low-pressure side of the turbine (outlet), after the economizer, and recirculated to the low-pressure side of the compressor (inlet), as reported in Fig. 14. For this reason, one of the main concerns of the technology is that it could lead to compressor failure, due the possible soot and condensate droplets which could damage the turbomachine (pitting and corrosion). Effective scrubbing and demisting systems are thus very important when considering this configuration. Another drawback of the LP EGR is related to the resulting bulkier system compared to the HP one, due to the lower pressures acting on the turbine outlet side, thus requiring more space for on-board installation. Moreover, OPEX (Operating Expenditure) is higher for LP-EGR, mostly due to the more expensive low sulphur fuel needed for operations without damaging the compressor.
However, the LP EGR architecture has also many other advantages. For example, it is simpler in structure compared to HP EGR, due to the lower system pressures involved and the lower temperatures, having also a lower CAPEX (Capital Expenditure). It requires a lower number of components, and the EGR cooler and the pre-scrubber are not needed. The EGR blower required power is lower compared to HP EGR, since the turbocharger suction pressure is used to draw gas through the compressor. The turbine operation is less affected compared to the HP EGR case because of all the exhaust gas is passed through in order to obtain the energy to run the compressor. However, a turbo-matching is still needed because of the possible increased boost required during EGR operations. In addition, just a simple valve is needed to divert exhaust gas to the EGR circuit, while for HP EGR more complicated control systems are needed.
On the waste heat recovery side, possible waste heat recovery systems (e.g. steam Rankine or ORC) are penalized, due to the absence of the EGR cooler heat rejection (possible bottoming cycle heat source at higher temperature) and to the lower temperatures available in the EGR line. However, all the exhaust mass flow can be fully exploited in the economizer for steam or electricity production, and an augmented SAC heat rejection could still be available to be recovered in a bottoming cycle.
MHI [80], during their LP EGR testing campaign, reported a NO_x reduction potential up to more than 80%, thus comparable with IMO Tier III emissions regulations. At the same time, MHI declared up to 91% soot removal and up to 99% SO_2 removal potential for their LP EGR scrubbing system, and compatibility with compressor clean operations. The fuel consumption increase is also reported to be lower than 1.5-2%, but the engine operating point has not been specified.
Finally, it is possible to observe how HP EGR should be more beneficial regarding combined emissions reduction technology and waste heat recovery systems use, mostly due to higher temperature involved in the processes and higher amount of heat available and a higher temperature. However, also LP EGR could show large benefits when considered in synergy with possible bottoming cycles, in order to recover the increase heat rejection expected at least in the SAC. Several different configurations for possible waste heat recovery bottoming cycles, such as steam Rankine and ORC, should be assessed, regarding the combined use of different heat sources (e.g. exhaust, SAC, EGR, coolant, lube oil), the choice of the right working fluid(s) and the proper cycle layout, in order to maximize the obtainable power output, with the scope of mitigating the adverse fuel consumption effect introduced with any of the considered emission reduction technologies.
For all these reasons, after a round-table discussion with the project partners Winterthur Gas & Diesel (WinGD) and National Technical University of Athens (NTUA), a LP EGR architecture has been chosen and investigated, together with the potential for waste heat recovery using ORC, as reported in section 6.3.

4.1.4 Typical Applications' Operating Profiles

In the first development stage of waste heat recovery systems for vehicles, or ships, applications, it is essential to study the real-life operating profiles, so to have a correct idea of which is the engine operating point (torque and speed) at which the heat recovery system must be designed and optimized. This optimum point is usually the point at which the engine spends most of his time during its duty cycle or the one allowing higher performance. In this section, an overview of typical operating profiles of heavy duty Diesel engines, in commercial vehicles and ships applications, has been reported, with the scope of understanding which is the best design point for a waste heat recovery system design and optimization. The reported data have been elaborated and published by the author also in [81].

4.1.4.1 Commercial Vehicles

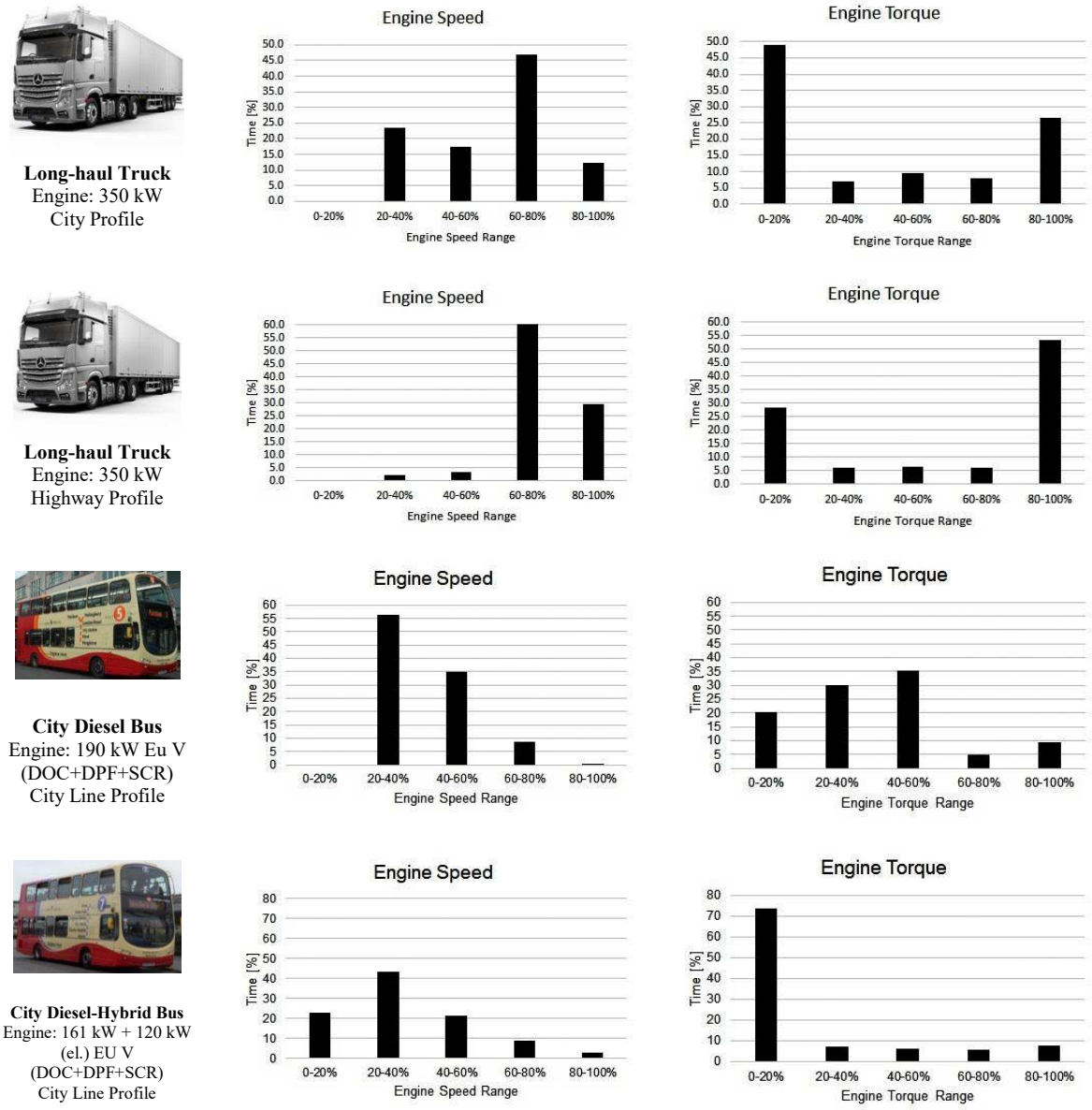

Fig. 16. Typical engine speed and torque time percentage distribution for on-highway vehicles

Agricultural Tractor
Engine: 300 kW
Mulching/Field Work Profile

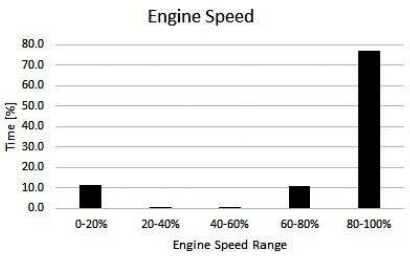

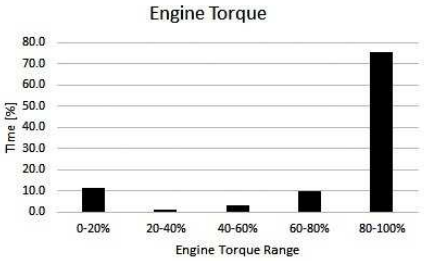

Backhoe Loader
Engine Power Range: 50 - 100 kW

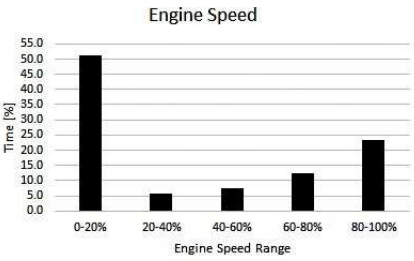

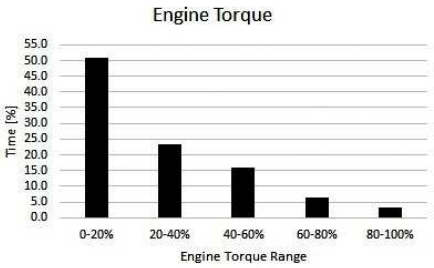

Crawler Loader / Dozer
Engine Power Range: 50 - 600 kW

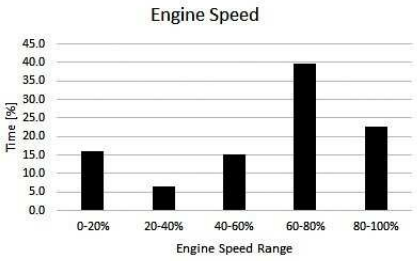

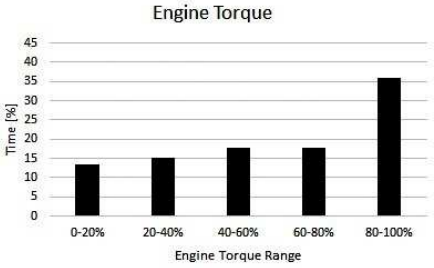

Excavator
Engine Power Range: 60 - 400 kW

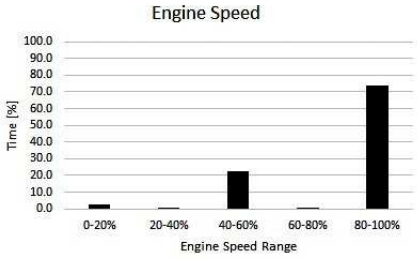

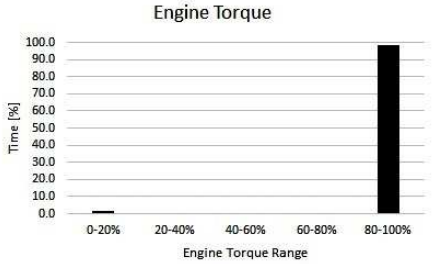

Wheel Loader
Engine Power Range: 50 – 400 kW

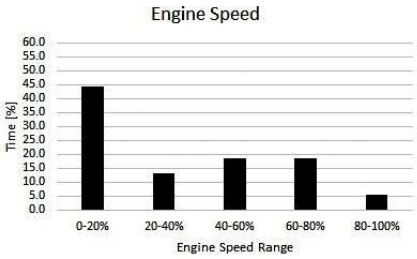

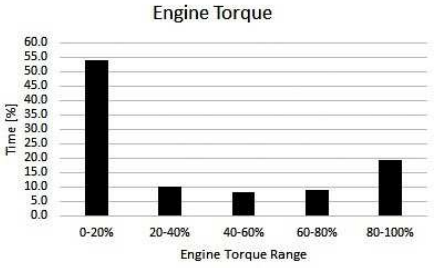

Skid Steer Loader
Engine Power Range: 40 – 80 kW

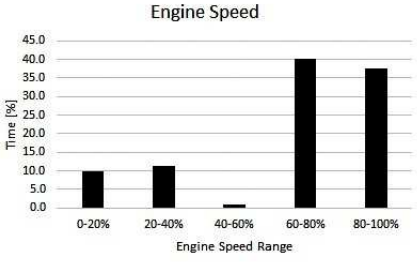

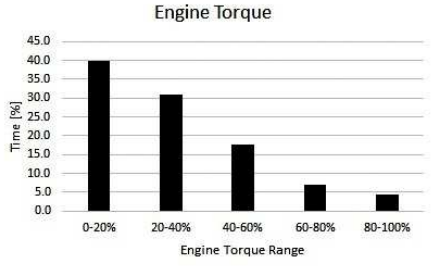

Fig. 17. Typical engine speed and torque time percentage distribution for off-highway vehicles

The data reported in Fig. 16 and Fig. 17 have been obtained from Ricardo's databases, and from EPA (United States Environmental Protection Agency) [82], and elaborated in the form of histograms of percentage of time spent in a certain engine speed and torque range.
Some considerations can be drawn from the histograms reported above.
A truck engine, in a typical city cycle, spends most of the time at medium-low speed levels, due to idle periods at traffic lights stops and in the traffic jam. In case of highway operating profile, the truck engine spends more time at medium-high speed levels (the vehicle is commonly at cruise speed), and the speed and torque profiles are quite constant over the time, being thus very suitable for waste heat recovery, due to the quite stable heat sources, e.g. exhaust gas and EGR, mass flow and temperature profiles.
In the case of the city bus, the engine runs most of the time at low-medium torque and speed levels with large amount of time spent at idle conditions (around 600 rpm) at the bus stops, traffic lights and in the city traffic jam. Moreover, it is possible to observe, especially in the case of the Euro V Diesel-hybrid bus, how the speed and torque histograms columns are more concentrated towards low values regions (0-20%). Indeed, for this application, the combustion engine is switched-off during a part of the operating profile, and the propulsion is supplied by the electrical engines. For these reasons, waste heat recovery bottoming cycles are more difficult to be developed in this case, because of the lower availability of exhaust gas mass flow at medium-high temperature (the engine is also smaller compared to the non-hybrid-Diesel bus). A possible benefit, in a hybrid application, could be related to the more stable and constant operating profile of the engine acting as power generator to supply energy for the batteries (transient behaviour is usually avoided, and steady state conditions are more common).
In the cases of off-highway vehicles, it is possible to observe stable high speed and torque profiles during operations for agricultural tractors and excavators, thus leading to the conclusion of a good potential for waste heat recovery systems implementation. The other vehicles show a wider distribution of speed and torque between different intermediate categories, suggesting more transient and variable profiles over the time.
However, in case of off-highway applications, the practical absence of ram air effect during vehicle operations, leads to higher cooling fan load and parasitic power consumption demands. In this case, indeed, the recovery of exhaust gas waste heat could be challenging since additional heat must be dissipated in the cooling system and in the cooling pack of the vehicle. EGR heat recovery, on the contrary, can be beneficial regarding vehicle thermal management, decreasing the amount of heat rejected from the cooler, that otherwise should be dissipated in the engine radiator. These issues have been investigated in the case study in section 6.1, introducing the problematic of engine-vehicle thermal management.

4.1.4.2 Ships

In order to design the most efficient and effective waste heat recovery system, it is necessary, also when considering the marine sector, to have a clear idea of which is the real operating profile of the ship application considered.
The design and optimisation of a waste heat recovery system for a ship engine is easier compared to automotive applications, mostly due to less stringent weight and space requirements (e.g. packaging), as well as, due to the more stable engine operational profile. Indeed, ship propulsion engines or power generators, usually operate for long periods at constant speed and load, showing transient operational behaviour only during manoeuvre operations (e.g. in the harbour), however with less marked variations compared to vehicle engines.
Nevertheless, also in ship applications, the most effective heat recovery design will lead to improved fuel economy benefits, which in turn, due to the high amount of fuel used, the costs and the large

number of operating hours per year, will turn into a concrete financial benefit for the ship operators and owners.
Two-stroke low speed Diesel propulsion engines, as those analysed in this work, usually operate over the so-called propeller curve, which correlates the engine rotational speed with the power required for the engine, to be delivered to the propeller, in order to reach a certain ship speed (with fixed pitch propeller) [62]:

$$\dot{W}_{shaft} = K \cdot N^3 \quad (9)$$

where $\dot{W}_{shaft}$ [kW] is the propulsion power, K is the propeller law constant and N is the engine rotational speed [rpm].
Several different considerations and effects affect typical ships speed, for example: air resistance, wave resistance, hull frictional resistance, hull design and also the choice of operating the ship in a so-called slow steaming operational mode.
Slow steaming is a strategy that can be implemented by fleet and ships owners in order to reduce fuel consumption and thus pollutants emissions, and it has been considered in this work due to the impact it can have on the application of waste heat recovery systems, because of the main engines running at different load and speed points, thus leading to complete different boundary conditions for the proper design of the heat recovery bottoming cycle.
Slow steaming is the practice, often used in the marine shipping industry, to decrease ships speed in order to reduce fuel consumption and emissions, at the price of delivering goods later than with common full steaming practices, due to the increased shipping time.
Indeed, ships fuel consumption is heavily dependent on vessel steaming speed (and engine operating point optimization). At the same time fuel costs represent most of the shipping operating costs. For this reason, usually, slow steaming strategies are applied depending on the fuel price, in order to save costs [83].
Slow steaming techniques tends to reduce ships speed from 23-25 knots to even 17-19 knots or less in case of extra slow steaming, and round-trip time is usually increased to 10 to 20% depending on route, weather conditions and port times [84].
A MAN survey analysis [85], conducted with 149 interviews of shipping container fleet respondents, showed how ships using slow steaming operations are running their engines at loads between 30 and 50%, while the majority of ship fleet companies which answered the survey declared also to combine slow steaming with full steaming operations, with only 6% employing only slow steaming, this leading to the need of designing engines capable of operating over a wide range of operational points in an effective way, as so the waste heat recovery systems also must be.
Slow steaming is beneficial regarding fuel cost savings but can lead to engine operating problems as for example: fouling of the exhaust boiler, low temperature in the exhaust gas boiler affecting possible waste heat recovery potential, soot deposit on moving parts, premature wear and tear of engine parts, under or over lubrication, lower engine performance and combustion efficiency, performance and combustion efficiency loss due to low-quality fuel.
Two operating profiles, obtained from a literature review, have been reported in Fig. 18, in order to show possible differences between full steaming and slow steaming operations, while, at the same time, showing typical ships duty cycles.
In particular, only the engine load profiles have been reported, for a Post-Panamax container ship designed for 24 knots cruise speed [86], and for an oil tanker, designed for medium-slow steaming conditions [87].
As already proposed for the commercial vehicles cases, also for the ship operating profiles it is possible to observe a concentration of load operational frequencies around medium-high loads in the first case (percentage of Maximum Continuous Rating, MCR), thus showing typical full steaming operations,

while a concentration of the main engine load peaks in the range between 50% and 75% in the second case, demonstrating possible slow steaming operations.

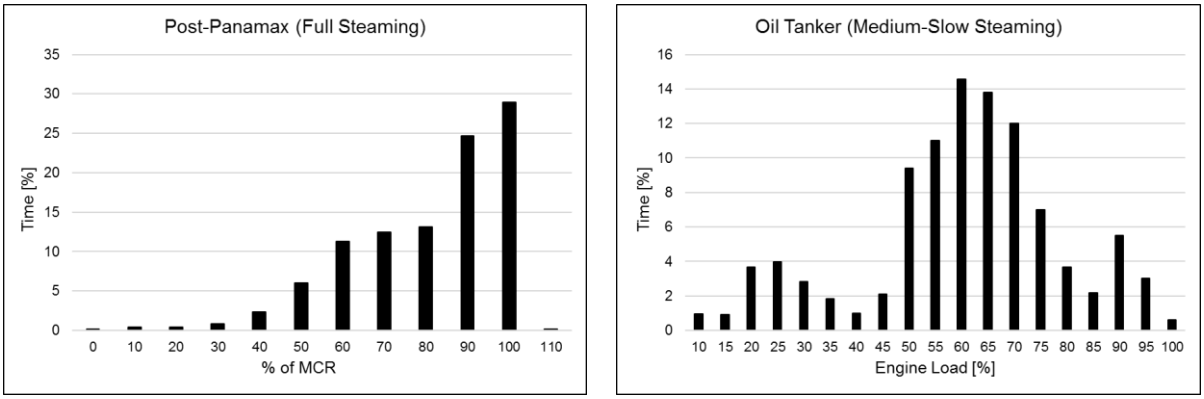

(a) **(b)**

Fig. 18. (a) Post-Panamax ship full steaming and (b) oil tanker ship medium-slow steaming main engine load operating profiles

Slow steaming operations have also impact on possible waste heat recovery systems, since lower scavenging air and exhaust gas mass flows and temperatures lead to lower waste heat recovery potential, and even sometimes the economizer, used to produce steam from tailpipe gas heat, should be by-passed due to too low exhaust temperatures and possible fouling problems. For ultra-slow steaming, auxiliary blowers could also be needed during operations in order to supply the right combustion scavenging air. Some typical heat sources data have been reported for different engine loads and speed for a two-stroke propulsion unit in Fig. 19, thus giving an idea of heat recovery potential at different operating points, especially when considering slow steaming strategies. The data have been reported for a Wärtsilä 6RT-flex58T-D, two-stroke, 13.6 MW brake power engine, with 1 stage turbocharger for IMO Tier II operations, and have been obtained and elaborated from the WinGD GTD software [60].

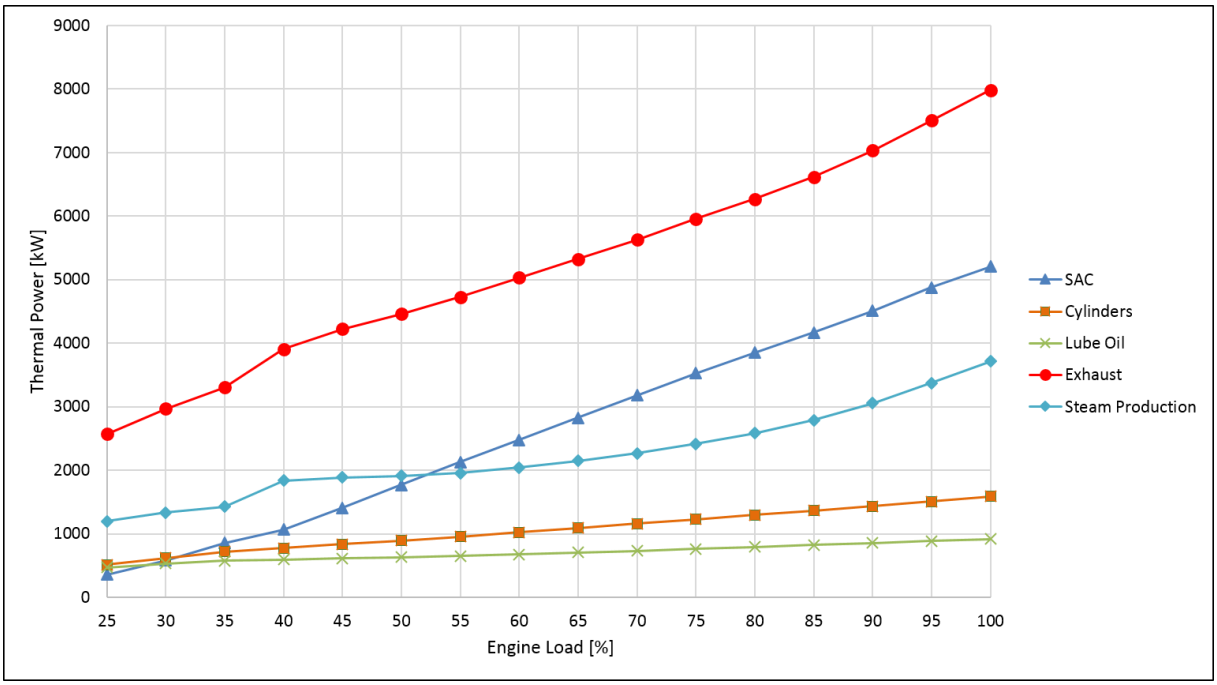

Fig. 19. Heat rejection and thermal power for different engine loads, for a Wärtsilä RT-flex58T-D, two-stroke 13.6 MW engine

As it can be observed in the graph reported in Fig. 19, with a reduction in engine load to 30-50% level, a sensible reduction in the thermal power available in all the possible heat sources that can be considered for waste heat recovery purpose can be evinced. The «Cylinders» heat source can be considered, in first approximation, as an estimation of the heat which is transferred from the cylinders to the cooling circuit of the engine, thus being an estimation of the coolant thermal power available to be recovered with possible waste heat recovery systems.
The engine fuel consumption benefit, due to possible slow steaming operations, can be evinced from the Tab. 7 and has also been reported in Fig. 20, showing a benefit especially when considering 50% load point. The engine, as already introduced, could be further optimized to run at slow steaming conditions. The data reported in the table and in the figure, are not for a slow steaming-optimized engine.
The steam production power term is calculated with an economizer outlet temperature of 170°C, and the data reported in Tab. 7 are a comparison with the 100% load point, showing a marked reduction of heat rejection for all possible bottoming waste heat recovery suitable heat sources.

Load	***30 %***	***50 %***
BSFC [g/kWh]	0.1 %	- 2 %
SAC [kW]	- 89 %	- 66 %
Cylinders [kW]	- 61 %	- 44 %
Lube Oil [kW]	- 42 %	- 32 %
Exhaust [kW]	- 63 %	- 44 %
Steam production [kW]	- 64 %	- 49 %
Exhaust Temperature [°C]	- 1 %	- 4 %
Exhaust Mass Flow [kg/s]	- 62 %	- 41 %

Tab. 7. Heat rejection and BSFC comparisons between 30% and 50% loads (referred to 100%) for a Wärtsilä RT-flex58T-D, two-stroke, 13.6 MW engine

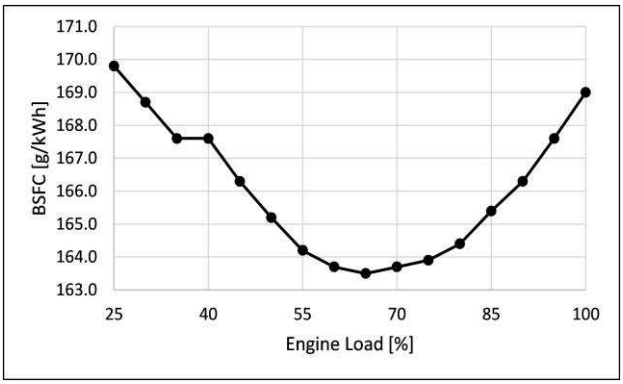

Fig. 20. BSFC at different load points for a Wärtsilä RT-flex58T-D, two-stroke, 13.6 MW engine

4.2 Waste Heat Recovery in HDDE

As already introduced in the previous sections, and as it can be observed from the proposed heat balances charts, 50% or more of the chemical energy introduced in the engine with the fuel is lost mostly as heat in the cooling and oil circuits and to the environment.
The main heat sources available for heat recovery in HDDE can be categorized in two classes, characterized approximately by the reported temperature ranges: [7]:

- Medium-high temperature heat sources (200 – 600°C):
  - Exhaust gas
  - Exhaust Gas Recirculation (EGR)
- Low temperature heat sources (60 – 200°C):
  - Coolant
  - Lubrication oil
  - Charge Air Cooling (CAC) or Scavenge Air Cooling (SAC)

In engine waste heat recovery systems studies and prototypes, exhaust gas and EGR heat sources are commonly exploited due to their high heat content and high temperatures, while only a lower amount of references about coolant, CAC and lubrication oil recovery are available in literature because of their lower temperature and potential [73] (even if the heat recovery could be beneficial for the whole vehicle thermal management and cooling circuit impact, especially for vehicles applications).
Recovery of several different heat sources is also not really practical in automotive applications, unless complicated and bulkier layouts are used (dual-loop pressures or cascade cycles, pre-heating, re-superheating), thus leading to increased weight, costs and space requirements, and more complicated control strategies implementations, with substantial decrease in reliability.
Recovering EGR heat (as well as cooling jacket water heat), however, is beneficial in particular for the vehicle cooling circuit, since the heat that should be rejected to the coolant (and then to the ambient through the cooling pack), is used to produce additional useful power.
In marine applications, where space and weight constraints are less of concern, more advanced layouts and thermodynamic cycles can be more easily considered.
It is out of the scope of this thesis to report all the possible waste heat recovery technologies which can be used in internal combustion engines applications. Just a tabulated qualitative overview has been proposed in Tab. 8, both for vehicles and ships applications, with some references from literature, main advantages and disadvantages, in case the reader wants to deepen the topics. The attention has been focused more on the Organic Rankine Cycle (ORC) technology, which has been described in the next sections. Some complete general overviews of waste heat recovery from internal combustion engines can be found in [88–92].

4.2.1.1 Commercial Vehicles

The oldest way to recover engine wasted heat in automotive applications is using the coolant heat for cabin heating purpose, while probably the most well-known technology for exhaust energy recovery in combustion engines is turbocharging. The exhaust gas drives a radial turbine, which is coupled with a radial compressor. The energy recovered by the turbine is supplied to the compressor which boosts the pressure of the engine incoming air, thus leading to increased volumetric efficiency, increased torque and power output.
As already introduced for marine applications in section 4.1.3.2, advanced turbocharging technologies are nowadays available, such as waste-gate (WG) and variable geometry turbines (VGT). Two-stage

turbocharging strategies are also used to increase the boosting efficiency over the entire engine operational regime and, recently, introduced also for vehicles applications.
Other technologies used or under development are: turbo-compounding (mechanical and electrical), Thermo-Electric Generators (TEG), Stirling engines, Brayton cycles, Ericsson engines, Atkinson engines, five or six stroke engines, absorption cycles, fuel reforming (Thermo-Chemical Recuperation, TCR) and Organic Rankine Cycles (ORC).
It is out of the scope of this work to describe all proposed technologies. For this reason and, as already stated in the previous section, the reader can deepen the topic starting from the short overview reported in Tab. 8. The benefit in fuel consumption (FC) of each technology, reported in percentage, comes from a Ricardo internal assessment, and must be considered just as a general trend to compare the different technologies.

4.2.1.2 Ships

Literature about waste heat recovery on board ships, with particular focus on two stroke propulsion units, is rather sparse [93].
The general trend is using a gas Power Turbine (PT) and/or a Steam Turbine (ST) as main waste heat recovery systems, together with steam production for general ships usage. A combination of the technologies can also be proposed as reported, for example, by MHI [94].
In the power turbine case, the kinetic energy of the engine exhaust gas is used to drive a gas turbine, in a comparable way of what can be done with a turbo-compound in vehicle applications. A parallel configuration with the turbocharger, or a series turbocharger-PT configuration are possible, depending on the engine architecture. By-pass valves can be used to control the flow through the turbocharger and PT. At partial load, in which most of the gas flow is needed to drive the turbo, the exhaust gas flow could be insufficient to operate also the PT. Mechanical or electrical coupling configurations with the main engine could be used, as in the case of a turbo-compound. Compared to ST, the PT has a lower capital cost (CAPEX) and shorter construction time and maintenance [93].
As reported by Choi *et al.* [95] the steam turbine (ST) configuration usually uses low temperature exhaust gas around 270°C (after the turbine) as a heat source. Superheated steam is produced exploiting a multi-step heat exchange through a high pressure and a low-pressure feed water heater, using then a mixed-pressure turbine.
Ma *et al.* [96] proposed a single pressure steam Rankine system, evaluating both design and part-load conditions, for a 9K98ME-C7 MAN two stroke engine. First and second law thermodynamic analysis have been considered. The results showed 8 bar as the most appropriate boiling pressure, showing an increased engine efficiency from 48.5% to 53.8%.
Dimopoulos *et al.* [97] proposed a detailed thermo-economic optimisation of a waste heat recovery system for a two stroke engine for container ships propulsion, while again Dimopoulos *et al.* [98] also investigated the exergy analysis as a way to optimize and further understand the combined Diesel engine-waste heat recovery system. Dimopoulos *et al.* [99], proposed also a tool, DNV COSSMOS, to model, simulate and optimise marine energy systems from and energetic and thermo-economic point of view, but with simplified engine models.
Several configurations are available from the main two stroke engines manufactures for waste heat recovery using PT and/or ST. Wärtsilä [45], for example, proposed mainly three different configurations, considering service steam production only, service steam production and a ST or a combined steam production ST-PT system, evaluating the possibility of producing electricity or re-inserting the generated power to the propeller shaft through the combined use of an electrical motor, and declaring a possible overall engine system thermal efficiency increase up to 11.4%.

MHI [94] also developed a combined PT-ST waste heat recovery system. For a 45.7 MW two-stroke engine they declared 5.5% maximum increased power production due to the ST, and 3.7% maximum power increase due to the PT.
MAN [41] also proposed mainly two configurations: a configuration with PT (or ST) only with steam production, and a configuration with combined PT-ST system, with a double pressure (or a single pressure) steam evaporator. Some results, reported in [100], show a possible increase in produced power between 7.3 and 8.3% compared to the baseline engine, without recovery system.
Larsen *et al.* [101] proposed a comparison between advanced heat recovery power cycles used in combined cycle configurations for large ships powered by two stroke Diesel engines. In particular, a Kalina cycle, a steam Rankine and an ORC have been evaluated, recovering exhaust gas and Charge Air Cooler (CAC) heat, showing how, in terms of performance, the Kalina cycle has no significant advantages compared to the ORC and the steam Rankine cycle, introducing even a more complicated system layout. The ORC, using R245ca as working fluid, contributed with 7% power increase compared to the baseline engine, while the Kalina and steam Rankine with 5%. A power turbine generator has also been considered leading to only 2.5% power increase.
As reported by Shu *et al.* [93] and Singh *et al.* [102], other waste heat recovery technologies, considered also for vehicles, can be used in ships applications, such as refrigeration (absorption or adsorption cycles) [103], Thermo-Electric-Generation (TEG) and desalination, while as already introduced above, also Kalina cycles [101,104–106] and Goswami cycles [107–109], could be developed and optimized in order to exploit wasted engine heat to produce additional power or combined power and cold energy for general ships usage. In particular, Kalina and Goswami cycles, due to their cycle complexity and bulkier system, are definitely more interesting for marine and stationary applications, leading to possible higher fuel consumption benefits, but also more complicated systems.
Moreover, in stationary heavy-duty Diesel cogenerative applications (CHP, Combined Heat and Power), the exhaust gas heat is recovered to produce hot water and vapour for industrial use.
Finally, a couple of words about a newly developed technology: the split cycle engine. The split cycle cannot be considered as a bottoming cycle for engine waste heat recovery. However, exhaust heat is recuperated in an innovative engine configuration in order to increase the internal combustion engine efficiency. The split cycle engine is based on the principle of separating compression and expansion strokes in different cylinders. In a first cylinder, the intake and compression processes happen, while, in a second cylinder, the combustion and expansion processes are carried out, and waste heat is recovered between the two [110].
Water or liquid nitrogen (LN_2) are, in some concepts, sprayed in the compression cylinder in order to obtain conditions similar to isothermal compression. Methods for vehicle on-board LN_2 production are explored by means of exhaust waste heat recovery. Computational models for split cycles architectures demonstrates up to 60% engine thermal efficiency could be possible [110]. The concept is under study, both for vehicle and stationary applications.
Ricardo in collaboration with University of Brighton is also developing a recuperated split cycle combustion engine [110], while the engine developer Scuderi group completed and patented its own split cycle prototype in 2009 [111].
Recently also ORC systems have been introduced in marine applications, in particular to consider low temperature heat sources in synergy with the already used PT and steam Rankine Cycles (or ST), or in order to be used instead of the steam turbine, fitted on the low temperature two stroke exhaust line [93,112]**.** An overview of studies about this type of systems for marine application is reported in the section 4.2.4.
As already introduced in the previous section, a non-exhaustive summary of the most common waste heat recovery technologies used and developed for automotive, marine and power generation applications has been reported in a tabulated form in Tab. 8.

Technology	Declared Range of FC Benefit (%)	Advantages	Disadvantages	Most Suitable Application	References
Mechanical Turbocompounding	3 - 5 %	Commercialized in premium HDDE powered vehicles Improved transient operations Compact system compared to other technologies	Increased engine backpressure Expensive gearbox system required Mechanical coupling more complicated than electrical Poor performance at low engine speed/load points	Vehicles	[22,113,114]
Electrical Turbocompounding	3 - 10 %	Commercially-ready, Hybrid-HDDE vehicles suitable Improved transient operations Better performance because of absence of gearbox	Increased engine backpressure Poor performance at low engine speed/load points Expensive high-speed generator	Vehicles	[22,113,114]
Thermo-electrics (TEG)	3 - 5 %	Simple, lightweight concept and architecture Compact system compared to other technologies No moving parts	Increased engine backpressure Poor performance with actual materials especially at low ΔT available Expensive materials required, thermal-fatigue issues	Vehicles	[23,24,115–117]
Stirling engine	6 - 12 %	High ideal thermal efficiency No pumping losses Reliable and silent	Not common in automotive applications Sealing problems, thermal stresses and high ΔT required Poor transient performance	Vehicles Ships Power generation	[118–120]
Brayton cycle	10 %	Can be used as engine retrofitting system Well known technology More suitable for high temperature heat recovery	Increased engine backpressure Expensive micro-gas-turbines required Vulnerability to avid corrosion and fouling	Vehicles Ships Power generation	[121–125]
Ericsson cycle	7 %	Heat exchangers are not un-swept volume as in Stirling systems Possibly compact layouts can be developed	Increased mechanical complexity Increased engine backpressure	Vehicles Ships Power generation	[119,126]
Atkinson cycle	2 - 8 %	Higher efficiency compared to common engines Used in hybrid-vehicles applications due to combined benefits at low-speed (Atkinson low power output)	Lower power density compared to common engines More complicated layouts or valve strategies Mostly developed and applied in gasoline Otto engines	Vehicles Ships Power generation	[127,128]
Five/six Stroke engine	9 %	Higher efficiency compared to common engines Reduced emissions Recovery stroke water injection possible	More complicated and bulky layouts In-cylinder corrosion problems in case of water injection Low power density	Vehicles Ships Power generation	[129–137]
Organic Rankine Cycle (ORC) and steam Rankine Cycle (RC)	6 - 10 %	Overall good fuel efficiency potential Simple layouts can lead to overall good performance Potential for low temperature heat recovery	Increased engine backpressure Complicated efficient layouts not suitable for vehicles Components must be optimized (cost, reliability)	Vehicles Ships Power generation	In the next sections in the details
Kalina, Goswami, absorption/adsorption refrigeration cycles	5 – 15 %	Cooling, or power-cooling combined effect in one system with weight and space benefits Increased system efficiency	Increased engine backpressure if exhaust heat is recovered Several additional components required in comparison to traditional ORC (cost, reliability, packaging, weight)	Ships Power generation	[101,103,104,106–109]
Thermo-Chemical Recuperation (TCR)	5 - 10 %	Potentially compact concept for vehicle applications Increased engine efficiency, reduced emissions Allows potential engine compression ratio increase	Increased engine backpressure Expensive converter-reformer required Potential boosting challenges	Vehicles Ships Power generation	[138,139]
Split cycle engine	>20 %	New engine concept, prototypes for stationary applications, concepts for automotive applications Net increase in main engine efficiency (up to 60%)	Technology development costs Reliability and cost Pumping losses between the cylinders	Ships Power generation	[140–143]

Tab. 8. Summary of most common waste heat recovery technologies for vehicles, ships and power generation applications, with relative fuel consumption expected benefit (literature data and Ricardo's analysis), advantages and disadvantages

4.2.2 Organic Rankine Cycles (ORC)

As suggested by Macchi [112], gas and steam cycles (Brayton and Rankine) are widely spread in the large scale stationary power generation sector, with energy conversion efficiencies which are difficult, at the current technology state, to rival.
However, there is a large variety of energy sources and applications (Fig. 21) which are not suitable to be harvested using the proposed cycles, mostly due to thermodynamic, technological and economic reasons. Indeed, for example, when the temperature and (or) the thermal power of an energy source is limited, the Organic Rankine Cycle (ORC) technology becomes much more interesting, and techno-economically valuable.

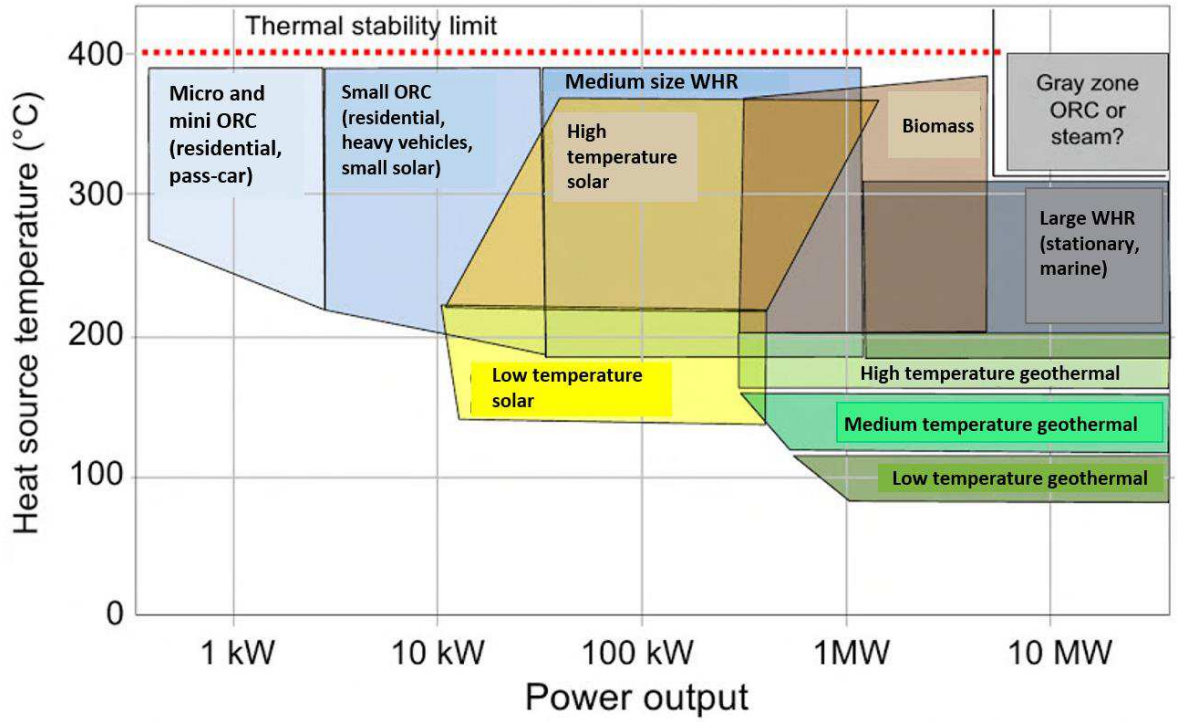

Fig. 21. ORC applications, heat source temperature and application power range. Elaborated from [112]

The precursor of the Organic Rankine Cycle (ORC) is for sure the traditional steam Rankine Cycle (RC), which has been intensively developed starting from the early 19th century, and later applied both in thermal plants, as well as in railway traction and ship propulsion (e.g. RMS Titanic). A quite exhaustive overview of the first developments of the ORC technology, as well as the main actual and past manufactures, can be found in Macchi [112] and is not reported here for the sake of brevity.
No matter if water steam is still often proposed as a suitable fluid for waste heat recovery from internal combustion engines, especially considering high temperature heat sources and exhaust gas and EGR, the choice of a steam Rankine Cycle compared to an ORC is most of the time discouraged when recovering other lower temperature heat sources (e.g. coolant, charge air cooling air, lubrication oil).
In Tab. 9, an overview of the main characteristics of steam Rankine Cycle and ORC has been reported, together with the typical shape of the temperature-entropy diagrams. The thermodynamics involved in the system processes has been considered more in the details in section 5.2, where the ORC modelling techniques adopted have been explained.

STEAM RANKINE CYCLE	ORGANIC RANKINE CYCLE
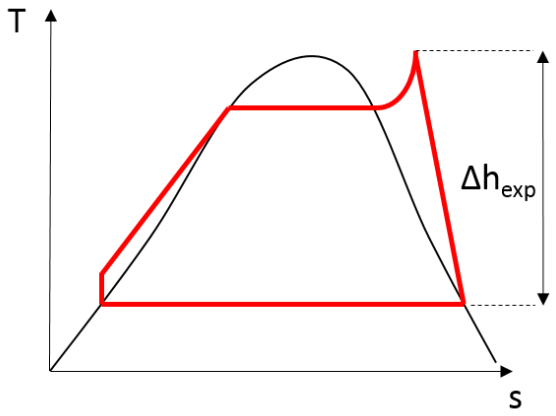	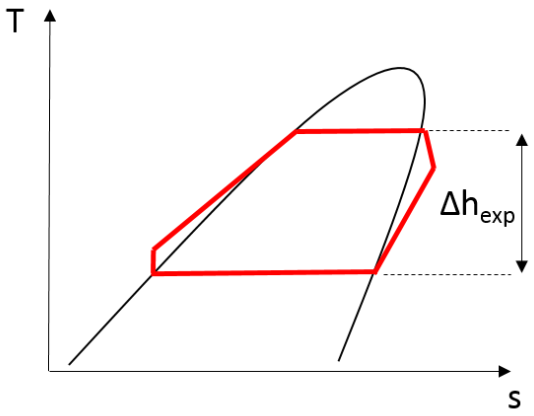
Convenient to recover high temperature heat sources High enthalpy drop (complex expansion machines) High level of superheating needed Risk of blade erosion – wet fluid Water treatment required Highly skilled personnel required High pressures and temperatures involved Convenient for high power plants (>10MW) Low flexibility Low performance at part load Well proven technology for large stationary applications	Convenient to recover low temperature heat sources Small enthalpy drop (simpler expansion machines) No need of high degree of superheat (limited heat exchangers dimensions) No risk of blade erosion - dry or isentropic fluids Minimum personnel requirements Completely automatic systems available High flexibility and good performance at part load Proven technology for stationary applications. Under development for smaller applications (e.g. vehicles) Suitable for small scale applications (kW size)

Tab. 9. Steam and Organic Rankine Cycle characteristics and typical Temperature-Entropy diagrams shapes

ORC technology is between the most promising technologies, in particular for applications such as geothermal, industrial heat recovery, biomass heat recovery, solar thermal and, as reported in this work, for engines waste heat recovery. In particular, recovering heat from stationary power generation engines (and gas turbines) is the predominant application concerning heat recovery solutions, as reported in Fig. 22 [144]. As already introduced, marine and commercial vehicles applications are not yet in large scale commercialization phase, but rather in a prototype testing and development status.

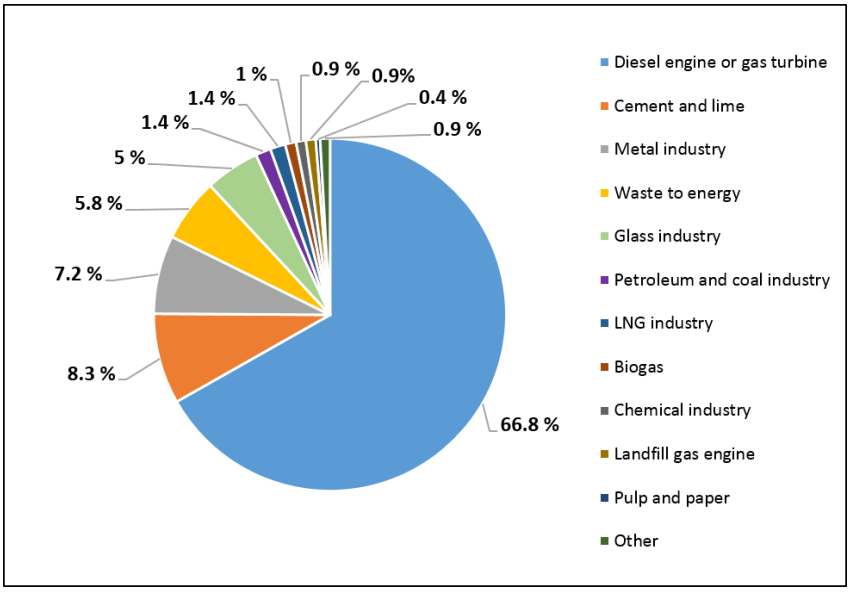

Fig. 22. ORC waste heat recovery applications. Elaborated from [144]

4.2.2.1 ORC Working Fluid Selection

The working fluid choice is one of the main issues when studying and developing ORC systems. The selection of the most appropriate working fluid depends on several considerations, not only related to the system thermodynamic performance, as for example:

- heat sources temperature;
- system operating temperature and pressure (evaporation and condensing sides);
- thermal match with the heat source (e.g. zeotropic mixtures);
- working fluid properties (e.g. thermal degradation and pressure compatibility);
- toxicity – health issues;
- flammability;
- chemical instability;
- serviceability and availability;
- environmental impact (considering indexes such as GWP, Global Warming Potential, or ODP, Ozone Depletion Potential);
- freezing point (of interest for vehicle applications under particularly cold environmental conditions);
- components' size;
- system and fluid costs;
- components' material compatibility (e.g. corrosion, sealing issues);

An applicable procedure for working fluid choice related to safety and environmental concerns (rather than thermodynamic performance) can be based on the categorization supplied by the NFPA (National Fire Protection Association) 704 Standard [145]. The working fluids are categorized [146] based on their Health (H), Flammability (F) and chemical Instability-Reactivity (R) hazards, and ranked with values from 1 (low hazard) to 4 (high hazard). Usually, fluids with values higher than 3 can be considered not suitable for vehicle applications, in which leakage and flammability concerns are very important in case of system failure or vehicle crash. In case of marine applications, limiting the presence on-board of dangerous fluids should also be considered.
Usually, considering waste heat recovery from high temperature heat sources, such as EGR and exhaust gas in case of internal combustion engines applications, alcohols (e.g. ethanol, methanol), water-steam and hydrocarbons (e.g. benzene, toluene, pentane, octane, cyclohexane, cyclopentane) can be considered good candidates, even tough, some of them show flammability concerns, thus leakage must be prevented.
Refrigerants, such as R-245fa (phased-out in the next future) and R-134a, are usually more suitable for lower temperature waste heat recovery, such as in the cases of CAC and coolant heat recovery.
Some examples of working fluids used in HDDE waste heat recovery studies have been reported in Tab. 11 and Tab. 12, together with some information about critical temperature and pressure, boiling temperature, freezing temperature, NFPA classification and environmental concerns. The available fluid properties have been obtained from several industrial technical and safety sheets, and from NIST REFPROP database [147]. For CO_2, in the boiling temperature column ($T_{boil,norm}$), the normal sublimation point has been reported, while in the freezing column (T_f), the melting/freezing point has been reported at 5.1 atm pressure.
As introduced above, the fluids have been divided in two categories: the first suitable for medium-high temperature heat recovery (typical of exhaust gas and EGR in engine applications), while the second suitable for low temperature heat recovery (e.g. coolant, CAC, oil).
Generally, medium-high temperature suitable fluids show high critical temperature and pressure, not always low freezing point, very often are flammable (e.g. hydrocarbons, alcohols). Blends with water or refrigerants are possible in order to reduce flammability issues.

Some working fluids (e.g. ammonia, HFE-7000, 3M Novec-649) have high health hazards, thus not being very suitable for vehicle applications, unless leakage is carefully avoided. CO_2 could be suitable for trans- or super-critical applications, but, in this case, high pressures lead to safety issues and costs. Anyway, carbon dioxide has less problems in case of flammability and health concerns. Ammonia and CO_2 are also still considered for HVAC (Heating, Ventilation and Air Conditioning) applications.
Ethanol, methanol, toluene and acetone are thermodynamically very suitable for high-to-medium temperature heat recovery applications, but they have flammability issues. Leakage must be avoided, especially in case of direct evaporation configurations, in which a possible contact with the hot exhaust gas could lead to fire hazards.
ODP and GWP are measures of the environmental impact of fluids. In particular, ODP is calculated with reference to R11, which has been defined with an ODP of 1, while GWP, usually calculated for a period of 100 years, is referred to CO_2 as a based unit. ODP refers to the influence on the ozone layer, while GWP rates the global warming contribution.
According to Montreal Protocol [148] on substances that deplete the ozone layer, the use of chlorofluorocarbons (CFCs), such for example R-113, has been completely banned since 2010, while Hydrochlorofluorocarbons (HCFCs), such as R-123, R-141b will be practically banned until 2020 due to the high ODP (even though they show good potential for low-medium temperature waste heat recovery). Moreover, the Kyoto Protocol [149] listed, but not banned, Hydrofluorocarbons (HFCs), such as R-245fa, R-245ca, R-134a and R-236fa as fluids with high GWP, and thus dangerous for the environment. For this reason, they will be soon probably banned, and new fluids are currently under development as substitutes: R1233zs(E) is being developed as substitute of R-245fa, while R-1234yf and R-1234ze, of R-134a (e.g. in air conditioning systems). Also in the case of refrigerants, such as high GWP R245fa or R134a, the use in mixtures with hydrocarbon can, at the same time, reduce flammability and reduce environmental issues.
Benzene and other hydrocarbons (HCs) commonly show good performance in medium-to-high temperature waste heat recovery applications, but they show also high toxicity and flammability issues, which could prevent them from vehicle applications use, unless adequate safety systems are considered.
MM, MDM and the other siloxanes reported in Tab. 12, are often considered also for medium-high temperature heat recovery, due their high critical temperature. However, the relatively low critical pressure leads to the need of pushing the evaporation pressure of the ORC system possibly above the critical level (super-critical or trans-critical systems) in order to allow a better thermal match with high temperature heat sources, thus discouraging the use in vehicles applications, because of safety reasons. Moreover, in particular MM, is very flammable, being also a big disadvantage in automotive applications.
Water-steam is also considered in many studies in literature about HDDE waste heat recovery in vehicle applications, since it shows good thermodynamic performance, especially for medium-high temperature heat sources (EGR and exhaust). However, it presents freezing issues in case of low ambient temperature conditions (de-freezing or warm-up systems could be considered in this case).
Mixtures are also being considered in several studies, especially zeotropic mixtures [150], because of their capabilities to evaporate at variable temperature, thus leading to a better match with the heat source profile and lower heat exchange irreversibilities, increasing heat transfer and overall system performance. However, also in this case, leakage must be prevented, because a change in composition could lead to completely different components behaviour and system performance.
Several publications are available in literature about ORC suitable working fluids. For example, Bao *et al.* [151] reported a complete overview of working fluids possibilities as well as ORC expanders considerations. Moreover, it is also possible to find publications regarding working fluids screening procedures and methodologies, as well as thermodynamic performance studies, in particular for medium-high temperature engine waste heat recovery. Some examples can be found in [152–155].

A couple of words need to be mentioned regarding the most cited fluid in literature, R245fa, and its future low GWP replacement, R1233zd(E), also because partially considered in this work.
In particular, the fluids present very similar thermodynamic properties, as denoted by the same Andrew's dome shape in the T-s diagram reported in Fig. 23, as well from a comparison of some properties in Tab. 10. The data have been obtained from again from REFPROP.

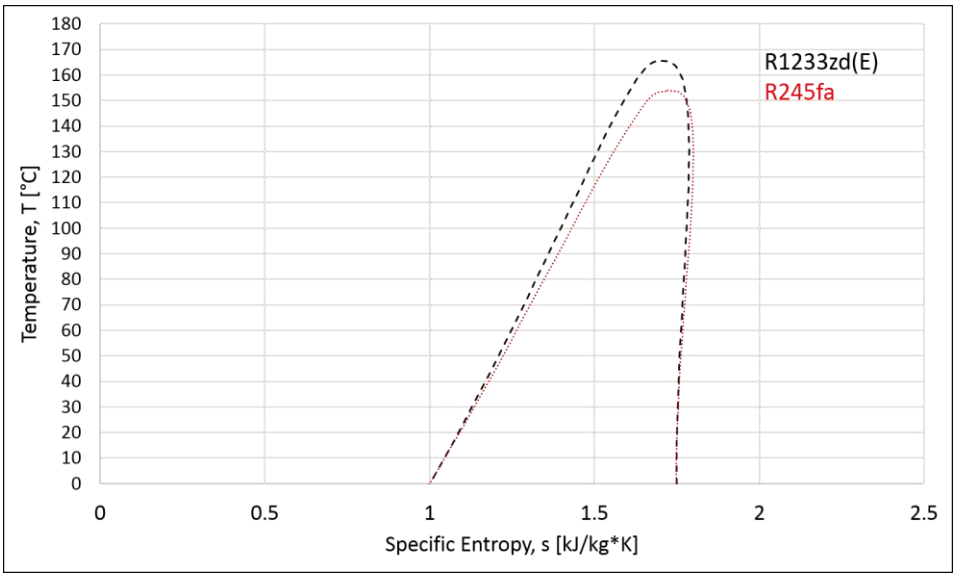

Fig. 23. T-s diagram comparison for R1233zd(E) and R245fa

	R1233zd(E)	**R245fa**
Chemical formula	$C_3ClH_2F_3$	$C_3H_3F_5$
Critical temperature, T_c [°C]	165.6	154
Critical pressure, p_c [bar]	35.7	36.5
Molecular mass, MW [kg/kmol]	130.5	134.03
Density, ρ [g/cm^3]	1.27	1.32
GWP (100)	1	1030
ODP	0	0.0003

Tab. 10. Properties comparison between R1233zd(E) and R245fa

As reported by Eyerer *et al.* [156], a characteristic influencing the produced power of the expansion machine in an ORC (an in particular a scroll machine) is the fluid density, which considering the same volumetric flow fixed for the operation, leads to a slightly lower power generation in the case of the R1233zd(E). Moreover, the saturation pressure, varying the saturation temperature, is always lower for the R1233zd(E), thus leading to a lower amount of power required for the liquid pumping. Higher cycle thermal efficiency is also expected for the R1233zd(E), compared to R245fa, however, attention should be paid to the material compatibility, and in particular the sealings, being the R1233zd(E) slightly more aggressive [156]. Generally, R1233zd(E) can be considered a good drop-in alternative to R245fa.

FLUID	CATEGORY	T_c [°C]	p_c [bar]	$T_{boil, norm}$ [°C]	T_f [°C]	NFPA			GWP (100)	ODP
PURE						H	F	R		
Water-vapour (R718)	Inorganic	374	220.6	100	0	0	0	0	< 1	0
Ethanol (ethyl alcohol)	Alcohol	241.6	62.7	78.4	-114.2	0	3	0	n.a.	n.a.
Methanol (methyl alcohol)	Alcohol	239.5	81	64.5	-97.5	1	3	0	< 3	n.a.
Benzene	Hydrocarbon	288.9	49.1	80.1	5.5	2	3	0	n.a.	n.a.
Toluene (methylbenzene)	Hydrocarbon	318.6	41.3	110.6	-95.2	2	3	0	2.7	n.a.
n-hexane	Hydrocarbon	234.7	30.4	68.7	-95.3	2	3	0	n.a.	n.a.
n-octane	Hydrocarbon	295.2	25	125.6	-56.6	1	3	0	n.a.	n.a.
p-xylene	Hydrocarbon	343	35.3	138.3	13.3	2	3	0	n.a.	n.a.
Cyclohexane	Hydrocarbon	280.5	40.8	80.7	6.3	1	3	0	n.a.	n.a.
Cyclopentane	Hydrocarbon	238.6	45.7	49.3	-93.5	1	3	0	n.a.	n.a.
Acetone	Organic compound	235	47	56.1	-94.7	1	3	0	0.5	n.a.
MIXTURES										
Ethanol/Water (0.5/0.5 mass)	Mixture	339.9	201.2	81.5	-32	n.a.	n.a.	n.a.	n.a.	n.a.
Benzene/R123 (0.7/0.3 mass)	Mixture HC+Refrig	272.5	49.4	59.4	n.a.	n.a.	n.a.	n.a.	n.a.	n.a.
Cyclohexane/R123 (0.7/0.3 mass)	Mixture HC+Refrig	263.6	42.6	56.4	n.a.	n.a.	n.a.	n.a.	n.a.	n.a.
Cyclopentane/R123 (0.7/0.3 mass)	Mixture HC+Refrig	228.3	44.6	42.3	n.a.	n.a.	n.a.	n.a.	n.a.	n.a.
Pentane/Hexane (0.5/0.5 molar)	Mixture of HCs	217.7	32.9	47.9	n.a.	n.a.	n.a.	n.a.	n.a.	n.a.

Tab. 11. Non-exhaustive list (with properties) of ORC working fluids for medium-high temperature engine waste heat recovery (e.g. exhaust gas and EGR)

FLUID	CATEGORY	T_c [°C]	p_c [bar]	$T_{boil, norm}$ [°C]	T_f [°C]	NFPA			GWP (100)	ODP
PURE						H	F	R		
R245fa (pentafluoropropane)	Hydrofluorocarbon	154	36.5	15.1	-102.1	2	1	0	1030	0
R245ca (pentafluoropropane)	Hydrofluorocarbon	174.4	39.4	25.3	-81.7	2	1	0	693	0
R134a (tetrafluoroethane)	Hydrofluorocarbon	101.1	40.6	-26.1	-103.3	2	1	0	1430	0
R236fa (hexafluoropropane)	Hydrofluorocarbon	124.9	32	-1.5	-93.6	1	0	0	9810	0
Iso-pentane (R601a)	Hydrocarbon	187.2	33.8	27.8	-160.5	1	4	0	4+/-2	0
n-pentane (pentane, R601)	Hydrocarbon	196.6	33.8	27.8	-129.7	1	4	0	4+/-2	0
Propane (R290)	Hydrocarbon	96.7	42.5	-42.1	-187.7	1	4	0	3.3	0
Isobutane (R600a)	Hydrocarbon	134.7	36.3	-11.8	-159.4	1	4	0	3	0
MM (hexamethyldisiloxane)	Siloxane - Silicone oil	245.6	19.4	100.3	-0.2	1	4	0	n.a.	n.a.
MDM (octamethyltrisiloxane)	Siloxane - Silicone oil	290.9	14.2	152.5	-86	0	2	0	n.a.	n.a.
MD2M (decamethyltetrasiloxane)	Siloxane - Silicone oil	326.3	12.3	194.4	-68	0	2	1	n.a.	n.a.
MD3M (dodecamethylpentasiloxane)	Siloxane - Silicone oil	355.2	9.5	229.9	-81.2	2	2	0	n.a.	n.a.
D4 (Octamethylcyclotetrasiloxane)	Siloxane	313.4	13.3	175.4	17.1	2	2	0	n.a.	n.a.
R141b (dichloro-1-fluoroethane)	Haloalkane	204.4	42.1	32.1	-103.5	2	1	0	725	0.12
R123 (Dichloro-2,2,2-trifluoroethane)	Hydrochloroflurocarbons	183.7	36.6	27.8	-107.2	2	0	1	77	0.02
HFE-7000 (3M NOVEC 7000)	Hydrofluoroheter	165	24.8	34	-122.5	3	0	0	370	0
HFE-7100	Hydrofluoroheter	195.3	22.3	61	-135	3	0	0	390	0
Ammonia (R717)	Inorganic	132.3	113.3	-33.3	-77.7	3	1	0	0	0
CO2 (R744)	Inorganic	31.1	73.8	-78.5	-56.6	2	0	0	1	0
COMMERCIAL NAMES										
Solkatherm (SES36)	Commercial/Mixture	177.6	28.5	36.7	n.a.	0	3	1	n.a.	n.a.
3M Novec-649	Commercial	169	18.8	49	n.a.	3	0	1	1	0
NEW (in development) – LOW GWP										
R1234yf (tetrafluoropropene)	Hydrofluoroolefin	94.7	33.8	-29.5	-53.2	2	2	0	6	0
R1234ze(E) (tetrafluoropropene)	Hydrofluoroolefin	109.4	36.4	-19	-104.5	2	1	0	4	0
R1336mzz-Z	Hydrofluoroolefin	171.3	29	33.4	-90.5	n.a.	n.a.	n.a.	2	0
R1233zd(E)	Hydrofluoroolefin	165.6	35.7	18.3	-107	2	0	0	1	0.0003

Tab. 12. Non-exhaustive list (with properties) of ORC working fluids for low temperature engine waste heat recovery (e.g. coolant, CAC and oil)

4.2.2.2 Combined Engine-ORC Architectures for Waste Heat Recovery

From a review of the literature about ORC vehicle implementations and studies, focusing on HDDE and on and off-highway commercial vehicles applications, it is possible to observe how the most developed ORC system layouts are simple cycles with one or maximum two evaporators to recover exhaust gas and EGR heat, which are the heat sources with higher potential, due to the higher temperatures involved in the thermodynamic processes. The configurations are mostly in series or in parallel, with the possibility of having recuperation of heat between the outlet of the expander and the inlet of the evaporator to increase system efficiency, in case of using dry or isentropic fluids. Examples of these layouts schemes have been reported in Fig. 24.

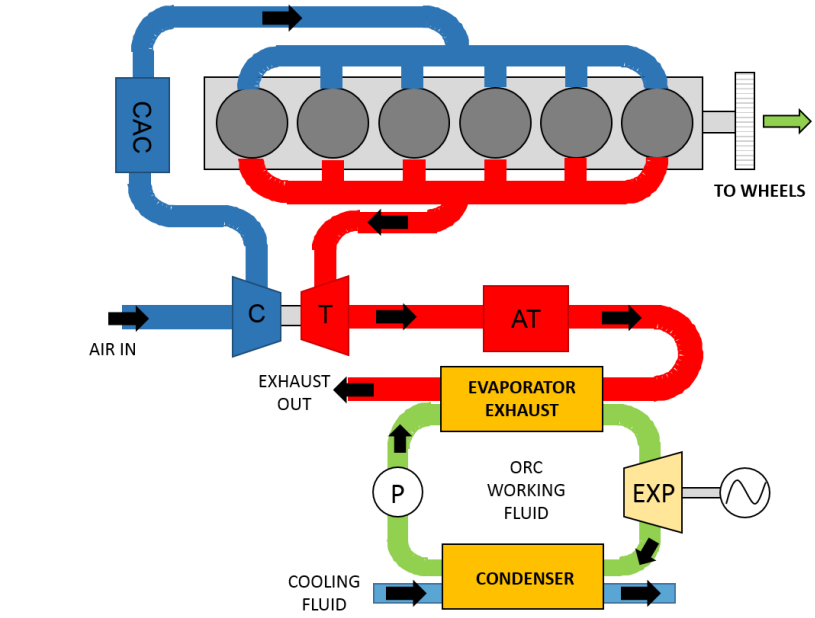

(a)

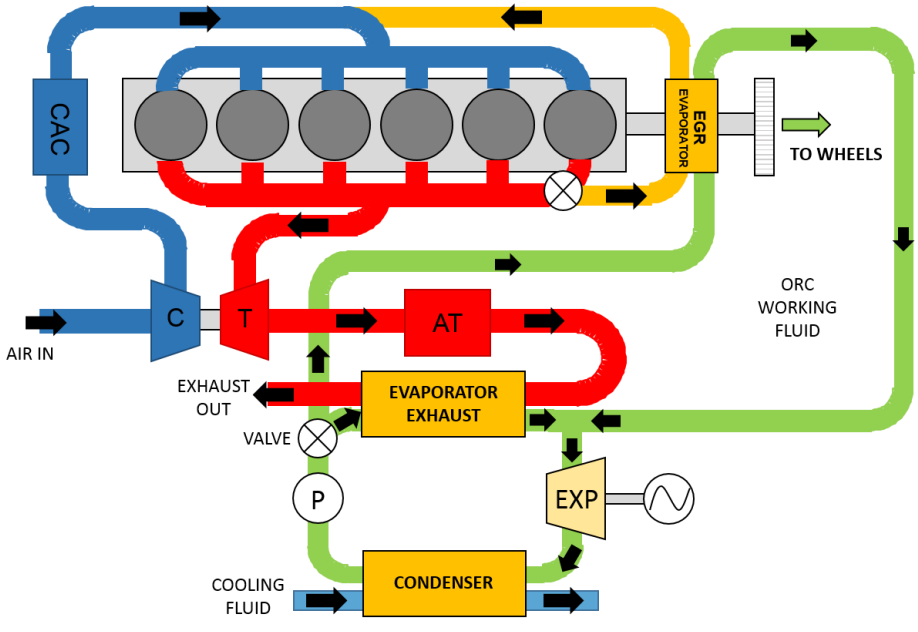

(b)

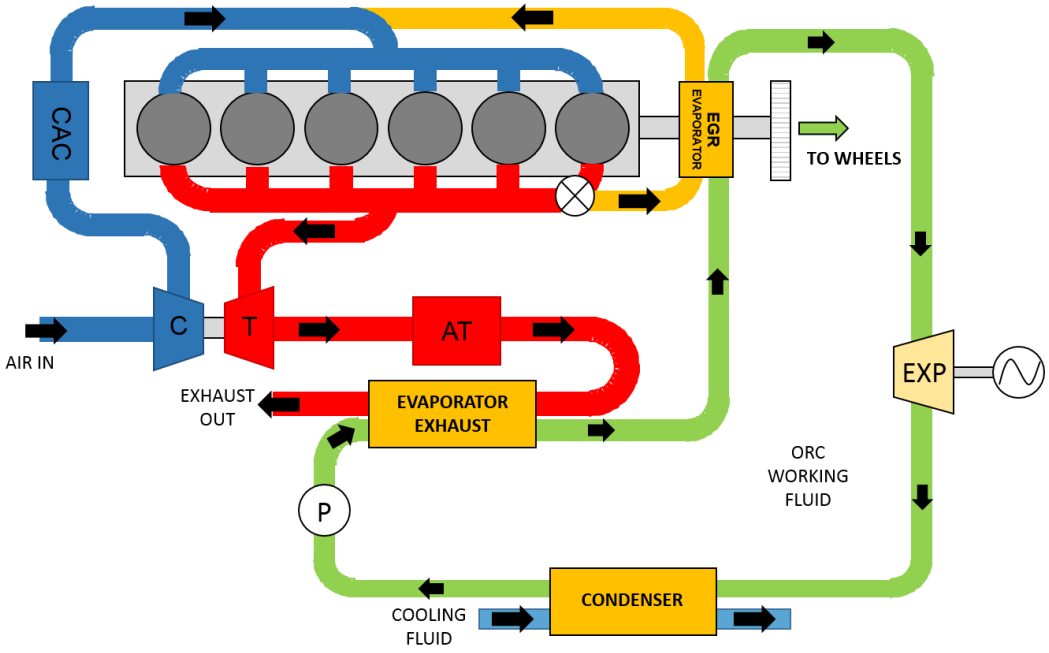

(c)

Fig. 24. Most common ORC layouts for HDDE on-off highway waste heat recovery: (a) simple tailpipe evaporator, (b) parallel exhaust gas-EGR evaporators and (c) series exhaust gas-EGR evaporators configurations

In the schemes proposed above, P stands for pump, EXP for expander. For the engine side, C is the turbocharger compressor, T the turbine, AT is the aftertreatment box, while CAC is the charge air cooler.

In the simple tailpipe evaporator configuration (Fig. 24-a), the ORC working fluid is fully evaporated using the exhaust gas heat, generally after the turbocharger and the aftertreatment box. In the parallel evaporators configurations (Fig. 24-b), often proposed by ORC developers in the sector, the ORC working fluid is split between the tailpipe and the EGR lines. This configuration is proposed when EGR is used as a method for NO_x abatement, and the evaporator on the recirculation line is installed instead of the common EGR cooler. In the configuration with series evaporator (Fig. 24-c), the exhaust gas is generally used to evaporate the ORC fluid, while the high temperature EGR to super-heat the fluid. Layouts with inverted series are also possible. Especially in the last two cases, the EGR cooling requirements for combustion must be respected, unless additional heat exchangers are installed. The first two layouts (*a* and *b*) have been assessed in the case study proposed in section 6.1.

Another possibility is using the engine coolant (or CAC) heat to preheat the working fluid before entering the evaporator.

In vehicle applications, packaging and weight constraints are also very important. For this reason, simple configurations are usually considered more suitable, rather than complicated multiple-loop or multiple-components systems. Integration of the system with engine, powertrain and vehicle thermal management are also of great importance.

The only heat sink which is available in a vehicle is the ambient air, which is supplied with the movement of the vehicle itself (ram air) or through the use of a fan (electric or coupled to the engine through a viscous clutch). Moreover, the vehicle cooling pack is usually made of the air conditioning condenser (AC), the oil cooler, the charge air cooler (CAC) and the engine radiator. For this reason, and considering packaging constraints, modifications of the cooling package of the vehicle can lead to problems in terms of space, cooling performance and increased fan parasitic power consumption (e.g. increase of the pressure drop to overcome over the overall cooling module). A solution, in order to supply enough cooling effect for the ORC systems, but at the same time reducing the impact on the

cooling module, is using the engine cooling circuit as a heat sink also for the ORC system itself, rejecting the overall heat to the ambient through the main radiator, as proposed by Edwards *et al.* [157]. This will generally increase the radiator heat rejection requirements, in terms, especially, of dimensions of the component, as assessed in the preliminary analysis proposed in section 6.1.
Another possibility is to propose a separated cooling circuit for the ORC system, with a dedicated ORC radiator (indirect condensation) or to directly condense the ORC fluid through the use of a AC-similar condenser. Innovative solutions to increase the vehicle heat rejection capabilities are currently under study as, for example, using part of the chassis body panels as heat exchangers, which are cooled through optimized air flows and aerodynamics.
In case of recovering EGR, part of the heat, which otherwise should be rejected into the engine cooling circuit and then to the ambient, is recovered and transformed in useful energy. For this reason, generally recovering EGR is beneficial regarding vehicle thermal management, compared to the case with exhaust gas, in which the rejected heat is just an additional load to the cooling package. Again, some of these issues have been addressed in the case study in section 6.1.
More complicated layouts or ORC evolutions studies are also available in literature, such as dual-loop or cascaded ORC (e.g. [158], [159],), two-stage pressurization ORC (some examples, referred to a two-stroke power unit have been reported in Fig. 25). These architectures are bulkier, more complicated, and are probably more suitable for stationary systems or marine ORC applications. The aim of these more complex layouts is to recover different heat sources, at different temperature levels (e.g. exhaust gas and engine coolant), in a unique architecture. They could present the potential to reach higher energy conversion efficiencies, but with bigger reliability issues, due to the increased system complexity. Some examples have been reported below, referring to a two-stroke marine engine.

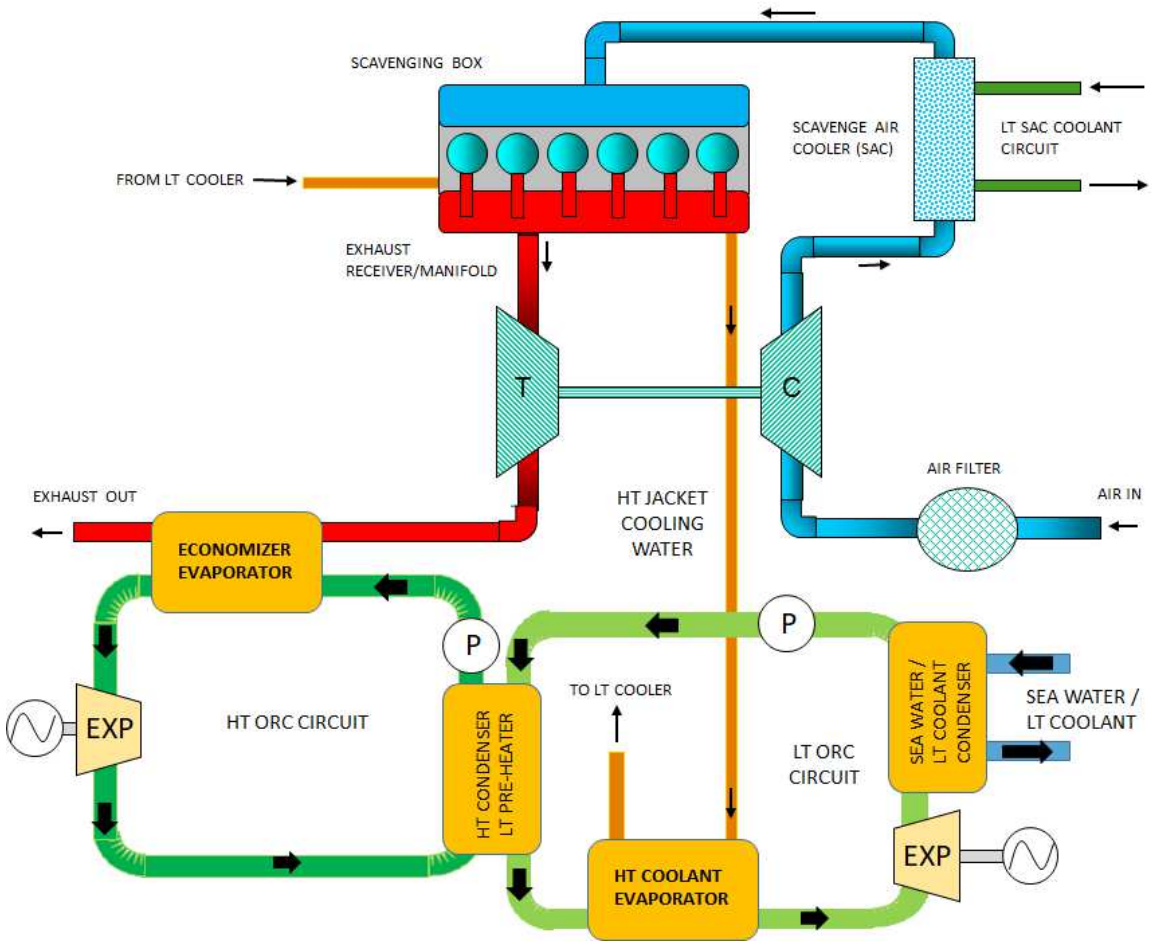

(a)

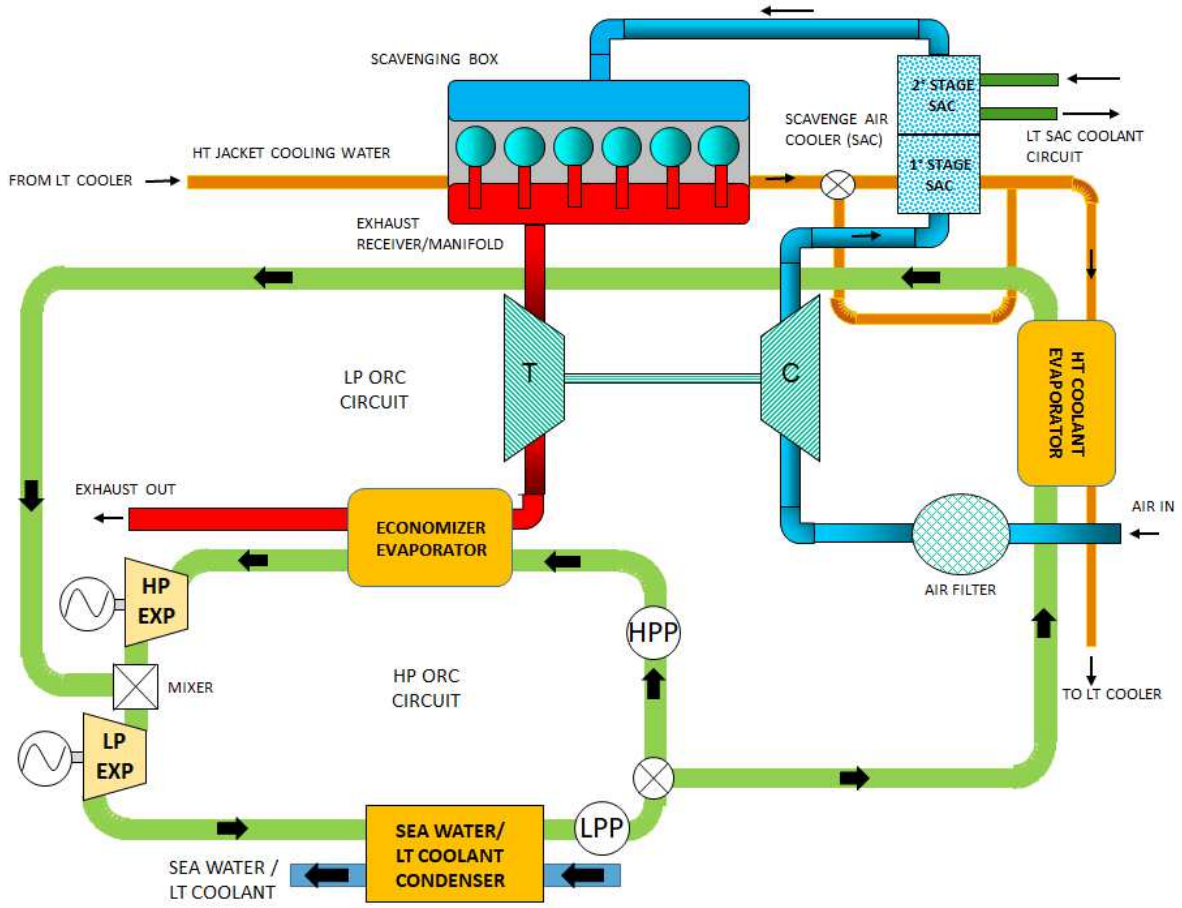

(b)

Fig. 25. More advanced ORC architectures: (a) dual-loop ORC and (b) two-stage pressurization ORC

In the dual-loop configuration example (Fig. 25-a), the exhaust gas heat is recovered through the use of a high temperature ORC loop using high temperature suitable working fluids (e.g. water or alcohols), while the coolant heat is recovered using a low temperature ORC loop, with lower temperature suitable working fluids (e.g. refrigerants). The two loops are connected through the high temperature loop condenser, which acts also as a preheater for the low temperature cycle.

In the two-stage pressurization example (Fig. 25-b), the ORC fluid is pumped to a certain pressure level, suitable for low temperature heat recovery (coolant in the example), through the use of a low-pressure pump (LPP), while part of the fluid is pumped to a higher pressure through a high-pressure pump (HPP) in order to recover the exhaust gas higher temperature heat. The ORC fluid is the mixed again after the high-pressure expander (HP EXP), and expander again in the low-pressure expander (LP EXP), before being condensed. In this case, a fluid capable of recovering both circuits heat should be considered. Literature information about this configuration are very poor.

Especially in marine applications, the choice of the right heat sink is less challenging compared to vehicles applications. Indeed, in ships, the availability of sea water, generally at quite low temperature, helps in rejecting the necessary heat for fluid condensation purpose. Dedicated fresh water intermediate circuits, or air-cooled condensers can also be considered in the first steps of a development project.

Additionally, some researchers propose also to directly recover engine block coolant heat with a suitable ORC working fluid which should, theoretically, be able to substitute actual engine cooling fluids, thus reducing system complexity and improving efficiency [160–162]. The proposed

architecture is very similar to the one reported in Fig. 25-b, with the fluid directly circulating into the engine jacket. However, boiling issues in the engine cooling jacket must still be assessed.
Other advanced ORC systems and architectures can also be considered, even if not directly analysed in this work. Some advantages and disadvantages of these systems have been presented in Tab. 13, while references have also been reported, in case the reader wants to deepen the topic. All proposed layouts and configurations can be assessed with the methodologies and analysis approach proposed in this work.
Some architectures between those reported in this section have been analysed, through the mean of thermodynamic simulation campaigns, in the case studies proposed in this work, with the scope of showing the possibilities offered by a combined engine-ORC simulation approach.
In particular, one architecture, proposed for the two-stroke engine case study, resulted to be very interesting because capable to achieve a good trade-off between power output and low system complexity. The layout has been reported in Fig. 26, and aims to recover both engine high temperature coolant heat and Scavenging Air Cooling (SAC) heat. The thermodynamic results for the cases analysed have been reported in section 6.3.

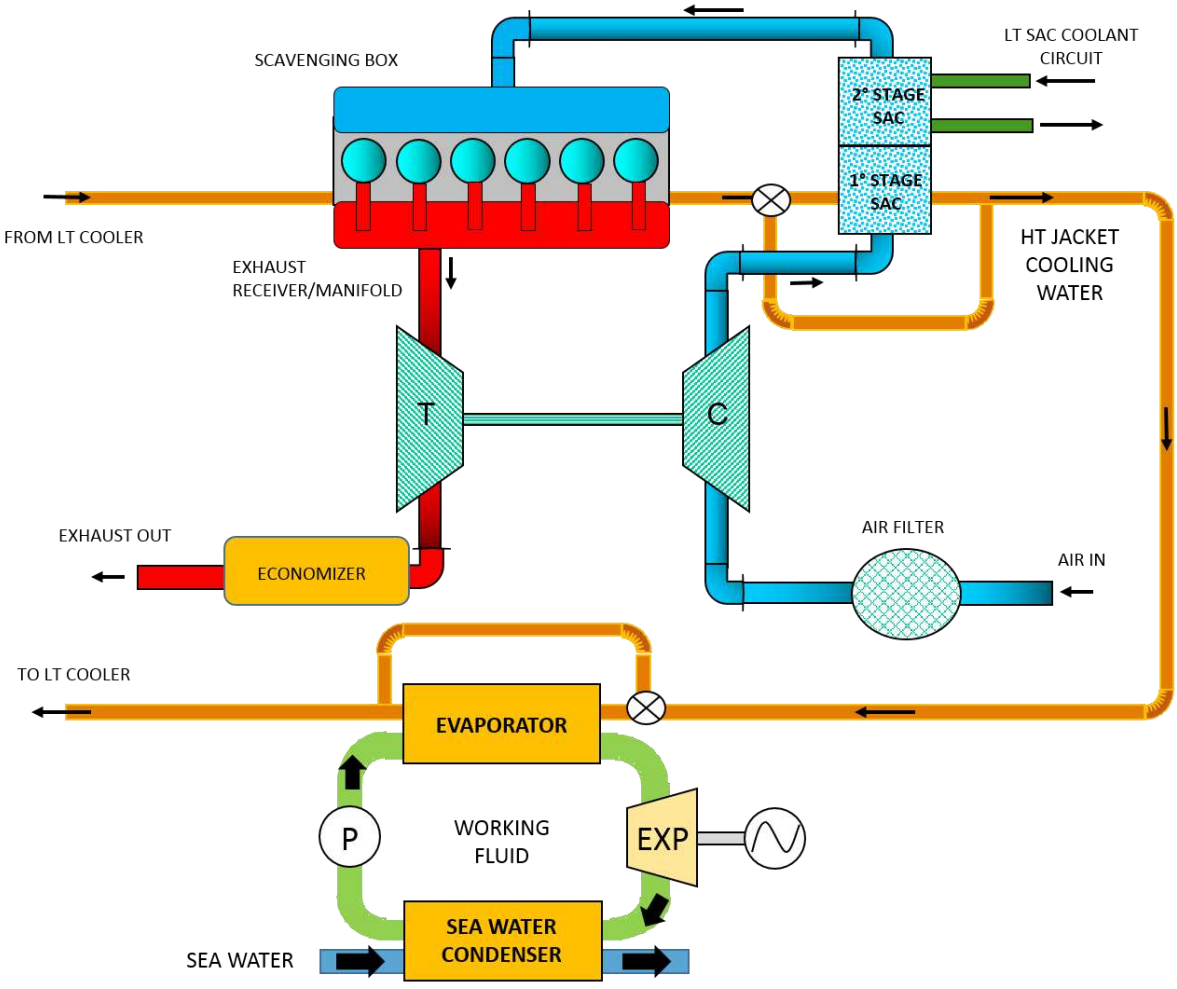

Fig. 26. ORC architecture to recover high temperature cooling water and SAC heat (two stroke propulsion unit)

Configuration	Short Description	Advantages	Disadvantages	References
Dual-loop ORC	Described in previous section (Fig. 25-a)	Increased system efficiency and fuel economy potential Potential to recover different temperature heat sources in a unique architecture	Increased engine backpressure Increased layout complexity (cost, weight, packaging, reliability) Not very suitable for vehicle applications	[163–169]
Two-stage pressurization ORC	Described in previous section (Fig. 25-b)	Increased system efficiency and fuel economy potential Potential to recover different temperature heat sources Potentially more compact than the dual-loop ORC	Increased engine backpressure Increased layout complexity (costs, weight packaging, reliability) Not very suitable for vehicle applications	[161,162,170,171]
ORC with ejector	The use of an ejector contributes to decrease the expander backpressure, thus improving system performance	Increased system efficiency and fuel economy potential compared to simple ORC Potentially compact solution for vehicle applications	Increased engine backpressure Additional components required (cost, weight, packaging, reliability) but more compact than dual-loop and two-stage configurations	[172–174]
Steam-Assisted Turbocharging (SAT)	Steam is evaporated through the use of the exhaust gas heat and used to drive the turbocharger turbine in synergy with exhaust gas	Increased boost and engine performance at high speed/load conditions	Increased engine backpressure Corrosion problems if wet steam is used Limited performance at low engine speed (<1000 rpm)	[175]
Open-steam power cycle and Engine-cylinder expansion ORC	Steam is evaporated through the use of the exhaust gas heat and used to drive the turbocharger turbine or expanded in one of the engine cylinders. Closed or open cycles possible.	Reduced emissions when using one cylinder as expander (sort of downsizing or cylinder deactivation effect)	Increased engine backpressure Limited performance at low engine speed (<1000 rpm) and load	[176–178]
Integrated coolant recovery ORC	The ORC working fluid is circulated into the engine cooling jacket and used directly to extract the heat from the engine	Beneficial for thermal management (vehicle) Possibly compact concept Lower number of heat exchangers used	Coolant boiling in the engine block can lead to engine failure Nucleate boiling strategies must be further studied	[160–162]
Trans-critical (TORC) and Super-critical ORC (SORC)	Typical ORC system with evaporation pressure above the critical one (transcritical). In the supercritical variant, also the condensation pressure is above the critical pressure	Increased system efficiency, better thermal match (especially for low temperature heat recovery) Beneficial for coolant waste heat recovery and thermal management	Increased engine backpressure if exhaust heat is recovered High pressures required for high temperature heat sources heat recovery Advanced components required (cost, reliability)	[179–183]
Trilateral Cycle (TLC) and Trilateral Rankine Cycle (TLRC)	ORC in which the expansion process starts from the saturated liquid state rather than vapour state	Increased thermal match with heat source Potentially compact system Potential for coolant waste heat recovery	Increased engine backpressure if exhaust heat is recovered Efficient expensive two-phase expanders required	[184–187]
Organic Flash Cycle (OFC)	Similar to TLC and TLRC, but with the use to a flash evaporator to avoid liquid during the expansion process	Expensive efficient two-phase expander not required Potential for coolant waste heat recovery	Increased engine backpressure if exhaust heat is recovered Flash evaporator required (cost, weight, packaging)	[188]

Tab. 13. Short overview of advanced ORC configurations with references from literature

4.2.2.3 ORC Components Overview

In this section, a brief overview of the main ORC components has been considered, with particular focus on marine and commercial vehicles applications. It is out of the scope of the work to consider the components in the details and, especially considering the overall system approach used in this research, the detailed description of the various technologies has been left to the various references reported in the following paragraphs.

Heat Exchangers

For engine waste heat recovery using ORC or Rankine cycles, usually shell-and-tubes, plate or compact finned-tubes (or finned-plates) heat exchangers are used. Shell-and-tubes types are mostly used in stationary applications and large systems (as in marine engine heat recovery) and they can tolerate high pressures, while, usually, plates heat exchangers are used when recovering heat from liquids fluids rather than gases (e.g. coolant, or in condensers using water as condensing medium) or in smaller applications due to their compactness [21]. Plate heat exchanger can withstand lower temperatures (around 250°C) compared to shell-and-tubes designs, because of plates deformations and gaskets-sealing problems [189], even though higher temperature suitable devices are under development. Metal foam heat exchangers [190] are also under study and can be used in vehicle waste heat recovery applications due to their compactness and enhanced heat transfer capabilities. Nevertheless, they result in being very expensive at the actual state of the art [189], and they lead to very high pressure drops on the engine exhaust gas side, with consequent increase in engine backpressure and decrease in performance [191].
In large ORC systems for stationary applications (e.g. biomass, stationary engines for power generation and marine applications), very often an intermediate oil circuit is used to separate the heat source from the working fluid. In case of hot engine flue gas waste heat recovery, this solution is used to avoid flammability and safety problems in case of working fluid leakage in the heat exchanger. In case of vehicle applications, it is useful, in order to decrease the system weight and cost, and to increase heat transfer efficiency, to directly transfer the heat from the heat source to the working fluid using a direct evaporation configuration. The heat exchanger installed on the heat source must tolerate high pressures (especially working fluid side), high temperatures, corrosion and fouling problems, especially when recovering heat from high sulphur content flue gases. In this case the exhaust gas must not be cooled down to a temperature below 90-130°C (depending on sulphur compounds amount), to avoid possible acid condensation and damaging of the heat exchanger. Currently, components able to better withstand acid condensation are under study and development (e.g. using stainless steel, [192]).
When sizing a heat exchanger, a right pinch point temperature difference between the heat source/heat sink and the working fluid must be chosen, usually as a trade-off between performance maximization and cost minimization (heat exchanger dimensions). Common pinch points trade-off values are 10 K for gas-to-gas heat transfer 5 - 10 K for liquid-to-gas or liquid-to liquid heat transfer.
In case of direct evaporation configuration, the gas-side pressure drop in the heat exchanger should be minimized in order to have a low impact on the engine backpressure, which increases engine pumping losses. Advanced turbocharging strategies have to be implemented in order to withstand this negative effect and counterbalance the engine performance, as proposed in the case study in section 6.2.
Several manufactures of thermal management components (e.g. Mahle-Behr, Modine, Borg Warner, TitanX) are working to replace EGR coolers and engine tailpipe section with ORC suitable evaporators, and to increase heat transfer performance and compactness. Hatami *et al.* [193] presented several techniques to increase heat transfer effectiveness for different heat exchangers designs. Most of these components are usually based on fin-tubes or fin-plates architectures.

Regarding condensers, a few condensing strategies possibilities are available in case of engine waste heat recovery in vehicle applications: indirect condensation using the engine cooling circuit as heat sink (average temperature range around 80-100°C), indirect condensation using a lower temperature cooling circuit (e.g. CAC coolant, average temperature level 40-70°C), or direct cooling using an ambient air condenser, similar to a AC condenser and installed in the vehicle cooling pack. In ORC vehicle applications, thermal management of the combined engine-ORC-powertrain system is of vital importance and must be analysed carefully both under steady-state and transient conditions. Advanced CFD models are used to optimize cooling package architectures. Space restrictions, as well as operational behaviour of the vehicle (speed, ram-air cooling effect) and ambient conditions (hot weather conditions are more challenging), are leading to severe cooling package sizing issues. A preliminary investigation of these issues has been considered in the case study proposed in section 6.1. Moreover, condensing pressures should be higher than ambient atmospheric pressure, to avoid air leaking into the system and expensive sealings. However, decreasing condensing pressure can lead to improved enthalpy drop over the expansion machine, thus increasing system performance. Condensing temperatures and pressures must also be chosen based on expected ambient conditions (e.g. to avoid inverse heat transfer during hot days).
In marine and stationary applications, condensation processes are less challenging, due to less space and weight constraints as well as to availability and lower cost of cooling medium, such as sea water. In this case, salty water corrosion problems must be taken into consideration. Air cooled designed units are also possible.

Pumps

An overview of the main pump technologies is reported in the scheme in Fig. 27, as proposed by Landelle *et al.* [194].

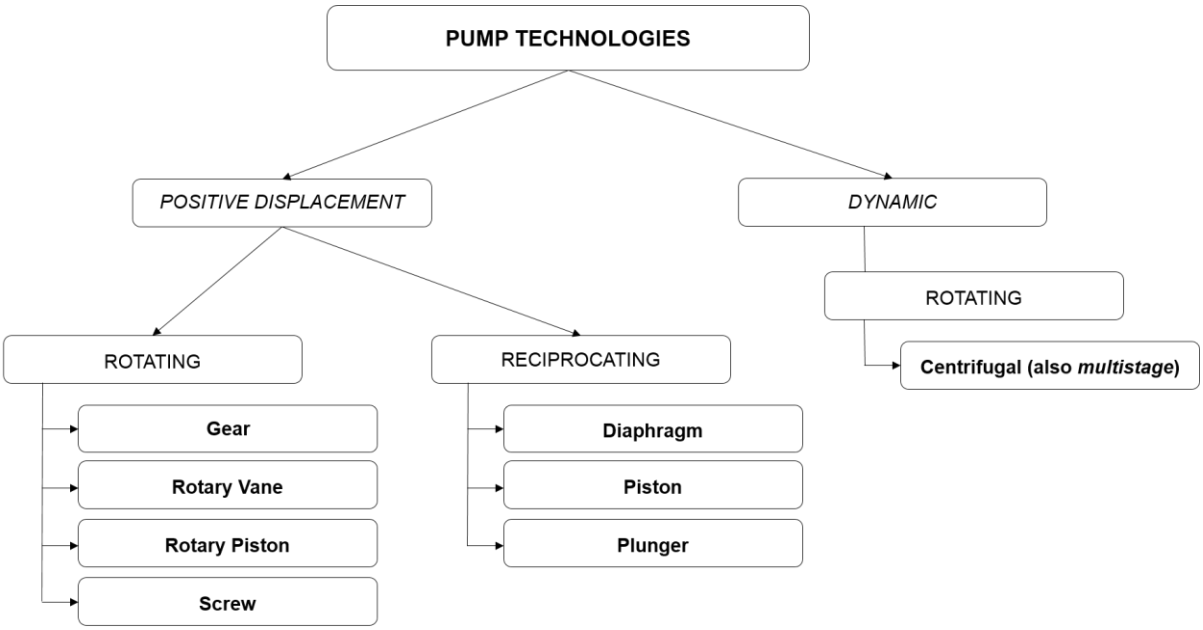

Fig. 27. Main ORC pump technologies

The pump in the ORC system is used to pressurize the working fluid from condensing to evaporation pressure and to control the working fluid mass flow rate in the circuit. A complete overview of the

main pumps requirements for ORC systems, such as controllability, efficiency, tightness, cavitation, has been reported by Quoilin *et al.* [21].
Different types of pumps could be suitable for ORC use. For example, positive displacement pumps (in which the working fluid flow rate in proportional to the rotational speed). An example of positive displacement pumps are diaphragm pumps, in which the contact between fluid and components is avoided and tightness of the system improved. Pulsed flow rate could be a drawback. Other examples are reciprocating piston pumps, or rotary pumps (e.g. screw, sliding or rotary vane, scroll, roots or gear pumps). Centrifugal pumps are also available. In this case the flow rate depends also on the pressure head between evaporation and condensing pressures. In some cases, the use of the most appropriate pump is a very important design choice, both in terms of system efficiency and costs.
The pump also controls the evaporation pressure in the system. The electrical motor driving the pump can be coupled with an inverter in order to change the rotational speed and control the working fluid mass flow. Magnetic coupling is often used to transfer torque from the electrical engine to the pump, thus not using sealings for the shaft (wear and fluid corrosion problems are avoided).

Expanders

The expander is one of the most critical components of an ORC, since the performance of the system are directly related to the performance of the expansion machine.
Two categories of expanders can be distinguished: turbo machines and positive displacement machines [21].
An overview of the main ORC suitable expansion machine technologies is reported in the scheme in Fig. 28, as proposed by Landelle *et al.* [194].

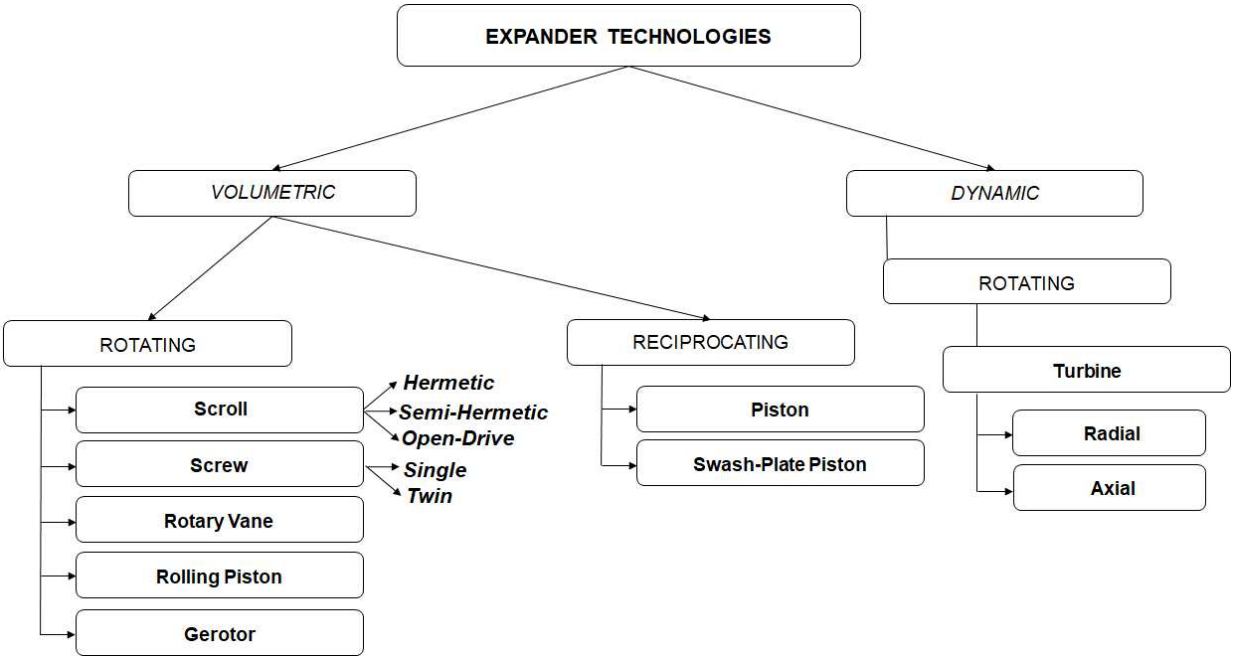

Fig. 28. Main ORC expander technologies

Turbo-expanders are more suitable for larger ORC systems and they show better performance when operating in a steady state condition at design point (off-design operations are less efficient compared to positive displacement type unless variable inlet guide vanes are used), with efficiencies which can

reach also values of 80 – 85 % [112]. They can be axial or radial turbines. The first type in mostly used in large waste heat recovery systems for stationary power generation applications with lower pressure ratios and high working fluid mass flow (e.g. some Turboden systems). Radial turbines are mostly used for high pressure ratios and lower working fluid flow rates. Axial turbines are more suitable to be assembled in several stages. Organic fluids suitable turbo-expanders have also more compact layouts and sizes compared to steam turbine, because of the higher density and lower specific volume of organic fluids compared to water-steam. Moreover, turbines used in ORC applications have lower enthalpy drops compared to steam, thus leading to the possibility of using only one or two expansion stages [151]. Turbomachines are not very suitable for small ORC systems, because of their very high rotational speed which could lead to structural problems, bearings failure, as well as to the need of very expensive high-speed generators for electricity production. Additionally, turbo-expanders do not tolerate high amounts of liquid during expansion, because of possible blade damaging problems, but advanced engineering activities are currently ongoing to mitigate all these risks and offer affordable and reliable turbo-machines as possible expansion devices for vehicle ORC. The high rotational speed in also detrimental when considering coupling the expander shaft to the engine shaft in case, for example, of vehicle mechanical energy utilization.

Positive displacement expander type examples are: reciprocating piston, scroll, screw, vane and Wankel expanders. A complete overview about these types of expanders, technical issues and considerations, as well as modelling techniques is presented by Lemort and Quoilin [195]. A review of working fluid and expander selection criteria is also reported by Bao and Zhao [151].

Reciprocating piston expanders are mostly developed for small-scale CHP and waste heat recovery systems (such as internal combustion engines applications). They can operate with large pressure ratios [196] because of their large volume ratios (or Built-In-Ratios, the ratio between expansion chamber volume at expansion end and expansion beginning), in practice around 6 to 14 or more. For this reason, the recovery of medium-high temperature heat sources in internal combustion engines, such as exhaust gas and EGR, seems to be a feasible application for this kind of technology, even though not many information and experimental activities are reported in literature, as can be evinced from Landelle *et al.* [194]. Some prototypes and commercial products are however available, as reported in Tab. 14. This type of expander requires precise timing for intake and exhaust valve, vibration control and balancing. Moreover, piston expanders show high frictional losses (e.g. piston rings-cylinder walls interactions), lubrication and sealing problems. They can tolerate high pressures and temperatures (70 bar, 560°C) and liquid phase during expansion is also well tolerated. Free-piston expanders are also under development (e.g. Libertine, UK [197]), while an example of swash plate axial-piston expander ORC vehicle implementation is reported by Endo *et al.* [198]. A commercial implementation of a reciprocating piston expander for ORC systems is the two-stroke SteamTrac model (Fig. 29-1) from Voith-SteamDrive [199], for on and off road, as well as marine and railway applications. No matter if the technology is still under development, it seems to be very promising, in particular for vehicle ORC applications.

Scroll type expanders can operate over a lower expansion ratio range due to their lower Built-In-Ratio (3.5 - 5), thus being more suitable for low temperature heat sources heat recovery (e.g. engine coolant). They undergo under-expansion or over-expansion losses as the reciprocating piston machines. Other important losses are due to friction (lubrication is needed), leakage and heat transfer. They can tolerate lower temperatures compared to piston type (215°C). It is very common that scroll devices for ORC applications are retrofitted from AC compressors for automotive applications, and mostly used for low temperature waste heat recovery (e.g. coolant). This allows cost savings during the system development, even though, well designed scroll for ORC applications promise better efficiencies. Also for scrolls, liquid phase during expansion is well tolerated and they can adapt to a wide range of operating conditions. Some oil-free models are under development. A review of scroll expanders for ORC systems is reported by Song *et al.* [200] and scroll performance issues are discussed in [201].

Scroll expansion machines, used in a series configuration, could allow higher expansion ratios to be achieved [202].
Screw-type (Lysholm) expanders (and twin-screw) has been also used as compressors in the past. They are mostly used in geothermal applications with medium-high power output (20 kW-1 MW). They show moderate Built-In-Ratios (5-8). Oil is needed for lubrication. Rotational speed is higher than for other expander types (reduction gearboxes are needed when using it in vehicle applications, feeding the recovered energy back into the crankshaft). Sealing is also very important to reduce leakage, especially in case of dangerous fluids. Manufacturers of ORC systems using screw expanders are, for example, Electratherm and Ormat, and they provide products for a power range starting from 50 kW_{el} [203]. Screw expanders are also generally bulkier, for this reason not being suitable for vehicle applications, but rather for stationary.
Vane-type expanders are also suitable for low power outputs ORC systems. They can have single acting or double acting configurations. They can tolerate a wide range of vapour qualities without damaging problems. They can be easily manufactured, and they provide smooth torque production. They can be suitable for engine mechanical coupling without gearbox due to their low rotational speed (3000 rpm). Little lubrication requirements as well as low level noise are other advantages. Leakage losses is a possible drawback, together with high pressure drops [189], due to the difficulty of vanes to maintain a good contact with the housing. The rotational speed is strongly affected by the pressure and flow rate of working fluid. Friction losses are also becoming important at higher speed rotational regimes. Generally, they tend to show lower efficiencies compared to scroll machines.
Wankel devices have been implemented in the past as air compressors or internal combustion engines. They are also suitable for low power output levels, they have simple configurations, but sealing and lubrication problems.
A study about the utilization of a roots expander for HDDE applications has been reported by Subramanian [204].
Some examples of commercial volumetric expanders, in the possible HDDE vehicle waste heat recovery power range (5-60 kW), have been reported in Fig. 29.

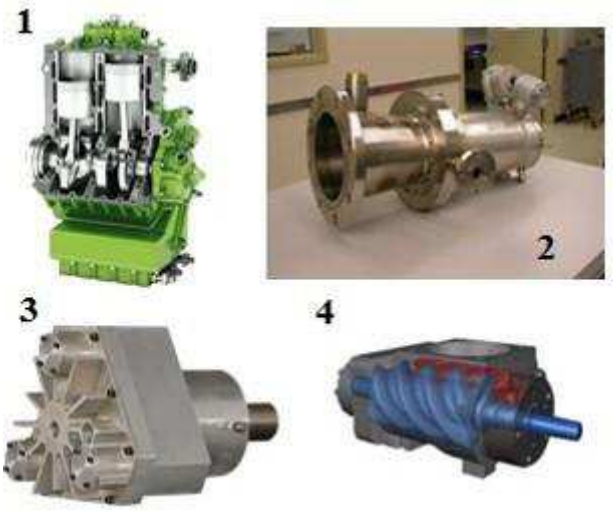

Fig. 29. SteamDrive SteamTrac piston expander (1, Courtesy of SteamDrive [205]*), Barber-Nichols radial expander (2, Courtesy of Barber-Nichols* [206]*), Air-squared scroll expander (3, Courtesy of Air-squared* [207]*), Electratherm twin-screw expander (4, Courtesy of Electratherm* [208]*)*

Another important issue regarding expanders in ORC engine waste heat recovery for vehicles implementations is the integration into the overall powertrain or driveline. Indeed, two possibilities are available: mechanical or electrical coupling (or energy generation).

In the first case, the expander produced net power is re-introduced into the crankshaft through the use of a gearbox or other type of transmissions, depending on the difference in rotational speed between expander shaft and engine shaft. A clutch can be inserted to disconnect the ORC expansion machine and the engine during, for example, downhill driving conditions, in which the engine load is not high enough to produce valuable exhaust gas heat to sustain the ORC operation [209].
In the second case, the expander is connected to a generator, and electrical energy is produced. The energy can be used to charge batteries, for auxiliary systems (AC, cooling refrigerators, on board electrical devices) or re-introduced into the powertrain in Diesel-hybrid vehicles configurations.
The two configurations have been reported in Fig. 30. The electrical configuration shows lower energy conversion efficiency (70 - 85%) compared to the mechanical one (90 – 98%), due to the need of going through all energy conversion steps ([112,210]). Similar configurations can be used also in case of marine applications. Some examples have been reported in section 6.3.

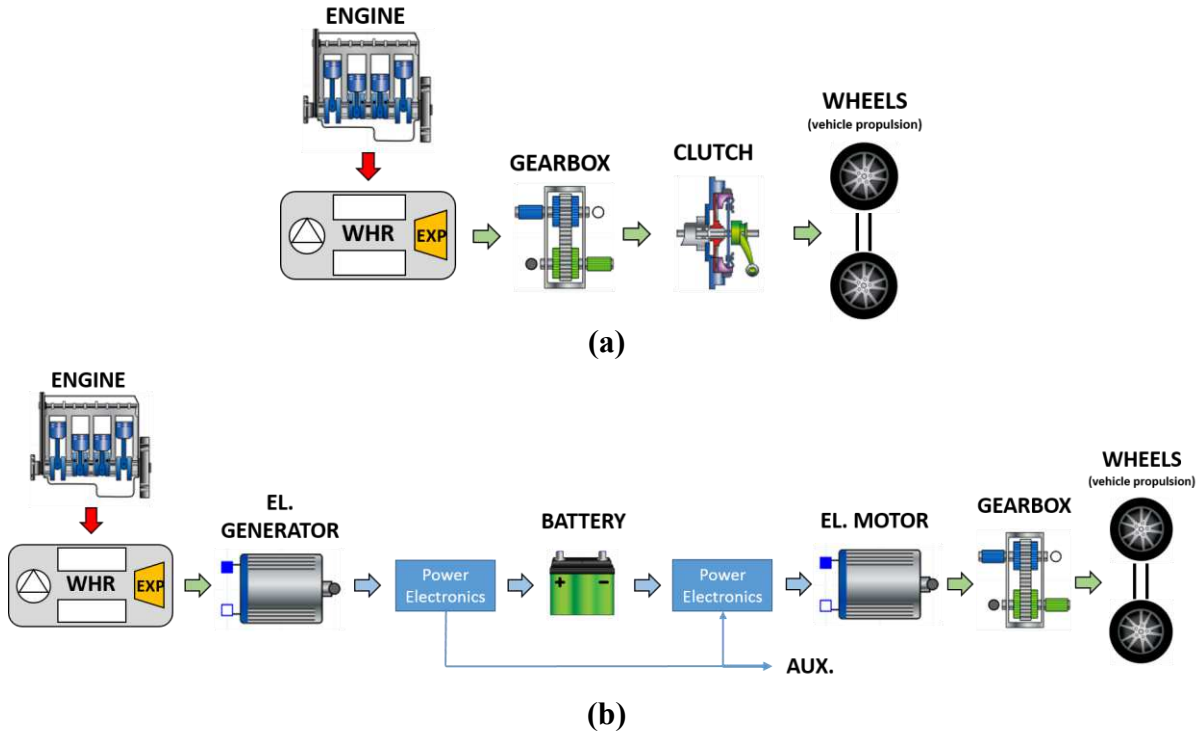

Fig. 30. Mechanical (a) and electrical (b) ORC driveline integration (vehicle example)

In the next section, in Tab. 15, a summary of heavy duty Diesel engine vehicle ORC implementations by automotive manufacturers and research institutions has been reported, focusing the attention on the expander technology tested and proposed, while in Tab. 14, an overview of different expander technologies available on the market in the power range for the considered vehicle applications has been reported.
Additional data, regarding pressure ratios and efficiency, for different expander technologies, and in particular scroll and piston, have been reported in section 5.3.1.2.

Company	Model	Working Fluid	ORC Power Range	Declared Eff. [%]	Expander Type	Speed [rpm]	Comments	Ref.
Verdicorp	n.a.	R245fa	30 - 180 kW	n.a.	Turbo/radial	n.a.	Conversion from air compressor	[211]
Barber Nichols	n.a.	Fluorinol-50, R245fa, toluene, water-steam, R134a	3 kW - 250 kW	85	Turbo/radial	up to 60000	Concept studies up to 250 kW range for stationary applications	[212]
Green Turbine	Green Turbine	water-steam, organic fluids	1.2 kW-15 kW	n.a.	Turbo/radial	up to 30000	/	[213]
Cummins	n.a.	R245fa	42 kW	77	Turbo/axial	80000	Development phase, HDDE truck suitable	[214]
Infinity Turbine LLC	IT01 / IT10 / IT50	R245fa	10 kW-3 MW	73	Turbo/radial	n.a.	/	[215]
Enogia	various	R245fa, Novec 649	5 – 100 kW	n.a.	Turbo/radial	n.a.	Commercial turbine coupled with high speed generator	[216]
Bosch	n.a.	Water, ethanol	2 – 18 kW	68	Turbo, double stage	150000	Prototypes tested	[217]
Borg Warner	n.a.	ethanol	3 – 20 kW	65	Turbo	n.a.	Electrical power production, 18:1 expansion ratio declared	[218]
Electratherm	n.a.	n.a.	35 - 110 kW	n.a.	Twin screw	n.a.	Available on the market mostly for stationary power generation applications	[219]
Air Squared	E15H022A-SH / E22H038A-SH	R245fa, R134a, other gases	1 - 5 kW	70 - 80	Scroll (oil-free or lubricated)	2600-3600	/	[220]
Eneftech	n.a.	R245fa	1 - 5kW	80	Scroll	2000-6000	for micro-CHP units	[221]
Liebherr	n.a. - Patent	R245fa, ethanol, water-steam	n.a.	n.a.	Rotary vane	n.a.	Patent, no other information available	[222]
SteamDrive GmbH	SteamTrac / SteamDrive	water-based medium	20 - 360 kW	> 65	Reciprocating piston	3600	/	[199]
Exoes	n.a.	Water-steam or ethanol	4 - 12 kW	40 - 45	Swashplate piston	1000-6000	Development phase, low power applications, development for trucks	[223]
Viking Development Group	CraftEngine	Organic fluid	2 - 40 kW	n.a.	Reciprocating piston	750-1500	Available on the market mostly for small CHP applications	[224]
Libertine	n.a.	ethanol	n.a.	n.a.	Free piston	n.a.	Prototypes available, still in development	[197]
Bosch	n.a.	water, ethanol	5 – 20 kW	n.a.	Piston, single cylinder, double acting	1500	Prototypes tested	[217]

Tab. 14. Commercialized or in-development expander technologies suitable for commercial vehicles ORC power range

4.2.3 Waste Heat Recovery in Commercial Vehicles using ORC - Literature Review

The first application of an ORC system used to recover engine wasted heat in a vehicle has been reported by Patel and Doyle [225] in 1976. They proposed to recover energy from the exhaust gas of a Mack 676 Diesel engine mounted on a long-haul truck, obtaining a gain of 13% in power without additional fuel at peak load conditions, using Fluorinol-50 as working fluid. Some additional testing results on the same system have been reported by Doyle *et al.* [209], together with a complete description of the hardware, considering also the system thermal management (using a compound radiator for the engine and the ORC). A 15% improvement in fuel efficiency is suggested to be possible for the combined system. DiBella *et al.* [226] reported additional results about the same system, regarding laboratory tests with improved components and implementation of control strategies. The authors reported an overall fuel consumption saving of 12.5% for a long-haul truck, with mechanical utilization of the additional recovered power, feeding it to the engine crankshaft using a gearbox.
More recently, Chammas and Clodic [227], in 2005, reported a concept study about the possibility of recovering exhaust and cooling circuit heat of an hybrid electric vehicle (HEV) powered by a gasoline 1.4 L engine. The recovered exhaust heat is transformed in electrical power through a turbine/generator and used for auxiliaries. Water-steam and organic fluids are evaluated through simulations. Water shows favourable performance (between 12 and 27% fuel economy declared) but also some issues, especially regarding complicated expanders designs. Favourable performance is obtained also using iso-pentane or R-245ca (17-32% fuel economy declared) but with more marked environmental and safety issues.
The engine manufacturer Cummins started, in 2005, to study an ORC system to recover heat from an ISX HDDE model. Nelson [228], in 2009 , reported a presentation regarding Cummins ORC activity, recovering mainly EGR and exhaust heat, stating that the development of efficient SCR after-treatment systems is supposed to decrease the benefit of an ORC fitted on the EGR, as already introduced also in section 4.1.3. Cummins claimed a potential improvement in engine total efficiency between 5 and 8%.
In 2006, Arias *et al.* [229] proposed different simulated ORC configurations to recover heat from exhaust, coolant and combined exhaust-engine coolant of a SI (Spark Ignition) engine installed on a hybrid passenger car. The configuration with working fluid pre-heating in the engine block and superheating with the exhaust gas, is found to be the most promising showing 8.1% cycle thermal efficiency.
Endo *et al.* (Honda) [198], in 2007, reported an implementation of a water-steam Rankine cycle to recover exhaust heat from a passenger car 2.0 L gasoline engine installed in a hybrid vehicle. The evaporator has been integrated in the catalytic converter to reduce the overall dimensions. The expander used is a volumetric swash plate axial piston-type, integrated with the generator. In the vehicle test, at constant speed of 100 km/h, an improvement of 3.8% of thermal efficiency has been claimed for the combined system compared to the baseline engine. Transient analysis and test bench results have been reported for the same system by Kadota *et al*. [230].
BMW ([231],[232]), in 2008 and 2009, reported the implementation of a Rankine cycle system, called "Turbosteamer", for the recovery of high temperature exhaust gas and lower temperature coolant for passenger cars applications. Water-steam was used in the high temperature loop, while ethanol in the low temperature loop. Vane expanders have been used for both the circuits. An increased power output of 15% with no additional fuel consumption has been obtained from tests, and, in general, a 10% value has been considered feasible under relevant stationary realistic conditions. Also, some simulations have been carried out using Dymola to assess different heat recovery systems based on Rankine cycles, and to carry out parametric studies regarding important system parameters such as evaporation and condensing pressure levels.
In 2009, Briggs *et al*. [233], from Oak Ridge National Laboratory, reported a publication about the experimental development of an ORC system applied to a four cylinders, 1.9 L light duty Diesel

engine, equipped with a variable geometry turbocharger and HP EGR, achieving a 45% combined system brake thermal efficiency, recovering heat only from the exhaust gas and using R-245fa as working fluid. The system used a turbo-expander connected to a generator.
Also Daimler and Detroit Diesel, in the frame of the DOE (US Department of Energy) Super Truck Program, investigated the possibility of recovering exhaust heat from a truck HDDE [234]. Heat sources recovered are EGR and exhaust gas, and the selected working fluid ethanol. Primary candidates for the expander choice are piston and scroll expanders, due to their ability of handling two-phase expansion. Different vehicle cooling strategies, components packaging, and weight issues have been investigated.
Behr reported also theoretical and experimental results about HDDE waste heat recovery for long-haul vehicle applications. Edwards *et al.* [157] presented simulation and steady-state components models validation results of a complete ORC waste heat recovery system coupled with vehicle thermal management, using an in-house developed simulation tool called BISS (Behr Integrated System Simulation). A 5% on-road fuel consumption improvement, based on the ESC cycle or a long-haul typical driving cycle, has been demonstrated to be possible. Schmiederer *et al.* [210] reported the results of the Behr experimental ORC cycle used to recover heat from an EURO VI truck engine. A newly developed control system implemented on the ORC system, and a piston type expander, allowed to recover up to 6% additional power. Tests under transient conditions have also been performed. Hybridization of the vehicle powertrain is suggested to be a new opportunity for further development of the technology, especially when considering electricity production from the bottoming cycle system.
Also Bosch presented simulation and experimental results about ORC waste heat recovery for commercial vehicle engine applications ([217],[235]). Two different expander technologies have been evaluated (piston-type and turbine). Exhaust gas and EGR have been recovered in a parallel configuration. Water-steam, ethanol, MM (hexamethyldisiloxane), R-245fa and toluene have been considered for the turbine case.
Eaton also carried out some concept work about implementing an ORC waste heat recovery system on a 470 kW, 13.5 L John Deere HDDE [204]. Simulation studies have been performed about engine performance and validated against experimental data. EGR and exhaust gas waste heat recovery has been simulated, using a layout with heat sources in series and recuperation. 6% BSFC improvement has been obtained. Single stage and multi-stage roots expander have been evaluated using ethanol as working fluid. Further engine integration steps are planned.
Hino reported the results of the design and implementation of a Rankine cycle to recover heat from the coolant of an HDDE for truck applications [236]. The energy of the coolant flow has been increased collecting the heat from exhaust and EGR flows, increasing coolant temperature up to 105°C. 7.5% improvement of fuel economy has been obtained from tests using HFE as working fluid (Hydro-Fluoro-Ether).
Also Ricardo plc has implemented an ORC system to recover EGR and exhaust gas from a 288 kW Volvo HDDE for trucks, using ethanol-water mixture as working fluid [237]. Thermodynamic system analysis, components commissioning, control strategies implementation and testing have been also performed. A piston expander has been used, and the recovered energy re-introduced in the drivetrain through mechanical coupling.
Ricardo plc has also worked on the demonstration of a waste heat recovery system applied to a double-deck Diesel-hybrid bus (2.4 L, EURO IV turbocharged Diesel engine), recovering coolant and exhaust heat with two separate ORC systems, in the frame of the TERS project (Thermal Energy Recovery System) [113,158,238–240]. In this case a scroll expander technology has been used and R-245fa as working fluid. From vehicle tests using off-the-shelf components, a 6% fuel economy has been achieved over a typical city bus driving cycle, being reduced to 2.7% considering that in the hybrid bus the internal combustion engine is switched on only for approximately 45% of the time. Additional benefits could be reached when using a cascaded ORC layout (or dual loop), recovering the rejected

heat from the topping exhaust ORC cycle to pre-heat the bottoming ORC working fluid used for the coolant heat recovery.
Some other studies have been carried out also by academic institutions. For example Katsanos *et al.* [72], reported a theoretical study about the possibility of recovering waste heat from an HDDE for truck applications using a steam Rankine cycle, investigating also the influence of the evaporator design, as well as the possibility of recovering exhaust gas and also EGR heat. In this study 7.5% improvement in BSFC has been obtained when recovering exhaust and EGR heat. The influence of fitting the ORC on the engine thermal management has been also considered, thus requiring a radiator with 20% increased heat rejection capabilities. Recovering EGR heat is beneficial to reduce the thermal load that must be rejected to the ambient by the cooling circuit.
In the study carried out by Hountalas *et al.* [73], also the possibility of recovering CAC heat has been evaluated, together with the investigation about the use of water-steam or an organic fluid (R-245ca). 11.3% improvement in BSFC has been obtained when using organic fluid, and 9% when using steam, in the configuration with EGR and CAC waste heat recovery. Radiator heat rejection capabilities have been investigated also in this study.
A parametric study has also been carried out by Katsanos *et al.* [241], again using water-steam or R-245ca as working fluids, to recover heat from an HDDE for truck applications. Different engine loads cases from 25 to 100% have been investigated.
Latz *et al.* [242] reported a theoretical study comparing different pure working fluids and zeotropic mixtures in sub-critical and supercritical Rankine cycles, considering both energy and exergy efficiencies. Considered pure fluids are: water, ammonia, ethanol, methanol, R-1234yf, R-123, R-152a. Considered mixtures are: R430A (R152a/R600a, 0.76-0.24 mass fractions), R431A (R290/R152a, 0.71-0.29), water-ammonia, water-ethanol, water-methanol. The outcome of the study is that recovering high temperature heat sources with supercritical cycles is not so beneficial compared to sub-critical. Supercritical systems may be beneficial for lower temperature heat recovery (e.g. coolant).
Dolz *et al.* [243] reported a study about different bottoming Rankine cycles setups with water-steam and organic fluids to recover waste heat from a two-stage turbocharged, 311 kW brake power, 12 L, HDDE. The work is divided into two parts. The first part reports an analysis of different heat sources and cycle layouts. Water-steam has been considered to be the best fluid choice when the engine is running at full load conditions, while organic fluids can be more suitable at partial loads operations.
In the second part of the work, Serrano *et al.* [243] investigated the possibility of recovering heat with a turbine expander and feeding the obtained power directly to the turbocharger-compressor eliminating the related turbine. This configuration has low advantages, in terms of performance, compared to the classical bottoming ORC configuration.
Moreover, Macián *et al.* [244] reported a methodology to design a bottoming Rankine cycle for waste heat recovery in vehicle applications. They applied their methodology to an HDDE. Water and R-245fa have been considered as working fluid possibilities. The outcome is that water-steam is more suitable over most of the operating points, while R-245fa is more feasible regarding components space requirement issues. 10% improvement in BSFC has been obtained considering the non-ideal behaviour of pump and expander.
Yang *et al.* [245], analysed the dynamic operating process of a Rankine bottoming cycle, applied to a 11.6 L HDDE model, under driving cycle operations. Low average efficiency during a Tianjin bus driving cycle has been reported (3.6%).
Amicabile *et al.* [246] proposed a comprehensive methodology for the design of ORC systems for automotive HDDE, considering heat sources and working fluid selection (also based on safety and environmental concerns), as well as some implemented costs correlations for the main components. Recuperated and non-recuperated cycles, as well as supercritical and sub-critical possibilities have been considered. Working fluid analysed are ethanol, R-245fa and pentane. The best performance has been obtained with ethanol and recuperative cycles.

Di Battista *et al.* ([247] and [248]) discussed the effects of the back-pressure increase due to the installation of an ORC system on the exhaust line of a turbocharged IVECO F1C engine for light-duty vehicle propulsion. The VGT (Variable Geometry Turbocharger) turbine operation can mitigate this drawback effect. Off-design evaporator operations have been also considered.
Allouache *et al.* [249] reported a study about fitting an exhaust heat exchanger on the tailpipe of a 6.7 L Cummins HDDE. The component has been tested for pressure drop optimization using R245fa as working fluid. An estimation of the recovery potential led to an overall 5% increase in brake thermal efficiency over the speed/load range of the considered engine.
Yamaguchi *et al.* [250] reported a study about recovering exhaust heat form a 6 cylinders HDDE with HP and LP EGR circuits, as well as two different boosting configurations (single-stage and two-stage turbocharged). Respectively 2.7% and 2.9% improvement in fuel consumption have been obtained at typical highway cruising conditions (80 km/h).
Latz *et al.* [251] proposed also experimental results about a water-based Rankine cycle recovering heat from the exhaust gas recirculation (EGR) of a 12.8 L HDDE engine installed on a test-bench. Deionized water, a 2-cylinder piston expander and a EGR boiler prototype have been used. 10% thermal efficiency has been declared for the ORC system.
Glover *et al.* [252] evaluated the possibility of using a supercritical ORC for vehicle waste heat recovery, considering multiple heat sources and working fluids. The simulation results show an efficiency between 5 and 23% for the ORC system and a possible gross fuel economy potential between 10 and 30%.
Pradhan *et al.* [253] investigated, through simulation, the possibility of pre-heating the working fluid with post-SCR heat and then evaporating it with EGR gas heat. Testing results from a MY2011 Mack MP8 engine have been used in order to evaluate transient heat sources behaviour and ORC power output. R123 and R245fa based systems demonstrated to be able to produce 56.2% and 37.6% more energy over a UDDS (Urban Dynamometer Driving Schedule) driving cycle as compared to thermal energy necessary to maintain the SCR in the adequate operational temperature range.
Grelet *et al.* [254] reported the development of controlling strategies for waste heat recovery Rankine based system in heavy duty engines for trucks applications. Again Grelet *et al.* [255] evaluated the transient performance of the ORC system comparing it with steady state data, and considering different cycle architectures and working fluids.
Feru *et al.* [256] presented an integrated energy and emission management strategy for an Euro VI Diesel engine with an electrified waste heat recovery system, with the purpose of optimizing the CO_2-NO_x trade-off with operational costs related to fuel consumption. Configurations with and without ORC and a recovery system with battery for energy storage have been considered. 3.5% CO_2 emission reduction and 19% particulate emission reduction have been obtained, while respecting NO_x emission limits, over a World Harmonized Transient Cycle (WHTC). The ORC system implementation leads to 3.5-4% fuel economy improvement during highway driving conditions.
Torregrossa *et al.* [257] reported results from the experimental testing of an ORC integrated in a 2 L turbocharged gasoline engine using ethanol as working fluid and a swash-plate expander. Transient tests with varying vehicle speed have been implemented with the purpose to evaluate expander controlling strategies over a New European Driving Cycle (NEDC).
Usman *et al.* [258] presented the analysis of a ORC system applied to a light duty vehicle, considering both positive and negative aspects of the system installation (e.g. net power output increase, weight increase, engine backpressure effect). The results show a 5.8 % engine power enhancement at vehicle speed of 100 km/h when considering negative effects (instead of previously calculated 10.9% not considering drawbacks). The conclusion of the study is also that at a speed lower than 48 km/h, the waste heat recovery system is not beneficial at all, even increasing engine power demand, thus discouraging the system installation in typical city driving cycle suitable vehicles.
In general, studies and developments about ORC for waste heat recovery in commercial engines applications are very common in literature in the last years, and the publications are growing in number

constantly, showing how the interest in the ORC technology is getting stronger, in order to further improve engine efficiency. In particular, heavy duty commercial vehicles seem to be still a promising application, due to the fact that hybridization of the powertrain, with consequent decrease of the thermal energy available for recovery systems, seems to be less effective than in the case of passenger cars, even though hybridization of trucks is under considerations, thus probably opening different scenarios for waste heat recovery systems.
Moreover, as evinced from the literature review, mostly on-highway applications are considered, not often evaluating the potential of the Rankine technology in the off-highway sector, which, even if challenging, could be a promising business case.
Anyway, as reported in section 5.3, most of the studies do not refer to economic considerations, which, at the end, are between the main driving forces regarding technology use and acceptance.
Moreover, most of the studies are also not considering the engine side as a possible part of a synergic optimization process, as it is proposed in this thesis work.
A summarized overview about some different vehicle ORC prototypes implementations available from literature has been reported in Tab. 15.

Company	Engine	Application	Engine Brake Power [kW]	Expander Type	Coupling / Energy Use	Working Fluid	Expander Isentropic Efficiency [%]	Max. Expander Power Output [kW]	Expander Speed [rpm]	References
Thermo-Electron	Mack 676 Diesel	Long-haul Truck	215	Turbo-expander	Mechanical	Fluorinol-50	n.a.	n.a.	37000	[225],[209],[226]
Cummins	Cummins ISX Diesel	Long-haul Truck	n.a.	Turbo-expander	Mechanical	R245fa	77	42	50000-80000	[259]
Honda	2.0 L Gasoline	Passenger Car-Hybrid	n.a.	Swash Plate Axial Piston Expander	Electrical	water-steam	n.a.	2.5	3000	[198],[230]
BMW	4 cyl. Gasoline	Passenger Car	n.a.	Vane Expander	Mechanical	water-steam / ethanol	n.a.	2	n.a.	[232]
Oak Ridge National Laboratory	1.9 L Gasoline	Passenger Car	66.7	Turbo-expander	Electrical	R245fa	n.a.	4	80000	[233]
BEHR	13 L Euro VI Diesel	Long-haul Truck	n.a.	Piston Expander	Mechanical / Electrical	water-steam / ethanol	n.a.	6% of engine break power	1400	[157],[210]
Bosch	12 L Diesel	Long-haul Trucks	n.a.	Piston / Turbo-expander	Mechanical / Electrical	water-steam / ethanol	70%**	12.3	150000**	[217],[235]
Eaton Corp.	13.5 L John Deere Diesel	Long-haul Truck	448	Roots Expander	n.a.	water-steam / ethanol	n.a.	n.a.	n.a.	[204]
Hino	n.a.	Long-haul Truck	n.a.	Turbo-expander	Electrical	HFE (not spec.)	n.a.	n.a.	n.a.	[236]
Ricardo plc - Volvo Trucks	12.9 L VOLVO D13 Diesel	Long-haul Truck	288	Piston Expander	Mechanical	ethanol-water mixture	70%	14***	1500	[260]
Ricardo plc - Wright Bus	2.4 L Ford Puma Diesel	City Bus – Diesel-Hybrid (REEV)	140	Scroll Expander	Electrical	R245fa	30%***	1.2	n.a.	[158]

Tab. 15. Summary of vehicle ORC implementations available in open literature

* In the tests, only mechanical power output considered
**Turbine expander data
***From Ricardo's tests

4.2.4 Waste Heat Recovery in Ships Using ORC – Literature Review

As already introduced in the previous sections, many articles have been published in literature about ORC as waste heat recovery systems for internal combustion engines, but only some works are available about systems on-board ships, since the application is still not well spread in the market but could show potential for future implementation.
Moreover, most on the works are related to heat recovery from four-stroke internal combustion engines for auxiliary power generation, while only a few publications and applications are related to two-stroke ship propulsion units.
The first ORC installed on-board ships has been used to recover heat from the engines of a car-truck carrier ship as reported by Öhman *et al.* [261], using an OPCON/Powerbox [262] unit, running with R236fa as working fluid (now banned due to environmental issues), engine cooling water as heat source and low temperature cooling water as heat sink, expecting a 4 - 6 % fuel saving.
Burel *et al.*[57] analysed the possibility to install an ORC in a tanker where Liquefied Natural Gas (LNG) is used as propulsion fuel, while Larsen *et al.* [263] proposed a generally applicable methodology based on natural selections principles, to optimise working fluid selection, boiler pressure and Rankine cycle process for marine engine heat recovery.
Again Larsen *et al.* [101] proposed a comparison of advanced heat recovery power cycles for large ships, modelling the systems in MATLAB environment, using a genetic algorithm for the optimisation procedure, and concluding that a Kalina cycle has no significant advantages compared to ORC and steam Rankine systems.
Bonafini *et al.* [264] proposed a study about recovering waste heat from the exhaust gas of marine dual-fuel engine with power output of 5.7 MW. The selected working fluid is toluene and a simple cycle architecture has been considered the most interesting in terms of increased power output benefits. A preliminary economic analysis has been performed.
Baldi *et al.* [265,266], in two different works, proposed the use of optimization techniques for Diesel engine-ORC waste heat recovery systems based on the analysis of typical ships operating profiles. The case studies use, as baseline engines, MaK 8M32C four-stroke Diesel engines with a power output of 3840 kW and some auxiliary units of about 683 kW. Fuel saving potential is considered for some typical vessels applications.
Song *et al.* [267] studied the waste heat recovery potential of an ORC to recover heat from the cooling water and the exhaust gas of a medium speed 996 kW marine Diesel engine produced by Hudong Machinery Co., Ltd. Economic evaluations as well as off-design conditions are considered. An optimized system using cyclopentane, cooling water as preheating source and exhaust gas as evaporating source for the working medium is proposed, obtaining only around 1.4 % lower power output compared to the separated bulkier systems.
Yun *et al.* [268] proposed a study about a dual loop ORC system with the aim of recovering waste heat in parallel from the exhaust gas of marine Diesel engines, with the highlighted benefit of being more versatile when operating at off design conditions. The conclusion is that the dual loop ORC has a power output which is between 3 and 15 % higher than a simple single loop system.
Yfantis *et al.* [269] proposed a thermodynamic model to study the first and second law of thermodynamics performance characteristics of a four-stroke marine Diesel engine equipped with a Regenerative Organic Rankine Cycle (RORC) to recover exhaust gas heat. Different engine operating loads are investigated, as well as R245fa, R245ca, isobutane and R123 as working fluids. A subcritical and saturated vapour regenerative cycle is found to have the best performance both from first and second law point of view.
Soffiato *et al.* [270] proposed an ORC system to recover jacket water heat, lubricating oil and CAC of the engines of a LNG carrier ship. In this case exhaust gas has been still used to generate steam. Simple, regenerative and two-stage evaporation architectures have been analysed obtaining a maximum net

power output of 820 kW achieved using the two-stage configuration and showing double the potential of the other architectures, but with higher structural complexity and reliability issues.
Sciubba *et al.* [271,272] analysed the comparison between a single loop and a dual loop waste heat recovery system for different power range marine engines (a yacht suitable non-supercharged 300 kW engine and a ship turbocharged 12.6 MW), using R245fa and R600 for the secondary recovery loop and water-steam for the primary loop, recovering engine exhaust gas and HT cooling water. Regeneration is also proposed to improve system efficiency. 8.1 % and 2.7 % improved electric power outputs have been achieved by simulation.
Michos *et al.* [273] analysed the engine fuel consumption effect of fitting an ORC boiler on the exhaust line of a turbocharged V12 engine used for marine auxiliary power generation. Different turbocharging strategies, such as Waste-Gate (WG) and Variable Turbine Geometry (VGT), have been investigated in order to counterbalance the detrimental effect of the increase exhaust line backpressure. Simple and recuperated ORC architectures have been investigated, through simulation, in order to assess the combined engine-ORC fuel economy improvement. A combined engine-ORC system using VGT turbine and acetone as ORC working fluid has been considered the most promising, leading to a possible improved fuel efficiency between 9.1 and 10.2 %, depending on the ORC boiler engine backpressure. The detailed results of the analysis have been proposed in this work is section 6.2.
Two-stroke ship propulsion units have also been considered in waste heat recovery studies, even if a lower number of works have been published.
Hountalas *et al.* [274] presented a theoretical study about a two-stroke 16.6 MW marine Diesel engine equipped with a Rankine cycle to evaluate the potential benefits for fuel consumption using a simulation model. Exhaust gas and SAC heat sources have been assessed, and a comparison performed between the use of steam and R245ca, obtaining 4.6 - 4.9 % and 5.0 - 5.2 % SFOC (Specific Fuel Oil Consumption) improvement. Pressure drop increase on the gas sides has been also considered.
Choi *et al.* [95] analysed the theoretical performance of a dual loop ORC with trilateral cycle applied to the exhaust gases of a two-stroke propulsion unit for a 6800 TEU (Twenty-foot Equivalent Unit) container ship, using water in the high pressure loop and R1234yf for the low pressure loop, obtaining a net power output of 2069.8 kW, with a maximum efficiency of 10.9 % and a 6 % fuel economy during actual operations.
Yang *et al.* [275] analysed the possibility of recovering jacket cooling heat of a large marine Diesel engine. Results show that R600a performs in the best way, followed by R1234ze, R1234yf, R245fa, R245ca and R1233zd, with very low evaporation temperature (58-68°C).
Wang *et al.* [276] simulated and analysed an ORC-desalination combined system driven by the SAC (Scavenging Air Cooler) heat of a two-stroke MAN 12S90ME-C9.2 ship engine, using R245fa as a working fluid for the ORC and obtaining up to almost 2800 kW and 245 t/day of desalinated water.
Grljusic *et al.* [277,278] proposed a supercritical ORC system operating with R123 or R245fa to recover scavenge air (SAC), jacket cooling water and exhaust gas of a two-stroke 18660 kW propulsion unit for a Suezmax oil tanker, concluding that the system can supply, at full load, enough electrical power for ship requirements, while at part load some additional fuel must be burned in order to reach the power target.
Calnetix [279] proposed an ORC system (Hydrocurrent^{TM} 125EJW ORC) to recover two-stroke jacket cooling water heat at 80-95°C, using sea water as cooling medium and a turbo-expander, obtaining around 120 kW net power output at design conditions, with a net thermal efficiency of 6.5 % and a declared turbine isentropic efficiency of 90 %. The working fluid used is R245fa.
Yang *et al.* [280] evaluated the economic performance of a Transcritical Rankine Cycle (TRC) using different low temperature suitable working fluids (R1234yf, R1234ze, R134a, R152a, R236fa and R290) obtaining the best results, and lowest levelized energy cost, with R236fa. Payback period, fuel oil savings and CO_2 emission reduction are also evaluated. Considered heat sources are exhaust gas, cylinder HT cooling jacket, scavenge air and lubrication oil.

Larsen *et al.* [178] also proposed a new concept of ORC system aiming at reducing the cost of the bottoming cycle installation using one of the cylinders of the large two-stroke engine for the expansion process. Numerical models have been used in order to assess the maximum power output of the proposed architecture, while 103 different fluids have been evaluated, obtaining the best results with R245fa and R1234ze(Z). The power output obtained from the ORC cylinder is declared to be similar to that obtainable from Diesel combustion, and an improvement of fuel economy of 8.3 % has been considered feasible.
Andreasen *et al.* [281] proposed a comparison between organic and steam Rankine cycle for waste heat recovery on large ships, obtaining, from a process simulation campaign, better results with steam as working fluid, at high load conditions, and better results with an organic medium at low load points. A turbine type expansion machine is considered in the study, and some preliminary design considerations have been proposed.
When considering ORC to recover waste heat from large low speed two-stroke marine Diesel engines, some peculiarities have to be considered compared to four-stroke engines. In particular, exhaust gas temperatures are much lower in two-stroke engines compared to four-stroke, even though mass flows are higher because of the large size of the engines, thus leading however to a high amount of heat that can be recovered with a bottoming cycle suitable for lower temperature heat sources, such an ORC.
Moreover, recently, some ORC manufacturers and shipping companies are considering using ORC technology in order to recover two-stroke waste heat. In particular, the challenge is recovering jacket coolant water of the engines, in the 80 - 90°C temperature range, which seems to become more attractive as a heat source, because basically freely available, easy to use and with less issues of flammability concerns in comparison to the gas exhaust line, in which a leakage from the ORC could become a problem. Recovering this heat could also have a positive effect on the sea water (or engine cooling water) pump parasitic power consumption, decreasing the cooling load of the engine.
Some ORC commercial-ready products for marine engine applications, and in particular two-stroke low speed engines, targeting mostly low temperature heat sources, have been reported in Tab. 16, even though the market in this sector can still be considered in a development phase.

Company	**Model**	**Heat Sources**	**Working Fluid**	**Power Output [kW_{el}]**	**Reference**
Opcon Marine	Powerbox™	coolant, SAC, exhaust gas	Ammonia	400 - 800	[21,262]
Calnetix	Hydrocurrent™ 125 EJW	coolant	R245fa	125	[279,282,283]
Climeon	Ocean™	Coolant, LT exhaust (after economizer)	n.a.	150 - 1000	[284]

Tab. 16. Commercial-ready ORC products examples for marine engine low-medium temperature waste heat recovery

5 Modelling and Analysis Approach

The main scope of the work reported in this thesis is to propose a new methodology for the design and analysis of combined engine-ORC systems in the preliminary phase of a project. For this purpose, the development and use of CAE (Computer Aided Engineering) software and process simulation techniques can be of vital importance in order to reduce development time and costs and to optimize the overall system.

In particular, in the common literature and commercial approach, ORC systems are developed considering the engine as just a system apart, supplying the thermodynamic boundary conditions to the waste heat recovery thermodynamic cycle. Indeed, most of the systems are currently only retrofitting existing engines, and room is still available for further improvement, in particular when proposing a complete combined optimization of the overall powertrain, considering all the sub-systems involved (e.g. engine, waste heat recovery, thermal management and power management). It is, indeed, for this purpose, that Second Law (exergy) analysis is becoming more popular, in close synergy with techno and thermo-economic and optimization techniques, as those considered in this work.

What is presented in this thesis is, indeed, the tentative of going beyond the common design methodology applied in the industry, showing the potential of the proposed combined approach, using CAE tools and process simulation techniques, to achieve a better comprehension of the overall system performance and operations. Moreover, the idea is also to assess different issues related to engine waste heat recovery systems analysis and development, particularly for marine and commercial vehicles applications, which are also the sectors of interest of the EU ECCO-MATE project, in the frame of which the proposed research activity has been carried out.

The first case study, reported in section 6.1, shows a common ORC analysis procedure, which considers the engine thermodynamic boundary conditions, for the most suitable heat sources and heat sinks, as already introduced in the previous literature review sections. The data have been obtained from engine dyno test campaigns carried out on a commercial vehicle four-stroke engine during Ricardo's project activities. The novelty, in this case, is the estimation of the performance of the proposed ORC systems also when considering vehicle thermal management issues, which are, as already introduced in section 4.2.2.2, not commonly considered in literature studies. Moreover, the off-highway agricultural tractor is an ORC application which is not commonly evaluated, while, at the same time, showing potential, in terms of system performance, mostly because of the high speed and high load, generally stable, engine operating profile.

The second case study, reported in section 6.2, assesses the thermodynamic performance of a marine MW size four-stroke power generator, recovering heat from the exhaust gas using an ORC system. In this case, the engine backpressure increase effect, due to the installation of the ORC evaporator on the tailpipe gas line, has been assessed, using Ricardo WAVE 1-D engine gas dynamic simulation software, while, at the same time, proposing different turbocharging strategies to counterbalance the observed loss in terms of engine performance. The combined turbocharging-ORC technological solutions have been also evaluated, showing the potential in fuel consumption reduction for this application.

The third case study, reported in section 6.3, aims to evaluate an innovative emission reduction strategy, using low pressure exhaust gas recirculation (LP EGR), while at the same time assessing the potential of ORC systems when recovering waste heat from a two-stroke, large bore, low speed marine propulsion engine, application which is not commonly proposed in literature studies. The Ricardo WAVE 1-D software has been used, also in this case, to calculate the thermodynamic performance of the engine when recirculating the exhaust gas to decrease pollutants emissions, and the boundary conditions have been obtained in order to run several ORC process simulations campaigns, assessing different layouts and working fluids, when considering engine operations under IMO Tier II or IMO Tier III emission levels. The impact of EGR on emissions has been assessed, in parallel during the ECCO-MATE project, in collaboration with the National Technical University of Athens (NTUA), by

means of a detailed 3D-CFD combustion analysis, performed on the same type of engine, and is not reported in this work, which focuses more on the waste heat recovery and thermodynamic analysis side. A common publication is expected as output of the collaboration.
The second and third case studies show how engine simulation tools can be used to assess the engine performance under different operational strategies, while at the same time supplying the right boundary conditions for the evaluation of the performance of the waste heat recovery system, saving time and expensive test campaigns. However, a more synergic approach should be considered, when evaluating the combined engine-ORC systems. For this reason, the last case study in section 6.4, aims to set the basics, and open the path, to a new methodology which can be helpful to understand the overall system and optimize its combined performance.
In particular, a four-stroke Diesel engine suitable for a medium- duty truck application has been used as baseline model, and fully equipped with sensors in Ricardo WAVE in order to extract the necessary thermodynamic parameters to calculate detailed First and Second Law analysis for every operating point which can be simulated. The innovative post-processing routines, developed in MATLAB, allows to assess the overall engine processes, thus properly understanding all energy and exergy streams in a detailed way, as well as giving insights on the efficiency of the different engine subsystems. Indeed, the calculation of every subsystem irreversibilities (or exergy destruction) allows to understand which processes are affecting more the engine performance, introducing system inefficiencies, wich are, inevitably, reflected into additional costs wasted.
To the author's knowledge, no commercial engine simulation software is programmed to perform such a detailed analysis.
The approach and modelling techniques applied in the four case studies have been explained in the details in the next sections, considering both engine and ORC systems' analysis approach, more detailed ORC components performance analysis and a description of the methodology proposed.

5.1 Engine Modelling

Except for the first case study, in which a steady-state engine test point has been used in order to obtain the boundary conditions for the ORC analysis, in the other case studies the Ricardo proprietary 1-D gas dynamic engine performance software Ricardo WAVE [11] has been used to assess the thermodynamic performance of the engine models evaluated.
From the dawn of the reciprocating combustion engines development, scientists, researchers and engineers tried to model the thermodynamic processes involved in engines operations, in order to better understand and develop the technology.
From the late 1800s ideal standard cycle models to the actual advanced 1-D and 3-D CFD simulations techniques, a lot of improvements have been achieved, and todays' commercial software, such as Ricardo WAVE and CFD techniques, are extensively utilized in every phase of the development of a combustion engine, allowing time and cost saving. A detailed overview of several aspects of engine simulation techniques is reported by Caton [10], reference which can be used by the reader to deepen the topic. Several benefits can be envisaged from engine simulations, such as:

- the potential to deeply understand the fundamentals of engine operations and to assess the complex interaction of the various thermodynamic and chemical processes, leading to engine performance and emissions results;
- the possibility of reducing experimental tests, which are usually very time and cost expensive. Testing campaigns cannot, however, be fully substituted by simulations. Both sides of the development must be carried out in parallel, using simulation as a guidance for further validation through adequate testing results;
- the possibility of assessing and obtaining some thermodynamic variables, which are otherwise difficult to study experimentally, such as in the case of entropy and enthalpy necessary for Second Law (exergy) calculations;
- the possibility to carry out extensive parametric studies and assessing new engine concepts in a preliminary phase of a development project;
- the opportunity to carry out optimization runs in order to assess several strategies to improve engine performance and emissions;
- the possibility to use thermodynamic simulations to develop control algorithms, taking profit of real-time capabilities (e.g. WAVE-RT). The engine models can be embedded in HiL (Hardware-in-the-Loop) or SiL (Software-in-the-Loop) architectures;

In this section, a short introduction about Ricardo WAVE has been proposed in order to describe the capabilities of the software. However, these types of commercial software are usually not developed to carry out Second Law analysis, based on exergy and entropy parameters, as well as they are usually not structured so to give an accurate idea of the energy and exergy balance of the overall engine. For these reasons, in this section, the methodology used to develop MATLAB-based routines for the complete, detailed, First (energy-based) and Second Law (exergy-based) analysis of the engine operations has been explained, with the scope of showing what could be the next step towards the implementation of more comprehensive software platform for the complete optimization of the overall powertrain.

5.1.1 Introduction to Ricardo WAVE

Ricardo WAVE is a 1-D CAE (Computer Aided Engineering) software developed by Ricardo [11]. It is widely used in the industry to assess the performance of theoretically any kind of internal combustion engine architecture, using the principles of gas dynamics.

It comprises a set of sub-models of typical engine components such as: engine block, engine cylinders, turbocharger compressor and turbine, injectors, valves, junctions and the ducts forming the engine piping and manifolds layout. A scheme of a typical WAVE model has been reported in Fig. 31, showing the different components and sub-models. Heat transfer, friction and combustion models are also implemented, while controlling strategies can be developed through the use the components available in a sub-library.

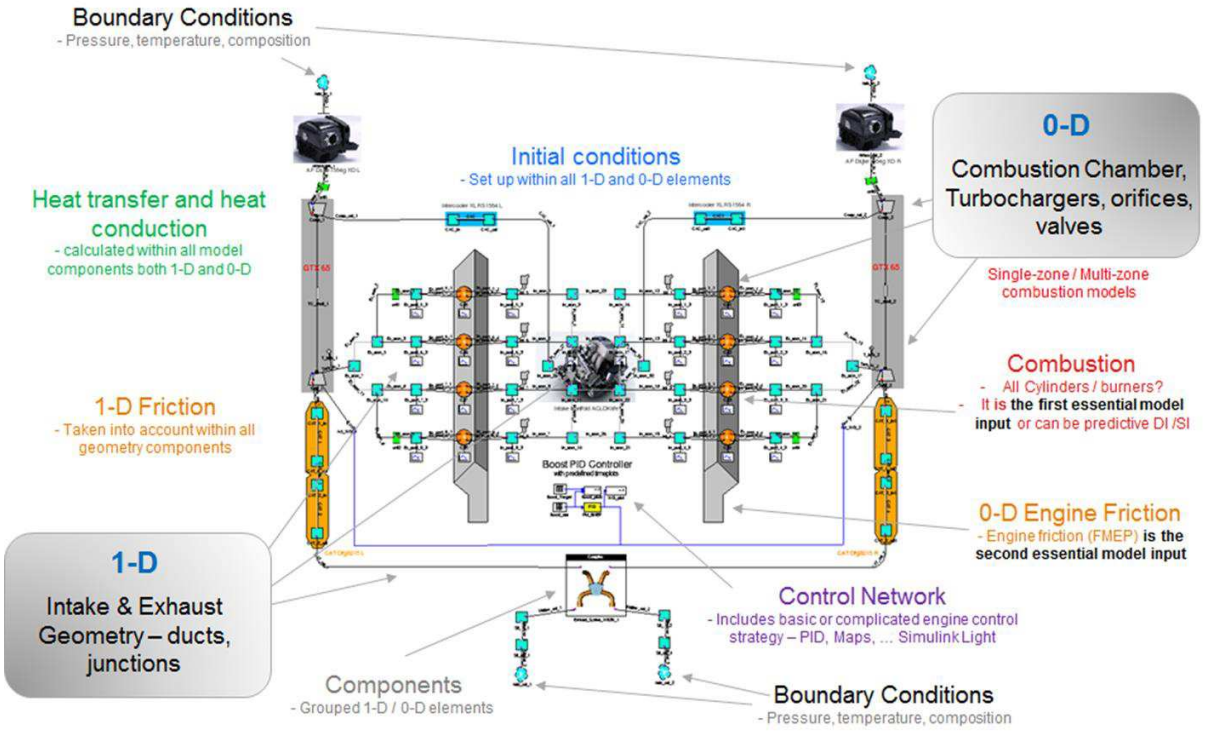

Fig. 31. A typical Ricardo WAVE engine model, with all main sub-systems and sub-models highlighted

As can be envisaged from the figure above, Ricardo WAVE, as also other competing commercial software, adopts a combined use of 0-D and 1-D modelling techniques. In particular, the combustion chamber is modelled as a 0-D reactor, in which the heat release analysis and the calculation of all combustion thermodynamic and chemical properties is carried out. While, the piping network is modelled using 1-D techniques with spatial and time discretization, assuming ideal gas properties and compressible fluid dynamics formulations (e.g. flow through the valves and orifices, calculation of pressure waves).
A short overview of the most important modelling techniques (sub-models) adopted in WAVE has been proposed in the following sections, because essential to understand the starting point of the following post-processing routines development. It is out of the scope of this thesis to supply a detailed description of how a thermodynamic engine performance software is developed. For more detailed information it is possible to refer to Caton [10] or Heywood [7], which provide more comprehensive and complete approaches.

5.1.1.1 Combustion Process

In 1-D engine performance commercial software, such as Ricardo WAVE, the First Law of Thermodynamics (mass, energy and momentum balances) is applied to an engine cylinder with volume

changes according to the crank-rod engine kinematics system. The First Law formulation is used to derive expressions for the time resolved (Crank-Angle-Degree, CAD) derivative of pressure, temperature and volume.
Generally, several models are available: single-zone, two-zone and multi-zone. In the first case, the formulations consider the cylinder as one region in which burned and unburned gases are assumed as a unique working fluid at same bulk temperature and pressure. In the second case, the cylinder is divided into burned and unburned zones, which share a common cylinder pressure but are considered separately. Multi-zone models are also available, considering more detailed description of the combustion region, always assuming a quasi-dimensional approach, in which there is not spatial context, but a sense of dimensionality can be perceived.
Two and multi-zone models are usually considered when emissions estimation must be carried out, because more precise in term of chemical reactions descriptions and species interactions. However, when more detailed emission studies must be carried out, a 3-D CFD approach (with detailed chemical kinetics) should be proposed, since capable of giving a more accurate description of the spatial and time distribution of the thermodynamic properties into the cylinder, which directly influence the emissions formation processes (e.g. NO_x formation is very dependent on the spatial distribution of temperature, with high-temperature regions producing more emissions). Coupled approaches with 1-D/3-D tools are nowadays possible.
One of the main parameters of a combustion analysis, as well as inputs for Ricardo WAVE simulations, is the mass fraction of fuel burned (x_{burned}), which is defined as:

$$x_{burned} = \frac{(m_{fuel})_{burned}}{(m_{fuel})_{total}} \quad (10)$$

With:

- $(m_{fuel})_{burned}$, mass of fuel burned [kg or g];
- $(m_{fuel})_{total}$, total mass of fuel injected [kg or g];

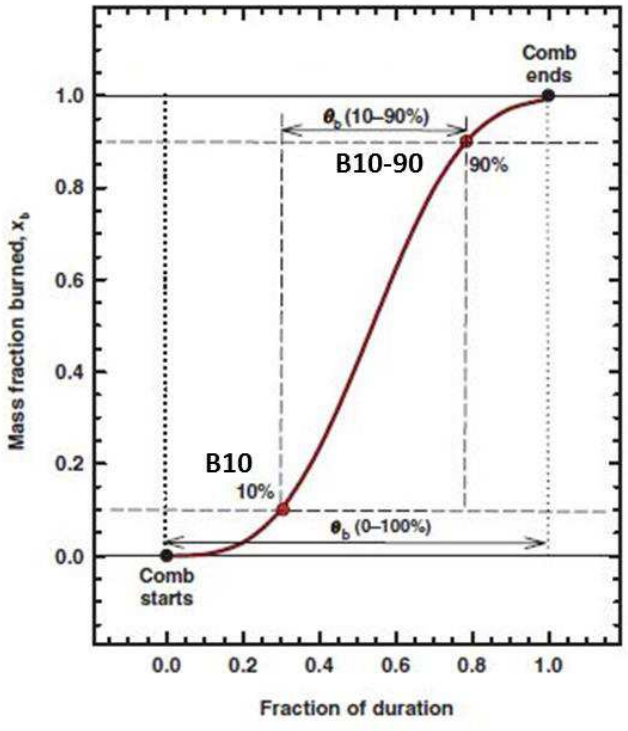

Fig. 32. Typical shape of the fuel mass fraction burned curve. Elaborated from Caton [10]

As can be observed from Fig. 32, some parameters can be used to obtain information about the combustion process development: the $\theta_b(0-100\%)$, which represents the overall combustion duration (CAD or radians), the $\theta_b(10-90\%)$, which represents the CAD interval in which the combustion happens between the 10 and the 90% of fuel mass fraction burned (in WAVE B10-90) and the B10, in WAVE representing the point (CAD or radians) in which 10% of the fuel has been burned. In WAVE, there are several possibilities to simulate the mass fraction burned: imposing directly a profile if available, using the so-called Wiebe function approach, or using the heat release analysis sub-model [7,10,11] from in-cylinder pressure data obtained from engine testing activities.

The Wiebe function has been used in the case study in section 6.4 to simulate a more detailed combustion profile, using the Multi-Wiebe WAVE model, which allows to over impose several different Wiebe curves to represent different phases of the engine combustion (e.g. pre-injection and the late combustion). The Multi-Wiebe model can also be used to simulate multi-fuel combustion (e.g. natural gas with diesel pilot injection). More detailed information about combustion can be obtained from a combined 3D-CFD analysis.

In particular, as already introduced and used in the case study in section 6.4, very often the Wiebe function approach [7,10] is used, to represent the mass fraction burned with the following function:

$$x_{burned} = 1 - exp\{-ay^{m+1}\} \quad (11)$$

with y a non-dimensional, crank-angle-based, time variable:

$$y = \frac{\theta - \theta_0}{\theta_b} \quad (12)$$

Where θ is the current crank-angle, θ_0 is the crank-angle of the Start of Combustion (SOC) and θ_b is the burn duration (crank-angle duration of combustion).

In equation (11) "a" and "m" are calibration parameters in order to match experimental data. In Fig. 32 they are set respectively to 5.0 and 2.0 as suggested by Heywood [7], and as it can be observed, the function is able to capture the main features of the combustion process, which begins slowly because of low initial cylinder temperature, and proceeds more rapidly due to the increase in temperature. In the end, when the reactants are finished, it becomes again slower. Generally, the total amount of burned fuel depends mostly from the parameter "a", which, with a value of 5.0, leads to a mass fraction burned of around 0.9933. In adequate Diesel combustion, generally unburned fuel is almost negligible, with an almost complete combustion to burned products.

Once the fuel mass burned fraction is available, the apparent heat release rate can be calculated as follows:

$$\frac{\delta Q}{\delta t} = \dot{x}_{burned} \cdot LHV \cdot m_{fuel,burned} \quad (13)$$

with:

- LHV, fuel Lower Heating Value [kJ/kg];
- $m_{fuel,burned}$, mass of fuel burned [kg];
- $\dot{x}_b$, time derivative of the fuel mass fraction burned [1/CAD], expressed as follows:

$$\dot{x}_{burned} = \frac{a(m+1)}{\theta_b} \cdot y^m \cdot exp\{-ay^{m+1}\} \quad (14)$$

However, as reported by Caton [10], the final net heat release rate must also account for the heat transfer ($\delta Q_{HT}/\delta\theta$), thus the final First Law expression for the closed system can be reported as follows:

$$\frac{\delta Q}{\delta\theta} = \frac{dU}{d\theta} + p_{cyl} \cdot \frac{dV}{d\theta} - \frac{\delta Q_{HT}}{\delta\theta} \quad (15)$$

with:

- $\frac{dU}{d\theta}$, internal energy variation with CAD;
- $p_{cyl}\frac{dV}{d\theta}$, term related to the work done on the piston, with V the cylinder volume, and p_{cyl} the cylinder pressure term;

As already introduced, for further deepening of the topic, the reader can refer to the relative literature already proposed.
Several different injectors can also be connected to the cylinders' components in WAVE in order to control the injection parameters (e.g. Air-Fuel-Ratio, injection ratio, mass flow rate of fuel, and so on).
The heat transfer-related term (with subscript "HT") is calculated using modelling techniques proposed in the next paragraph.

5.1.1.2 Cylinder Heat Transfer

The cylinder heat transfer processes are complex phenomena which are still an active area of engine research and development, and often assessed through the combined use of 3D-CFD techniques. Also in this case, additional information can be found in the consistent literature (e.g. Heywood [7]).
In 1-D commercial software, the cylinder heat transfer calculation is usually based on empirically derived correlations which are used to calculate the convective heat transfer coefficient in the engine. Conduction sub-models can also be used to calculate in-cylinder surface temperatures to improve the boundary conditions for the in-cylinder heat transfer models and assist in engine components design [11]. Additionally, some more advanced cylinder models are available in WAVE, providing a radiation model to predict the contribution of radiation to the overall heat transfer of the cylinder (which is however generally low compared to the convective one). However, these models have not been used or considered for the work reported in this thesis.
The convective heat transfer is the dominant mechanism of the cylinder heat transfer process, and it is mainly due to the motion of air and fuel mixture inside the cylinders and combustion chambers. It is also related to the shape of the combustion chamber and manifolds, as well as to the characteristics of the mixture. The general form of the convective heat transfer is:

$$\dot{Q} = h_c \cdot A(\theta) \cdot (T_{wall} - T) \quad (16)$$

with:

- h_c, instantaneous convective heat transfer coefficient [W/m^{2}K];
- $A(\theta)$, instantaneous surface area exposed to the cylinder gases (varying with cylinder volume and crank-rod kinematics) [m^2];
- T_{wall} and T, respectively the cylinder walls temperature and the gas bulk temperature [K];

The heat transfer coefficient is generally a function of the Reynolds (*Re*) and Nusselt (*Nu*) numbers, as reported by Caton [10], following the below-reported expression:

$$Nu = \frac{h_c \cdot L}{k_{gas}} = a \cdot Re^b = a \cdot \left(\frac{w_c L_c}{\nu}\right)^b \quad (17)$$

with:

- k_{gas}, thermal conductivity of the gas [W/mK];
- w_c and L_c, characteristic velocity and length [m/s and m];
- ν, kinematic viscosity [m^2/s];
- a and b, calibration parameters [-];

Generally, between the most used correlations is the one from Woschni [7,10,11], which is also extensively used in the models proposed in this work. The correlation has been reported below in the form used in Ricardo WAVE:

$$h_c = 0.0128 \cdot D^{-0.20} \cdot {p_{cyl}}^{0.80} \cdot T^{-0.53} w_c^{0.8} \cdot C_{enht} \quad (18)$$

With:

- D, cylinder bore [m];
- p_{cyl}, cylinder pressure [Pa];
- T, cylinder temperature [K];
- w_c, characteristic velocity [m/s];
- C_{enht}, user-entered heat transfer multiplier [-];

Other correlations for the calculations of the convective heat transfer coefficient are available in WAVE, such as Annand and Colburn. For additional information refer to Ricardo WAVE [11] and more complete references about the topic [7,10].

5.1.1.3 Friction

Engine friction energy dissipation is due to several processes and components, for example: gas pressure, piston rings, bearings, valvetrain, crankshaft and auxiliaries (e.g. pumps, fans, alternator). Often, in engine thermodynamic simulations, the friction term refers to the Friction Mean Effective Pressure (FMEP, bar), as already introduced in section 4.1. The FMEP is often calculated using the Chen-Flynn correlation [285], which is implemented in WAVE in a slightly modified form:

$$FMEP = ACF + \frac{1}{n_{cyl}} \cdot \sum_{i=1}^{ncyl} \left[BCF \cdot (p_{max})_i + CCF \cdot \left(S_{fact}\right)_i + QCF \cdot \left(S_{fact}\right)_i^2\right] \quad (19)$$

with:

$$S_{fact} = N \cdot \frac{S}{2} \quad (20)$$

As it can be observed, the formulas (19) and (20) are composed of different terms:

- ACF, constant term for accessory frictions $[bar]$;

- BCF, term which varies with peak cylinder pressure p_{max}, which is expressed in $[bar]$;
- CCF, term linearly dependent on mean piston velocity $[Pa\frac{min}{m}]$. This term considers the hydrodynamic friction in the cylinder;
- QCF, term which varies quadratically with the piston speed $[Pa\frac{min^2}{m^2}]$. This is referred to the windage losses (air resistance on the shaft) in the cylinder;
- N, engine rotational speed $[rpm]$;
- n_{cyl}, number of cylinders;
- S, engine stroke $[m]$;

Data for the FMEP can be also used as constants when available from testing.

5.1.1.4 Turbocharger

As already introduced in this thesis, the turbocharger is made mostly of a compressor and a turbine, which are interconnected with a shaft.
In WAVE, the turbo-junctions are generally simulated using steady-state maps, obtained from an interpolation of experimental data coming from tests. Some examples of compressor and turbine maps have been reported in Fig. 33 and Fig. 34, and are representative of the components simulated in the engine model considered in section 6.4.
VGT and WG turbochargers can be also simulated with appropriate settings in WAVE. Fixed efficiency approach can be also proposed in the preliminary stage of a project.

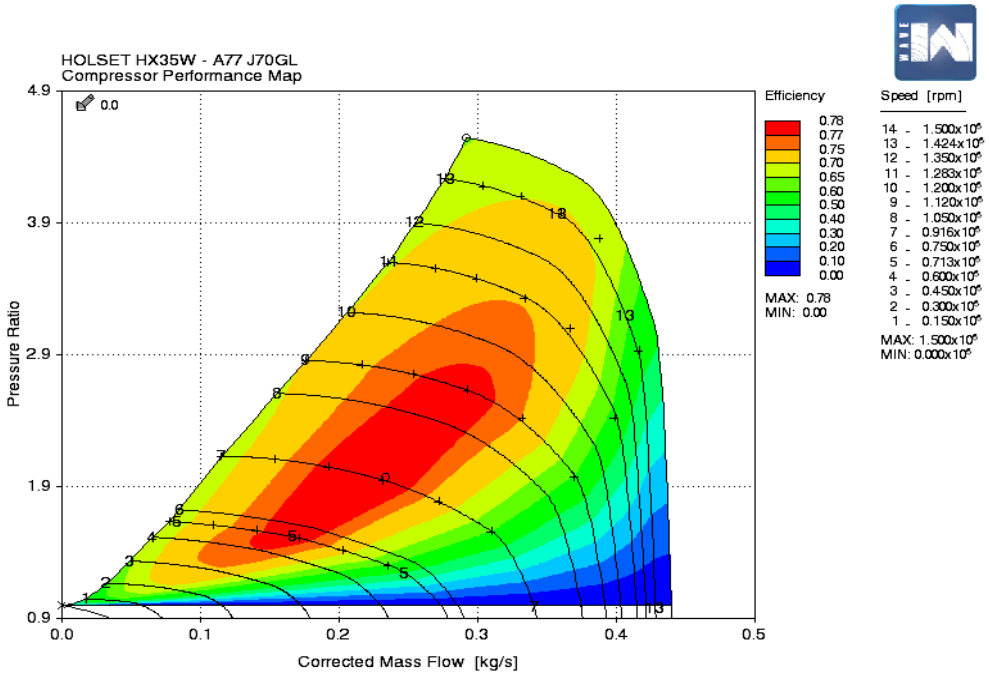

Fig. 33. Typical turbocharger compressor performance map

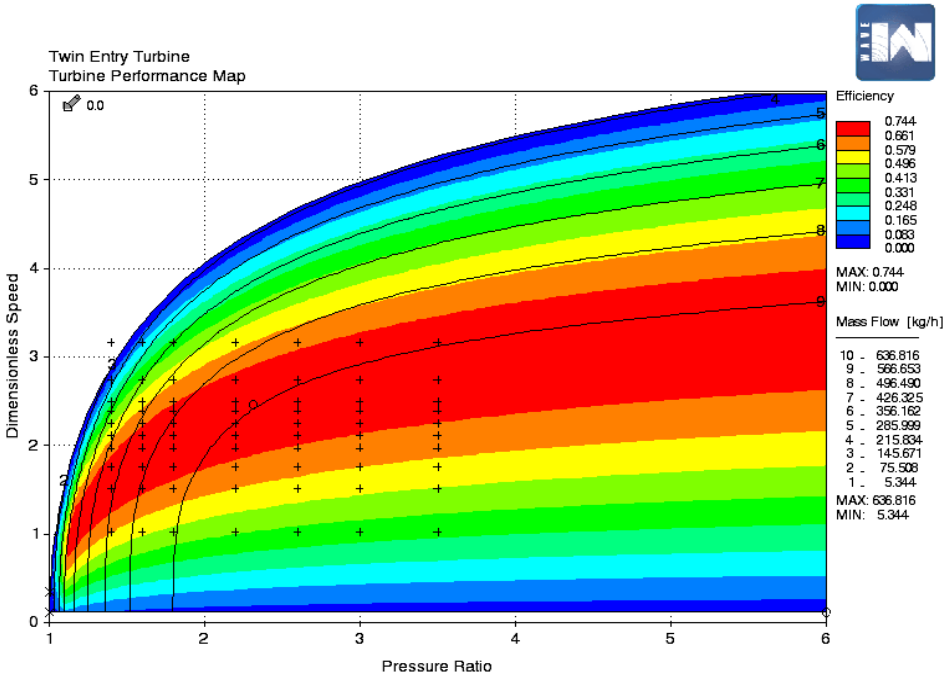

Fig. 34. Typical turbocharger turbine compressor performance map

5.1.1.5 Valves

In this paragraph, just a very short explanation about how cylinder valves are modelled in Ricardo WAVE, because generally common practice in these kinds of commercial software.
In the energy and mass balance equations for the cylinders also the mass flow rates entering and exiting the control volume must be considered. These are, indeed, dependent on the valves behaviour. Generally, the following assumptions are used: the flow is quasi-steady, one-dimensional, reversible, adiabatic and the flow discharge coefficients are assumed constants or as a function of the valve lift profile, which can be set as an input in WAVE. Some examples of valve lift profiles have been reported in the case study in section 6.3. The valves parameters, such as Inlet Valve Opening (IVO), Inlet Valve Closing (IVC), Exhaust Valve Opening (EVO) and Exhaust Valve Closing (EVC), can be controlled in WAVE in order to perform parametric studies and optimize the charge exchange processes. The shape and lift of the valves can also be modified in order to simulated different types of valves.
To account for the losses in a realistic engine, the assumptions reported above are generally corrected using an empirical discharge coefficient, C_D, which represents the ratio between the actual mass flow rate and ideal mass flow rate through the valve.
The mass flows through the valves are calculated using the expressions for a subsonic or sonic flow through an orifice. The overall formulations are extensively described in common internal combustion engine literature references [7–10].

5.1.1.6 Ducts, Space-Time Discretization and Species Considered in WAVE

In this paragraph, a short introduction about the discretization procedure, as well as the chemical species adopted in WAVE has been proposed.

This is indeed essential to properly understand how the engine post-processing routines, for First and Second Law analysis, have been developed.
Ducts and pipes in WAVE are discretized into a series of small volumes and governing equations are applied and solved using the finite difference method, while time differencing is based on the explicit Euler scheme.
Conduction and convection heat transfer models are available also for the ducts components, as well as heat exchangers (e.g. CAC or EGR coolers), or mufflers, receivers and silencers, can be modelled using appropriate ducts and junctions' networks.
In mathematics, the discretization process is used in order to represent a continuous function, such as a pressure wave for example, as a finite discrete counterpart, which can be solved using numerical methods. The purpose of the discretization is also to achieve a better resolution and accuracy of the changes in the calculated thermodynamic state of the fluid into the engine network. The smaller is the discretization of the ducts the higher is the accuracy with which, for example, the pressure waves are modelled. For the same reasons, an improved discretization will also allow to calculate more precise First and Second Law balances of the entire engine model. At the same time, however, a very small spatial discretization will also increase the overall computational time. For this reason, a trade-off must be found between the results accuracy required and the calculation time.
In a software like WAVE, directly related to the spatial discretization is also the time step discretization (*dt*, for an engine cycle CAD, Crank-Angle-Degree, resolution). In WAVE, the time step size is not constant, but rather it changes based on the so-called Courant condition, which is applied to determine the maximum allowed time step size, following the below-reported formula:

$$dt = CFL \cdot \frac{dx}{(c + |w|)} \qquad (21)$$

with:

- dt, time step discretization (CAD, Crank-Angle-Degree step-size);
- CFL, user-imposed multiplier to reduce the time-step and improve simulation stability (0.8 usually suggested);
- dx, spatial ducts discretization [mm];
- c, instantaneous speed of sound [m/s];
- w, instantaneous gas velocity [m/s];

The Courant condition does not allow a complete control on the simulation, and in particular on the choice of the time-step, which, at the same time, has an impact on the crank-angle discretization of the required thermodynamic variables. This aspect can influence also the results of the proposed energy and exergy balances, since in order to obtain the cycle average values for the thermodynamic properties, a trapezoidal numerical integration method has been implemented in MATLAB. In this case, a higher number of time-steps (CA steps) will lead to a more accurate calculation. In the case study proposed in section 6.4, a spatial discretization of $dx = 10\ mm$ has been chosen, thus leading to a quite accurate calculation of the balances, even though, the Courant condition and the different speed of the gas for every simulated case, which is directly related to the engine rotational speed, leads to different time-step discretization, which are however enough to provide accurate data.
Another important information to know when calculating the energy and exergy balances from the WAVE outputs is the position of the thermodynamic variables in the ducts network. Indeed, not all the variables are defined in the centre of the discretized control volume. The location of the main parameters and variables is represented in the scheme reported in Fig. 35.

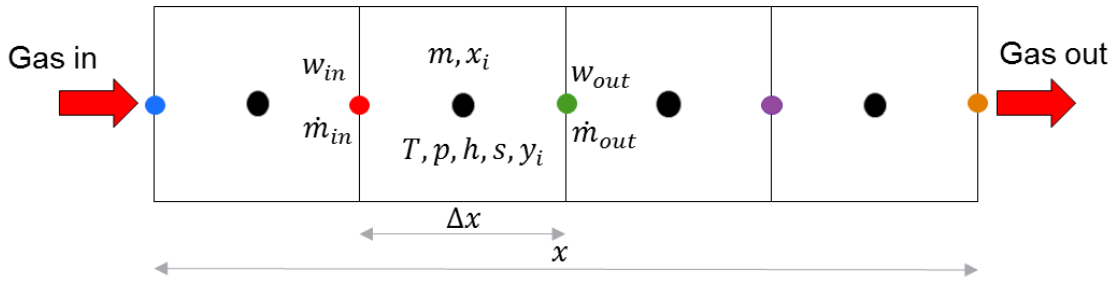

Fig. 35. Location of the main variables in the discretized control volumes

As it can be observed from the proposed scheme, temperature, pressure, enthalpy, entropy, mass and chemical species mass and molar fractions are located in the centre of the discretized sub-volume, while velocity and mass flow rate are defined in the boundaries. For this reason, mass and energy balance equations are solved in the volume centroid, while momentum equations are solved for each boundary between the volumes.
One of the most important features in a code like WAVE, is the calculation of the working fluids thermodynamic properties. Various detailed explanations have been proposed in references such as [7–10]. In particular, in WAVE the main thermodynamic properties are calculated through the use of the NASA-JANAF polynomials for ideal gas formulations, using tabulated data, which are interpolated during the simulations in order to increase the computational speed [286,287].
The chemical species considered in WAVE are 11: CO_2, H_2O, CO, H_2, O_2, N_2, OH, NO, O, H, N. These species are forming generally the burned and unburned mixture.
In WAVE, the overall mixture is made of 5 constituents, which are considered in the development of the post-processing routines when calculating several different properties from the output of the WAVE simulations: fresh air, unburned liquid fuel, unburned vapor fuel, burned fuel and burned air.

5.1.1.7 SDF Functions for WAVE-MATLAB Data Exchange

Most, but not all of the parameters required for the First and Second Law analysis are directly provided by the WAVE simulations in the text output file with extension *.wvd*. These parameters and outputs must be extracted from the file and sent to the MATLAB workspace to be used by the developed post-processing routines. For this reason, with the installation of WAVE, some functions have been provided for this purpose: *.sdf* functions. These functions allow to open the right .wvd file (*sdf_open*), to list the various parameters available (*sdf_list*) and to transfer them into the MATLAB workspace (*sdf_data*), following a code structure such as the one proposed below for the crank-angle-step discretized vector:

```
% Opening an SDF file (.wvd)for read
fp = sdf_open('6_0L_I6_Truck_Turbo_single_zone_v13.wvd');
% Listing datasets available from .wvd file - All variables datasets
names = sdf_list(fp);
% Crankangle rotational position [°CA]
CA = sdf_data(fp,'WAVE:CASE1_0:BASIC:CRANKANGLE:CLOCK');
```

The properties could be, theoretically, extracted also during the WAVE simulation, however this requires the use of Simulink-based models and calculations, increasing the computational time. This approach could be used, for example, for transient simulations, but it is not proposed in this thesis, leaving it for future developments with possible Real-Time capable tools.

5.1.1.8 Enthalpy and Entropy at Reference State Calculation

Both for the First and Second Law balances calculations, it is necessary to calculate the enthalpy (h_0) and entropy (s_0) at the reference state (T=298.15 K, p=1.01325 bar), assumed to be, basically, ambient standard (ISO) conditions.
The calculation of these thermodynamic parameters is not available in a commercial software as WAVE, thus external functions are needed in order to carry out the task, utilizing some thermodynamic outputs which can be extracted from WAVE using the proposed SDF functions.

Enthalpy at Reference State

In order to calculate both First and Second Law analysis, the value of the specific enthalpy at reference state, h_0 $[J/kg]$, needs to be calculated in the MATLAB developed post-processing routines, using the *PROP function*, supplied by Ricardo software, and called in MATLAB through a *.mex* file. The inputs required for this function are:

- *fuel file*: the file is provided in WAVE and is a text file containing tabulated properties for the fuel and the overall gas mixture, for different combustion settings;
- T_0: reference state temperature (298.15 K used);
- p_0: reference state pressure (101325 Pa = 1.01325 bar used);
- mass fractions, x_i, of the five mixtures constituents considered in WAVE with the following order:
  - *Fresh air (unburned)*
  - *Vaporized fuel (unburned)*
  - *Burned air*
  - *Burned fuel*
  - *Liquid fuel (unburned)*

The value of h_0 is calculated, from the data extracted from WAVE, for every crank-angle step, considering the variations of mass flow, temperature, pressure and species concentration during all the phases of the engine cycle.

Entropy at Reference State

The specific entropy at reference state, s_0 $[J/kg \cdot K]$, is an essential parameter for the Second Law analysis, which is not directly calculated in WAVE. For this reason, it has been necessary to develop a function in MATLAB (*Ideal_Gas_Prop_refstate_s0.m*) which is able to calculate the required values on a crank-angle step base, as done using the PROP function, following the ideal gas formulations. In this case the required inputs are:

- y_i: molar fractions of the 11 chemical species which are involved in the combustion process and in the WAVE simulations. The values can be extracted from WAVE, in every location of the developed model, through the use of sensors with the appropriate settings;
- $x_{liq,fuel}$: mass fraction of unburned liquid fuel. The value can be extracted from WAVE through a sensor;

- $x_{vap,fuel}$: mass fraction of unburned vaporized fuel. The value can also be extracted from WAVE through a sensor;
- R: the mixture specific gas constant $[J/mol \cdot K]$, provided by the PROP function;

As reported by Ferguson [8], the calculation of the specific entropy at the reference state, on molar base $[J/mol \cdot K]$, for an ideal gas mixture (i=11 species), is based on the following equation:

$$\bar{s}_{0,IG} = -\bar{R} \cdot ln\left(\frac{p_0}{p_0}\right) + \sum_{i=1}^{11} y_i \cdot \left[\bar{s}^0_{0,i} - \bar{R} \cdot ln(y_i)\right] = \sum_{i=1}^{11} y_i \cdot \left[\bar{s}^0_{0,i} - \bar{R} \cdot ln(y_i)\right] \quad (22)$$

with:

- $\bar{R}$: universal gas constant on molar base ($8.314\ J/mol \cdot K$);
- $\bar{s}^0_{0,i}$: specific entropy of formation on molar base $[J/mol \cdot K]$ of the eleven species at the reference conditions T_0 and p_0. The values, together with the values of the Molar Weight (MW_i) of the species, have been retrieved from the NIST Chemistry Webbook database [288];

On a mass base $s_{0,IG}$ $[J/kg \cdot K]$, the conversion can be done as follows, being the MW_{mix} the molar weight of the overall mixture composed of the 11 species:

$$s_{0,IG} = \left(\frac{\bar{s}_{0,IG}}{MW_{mix}}\right) \cdot 1000 \quad (23)$$

To calculate the specific entropy at reference state of the overall mixture, composed also of unburned quantities of vapour and liquid fuel, it has been necessary to obtain additional information about the specific entropy of these components at reference state, $s^0_{0,vap,fuel}$ and $s^0_{0,liq,fuel}$, extracted directly from the fuel file in WAVE.
Indeed, the equation for the calculation of the specific entropy at reference state of the overall mixture can be written as follows:

$$s_{0,mix} = \left(1 - x_{vap,fuel} - x_{liq,fuel}\right) \cdot s_{0,IG} + x_{vap,fuel} \cdot s_{0,vap,fuel} + \\ + x_{liq,fuel} \cdot s^0_{0,liq,fuel} \quad (24)$$

with:

- $s_{0,vap,fuel} = s^0_{0,vap,fuel} - \left[R_{vap,fuel} \cdot ln\left(y_{vap,fuel}\right)\right]$: the specific entropy at the reference state of the vapour fuel $[J/kg \cdot K]$. The term in the brackets considers also the partial pressure;
- $R_{vap,fuel} = \frac{\bar{R}}{MW_{fuel}}$: the specific gas constant of the fuel vapor on mass base $[J/kg \cdot K]$;
- $y_{vap,fuel}$: the molar fraction of the unburned vapor fuel, calculated from the mass fraction and the molar weight;

The proposed function, called in the post-processing routine developed in MATLAB for the Second Law analysis, allows to calculate the specific entropy term at the reference state (0) in all the model locations in which is needed, allowing at the same time to calculate the exergy terms, which are directly dependent to it and not considered in common commercial software.

5.1.2 First Law Analysis Applied to the Engine

As already introduced in the literature review part, the internal combustion engine is a device, based on a thermodynamic open cycle, which converts the chemical energy stored in the fuel chemical bonds into useful work for propulsion or electricity generation purposes. The process happens through the combustion of the fuel with aspirated ambient air as oxidizer.
However, not all the energy stored in the fuel is converted into brake power, as part of it is rejected into the oil and cooling systems, or to the surrounding environment through convection and radiation, or exhaust gas.
The First Law of Thermodynamics, proposed in this section, states that the total energy of an isolated system is constant and cannot be destroyed but just converted in different forms (work and heat). This important law allows, through the energy conservation principle application, to obtain a global overview of the transformations which happen in the system, giving an idea of the work and heat flows through the overall system architecture.
Advanced gas dynamic engine performance simulation software, such as Ricardo WAVE, allows to perform this kind of calculations for detailed and complicated engine architectures, being versatile and modular. However, these software packages are not programmed to supply the overall energy balance of the system, while this could, at the same time, give a better indication of the energy flows, thus being suitable, for example, for engine thermal management developments.
A "conventional" use of WAVE is proposed in the second and third case studies, in which the software has been used to perform simulations about different engine operating strategies and architectures, at the same time, supplying the boundary conditions for ORC thermodynamic analysis and optimization. A complete heat balance approach has been proposed in section 6.4.
Indeed, in order to explain how the overall energy balance of the engine has been calculated and post-processed, the engine model proposed in the fourth case study has been taken as a reference in the development of all the post-processing routine and methodology. However, the approach can be used for any kind of architecture which can be simulated in WAVE. Further embedding of a faster calculation of the parameters required, directly in WAVE, could also be envisaged for future developments of the software platform, thus avoiding to code post-processing routines, which take a sensible amount of time and efforts.

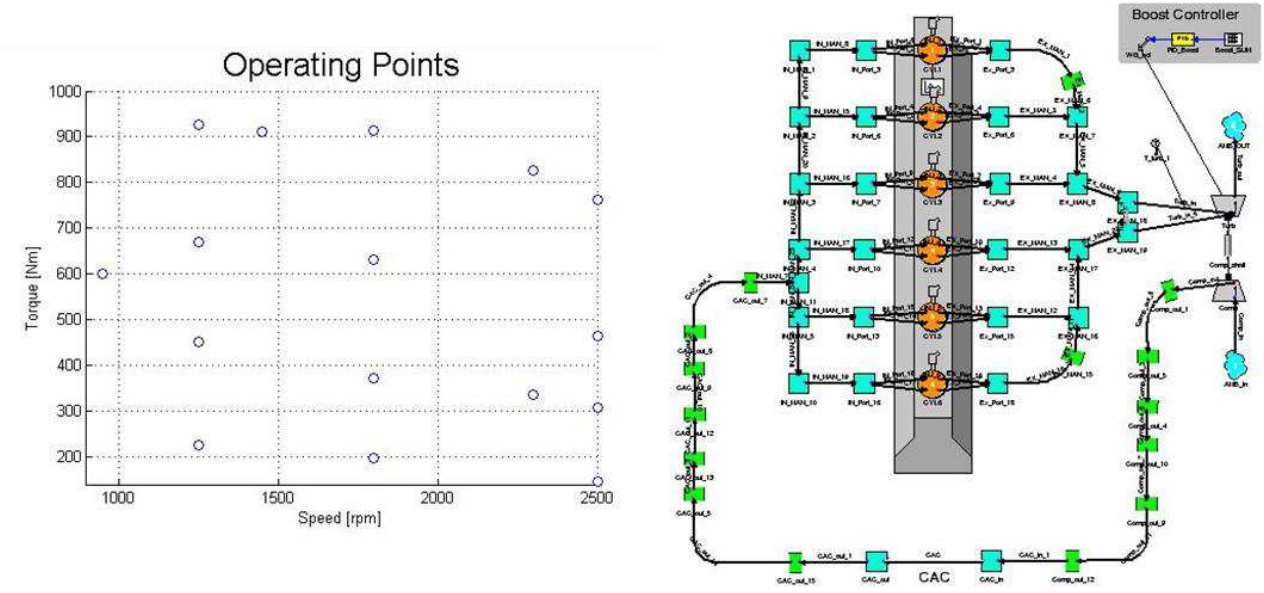

Fig. 36. WAVE engine model used for the post-processing routines development and operating points simulated

The engine model used for the development of the routines is a validated model of a six-cylinders, medium-duty, direct injection, charge-air-cooled (CAC), Diesel engine, with 5.9 L displacement, Waste-Gate turbocharger, and around 200 kW brake power at full load and full speed. Further information about the engine have been reported in section 6.4. The engine is typical for a medium-duty truck, as the application proposed in the fourth case study, or for small recreational marine applications. In this case, the engine has no EGR, but has been used because freely available between the WAVE models' examples and because validated not only for the full load curve, but also at 16 different part load points (Fig. 36) which are essential when considering applications, such vehicles, which are not expected to run the whole time at steady-state full load points. The absence of EGR excludes one of the sensible heat sources for waste heat recovery, however, the model has been considered enough to show how to apply the methodology. More advanced models, with EGR and multiple stage turbochargers can be proposed for future developments and analysis.
Compared to the Second Law analysis, described in section 5.1.3, for the First Law analysis a unique control volume (CV) has been adopted, which considers the overall engine and not the single sub-systems, from the intake air inlet to the exhaust gas outlet after the turbine. Then, all contributions have been separated, as for the Second Law analysis, in order to demonstrate the various heat and work streams contributions and compare the two laws balances, as reported in Fig. 37, which clarifies most of the parameters required to be sent from the WAVE simulations outputs to the MATLAB post-processing routines.

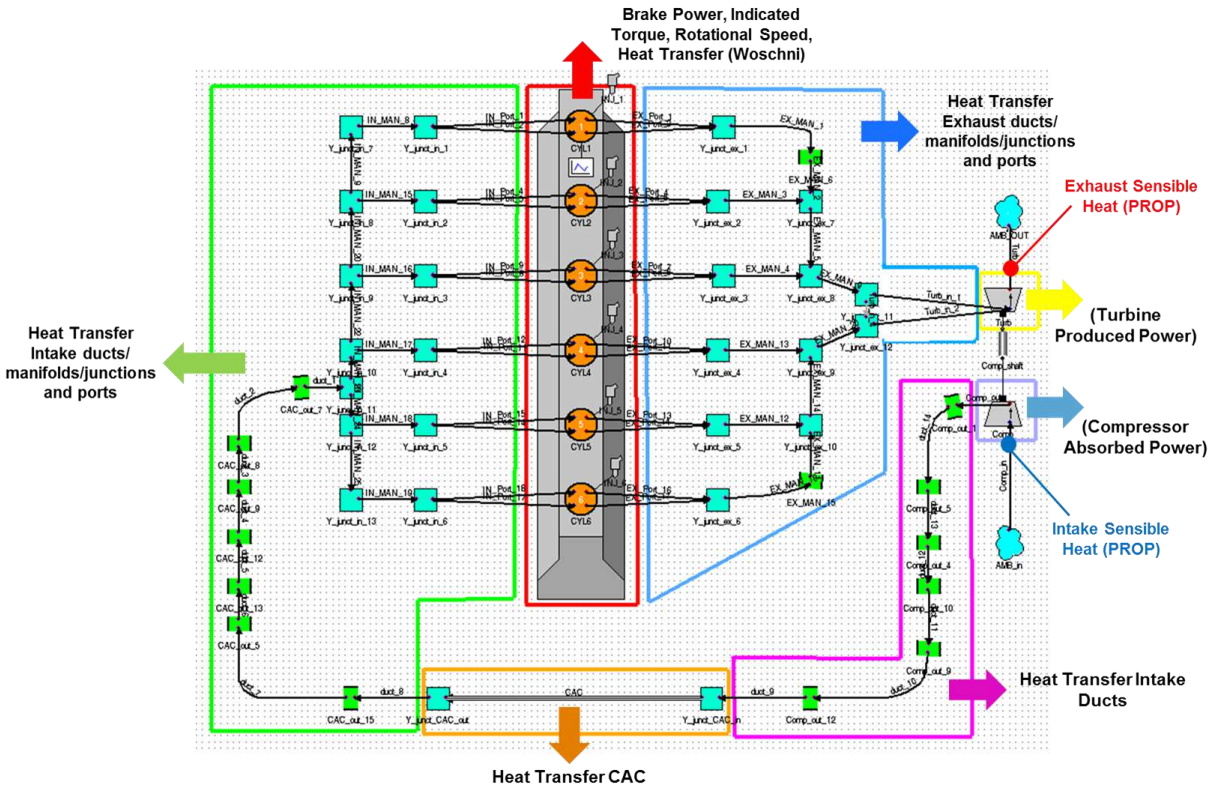

Fig. 37. WAVE model with all First Law contributions

WAVE does not consider any cooling circuit or oil circuit data (unless assumptions are considered, and a conduction model is used). For this reason, when calculating the First Law energy balance, only the gas side balance has been considered. When estimating heat rejection contributions to coolant and oil, adequate assumptions must be considered, possibly supported by experimental data, regarding the contributions of heat transfer and friction terms.

Following what reported by Ferguson [8], a power balance ([kW]) has been implemented considering the overall CV:

$$\dot{Q}_{CV} - \dot{W}_{CV} = \left(\frac{dU}{dt}\right) + \sum_{out} \dot{m}_{out} \cdot h_{out} - \sum_{out} \dot{m}_{in} \cdot h_{in} \qquad (25)$$

with:

- (dU/dt): the variation of internal energy. Integrating over and engine's cycle the term goes to zero
- $\dot{m}_{in}$, $\dot{m}_{out}$: mass flows of the streams entering and exiting the cv [kg/s];
- h_{in}, h_{out}: specific enthalpy of the streams [J/kg];
- $\dot{Q}_{CV}$: heat streams entering (or exiting) the CV [W], with their relative signs;
- $\dot{W}_{CV}$: work term [W];

Following what reported by Payri *et al.* [289], and considering that all parameters are referred to the ambient conditions as reference state (T=298.15 K, p=1.01325 bar), it has been necessary to consider the sensible specific enthalpy contributions (h_i^{sens}) at the inlet and outlet of the overall control volume. In this way, the overall energy balance, at steady state, considering all terms that can be obtained from WAVE calculations outputs, has become:

$$\begin{aligned} \dot{m}_{fuel,inj} \cdot LHV(298.15\ K) + \dot{m}_{fuel,inj} \cdot h_{fuel,sens} + \dot{m}_{air} \cdot h_{air}^{sens} = \\ = \dot{W}_{brake} + \dot{W}_{frict} + \dot{Q}_{HT} + \dot{m}_{exh} \cdot h_{exh}^{sens} + \dot{H}_{exh,ic} + \dot{\varepsilon} \end{aligned} \qquad (26)$$

All parameters reported in the above formula have been treated as cycle average values, integrating, over an entire engine cycle (720°CA for a four-stroke engine), the crank-angle resolved parameters obtained from WAVE's output, through the SDF functions. The parameters used in the formula are:

- $\dot{m}_{fuel,inj}$: fuel mass flow injected per engine cycle [kg/s];
- $LHV(298.15\ K)$: Lower Heating Value of the fuel at reference temperature [J/kg]. In the proposed case, the fuel is a Diesel blend with chemical formula $C_{15}H_{25.5}$ and LHV 42800 [kJ/kg];
- $h_{fuel,sens}$: sensible specific enthalpy of the fuel [J/kg]. The term $\dot{m}_{fuel,inj} \cdot h_{fuel,sens}$ is used in case the fuel is injected at a temperature higher then reference ambient temperature. This term is, however, almost negligible in comparison to the other terms and can be often be neglected, as done in this work, in which the fuel is injected at reference temperature;
- $\dot{m}_{air}$: mass flow of aspirated intake air [kg/s];
- $h_{air}^{sens} = h_{air}(T_{air}) - h_{air}^{0}(298.15\ K)$: sensible specific enthalpy of the incoming intake air [J/kg]. The term $h_{air}(T_{air})$ is the absolute enthalpy of the air mixture and is provided by WAVE's outputs, while $h_{air}^{0}(298.15\ K)$ is the specific enthalpy of the air mixture at the reference temperature (298.15 K), and it is calculated using the already described PROP function;
- $\dot{W}_{brake}$: engine brake power [W]. This value is directly provided from WAVE simulations and imported in MATLAB through the SDF functions;
- $\dot{W}_{frict}$: power losses due to friction [W]. In the MATLAB post-processing routine this contribution is calculated as the difference between the indicated ($\dot{W}_{ind}$, [W]) and brake power. The indicated power is calculated from the indicated torque, T_{ind} [Nm], and the rotational speed, N [rpm], through the following formula:

$$\dot{W}_{ind} = \left(\frac{2 \cdot \pi \cdot N}{60}\right) \cdot T_{ind} \quad (27)$$

- $\dot{Q}_{HT}$: total amount of heat transfer contributions [W]. This term is obtained through the sum of various terms obtained for ever component in the WAVE model. In particular:
  - $\dot{Q}_{ports}$: heat losses in the intake and exhaust ports next to the cylinders [W];
  - $\dot{Q}_{junctions}$: heat losses in the junctions between the pipes [W];
  - $\dot{Q}_{manifolds}$: heat losses in the intake and exhaust manifolds [W];
  - $\dot{Q}_{CAC}$: heat transfer in the heat exchanger representing the Charge Air Cooler (CAC) [W];
  - $\dot{Q}_{pipes}$: heat losses in the remaining pipes [W];
  - $\dot{Q}_{cyl,i}$: heat transfer from the i-cylinder component [W]. This term is calculated through the Woschni model. The term can be divided into three main contributions: the heat directed to the liner ($\dot{Q}_{liner,i}$), the heat directed to the piston ($\dot{Q}_{piston,i}$) and the heat directed to the cylinder head ($\dot{Q}_{head,i}$). Generally, the liner and head contributions can be representative, in first approximation, of the heat transmitted to the cooling jacket and the cooling circuit, while the piston contribution to the oil circuit. An approach based on experimental data, dividing the contribution percentages between the two circuits can be also used when enough data are available;
- $\dot{m}_{exh}$: mass flow of exhaust gas (after the turbine) [kg/s];
- $h_{exh}^{sens} = h_{exh}(T_{exh}) - h_{exh}^{0}(298.15\ K)$: as for the intake air contribution, this term is the sensible specific enthalpy of the exhaust gas [J/kg]. The term $h_{exh}(T_{exh})$ is the absolute enthalpy of the exhaust gas mixture and is provided by WAVE's outputs, while $h_{exh}^{0}(298.15\ K)$ is the specific enthalpy of the exhaust gas mixture at the reference temperature (298.15 K), and it is calculated using the already described PROP function;
- $\dot{H}_{exh,ic}$: is the thermal power lost due to unburned fuel (incomplete combustion, *ic*) [W]. Considering the lean burning combustion of Diesel engine such as those reported in this work (with excess air), this term is very small and could be often be neglected, unless incomplete combustion is expected;
- $\dot{\varepsilon}$: this term represents an error due to numerical approximations and the cycle integration procedure with the trapezoidal rule. For all the heat balances calculated for the proposed engine model, an error lower than approximately 0.1% has been obtained, closing the balance always to a value very next to 100%, at the cost of slower simulations due to the very small piping numerical discretization.

The heat losses associated to the turbocharger components (turbine, compressor and shaft) are not considered, because the components are assumed, in WAVE, to be adiabatic.
Cylinders blow-by losses are also not considered in this work. When using an IRIS cylinder, these terms can be considered, even though generally very small in absolute values compared to the other balance contributions.
The results of the First Law analysis for the proposed engine model at the simulated operating points have been reported in section 6.4. A single-zone combustion model has been used in the simulations, using a Multi-Wiebe approach.
Sweeps and parametric analysis of all the main quantities reported in the balance (e.g. heat transfer, brake power, exhaust gas thermal power, friction) can be carried out with the proposed post-processing routines, thus allowing to quickly have an idea of what is happening when changing important operational parameters, such as equivalence ratio (AFR), rotational speed, Start of Injection (SOI). For every operating point, it is then straight forward to obtain the overall complete heat balance.

An example of engine rotational speed sweep analysis has been reported in Fig. 38, for a one-cylinder engine example, operating at Air-Fuel-Ratio of 20.9 (equivalence ratio, φ, of 0.68), with Start of Injection (SOI) of -11 CAD (Crank-Angle-Degrees) BTDC (Before Top Dead Centre). The heat balance small chart is reported just to give and idea of the outputs which can be obtained for every parametric point.

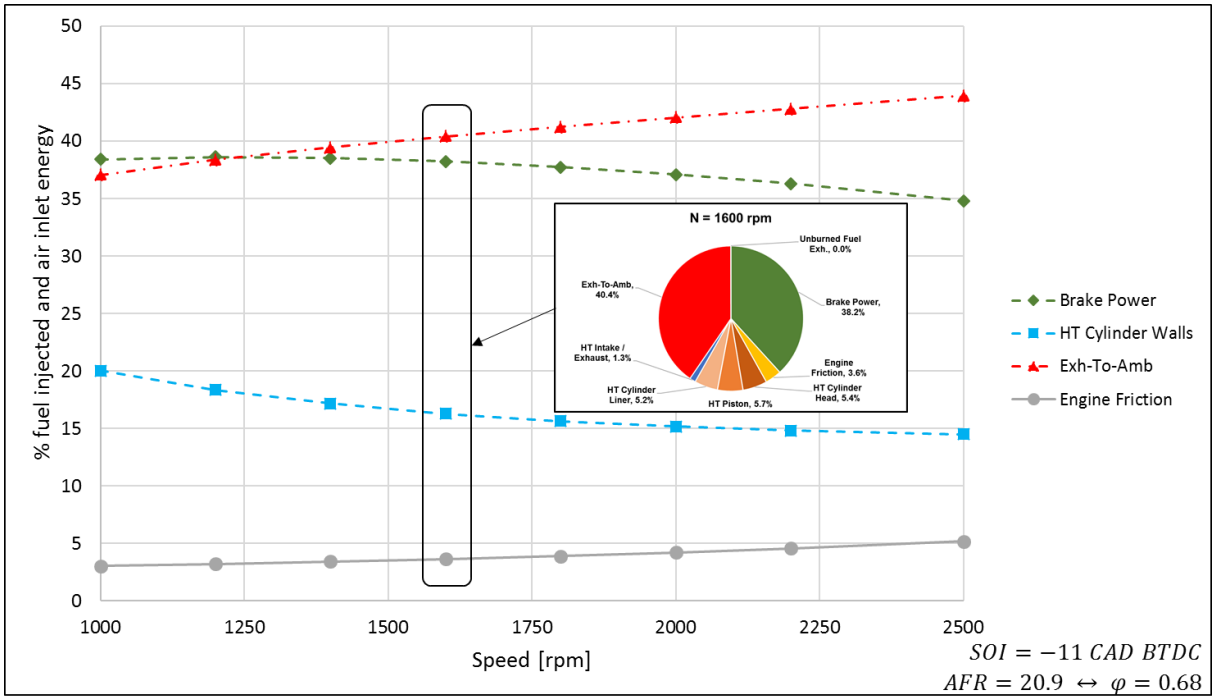

Fig. 38. Example of First Law parametric sweep analysis (rotational speed [rpm])

In this case, for example, an increase in engine rotational speed causes an increase in mechanical friction, as can be evinced also from the Chen-Flynn correlation reported in section 5.1.1.3. The combustion becomes also less efficient, since there is less time for a proper combustion, thus cylinder pressure becomes also lower, with consequent decrease in brake power output achieved. The lower combustion efficiency leads also to a higher amount of thermal power lost in the exhaust gases (*Exh-to-Amb* term). The cylinder heat transfer term (*HT Cylinder Walls*) tends also to decrease, mostly due to two main consequences of the increased rotational speed. First of all, the cylinder heat transfer increases due to the more intense motion of the gas mixture in the cylinder (gas velocity), but, at the same time, the duration of the transfer process is shorter. This second effect is predominant, thus leading to an overall decrease of heat transfer to the cylinder walls with increased rotational speed.
These results are in agreement with what reported, for a similar Diesel engine, by Rakopoulos *et al.* [290,291], who proposed an engine analysis using a code developed for non-commercial purposes.
Additional results for complete First Law energy balances have been reported in the case study in section 6.4.

5.1.3 Second Law Analysis Applied to the Engine

The First Law of Thermodynamics states the equivalence between work and heat exchanged by a system, clarifying that energy can be transferred and converted by a form to another, but never destroyed.
However, heat cannot be converted completely and continuously into work (Carnot). That is why the thermal efficiency of a closed heat engine cannot even approach 1 (100%). This is because of the so-called irreversibilities in the processes. However, as reported by Caton [10] and other scientists, the internal combustion engine is not an heat engine, and is not theoretically limited by the Carnot efficiency. Even though this limitation does not exist, it is still not possible to approach 100% efficiency due to the inefficient processes intrinsic to engine operations.
It is in order to investigate these inefficient processes, which a Second Law of Thermodynamics analysis becomes useful, and essential, in order to open the path to the development of more efficient engines and combined powertrains, and to push the limits of the system efficiency.
The main irreversibilities and losses in an internal combustion engine are:

- Friction and mechanical;
- Fluid flow losses (pipes);
- Throttling and valves;
- Pumping work;
- Combustion (generally 20-25% of total irreversibilities at full load);
- Heat transfer (coolant, oil, CAC, EGR);
- Heat losses to the environment;
- Exhaust gas heat lost to the environment;
- Expansion and compression losses (turbocharger);

It is in order to study and optimize all these processes, that a Second Law analysis becomes important, especially when coupling the engine system with a possible waste heat recovery system, such an ORC. The concepts of Second Law analysis are not well understood and spread in the industrial sector, and this is also represented by the fact that, for example, commercial engine performance simulation software, such as Ricardo WAVE, which are widely utilized tools in all engine development phases, are not programmed to perform a Second Law analysis, but are rather used in the way proposed in the second and third case studies in this work. Indeed, these software packages consider energy fluxes with the same potential of producing work. However, this is not true, because of the already cited irreversibilities.
Many scientists, in particular in the academic sector, proposed publications and research activities related to engine Second Law analysis. A quite complete overview is proposed by Rakopoulos *et al.* [290] and Caton [10], who cite different research groups and authors. However, generally all the proposed research is mostly focused on the combustion side of the engine operations, while not considering the overall engine processes and sub-system (but in some rare cases) and possible more advanced engine-waste heat recovery powertrains. Moreover, to the author's literature knowledge, only Edwards *et al.* [292], tried to applied the proposed researches using industry standard engine performance simulation software, such as Ricardo WAVE, demonstrating a methodology similar to the one proposed in this work, but without considering the waste heat recovery side and also an economic analysis of the concepts.
Directly connected to the Second Law analysis is the concept of exergy (or availability, A) which has been introduced in the next section.

5.1.3.1 The Concept of Exergy (Availability)

Exergy, or often called availability, A [J], is a thermodynamic extensive property, with a value greater or equal to zero, depending not only on the state of the system, but also on an arbitrary reference state. The exergy represents the maximum useful work that can be extracted from a process if all the transformations would occur in a reversible way (without irreversibilities) towards equilibrium.
Exergy is also directly correlated (and calculated) with entropy, which is commonly understood as a measure of disorder and associated to the irreversibilities. For this reason, exergy can be considered as the "quality of energy".
Unlike energy, exergy can be destroyed during the thermodynamic processes, because of the irreversibilities (exergy destruction terms, $\dot{I}$ [W]). It can also be transferred from a system to another (e.g. from the engine to the waste heat recovery system or the cooling and oil circuits) or to the surroundings (in this case being a loss). For these reasons, between the goals of a Second Law analysis is the reduction of irreversibilities and exergy losses, identifying the main sources and proposing improvements.
There is also a link between exergy (quality of the energy) and economic value (costs) as it has been introduced in section 5.3 and in the case study in section 6.4.
Exergy is calculated referring to a reference state, which is essentially a system which stays always at the same conditions even if energy and mass flow towards it. The main characteristics of the reference state are generally to be of bigger dimensions compared to the system studied, to have a homogeneous distribution of temperature and pressure, and to exchange energy without varying the intensive properties, so that its temperature and pressure are always the same. When a system is at thermo-mechanical (temperature and pressure) equilibrium with the environment, it is said to be in a restricted dead state, while when there is also chemical equilibrium it is said to be in a true dead state.
For the proposed work, and considering, as reported by Rakopoulos *et al.* [290], that it is very difficult to extract work from the difference in partial pressures of the chemical species (complicated devices or membranes would be needed), a restricted dead state has been considered, with values of $T_0 = 298.15\ K$ and $p_0 = 1.01325\ bar$, representing ISO ambient conditions, as often done in literature.
According to Rakopoulos *et al*. [290], the total availability can be divided into two terms: the thermo-mechanical availability and the chemical availability, which are considered separately, and depend on the chosen restricted or true dead state.
For the thermo-mechanical availability [J], the following formulation, for a closed system without flow, can be used:

$$\begin{aligned} A^{tm} &= (E - U_0) + p_0 \cdot (V - V_0) - T_0 \cdot (S - S_0) \\ &= (H - H_0) - T_0 \cdot (S - S_0) + E_{kin} + E_{pot} \end{aligned} \quad (28)$$

with:

$$E = E_{kin} + E_{pot} + U \quad (29)$$

and:

- E_{kin}: kinetic energy [J], often neglected;
- E_{pot}: potential energy [J], often neglected;
- U, U_0: internal energy and internal energy at reference state [J];
- p_0, T_0: pressure [Pa] and temperature [K] at reference state;
- V, V_0: actual and reference state volume of the system considered [m^3];
- S, S_0: entropy and reference state entropy [J/K];

- H, H_0: enthalpy and reference state enthalpy [J];

As already introduced, the chemical exergy has not been considered in this work, because, as stated by Rakopoulos *et al.* [290] and Flynn *et al.* [293], considering typical lean operations of Diesel engines, there are practically no partial products in the exhaust gas that could contain substantial chemical exergy (e.g. can be further oxidized or reduced). Furthermore, chemical availability is usually useless due to difficulty of recovery, at least in mobile applications (e.g. complicated membranes to exploit the potential difference in concentrations between the various species should be developed).

5.1.3.2 Thermodynamic Formulation of the Second Law

Once the thermodynamic properties at the actual state and at the reference dead state are extracted or evaluated, in every point of the model where it is required, it is possible to calculate the availability in the various engine sub-systems. The general formulation of the availability balance for an open system (control volume, CV), with exchange of mass with the surroundings, can be written as follows [290]:

$$\frac{dA_{cv}}{dt} = \int \left(1 - \frac{T_0}{T_j}\right) \cdot \dot{Q}_j - \left(\dot{W}_{cv} - p_0 \cdot \frac{dV_{cv}}{dt}\right) + \sum_{in} \dot{m}_{in} \cdot b_{in} - \sum_{out} \dot{m}_{out} \cdot b_{out} - \dot{I}_{cv} \qquad (30)$$

with:

- dA_{cv}/dt: time rate of change of the availability of the CV contents [kW];
- $\int \left(1 - \frac{T_0}{T_j}\right) \cdot \dot{Q}_j$: availability term related to the heat transfer rate $\dot{Q}_j$ [kW]. T_j [K] is the temperature at the boundary of the system (often assumed the working fluid bulk temperature) at which the heat is transferred. The formulation clearly shows how the "exergetic value" of the stream increases with increasing temperature;
- $\dot{W}_{cv} - p_0 \cdot \frac{dV_{cv}}{dt}$: availability associated with mechanical work transfer [kW]. $\dot{W}_{cv}$ is the work transferred [kW]. $\frac{dV_{cv}}{dt}$ is time-based variation of the CV volume (e.g. the cylinder's volume in case of the cylinder CV, [m^3/s]);
- $\sum_{in} \dot{m}_{in} \cdot b_{in}$: flow availability associated with the inflow mass flow $\dot{m}_{in}$ [kW];
- $\sum_{out} \dot{m}_{out} \cdot b_{out}$: flow availability associated with the outflow mass flow $\dot{m}_{out}$ [kW];
- $\dot{I}_{cv}$: rate of irreversibilities production for the considered CV;
- b_{in}, b_{out}: flow specific availability terms [J/kg] at inlet and outlet of the CV. Considering only the thermo-mechanical availability, the terms can be expressed as follows:

$$b = (h - h_0) - T_0 \cdot (s - s_0) \qquad (31)$$

With:

- h: specific enthalpy [J/kg] of the working fluid mixture at temperature T;
- s: specific entropy [J/kgK] of the working fluid mixture at temperature T and pressure p;
- h_0: specific enthalpy [J/kg] of the working fluid mixture with the same chemical composition but brought to the reference state (T_0);
- s_0: specific entropy [J/kgK] of the working fluid mixture with the same chemical composition but brought to the reference state (T_0, p_0).

Generally, all the terms in equation (30) are known from the thermodynamic calculations, while the only unknown is the irreversibilities production term, $\dot{I}_{cv}$, which can be calculated from the availability balance for every CV considered. This is, indeed, one of the most important outputs of a Second Law analysis, which cannot be evaluated just with a traditional, First Law-based, simulation approach.

5.1.3.3 Application of the Second Law Analysis to the Considered Engine Model

In this section, a detailed description of the application of the Second Law analysis, as proposed in equation (30), has been reported, with the scope of showing a methodology which is applied to the same engine model used for the First Law analysis in section 5.1.2 (and as a case study in section 6.4), but which can be applied to any engine model which can be simulated in WAVE, once the procedure is automatized and embedded directly in WAVE or another co-simulation canvas.
The aim of the analysis is to calculate the irreversibilities production rate of every engine sub-system (CV), as well as all the exergy streams of the engine, in order to have a full overview of the thermodynamic processes, from both a First and Second Law point of view. The successive steps are then the implementation of bottoming waste heat recovery cycles models and a techno and thermo-economic exergy-based approach, in order to open the way to a more synergic way of designing combined systems.
As already reported for the First Law case, for the Second Law, the availability balance has been applied for all the control volumes reported in Fig. 39: cylinders/engine block, intake, exhaust, Charge Air Cooler (CAC), inlet ducts, compressor and turbine.

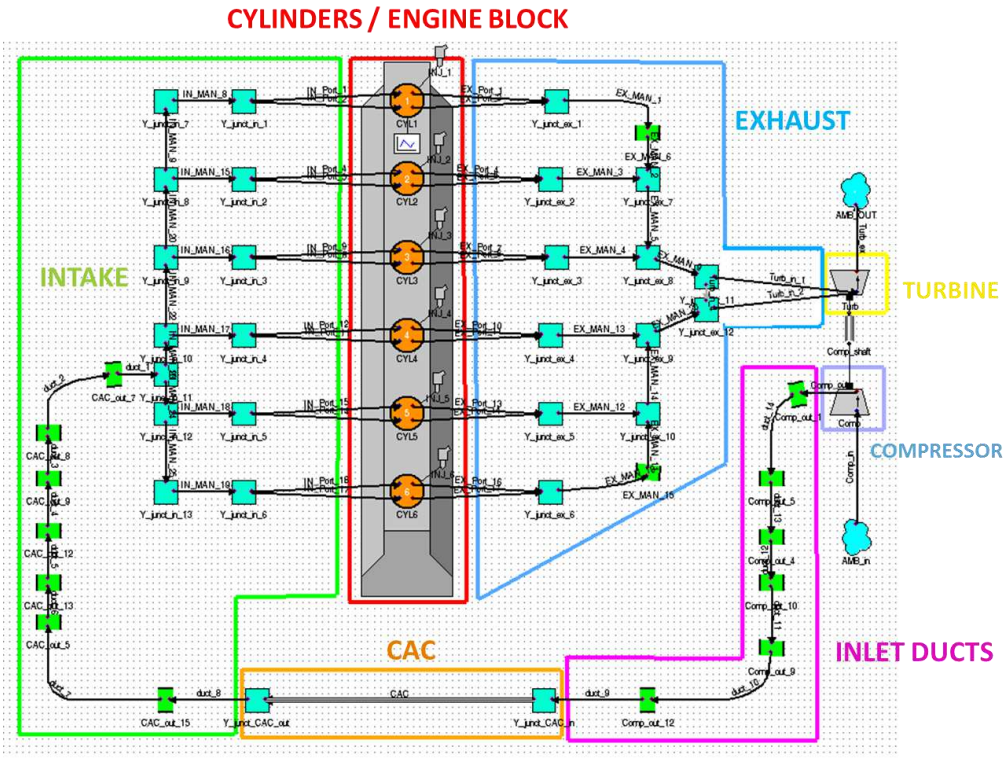

Fig. 39. Engine WAVE model control volumes (CV)

Also in this case, the analysis has been carried out on crank-angle-degree (CAD, θ) step base, and then the terms have been integrated over a cycle in order to calculate the average values. The solution, in particular for the internal CV availability term, has been reported in CAD resolution only for the

cylinders, while for the other CVs only cycle average values have been calculate, especially considering that in steady-state, the terms on the left-hand side of equation (30) are summing up zero over an engine cycle.

Cylinders / Engine Block

The cylinders / engine block control volume is the most complicated between those considered and the one calculated more in the details. It takes in consideration also the initial discretized parts of the intake and exhaust ports, thus considering also valves losses and irreversibilities.
The general form of the availability balance [J/CAD] can be written as follows for the j-cylinder (j=6 in the model proposed):

$$\frac{dA_{cyl}}{d\theta} = \frac{\sum_i \dot{m}_{in} \cdot b_{in} - \sum_i \dot{m}_{out} \cdot b_{out}}{6N} - \frac{dA_{work,brake}}{d\theta} - \frac{dA_{frict}}{d\theta} - \frac{dA_{HT}}{d\theta} + \frac{dA_{fuel,burned,ch}}{d\theta} - \frac{dI_{cyl}}{d\theta} \quad (32)$$

with:

- $\dot{m}_{in}$, $\dot{m}_{out}$: incoming and outgoing mass flow rates for all the ports/valves of the j-cylinder [kg/s]. In the case study considered in this work the incoming mass flow is just pure air, but in the case of EGR, a certain amount of recirculated exhaust gas is present;
- b_{in}, b_{out}: specific flow availability terms [J/kg], referred to the inflow and outflow masses;
- N: engine rotational speed [rpm];
- $\frac{1}{6N} = \frac{60}{N}\frac{1}{360}\frac{s}{CAD}$: a conversion parameter has been used in the MATLAB routine in order to convert all the data from the time base to CAD base;
- $\frac{dA_{work,brake}}{d\theta}$: the availability term due to the brake work produced by the cylinder;
- $\frac{dA_{frict}}{d\theta}$: the availability term due to friction, calculated from the output of the Chen-Flynn correlation and from the indicated work as:

$$\frac{dA_{frict}}{d\theta} = \frac{dA_{work,ind}}{d\theta} - \frac{dA_{work,brake}}{d\theta} \quad (33)$$

with (j-cylinders and overall indicated power):

$$\frac{dA_{work,ind,j}}{d\theta} = \left(p_{cyl,j} - p_0\right) \cdot \frac{dV_{cyl,j}}{d\theta} \quad \rightarrow \quad \frac{dA_{work,ind}}{d\theta} = \sum_j \frac{dA_{work,ind,j}}{d\theta} \quad (34)$$

with:

- $p_{cyl,j}$: in-cylinder pressure of the j-cylinder [Pa];
- $\frac{dV_{cyl,j}}{d\theta}$: differential of the j-cylinder volume [m^3/CAD];
- $\frac{dA_{HT}}{d\theta}$: the availability transferred to the cylinder walls due to the heat transfer:

$$\frac{dA_{HT}}{d\theta} = \frac{dQ}{d\theta} \cdot \left(1 - \frac{T_0}{T_{cyl}}\right) \quad (35)$$

with:

- $\frac{dQ}{d\theta}$: the heat transfer rate [J/CAD] calculated through the Woschni model;
- T_{cyl}: the instantaneous in-cylinder gas contents temperature [K];

- $\frac{dA_{fuel,burned,ch}}{d\theta}$: the chemical availability provided with the fuel burned, written as:

$$\frac{dA_{fuel,burned,ch}}{d\theta} = \frac{dm_{fuel,burned}}{d\theta} \cdot a_{fuel,ch} \quad (36)$$

In this case, as reported by Rakopoulos *et al.* [290], an approximation for fuels in liquid state, with chemical formula $C_z H_y$ ($C_{15}H_{25.05}$ for the diesel fuel used in WAVE), proposed by Moran *et al.* [294] has been used:

$$a_{fuel,ch} = LHV \cdot \left(1.04224 + 0.011925 \cdot \frac{y}{z} - \frac{0.042}{z}\right) \quad (37)$$

with:

- LHV: Lower Heating Value. For the $C_{15}H_{25.05}$ diesel, 42800 [kJ/kg] as from the "diesel.fue" fuel file of WAVE;
- $\frac{dm_{fuel,burned}}{d\theta}$: burned fuel mass per CAD [kg/CAD]. Compared to the First Law analysis, in this case only the part of fuel burned contributes to supply availability to the system, instead of the total fuel mass injected. Generally, however, especially with lean burn operations typical of Diesel engines, almost all the fuel is burned, with low amount of residual unburned fuel remining. To obtain this value, the mass fraction burned rate provided in the WAVE outputs has been multiplied for the total amount of fuel injected per CAD. In the case of a preheated fuel, the thermal availability is usually neglected because not greater of 0.2% of the total chemical availability, as reported by Rakopoulos *et al.* [290].

- $\boldsymbol{\frac{dI_{cyl}}{d\theta}}$: the in-cylinder irreversibilities production rate and the unknown of the problem. In particular, the cylinder's control volume is the one producing more irreversibilities in the engine. The dominant processes responsible of the destruction of exergy are the combustion, followed by viscous dissipation, turbulence due to valves throttling and the mixing of the incoming air with the cylinder residuals. As reported by Rakopoulos *et al.* [290], typical values of the in-cylinder irreversibilities are around 20-25% of the inserted fuel availability in the case of full load, Diesel, four stroke engine turbocharged operations. In the case of spark ignited engines or low load operations, these values can up to more than 40%.

In order to solve the equation (30), it is necessary to calculate the left-hand side term, which represents the rate of change of the total availability inside the cylinder and can be written in an explicit form as follows [290]:

$$\frac{dA_{cyl}}{d\theta} = \frac{dU_{cyl}}{d\theta} + p_0 \cdot \frac{dV_{cyl}}{d\theta} - T_0 \cdot \frac{dS_{cyl}}{d\theta} - \sum_i \frac{dm_i}{d\theta} \cdot \mu_i^0 \quad (38)$$

with:

- $\frac{dU_{cyl}}{d\theta}$: internal energy rate of change of the cylinder contents. The value of U is not provided directly from the WAVE outputs, but must be calculated from the total enthalpy, extracted from WAVE, through the well-known formula:

$$U_{cyl} = H_{cyl} - R \cdot T_{cyl} \quad (39)$$

In which H_{cyl} is the enthalpy of the entire mixture in the combustion chamber/cylinder [J], R is the gas constant ($8314\ J/(mol \cdot K)$), and T_{cyl} is the actual temperature inside the cylinder [K]. All the parameters required are provided by WAVE using the SDF functions and directly imported into the MATLAB routine.

- $\frac{dS_{cyl}}{d\theta}$: the entropy rate of change of the cylinder contents [J/(K·CAD)]. The S values is provided directly by WAVE and needs just to be differentiated, as the other terms;
- $\sum_i \frac{dm_i}{d\theta}\mu_i^0 = \frac{dG_0}{d\theta}$: free Gibbs enthalpy rate of change at the reference state conditions. This term can be considered as the maximum amount of mechanical work which can be obtained from a given quantity of a certain substance, in this case, at reference conditions. $\frac{dm_i}{d\theta}$ is the rate of change of the mass of the single eleven chemical species considered in WAVE, which interact between each other in the combustion process, crank-angle per crank-angle. μ_i^0 is the chemical potential [J/kg] of the single i-specie, and can be calculated as follows [290]:

$$\mu_i^0 = g_i(T_0, x_i p_0) = h_i(T_0) - T_0 \cdot s_i(T_0, x_i p_0) \quad (40)$$

It is possible to observe that the enthalpy and entropy at reference state are required for the calculations in equation (40). As already introduced, these parameters are not available in WAVE and must be calculated through the already proposed functions.

It is important, especially in order to double-check the performed calculations, that the term $\frac{dA_{cyl}}{d\theta}$, in a cyclic steady-state simulation process, must satisfy the relation $\int_0^{720} \frac{dA_{cyl}}{d\theta} d\varphi = 0$ when integrating over the cycle. From all performed simulation cases, the average cycle value is slightly different from zero, due to numerical approximations. However, is approaches zero always.

As already introduced, in the case of the cylinder / engine block CV, a detailed crank-angle-degree resolved analysis has been proposed, and an example of this kind of output can be observed in Fig. 40, in which the case at 100% load and 2500 rpm has been reported, proposing the evaluation of the crank-angle instantaneous exergy contributions.

In WAVE, the cycle simulation starts at the Inlet Valve Closing (IVC) event. Until the Start of Combustion (SOC) event is reached, the availability of the cylinder contents ($dA_{cyl}/d\theta$) increases due to the compression work supplied by the piston to the working fluid. In this crank-angle range it is possible that the air (or gas mixture) is at lower temperature, especially at the beginning, compared to the surrounding walls, thus receiving heat and availability, until a certain point, in which the heat transfer reverses because of the increase of the in-cylinder gas temperature. In this part of the cycle, the irreversibilities are near to zero, since they are mostly due to the rate of change of the molar quantities of the working medium species and some preliminary chemical reactions.

When injection begins, a small drop can be observed for the cylinder term ($dA_{cyl}/d\theta$), mostly due to the ignition delay and the evaporation of the injected fuel, due to the high temperatures, which subtract heat from the mixture.

When combustion starts, the increase in pressure and temperature, due to the burning fuel, leads to a drastic increase of the cylinder availability term and also to the increase of the term related to the

cylinder walls availability transfer. At the same time, the irreversibilities term shows also a considerable increase due to the combustion event and the chemical dissociation reactions.
Towards the end of combustion, when the pressure and the temperature decrease, due to the expansion event, the irreversibilities term tends to decrease, together with the cylinder availability term, since the working fluid availability is returned as indicated work, heat transfer and irreversbilities, explained in the exergy balance formulation. The same trend can be observed for the cylinder heat transfer term, while, as already introduced, the indicated work increases due to the expansion stroke, which produces useful work (during the compression stroke, this term is correctly negative). The fuel burned availability goes to zero as soon as the combustion event is finished, and the fuel is almost completely burned (especially during lean-burn diesel operations). At the Exhaust Valve Opening (EVO) event, the exhaust gas availability increases, due to the blow-down period in which the gas is expelled from the cylinder, and subsequently tends to go to zero at Exhaust Valve Closing (EVC). All the availability terms tend then to the same values of the beginning of the cycle, in steady-state conditions, going through EVC and Inlet Valve Opening (IVO) events.

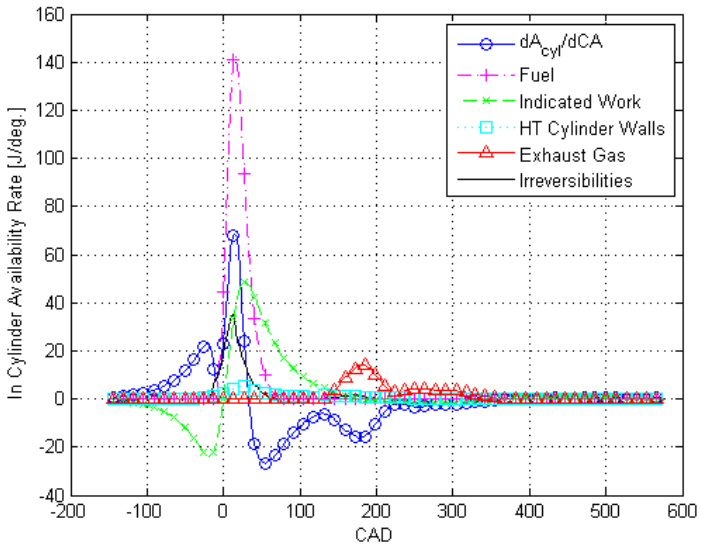

Fig. 40. In-cylinder availability terms calculated with the developed post-processing routine (100% Load, 2500 rpm)

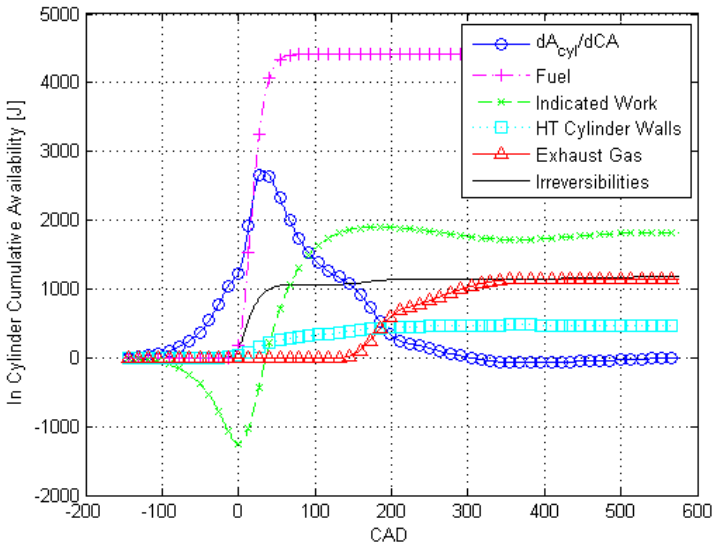

Fig. 41. In-cylinder availability cumulative terms calculated with the developed post-processing routine (100% Load, 2500 rpm)

The post-processing routine calculates also the cumulative trends, reported in Fig. 41. This shows also how the in-cylinder term ($dA_{cyl}/d\theta$ or dA_{cyl}/dCA in a discretized form) goes to zero at the end of a steady-state cycle.
The obtained in-cylinder availability charts are in very good agreement with what reported by Rakopoulos *et al.* [290] for a comparable engine model to the one considered in this work.
The outcomes of the analysis are very interesting since, through a combined use of 1-D and 3D-CFD in-cylinder simulation tools, it is possible, in an iterative way, to assess new combustion strategies, obtaining the heat release and burn rate from the CFD calculations, and then using the 1-D approach to address new combustion concepts in order to reduce the irreversibilities.
This is however out of the scope of this work and is left to future developments.
It is the case also to remember that, in the approach followed, the valves throttling irreversibilities are considered to be part of the cylinders / engine block CV.
A sweep parametric analysis is also possible, as proposed in the case of the First Law.

Inlet Ducts

The control volume related to the inlet ducts includes all the duct between the compressor outlet and the Charge Air Cooler (CAC) inlet. The availability balance can be written as follows [J/CAD] (the work term is not present since no work is exchanged):

$$\frac{dA_{ducts}}{d\theta} = \frac{\dot{m}_{ducts,in} \cdot b_{ducts,in} - \dot{m}_{ducts,out} \cdot b_{ducts,out}}{6N} - \frac{\sum_k dA_{HT,ducts,k}}{d\theta} - \frac{dI_{ducts}}{d\theta} \qquad (41)$$

with:

- $\frac{dA_{ducts}}{d\theta}$: the control volume availability accumulation term [J/CAD]. Considering a steady-state simulation, the term has been imposed to be zero;
- $\dot{m}_{ducts,in}$, $\dot{m}_{ducts,out}$: mass flows [kg/s] at the inlet and outlet boundaries of the CV;
- $b_{ducts,in}$, $b_{ducts,out}$: specific flow availabilities [J/kg] of the incoming and outgoing mass flows. The enthalpy and entropy terms at reference dead state are calculated through the *PROP* and *Ideal_Gas_Prop_refstate_s0* functions;
- N: engine rotational speed [rpm];
- $\frac{dA_{HT,ducts}}{d\theta}$: the availability due to heat transfer, calculated as follows for the k-duct:

$$\frac{dA_{HT,ducts,k}}{d\theta} = \frac{dQ_{ducts}}{d\theta} \cdot \left(1 - \frac{T_0}{T_{duct,avg,k}}\right) \qquad (42)$$

with:

- $\frac{dQ_{ducts}}{d\theta}$: rate of heat transfer per CAD [J/CAD], calculated from the heat transfer rate [W] obtained from WAVE for every k-duct;
- $T_{duct,avg,k}$: k-duct bulk gas average temperature between inlet and outlet [K];

$\frac{dI_{ducts}}{d\theta}$ are the irreversibilities of the inlet ducts control volume, which are generally minimal due to the small dimensions of the control volume, and the low heat and pressure losses. The irreversibilities are mostly due to the gas friction in the ducts.

Charge Air Cooler (CAC)

The control volume of the CAC includes the CAC duct (modelled as a multiple-pipes duct) and the two junctions representing the heat exchanger headers. The availability balance can be written as follows [J/CAD] (the work term is not present since no work is exchanged):

$$\frac{dA_{CAC}}{d\theta} = \frac{\dot{m}_{CAC,in} \cdot b_{CAC,in} - \dot{m}_{CAC,out} \cdot b_{CAC,out}}{6N} - \frac{dA_{HT,CAC}}{d\theta} - \frac{dI_{CAC}}{d\theta} \quad (43)$$

with:

- $\frac{dA_{CAC}}{d\theta}$: the control volume availability accumulation term [J/CAD]. Considering a steady-state simulation, the term has been imposed to be zero;
- $\dot{m}_{CAC,in}$, $\dot{m}_{CAC,out}$: mass flows [kg/s] at the inlet and outlet boundaries of the CV;
- $b_{CAC,in}$, $b_{CAC,out}$: specific flow availabilities [J/kg] of the incoming and outgoing mass flows. The enthalpy and entropy terms at reference dead state are calculated through the *PROP* and *Ideal_Gas_Prop_refstate_s0* functions;
- N: engine rotational speed [rpm];
- $\frac{dA_{HT,CAC}}{d\theta}$: the availability due to heat transfer, calculated as follows for the k-duct:

$$\frac{dA_{HT,CAC}}{d\theta} = \frac{dQ_{CAC}}{d\theta} \cdot \left(1 - \frac{T_0}{T_{CAC}}\right) \quad (44)$$

with:

- $\frac{dQ_{CAC}}{d\theta}$: rate of heat transfer per CAD [J/CAD], calculated from the heat transfer rate of the CAC [W] obtained from WAVE;
- T_{CAC}: k-duct bulk gas average temperature over the CAC [K];

$\frac{dI_{CAC}}{d\theta}$ are the irreversibilities of the CAC control volume, which are mostly due to the gas friction in the ducts.

Intake Manifolds

The intake (manifolds) control volume includes the intake ports (until the beginning of the engine control volume), the intake manifolds and junctions and the ducts from the CAC outlet to the cylinders' inlets. The availability balance can be written as follows [J/CAD] (the work term is not present since no work is exchanged):

$$\frac{dA_{int}}{d\theta} = \frac{\dot{m}_{int,in} \cdot b_{int,in} - \sum_i \dot{m}_{int,out,i} \cdot b_{int,out,i}}{6N} - \frac{\sum_k dA_{HT,int,k}}{d\theta} - \frac{dI_{int}}{d\theta} \quad (45)$$

with:

- $\frac{dA_{int}}{d\theta}$: the control volume availability accumulation term [J/CAD]. Considering a steady-state simulation, the term has been imposed to be zero;
- $\dot{m}_{int,in}$, $\dot{m}_{int,out,i}$: mass flows [kg/s] at the inlet and outlet boundaries of the CV (i-intake ports);

- $b_{int,in}$, $b_{int,out,i}$: specific flow availabilities [J/kg] of the incoming and outgoing mass flows (i-intake ports). The enthalpy and entropy terms at reference dead state are calculated through the *PROP* and *Ideal_Gas_Prop_refstate_s0* functions;
- N: engine rotational speed [rpm];
- $\frac{dA_{HT,int,k}}{d\theta}$: the availability due to heat transfer, calculated for the k-duct / junction / manifold as done for the inlet ducts control volume;

$\frac{dI_{int}}{d\theta}$ are the irreversibilities of the intake control volume and consider mainly mixing of the incoming air with the intake contents and friction in the ducts.

Exhaust Manifolds

The exhaust manifolds control volume includes the exhaust ports (from the end of the engine control volume), the exhaust manifolds and junctions and the ducts until the turbine inlets. The availability balance can be written as follows [J/CAD] (the work term is not present since no work is exchanged):

$$\frac{dA_{exh}}{d\theta} = \frac{\sum_i \dot{m}_{exh,in,i} \cdot b_{exh,in,i} - \sum_j \dot{m}_{exh,out,j} \cdot b_{exh,out,j}}{6N} - \frac{\sum_k dA_{HT,exh,k}}{d\theta} - \frac{dI_{exh}}{d\theta} \qquad (46)$$

with:

- $\frac{dA_{exh}}{d\theta}$: the control volume availability accumulation term [J/CAD]. Considering a steady-state simulation, the term has been imposed to be zero;
- $\dot{m}_{exh,in,i}$, $\dot{m}_{exh,out,j}$: mass flows [kg/s] at the inlet and outlet boundaries of the CV (i-exhaust ports, j-exhaust CV outlet ducts entering the turbine);
- $b_{exh,in,i}$, $b_{exh,out,j}$: specific flow availabilities [J/kg] of the incoming and outgoing mass flows (i-exhaust ports, j-exhaust CV outlet ducts entering the turbine) The enthalpy and entropy terms at reference dead state are calculated through the *PROP* and *Ideal_Gas_Prop_refstate_s0* functions;
- N: engine rotational speed [rpm];
- $\frac{dA_{HTexh,k}}{d\theta}$: the availability due to heat transfer, calculated for the k-duct / junction / manifold as done for the inlet and intake ducts control volumes;

$\frac{dI_{exh}}{d\theta}$ are the irreversibilities of the intake control volume and consider mainly mixing of the exhaust gas with the exhaust ports contents and friction in the ducts.

Compressor

The compressor control volume considers the compressor component plus the first centroid of the compressor inlet and compressor outlet, due to the discretization in the model. However, the heat transfer contributions of these infinitesimal parts of the ducts are neglected for simplicity, not leading to big inaccuracies, especially considering the low heat transfer rate expected in the nearby of the compressor. The compressor is modelled, in WAVE, as a steady-state map and considered adiabatic

towards the environment. The availability balance can be written as follows [J/CAD], in this case directly resolved for the irreversibilities:

$$\frac{dI_C}{d\theta} = \frac{\dot{m}_{C,in} \cdot b_{C,in} - \dot{m}_{C,out} \cdot b_{C,out}}{6N} - \frac{\dot{W}_C}{6N} \quad (47)$$

with:

- $\dot{m}_{C,in}$, $\dot{m}_{C,out}$: mass flows [kg/s] at inlet and outlet of the compressor CV. $\dot{m}_{C,in}$ is also the mass flow at the inlet of the overall engine CV;
- $b_{C,in}$, $b_{C,out}$: specific flow availabilities [J/kg] of the incoming and outgoing mass flows. The enthalpy and entropy terms at reference dead state are calculated through the *PROP* and *Ideal_Gas_Prop_refstate_s0* functions;
- N: engine rotational speed [rpm];
- $\dot{W}_C$: compressor absorbed power [W], obtained from WAVE outputs.

$\frac{dI_C}{d\theta}$ are the irreversibilities of the compressor control volume and are mostly due to the flow losses because of fluid shear and throttling through the compressor blades.

Turbine

The turbine control volume considers the turbine component plus the first centroid of the turbine inlet and turbine outlet ducts, in which the flow availabilities are considered. Also in this case, the heat transfer contributions of the infinitesimal ducts parts are neglected for simplicity, especially considering that, no matter the high temperatures in the line, the not considered heat transfer is minimal. The turbine is also modelled in WAVE as a steady-state map and considered adiabatic towards the environment. The availability balance can be written as follows [J/CAD], in this case directly resolved for the irreversibilities:

$$\frac{dI_T}{d\theta} = \frac{\sum_i \dot{m}_{T,in,i} \cdot b_{T,in,i} - \dot{m}_{T,out} \cdot b_{T,out}}{6N} - \frac{\dot{W}_T}{6N} \quad (48)$$

with:

- $\dot{m}_{T,in,i}$, $\dot{m}_{T,out}$: mass flows [kg/s] at inlet(s) and outlet of the turbine CV. $\dot{m}_{T,out}$ is also the mass flow at the outlet of the overall engine CV;
- $b_{T,in,i}$, $b_{T,out}$: specific flow availabilities [J/kg] of the incoming and outgoing mass flows. The enthalpy and entropy terms at reference dead state are calculated through the *PROP* and *Ideal_Gas_Prop_refstate_s0* functions;
- N: engine rotational speed [rpm];
- $\dot{W}_T$: turbine produced power [W], obtained from WAVE outputs.

$\frac{dI_T}{d\theta}$ are the irreversibilities of the compressor control volume, and are, also in this case, mostly due to the flow losses because of fluid shear and throttling through the turbine blades.

Exhaust Unburned Fuel

The last term of the balance is related, as for the First Law case, to the unburned fuel availability, which is lost through the exhaust. This term, even if almost negligible due to the lean-burn diesel operations, has been estimated starting from the liquid and vapor unburned fuel mass flows extracted from the wave turbine outlet CV as follows:

$$\frac{dA_{unb,fuel,exh}}{d\theta} = \frac{\dot{m}_{liq,unb,fuel,exh}}{6N} \cdot a_{fuel,liq,ch} + \frac{\dot{m}_{vap,unb,fuel,exh}}{6N} \cdot a_{fuel,vap,ch} \qquad (49)$$

with:

- $\dot{m}_{liq,unb,fuel,exh}$: exhausted mass flow of unburned liquid fuel (almost negligible amount) [kg/s];
- $\dot{m}_{vap,unb,fuel,exh}$: exhausted mass flow of unburned vaporized fuel [kg/s];
- $a_{fuel,liq,ch}$: liquid fuel availability [J/kg], as calculated with equation (37);
- $a_{fuel,vap,ch}$: vapour fuel availability [J/kg], calculated with the same formula in equation (37), but using the Lower Heating Value of the vapour fuel (LHV_{vap}), calculated as the difference between the LHV of the liquid fuel (42800 kJ/kg for the assumed diesel) and the enthalpy of vaporization of the fuel (220 kJ/kg for the assumed diesel).

The final WAVE model, developed in order to carry out the detailed First and Second Law analysis, using the proposed MATLAB post-processing routines, results in being a very highly discretized model, with multiple so-called "sensors" components, which are used to extract the required parameters from the model, especially when not available directly in the output .wvd file. Between these parameters, the most important are the heat transfer rates of all the pipes, junctions and various components, and the molar fractions of the eleven species in every location of the model in which the specific enthalpy and entropy at reference state need to be calculated. This results in an "heavily-sensored" and detailed model, which at the same time, results in high computational time, in order to achieve accurate results. The final model has been reported in Fig. 42, as an example of the model complexity. A trade-off between simulation speed and results accuracy must be considered when carrying out the analysis, especially if industrial project time constraints need to be applied.

What proposed in this work is the attempt to open a new path for a synergistic simulation (or co-simulation) approach using the principles of exergy analysis, and as a second step, techno and thermo-economics.
Further developments, in collaboration with software development experts, should be carried out in order to embed the proposed approach into a more complete tool, maybe in a modular way. Already implementing the possibility of calculating the gas properties at the reference dead state, would allow the user to get rid of many of the sensors, thus reducing the complexity of the overall model, which at the actual status of development results in being very complex (as can be evinced from Fig. 42).
If the proposed methodology would be implemented directly in WAVE, or in a more advanced simulation platform, such as IGNITE [295], the handling of the overall process could become easier, enhanced by an user-friendly GUI, speeding-up the entire analysis process, and allowing the combined use of advanced optimization techniques in a unique canvas. Transient simulation approaches could also be proposed, with the scope of minimizing irreversibilities production during transitory engine operations and operating cycles' analysis.
A methodology as the one proposed in this work could allow to open the path to a new engine development approach, not yet used in the industry, taking profit not anymore only of the First Law

information, but also the Second Law. An additional economic analysis could even allow to design not only efficient engines, but also feasible from an investment cost point of view.

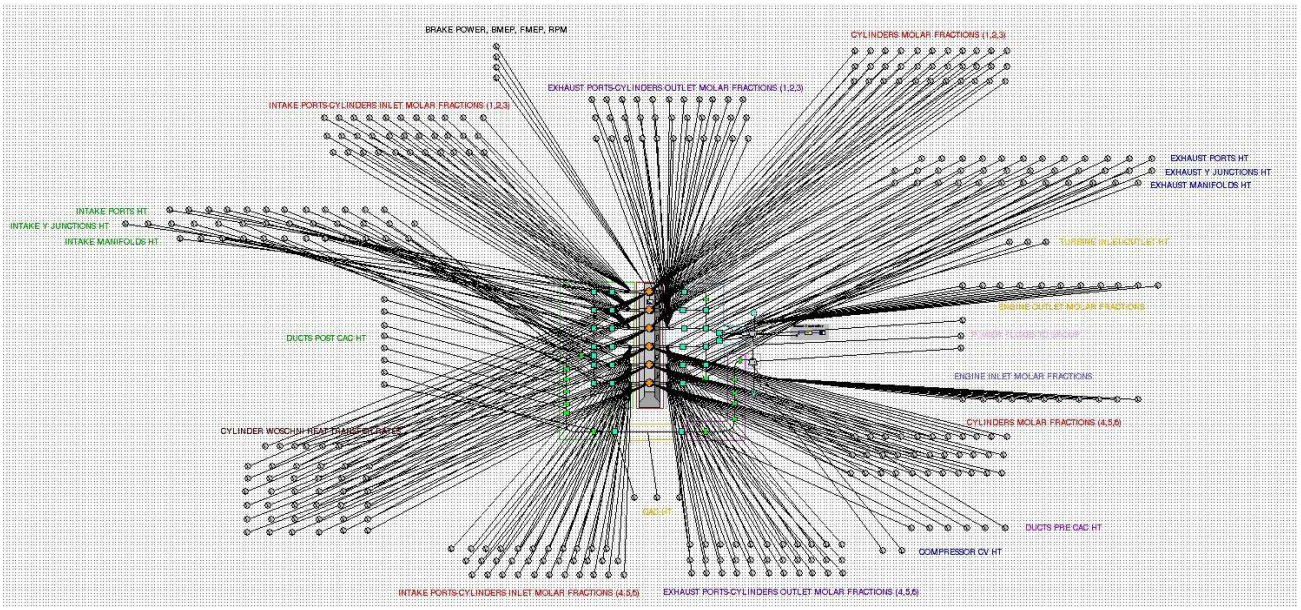

Fig. 42. Fully sensored WAVE model ready for First and Second Law analysis

5.2 ORC Modelling

Different levels of modelling complexity can be considered when analysing Organic Rankine Cycles (ORC) and, in general, engine-bottoming waste heat recovery systems. No matter if the ORC is a well-known and studied technology, mostly due to the quite simple operating principles, similar to common steam Rankine cycles, the design and modelling of ORCs can be challenging, especially when considering transient conditions, which are simulated, very often, for the purpose of developing adequate controlling strategies, for off-design conditions. In these case, more detailed 1-D and 3-D modelling approaches must be proposed in order to model more in the details the physics of the components, compared to what presented in this work.
A quite interesting and detailed overview of modelling challenges related to ORC systems is reported by Ziviani *et al.* [296], who proposed a list of different software or coding languages generally used for ORC models development.
However, for the purpose of this work, and considering that the proposed methodology can be generally applied in the first phases of a development project, in order to decide between different fluids, cycle architectures and engine-ORC configurations and operational parameters, a detailed, components-oriented approach, has not been proposed, rather using thermodynamic 0-D formulations, for mass, energy and exergy balances of the main components of the system (e.g. pumps, evaporators, condensers, expanders), choosing a more holistic simulation approach. The introduction of detailed components models can be proposed in the future in order to improve the accuracy of the analysis getting rid of some of the proposed ORC components' performance assumptions, but at the same time increasing the overall computational cost, due to the needs of operating co-simulation between different detailed modelling platforms.
As already introduced for the engine case, the application of the principles of the First Law of Thermodynamics is not enough to reach a complete understanding of the processes happening in the ORC system. Indeed, also for the waste heat recovery system case, the application of the principles of the Second Law (exergy balances) is needed, in order to understand which components are introducing more inefficiencies. This step is also necessary to apply a combined thermo-economic approach, as introduced in section 5.3.

5.2.1 First Law Analysis Applied to the ORC

As introduced, the first step of the analysis has been proposed using the principles of First Law of Thermodynamics, calculating mass and energy balances for the main components of the Organic Rankine Cycle (ORC) system.
The boundary conditions for the analysis are obtained from the engines analysed in this work, in particular for the main possible heat sources (exhaust gas, EGR, coolant, Charge Air Cooling heat, Scavenge Air Cooling heat and lubrication oil). Regarding the heat sink at the ORC condensing side, the boundary conditions are obtained from the environmental conditions (e.g. sea water, ambient air), or the engine cooling circuit or cooling package, especially for vehicles applications, with feasible assumptions proposed.
The working fluids thermodynamic properties (e.g. specific enthalpy, specific entropy, specific volume, density and so on) have been retrieved directly from EES (Engineering Equation Solver, [297]) internal database, or using the NIST REFPROP software ([147]).
The codes used to evaluate the performance of the different ORC concepts have been developed using EES or MATLAB [298] programming languages. In particular, the first three case studies have been simulated using EES, while the last case study using MATLAB, in order to exploit the improved optimization software coupling capabilities of the software, and the possibility of a future better

interface with Ricardo tools, such as WAVE and IGNITE. In this last case, the working fluids properties have been retrieved using REFPROP wrapper interfaces available for MATLAB.
Generally, in first approximation, and in order to simplify the model, the thermodynamic properties of the Diesel engine exhaust gas are approximated with those of air, since they are not expected to vary much [299]. When fully integrating the engine and ORC routines, the properties could be directly obtained from WAVE.
As a second analysis layer, the exergy balances (Second Law) have been applied, with the scope of calculating the exergy fluxes and the irreversibilities all-over the ORC system. This will allow to have the full overview of the exergy fluxes in the combined engine-ORC powertrain system, in order to apply the thermo-economic analysis step.
The first three case studies have been studied using only a First Law formulation, while the last and fourth case study, with a complete techno and exergo-economic (or thermo-economic) approach, in order to show an increasing level of synergy of the proposed methodology.
An example of simple ORC architecture, together with a possible T-s diagram process explanation chart, has been reported in Fig. 43, with the purpose of showing the main ORC thermodynamic processes.

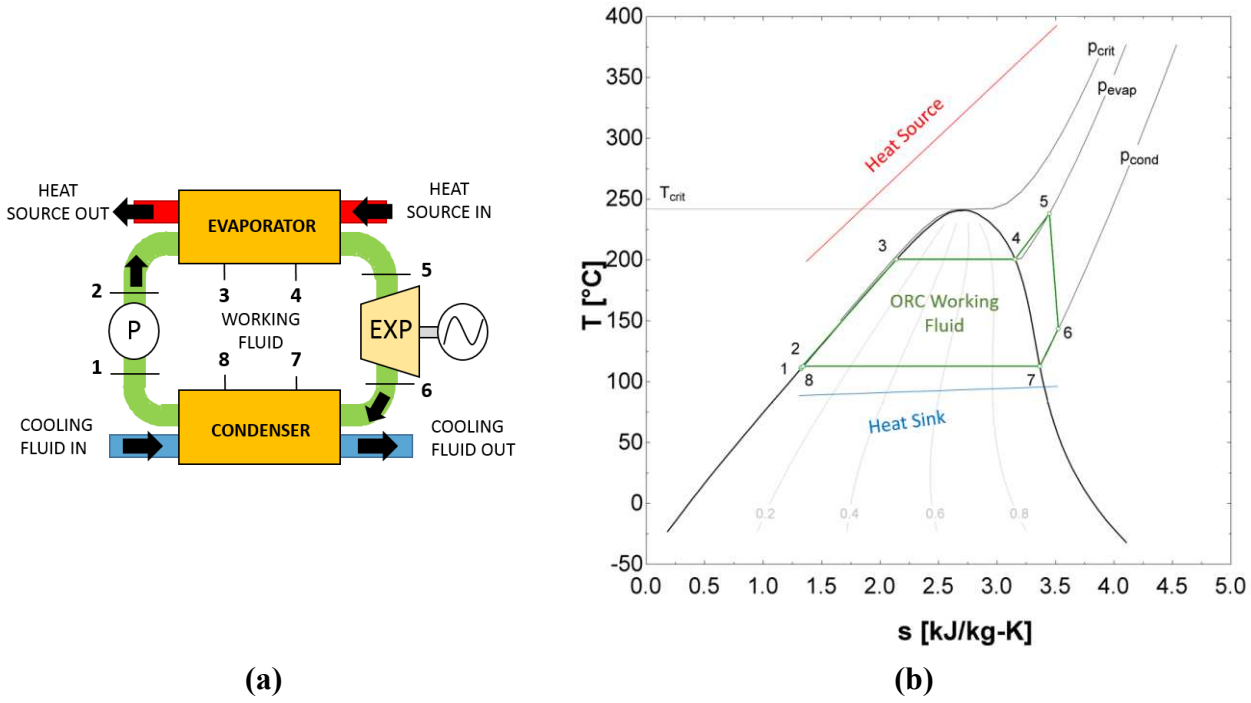

Fig. 43. (a) Scheme of a simple ORC architecture and (b) relative T-s diagram example

- **1 – 2:** pumping of the working fluid from the low-pressure to the high-pressure side (from condensing to evaporation pressure). "P" stands for pump;
- **2 – 3:** pre-heating of the working fluid without phase-change (pre-heater);
- **3 – 4:** evaporation of the working fluid from saturated liquid to saturated vapour with phase-change (evaporator);
- **4 – 5:** superheating of the working fluid to superheated vapour (super-heater). This process is often carried out, in particular in steam plants, to avoid having liquid at the outlet of the expansion machine, which could damage the blades of a possible turbo-expander, due to liquid droplets high-speed impingement (pitting);
- **5 – 6:** expansion of the working fluid in the expansion machine (expander, EXP);
- **6 – 7:** de-super-heating of the working fluid from superheated vapour to saturated vapour (de-super-heater);

- **7 – 8:** condensation of the working fluid from saturated vapour to saturated liquid (condenser);
- **8 – 1:** sub-cooling of the working fluid from saturated liquid to sub-cooled liquid (sub-cooler). This process is usually carried out in order to avoid having vapour phase at the pump inlet, which could lead to cavitation problems.

The architecture with parallel evaporators (e.g. exhaust and EGR gas heat recovery) follows the same principles, with the difference that a working fluid split valve has been proposed right after the pump, to divide the fluid between the exhaust and EGR circuits/evaporators.
Some other assumptions have been proposed when developing the models:

- The evaporator and the condenser heat exchangers have been divided in the proposed three zones and a fixed boundary modelling technique has been applied;
- Heat exchangers with no phase change (e.g. recuperator, exhaust-to-thermal oil) have been modelled with only one zone;
- The heat exchangers have been considered to have a parallel counter-flow configuration;
- Pressures drops, and heat losses have not been considered in the components and in the pipes;
- A fixed pump isentropic efficiency, $\eta_{is,P}$, has been always imposed (with values between 60 and 70% at design points);
- A fixed expander isentropic efficiency, $\eta_{is,EXP}$, has been always imposed (with values between 70 and 80% at design points). Further detailed components performance should be considered for future developments of the methodology;
- A fixed energy conversion (e.g. mechanical or electrical coupling) efficiency, η_{conv}, has been always considered, depending on the application and size of the system;
- A sub-cooling temperature difference, $\Delta T_{sub-cool}$, of 2°C has been always imposed. The fluid reservoir has not been modelled;

The mathematical modelling of the main processes has been proposed below, using the numeration proposed in Fig. 43.

Pump

The condensing pressure, p_{cond} (p_1), is fixed based on the heat sink temperature and pressure levels. The pressure ratio over the pump (and considering no pressure losses, over the expander), PR, is also imposed, in order to calculate the evaporation pressure ($p_{evap} = p_2$):

$$p_{evap} = p_{cond} \cdot PR \quad (50)$$

The pump isentropic specific work, $w_{is,P}$ [J/kg], can be calculated from the specific volume at the pump inlet, v_1 [m^3/kg] (assuming incompressible fluid, $v_1 = v_2$) and the pressure difference [Pa]:

$$w_{is,P} = v_1 \cdot (p_2 - p_1) \quad (51)$$

Once the isentropic efficiency of the pump is assumed, the actual specific work of the pump [J/kg] can be calculated as:

$$w_P = \frac{w_{is,P}}{\eta_{is,P}} \quad (52)$$

and the power absorbed [W], multiplying for the working fluid mass flow, $\dot{m}_{wf}$ [kg/s], as:

$$\dot{W}_P = w_P \cdot \dot{m}_{wf} \quad (53)$$

The specific enthalpy [J/kg] at point 2 (pump outlet, pre-heater inlet) can be then calculated as:

$$h_2 = h_1 + w_P \quad (54)$$

All other thermodynamic properties of point 2 can be obtained knowing the pressure and the specific enthalpy, using the fluids properties routines from EES or REFPROP.

Evaporator

As already introduced, the evaporator has been divided, for modelling reasons, in three zones and a fixed boundary approach has been applied, calculating mass and energy balances for: pre-heater (*preh*, 2-3), evaporator (*evap*, 3-4) and super-heater (*suph*, 4-5).
A superheating temperature difference is imposed as one of the inputs of the model (ΔT_{suph} [°C]), in order to fix the expander inlet temperature.
The following energy balances have been applied, in order to calculate the heat source (*hs, e.g. exhaust gas*) temperature at the outlet of every section, starting from the thermodynamic states fixed on the ORC working fluid side (*wf*) and the heat source evaporator inlet temperature ($T_{hs,5}$). A formulation with specific enthalpy or with average fluid specific heat, cp_i, multiplied by the temperature difference, is possible.

$$suph: \quad \dot{m}_{hs} \cdot (h_{hs,5} - h_{hs,4}) = \dot{m}_{wf} \cdot (h_{wf,5} - h_{wf,4}) \rightarrow h_{hs,4} \rightarrow T_{hs,4} \quad (55)$$

$$evap: \quad \dot{m}_{hs} \cdot (h_{hs,4} - h_{hs,3}) = \dot{m}_{wf} \cdot (h_{wf,4} - h_{wf,3}) \rightarrow h_{hs,3} \rightarrow T_{hs,3} \quad (56)$$

$$preh: \quad \dot{m}_{hs} \cdot (h_{hs,3} - h_{hs,2}) = \dot{m}_{wf} \cdot (h_{wf,3} - h_{wf,2}) \rightarrow h_{hs,3} \rightarrow T_{hs,2} \quad (57)$$

The evaporator recovered heat [W], which is also the heat entering the ORC system, can be calculated as:

$$\dot{Q}_{ORC,in} = \dot{Q}_{preh} + \dot{Q}_{evap} + \dot{Q}_{suph} \quad (58)$$

Once all the temperatures are known, from the heat balances, it is possible to evaluate the pinch point temperature difference, as the minimum value between the differences of the temperature of the heat source and the working fluid in every section in which the heat exchanger is divided. This allows to constrain these values to be higher than a certain quantity (e.g. 5-10°C) during the simulations, in order to have suitable heat transfer performance (example in Fig. 44).
All the properties can be calculated, using EES or REFPROP routines, for the points 2-3-4-5.

Expander

The expansion machine converts the fluid energy into mechanical power, proportionally to the enthalpy drop between the outlet and the inlet of the expander. However, the whole enthalpy drop cannot be converted into useful work, due to the machine inefficiencies. This is considered through the assumption of the expander isentropic efficiency:

$$\eta_{is,EXP} = \frac{h_6 - h_5}{h_{6is} - h_5} \quad (59)$$

Starting from an isentropic process ($s_6 = s_{6,is}$), and the expander outlet pressure (p_{cond}, without pressure losses), it is possible to calculate all thermodynamic properties at the expander isentropic outlet. The expansion machine isentropic specific work [J/kg] can then be calculated as:

$$w_{is,EXP} = h_5 - h_{6,is} \quad (60)$$

As done for the pump, imposing the isentropic efficiency, it is possible to obtain the actual expander specific work [J/kg]:

$$w_{EXP} = w_{is,EXP} \cdot \eta_{is,EXP} \quad (61)$$

And the power [W] produced by the expander:

$$\dot{W}_{EXP} = w_{EXP} \cdot \dot{m}_{wf} \quad (62)$$

In a reverse way, the specific enthalpy at the actual expander process outlet, can be calculated as:

$$h_6 = h_5 - w_{EXP} \quad (63)$$

All other properties at point 6 can then be calculated through the use of the EES or REFPROP fluid properties routines.

Condenser

A simple procedure has been implemented to control the position of point 7, depending if the end of the expansion process is inside or outside the dome (vapour quality, x_6, presence of liquid at the end of the expansion). The procedure fixes the positions of point 7 (beginning of the condensation process) of consequence, in the two-phase or superheated regions, or as saturated vapour. Subsequently, the thermodynamic properties at point 7 can be calculated from $p_7 = p_{cond}$ and x_7.
A sub-cooling temperature difference is imposed as one of the inputs of the model ($\Delta T_{sub-cool}$ [°C]), in order to fix the pump inlet temperature for the subsequent calculations.
As for the evaporator, the condenser is also divided in three zones, and a fixed boundary approach applied for the three sections, using an energy balance. The three sections are: de-super-heater (*desuph, 6-7*), condenser (*cond, 7-8*) and sub-cooler (*sub-cool, 8-1*). The same approach used for the evaporator case, is used to calculate the heat sink (cooling fluid) temperatures at the outlet of every section, starting from the points fixed for the working fluid thermodynamic properties, and the cooling fluid (*cf*) inlet temperature ($T_{cf,1}$):

sub-cool: $\dot{m}_{cf} \cdot (h_{cf,8} - h_{cf,1}) = \dot{m}_{wf} \cdot (h_{wf,8} - h_{wf,1}) \rightarrow h_{cf,8} \rightarrow T_{cf,8}$ (64)

cond: $\dot{m}_{cf} \cdot (h_{cf,7} - h_{cf,8}) = \dot{m}_{wf} \cdot (h_{wf,7} - h_{wf,8}) \rightarrow h_{cf,7} \rightarrow T_{cf,7}$ (65)

desuph: $\dot{m}_{cf} \cdot (h_{cf,6} - h_{cf,7}) = \dot{m}_{wf} \cdot (h_{wf,6} - h_{wf,7}) \rightarrow h_{cf,6} \rightarrow T_{cf,6}$ (66)

The same approach has been used to calculate the pinch point temperature difference in the case of the condenser heat exchanger.
The condenser rejected heat [W], which is also the heat exiting the ORC system, can be calculated as:

$$\dot{Q}_{ORC,out} = \dot{Q}_{de-suph} + \dot{Q}_{cond} + \dot{Q}_{sub-cool} \quad (67)$$

The calculations for the condenser close the cycle, which starts again from the pump inlet point (1).

Recuperator

Especially in the case of dry or isentropic fluids, in which the expansion end is almost always in the superheated region, the heat at the expander outlet can be used to pre-heat the working fluid at the pump outlet. Indeed, the effect of the evaporator is, generally, to reduce the heat recovered from the heat source, for an equal system power output. This will have the secondary effect of increasing the system thermal efficiency and reduce the heat which must be rejected to the heat sink, thus being particularly useful in applications such as vehicles, in which reducing the heat rejected will have a positive impact on the vehicle cooling package performance. A trade-off with the increased system costs and weight should be however considered.
The recuperator is solved in EES using its embedded solver capabilities (acausal solver). Indeed, the equations can be entered without the need of an order, and the solver will solve them using an iterative procedure to convergence. In the case of MATLAB, an iterative (while cycle) procedure has been implemented, however leading to the same results. A recuperator average effectiveness, ε_{recp}, has been imposed to be equal to 80% (0.8).
A maximum temperature difference over the recuperator is calculated, considering the hot (turbine outlet) and cold (pump outlet) sides, as:

$$\Delta T_{max,recp} = T_{hot,recp,in} - T_{cold,recp,in} \quad (68)$$

and a guess temperature at the recuperator hot side outlet is assumed as $T_{hot,recp,out} = T_{exp,out}$, as the same of the expansion process outlet, in first approximation.
A temperature step and a tolerance have been set for the iterative calculation, in order for the simulation to converge.
In the iterative procedure, the specific enthalpy at the hot side outlet of the recuperator can be calculated from the guessed $T_{hot,recp,out}$ and the condensing pressure.
The specific heat [J/kg] transferred from the hot side (to the cold side) of the recuperator is calculated as:

$$q_{recp} = h_{hot,recp,in} - h_{hot,recp,out} \quad (69)$$

While, from the enthalpy balance over the recuperator, the enthalpy at the cold outlet is calculated [J/kg] (as well as the temperature):

$$h_{cold,recp,out} = h_{hot,recp,in} - h_{hot,recp,out} + h_{cold,recp,in} \quad \rightarrow \quad T_{cold,recp,out} \tag{70}$$

Once all the four inlet and outlet temperatures are estimated or known, for every cycle, the average cold and hot side specific heats [J/kgK] can be calculated, and the minimum specific heat addressed (c_{min}). The specific heat exchanged by the recuperator [W] can then be again recalculated as:

$$q'_{recp} = \varepsilon_{recp} \cdot c_{min} \cdot \Delta T_{max,recp} \tag{71}$$

The converge criteria is then evaluated as:

$$conv\_crit = \left| \frac{q_{recp} - q'_{recp}}{q_{recp}} \right| \leq tolerance \tag{72}$$

Once the converge criteria is satisfied, the outlet final cold and hot side outlet temperatures are finally calculated, and the heat recuperated by the recuperator [W] evaluated as:

$$\dot{Q}_{recp} = q_{recp} \cdot \dot{m}_{wf} \tag{73}$$

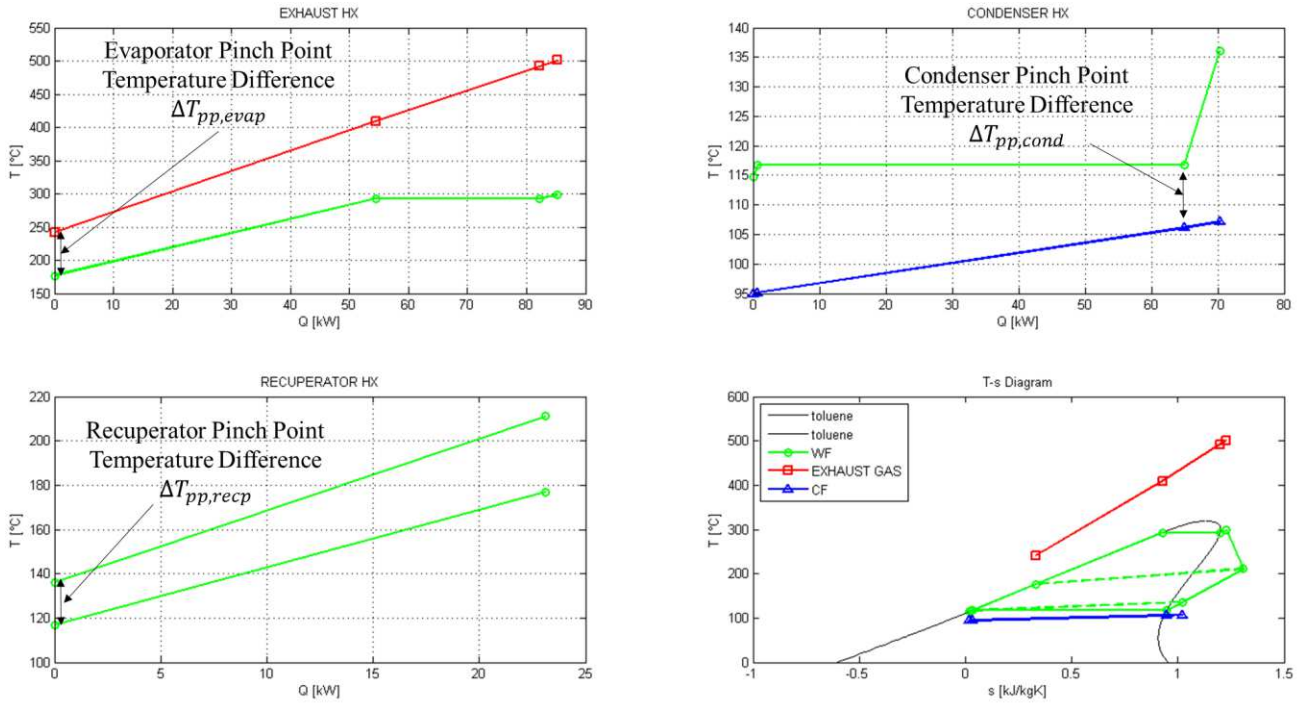

Fig. 44. Example of graphical outputs from the MATLAB ORC routine (recuperated cycle). The pinch point temperature difference for the various heat exchangers can be observed

5.2.2 Second Law Analysis Applied to the ORC

As already introduced, the First Law analysis is not enough to supply all the information needed to fully understand the thermodynamic processes. Because of this, a Second Law analysis has been proposed also for the main components of the ORC system, starting from the thermodynamic calculation results of the First Law.
A complete exergy balance has been applied to the components' control volumes (CV). For the general CV, the availability (or exergy) balance can be written (in steady-state), in a similar way as done for the engine (eq. (30)), as reported in [300]:

$$0 = \sum_j \left(1 - \frac{T_0}{T_j}\right) \dot{Q}_j - \dot{W}_{cv} + \sum_{in} \dot{m}_{in} b_{in} - \sum_{out} \dot{m}_{out} b_{out} - \dot{I}_{cv} \qquad (74)$$

In the next paragraphs, a short description of the application of the proposed balance to the various components has been reported, considering the reference numbers of Fig. 43. For a parallel evaporators system, or different, more complicated, architectures, the same principles and methodology can be applied.

Pump

In the case of the pump, the CV supplied exergy/availability is given by the pump absorbed power: $\dot{A}_P = \dot{W}_P$ [W].
For the calculation of the irreversibilities [W], using the availability balance approach, it is possible to write ($\dot{W}_P$ assumed with positive sign):

$$\dot{I}_P = \dot{m}_{wf} \cdot \left[\left(h_{wf,1} - h_{wf,2}\right) - T_0 \cdot \left(s_{wf,1} - s_{wf,2}\right)\right] + \dot{W}_P \qquad (75)$$

Evaporator

Also the evaporator has been considered adiabatic towards the environment, so the heat transfer term in eq. (74) is set to zero. Extending the equation, using the thermodynamic properties calculated from the First Law analysis, the final formulation is simplified as follows:

$$\begin{aligned} \dot{I}_{evap} = {} & \dot{m}_{hs} \cdot \left[\left(h_{hs,5} - h_{hs,2}\right) - T_0 \cdot \left(s_{hs,5} - s_{hs,2}\right)\right] + \\ & + \dot{m}_{wf} \cdot \left[\left(h_{wf,2} - h_{wf,5}\right) - T_0 \cdot \left(s_{wf,2} - s_{wf,5}\right)\right] \end{aligned} \qquad (76)$$

In order to carry out a thermo-economic analysis, introduced further in the thesis, also the availability terms at the inlet and outlet of every stream across the evaporator must be known, since the costs will be associated to these streams.
The proposed sketch (Fig. 45) can be considered, in order to have a clear idea of the balances applied.

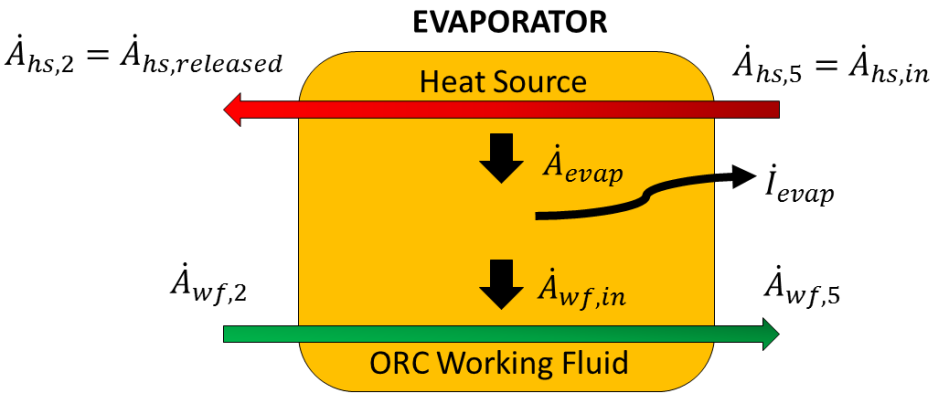

Fig. 45. Evaporator availability streams scheme

Once the irreversibilities are calculated, the availability flowing into the working fluid system [W] can be calculated as follows:

$$\dot{A}_{wf,in} = \dot{m}_{wf} \cdot \left[\left(h_{wf,5} - h_{wf,2}\right) - T_0 \cdot \left(s_{wf,5} - s_{wf,2}\right)\right] \quad (77)$$

and the availability transferred from the heat source [W] (entering the ORC system) from the balance:

$$\dot{A}_{evap} = \dot{A}_{wf,in} + \dot{I}_{evap} \quad (78)$$

The availability still available in the heat source after the ORC [W] is also calculate from the balance:

$$\dot{A}_{hs,released} = \dot{A}_{hs,in} - \dot{A}_{evap} \quad (79)$$

The availability term $\dot{A}_{hs,in}$ is calculated directly from the engine routines (e.g. $\dot{A}_{ENG,exh}$, availability in the engine exhaust gas after the turbine, if, for example, recovering exhaust gas).
While the last two terms related to the availabilities at the inlet and outlet of the working fluid path are calculated from the availability definition:

$$\dot{A}_{wf,i} = \dot{m}_{wf} \cdot \left[\left(h_{wf,i} - h_{0,wf,i}\right) - T_0 \cdot \left(s_{wf,i} - s_{0,wf,i}\right)\right] \quad (80)$$

With the terms $h_{0,wf,i}$ and $s_{0,wf,i}$ calculated at the reference dead state.

Expander

The expander has been considered adiabatic as done for the pump. The useful availability stream is, in this case, the produced power (or produced availability): $\dot{A}_{EXP} = \dot{W}_{EXP}$ [W].
For the calculation of the irreversibilities [W], using the availability balance approach, it is possible to write ($\dot{W}_{exp}$ assumed with positive sign):

$$\dot{I}_{EXP} = \dot{m}_{wf} \cdot \left[\left(h_{wf,5} - h_{wf,6}\right) - T_0 \cdot \left(s_{wf,5} - s_{wf,6}\right)\right] - \dot{W}_{EXP} \quad (81)$$

Condenser

Similar to what has been done for the evaporator, considering the availability balance, the irreversibilities [W] can be calculated as follows (*cf* = cooling fluid):

$$\dot{I}_{cond} = \dot{m}_{wf} \cdot \left[\left(h_{wf,6} - h_{wf,1}\right) - T_0 \cdot \left(s_{wf,6} - s_{wf,1}\right)\right] + \\ + \dot{m}_{cf} \cdot \left[\left(h_{cf,1} - h_{cf,6}\right) - T_0 \cdot \left(s_{cf,1} - s_{cf,6}\right)\right] \quad (82)$$

As done for the evaporator, the availability streams must be calculated also for the condenser, in order to associate the costs to every stream when applying the thermo-economic analysis layer.
A scheme has been proposed also in this case (Fig. 46).
Once the irreversibilities are calculated, the availability flowing outside the working fluid system [W] can be calculated as follows:

$$\dot{A}_{wf,out} = \dot{m}_{wf} \cdot \left[\left(h_{wf,6} - h_{wf,1}\right) - T_0 \cdot \left(s_{wf,6} - s_{wf,1}\right)\right] \quad (83)$$

and the availability entering the cooling fluid system [W] from the balance:

$$\dot{A}_{cond} = \dot{A}_{wf,out} - \dot{I}_{cond} \quad (84)$$

In the same ways as done for the evaporator, the other streams are then calculated from the balance or the definition of availability, in order to be used for the thermo-economic analysis.
In case the cooling fluid is the engine coolant, the availability term calculated from the engine routines must be used for the term $\dot{A}_{cf,in}$.

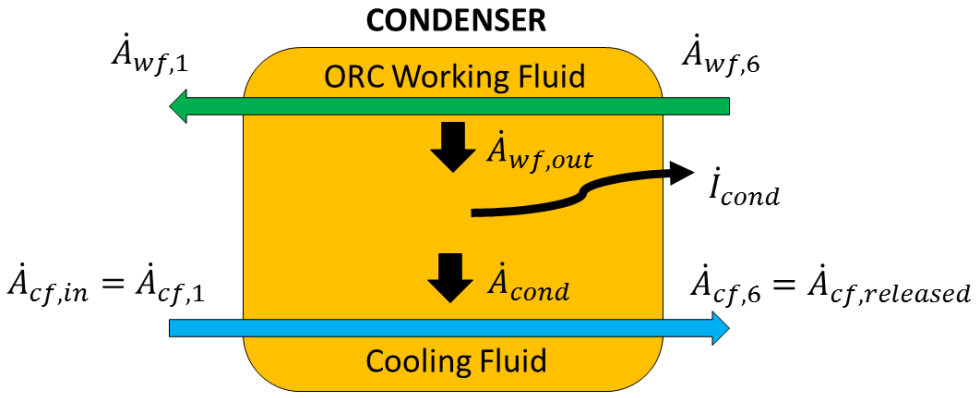

Fig. 46. Condenser availability streams scheme

Recuperator

For the recuperator, the same approach used for the other heat exchangers has been used:

$$\dot{I}_{recp} = \dot{m}_{wf} \cdot \left[\left(h_{wf,hot,in} - h_{wf,hot,out}\right) - T_0 \cdot \left(s_{wf,hot,in} - s_{wf,hot,out}\right)\right] + \\ + \dot{m}_{wf} \cdot \left[\left(h_{wf,cold,in} - h_{wf,cold,out}\right) - T_0 \cdot \left(s_{wf,cold,in} - s_{wf,cold,out}\right)\right] \quad (85)$$

A 0-D thermodynamic modelling approach, as the one proposed, has some limitations, due especially to the assumptions regarding components performance (e.g. expander, pump and heat exchangers). A 1-D physical, or semi-empirical, modelling approach could allow to get rid of some of the proposed assumptions (as in the case of the validated engine model), however increasing the overall computational time. The proposed methodology can however be applied also when using more advanced models, being a post-processing-based approach.
A 0-D modelling approach can be useful, in the first stages of a project, to evaluate and screen different working fluids and combined engine-ORC architectures, while, at the same time, keeping the computational efforts at reasonable levels.
All the proposed calculations can be applied also for more advanced cycle architectures. Generally, as often reported in literature, complicated layouts could lead to calculation instability problems, thus requiring an object-oriented simulation approach, using more advanced commercial software or coding platforms, which are more modular and robust (e.g. Amesim, Modelica-based software).
Once all the various First Law and Second Law related calculations have been performed, the model is ready to calculate the overall engine-ORC combined performance, as well as, it is ready to supply all necessary information for the application of the thermo-economic analysis, which has been described in section 5.3.

5.2.3 Combined Engine-ORC System 1st and 2nd Law Performance Analysis

In this section, some of the main performance parameters, related to the First and Second Law analysis, of engine, ORC and combined engine-ORC have been reported. All these parameters have been intensively used in all the four case studies in order to evaluate the performance of the analysed concepts.
For the engine, Brake Specific Fuel Consumption [g/kWh] and thermal efficiency, $\eta_{th,ENG} = \eta_{ENG,I}$ (or engine First Law efficiency), have already been introduced in section 4.1.2.
For the ORC, the net power output obtained can be calculated as follows:

$$\dot{W}_{ORC,net} = \dot{W}_{EXP} - \dot{W}_{P} \quad (86)$$

and, considering the energy conversion efficiency (mechanical or electrical coupling), the effective power available can be estimated as:

$$\dot{W}_{ORC,net,mech/el} = \dot{W}_{ORC,net} \cdot \eta_{conv} \quad (87)$$

The ORC thermal efficiency (First Law) is calculated as:

$$\eta_{th,ORC} = \eta_{ORC,I} = \frac{\dot{W}_{ORC,net}}{\dot{Q}_{ORC,in}} \quad (88)$$

The combined engine-ORC First Law efficiency can be finally calculated as:

$$\eta_{ENG+ORC,I} = \frac{\dot{W}_{brake} + \dot{W}_{ORC,net,mech/el}}{\dot{m}_{fuel,inj} \cdot LHV} \quad (89)$$

while the combined engine-ORC BSFC [g/kWh] as:

$$BSFC_{ENG+ORC} = \frac{\dot{m}_{fuel,inj}}{\dot{W}_{brake} + \dot{W}_{ORC,net,mech/el}} \quad (90)$$

The percentage improvement, $BSFC_{impr}$, compared to the engine without ORC can be calculated as the relative difference between the two values, as also proposed by Yang *et al.* [301]. The final effect is obtaining more useful power, for the same injected fuel, even though, sometimes, the goal could be obtaining a fuel injection reduction for the same power output. In first approximation, in this work, the first approach has been used.
For the Second Law analysis, a very similar approach is used. The engine Second Law efficiency is calculated considering the injected fuel availability as:

$$\eta_{ENG,II} = \frac{\dot{W}_{brake}}{\dot{m}_{fuel,inj} \cdot a_{fuel,ch}} = \frac{\dot{W}_{brake}}{\dot{A}_{fuel,ch,inj}} \quad (91)$$

While, for the ORC, in a similar way, considering the recovered availability, $\dot{A}_{ORC,in}$,:

$$\eta_{ORC,II} = \frac{\dot{W}_{ORC,net}}{\dot{A}_{ORC,in}} \quad (92)$$

Finally, also the combined engine-ORC system Second Law efficiency can be calculated as:

$$\eta_{ENG+ORC,II} = \frac{\dot{W}_{brake} + \dot{W}_{ORC,net,mech/el}}{\dot{m}_{fuel,inj} \cdot a_{fuel,ch}} = \frac{\dot{W}_{brake} + \dot{W}_{ORC,net,mech/el}}{\dot{A}_{fuel,ch,inj}} \quad (93)$$

Other specific parameters can be used to evaluate the performance, in particular, of the ORC systems. Some examples can be found in Branchini *et al.* [302] and in the proposed case studies.

As already introduced, the First and Second Law analysis are necessary steps in order to implement a techno and thermo-economic analysis.
A short overview of the principles of techno ad thermo-economics has been proposed in the next section, focusing, in particular, on engine-ORC applications. However, the same ideas can be adapted to any kind of thermodynamic system, and usually the most considered applications are those related to stationary power generation systems, as reported by Bejan *et al.* [303].

5.3 Techno and Thermo-Economic Analysis Approach

Thermo-economics (or sometimes called exergo-ecomomics) is the science which combines together exergy (Second Law) analysis with conventional cost analysis, in order to assess and optimize the performance of energy conversion systems both from a thermodynamic and financial perspective. Even though in literature the terms are often interchanged, thermo-economics should not be confused with techno-economics, which does not refer to exergy-based methodologies.
Exergy-based analysis, as the one proposed in the previous sections, helps to understand where inefficiencies concentrate in the system, calculating exergy streams, exergy destruction and exergy losses terms. However, only Second Law analysis does not help in understanding how much the inefficiencies' cost impact on the system design is, as well as the cost of production of the system main product streams (e.g. engine brake power or ORC net power output in the case of the systems proposed in this work). With a thermo-economic approach it is also possible to understand the cost formation process and the flow of costs in the system, optimize specific variables or single components, design cost-efficient systems in the first phases of a project or, even diagnose system inefficiencies, defect or faults, and propose solutions to improve the performance (Bejan *et al.* [303]).
The common ORC design approach, for engine waste heat recovery, is usually based on the following steps:

- assessment of the engine available heat sources and thermodynamic boundary conditions;
- preliminary thermodynamic feasibility study (layout and working fluid choice/optimization, performance evaluation);
- main components choice and accurate modelling;
- development of adequate controlling strategies;
- prototype implementation and system testing;

However, the common procedure has some drawbacks, because the ORC system will result in just a retrofitting of the existing engine, thus leading to non-optimized combined engine-ORC powertrain performance.
For this reason, the application of energy, exergy, techno and thermo-economic techniques can help to develop more efficient and optimized combined engine-ORC powertrain concepts. Indeed, a detailed Second Law analysis can assess the combined system irreversibilities, while a techno and thermo-economic approach can assess and optimize concept costs, still considering the thermodynamic performance of the system.
During a system thermodynamic analysis, when we think about energy (First Law), we think about "quantity", while exergy (Second Law) introduces a concept linked to the potential useful work of a certain energy stream, thus allowing also to introduce the concept of "quality", as reported by Valero *et al.* [304].
As introduced by Valero *et al*., many researchers and authors agree that exergy, and not energy, is the right thermodynamic property to which costs must be allocated, because it accounts for the quality of the energy, and often, also the in the human society, the cost is associated to the quality of a product. An example, indeed, could be a CHP plant (Combined Heat and Power), in which, in general, the electricity is sold at a much higher price than heat. This is also reflected in the exergy accounting of the two energy streams. Two streams are indeed thermodynamically equivalent, or it is possible to get one from the other without additional consumption of energy resources if, and only if, they have the same exergy content. This is generally not valid, for example, for heat and work.
Moreover, as proposed by Rosen *et al.* [305], exergy can be more easily linked to environmental analysis (exergo-environmental analysis), since it is a measure of the departure of a thermodynamic process from the environmental conditions, thus also allowing to link the overall analysis to, for example, an emission impact evaluation (through a combined use of also LCA analysis, Life-Cycle-Analysis).

It is out of the scope of this work to report all theory and history about thermo-economic methodologies, which can be deepened by the reader, from authors such as Bejan, Valero, Frangopoulos, Von Sparkowsky, Tsatsaronis. Just an example of cost allocation using energy and exergy has been reported in Fig. 47, for a cogeneration plant producing steam, in order to show the differences when using one or the other thermodynamic parameter [303].

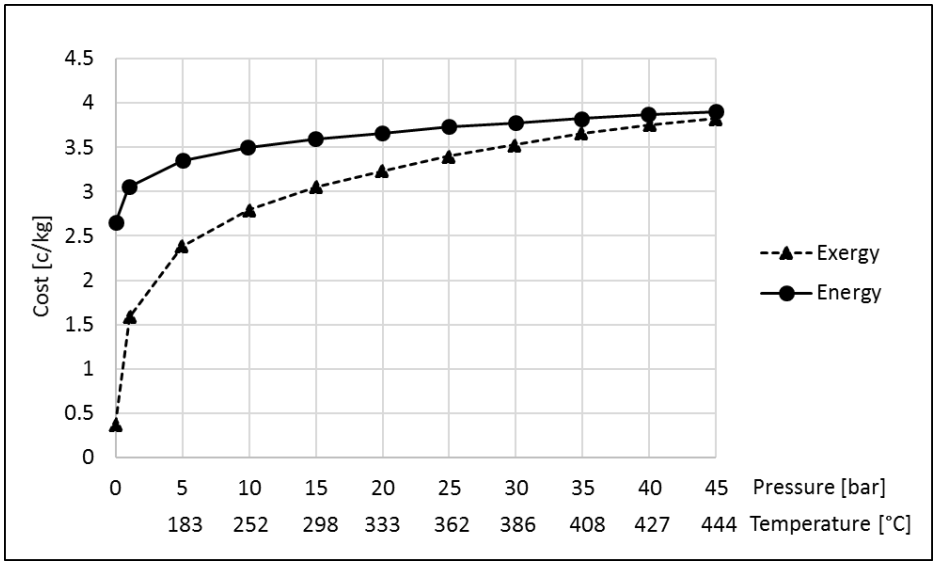

Fig. 47. Example of difference between energy and exergy costing. Cogenerating steam production specific cost vs turbine outlet pressure (or temperature). Elaborated from Bejan et al. [303]

As can be evinced, at very low pressure of 1 bar, the unit cost, on energy basis, for steam is close to 3, even though the produced steam has very limited usefulness due to the low pressure and temperature (low quality). Unlike exergy, energy costing, indeed, does not make distinctions about the usefulness of the energy transfer process (it is not sensible to the quality of the steam), still addressing a high cost to the poor-quality steam. Unlike energy, the exergy costing basis shows that high-pressure (and high-temperature) steam has a much higher value per unit of mass compared to the low-pressure (and low-temperature) steam. In case of exergy basis, the cost per unit mass also approaches rapidly zero, as the thermodynamic usefulness of steam (exergy) goes towards zero (dead state). As proposed by many researchers, this should be the right behaviour that would be expected from a rational thermodynamic costing approach.
Before applying a techno or thermo-economics approach, as a preliminary step, the main ORC components (in particular heat exchangers and expansion machines) performance should be assessed more in details, in order to extract some analysis parameters which, in fact, represent the dimensions/performance of the components (e.g. heat transfer area for the heat exchanger, power or volume flow for the expander and the pump). These parameters are then, in literature, usually associated to suitable cost correlations which allow to estimate the cost of the components (economic analysis), varying the design operating conditions chosen.

5.3.1 Components Performance Analysis

As introduced in the previous section, in order to apply a techno or thermo-economic methodology, it is necessary to assess the performance of the main components more in the details.
The best solution would be to develop detailed 1-D physical (or semi-empirical) models for the heat exchangers and more advanced and accurate models for the expansion machine (and eventually the

pump). Several publications are available in literature about the topics. However, for the first stages of a project, in which a clear architecture and the different components types are not yet chosen, and in order not to dramatically increase the simulation computational efforts, it is enough, especially when comparing different ORC (and engine) concepts and working fluids, to stick to 0-D thermodynamic formulations, while, at the same time, introducing some parameters able to describe a bit more in the details the components performance, as proposed also by Panesar [306] and Bejan *et al.* [303]. For the next stages of a development project, more detailed components models are needed to assess the system with a higher level of accuracy. This is left for future developments (e.g. Ricardo is planning to embed Modelica models into the IGNITE simulation platform in order to allow to accurately model different physical sub-systems in an overall powertrain co-simulation approach).

5.3.1.1 Heat Exchangers

In order to calculate the heat exchanger heat transfer area, A_{HX} [m^2], which then is used as main dependent variable to calculate the component's cost, through the use of appropriate cost correlations, it is necessary to estimate the overall heat transfer coefficient, U_{HX} [W/m^{2}K], which is used in the following formula, in order to estimate the heat transfer area [303,307]:

$$\dot{Q}_{HX} = U_{HX} \cdot A_{HX} \cdot \Delta T_{LMTD} \cdot F \qquad (94)$$

with:

- $\dot{Q}_{HX}$: heat transferred (thermal power) [kW]. Calculated from the First Law analysis, applying adequate energy balances over the entire heat exchangers;
- U_{HX}: overall heat transfer coefficient [W/m^{2}K];
- A_{HX}: heat transfer area [m^2];
- ΔT_{LMTD}: Log Mean Temperature Difference [°C or K];
- F: correction factor, dependent on the heat exchanger configuration (1 assumed for complete counter-flow arrangement);

Considering a counter-flow heat exchanger, in first approximation, the Log Mean Temperature Difference can be calculated as [307] (considering the inlet and outlet temperatures of the hot and cold streams):

$$\Delta T_{LMTD} = \frac{\left(T_{hot,in} - T_{cold,out}\right) - \left(T_{hot,out} - T_{cold,in}\right)}{ln\left(\frac{T_{hot,in} - T_{cold,out}}{T_{hot,out} - T_{cold,in}}\right)} \qquad (95)$$

Typical overall heat transfer coefficients for different heat transfer conditions (e.g. gas-liquid, liquid-liquid, etc) and heat transfer equipment (e.g. plate, shell & tube, air-condensers, etc) can be found in literature, and can be used in first approximation as a starting point, assuming a constant overall heat transfer coefficient, in order to propose different concepts comparisons.

As already introduced, for more detailed calculations, the detailed geometry of the particular type of heat exchanger should be taken into consideration, applying convective and conductive heat transfer correlations for the mono-phasic and bi-phasic zones, fouling factors and calculating the thermodynamic and transport properties of the working fluids along the heat exchanger dimensions.

In this work, and considering the preliminary phases of a project proposed in the described methodology, the first approach has been used, and a review of the literature has been carried out, in order to create a quite complete summary of different heat transfer scenarios (type of heat exchanger

and type of heat transfer process), in order to then extract a feasible average value of the overall heat transfer coefficient to be used in the heat transfer areas evaluations.
Some examples have been reported in Fig. 48 and Fig. 49. In order to keep the analysis results short, the other values and ranges, together with the references have been reported in Tab. 17, to summarize the data which can be considered, in first approximation, for the heat transfer performance.

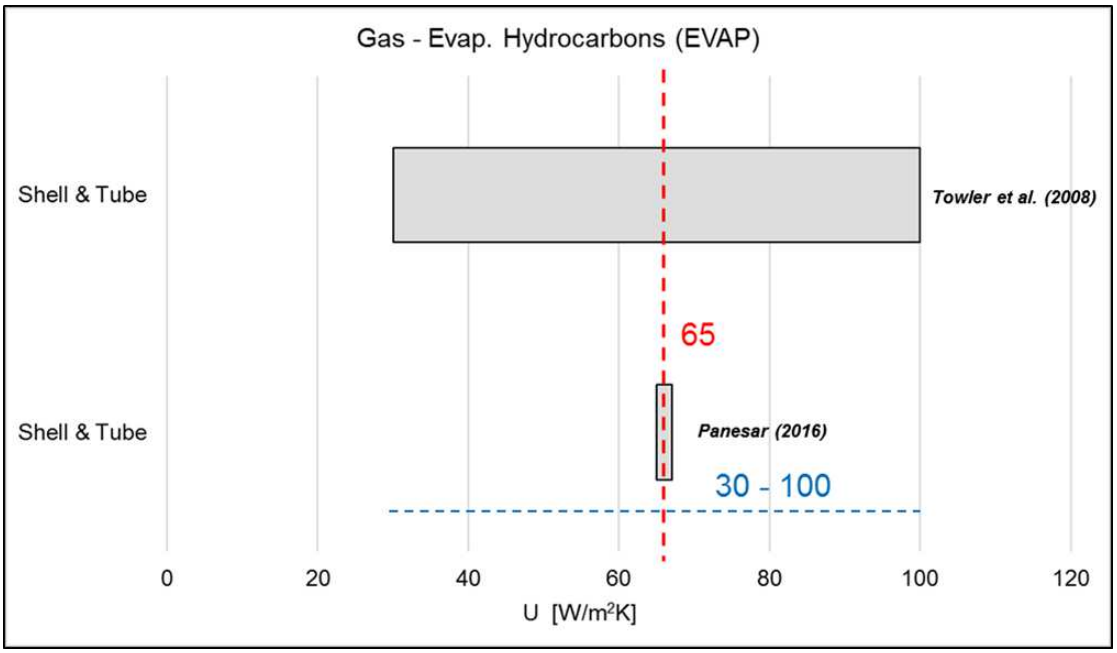

Fig. 48. Overall Heat Transfer Coefficient (U) for Gas - Evaporating Hydrocarbons (Evaporator)

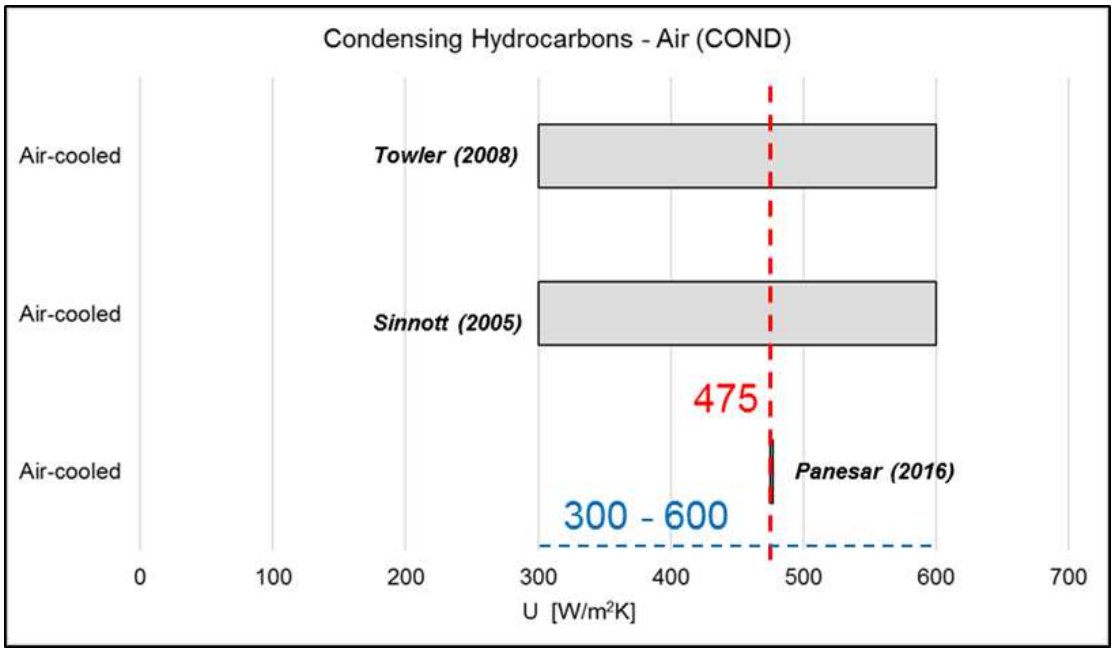

Fig. 49. Overall Heat Transfer Coefficient (U) for Condensing Hydrocarbons - Air (Condenser)

Heat Exchanger	Type	Hot Fluid	Cold Fluid	U_{HX} Range [W/m^{2}K]	U_{HX} Assumed Value [W/m^{2}K]	References	
Evaporator	S&T	Gas	Water-Steam	105	105	Shah *et al.* (2003)	[308]
Evaporator	S&T	Gas	Organic Fluids	93 – 101	97	Astolfi (2014) Shah *et al.* (2003)	[308,309]
Evaporator	S&T	Gas	Evap. Hydroc.	30 – 100	65	Towler *et al.* (2008) Panesar (2016)	[306,310]
Evaporator	Coaxial Coil-Tubes	Water	Organic Fluids	59 – 263	161	Eyerer *et al.* (2016)	[156]
Evaporator	S&T	Water	Organic Fluids	500 – 600	550	Astolfi (2014) Shah *et al.* (2003)	[308,309]
Evaporator	Plate	Water	Organic Fluids	2000 – 9000	5500	Hu *et al.* (2015) Fu (2016)	[311,312]
Condenser	S&T	Organic Fluids	Water	250 – 1200	852	Suarez *et al.* (2016) Sinnott (2005) Incropera et al. (2007) VDI Atlas (2010) Perry's (1999) Peters (1991) Towler (2008)	[307,310,313–317]
Condenser	Air-cooled (Coils)	Organic Fluids (Refrig.)	Air	4 – 46	25	Eyerer *et al.* (2016)	[156]
Condenser	Air-cooled (AC)	Organic Fluids (Refrig.)	Air	400 – 1000	700	Yeon Yoo *et al.* (2004)	[318]
Condenser	Air-cooled (AC)	Cond. Hydroc.	Air	300 – 600	475	Panesar (2016) Sinnott (2005) Towler *et al.* (2008)	[306,310,314]
Condenser	S&T	Cond. Hydroc.	Water	764	764	Shah *et al.* (2003)	[308]
Condenser	S&T Plate	Water Steam	Water	500 – 6000	4000	Suarez *et al.* (2016) Sinnott (2005) Shah *et al.* (2003) Astolfi (2014) Incropera et al. (2007) VDI Atlas (2010) Perry's (1999) Peters (1991) Towler (2008)	[307–310,313–317]
Heat Exchanger	S&T	Water	Water	800 – 2839	1820	Sinnott (2005) Shah *et al.* (2003) Incropera et al. (2007) Peters (1991) Towler *et al.* (2008)	[307,308,310,314,317]
Heat Exchanger	Plate	Water	Water	5000 – 7500	6250	Sinnott (2005) Towler *et al.* (2008)	[310,314]
Heat Exchanger	S&T	Organic Fluids	Organic Fluids	100 – 500	300	Suarez *et al.* (2016) Sinnott (2005) Shah *et al.* (2003) Perry's (1999) Peters (1991) Towler (2008)	[308,310,313,314,316, 317]
Heat Exchanger	Plate	Organic Fluids	Organic Fluids	2500 – 5000	3750	Sinnott (2005) Towler (2008)	[310,314]
Heat Exchanger	S&T (Econ.)	Gas	Water	20 – 426	223	Suarez *et al.* (2016) Shah *et al.* (2003) Peters (1991) Towler (2008)	[308,310,313,317]
Heat Exchanger	Plate (Econ.)	Gas	Water	20 – 60	40	VDI Atlas (2010)	[315]
Heat Exchanger (e.g. RECP)	Plate	Vap. Hydroc.	Liq. Hydroc.	200	200	Panesar (2016)	[306]
Heat Exchanger	S&T	Gas	Organic Fluid	99	99	Shah *et al.* (2003)	[308]
Heat Exchanger	S&T	Gas	Oil	120	120	Suarez *et al.* (2016)	[313]
Heat Exchanger	S&T	Organic Fluids	Water	250 – 852	551	Shah *et al.* (2003) Peters (1991) Towler (2008)	[308,310,317]

Heat Exchanger	Plate	Organic Fluids	Water	2000 – 4500	2350	Sinnott (2005) Towler (2008)	[310,314]
Radiator	Finned Tube	Water	Air	25 – 50	38	Incropera et al. (2007)	[307]

Tab. 17. Data summary for preliminary heat transfer performance estimations

Generally, for gas-liquid heat transfer, shell & tube (S&T) and fin and tube heat exchangers are more suitable than plate heat exchangers and have higher heat transfer performance. For example, for engine exhaust gas heat recovery, usually fin and tube or shell & tube heat exchangers are used. For liquid-liquid heat transfer, plate heat exchangers are more compact and have higher performance compared to shell & tube.
The change of phase (evaporation or condensation) enhances the performance (higher overall heat transfer coefficient) respect to the cases without phase change.
Air-cooled heat exchangers are generally less performant than water-cooled one. For this reason, fins are usually used in order to increase the heat transfer area and improve the process, at the same time trying to keep the heat exchanger compact (e.g. radiators and AC condensers).
The same is proposed, as already introduced, for gas-fluids evaporators (e.g. exhaust gas driven boilers, or ORC engine-tailpipe evaporators). In order to avoid bulkier components, fin & tube heat exchangers are under development and optimization, in automotive applications, following the direction of what is done for EGR coolers. Reliability, leakage-free capabilities and capacity of achieving ORC fluid side high evaporation pressure levels are characteristics which are essential in order to develop efficient and compact automotive waste heat recovery systems.
Of course, when considering in the analysis the evaporator-engine backpressure effect, more appropriate and accurate models should be used and developed, rather than preliminary overall heat transfer coefficients data. When detailed geometry-dependent models are available, also a more accurate heat transfer area estimation is possible, but generally increasing the computational time required for the analysis.

5.3.1.2 Expanders

One of the most important components of an ORC system is the expansion machine, which drastically influences the performance of the overall system, depending on the achievable component's efficiency. An introduction about several different expansion machine technologies has been already proposed in section 4.2.2.3. The purpose of this section is giving some hints about the possible performance and efficiency levels expected for this component in order to proposed reliable assumptions during the overall system simulations.
It is out of the scope of this work to investigate in the deep the expansion machine performance, an analysis of which, through adequate validated models and experimental campaigns, is however required when evaluating the performance of the entire ORC system under off-design conditions. This could be considered a step ahead compared to the methodology proposed, which is more useful when investigating different engine-ORC combined concepts, in order to choose the most appropriate for further developments and detailed evaluations.
Between the most used and considered expansion machine technologies for marine and commercial vehicles applications are turbo-expanders, piston expanders and scroll expanders. The first is usually used for higher expansion ratios and generally higher power output systems (e.g. marine applications), while the second and third are generally considered for smaller applications such as automotive of

micro-ORC (e.g. solar, residential), in which smaller power outputs (and possibly lower expansion ratios) can be expected.
As reported also by Lemort *et al*. [319], different possibilities are available to evaluate the performance of an expansion machine, based on the overall cycle thermodynamic boundary conditions:

- using models:
  - *empirical*: characterized by low computational time, but strictly linked to the calibration conditions used and not accurate out of the calibration range;
  - *semi-empirical*: characterized by an improved physical meaning and more accurate out the calibration range, but more computationally expensive;
  - *deterministic*: characterized by the application of mass and energy balances, but more computationally expensive than the previous mentioned models. Generally used in the development phases of the physical components;
- using correlations and values from the analysis of experimental data and data available from literature. This approach has been used in this work in order to propose feasible assumptions for the isentropic efficiency parameter used in the proposed cycle simulation models;

Examples of models of expansion machines and, in particular, for scroll and piston expanders have been proposed in literature by several authors, such as Clemente *et al.* [196,201] or Glavatskaya *et al.* [320].
The optimal expansion ratio at which the expansion machine shows the best performance (e.g. highest isentropic efficiency) depends on the geometrical properties of the expander itself and it is a common characteristics of every positive displacement expander, such as, for example, piston and scroll expanders. This optimal pressure ratio is often called built-in expansion ratio ($r_{p,opt}$) and should match the ORC cycle operational pressure ratio ($p_{exp,in}/p_{exp,out}$), in order to achieve the best system performance. Indeed, the more the cycle pressure ratio differs from the built-in expansion ratio, the more the component (and system) performance will be affected, due mostly to two sources of losses: the over-expansion losses ($p_{exp,in}/p_{exp,out} < r_{p,opt}$) and the under-expansion losses ($p_{exp,in}/p_{exp,out} > r_{p,opt}$). Generally, the over-expansion losses are more critical than the under-expansion losses regarding the impact on the expander isentropic efficiency. For this reason, it is usually better, when not knowing exactly the expected cycle design pressure ratio, to choose, or design, an expansion machine which possibly operates in the under-expansion losses region, rather in the over-expansion losses region, if an optimal expansion machine cannot be envisaged, due for example, to very variable operating conditions.
Due to this typical trend of the positive displacement expander isentropic efficiency, it is very difficult, in the cycle design phases of a project (as those proposed for the developed methodology explained in this work) to have an accurate idea of the component realistic performance. For this reason, usually, in thermodynamic feasibility studies, a fixed isentropic efficiency is imposed, sticking to feasible values from literature data. Once the cycle has been designed and the expander chosen (or designed), based on the heat source and sink boundary conditions, a more detailed analysis of the expansion machine processes should be performed in order to analyse the off-design conditions performance (at least using polynomial regression forms coming from experimental data).
For these reasons, in the proposed case studies, considering the design conditions assumed (no off-design analysis), a fixed isentropic efficiency approach has been used in order to simulate the expander machine performance. The assumptions used are based on literature data, some of which have been reported, as a summary, for scroll and piston expansion machines in the following graphs and tables, to visualize in which ranges of values are the performance of the expander expected to fall. Some preliminary ranges of values can be also envisaged from Macchi *et al.* [112] and have been reported in Tab. 18.

Technology	Isentropic Efficiency at Design [-]
Piston / Scroll (positive displacement)	0.65 – 0.80
Turbo	0.70 – 0.85

Tab. 18. Ranges of typical expander isentropic efficiency values at design conditions

Piston

The data gathered from literature have been reported in Tab. 19 and Fig. 50, and they are related to both experimental and modelling results.

References	Built-In Exp. Ratio	Temperature Range [°C]	High Pressure Range [bar]	Power Output [kW]	Rotational Speed [rpm]	Model / Experiment	Fluid
Winandy *et al.* [321] (compressor)	n.a.	30 - 50	18	6	366 - 665	Experiment / Model	Refrigerant (n.a.)
Clemente *et al. (2011)* [196]	5 - 7	150 - 200	n.a.	1 - 4	1500	Model	R245fa / isopentane
Glavatskaya *et al. (2012)* [320]	n.a.	280 – 320	n.a.	2 - 7	500 - 6000	Semi-emp. Model	Water
Kim *et al. (2014)* [322]	10	300	35	3 - 4	2450	Model / Theoretical	Water
Oudkerk *et al.(2015)* [323]	n.a.	n.a.	30	2	1000 - 4000	Experiment / Semi-emp. Model	R245fa
Oudkerk (2016) [324]	n.a.	n.a.	30	2	1000 - 4000	Experiment / Semi-emp. Model	R245fa

Tab. 19. Gathered data for piston expanders performance

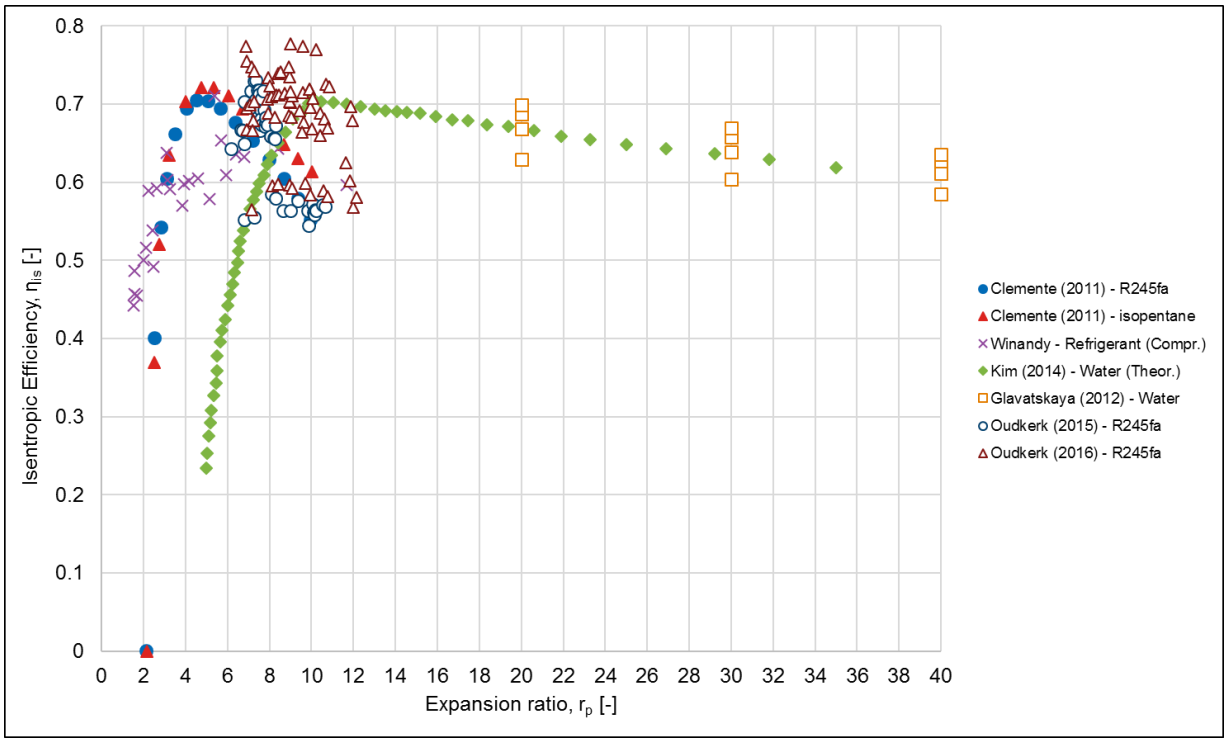

Fig. 50. Graphical representation of piston expanders isentropic efficiency vs expansion ratio (literature data)

Scroll

Source	Built-In Exp. Ratio	Temperature Range [°C]	Pressure Range [bar]	Power Output [kW]	Rotational Speed [rpm]	Model / Experiment	Fluid
Winandy et al. (2002) [325]	n.a.	18 - 140	2.4 – 25.3	11	2800 - 2900	Exp. / Semi-Emp. model	R22
Lemort et al. (2009) [326] Quoilin et al. (2010) [327]	4.05	66.4 – 165	1.4 – 11.1	1.8	1771 – 2660	Exp. / Semi-Emp. model	R123
Clemente et al. (2012) [201]	3.5	40 – 200	n.a.	1.5	3000	Model	R245fa / isopentane
Declaye et al. (2013) [328]	3.95	150	30	2	2000 – 3000	Exp. / Pacejka's Equation empirical regression	R245fa
Mendoza et al. (2014) [329]	1.9	27 – 91	1 – 4	0.3 – 0.8	2000	Exp.	Air / Ammonia
Giuffrida (2014) [330]	4.5	101 – 165	5.5 – 11.1	2	1771 – 2660	Model	4 refrig.
UniTS (2014)	*4*	*25 – 150*	*7 - 16*	*1 - 2*	*5000 - 7750*	*Exp.*	*R245fa*
Usman et al. (2015) [331]	3.5	70 – 135	1 - 12	1	3400 – 3500	Exp.	R245fa
Yun et al. (2015) [332]	4.5	24 – 120	13	1.8	1200	Exp.	R245fa
Taccani et al. (2016) [333]	*4*	*90 – 150*	*n.a.*	*0.4 – 0.7*	*5000 – 7750*	*Exp.*	*R245fa*
Braimakis et al. (2017) [334]	3.5	40 – 200	n.a.	n.a.	3000	Model regression	R245fa

Tab. 20. Gathered data for scroll expanders performance

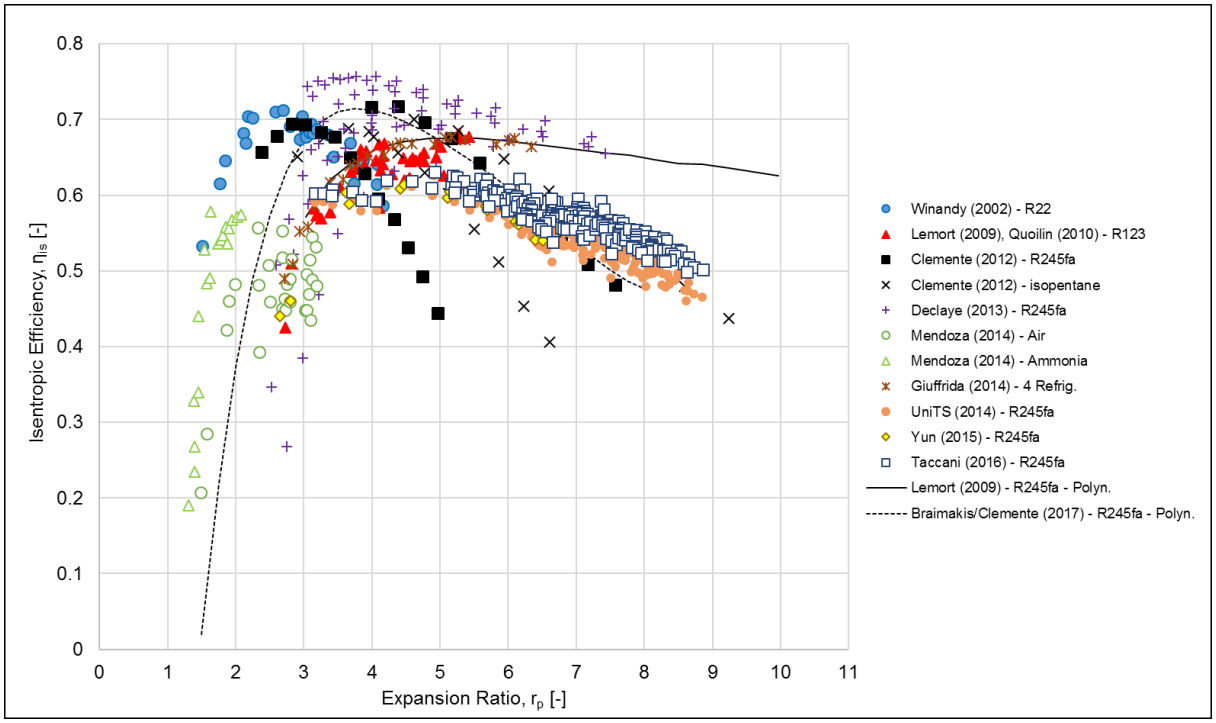

Fig. 51. Graphical representation of scroll expanders isentropic efficiency vs expansion ratio (literature data)

The data for scrolls have been reported in Tab. 20 and Fig. 51. Some of the measured performance of the scroll machines derive also from tests carried out on test bench (or experimental activities) of the

University of Trieste in the *Enesys Lab* laboratory (reported in *italics* in the table), and are comparable, at least in range, to possible expected engine coolant heat recovery temperature conditions.
Both scroll and piston expanders show maximum isentropic efficiency values (at the built-in expansion ratio) around 70% or slightly higher for optimized components. The values of the efficiency are then decreasing for higher or lower expansion ratios due to the under and over-expansion losses (and due also to other losses such as leakage, friction and thermal losses). For these reasons, scroll expanders are generally more suitable for low temperature heat recovery through small systems (below 5 kW), while piston expanders can be more suitable for higher temperature heat recovery systems as those proposed for commercial vehicles applications (up to maximum 20 kW). Turbo-expanders can be considered a better choice for higher power output systems, such as those for marine or stationary applications.
Scroll expanders show generally built-in expansion ratios between 3 and 5, while piston expanders show tendentially higher values, from 6 to 14, but theoretically being able to ensure a high isentropic efficiency (above 60-70%) also at higher ratios up to 20 or slightly more.
For higher pressure ratios, generally turbo-expanders should be used, with isentropic efficiencies which could theoretically reach levels up to 85%, as reported by Macchi *et al.* [112], for well-designed and controlled machines at the design speed. Multiple stages expansion machines could be required.
In the case studies reported in this work, isentropic efficiencies at design point of around 70 to 80% have been considered, depending if positive displacement or turbo-machines are assumed. Sometimes values of 70% have been assumed for turbo-machines also, in order to account for possible inefficiencies and stick to more realistic values (precautionary assumption).
For the pump, usually, a constant value of 60% has been used, especially considering that the pump power consumption is generally much lower than the expander generated power, thus with lower impact on the overall system power balance.
As already introduced, when considering off-design system analysis, a more detailed expansion machine performance assessment is required, for example, through the development and validation of appropriate semi-empirical or deterministic models.

5.3.2 Economic Analysis

After having estimated the performance and dimensions of the components, extracting the main representative parameters (e.g. heat transfer area, power absorbed or produced, volume flows) it is necessary to proceed with an economic analysis, developing reliable cost correlations which allows the designer to estimate the costs of the overall system and of the single components.
In order to compare the various system cost-to-performance benefit, very often in literature the SIC parameter is used (Specific Investment Cost, [$/kW or €/kW]). This parameter is usually calculated as the ratio between the investment cost of the system [$ or €] and the net power output produced [kW], as:

$$SIC = \frac{C_{inv}}{\dot{W}_{net}} \tag{96}$$

The investment cost of the system is usually the sum of several different cost voices such as [303]: PEC (Purchased Equipment Cost) of the main components, maintenance, instrumentation and controls, electrical equipment and materials, services, facilities, engineering and supervision, contractors, contingencies, start-up costs, licensing, research and development, and so on.

All these costs are sometimes difficult to be estimated, and some methodologies, not described in this work, can be found is references such as: Turton [335], Peters [317], Bejan [303], Towler [310]. These references allow to calculate the PEC for the main system components through appropriate cost correlations and factors related to operational system behaviour (pressures, temperatures, materials). The other costs can also be estimated, mostly based on some percentage assumptions.
In many ORC related techno and thermo-economic studies in literature, the Turton reference is very often used. However, the correlations proposed are coming from the chemical industry sector, thus being not completely suitable for ORC systems, or at least, being more compatible with large systems as those developed for stationary, marine and geothermal applications. Moreover, Bejan *et al.* [303] and Lemmens [336,337] declare how the cost estimations can deviate from the real cost data up to ±50%, thus being suitable mostly for the preliminary estimation phases of a project, when different concepts are evaluated and compared.
When considering smaller size applications, such as small CHP units or automotive ORCs (e.g. commercial vehicles as the application proposed in the fourth case study in this work), cost correlations literature is rather poor, due to the development phase in which these systems, and the relative components, are. Moreover, in order to have an accurate estimation of the main components' costs, a detailed suppliers' analysis should be carried out, trying to keep data always as more up-to-date as possible. Finally, but not less important, a scale economy due to the expected large mass production of the proposed systems should be considered, leading to a general cost decrease effect, which can again be observed from a detailed suppliers' market analysis.
For all these reasons, in automotive ORC techno and thermo-economic studies, the best choice should be the use of correlations developed from suppliers' quotations and developing/consulting companies' analysis. However, these data are generally kept confidential. In this work, some correlations from literature have been used, corrected following Ricardo's suppliers' analysis experience, in order to reflect in a more accurate way the range of costs expected for a system developed for commercial vehicles applications. However, the methodology proposed can be used also for other applications (e.g. marine, stationary, geothermal, biomass) when adequate cost correlations are available.
Moreover, in the application proposed in the fourth case study, only the PEC for the main ORC components have been used in order to estimate the cost of the ORC system, not considering maintenance and other costs. PEC should be, however, the main voice of cost.
The main source of the cost correlations used in the fourth case study is the work reported by Panesar [306], who is proposing cost formulas for ORC systems components to be applied to automotive HDDE applications (in particular trucks).From a discussion with the author, the correlations are declared to come from a review of data coming from commonly used books (as those already cited) and journals data, and adjusted based on a suppliers' data analysis and enquiries but, at the same time, considering other possible similar industry sectors (in particular turbochargers and refrigeration systems manufacturers). The large amount of data collected has been then fitted with adequate regression equations (±20% variations declared) accounting also for a mass production scenario.
Other correlations have been considered, in particular for a possible scroll expansion machine, retrofitted from an AC compressor, and for the pump, from Quoilin *et al.* [338].
However, especially regarding the correlations proposed by Panesar, after an internal discussion in Ricardo, it has been decided to scale the correlations based on the data from Ricardo suppliers' analysis experience, from previous projects such as the TERS and the Volvo ones [260,339]. Indeed, the results reported by Panesar leads to a general SIC range of values (around 1792 - 2906 $/kW) which has not been considered adequate for a scale economy-developed automotive ORC system. The proposed considerations are also supported by the data related to systems developed by AVL, reported in open literature [340,341]. Other considerations about possible SIC values and different applications have been reported in section 5.3.3.
The main ORC modified cost correlations, together with some other fixed costs for other sub-systems or components, from Ricardo's experience, have been collected in Tab. 21. The costs have been all

reported in US dollars [$], and when a Euro-to-Dollar conversion was needed, a factor of 1.15 has been used. The costs have been considered at the actual time in which the work described in this thesis has been carried out, and no actualization index, such as the CEPCI (Chemical Engineering Plant Cost Index), has been used, as often reported in literature.
The cost correlations have been considered suitable for the range of operating parameters expected for an ORC recovering waste heat from a medium-heavy duty commercial vehicle engine, as declared also by Panesar [306].

Component	Type/Design	Reference Parameter	PEC Cost Correlation [$]	Reference
Evaporator	S&T	A_{evap} [m^2]	$400 + 30 \cdot A_{evap}$	Panesar [306] (modified Ricardo)
Evaporator / Condenser / Recuperator	Plate	A_{HX} [m^2]	$600 + 12.2 \cdot A_{HX}$	Panesar [306]
Condenser	Air-cooled	A_{cond} [m^2]	$190 \cdot A_{cond}^{0.42}$	Panesar [306] (modified Ricardo)
Expander	Piston	$\dot{W}_{exp}$ [kW]	$500 + 12.5 \cdot \dot{W}_{exp}$	Ricardo / AVL [341]
Expander	Scroll	$\dot{V}_{exp,in}$ [m^3/s]	$1.15 \cdot 1.5 \cdot (225 + 170 \cdot \dot{V}_{exp,in})$	Quoilin *et al.* [338]
Expander	Turbo	$\dot{W}_{exp}$ [kW]	$1000 + 40 \cdot \dot{W}_{exp}$	Panesar [306] (modified Ricardo)
Pump	Radial	$\dot{W}_{pump}$ [kW]	$500 \cdot \left(\frac{\dot{W}_{pump}}{300}\right)^{0.25}$	Quoilin *et al.* [338] Bejan *et al.* [303]
Fluid tank	/		290	Ricardo
Valves	/		750	Ricardo
Piping	/		230	Ricardo
Control & Instrumentation	/		230	Ricardo

Tab. 21. Cost correlations and fixed costs used for the techno and thermo-economic study in case study 4 (commercial vehicle application)

For the piston expander, the correlation has been considered linear based on the expander power, with absolute values trends reflecting data reported by AVL and by Ricardo costs estimation for a 2 cylinders' engine without injector and spark-plug.
All expansion machines have been considered with mechanical power production coupled to the engine crankshaft. Following Ricardo suppliers' analysis, if considering electricity production through a generator, a factor of 1.6 should multiply the cost correlation, reflecting the increased cost of a system with electricity generation.
From Ricardo's analysis, it is also possible to observe how, generally, system valves are leading to non-negligible costs.
The fluids tank, valves, piping and control and instrumentation costs have been estimated from Ricardo's previous projects data and have been considered fixed for every ORC concept analysed in case study four, supposing the systems would be very similar in terms of size. The approximation is feasible for a first project phase estimation.

As reported by Panesar [306], ORC fluids costs are generally low compared to the components' costs, but should be also considered in the analysis. The costs of some the considered fluids have been reported in Tab. 22. The cost of R245fa and R1233zd(E) has been considered the same in first approximation.

Fluid	PEC fluid ($/L)	References
Toluene	5.1	Panesar [306]
MM	7.5	Panesar [306]
Water	0	Assumed free-of-charge
Ethanol	2	Astolfi [309], marked prices for ethanol
R245fa	20	University of Trieste experience, Astolfi [309]
R1233zd(E)	20	

Tab. 22. ORC working fluids costs

In the proposed fourth case study, a fixed 20 L volume of working fluid has been assumed, after internal Ricardo discussion.
For the purpose of the thermo-economic analysis, also the engine cooling circuit water coolant and, of course, the ambient cooling air, have been considered to be freely available (or already accounted in the engine cost for the coolant).
When considering a complete combined engine-ORC architecture, in which also the engine side components can influence both the performance and the cost of the overall powertrain, an analysis also of the engine main components' costs should be carried out (mostly done during common engine developments projects), in particular for:

- main engine components (block, cylinders head, liners, conrod, crankshaft, valvetrain, injectors and so on);
- turbocharger;
- heat exchangers (EGR cooler(s), CAC, SAC);
- aftertreatment devices (SCR, DPF, DOC, urea tank, and so on);
- piping and manifolds;
- valves;
- innovative technologies;

However, these data are kept confidential by developing companies and cost correlations are almost impossible to find in open literature.
When this information is available, the combined approach methodology proposed in this work could be implemented also for the engine side, studying which could be the influence of improving and changing all powertrain components, and subsystems, and not only the ORC. Indeed, as done for the ORC, cost correlations could be also developed for the main engine components once suitable dependent variables are estimated from Ricardo WAVE simulations.
What proposed above is left to future developments and is reported just to give the idea in which direction could the methodology be used, in a more complete and powerful way. In this work the engine system, simulated in WAVE, has been considered as a "black box" with multiple energy, exergy and mass streams entering and exiting the system, but the cost of the engine itself has been considered constant and assumed to be 15000 € for an engine with around 200 kW brake power output, as the one proposed in the fourth case study, with a complete EURO VI compliant aftertreatment system (Ricardo engine development experience).

As a last input, especially for a thermo-economic analysis or an operational cost saving analysis, the cost of the automotive diesel fuel should be considered. An average cost of 1.22 €/L has been assumed

(1/05/2017) based on the data available from the European Environment Agency [342]. A factor of 1.15 has been used for all Euro-Dollars conversions.

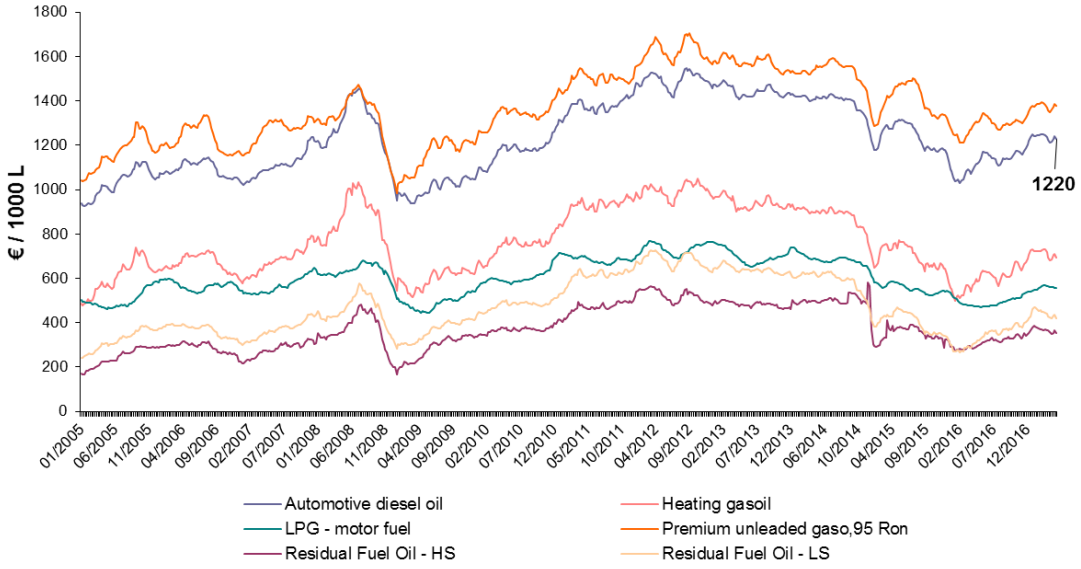

Fig. 52. Transport fuel prices (European Environment Agency) [342]

5.3.3 Techno-economic Analysis

As already introduced, a techno-economic analysis considers only the energy and economic considerations, without introducing the concept of exergy. Generally, a techno-economic analysis is what is more common in the industrial sector, where an exergy analysis is not well-spread and, very often, also not well understood.
In this work, as techno-economic indicators, mostly the Specific Investment Cost (SIC, [$/kW]) and the total ORC components Purchased Equipment Cost (PEC, [$]) have been considered, because between the most spread in literature, and often used to assess the system performance and economic trade-off in the industrial sector.
In the analysis proposed in the fourth case study, these indicators, together with the net ORC power output, have been used in order to assess the techno-economic performance of the systems analysed.
A mono or multi-objective optimization, aiming at finding the best trade-off between performance and costs, can be proposed, when a simulation code has been developed and coupled with powerful optimization algorithms.
In particular, in this work, the techno-economic analysis has been applied mostly to the ORC side of the overall engine-ORC powertrain, since, as already mentioned, the engine investment cost has been considered constant. When adequate engine sub-systems costs correlations would be available and implemented in the post-processing routines, an overall total engine-ORC system techno-economic optimization could be carried out, for every operating point, layout and working fluid configurations which could be proposed and simulated in the combined co-simulation approach.
Some data regarding SIC and PEC values for different ORC applications and cost percentage split, available in the open literature, can be observed in the charts reported in Fig. 53, as an idea of the values expected. Some Ricardo's data have been also reported, in particular for truck applications (note

very common in literature). Some other interesting overviews and consideration have also been reported by Lemmens [337].

Industrial WHR (a)

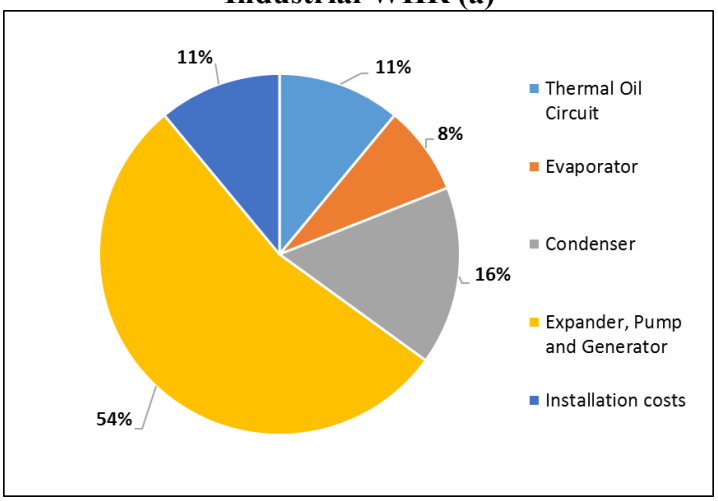

ORC description:

- Temperature levels: 150 – 250°C
- Power output: n.a.
- Intermediate oil-loop
- Turbo-radial expansion machine
- Plate evaporator
- Air-cooled condenser
- Fluid: n.a.
- **SIC = 4216 €/kW (2016)**
- Total PEC = n.a.
- Cost sources: suppliers' data
- Reference: Lemmens [337]

Marine four-stroke engine WHR (b)

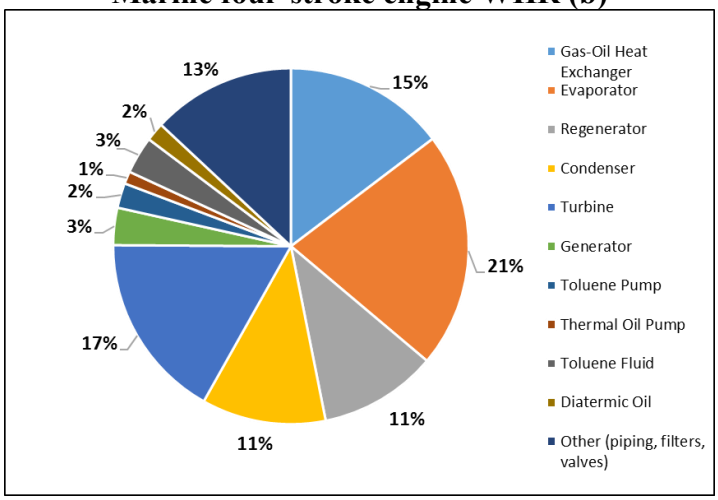

ORC description:

- Engine: four-stroke Wärtsilä DF 6L50DF, 5.7 MW
- Temperature levels: exhaust gas compatible
- Power output = 400 kW
- Intermediate oil-loop
- Turbo-expander
- Recuperated cycle
- Fluid: toluene
- **SIC = 2214 €/kW (2010)**
- **Total PEC = 885500 €**
- Cost sources: Aspen Tasc, Aspen Hysys, manufacturers data
- Reference: Bonafin *et al.* [264]

Small scale solar (c)

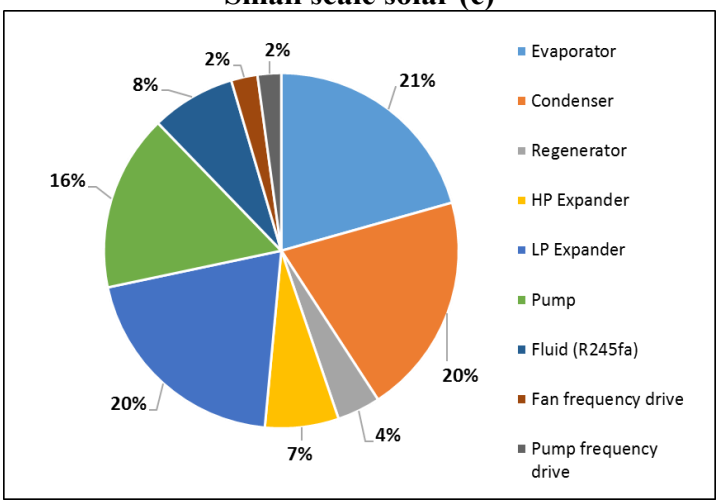

ORC description:

- Temperature levels: solar thermal collectors' compatible
- Power output = 5.5 kW
- Intermediate oil-loop
- 2 scroll expansion machines in series
- Diaphragm pump
- Plate heat exchangers
- Recuperated cycle
- Fluid: R245fa
- **SIC = 2600 €/kW (2013)**
- **Total PEC = 14321 €**
- Series off-the-shelf components used
- Reference: Georges *et al.* [343]

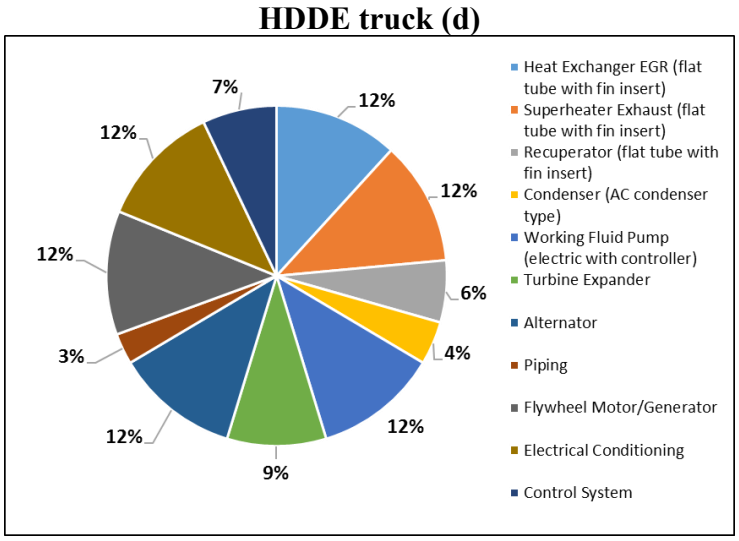

ORC description:

- Engine: 10.8 L Cummins
- Temperature levels: exhaust gas and EGR compatible
- Max. power output tested = 12.5 kW
- Exhaust gas an EGR heat recovery with series configuration
- Turbo-expander, retrofitted from Garrett GT-25 modified turbocharger with electrical power generation
- Electric pump with controller
- Finned-tube evaporators
- AC automotive-type air-cooled condenser
- Recuperated cycle
- Fluid: ethanol
- **SIC = 560 €/kW (2011),** at high load – high speed points, estimated
- **Total PEC = 8500 $**
- Cost sources: suppliers' analysis
- Reference: Park *et al.* [340]

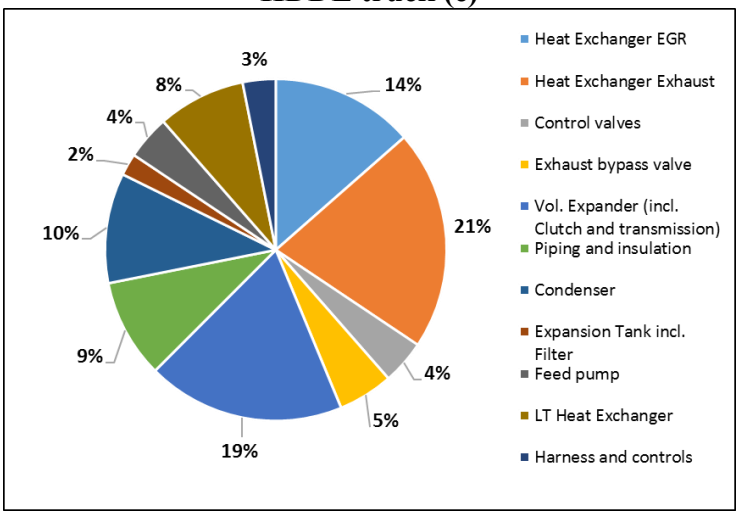

ORC description:

- Engine: n.a.
- Temperature levels: exhaust gas and EGR compatible
- Max. power output tested = n.a.
- Exhaust gas an EGR heat recovery with parallel configuration
- Piston expander with mechanical coupling with engine crankshaft
- Fluid: ethanol
- SIC = n.a
- **Total PEC = 2800 €** (maximum system target cost declared in 2013)
- Cost sources: suppliers' analysis
- Reference: Walter [341]

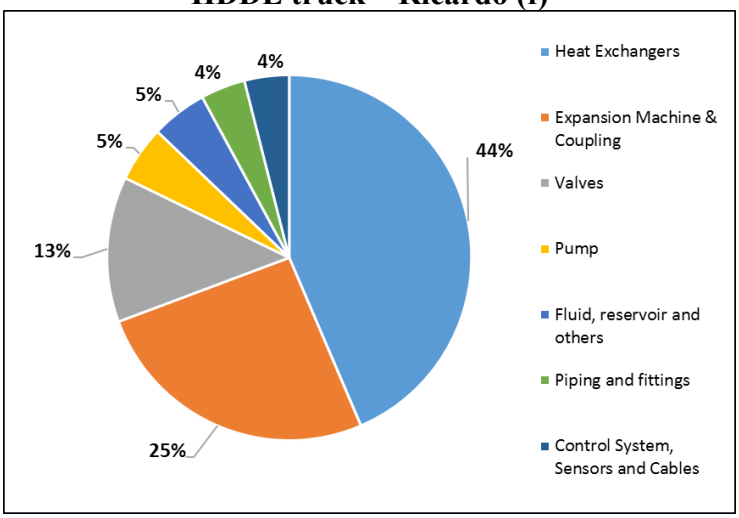

ORC description:

- Engine: n.a.
- Temperature levels: exhaust gas and EGR compatible
- Max. power output tested = 18 kW
- Exhaust gas an EGR heat recovery
- Turbo-expander with mechanical coupling
- Fluid: n.a.
- **SIC = 278 €/kW** estimated at high ORC power output (high load – high speed engine operating conditions)
- **Total PEC = 4000-5000 €**
- Cost sources: suppliers' analysis and internal Ricardo analysis
- Reference: Ricardo internal projects
- Return of Investment (ROI) declared: 1.8 – 2.8 years required

Fig. 53. Typical techno-economic data for several different ORC waste heat recovery applications (literature and Ricardo's data)

From the charts reported in Fig. 53 it is possible to observe how, generally, systems developed and built for large stationary or marine applications show higher values of SIC, but they are still competitive because of the large amount of power output they produce proportionally to the invested costs. The investment must be done also just once, and a scale economy due to high mass production is not possible, as in the case of traditional power plants.
Small scale ORC applications, such as for the solar system reported, or for small residential systems, show also high values of SIC, even though, of course, the investment costs result in being lower. This is mostly due to the fact that, again, a scale economy factor cannot be considered at the actual status of technology development, while at the same time, the systems are generating a low amount of power, compared to the average proportionally high investment costs required. The technology, in these sectors, is expecting to enter a competitivity range in the next years, together with a reduction of investment costs and an improvement in main components' efficiency, leading to a possible decrease in typical SIC values.
As demonstrated for the last three charts, in the case of HDDE truck on-highway applications, recent developments are pushing the technology towards a competitive SIC range. These systems are expected to enter the market around 2020, following Ricardo's analysis and roadmaps. Indeed, competitive SIC and PEC values are essential for the ORC technology in order to be able to be accepted in the automotive market.
Following Ricardo's analysis and internal discussions, ORC systems for automotive on-highway applications are expected to enter the market in the "elite-truck segment", with an estimated mass production per year of around 30000-50000 units.
At the actual technology status, SIC values in the range between 300 – 1000 $/kW can be achieved, at optimal, full-speed/full load engine operating points, in which a high amount of heat can be recovered from exhaust and EGR, thus leading to good ORC performance in terms of net power output achievable. At optimal operating points, minimum SIC values of around 300 $/kW or lower can be expected, but are generally far from real world operations, in which the truck operating profile results in very transient operations and generally mid-speed/mid-load highway conditions as expected most used operating point (highway cruise).
For full technology competitivity, SIC values, at best conditions, of 200 – 300 $/kW should be achieved, improving the components efficiency-cost trade-off and overall system performance.
The cost correlations proposed in this work, obtained from literature and modified based on Ricardo's experience, reflect these trends.
A graphical overview of the considerations proposed in this section can be observed in Fig. 54.

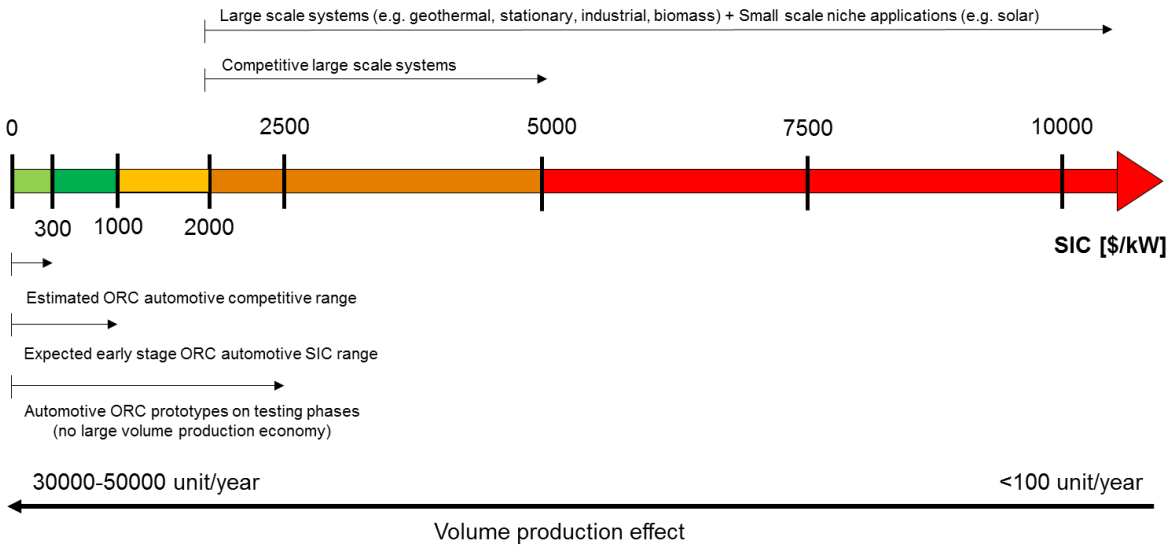

Fig. 54. Graphical overview of the SIC ranges expected for different ORC applications

5.3.4 Thermo-economic Analysis

As already introduced, thermo-economics is the discipline which uses together exergy and economic analysis in order to extract more information about the system analysed, both from a thermodynamic and economic point of view, considering the fact, as already mentioned at the beginning of section 5.3, that exergy, and not energy, is the right parameter to which costs should be associated.
As reported by Tsatsaronis [344], in the development and optimization of a thermodynamic system, the following questions should be answered:

1. Where the thermodynamic inefficiencies in the system occur, how high are they, and what causes them?
2. What measures or alternative designs would improve the efficiency of the overall plant?
3. How high is the required total investment and the PECs of the most important plant components?
4. How much do the thermodynamic inefficiencies cost the plant operator or developer?
5. What measures would improve the cost effectiveness of the overall plant?

The scheme in Fig. 55, clarifies which kind of analysis are needed in order to answer the proposed questions, showing clearly how a thermo-economic (and techno-economic) approach helps in the required tasks.

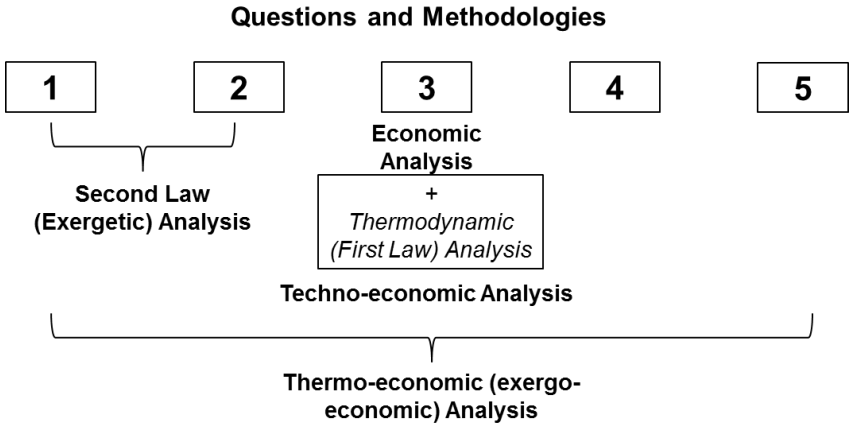

Fig. 55. Design and optimization questions and useful approaches

It is out of the scope of this work to present a detailed overview of thermo-economic methodologies developments. In order to deepen the topic, the author suggests references such as Valero *et al.* [304], Tsatsaronis [345], Abusoglu [346] and Bejan *et al.* [303]. It is however clear, from a literature review, that thermo-economic methodologies are not commonly applied to internal combustion engines and vehicles-related waste heat recovery systems, but rather to power plants, cogeneration systems, gas turbine systems and industrial thermal processes. New optimization techniques are also often proposed in synergy with thermo-economics.
In this work, a thermo-economic methodology is proposed applied to combined engine-ORC systems in order to show the potential of the approach for the development of more optimized and cost-effective systems, using process simulation techniques and powerful engine gas dynamic simulation software as Ricardo WAVE, which even if very well-spread in the industry engine development processes, are, however, not programmed to perform this kind of analysis. For this reason, further developments are needed, and this work aims at showing the potential and what could be done with an optimized combined tool, able to perform energy, exergy, techno and thermo-economic analysis, together with optimization, in a unique combined simulation environment, to answer many of the possible developers' questions.

The thermo-economic methodology applied in this work is based on the so-called SPECO approach (Specific Exergy Costing). References such as Bejan *et al.* [303] and Lazzaretto *et al.* [347] refer to the above-cited methodology and explain the main theoretical principles and background.
To the author's knowledge, just some references are available in literature about the application of the SPECO thermo-economic approach to ORC engine waste heat recovery case studies, such as Abusoglu *et al.* [348,349], Seyyedvalilu *et al.* [350], Khaljani *et al.* [351], Xia et al. [352]. However, the authors of these publications are generally focusing on CHP stationary applications, using cost correlations coming from the chemical sector. Thermo-economic studies about commercial vehicles medium or heavy-duty engine applications are, to the author's knowledge, not available in literature. When the proposed application is considered, generally just a techno-economic approach is applied, and the engine side is generally not considered in the overall analysis (e.g. Lemort *et al.* [353]). While, the methodology proposed in this work, aims to open the way to a more complete optimization approach, considering both engine and waste heat recovery sides at the same time, and can be applied to any case in which an engine is used as a topping cycle and whatever waste heat recovery technology as a bottoming one.

As already mentioned, compared to a techno-economic approach, the thermo-economic one requires an additional "exergy calculation layer", because costs are associated to the exergy (and not to energy) streams.
In particular, three main steps are needed for the overall analysis:

1. Identification of the exergy (or availability, $\dot{A}_i$, [kW]) and irreversibilities ($\dot{I}_i$) streams. Detailed exergy analysis of the combined engine-ORC powertrain, using Ricardo WAVE and the engine post-processing and ORC codes developed in MATLAB (or EES) environment;
2. Definition of *fuels* and *products* for every investigated system component (in this case the engine as a "black box" and all the main components of the ORC system);
3. Development of cost balances and auxiliary equations for every component. The equations obtained form a linear algebraic system which is solved in MATLAB.

Usually it is possible to differentiate between *exergy cost* and *exergo-economic cost*.
The *exergy cost,* of a mass or energy stream, is the exergy amount required to produce it. For example, in a cogeneration plant, the exergy cost of the net electrical output, is the amount of coal or natural gas exergy required to produce it.
The *monetary cost or exergo-economic cost*, considers the economic cost of the consumed *fuel* c_F [$/GJ or $/kJ] and also the levelized cost of the *installation* and *operation* of the plant $\dot{Z}$ [$/h], and the outcome of the analysis, could be, for example, the amount of money needed to generate a certain mass or energy/exergy flow (average cost of the *product* per unit exergy, c_P [$/GJ], or the cost of the product stream $\dot{C}_P$, [$/h]).
For this reason, in a thermo-economic analysis, it is important, for every component and for the overall system, to address the fuel and cost streams, entering and exiting the control volume.
According to exergy-costing techniques (such as SPECO), the cost stream associated with an exergy stream can be written as [303]:

$$\dot{C}_i = c_i \cdot \dot{A}_i \qquad (97)$$

with:

- c_i: average cost per unit exergy of the stream [$/GJ or $/kJ];
- $\dot{A}_i$: exergy of the stream (availability) [kW];
- $\dot{C}_i$: exergo-economic cost of the stream [$/h];

For every k-th component (or control volume), an exergo-economic cost balance can be applied, as suggested by Bejan *et al.* [303]. The sum of the exiting cost streams (*out*) equals the sum of the entering

cost streams (*in*) plus the change due to the capital investment ($\dot{Z}_k^{CI}$) and operating and maintenance costs ($\dot{Z}_k^{OM}$). The sum of the costs is often reported in literature as ($\dot{Z}_k$) and is a levelized cost based on a certain time interval and some assumptions, clarified later in this section, for the proposed application. The cost balance for the k-th component, in case, for example, of a component in which heat is supplied ($\dot{C}_{q,k}$) and work produced ($\dot{C}_{W,k}$), can be written as:

$$\sum_{out} \dot{C}_{out,k} + \dot{C}_{W,k} = \dot{C}_{q,k} + \sum_{in} \dot{C}_{in,k} + \dot{Z}_k \quad (98)$$

Components Levelized Costs

The levelized cost of the k-th component ($\dot{Z}_k$, [$/h]) can be calculated as follows [303]:

$$\dot{Z}_k = PEC_k \cdot CRF \cdot \frac{mf}{n_h} \quad (99)$$

with:

- PEC_k: Purchased Equipment Cost of the k-th component [$];
- CRF: Capital Recovery Factor;
- mf: maintenance factor;
- n_h: annual number of system operating hours [h/year]. In the case study proposed in section 6.4, a value of 2600 h/year has been assumed considering a truck driving 5 days/ week, 10 h/day and 52 weeks/year. Different operational scenarios can be considered using this parameter and the right assumptions;

The CRF parameter can be calculated as [303]:

$$CRF = \frac{i \cdot (1+i)^{LT}}{(1+i)^{LT} - 1} \quad (100)$$

with:

- i: interest rate (assumed ad 10% = 0.10);
- LT: life-time of the system (assumed 8 years from Ricardo's experience) [years];

Cost per Unit Exergy of Diesel Fuel

One of the first inputs of the combined engine-ORC thermo-economic analysis is the average cost per unit exergy of the engine diesel fuel, c_{fuel} [$/GJ or $/kJ].
The calculations are based on the assumed cost per litre from [342], reported in Fig. 52 using, as already mentioned, a 1.15 factor for the conversion to US dollars, an average density of the fuel at ambient conditions of 762.6 kg/m^3 and the LHV of 42800 kJ/kg from the WAVE fuel file, obtaining a value for the c_{fuel} of approximately 43 $/GJ. Often, in literature studies, values of average cost per unit exergy of the fuel around 4.0-7.0 $/GJ are used, but they are usually referred to methane for power generation, which is generally much cheaper than the diesel for automotive traction.

The supplied fuel cost stream can then be calculated using the exergy formulation for the chemical exergy of the engine fuel already proposed in eq. (37) and the formula:

$$\dot{C}_{fuel} = c_{fuel} \cdot a_{fuel} \cdot \dot{m}_{fuel} = c_{fuel} \cdot \dot{A}_{fuel} \qquad (101)$$

Cost Balance for the Engine System

As already mentioned, the engine system has been considered, in this work, as a "black-box" with entering and exiting mass and energy (as well as exergy) streams, which are calculated using the developed post-processing routines from the WAVE simulations' outputs.
However, when appropriate cost correlations for the main engine sub-systems would be available, the approach proposed for the ORC side could be also applied to the engine side.
A scheme for the engine "black-box" approach has been reported in Fig. 56.

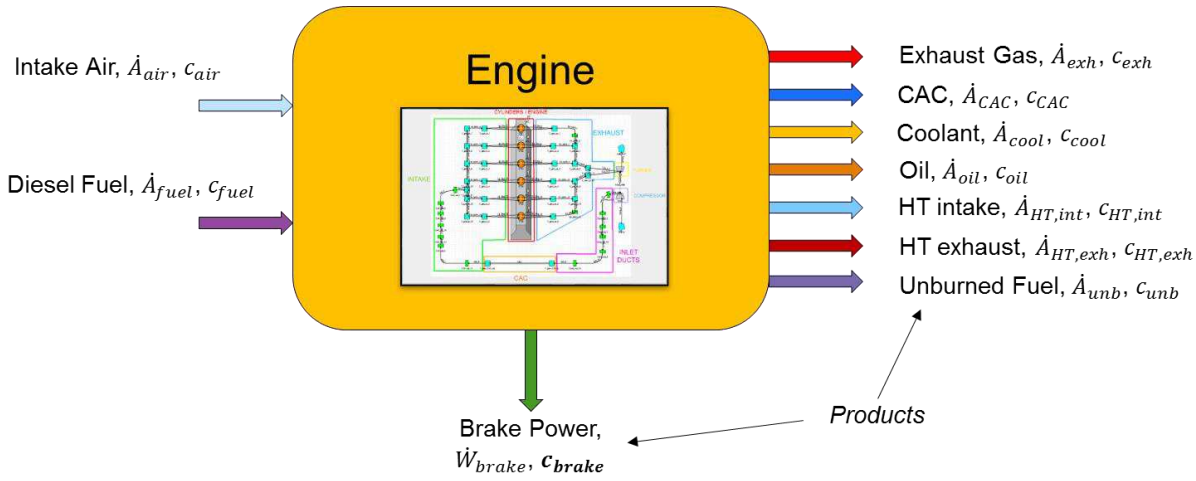

Fig. 56. Scheme for the engine thermo-economic "black-box" analysis approach

In the scheme reported above, "HT" stands for Heat Transfer, and is mostly related to the heat losses of the engine in the intake and exhaust manifolds.
Following what described previously, the cost balance for the engine overall system can be written as:

$$\dot{C}_{brake} + \dot{C}_{exh} + \dot{C}_{CAC} + \dot{C}_{cool} + \dot{C}_{oil} + \dot{C}_{HT,exh} + \dot{C}_{HT,int} + \dot{C}_{unb} = \\ = \dot{C}_{air} + \dot{C}_{fuel} + \dot{Z}_{ENG} \qquad (102)$$

In the formula, the terms $\dot{C}_i$ are the cost rates [$/h] associated with all the engine exergy (availability, $\dot{A}_i$) streams.
The average cost per unit exergy of the intake air has been considered 0, for this reason the term $\dot{C}_{air}$ can be directly neglected.
The control volume considered has eight exiting streams. For this reason, as proposed by Bejan *et al.* [303], $N_{aux,eq} = 8 - 1 = 7$ auxiliary equations are needed in order to close and solve the linear sub-system.
Some references in literature (e.g. Xia *et al.* [352]) suggest how the streams which could recovered, as exhaust gas, CAC, coolant and oil should be considered as free-of-charge, thus addressing to them a 0

$/GJ average cost per unit exergy. However, Bejan *et al.* [303] suggest, when studying the overall cost formation process, that the average cost per unit exergy of the fuel, c_{fuel}, should be better used, usually addressing 0 $/GJ only to the streams which are directly discharged to the environment and thus with no possibility of being utilized anymore. Considering what reported, the c_{fuel} has been addressed to the exhaust, coolant, oil, CAC and unburned streams, which could be still recovered, while a 0 $/GJ has been addresses to the intake and exhaust heat losses contributions, which are directly discharged into the environment. With the following assumptions, the auxiliary equations for the engine system are:

$$\begin{aligned} c_{exh} &= c_{fuel} \\ c_{CAC} &= c_{fuel} \\ c_{cool} &= c_{fuel} \\ c_{oil} &= c_{fuel} \end{aligned} \qquad \begin{aligned} c_{unb} &= c_{fuel} \\ c_{HT,int} &= 0 \\ c_{HT,exh} &= 0 \end{aligned} \qquad (103)$$

Inserting the proposed equations in the cost balance, it is possible to simplify the overall engine formulation and solve for the brake power average cost per unit exergy, as:

$$c_{brake} = \frac{c_{fuel} \cdot \left(\dot{A}_{fuel} - \dot{A}_{exh} - \dot{A}_{CAC} - \dot{A}_{cool} - \dot{A}_{oil} - \dot{A}_{unb}\right) + \dot{Z}_{ENG}}{\dot{W}_{brake}} \qquad (104)$$

As it can be observed from the cost balance, the cost associated to the irreversibilities is not part of the overall balance (it is an hidden cost, as declared by Bejan *et al.* [303]), but it is a very important output of a thermo-economic analysis, and can be calculated as follows:

$$\dot{C}_{irr,eng} = c_{fuel} \cdot \dot{I}_{ENG} \qquad (105)$$

Considering the "black-box" approach adopted for the engine, the irreversibilities have been summed for all the engine sub-systems, $\dot{I}_{ENG} = \sum \dot{I}_i$ [kW].

Cost Balance for the Heat Exchangers

The approach proposed in Bejan *et al.* [303] has been used for the heat exchangers, and in particular the evaporator and condenser.
The scheme of the component has been reported in Fig. 57. The exergy streams are calculated through the routines developed in MATLAB with REFPROP interface in order to retrieve the working fluids properties.
The cost balance for a typical heat exchanger (*HX*), can be written, considering the generic *hot* and *cold* streams, as:

$$\dot{C}_{cold,out} + \dot{C}_{hot,out} = \dot{C}_{cold,in} + \dot{C}_{hot,in} + \dot{Z}_{HX} \qquad (106)$$

The generic heat exchanger control volume has two exiting streams. For this reason, $N_{aux,eq} = 2 - 1 = 1$ auxiliary equation is needed to close the linear sub-system. As proposed by Bejan et al. [303], the average cost per unit exergy remains the same from the inlet to the outlet of the hot stream:

$$c_{hot,out} = c_{hot,in} \quad (107)$$

The general purpose of a heat exchanger is to provide heating of the cold stream, transferring energy (and exergy), from the hot one. For this reason, the system can be solved for the average cost per unit exergy of the cold stream at the component outlet [$/GJ]:

$$c_{cold,out} = \frac{c_{cold,in} \cdot \dot{A}_{cold,in} + c_{hot,in} \cdot \left(\dot{A}_{hot,in} - \dot{A}_{hot,out}\right) + \dot{Z}_{evap}}{\dot{A}_{cold,out}} \quad (108)$$

In the case of the evaporator, $c_{hot,in} = c_{fuel}$, while in the case of the condenser, $c_{cold,in} = 0$ (if the cooling fluid is ambient air) or $c_{cold,in} = c_{fuel}$ (if the cooling fluid is the engine coolant circuit).
Again, the cost rate associated to the irreversibilities [$/h] is not part of the balance, however, can be calculated considering the average cost per unit exergy of the component's fuel (generally the hot stream) and the irreversibilities calculated from the Second Law analysis:

$$\dot{C}_{irr,HX} = c_{hot,in} \cdot \dot{I}_{HX} \quad (109)$$

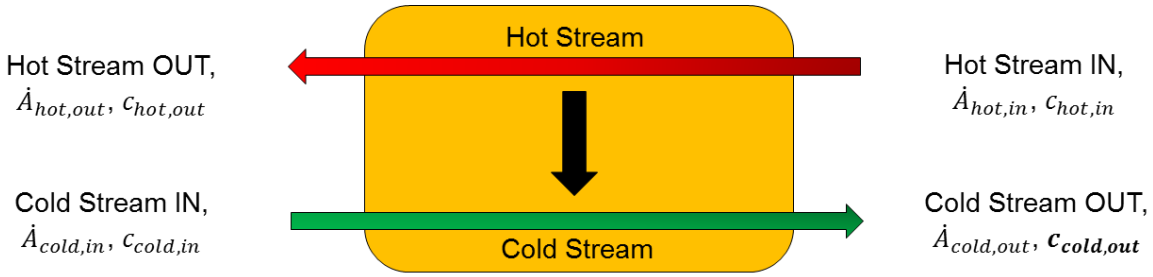

Fig. 57. Scheme for generic heat exchanger thermo-economic analysis

Cost Balance for the Pump

The pump control volume can be schematized as in Fig. 58.

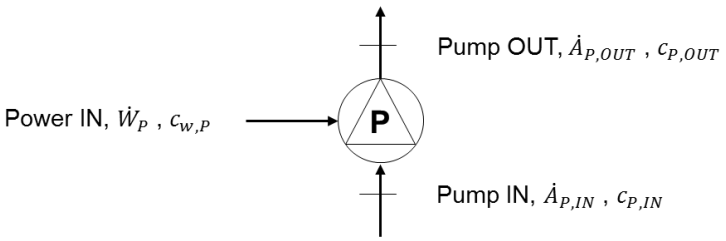

Fig. 58. Scheme for pump thermo-economic analysis

Also for the pump, the cost balance can be written as:

$$\dot{C}_{P,out} - \dot{C}_{P,in} = \dot{C}_{w,P} + \dot{Z}_P \quad (110)$$

In this case, the pump control volume has just one exiting stream, thus not requiring any auxiliary equation to be solved. In first approximation, the average cost per unit exergy of the power supplied to the pump to pressurize the fluid has been imposed as the one calculated for the engine brake power, supposing the pump is rotated by the energy subtracted from the engine crankshaft: $c_{w,P} = c_{brake}$. The balance can be then solved for the pump outlet average cost per unit exergy [$/GJ]:

$$c_{P,out} = \frac{c_{w,P} \cdot \dot{W}_P + c_{P,in} \cdot \dot{A}_{P,in} + \dot{Z}_P}{\dot{A}_{P,out}} \quad (111)$$

As well as the irreversibilities cost rate [$/h] as:

$$\dot{C}_{irr,P} = c_{w,P} \cdot \dot{I}_P = c_{brake} \cdot \dot{I}_P \quad (112)$$

Cost Balance for the Expander

The expander control volume can be schematized as in Fig. 59.

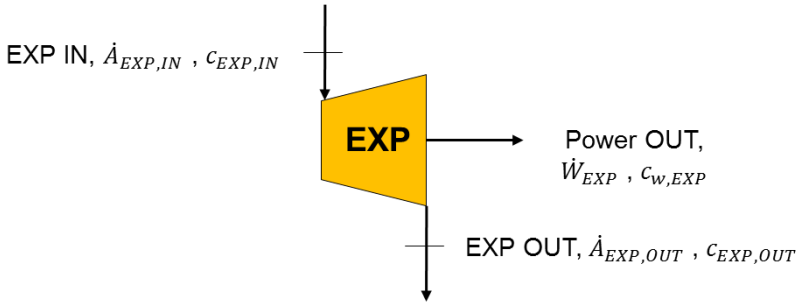

Fig. 59. Scheme for expander thermo-economic analysis

Also for the expander, the cost balance can be written as:

$$\dot{C}_{w,EXP} = \dot{C}_{EXP,in} - \dot{C}_{EXP,out} + \dot{Z}_{EXP} \quad (113)$$

The expander control volume has two exiting streams. For this reason, $N_{aux,eq} = 2 - 1 = 1$ auxiliary equation is required to solve the linear sub-system. Following the guidelines from Bejan *et al.* [303], the auxiliary equation has been chosen as:

$$c_{EXP,out} = c_{EXP,in} \quad (114)$$

Solving for the average cost per unit exergy of the extracted expander power [$/GJ], which is one of the most important thermo-economic outputs of the analysis, it is possible to write:

$$c_{w,EXP} = \frac{c_{EXP,in} \cdot \left(\dot{A}_{EXP,in} - \dot{A}_{EXP,out}\right) + \dot{Z}_{EXP}}{\dot{W}_{EXP}} \quad (115)$$

While the irreversibilities cost rate [$/h] can be written as:

$$\dot{C}_{irr,EXP} = c_{EXP,in} \cdot \dot{I}_{EXP} \quad (116)$$

Solving the Linear System

After having written all the cost balances and auxiliary equations for all the ORC main components (or control volumes), it is possible to order all the equations obtained in the form of a linear system:

$$A \cdot x = B \quad (117)$$

with:

- A: matrix (n x n) of the coefficients of the equations, which are the availability terms [kW] of all the streams in the system;
- x: unknowns of the problem. This is the vector (n x 1) containing all the average costs per unit exergy of all the streams in the system [$/GJ or $/kJ]. The system must be solved in order to find the required values for all the streams;
- B: known terms of the problem. This is the vector (n x 1) containing all the known terms, and in particular the levelized costs of the components [$/h] and some known availability terms [kW] and average costs per unit exergy [$/GJ or $/kJ];

The system, in the proposed work, has been solved, for different ORC layouts configurations (e.g. simple, recuperated) using adequate MATLAB embedded routines.

Thermo-economic Analysis Outputs

As already mentioned, the immediate output of a thermo-economic analysis is the calculation of the average costs per unit exergy of the various exergy streams of the combined engine-ORC system.
Between the main outputs of a thermo-economic analysis are also the cost rates [$/h] of the products of the system: in this case the useful power output of the combined engine-ORC system.
For the engine side, the cost rate of the engine brake power produced [$/h] can be written as:

$$\dot{C}_{brake} = c_{brake} \cdot \dot{W}_{brake} \quad (118)$$

while for the ORC side, the expander produced power cost rate [$/h]:

$$\dot{C}_{w,EXP} = c_{w,EXP} \cdot \dot{W}_{EXP} \quad (119)$$

and, considering the ORC net power output, estimated after the mechanical (or electrical) energy conversion stage [$/h]:

$$\dot{C}_{ORC,net,mech} = c_{w,EXP} \cdot \dot{W}_{ORC,net,mech} \quad (120)$$

Regarding the irreversibilities cost rates, for the engine, assuming the "black box" approach, they can be summed up for all the control volumes (i), assuming as average cost of unit exergy the cost of the diesel fuel, c_{fuel} [$/GJ]. This approach, as explained by Bejan et al. [303], basically considers that the effect of the irreversibilities is to increase the costs related to the fuel used, which is additionally wasted because of the destruction of exergy in the system [$/h]:

$$\dot{C}_{irr,ENG,TOT} = \sum_i \dot{C}_{irr,ENG,i} \quad (121)$$

In the same way, for the ORC system, assuming the as average costs per unit exergy the various values for the fuel streams of the ORC components (j), calculated from the resolution of the linear system, and summing up all the contributions [$/h], it is possible to write:

$$\dot{C}_{irr,ORC,TOT} = \sum_j \dot{C}_{irr,ORC,j} \quad (122)$$

With the right assumptions regarding the various streams average costs per unit exergy calculated from the linear system, it is possible also, in the same way, to calculate all the cost rates of the various exergy streams (e.g. the released exhaust gas after the ORC evaporator, the contributions to the engine coolant, CAC, and oil, and the ORC condenser released cooling stream).
Other parameters, such exergo-economic factor and relative cost difference, are often proposed for a thermo-economic analysis (Bejan *et al.* [303]) but have not been considered in this work, which aim is to demonstrate the proposed methodology.
Generally, as proposed by Bejan et al. [303], the various non-useful exergy streams cost rates should be minimized in order to lead to a system which dissipates the lowest costs per hour possible. Also, the useful streams cost rates should be minimized, thus leading to a system which produces, for example, power at the minimum cost per hour possible.
When a certain investment cost cannot be avoided, because of the required system components investment, it would be generally better to design a system which has higher cost rates "invested" in the production of a real useful output (e.g. power) than "wasted" in the production of non-useful streams (e.g. cooling medium, exhaust released gas and so on) or irreversibilities.
More complex bottoming systems, such as dual loop and two-stage pressurization, could be analysed with this approach in order, for example, to recover costs (and exergy/energy) from generally not-used streams (e.g. coolant, CAC), addressing also the trade-off with their possible thermodynamic performance (First Law analysis) and Specific Investment Costs (techno-economic analysis).
Different optimization strategies can be used for these purposes. Some of them have been proposed in the last case study in section 6.4 as an example of what can be done.
However, the possibilities which can be envisaged with this combined approach are multiple and generally left to the goal of the project itself and to the choice of the developer.
What reported in this work is just an example of the potential of such a combined analysis methodology.

6 Case Studies and Results Discussions

The four case studies evaluated in this work have been reported in the next sections, considering an introduction to the specific application, the type of engine evaluated, the calculations performed, together with a critical discussion of the results obtained. The case studies have been reported in the chronological order in which they have been developed in the frame of the doctoral work and ECCO-MATE project, in order to show an increasing level of synergy between the various tools, approaches and methodologies proposed.

6.1 Case Study 1: Off-highway Application - Agricultural Tractor

Many studies reported in literature about ORC waste heat recovery for vehicles are related to passenger cars (diesel or gasoline), on-highway trucks, stationary power generation, or marine applications, but off-highway applications, as earth moving machines or agricultural tractors, are not commonly investigated. Even though, engine and powertrain thermal management in off-highway vehicles is very problematic, due to low ram air effect for cooling purpose and high parasitic fan power consumption, the operating profile is very suitable for waste heat recovery bottoming cycles implementation, due to the high engine speed and load stable conditions, and the availability of valuable medium-high temperature heat in the exhaust and EGR as already introduced in section 4.1.4.1.
For these reasons, the work proposed in the first case study investigates the possibility of recovering heat from exhaust gas and EGR of a commercial HDDE for an agricultural tractor, considering also the impact of fitting the ORC system on the radiator dimensions and, thus, on the vehicle cooling system performance, an issue often not considered in literature. Two different heat sink configurations are investigated: a higher temperature (HT) engine cooling circuit or a lower temperature ORC-only additional cooling circuit (LT).
The performance of the different ORC architectures, and of the proposed cooling strategies, have been investigated through the use of a process simulation model developed in Engineering Equation Solver [297], while cycle parameters have been optimized using a Genetic Algorithm [354] and a Nelder-Mead Simplex algorithm [355], with the purpose of maximizing the overall powertrain fuel consumption benefit and to assess the possible power output that can be expected.
The work proposed in this case study has been published by the author in [75,356].

6.1.1 Reference Engine and Design Point Choice

The reference engine considered in this study is a heavy duty direct injection 6 cylinders in-line Diesel engine with a brake power output of 302 kW. The engine configuration is two-stage turbocharged with intercooling and is fulfilling the Tier 4 final emissions regulation for off-highway vehicles, using cooled High Pressure (HP) EGR and a complete aftertreatment system composed by Diesel Oxidation Catalyst (DOC), Diesel Particulate Filter (DPF) and Selective Catalytic Reduction (SCR) with urea injection.
To choose the most appropriate design point for the ORC system, it is necessary to investigate the application specific operating profile. An example of engine speed (N) and engine torque (τ) profiles for a typical agricultural tractor operating cycle has been already reported in Fig. 17, in section 4.1.4.1. From the operating cycle reported in the cited figure, it is possible to observe how the engine spends most of the time at full load and medium-high speed conditions, thus leading to the availability of a

high amount of exhaust gas at medium-high temperature, suitable for heat recovery using bottoming cycles. For this reason, the design point for the ORC system calculations has been chosen in this engine operating range, expecting also a quite high amount of recirculated gas in the EGR circuit.
The data used to carry out the ORC analysis are experimental data at design load and speed conditions, obtained from engine test campaign on the dynamometer at Ricardo's facilities, and have been reported, just for the selected point, in Tab. 23.

Engine-ORC Design Point (Test Data)	**Symbol**	**Unit**	**Value**
Engine brake power	P_{ENG}	kW	302
Engine speed	N	rpm	2000
Engine torque	τ	Nm	1443
Exhaust gas mass flow rate	$\dot{m}_{exh}$	kg s^{-1}	0.36
Exhaust gas temperature (after low pressure turbine)	T_{exh}	°C	509
Exhaust gas thermal power (cooling limit to 90°C)	$\dot{Q}_{exh}$	kW	186
EGR gas mass flow rate	$\dot{m}_{EGR}$	kg s^{-1}	0.12
EGR gas temperature (EGR cooler inlet)	$T_{EGR,in}$	°C	699
EGR gas temperature (EGR cooler outlet)	$T_{EGR,out}$	°C	145
EGR cooler thermal power	$\dot{Q}_{EGR}$	kW	81

Tab. 23. Engine-ORC design point. Test data for the 302 kW brake power two-stage turbocharged tractor engine at full-load (case study 1)

The exhaust gas thermal power is calculated imposing as lower cooling limit 90°C, considering a low-sulphur content diesel fuel, in order to avoid acid condensation problems in the ORC exhaust heat exchanger.
Temperature data for the exhaust line of the reference engine are available only until the low-pressure turbine outlet, not considering the aftertreatment system. However, from what reported by Qiu *et al.* [357], and analysing some other steady-state proprietary Ricardo HDDE test data, in which temperatures in the aftertreatment are measured, it is possible to assume no temperature change over the aftertreatment system in first approximation, especially in the engine high speed and torque range considered in this study.

6.1.2 ORC and Heat Sink Architectures

In this work, two ORC architectures have been considered: a simple evaporator configuration (SC, Simple Cycle) to recover heat from tailpipe exhaust gas, and a parallel evaporator configuration (PC, Parallel Cycle) to recover heat both from exhaust and EGR gas.
The engine and the main ORC components, evaporator, condenser, pump (P) and expander (EXP) can be observed in Fig. 60(a-d), which reports both the Simple Cycle (SC) and the Parallel Cycle (PC) ORC architectures, and the two different heat sink configurations: the Indirect Condensation 1 (IC 1), using the engine high temperature cooling circuit, and the Indirect Condensation 2 (IC 2), using a dedicated ORC lower temperature circuit.
The evaporators are placed after the aftertreatment system and instead of the EGR cooler. In this preliminary study, the increased backpressure effect of the boilers on the engine has not been considered.
The two investigated heat sink solutions can also be observed in the schemes reported in Fig. 60: Indirect Condensation 1 (IC1), a configuration using the engine and EGR high temperature cooling

circuit as heat sink for the ORC system, and Indirect Condensation 2 (IC2), a configuration using a lower temperature cooling circuit with the purpose of increasing the net power output of the bottoming cycle, allowing a higher enthalpy drop in the expander. In this second case, an additional radiator is needed. The two ORC architectures are evaluated with both heat sink configurations, for a total of four cases, as reported in the figures.
The main data for the heat sink configurations have been reported in Tab. 24 and used as boundary conditions for the ORC analysis. The coolant is a mixture of water and ethylene-glycol with a 50% mass composition for the two components. The mass flow, in the IC2 case, has been considered as a variable in the optimization process, and the ORC condenser inlet temperature has been fixed to 50°C. The thermodynamic properties for the coolant mixture, as well as the ORC working fluids, are obtained from Engineering Equation Solver (EES) internal database [297].

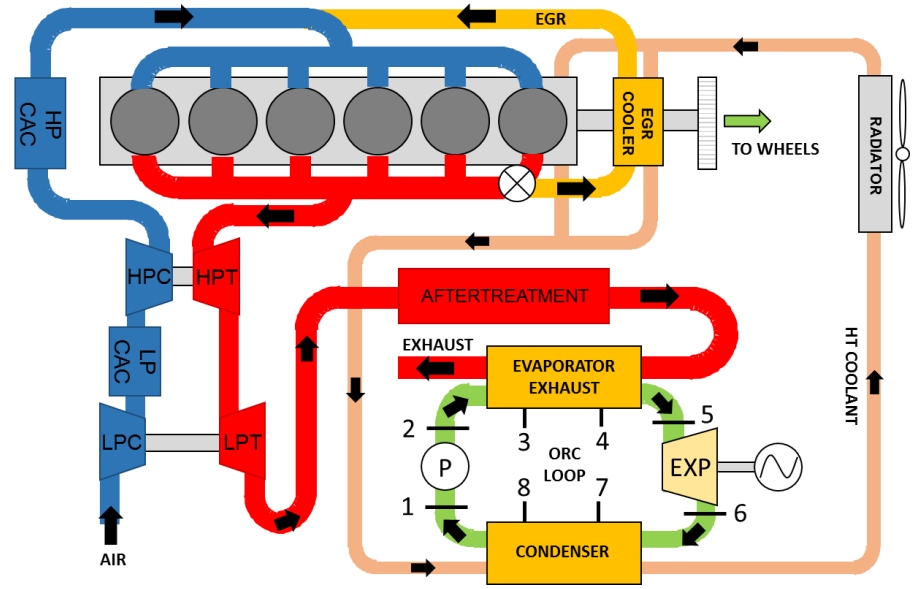

(a)

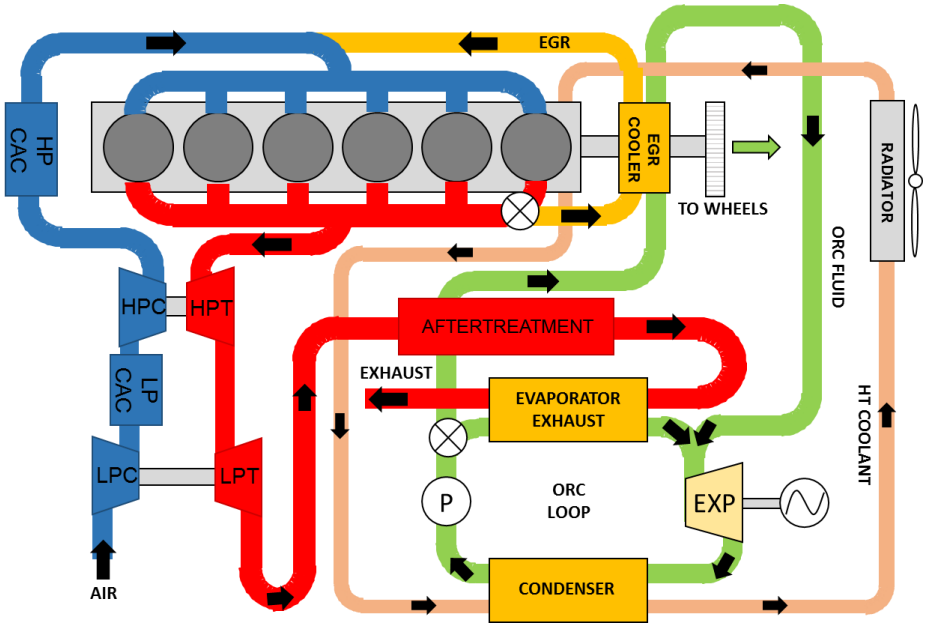

(b)

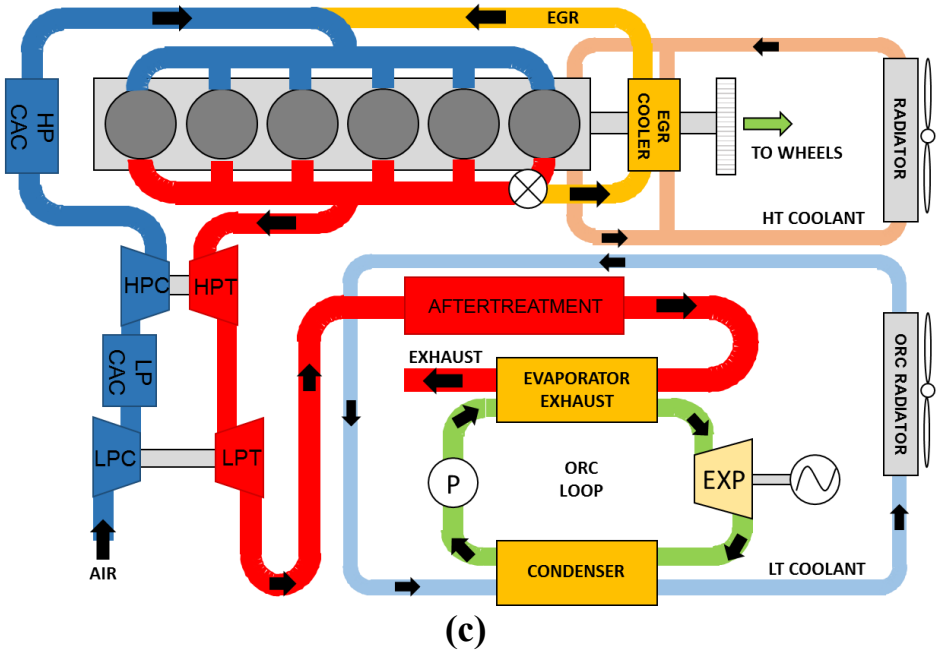

(c)

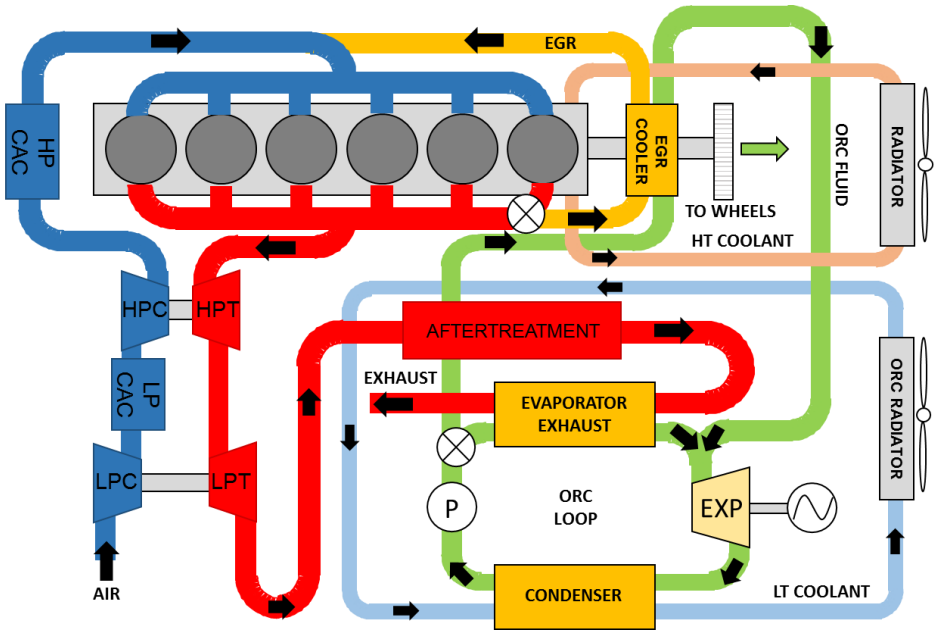

(d)

Fig. 60. Simple Cycle (SC) and Indirect Condensation 1 (IC 1) architecture (a). Parallel Cycle (PC) and Indirect Condensation 1 (IC 1) architecture (b). Simple Cycle (SC) and Indirect Condensation 2 (IC 2) architecture (c). Parallel Cycle (PC) and Indirect Condensation 2 (IC 2) architecture (d) – (case study 1)

Heat sink data	**Symbol**	**Unit**	**IC1**	**IC2**
Coolant mass flow rate	$\dot{m}_{cf}$	kg s^{-1}	3.2	var.
Coolant temperature at the ORC condenser inlet	$T_{cf,in}$	°C	93.6	50

Tab. 24. Heat sink data (case study 1)

The following assumptions have been used in the process simulation model:

- pressure drops and heat losses have not been considered in the components and in the pipes;

- pump isentropic efficiency, $\eta_{is,P}$, has been set to 70%;
- expander isentropic efficiency, $\eta_{is,EXP}$, has been set to 80%, considering the possibility of using a turbo-expander, due to the stable operating profile (efficiency generally higher than for volumetric expansion machines);
- expander mechanical efficiency, $\eta_{mech,EXP}$, has been set to 85%, considering possible mechanical coupling with the engine crankshaft using a belt. Electrical coupling could also be assumed, in first approximation, to have a similar efficiency value when considering the electric generator and a driving belt. Higher coupling efficiency levels could be expected (up to 95%);
- heat exchangers are counter-flow, divided in single-phase and two-phase zones and modelled with fixed boundaries technique;
- a sub-cooling degree, $\Delta T_{sub-cool}$, of 2°C has been imposed at the outlet of the condenser in order to obtain working fluid always in a liquid state at the pump inlet and avoid cavitation problems. A fluid reservoir is not modelled in this preliminary study;
- in first approximation, exhaust gas and EGR gas are assumed to have the same properties of dry air;
- the circulator pumps of the cooling circuits are not considered in the overall power balance. However, the high temperature coolant circuit has already a circulator pump, while the low temperature cooling circuit pump is not expected to consume a lot of power, due to the low pressure drop and mass flows considered;

The single and parallel evaporators ORC architectures have been modelled using the Engineering Equation Solver (EES) software, following the methodology described in section 5.2.1.
Some additional performance indexes have been used to investigate the overall cycle, as well as the individual components [302]. The indexes considered have been reported in Tab. 25. Some of the them have already been introduced in section 5.2.3.

Parameter	Component/System	Description
$P_{ORC,net}$	ORC System	ORC net power output
η_{ORC}	ORC System	ORC efficiency
$BSFC_{impr}$	Combined System	BSFC improvement compared to baseline engine
$\dot{Q}_{ORC,out}$	ORC System	ORC rejected heat in the condenser
$\sum_i U_i A_{HX,i} = \frac{1}{\dot{m}_{exh/EGR}} \sum_i \left(\frac{\dot{Q}_{HX,i}}{\Delta T_{LMTD,i}} \right)$	Heat Exchangers	Sum of the conductance of the HXs (global surface index) per unit recovered mass flow

Tab. 25. ORC performance parameters (case study 1)

The last parameter presented in the table above gives an idea of the dimensions, and thus the cost, of the heat transfer equipment, and is calculated using the Log Mean Temperature Difference method (LMTD) [307].

6.1.3 Heat Sink and Radiator

The radiator has also been modelled using EES. The configuration is a single-pass cross-flow compact fin and plate heat exchanger, with rectangular coolant plate flow areas and triangular fins geometry, in which the coolant flows only in the direction from the top to the bottom of the heat exchanger, in a so-called *I* configuration. The air is considered to be homogeneously distributed over the radiator frontal area, as the coolant in the pipes.
The modelling theory guidelines have been taken mainly from Cowell [358] and Ricardo internal guidelines, following typical compact heat exchangers modelling techniques [359]. The coolant is considered to be a mixture of water and ethylene-glycol (0.5/0.5 in mass composition), while the coolant heat transfer and pressure drop correlations have been obtained from EES internal procedures, based on laminar or turbulent flow regimes. For the air side, the Colburn factor and friction coefficient have been obtained from Cowell [358] and used as a lookup table in the calculations. The performance of the radiator, in term of heat rejection capabilities based on main component dimensions, supplied as inputs (Fig. 61), are calculated based on the $\varepsilon - NTU$ method [307].

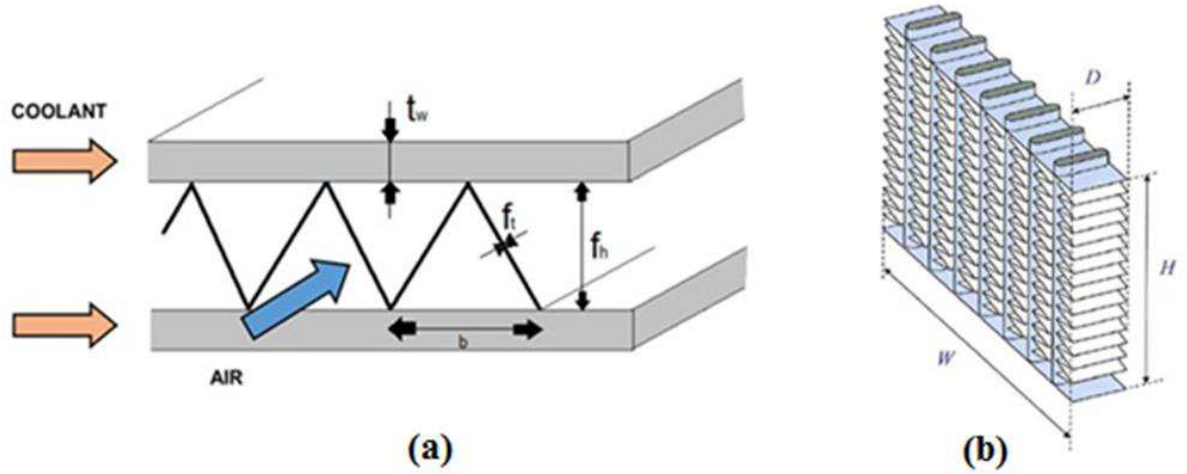

Fig. 61. Radiator fin-and-plate dimensions (a) and main geometry dimensions (b). Elaborated from [358] *(case study 1)*

In particular, for the coolant plates side, the EES implemented procedure "DuctFlow" [360] has been used to obtain the average convective heat transfer coefficient. This procedure has been considered more accurate than using the Dittus-Boelter (fully turbulent flow) correlation [359]. Indeed "DuctFlow" determines if the flow is laminar or turbulent (or transitional between 2300 and 3000 Re) and applies the right correlations regarding heat transfer and pressure drops.
For the air side, the Colburn factor and the friction coefficient, together with the specification of the main geometry parameters, have been used with the final purpose of investigating the heat transfer and the air pressure drop over the radiator core geometry.
In particular, once the overall conductance UA has been calculated (neglecting the conductance in the plates thickness), the ε-NTU method has been applied to obtain the radiator effectiveness and then estimate the heat transfer rate between coolant and air sides.
The procedure is applied using the coolant and air mean temperature values, between inlet and outlet, but since the outlet temperatures of the two flows are not known at the beginning, an iterative process has been implemented exploiting the solver capabilities of EES.
For the estimation of the fan parasitic power consumption, the fan static efficiency, η_{fan}, has been imposed to 60%, considering big heavy-duty cooling fan applications. This number has been compared with the data from Multi-Wing fan manufacturer software [361] obtaining a good match for big diameters (700-800 mm) fan models, expected for these kind of applications.

The fan power consumption has then been estimated with the following formula:

$$P_{abs,fan} \cong \frac{\dot{m}_{air} \cdot \Delta p_{air}}{\rho_{air,avg} \cdot \eta_{fan}} \quad (123)$$

considering the required cooling air mass flow $\dot{m}_{air}$, the total radiator core air side pressure drop, Δp_{air}, the average air density, $\rho_{air,avg}$, and the fan efficiency, η_{fan}.
The radiator fins density has been kept fixed to 8 fins/inch, considered suitable for off-highway applications operating in dusty conditions, and the material is aluminium.
As first step, since no real data were available, the baseline engine radiator (without ORC) has been sized, considering radiator core height (H), width (W) and depth (D), in order to keep the frontal area 1 m^2 and reject 202.5 kW heat to the ambient, to cool the cooling fluid from a radiator inlet temperature of 95.7°C to 84°C (engine inlet temperature), as required during Ricardo testing campaigns. The cooling air inlet temperature has been imposed to the average fixed value of 50°C, considering an ambient temperature of 40°C to simulate particularly critical hot conditions for the cooling package, and assuming the radiator in series after CAC, oil cooler and air conditioning condenser, in a traditional cooling package configuration. For the air conditioning condenser, 5 kW average heat rejection has been assumed, as reported in [362], in order to estimate the temperature drop over the AC cooler and the temperature at the engine radiator inlet. The data for the baseline radiator have been reported in Tab. 26.

Baseline engine radiator data	**Symbol**	**Unit**	**Value**
Coolant volume flow	$\dot{V}_{cf}$	$m^3\ s^{-1}$	4.8
Coolant radiator inlet temperature	$T_{cf,air,in}$	°C	95.7
Cooling air volume flow	$\dot{V}_{air}$	m^3/s	11.8
Cooling air radiator inlet temperature (after CAC and AC HX)	$T_{air,rad,in}$	°C	50
Radiator heat rejection	$\dot{Q}_{rad}$	kW	202.5
Radiator height	H	m	1.13
Radiator width	W	m	0.89
Radiator depth	D	m	0.08
Radiator core frontal area	$A_{f,rad}$	m^2	1
Radiator core volume	V_{rad}	m^3	0.08
Fan power consumption	P_{fan}	kW	21

Tab. 26. Baseline engine radiator data (case study 1)

When fitting the ORC, two different heat sink configurations have been considered for the two cases IC1 (Indirect Condensation 1) and IC2 (Indirect Condensation 2). The two configurations are influencing the cooling air temperature at the inlet of the radiator, and thus, the radiator performance. The schemes, together with a simplified vehicle sketch, have been reported in Fig. 62, to give an idea of how the design could look like.

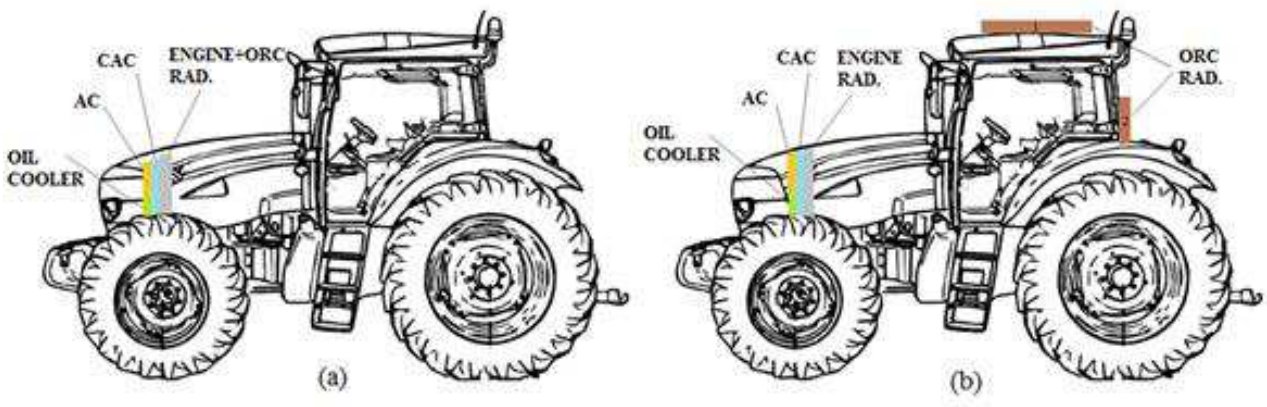

Fig. 62. Heat sink configurations IC1 (a) and IC2 (b) and vehicle sketches (case study 1)

The configuration *(a, IC1)* is similar to the baseline and is the most compact, since the same cooling circuit is used to cool both engine and ORC, and the coolant is then cooled in a combined engine-ORC radiator. However, the cooling air high temperature at the inlet of the combined radiator decreases the heat rejection capabilities of the heat exchanger, thus requiring higher dimensions and more cooling air volume flow, with increased fan parasitic power consumption when increasing the heat that must be rejected due to the ORC system installation. An additional ORC-only separated radiator, positioned in series after the engine radiator, would have been probably affected by too high cooling air inlet temperature. For this reason, this configuration has not been considered.
The configuration *(b, IC2)* needs additional piping and more complicated system layout. The position of the ORC radiator behind the cabin can create visibility problems when the tractor works in reverse direction or when controlling PTOs. The roof-top position could be more interesting and could lead to less issues (resistance of the cabin must be assessed, and components probably reinforced). However, this configuration benefits from the lower temperature of the cooling air, which has not to pass through the cooling package before cooling the ORC radiator, and can, in first approximation, be considered at the same temperature of ambient air. However, an additional electrically driven fan must be considered in this case, thus impacting the overall vehicle power balance.
In total, four cases have been considered for the heat sink study of the combined engine-ORC system (Tab. 27).

Case	Configuration ORC-Heat sink	Heat sink position
1	Simple Cycle (SC) – IC1	a
2	Parallel Cycle (PC) – IC1	a
3	Simple Cycle (SC) – IC2	b
4	Parallel Cycle (PC) – IC2	b

Tab. 27. Considered combined ORC architecture-heat sink configurations (case study 1)

6.1.4 Working Fluid Selection

A literature review of the most used ORC fluids for medium-high temperature waste heat recovery has been carried out, as already reported in section 4.2.2.1. After this first step, a final list of ten fluids has been finalized, considering only the fluids which fulfilled some requirements on the base of the NFPA 704 classification, from the National Fire Protection Association [145], and on the base of the low Global Warming Potential at 100 years (GWP 100), in order to use fluids not very harmful for the

environment [363]. The limits for the health hazard (H) has been set to 2, the one for flammability (F) to 3 and the GWP 100 to 1300. The freezing point limit has been assumed to be 0°C (water steam) to avoid fluid freezing problems in cold ambient conditions. The final list of fluids evaluated is reported in Tab. 28, together with the main properties obtained from NIST REFPROP [364].

Working fluid	T_c [°C]	p_c [bar]	T_{boil} [°C]	T_f [°C]	Health hazard (H)	Flammability Hazard (F)	GWP (100)
ethanol	241.6	62.7	78.5	-114.2	0	3	n/a
methanol	239.5	81	64.5	-97.6	1	3	2.8
toluene	318.6	41.3	110.6	-95.2	2	3	2.7
cyclopentane	238.6	45.7	49.3	-93.5	1	3	n/a
MDM	290.9	14.2	152.5	-86	0	2	n/a
acetone	235	47	56.1	-94.7	1	3	0.5
R-141b	204.4	42.1	32.1	-103.5	2	1	725
R-123	183.7	36.6	27.8	-107.2	2	0	77
R-245fa	154	36.5	15.1	-102.1	2	1	1030
water-steam	374	220.6	100	0	0	0	<1

Tab. 28. Working fluids evaluated (case study 1)

6.1.5 Optimization Procedure

For all the four cases evaluated, the chosen ten fluids have been thermodynamically assessed in order to obtain the best BSFC improvement ($BSFC_{impr}$) for the combined engine-ORC system.
First of all, the *independent variables* for the optimization process have been identified and are reported in Tab. 29, divided for type of cycle architecture.

Independent Variable	Unit	Simple Cycle (SC)	Parallel Cycle (PC)
Working fluid mass flow	kg s^{-1}	$\dot{m}_{wf}$	$\dot{m}_{wf}$
Condensing pressure	bar	p_{cond}	p_{cond}
Pressure ratio	-	PR	PR
Superheating degree in the ORC exhaust circuit	°C	$\Delta T_{suph,exh}$	$\Delta T_{suph,exh}$
Superheating degree in the ORC EGR circuit	°C	-	$\Delta T_{suph,EGR}$
Cooling fluid mass flow	kg/s	$\dot{m}_{cf}$	$\dot{m}_{cf}$
Working fluid rate in the ORC EGR circuit	%	-	a_{EGR}

Tab. 29. Independent variables for the optimization procedure (case study 1)

The cooling fluid mass flow variable is optimized only in heat sink layout IC2, because in the layout IC1, the parameter is fixed as the same for the engine cooling system.
As a second step, the *constraints* for the optimization process have been identified, and are presented in Tab. 30.

Variable	Unit	Simple Cycle (SC)	Parallel Cycle (PC)
Pinch point temperature difference in the evaporators and condensers	°C	$\Delta T_{PP,evap/cond} \geq 10$	$\Delta T_{PP,evap/cond} \geq 10$
Superheating level in the ORC exhaust and EGR circuits	°C	$\Delta T_{suph,exh/EGR} \leq 100$	$\Delta T_{suph,exh/EGR} \leq 100$
Evaporation pressure	bar	$p_{evap} \leq 30$ (or $0.9 \cdot p_c$)	$p_{evap} \leq 30$ (or $0.9 \cdot p_c$)
Condensing pressure	bar	$p_{cond} \geq 1.2$	$p_{cond} \geq 1.2$
Evaporation temperature	°C	$T_{evap} \geq 50$	$T_{evap} \geq 50$
Condensing temperature	°C	$T_{cond} \geq 50$	$T_{cond} \geq 50$
Exhaust gas temperature at evaporator outlet	°C	$T_{exh,out} \geq 90$	$T_{exh,out} \geq 90$
EGR gas temperature at EGR cooler outlet	°C	-	$T_{EGR,out} = 145$
Vapour quality at expansion outlet	-	$x_{EXP,out} \geq 0.9$	$x_{EXP,out} \geq 0.9$
Cooling fluid temperature at condenser outlet	°C	$T_{cf,cond,out} \leq 125$	$T_{cf,cond,out} \leq 125$
Maximum working fluid temperature (expander inlet)	°C	$T_{wf,EXP,in} \leq T_c$	$T_{wf,EXP,in} \leq T_c$
Cooling fluid mass flow	kg s^{-1}	$\dot{m}_{cf} \leq 5$	$\dot{m}_{cf} \leq 5$

Tab. 30. Constraints for the optimization procedure (case study 1)

Some considerations can be drawn about the imposed constraints:

- the pinch point value of 10°C has been considered as a trade-off between heat exchanger performance and cost-dimensions, as often proposed in literature;
- the working fluid evaporation pressure has been limited to 30 bar or 90% of the fluid critical pressure due to safety reasons and possible fluid chemical instability;
- the working fluid condensing pressure has been imposed to be higher than 1.2 bar in order to avoid ambient air leaking into the system and expensive sealing;
- the evaporating and condensing temperatures have been imposed higher than 50°C in order to avoid inverse heat transfer during particularly hot ambient conditions;
- the exhaust gas temperature at the outlet of the evaporator has been limited to 90°C in order to avoid acid condensation and corrosion problems (low sulphur content diesel fuel assumed);
- the EGR cooler gas outlet temperature has been fixed to 145°C in order to fulfil combustion requirements for the engine. This basically means EGR heat must be fully recovered due to recirculated gas cooling requirements;
- the coolant temperature at the condenser outlet has been limited to 125°C to avoid the cooling mixture to boil. In the IC2 heat sink layout, the coolant mass flow has been imposed lower than 5 kg/s to keep the design similar to the main engine cooling circuit;
- the vapour quality at the expander outlet has been imposed to be higher than 0.9 in order to avoid liquid droplets formation and possible damaging problems, especially when using turbo-expanders;

As last step, as *objective function*, it has been chosen to maximize the $BSFC_{impr}$ parameter (improvement of BSFC in comparison to the baseline engine without ORC), in order to obtain the best Brake Specific Fuel Consumption improvement when recovering heat from the engine with the ORC system.
The optimization process has been carried out using EES Optimization Toolbox, and the procedure developed in two steps:

1) A *Genetic Algorithm (GA)* [354] is used to obtain a first global best solution, exploiting the characteristics of the GA of being robust to find a global optimum, but slow and not very accurate. This will guarantee to be close to the global optimal point;
2) A *Nelder-Mead Simplex Algorithm* [355] is used as second step, starting from the GA solution, to find a more accurate best BSFC improvement value, thus refining the search, exploiting the properties of this type of algorithm of being more accurate and fast converging to the solution, but being less robust in finding a global solution;

Once obtained the best solutions for all the examined cases, the heat sink analysis has been carried out on the most promising configurations. The results of the overall procedure are reported in the next section.

6.1.6 Results and Discussion

The results of the optimization have been proposed in this section, divided between Simple Cycle (SC) and Parallel Cycle (PC) ORC layouts, reporting both the heat sink configurations, IC1 (higher temperature engine cooling circuit) and IC2 (lower temperature ORC-only cooling circuit).

6.1.6.1 ORC Performance Optimization

In the next sections, the results regarding the ORC simulations for the two different cycle architectures have been proposed.

Simple Cycle (SC) – Exhaust Gas Heat Recovery

Simple Cycle (SC) - BSFC improvement [%]			
IC1		**IC2**	
water-steam	6.4	methanol	7.7
toluene	6.3	acetone	7.6
ethanol	5.1	ethanol	7.1
acetone	4.9	cyclopentane	7.0
methanol	4.8	water-steam	6.7
cyclopentane	4.6	R-141b	6.3
R-141b	3.7	toluene	6.3
R-123	3.1	R-123	5.7
MDM	2.8	R-245fa	4.4
R-245fa	1.7	MDM	2.8

Tab. 31. Simple Cycle (SC) BSFC improvement (%) for IC1 and IC2 heat sink configurations (case study 1)

For the Simple Cycle (SC) layout, the working fluids giving the best BSFC improvement (Tab. 31) are water-steam for Indirect Condensation 1 (IC1) heat sink configuration (6.4%) and methanol for Indirect Condensation 2 (IC2) configuration (7.7%). The net power generated is almost in all fluids cases higher when IC2 heat sink is used, due to the lower condensing temperature and higher pressure

ratio available through the expander (e.g. + 46% for methanol from IC1 to IC2 configurations as reported in Fig. 63).

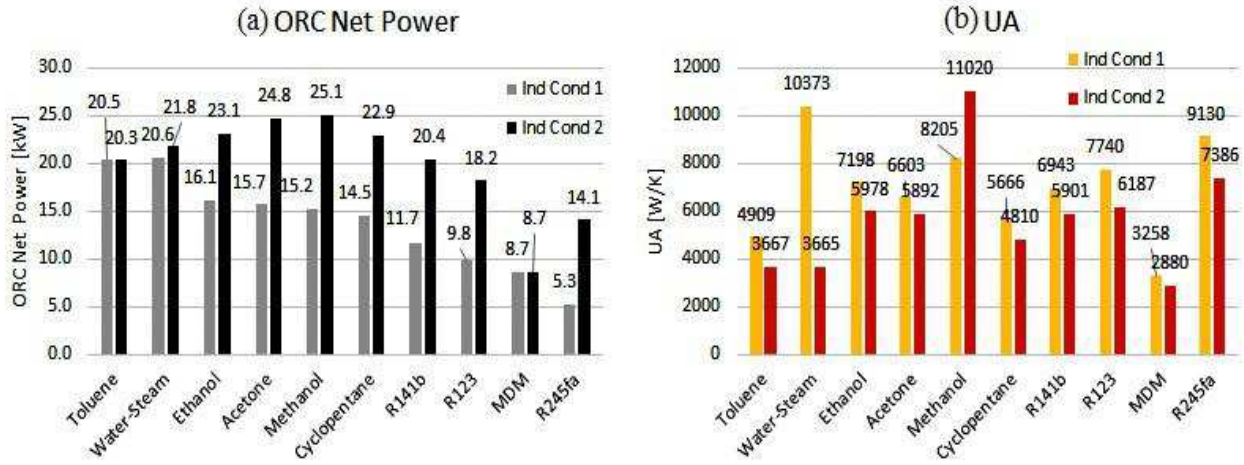

Fig. 63. (a) ORC net power output, (b) heat exchangers UA coefficient for Simple Cycle (SC) – (case study 1)

The $\sum U_i A_{HX,i}$ index gives an idea of the dimensions of the heat exchangers, and thus is also a global indicator of the cost of the heat transfer equipment. For example, in case of R-245fa, R-141b and R-123, the power generated is low compared to other fluids examined, and the heat transfer index is proportionally high, thus leading to bulky heat transfer equipment in comparison to the net power obtained. The same problem can be faced in case of methanol: BSFC improvement is high (7.7% in IC2) but $\sum U_i A_{HX,i}$ reveals the need of bulky heat exchangers to achieve this performance, compared to other fluids. Water-steam reveals a good compromise between ORC net power generated and heat transfer equipment dimensions, especially in IC2 configuration (IC1 shows quite high heat exchangers *UA*), and has no flammability and health issues, however it can lead to freezing problems in particularly cold weather conditions due to the high melting point. Toluene, ethanol, acetone, methanol and cyclopentane, even if with good BSFC improvement potential, still present flammability issues, and a mixture with other fluids, capable to mitigate the problem (e.g. water), could be considered in future studies, especially in case of direct evaporation configurations, in which possible fluid leakage could lead to ignition problems. MDM, even if leading to less bulky equipment and mass flow needs, leads also to low BSFC improvement (2.8% in both IC configurations). MDM seems to be more suitable in case of medium-low temperature heat recovery and the condensing temperature (at 1.2 bar condensing pressure) is also very high, thus leading to decreased pressure ratio available through the expander and decreased net power produced.

Parallel Cycle (PC) – Exhaust Gas and EGR Heat Recovery

For the Parallel Cycle (PC) ORC layout, the working fluids giving the best BSFC improvement (Tab. 32) are toluene for Indirect Condensation 1 (IC1) heat sink configuration (9.2%) and methanol for Indirect Condensation 2 (IC2) configuration (10.6%). Also in this case, there is a sensible increase in the net power generated from IC1 to IC2 (e.g. +57% in case of methanol, as reported in Fig. 64).
Generally, the same conclusions of SC cases can be drawn for the PC layout cases, with the difference that the PC layout leads to increased heat recovery, increased net power output and thus increased

BSFC improvement potential compared to SC. Even though the PC layout leads to an increase in heat rejection compared to the SC layout, it also allows the ORC to recover the EGR heat to produce additional useful power. If not recovered, this heat would have impact on the overall vehicle thermal management, since it would need to be rejected, in the EGR cooler, to the cooling system and then to the ambient through the cooling package, requiring additional fan parasitic power consumption and cooling package dimensions' requirements. Moreover, water-steam, despite his problems of freezing in case of low ambient temperatures, shows a very good potential (high BSFC improvement and low heat rejection compared to other fluids, due to higher cycle thermal efficiency). However, in case of IC1 heat sink layout, the heat exchangers result in being quite bulky.

Parallel Cycle (SC) - BSFC improvement [%]			
IC1		**IC2**	
toluene	9.2	methanol	10.6
water-steam	9.1	acetone	10.2
ethanol	6.8	water-steam	10.0
acetone	6.6	cyclopentane	9.9
cyclopentane	6.3	ethanol	9.9
methanol	5.9	toluene	9.2
R-141b	4.9	R-141b	8.7
MDM	4.2	R-123	7.7
R-123	4.1	R-245fa	6.1
R-245fa	1.9	MDM	4.2

Tab. 32. Parallel Cycle (PC) BSFC improvement (%) for IC1 and IC2 heat sink configurations (case study 1)

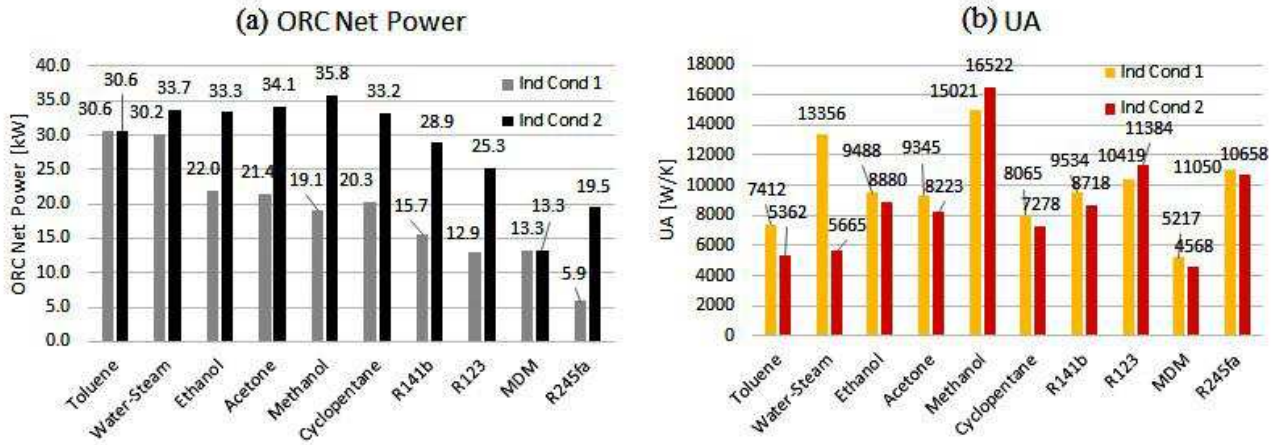

Fig. 64. (a) ORC net power output, (b) heat exchangers UA coefficient for Parallel Cycle (PC) – (case study 1)

From the analysis carried out with ten different working fluids, it has been confirmed that R-245fa, R-141b, R-123 and MDM are not suitable for medium-high temperature heat sources such as exhaust gas and EGR. Toluene, ethanol, methanol, acetone, cyclopentane and water-steam have been considered possible choices for a preliminary ORC concept, based on the prescribed boundary conditions, and are evaluated in the heat sink study reported in the next section.

6.1.6.2 Heat Sink Study

The heat rejected by the ORC system at the condenser must be transferred to the cooling loops and then to the ambient through the radiator (or through the two separated radiators in the case of IC2 heat sink configuration).
In Tab. 33, the heat rejected by the ORC systems in the various considered configurations is reported.

$\dot{Q}_{ORC,out}$ (kW)				
Fluids	**SC – IC1**	**SC – IC2**	**PC – IC1**	**PC – IC2**
toluene	128.2	128.4	191.5	191.5
water-steam	107.9	107.8	171.8	171.1
ethanol	135	138.9	200.7	202.2
acetone	135.4	137.5	201.4	201.9
methanol	136	137.2	203.6	200
cyclopentane	137	138.2	203.3	202.8
R141b	139.9	142	207.9	207.8
R123	142	142.2	211	211.9
MDM	125.4	125.4	192.1	192.1
R245fa	147.4	150	205.1	218.7

Tab. 33. ORC system heat rejection for the four cases evaluated and the working fluids considered (case study 1)

The data reported in Tab. 33 show a higher heat rejection in the PC layout (+40-60% if compared to SC), mostly due to the heat recovered in the EGR and introduced in the cycle. However, the EGR heat, if not recovered, should be anyway rejected to the ambient, thus being an additional thermal load for the vehicle thermal management system.
The EES code developed has been used in order to assess the heat rejection capabilities and dimensions needed for the combined engine-ORC radiator (IC1 configuration) or for the ORC rooftop radiator (IC2). In case of IC2 configuration, an additional fan is required to cool the ORC radiator, but still the conventional fan is used to cool the engine cooling package. In case of SC layout, the engine radiator must reject both engine and EGR heat, while in case of PC layout, only the engine heat, since the EGR heat is recovered by the ORC. The fan consumption of the baseline engine radiator must anyway be considered in the power balance analysis.
In case of IC1 configuration, the power balance can be reported as:

$$\Delta\dot{W} = \dot{W}_{ORC,net} - \dot{W}_{ENG/ORC,fan} \quad (124)$$

With $\dot{W}_{eng/ORC,fan}$ the power consumption of the fan of the combined engine-ORC radiator.
In the case of the IC2 configuration, in addition to the separate rooftop ORC fan consumption ($\dot{W}_{ORC,fan}$) also the fan consumption of the baseline engine radiator has to be considered ($\dot{W}_{ENG,fan}$, with or without EGR heat rejection depending on the ORC layout):

$$\Delta\dot{W} = \dot{W}_{ORC,net} - \dot{W}_{ORC,fan} - \dot{W}_{ENG,fan} \quad (125)$$

These power balances must be maximized in order to obtain the best benefit, considering also that increasing the radiator dimensions usually decreases the fan power consumption, but increases space and design issues.

In this study, however, no optimization algorithm has been used to size the radiator, but the main dimensions, width (W), height (H) and depth (D), have been swept and the fan power consumption estimated, always considering radiator shape and size having in mind an actual and feasible implementation, especially when using the configuration IC1 with a combined engine-ORC radiator, which must still fit in the engine under hood compartment.
In particular, for IC1 configuration, a maximum of 10-30 cm increase in height (H) and width (W), and 4-5 cm in depth (D) has been considered in this study.
For configuration IC2 (rooftop installation), an increase of maximum 50 cm in height and width, and 7 cm in depth has been tolerated, due to less stringent space constraints.
The new radiator dimensions have then been compared to the engine baseline radiator, with frontal area, $A_{f,rad}$, of 1 m^2, and the core volume, V_{rad}, of 0.08 m^3.

Simple Cycle – Indirect Condensation 1 (SC - IC1)

The best trade-off between radiator dimensions and fan parasitic consumption has been obtained with water-steam as working fluid, 40% percentage increase in radiator frontal area and 90% in radiator volume (calculated as difference between new and baseline radiator dimensions), with an estimated fan consumption of around 13 kW, reduced in comparison to the engine-only radiator due to the increased dimensions. Toluene can lead also to a good compromise (40% frontal area and 110% volume increase), but with increased fan consumption (17.3 kW) when considering almost the same increase in component dimensions. Toluene is also not as safe as water, due to flammability problems. For the other fluids considered, the compromise cannot be considered as good. Indeed, in these cases, it is necessary to further increase the radiator dimensions in order to achieve positive trade-off values. The IC1 heat sink configuration is the most compact solution, when trying to fit the ORC thermal management components in the vehicle cooling package, as well as the most compact in terms of ORC components dimensions.
In every case evaluated it is not possible to achieve the required heat rejection performance using the same baseline engine radiator dimensions.

Parallel Cycle – Indirect Condensation 1 (PC - IC1)

This configuration is beneficial regarding both ORC performance and thermal management. Indeed, EGR heat is recovered by the ORC system, thus producing net power from the heat that otherwise should be rejected in the engine cooling circuit, and then to the ambient through the radiator.
Also in this case, the best trade-off between radiator dimensions and fan parasitic power consumption can be obtained with water-steam. With the same percentage increase in frontal area (40%) and volume (90%) of SC case, the fan consumption drops from 13 kW to 6.2 kW, while the net ORC power generated increases from 20.6 kW to 30.2 kW. In this case, it would be also possible to decrease the combined engine-ORC radiator dimensions still keeping a good compromise between dimensions and parasitic fan consumption. Also in this case, the second-best choice is toluene (30.6 kW ORC net power and 8.2 kW fan consumption), while the other fluid still gives acceptable compromises compared to the SC-IC 1 case.
Generally, even if adding an additional heat exchanger (EGR boiler) is detrimental regarding packaging, cost, weight and system complexity issues, the compromise between performance and thermal management is better than in the case of the SC layout, when using IC1 heat sink configuration, or compared to the baseline configuration without ORC system.

Simple Cycle – Indirect Condensation 2 (SC – IC2)

In case of using the lower temperature cooling circuit, even though the ORC condensing temperature can be decreased, the temperature difference between the coolant and the ambient air is also smaller, thus leading to the need of drastically increasing the radiator dimensions in order to keep a good compromise with fan parasitic consumption (100% percentage increase in frontal area and 275% in volume). Furthermore, the positive effect of using the ORC, is almost completely overcome by the need to reject a high amount of heat to the ambient when recovering exhaust gas but not EGR. For this reason, SC-IC2 configuration gives basically no benefits, being the ΔP parameter basically always negative when considering even consistent radiator dimensions increase.

Parallel Cycle – Indirect Condensation 2 (PC -IC2)

In this case, considering the same frontal area and volume dimensions' increase compared to engine baseline radiator used in SC-IC2 configuration, the best trade-off is given by ethanol (33.3 kW ORC net power generation and 15.1 kW fan consumption). This is because the coolant mass flow required for ethanol case is lower than for water-steam or other fluids, while the coolant temperature at the radiator inlet is higher, thus leading to a higher ΔT with the cooling ambient air and smaller radiator dimensions-fan parasitic consumption compromise. Water-steam still gives a good compromise, but with higher fan consumption (19.4 kW), even if with similar ORC net produced power (33.7 kW). Other fluids lead to not comparable benefits.
Also in this configuration, increasing the radiator dimensions is beneficial in order to reduce fan power consumption. This could be compatible with a rooftop installation, however, weight and cabin resistance issues must be assessed, as well as layout complexity.

6.1.6.3 Overall Results

The first six best configurations, and relative power balance and radiator dimensions' increase, obtained after the heat sink study are reported in Tab. 34.

Fluid	**Config.**	$A_{f,rad,incr}$ **[%]**	$V_{rad,incr}$ **[%]**	$\dot{W}_{fan}$ **[kW]**	$\dot{W}_{ORC,net}$ **[kW]**	**Δ [kW]**
water-steam	PC-IC1	40	90	6.2	30.2	24.0
toluene	PC-IC1	40	90	8.2	30.6	22.4
ethanol	PC-IC2	100	275	15.1	33.3	18.2
acetone	PC-IC1	40	90	9.3	21.4	12.1
cyclopentane	PC-IC1	40	90	9.7	20.3	10.6
methanol	PC-IC1	40	90	9.7	19.1	9.4

Tab. 34. ORC-heat sink study best configurations

From a comparison of the results, it emerges how the Parallel Cycle (PC) ORC layout is always the best choice compared to the Simple Cycle (SC) regarding ORC and heat rejection performance.
In particular, for IC1 heat sink configuration (engine cooling circuit), the recovery of EGR heat is beneficial also for thermal management, since the heat, that otherwise has to be rejected to the engine cooling circuit and then to the ambient through the radiator, is used to produce additional net power in the ORC. EGR recovery allows also smaller radiator dimensions and a better compromise with fan consumption, due to the fact that part of the EGR recovered heat is converted into useful power in the

ORC, and a lower amount of heat is then rejected to the coolant, thus reducing the impact on the vehicle thermal management system.
IC2 heat sink configuration (LT cooling circuit) is not very beneficial. This is mainly due to the fact that a lower coolant temperature leads to a lower temperature difference between coolant and cooling air in the radiator, and thus higher heat transfer area requirements. This configuration could be used when lower ambient temperature conditions are expected and when ethanol is used.

6.1.7 Conclusions

The results of the case study show how the choice of the best ORC solution, especially in vehicle applications such the one proposed, is always a trade-off between several considerations: ORC performance, heat rejections capabilities and vehicle thermal management, fluids properties (safety, flammability, availability and environmental impact), packaging and weight constraints, components choice and performance, engine and ambient boundary conditions.
In the cases analysed, even if methanol or acetone in PC-IC 2 configuration, give the best BSFC improvement potential (respectively 10.6% and 10.2%), fan consumption and radiator dimensions are higher than in the case of water-steam, toluene or ethanol, leading to an overall reduced benefit when considering engine cooling needs. Water-steam, even with possible freezing problems, can be a valuable choice regarding performance and thermal management. Water has a very high potential for waste heat recovery in the temperature range considered in this application (500-600°C, exhaust gas and EGR), is safe in operations, readily available, non-toxic, chemically stable and environmentally friendly. Toluene and ethanol, even if with more safety and flammability concerns, present less freezing issues and still good thermodynamic performance. Ethanol is indeed one of the fluids considered by OEMs and system developers.
Recovering EGR heat is beneficial both regarding ORC performance and vehicle thermal management because, particularly with heat sink IC1 configuration, it allows to reduce combined engine-ORC radiator dimensions and fan power consumption and, at the same time, to improve the overall powertrain performance at the expense of a slightly more complicated architecture, due to the ORC components installation. However, the engine cooling layout remains similar to the baseline one.
The IC2 configuration is not very beneficial. Indeed, in case of ethanol and PC layout, the overall powertrain will benefit from an increased power output but encompassing a bulkier and more complicated cooling system, and an increased fan parasitic consumption.
A recuperated cycle could be proposed when using dry fluids (e.g. toluene), thus allowing to reduce the heat rejection to the cooling package but increasing the overall system complexity and cost.
Regarding heat rejection, Ricardo guidelines often suggest limiting the heat recovery (and thus the heat rejection at the condenser side) due to cooling package dimensions' requirements. This will limit also the ORC net power achievable to maximum values declared to be around 20 kW. After this limit, usually the exhaust boiler is by-passed.
Furthermore, heat and pressure losses, combined engine backpressure effects and a cost analysis and feasibility are not assessed in this study but must be considered for future research and development activities. For example, the backpressure issue has been assessed in the second case study, referred to a marine four stroke power generator.

6.2 Case Study 2: Marine Four-Stroke Power Generator

In literature, several studies are available about the introduction of ORC systems in marine applications, as already reported in the overview in section 4.2.4, but not all of them consider also the mutual effect on the internal combustion engine.
In this work, the interactions between a modern marine turbocharged Diesel power generation unit and a possible exhaust gas driven ORC system, for combined system efficiency improvement, have been investigated through simulation.
In particular, both internal combustion engine and ORC sides have been investigated in this case, considering different engine turbocharging strategies and the optimization of the ORC cycle parameters in order to obtain the best combined fuel consumption reduction with the fluids examined.
On the engine side, the adverse backpressure effect of fitting an exhaust gas driven ORC evaporator on the engine breathing capabilities, is investigated using Ricardo proprietary 1-D engine performance simulation software Ricardo WAVE [11]. Fixed geometry, Waste-Gate (WG) and Variable Geometry Turbocharger (VGT) boosting technologies have been evaluated in order to withstand the increased engine pumping losses due to the waste heat recovery boiler installation.
On the ORC side, for each of the three investigated turbocharging system scenarios and for a moderate exhaust gas backpressure, which corresponds to specific exhaust gas characteristics (mass flow rate and temperature), the power output of optimized, in terms of thermodynamic cycle parameters, simple and recuperated exhaust gas driven ORC layouts has been computed using Engineering Equation Solver (EES, [365]) for a set of working fluids (n-hexane, n-octane, acetone, toluene, ethanol and MDM) selected after a screening procedure, which, as already proposed in the previous case study and in the literature review section, considers not only thermodynamic performance, but also environmental, flammability and safety issues. After identifying the most promising turbocharging system-ORC configuration, in terms of combined system fuel economy improvement for the moderate backpressure case, further simulations of this system have been performed for a range of backpressure values in order to evaluate the corresponding expected range of fuel economy benefit for all possible heat exchangers hardware designs.
The work proposed in this case study has been co-published by the author in Michos *et al.* [273].

6.2.1 Reference Engine and Design Point Choice

The simulation model has been implemented using Ricardo WAVE [11], considering a 1.5 MW high speed Diesel engine (120 kW/Cylinder at 1500 rpm) running at full load conditions.
The engine configuration is a V12, with single-stage turbocharging and aftercooler, employing Miller inlet valve timing for reduced NO_x emissions. The engine is used in the power generation or marine sector as a generator set and equipped with a Selective Catalytic Reduction (SCR) system for compliance with IMO (Internal Maritime Organization) Tier III NO_x emissions regulations [3] (Tab. 3). Some of the basic geometric features and full load performance data of the engine at ISO ambient conditions (25°C, 1 bar) have been reported in Tab. 35. Some other more detailed engine information has not been reported due to confidentiality reasons.
It is assumed that, at the above reported ambient conditions, the pressure drops of the SCR system and the Charge Air Cooler (CAC) are respectively 120 mbar and 100 mbar, while the outlet temperature of the CAC and the efficiency of the SCR system are always constant, being respectively 55°C and 65%. It has to be noted that the SCR efficiency determines the maximum allowable engine NO_x emissions, which are in turn controlled in the engine WAVE model by regulating the injection timing. This parameter is also controlled in order to avoid having peak cylinder pressures higher than 230 bar.

All these assumptions have been fixed based on the information coming from Ricardo project analysis, regarding the proposed type of engine.
Another constraint, related to safe turbocharger turbine steady-state operations, is that the inlet temperatures should not be higher than 700°C. All the parameters and constraints have been controlled using adequate controlling strategies implemented in the engine WAVE model.

Displacement/cylinder (l)	V_d	4.31
N° of cylinders	n_{cyl}	12
Speed (rpm)	N	1500
Brake Mean Effective Pressure (bar)	$bmep$	22
AFR trapped (-)	AFR	27
IMO Tier III NOx limit (g/kWh)	-	2.0
Baseline turbocharging efficiency (%)	η_{TC}	59.0

Tab. 35. Basic engine features and full load performance data at ISO ambient conditions (baseline engine case, case study 2)

The model simulates the combustion process in a simplified way, using an experimentally derived, non-dimensional burn rate profile, which is valid under the examined engine speed, trapped Air-Fuel-Ratio (AFR) and typical start of injection (SOI) timings. To simplify the calculations, it has been assumed that the turbocharger efficiency remains constant. The turbine and compressor have been modelled with a quasi-steady approach, calculating the mass flow and enthalpy rise across the components, simulated as an orifice, as well as the torque produced or absorbed.

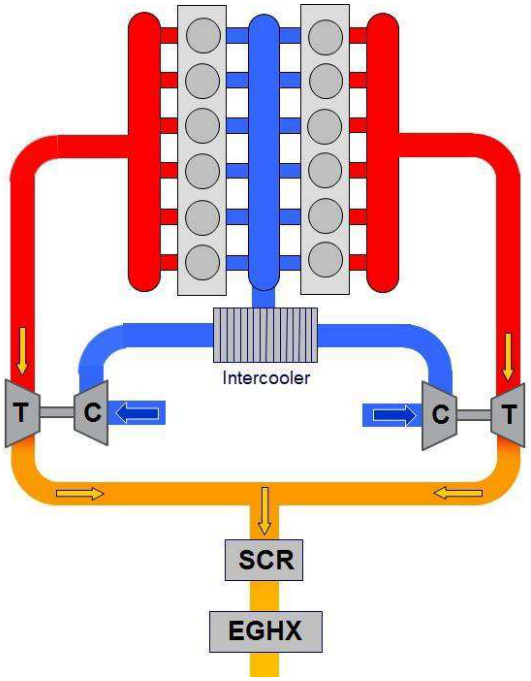

Fig. 65. Combined engine-ORC EGHX layout scheme (case study 2)

Considering that the SCR thermochemical performance has not been modelled and considered in this work, it has been assumed that, under steady-state operating conditions, the exhaust gas temperature downstream the turbocharger turbine is equal to the inlet temperature of the Exhaust Gas Heat Exchanger (EGHX or boiler) of the ORC system (no temperature change is assumed over the SCR system, following what reported by Qiu *et al.* [357]).

The ORC boiler is installed downstream the SCR system, as reported in Fig. 65, which describes the layout of the combined Engine-EGHX. The sketch of the WAVE model has not been reported because of confidentiality reasons.

6.2.1.1 Turbocharging Systems Description

In a common turbocharger design for large four-stroke engines, an exhaust gas driven radial or axial turbine is coupled to a centrifugal air compressor. The engine exhausted gas drives the turbine which is coupled to the compressor in order to increase the intake boost pressure, thus also increasing engine volumetric efficiency and performance [62].
Three turbocharging systems are analysed: 1) fixed geometry turbine, 2) Waste-Gate (WG) and 3) Variable Geometry Turbocharging (VGT). Some of the features have been already described in section 4.1.3.2, however, a short overview of the considered technologies has been proposed in the next paragraphs, describing which considerations have been used in the simulation campaigns.
The simplest turbocharger configuration is with fixed geometry for both compressor and turbine. In this case, there is no boost control possibility, and the boost level is directly related to the exhaust gas flow and to the turbocharger characteristics. The enthalpy to drive the turbine is directly dependent on the combustion performance.
The WG turbocharging strategy uses a waste gate valve to bypass the turbine in order to control the rotational speed of the turbocharger, thus regulating the boost pressure of the engine. Adding a by-pass valve to the fixed geometry turbocharger is the easiest implementable strategy to improve engine control over a more severe transient operational profile or over more variable backpressure conditions. However, typically, WG turbochargers increase the exhaust losses, thus leading to decreased turbocharger efficiency [64].
The VGT operates altering the geometry of the effective turbine area in order to reach the requested boost pressure for the compressor, but still handling all the exhaust flow, which does not bypass the turbine. This turbocharging strategy usually allows better control of boost pressures at low engine loads and speeds. In particular, for large medium-low speed Diesel engines as the one considered in this study, the VGT is equipped with a nozzle ring with movable vanes which direct the exhaust gas flow through the turbine blades. The angle of the vanes is controlled at different engine speeds in order to optimize the flow through the turbine [366]. A precise control of AFR can be obtained with this strategy, as well as losses associated with the Waste-Gate valve are eliminated and engine control improved [62]. Drawbacks of VGT are the increased cost and vanes fouling problems when using heavy fuel oils [64].
In this preliminary study, a parametric analysis of the ORC boiler backpressure effect has been carried out considering the three turbocharging solutions and assuming the engine operating at full load constant conditions.
The backpressure range considered is from 0 to 100 mbar in order to study different boiler designs.
When considering the Waste-Gate solution (Case 2), the turbocharger is dimensioned, at the highest backpressure case (100 mbar), with fully closed waste gate valve, thus resulting in a smaller turbine than that used in Case 1 with fixed geometry turbocharger. The dimensioning aims also to maintain the AFR at the design point value. Then, as the backpressure is reduced, the waste gate valve is gradually opened in order to keep the requested AFR always constant.
In the Case 3, the turbine nozzle area of the VGT turbocharger is controlled in order to keep, again, the AFR constant, independently of the EGHX backpressure imposed.

6.2.2 ORC Architectures

In terms of ORC system layouts, a simple and a recuperated cycle have been examined in this case study, both employing an intermediate thermal oil circuit [367], to avoid the contact between exhaust gas and possibly flammable working fluids.
The cooling medium in the condenser is water, which could hypothetically be sea water, and easily available on-board ships.
The schemes of the two cycle architectures considered have been reported in Fig. 66.

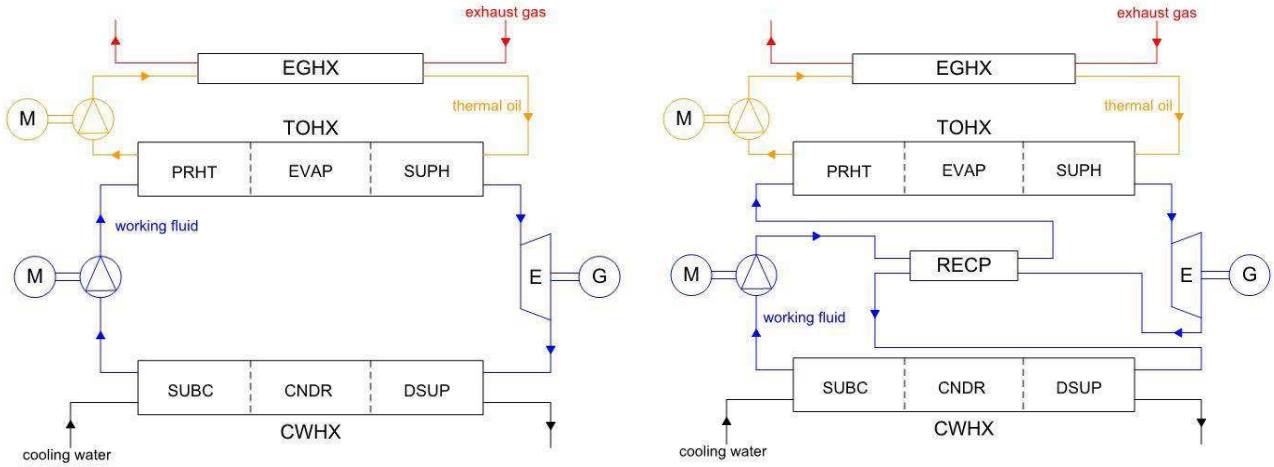

Fig. 66. Schemes of the simple (a) and recuperated (b) ORC layouts (case study 2)

For modelling reasons, the Thermal Oil Heat Exchanger (TOHX) and the Cooling Water Heat Exchanger (CWHE) are divided respectively in three regions, in which preheating (PRHT), evaporation (EVAP), superheating (SUPH), de-superheating (DSUP), condensing (CNDR) and sub-cooling (SUBC) processes happen, as already introduced in section 5.2.
For every region, a fixed boundary modelling technique have been applied, as well as mass and energy balances.
In the case of the Exhaust Gas Heat Exchanger (EGHX), a unique region has been considered, since no phase change is happening. The same approach is used for the recuperator (RECP).
All the heat exchangers have been considered to have a counter-flow configuration in order to increase heat transfer efficiency.
The pump and expander (E) have been modelled with a simple fixed isentropic efficiency, considered for steady-state full load operations (the efficiencies have been reported in Tab. 39).
Two examples of T-s diagrams have been reported in Fig. 67 in the case of n-hexane working fluid, for the simple and recuperated cycles.
In the case of the recuperated cycle, a recuperator (RECP) has been added in order to partially preheat the liquid working fluid downstream the pump using the heat rejected from the superheated vapour at the expander outlet. The purpose of this second configuration is to increase the ORC system efficiency thus leading to a better utilization of the engine recovered heat. This will also lower heat rejection at the condenser side for the same power output generated. The solution is suitable in particular for dry fluids. The ORC has been modelled through the use of energy balances as reported already in section 5.2.1, using EES. In this case, the properties of the intermediate thermal oil and, in particular, the specific heat for the heat balances calculations, have been obtained from [367], and a correlation has been calculated based on the temperatures at the inlet and outlet of the heat exchangers and pump of the oil circuit:

$$c_{p,TO} = 0.003 \cdot T_{TO} + 1.6017 \quad (126)$$

An average specific heat value [kJ/kgK] has been used, between inlet and outlet of the heat exchangers components, in order to calculate the heat balances (the exhaust gas specific heat has been considered constant in first approximation).

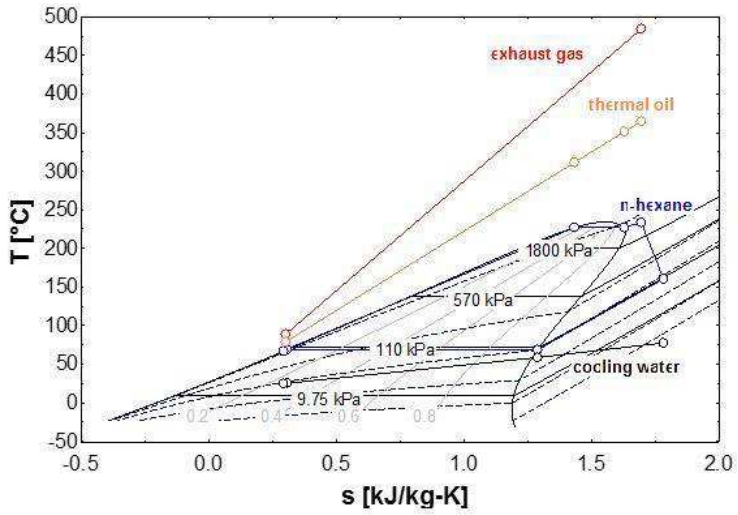

(a)

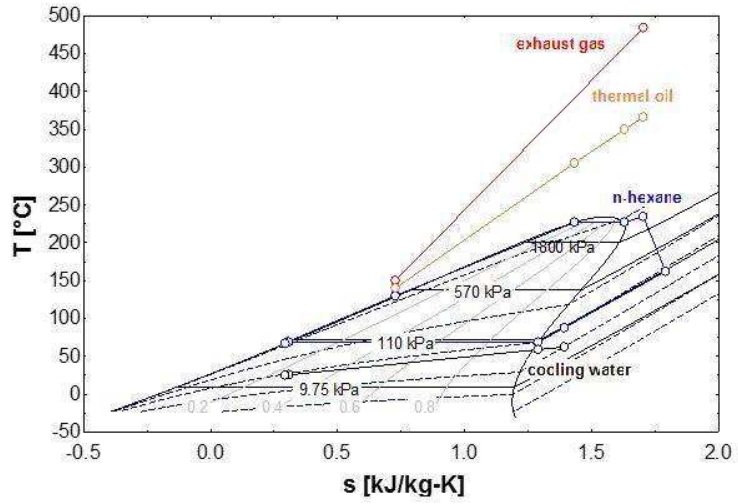

(b)

Fig. 67. n-hexane T-s diagram examples for simple (a) and recuperated (b) ORC (case study 2)

In the case of the recuperated ORC system (RECP), the heat exchanged between the liquid and vapour sides of the heat exchanger has been calculated from an iterative procedure solved in EES, in order to obtain the vapour side outlet temperature $T_{vap,RECP,out}$ and the liquid side outlet temperature $T_{liq,RECP,out}$. The considered specific heat is the minimum between the average values calculated at the liquid and vapour sides, and it is dependent on the outlet temperatures. The balance over the recuperator has been calculated with the following formula, assuming a fixed heat exchange effectiveness, ε_{RECP}, of 80%:

$$q_{RECP} = \varepsilon_{RECP} \cdot c_{p,min} \cdot \left(T_{vap,RECP,in} - T_{liq,RECP,out}\right) \quad (127)$$

The thermal oil circuit pump power consumption has been estimated based on an assumed averaged 80 mbar pressure drop over both the two heat exchangers, from the following formula:

$$\dot{W}_{P,TO,is} = \frac{\left(\Delta p_{TO,TOHX} + \Delta p_{TO,EGHX}\right) \cdot \dot{m}_{TO}}{\rho_{TO} \cdot \eta_{P,TO}} \quad (128)$$

The thermal oil pump fixed isentropic efficiency ($\eta_{is,P,TO}$) is 60%.

The thermal oil density has been calculated [kg/m^3], as previously done for the specific heat, with the following formula, fitted from the curve reported in [367]:

$$\rho_{TO} = -0.7543 \cdot T_{TO} + 979.25 \quad (129)$$

6.2.3 Working Fluid Selection

In order to limit the number of working fluids to be investigated through simulation, a selection procedure has been conceived and applied, based on environmental (legislative), safety, usage and thermodynamic requirements, as already introduced in section 4.2.2.1.
Based on these environmental limitations already considered in the theory section, various working fluids (pure substances and mixtures) from the relevant literature as well as from real applications for low- [149] and high-temperature [153] ORC applications have been considered at the starting point of the selection procedure and categorised into families, as shown in Tab. 36.

Linear and branched hydro-carbons	*Aromatic hydro-carbons*	*HFCs*[1]	*Fluoro-Carbons*	*Inorganic fluids*	*Alcohols*	*Siloxanes*	*Zeotropic mixtures*
i-butane	cyclopropane	R134a	C5F12	water	ethanol	MDM	ammonia/water 20/80
pentane	benzene	R236fa	RC318	ammonia		MM	R32[1]/R134a[1] 30/70
n-hexane	toluene	R245fa					R125[1]/R245fa[1] 90/10
n-octane	p-xylene	R365mfc					R245fa[1]/R152a[1] 45/55
acetone							R245fa[1]/pentane 50/50
[1] *Listed in the Kyoto Protocol*							

Tab. 36. Working fluids considered at the starting point of the selection procedure (case study 2)

Due to safety issues, the environment in which the ORC system is going to operate should always be taken into consideration. For this reason, the generally applicable NFPA 704 Standard has been used in this work to characterise the severity level of each working fluid in terms of health, flammability, and instability hazards [368]. As a rule, working fluids with 'Health Hazard' higher than 2 and 'Flammability Hazard' higher than 3 have been excluded and not considered in the simulation work.

In terms of usage requirements, working fluids with freezing temperatures higher than approximately - 30°C should be also excluded, in order to avoid freezing problems during very cold days, unless the ORC is installed in temperature-controlled environment. For this reason, in this case water-steam has not been evaluated, even though it could be suitable for the application and temperature ranges, as demonstrated in the other case studies.
Specific thermodynamic requirements must also be considered in the simulations.
At the low-pressure side of the ORC system, the condensation pressure should be higher than the ambient pressure in order to avoid air infiltration into the system, while the condensation temperature should be higher than approximately 50°C, to prevent reverse heat transfer from ambient to the working fluid during very hot days. These constraints have been graphically reported in Fig. 68, where the saturation curves of most of the considered fluids of Tab. 36 are presented (NIST REFPROP data, [147]). The constraints could however vary from case to case examined and based on the boundary conditions assumed.
As shown, the upper right (white) window represents the practical condensation region of the various fluids. In particular, regarding HFCs and fluorocarbons, it can be observed that the condensation pressure must be relatively high, resulting consequently in reduced available expansion ratios for the ORC expander and consequently lower power production.

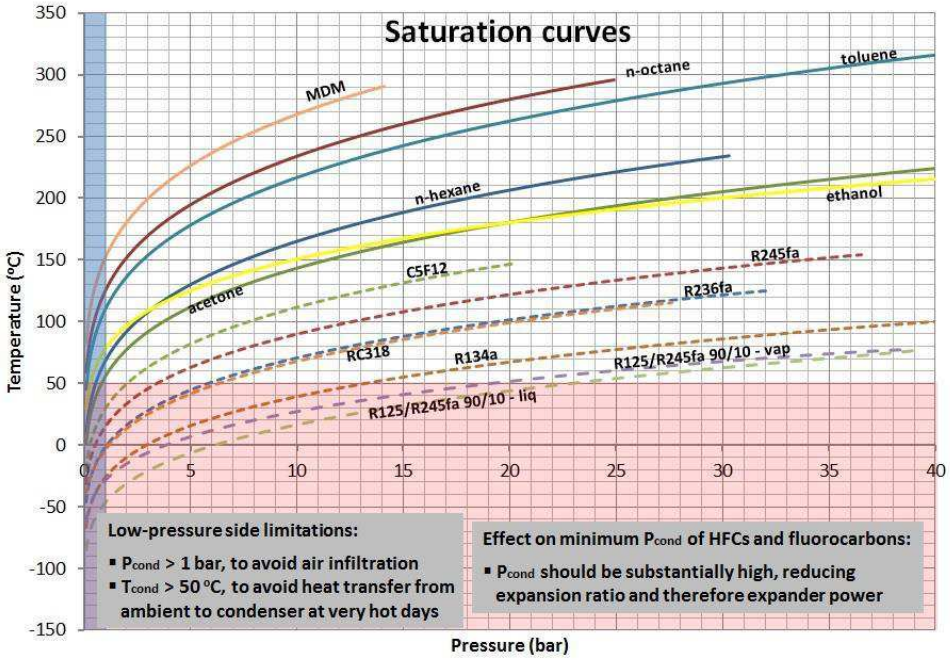

Fig. 68. ORC system low pressure side limitations on working fluids saturation curve diagram (case study 2)

With similar considerations, at the high-pressure side, the evaporation pressure should be lower than the critical pressure of the working medium, in order to avoid fluid degradation effect, as well as a limit of 30 bar for the maximum cycle pressure has been set to avoid material strength and possible safety issues. Moreover, the evaporation temperature should be higher than 50°C to again prevent reverse heat transfer during operations in very hot environments or climate conditions.
As an appropriate guideline, fluids whose critical temperature is higher than 200°C should be considered suitable for medium-high temperature ORC applications such as in the considered case study.
All previously described requirements and constraints, applied separately to each of the various fluids of Tab. 36, have been collectively presented in Tab. 37. Each fluid has been evaluated against the

requirements successively and, when not passing one of them, it has been discarded and not analysed in the following simulation work. From the original set of candidate fluids, it can be seen that only six of them are appropriate for the developed case study, considering the described constraints assumed. The appropriate fluids have been reported in bold letters in Tab. 37 and in Tab. 38 with the respective main properties, obtained from NIST REFPROP [147].

Working Fluid	**Health hazard**	**Flammability hazard**	**Freezing temperature T_f**	**Condensation pressure p_{cond}**	**Evaporation pressure p_{evap}**	**Critical temperature T_c**
	-	**-**	**°C**	**bar**	**bar**	**°C**
Requirement	*≤ 2*	*≤ 3*	*< -30 °C*	*available range should be significant*		*> 200 °C for high temp. applications*
i-butane	1	4	-	-	-	-
Pentane	1	4	-	-	-	-
n-hexane	**2**	**3**	**-95.3**	**> 1**	**< 30**	**234.7**
n-octane	**1**	**3**	**-56.6**	**> 1**	**< 25**	**295.2**
acetone	**1**	**3**	**-94.7**	**> 1**	**< 30**	**235**
cyclopentane	1	4	-	-	-	-
benzene	2	3	5.5	-	-	-
toluene	**2**	**3**	**-95.2**	**> 1**	**< 30**	**318.6**
p-xylene	2	3	13.3	-	-	-
R134a	1	0	-103.3	>13.2	< 30	101.1
R236fa	1	0	-93.6	> 5.9	< 30	124.9
R245fa	2	0	-102.1	> 3.5	< 30	154
R365mfc	0	4	-	-	-	-
C5F12	1	1	-120	> 2.1	< 20.5	147.4
RC318	2	0	-40	> 6.5	< 27.8	115
water	0	0	0	-	-	-
ammonia	3	-	-	-	-	-
ethanol	**2**	**3**	**-114.2**	**> 1**	**< 30**	**241.6**
MDM	**0**	**3**	**-86**	**> 1**	**< 14.2**	**290.9**
MM	1	4	-	-	-	-
ammonia/water 20/80	3/0	-	-	-	-	-
R32/R134a 30/70	1/1	4/0	-	-	-	-
R125/R245fa 90/10	1/2	0/0	-107	> 22.9	< 30	-
R245fa/R152a 45/55	2/1	0/4	-	-	-	-
R245fa/pentane 50/50	2/1	0/4	-	-	-	-

Tab. 37. Working fluid selection procedure (case study 2)

Working Fluid	T_c [°C]	p_c [bar]	T_{boil} [°C]	T_f [°C]
n-hexane	234.7	30.4	68.7	-95.3
n-octane	295.2	25	125.6	-56.6
acetone	235	47	56.1	-94.7
toluene	318.6	41.3	110.6	-95.2
ethanol	241.6	62.7	78.4	-114.2
MDM	290.9	14.2	152.5	-86

Tab. 38. Working fluids evaluated for the simulation work (case study 2)

6.2.4 Optimization Procedure and Performance Indexes

The basic assumptions and constraints for the ORC investigated in this work have been presented in Tab. 39. The cycle independent variables for the optimization procedure have been reported in Tab. 40. A Genetic Algorithm has been applied, with the purpose of maximizing the ORC net power output. The ORC engine exhaust gas boundary conditions are reported, for every turbocharging case evaluated, in Fig. 69 (k to l).

Parameter	Symbol	Value
Thermal oil pump isentropic efficiency	$\eta_{P,TO}$	60%
Working fluid pump isentropic efficiency	η_P	60%
Expansion machine isentropic efficiency	η_{EXP}	70%
Mechanical and electrical efficiencies of machines	η_{mech}, η_{el}	100%
RECP effectiveness	η_{RECP}	80%
Exhaust gas specific heat capacity under constant pressure	$c_{p,exh}$	1.15 kJ/kg/K
Cooling water specific heat	$c_{p,cool}$	4.19 kJ/kg/K
Piping pressure losses in thermal oil, working fluid and cooling	Δp_{pipes}	0 (not considered)
Thermal oil pressure losses in EGHX	$\Delta p_{TO,EGHX}$	80 mbar
Thermal oil pressure losses in TOHX	$\Delta p_{TO,TOHX}$	80 mbar
Working fluid pressure losses in TOHX, CWHX and RECP	$\Delta p_{wf,i}$	0 (not considered)
Cooling water pressure losses in CWHX	Δp_{cool}	0 (not considered)
Heat losses in piping and components	$\dot{Q}_{HT,i}$	0 (not considered)
Sub-cooling (1)	$\Delta T_{sub-cool}$	2 °C
Condensation pressure	p_{cond}	1 bar
Cooling water inlet temperature	$T_{cool,in}$	25 °C
Exhaust gas temperature downstream EGHX (2)	$T_{exh,EGHX,out}$	> 85 °C
EGHX, TOHX, CWHX pinch point temperature diff.	$\Delta T_{pp,i}$	> 10 °C
Evaporation pressure	p_{evap}	< min (0.9×p_c, 30 bar)
Maximum working fluid temperature	$T_{wf,max}$	< T_c

Tab. 39. Assumption and constraints for the ORC system optimization (case study 2)

Thermal Oil Mass Flow [kg/s]	$\dot{m}_{TO}$
Thermal Oil EGHX Inlet Temperature [°C]	$T_{TO,in}$
Pump Pressure Ratio [-]	PR
ORC Working Fluid Mass Flow [kg/s]	$\dot{m}_{wf}$
Superheating [°C]	ΔT_{suph}
Cooling Water Mass Flow [kg/s]	$\dot{m}_{cool}$

Tab. 40. Independent variables for optimization procedure (case study 2)

Regarding the condenser, a slight sub-cooling is usually applied to ensure that the working fluid, at the inlet of the pump, is in a liquid state, even if the fluid receiver is not modelled in this study for simplicity reasons.
Regarding the exhaust gas temperature downstream the EGHX (2), it should be usually higher than the acid dew point temperature of the gas, in order to ensure that no condensation of corrosive sulphuric acid occur on the last section of the heat exchanger. For IMO Tier III complying marine Diesel generators, where the equivalent sulphur mass fraction in the fuel must be as low as 0.1% in the Emission Control Areas (ECAs), an acid dew point temperature in the range of 85-90°C can be expected and has been assumed as constraint in this study.
Together with the evaluation of the ORC net power output, which is used to compute the BSFC improvement of the combined engine-ORC configuration, various comprehensive ORC system performance indexes have been also calculated, characterising the efficiency of the exploitation of the engine waste heat energy and the size and economics of the ORC system. Most of the indexes have been obtained or re-elaborated from Branchini *et al.* [302], and have been reported in Tab. 41.

Index	**Symbol**	**Significance**	**Aspect**	**Favorable trend**
Thermal efficiency	$\eta_{ORC,th} = \frac{w_{ORC,net}}{q_{in}}$	conversion efficiency of absorbed exhaust gas heat into useful power output	system efficiency	high
Specific work	$w_{ORC,net} = w_{EXP} - w_P$	amount of organic fluid required for an assigned power output	system efficiency	high
Organic fluid to exhaust gas mass flow ratio	$MFR = \frac{\dot{m}_{wf}}{\dot{m}_{exh}}$	amount of organic fluid required per unit of exhaust gas mass flow	system size	low
Recovery efficiency	$\eta_{rec} = = MFR \cdot \frac{w_{ORC,net}}{c_{p,exh} \cdot (T_{exh,in} - T_{exh,out,min})}$	conversion efficiency of available exhaust gas heat into useful power output (proportional to the product of thermal efficiency and heat recovery process effectiveness)	system efficiency	high
Expander volumetric expansion ratio	$VER = \frac{v_{out}}{v_{in}}$	expansion machine sizing (and possibly type) – ratio of specific fluid volumes over the expander	system size	low
HXs surface index	$SI_{HX,ORC} = \frac{\sum_i UA_i}{\dot{m}_{exh}}$	sum of HXs surface	system size	low

Tab. 41. ORC system performance indexes (case study 2)

In particular, the last index concerning heat transfer equipment dimensions, can be very useful, since the final decision regarding the selection of the most favourable cycle layout and organic working fluid, for the investigated turbocharging system scenarios and the relative engine configuration, should be ultimately based on a thermo-economic assessment, as reported by Quoilin *et al.* [338], followed by multi-criteria evaluation, as exemplified by Frangopoulos *et al.* [369], using technical, economic and environmental parameters.
The heat exchanger conductance UA_i has been calculated using the Log Mean Temperature Difference method (LMTD) [307].

6.2.5 Results and Discussion

In the following paragraphs, the results of the thermodynamic process analysis and optimization of the engine and ORC systems have been presented and discussed, with the purpose of finding the best configuration to increase the overall powertrain fuel efficiency.

6.2.5.1 Engine and Turbocharging Systems

Fig. 69 (a to l) show various engine and turbocharging system parameters for the three investigated turbocharging systems (fixed turbine, Waste-Gate and VGT), considering the effect of the increased backpressure due to the installation of the ORC boiler (ORC EGHX).

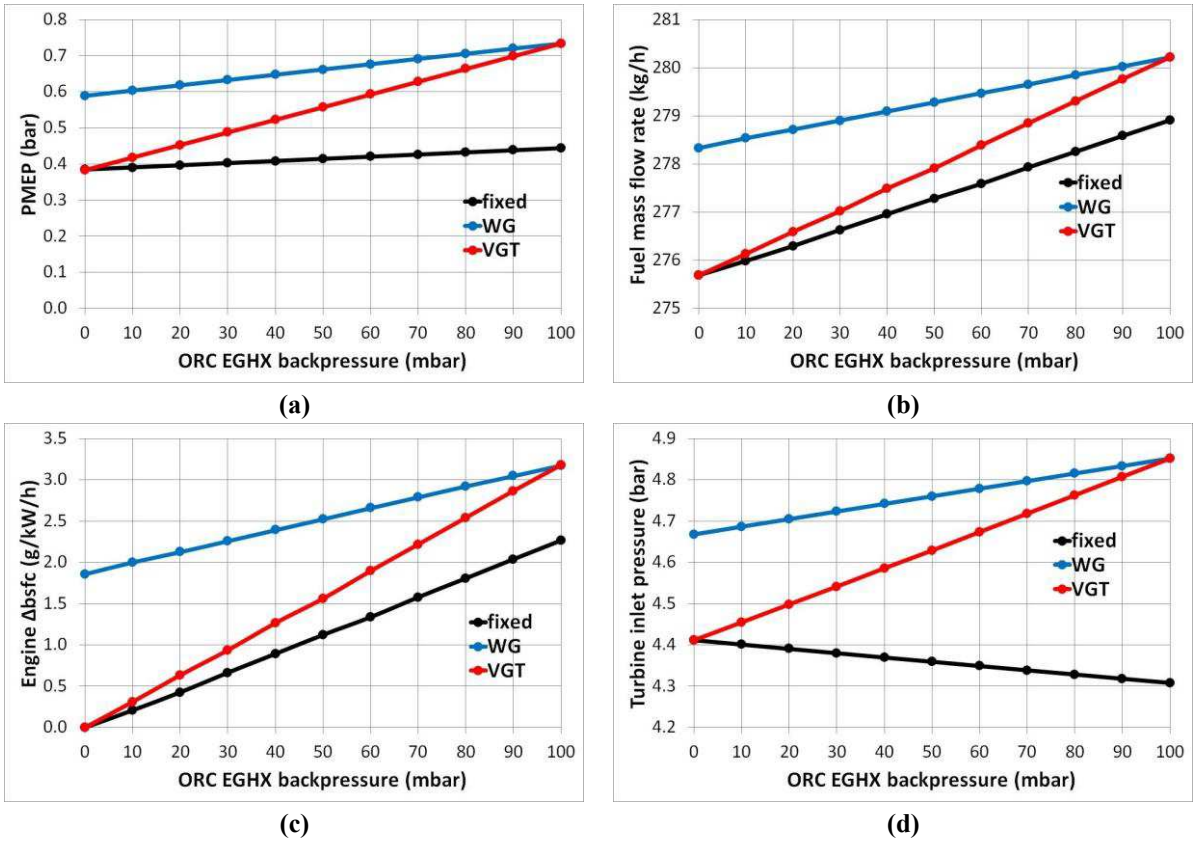

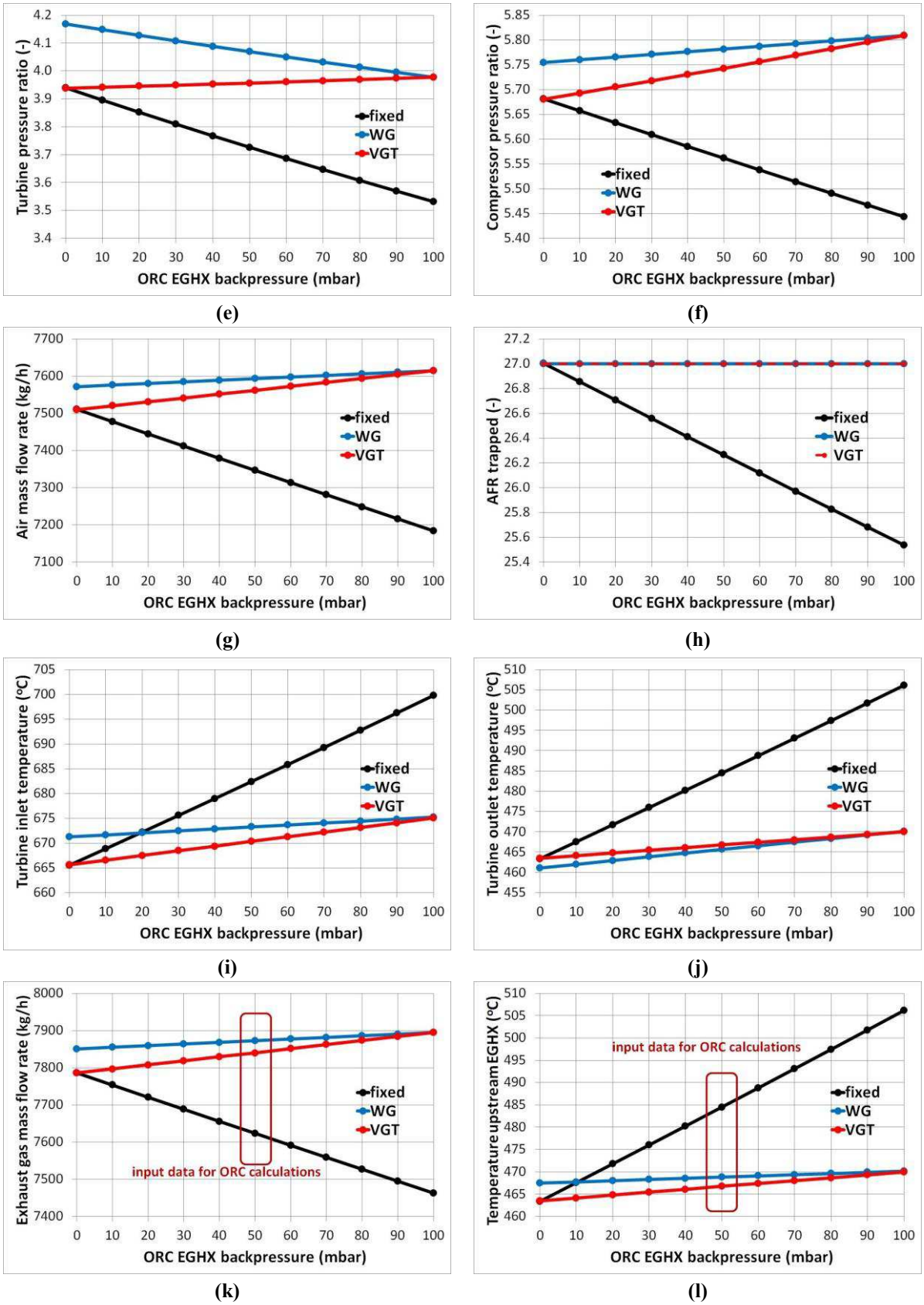

Fig. 69. PMEP (a), fuel mass flow rate (b), engine Δbsfc (c), turbine inlet pressure (d), turbine pressure ratio (e), compressor pressure ratio (f), air mass flow rate (g), AFR trapped (h), turbine inlet temperature (i), turbine outlet temperature (j), exhaust gas mass flow (k) and temperature upstream the EGHX (l), against ORC EGHX backpressure for the three different turbocharging scenarios (case study 2)

In order to facilitate the understanding of the results reported in the ORC section, the operating conditions for the considered simulated cases have been extracted from Fig. 69 (k-l) and reported in Tab. 42.

Parameter	**Fixed Geometry Turbine**	**Waste-Gate (WG) Turbine**	**Variable Geometry Turbine (VGT)**
Exhaust Gas Mass Flow, $\dot{m}_{exh}$ [kg/h]	7623.6	7872.6	7839.6
Exhaust Gas Temperature, $T_{exh,EGHX,in}$ [°C]	484.5	468.9	466.8

Tab. 42. ORC boundary conditions for exhaust gas mass flow and temperature (case study 2)

The case of the fixed turbocharging system can be used for the explanation of the main effects of the increasing backpressure. On the one hand, since the engine has to overcome higher pumping losses, while maintaining a constant brake load, more fuel has to be consumed resulting in the increase of the engine bsfc (positive Δbsfc, compared to reference base case engine bsfc). On the other hand, the turbine and, consequently compressor pressure ratios, are reduced, reducing accordingly the air mass flow through the engine. As a result, the trapped AFR is reduced, deteriorating the combustion quality. Moreover, the increased exhaust temperatures, due to richer combustion, increase the thermal loading of the engine, which in turn can cause thermal failure of the pistons, cylinder heads and valves, as well as breakdown of the oil film, with adverse wear consequences on pistons and cylinder walls. However, the turbine inlet temperature never exceeds its allowable limit.
The first alternative to the fixed turbocharger, with the purpose of decreasing exhaust temperatures and maintaining the base case trapped AFR, is the use of a smaller turbine to increase the boost pressure, and therefore the engine air mass flow, equipped with a Waste-Gate (WG) valve in order to bypass some of the exhaust gas around the turbine at the lower backpressure cases, when the requirements for increased boost pressure are reduced. The WG opening area is controlled so as to preserve, in all backpressure cases, the base case AFR. In comparison to the fixed turbocharger case, the pumping losses (PMEP, bar) are now increased, increasing fuel consumption in order to maintain the constant brake load, therefore resulting also in increased bsfc. As expected, the turbine pressure ratio is now increased, due to the smaller turbine size. As backpressure increases, the closing of the WG valve results in the increase of the pressure upstream the turbine. However, the turbine pressure ratio is continuously decreasing. Compressor pressure ratio is higher than that of the fixed turbocharger case, however this increases with backpressure, increasing respectively the air flow to such extent so as to keep the AFR fixed. Even though the bsfc of the engine is now higher, turbine inlet temperatures are in general lower than those of the fixed turbocharger case due to the higher AFRs, with this trend being reversed at the low backpressure cases, where the AFR of the fixed turbocharger case is still high and close enough to the base case value. Due to the higher turbine pressure ratio, turbine outlet temperatures are now reduced. However, finally due to the mixing with the hot bypass exhaust gas as backpressure reduces, the temperature upstream the EGHX is getting slightly higher, compared to the case of fixed turbine, at the low backpressure cases, however, with not very marked effect.
To reduce the increased bsfc due to the smaller turbine (and thus increased pumping losses) of the WG turbocharger case, while still maintaining the base case AFR, the solution of a VGT turbocharger has been considered and applied. The flexibility offered by the variable turbine nozzle area of the VGT turbocharger, being this practically correspondent to different turbine sizes for the various backpressure cases, results, on the one hand, in a turbine size equal to that of the fixed turbocharger at

the 0 mbar backpressure case and, on the other hand, in a turbine size equal to that of the WG turbocharger at the 100 mbar backpressure case. In the intermediate backpressures, the turbine nozzle area of the VGT turbocharger is adjusted linearly between the two extreme cases. This trend for the VGT turbocharger, between the fixed and WG turbochargers at the 0 mbar and 100 mbar backpressure cases, respectively, can be obviously observed in the graphs of PMEP, fuel mass flow rate and engine Δbsfc. Therefore, in terms of engine efficiency, the VGT turbocharger offers a clear benefit over the WG for the investigated ORC backpressure effect. Additionally, it is observed that, as backpressure increases, the decrease of the turbine nozzle area throttles the exhaust gas flow to such an extent so that the turbine pressure ratio, even if slightly, increases continuously. Accordingly, the compressor pressure ratio and engine air mass flow are increased to maintain the base case AFR, following the above-mentioned correlation between the fixed and WG turbochargers extreme backpressure cases. The turbine inlet temperature is reduced even further in comparison to the WG turbocharger case, following the relevant bsfc trends, since AFR is the same. However, the temperatures at the turbine outlet appear to be higher than those of the WG turbocharger case due to the lower pressure ratio of the VGT turbocharger turbine, especially at low backpressure levels.
From the engine operation point of view, it can be stated that, among the investigated turbocharging system scenarios, the VGT turbocharger seems to be the most favorable solution, alleviating at the most the adverse effect of the ORC EGHX backpressure on engine efficiency, while at the same time fulfilling the requirements for constant AFR and relatively low and safe exhaust temperatures. The VGT turbocharger offers also a more advanced controllability and flexibility in operations.
As already introduced, in Fig. 69 (k to l) and in Tab. 42, the boundary conditions, regarding engine tailpipe temperatures and mass flow rates, for the ORC simulations have been reported for the three considered turbocharging strategies assessed.

6.2.5.2 ORC

In addition to the analysis of the backpressure effect on the engine side operations, it is useful to carry out a performance evaluation of the combined engine-ORC system, considering also the qualitative comparison of the trends of the ORC system performance indexes in the simulated cases. For this purpose, the results of the 1-D engine analysis, for a moderate EGHX backpressure of 50 mbar, have been used as input for the ORC calculations, which consider a simple and a recuperated cycle layouts and n-hexane, n-octane, acetone, toluene, ethanol and MDM as working fluids. An optimization of the relevant cycle parameters with the purpose of maximizing the ORC net power output has been carried out.
Fig. 70 (a to h) show the combined system Δbsfc reduction, the exhaust gas temperatures at the EGHX outlet, as well as the ORC system efficiency and size performance indexes for the investigated fluids and layouts combinations. As it can be observed, the main factor determining the combined system Δbsfc is the working fluid choice for the ORC system. In addition, as a general trend, it is observed that the recuperated cycle offers greater fuel economy, resulting at the same time in higher exhaust gas temperatures downstream the EGHX. Therefore, in this case, the exhaust gas can be further utilized. The VGT turbocharger, as well, provides always larger fuel economy benefits for the combined system than the WG turbocharger independently of cycle layout and working fluid, with the fixed turbocharger excluded from the comparison due to its inability to keep AFR constant, thus also influencing combustion efficiency and emissions patterns.
From the combined system efficiency point of view, it can be inferred that the largest fuel economy benefits are obtained with the recuperated cycle operating on acetone, with a VGT turbocharger on the engine side in order to keep the AFR constant, thus preserving a good combustion quality. Cases with fixed turbine show a combined system fuel saving potential slightly higher, however not preserving

AFR values and thus combustion requirements. According to the results, the acetone-VGT system shows the potential of reducing the bsfc approximately of 18.9 g/kWh (9.8% reduction), with the assumption of 50 mbar EGHX backpressure. This is mainly a result of the increased thermal and recovery efficiencies of this particular ORC system. As far as size and economics indexes are concerned, the recuperated acetone cycle presents relatively moderate requirements of expansion machine size and general system size (mass flow ratio, MFR index). However, its implementation involves relatively large, and therefore costly, heat exchangers.

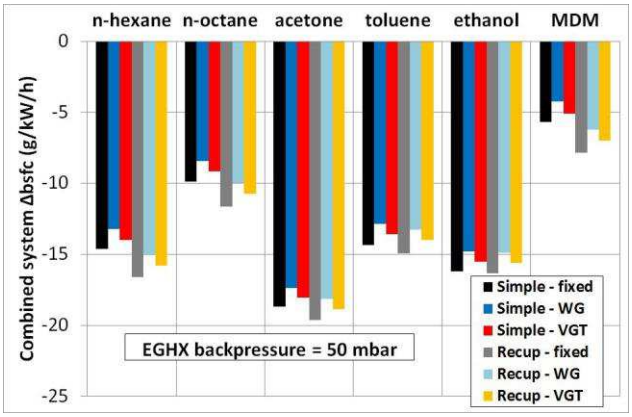

(a)

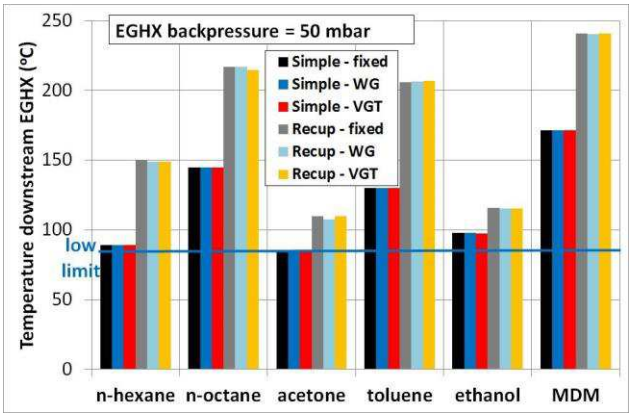

(b)

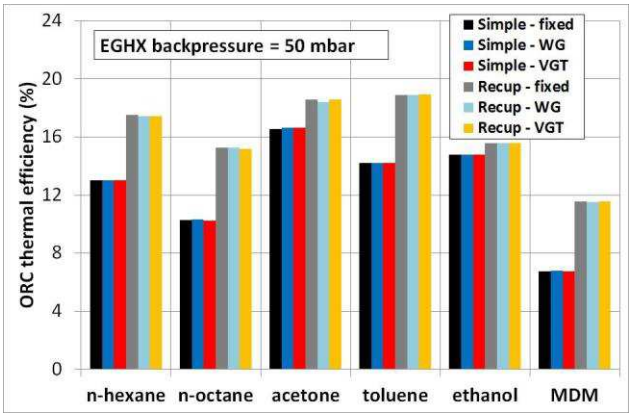

(c)

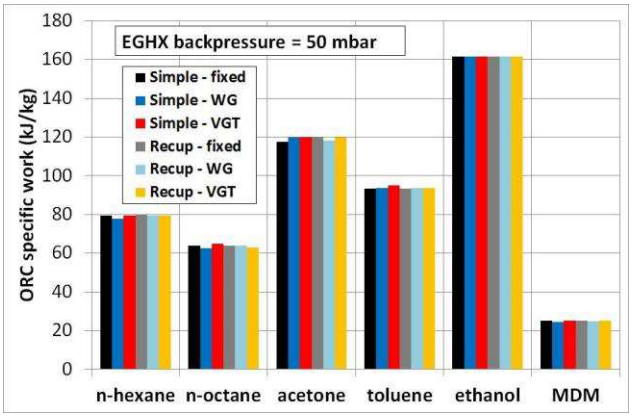

(d)

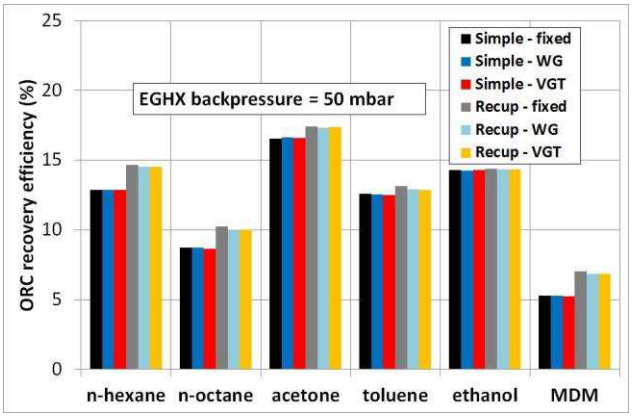

(e)

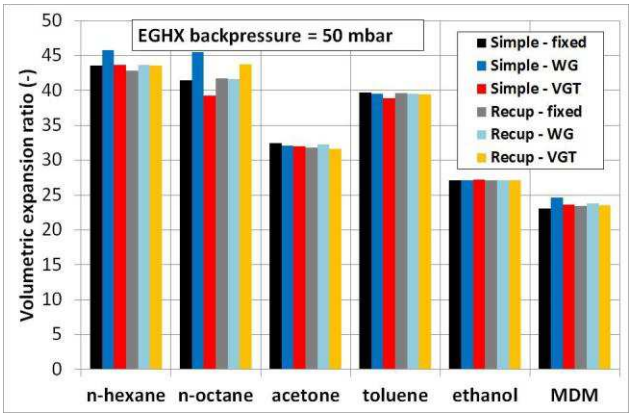

(f)

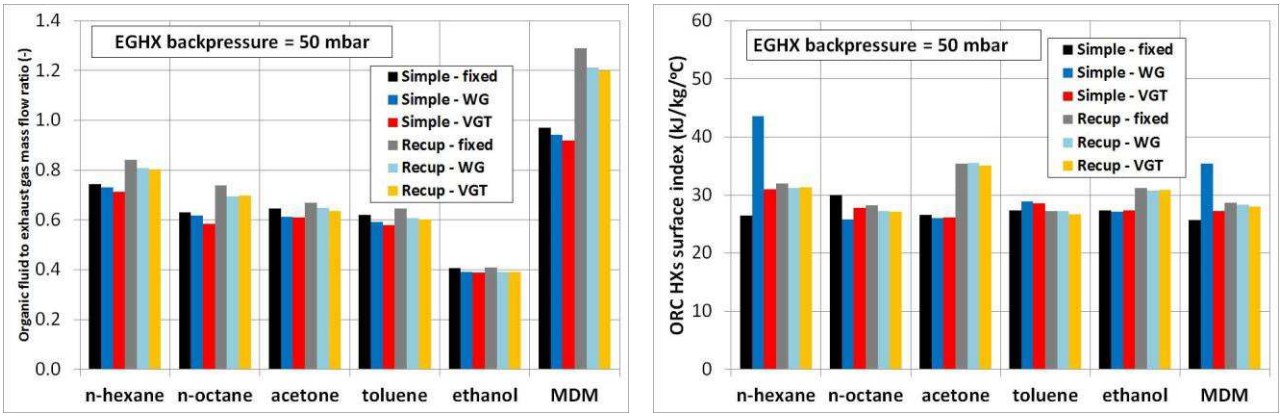

(g) **(h)**

Fig. 70. Combined engine-ORC system Δbsfc (a), exhaust gas temperature downstream EGHX (b), ORC thermal efficiency (c), ORC specific work (d), ORC recovery efficiency (e), expansion machine volumetric expansion ratio (f), organic fluid to exhaust gas mass flow ratio (g) and ORC heat exchangers (HXs) surface index (h) for the analysed working fluids and the simple and recuperated cycle layouts, with optimized cycle parameters, fixed, WG and VGT turbocharging scenarios (case study 2)

After the identification of the most promising, in terms of combined system efficiency, turbocharging-ORC system configuration, based on the 50 mbar EGHX backpressure assumption, additional performance simulation runs of this system have been conducted for the complete EGHX backpressure range, in order to evaluate a sensitivity analysis on the respective fuel economy benefit range that can be expected for any possible EGHX hardware design. According to Fig. 71, which presents the Δbsfc achieved by this particular combined system for the various EGHX backpressure values, it is shown that the effect of the EGHX design on the fuel consumption improvement is relatively weak, since the bsfc reduction that can be obtained lies between 17.7 and 19.7 g/kWh (9.1 to 10.2%).

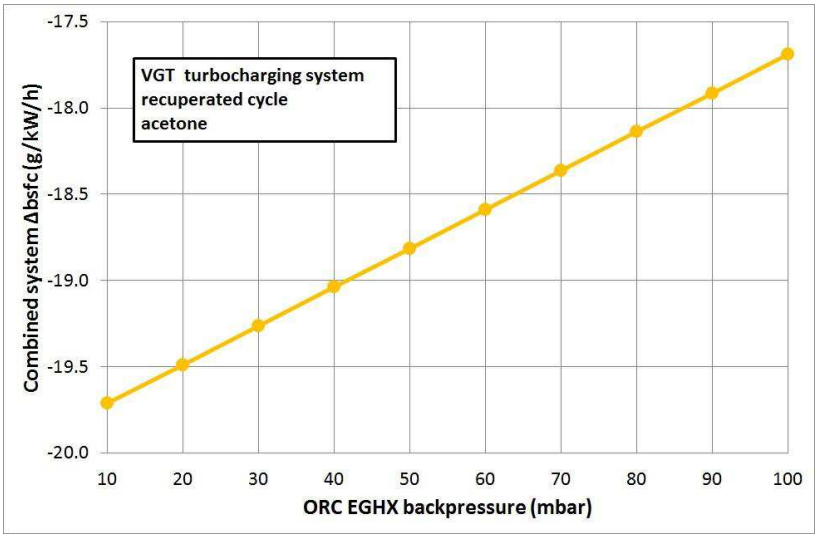

Fig. 71. Combined engine-ORC system Δbsfc against EGHX backpressure for the VGT turbocharging system with optimised recuperated ORC layout operated on acetone (case study 2)

6.2.6 Conclusions

The work reported in this second case study investigates the possibility of introducing an ORC to improve the performance of a high-speed Diesel engine used in marine and power generation applications. In particular, the effects of introducing the ORC evaporator on the engine exhaust gas line backpressure have been considered.
Three turbocharging systems have been assessed: a fixed geometry turbocharger, a turbocharger with a Waste-Gate and a VGT turbocharger.
Some main considerations can be drawn:

- from the engine operation point of view, the VGT turbocharger is the most favourable solution, since it alleviates at the most the adverse effect of the ORC evaporator backpressure on engine efficiency while, at the same time, it fulfils the requirements for constant AFR and relatively low and safe exhaust temperatures;
- from the combined engine-ORC system efficiency point of view, the combination of the VGT turbocharger with a recuperated cycle operated with acetone provides the greatest benefits, reducing the fuel consumption of the combined system of 17.7-19.7 g/kWh (9.1 to 10.2%), depending on the EGHX backpressure. This is mainly due to the relatively high thermal and recovery efficiencies of this particular ORC configuration. In terms of size/economic issues, the selected ORC system presents relatively moderate requirements of expansion machine size and general system size in comparison to the other candidate solutions. However, its implementation requires the use of relatively large and costly heat transfer equipment;
- in general, the efficiency of the combined system depends mainly on the used organic working fluid, with the influence of the cycle layout and turbocharging system coming as subsequent requirements;
- in terms of cycle layouts, recuperated ORC configurations present clear efficiency benefits over their simple cycle counterparts, resulting also in favourably higher exhaust gas temperatures at their exhaust gas outlet for further use in typical cogeneration configurations;
- most of the fluids considered in this study are however generally flammable and, even though a thermal oil loop has been interposed between the exhaust gas and the ORC fluid, flammability issues could discourage the use of this substances in closed environments such as those on-board ships.

In this case study, the internal combustion engine simulation has been carried out using fixed engine parameters. As a future work, engine parameters optimization could be carried out on the selected solution (VGT). Engine parameters to be considered are, for example, the valve timing, valve diameters, injection timing and compression ratio.
For the final selection of the most favorable cycle layout and working fluid, a techno or thermo-economic assessment, followed by a multi-criteria evaluation of the investigated ORC systems, could integrate the thermodynamic results of this work. For this reason, the technical parameters computed could be used as input into cost functions of the ORC components to evaluate relevant economic parameters, as it has been proposed in the last case study, in which the path to a more complete, combined and synergistic methodology has been presented. Subsequently, technical, economic and environmental parameters could be introduced using an appropriate multi-criteria evaluation procedure in order to obtain an index to be used for the final quantitative comparison of the various examined system configurations.

6.3 Case Study 3: Marine Two-Stroke Ship Main Propulsion Unit

As can be observed in Fig. 1, in the introduction of this thesis, the Third IMO GHG study reports the fuel consumption and CO_2 emissions estimated for different types of ships used in the marine shipping sector in 2012. It is, indeed, possible to infer that the ships which emit more CO_2 and use more fuel are: container ships, bulk carriers, oil tankers, general cargo ships and chemical tankers. These types of ships are typically powered by low speed two-stroke propulsion units, which have been intensively studied in this proposed third case study.
Indeed, in the frame of the EU ECCO-MATE project, and in particular of the Working Package 1 (WP1) led by Ricardo, one of the scope of the research carried out has been the study of innovative engine air management architectures, as for example Exhaust Gas Recirculation (EGR), in order to decrease marine Diesel engine emissions, such as the harmful nitrogen oxides (NO_x). At the same time, however, when developing an engine, it is important to try to keep the performance at reasonable high levels, without impacting too much on the fuel consumption. For this reason, waste heat recovery technologies, such as Organic Rankine Cycles (ORC), have been investigated, using a thermodynamic process simulation model, in order to recover engine waste heat with the final scope of increasing the system overall efficiency.
In this work, a 1-D gas dynamic model of a two-stroke, crosshead, low speed, 13.6 MW marine Diesel engine for ship main propulsion, has been developed using Ricardo WAVE, in collaboration with the National Technical University of Athens (NTUA-DME). The model has been built and validated based on the data supplied by the project partner Winterthur Gas & Diesel (WinGD, former Wärtsilä two-stroke division). A Low Pressure (LP) EGR architecture has been then implemented (section 4.1.3.2), starting from the validated baseline model, in order to assess the engine performance under possible IMO Tier III operating conditions (section 4.1.1.2).
The boundary conditions, regarding the engine heat rejection, in particular for exhaust gas economizer, Scavenge Air Cooler (SAC) and High Temperature (HT) jacket cooling water, have been estimated from the 1-D models, both for the baseline case (IMO Tier II) and the case with LP EGR (IMO Tier III).
The data have been used as inputs for a thermodynamic process simulation model, developed in Engineering Equation Solver (EES), able to assess the performance of different Organic Rankine Cycles (ORC) architectures and working fluids, with the scope of obtaining the maximum net power output achievable from all engine operating points considered.
The outcome of the proposed case study is that, through the combined use and integration of innovative emissions reduction strategies, such as LP EGR, and waste heat recovery systems, such as ORC, it is possible to develop marine Diesel engines which, at the same time, can show high efficiency and reduced pollutants emissions.
The proposed case study has been part of one of the deliverables of the ECCO-MATE project, in collaboration with NTUA and WinGD. An introduction to the work carried out in the frame of the project has been proposed by the author in [370]. Further joint publications have been considered at the time in which this thesis has been submitted.

6.3.1 Reference Engine and Modelling Approach

The engine considered in this case study is a 13.6 MW brake power, two-stroke, low speed, uniflow scavenged, crosshead Wärtsilä 6RT-flex58T-D V2, Diesel ship main propulsion engine, still available on market, but not between the newest of the line currently proposed by Winterthur Gas & Diesel

(WinGD), project partner of Ricardo and University of Trieste in ECCO-MATE. The baseline engine is fulfilling the IMO Tier II emission regulation standards.
The engine has the following main specifications, reported in Tab. 43, while a graphical representation of the engine architecture has been proposed in Fig. 72:

N° of cylinders	6
Bore [mm]	580
Stroke [mm]	2416
Displacement [L]	1585
Connecting Rod Length [mm]	2242
Geometric Compression Ratio [-]	18
Brake Power (@ full load) [kW]	13560
Brake Torque (@ full load) [kNm]	1233
Rotational Speed (@ full load) [rpm]	105
BMEP (@ full load) [bar]	20.2

Tab. 43. Baseline engine specifications (case study 3)

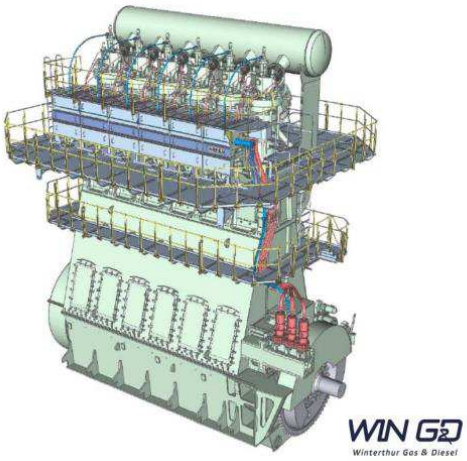

Fig. 72. Baseline engine representation (courtesy of WinGD) – (case study 3)

6.3.1.1 Supplied Data

The main geometrical data have been supplied by the project partner Winterthur Gas & Diesel (WinGD) in order to develop a thermodynamic model using the 1-D Ricardo WAVE engine simulation software.
The data, concerning engine performance and intake and exhaust lines pressures and temperatures, have also been supplied by WinGD in order to validate the model. WinGD declared that the data come from an in-house developed 0-D simulation tool, validated with engine experimental data. For this reason, a tolerance of ±5% has be declared to the sufficient during the validation process. All data have been supplied for four different operating points: 100%, 75%, 50% and 25% loads.
Considering that at 25% load the turbocharger is not able to supply the necessary intake air mass flow and boost pressure, and that an auxiliary blower is needed in order for the engine to properly work, it has been decided not to simulate the mentioned operating point, especially observing that, due to the low amount of heat rejected during this load point operations, a possible waste heat recovery system would not show adequate performance and would be probably switched off.
The BSFC (Brake Specific Fuel Consumption, g/kWh) data of the baseline engine have been obtained from the WinGD GTD software [60] available online. The fuel mass flow has been then calculated, and verified with WinGD, based on the BSFC formula (6) in section 4.1, knowing the brake power output at the simulated operating point.
The intake air mass flow data, $\dot{m}_{air}$, have been supplied by WinGD just for one cylinder. The value has been multiplied for six, considering homogeneous air distribution to all six cylinders, in order to obtain the overall intake mass flow.
WinGD supplied also the baseline engine data regarding intake ports effective area, exhaust valve lift profile and flow coefficient, engine friction (FMEP, Friction Mean Effective Pressure, bar) and combustion data.
Indeed, the engine configuration for the considered two-stroke, crosshead, uniflow propulsion unit is quite different compared to the common four-stroke architectures with poppet intake and exhaust

valves. As a clarification of what reported, a sketch for a typical two-stroke large marine engine configuration, as the one considered in this work, has been reported in Fig. 73.

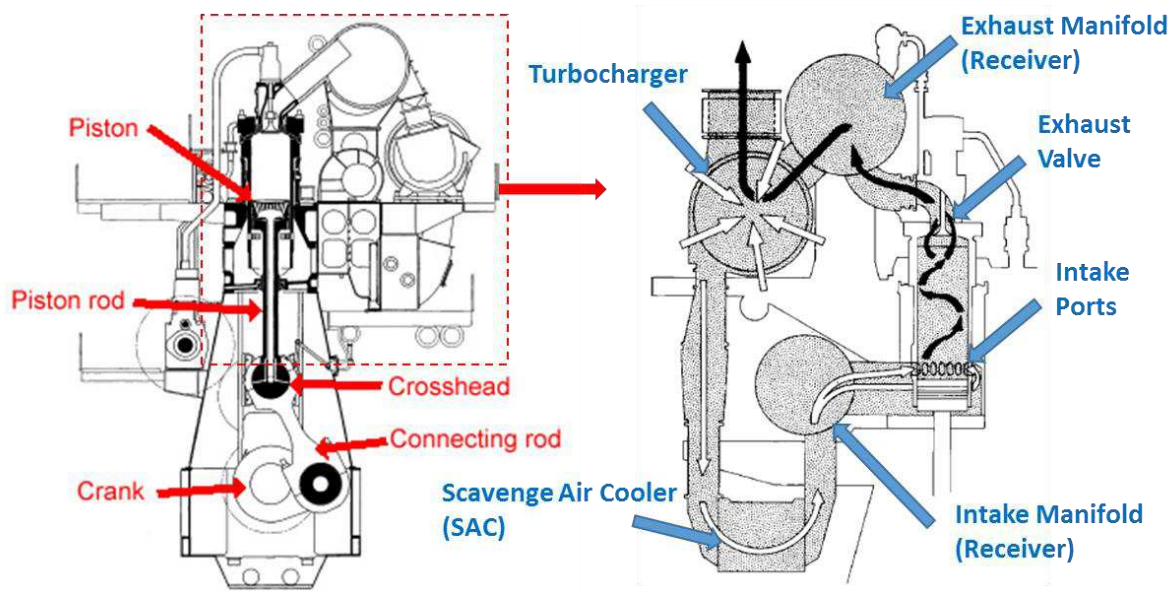

Fig. 73. Sketches of a two-stroke, crosshead, uniflow large marine Diesel engine propulsion unit and its gas lines systems. Elaborated from [62] *(case study 3)*

Concerning the *intake ports* data, the effective area with CAD (Crank-Angle-Degree) variation has been supplied in the form of values normalized by the engine piston area and considering a constant discharge coefficient C_D of 0.9. The piston area has been estimated, from the bore, to be around 264208 mm^2 and the total effective area with CAD variation has been reported in Fig. 74, considering all 30 intake ports disposed along the liner circumference near the BDC (Bottom Dead Centre).

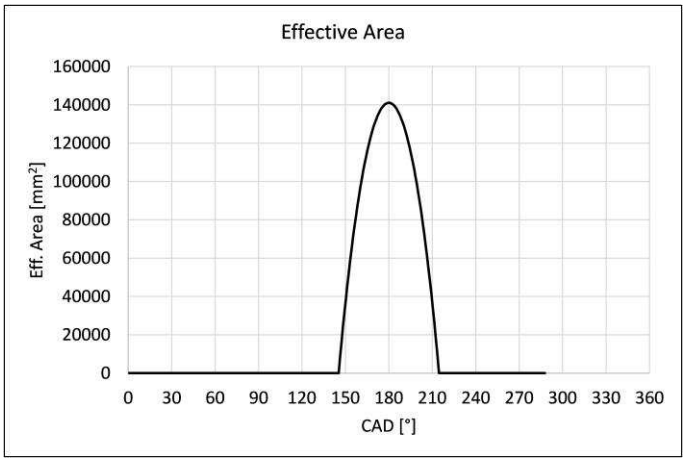

Fig. 74. Intake ports effective area vs CAD (case study 3)

The *exhaust valve* is a poppet-type valve which is located on the top of the cylinder head. The lift profile with CAD variation has been supplied by WinGD for all the operating points simulated. An example for the 100% load case has been reported in Fig. 75. Also, the forward discharge coefficient profile for the valve has been provided by WinGD.

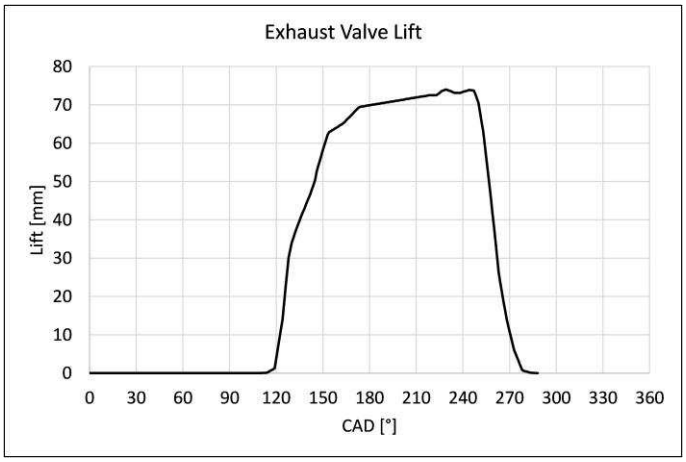

Fig. 75. Exhaust valve lift profile at 100% Load case (case study 3)

WinGD supplied also the *engine friction data (FMEP)* which have been used as inputs for the model developed in WAVE. FMEP data for all considered operating points have been reported in Fig. 76. *Combustion data* have been also provided. The burning rate and in-cylinder pressure profiles for the 100% load case are reported in Fig. 77(a-b).

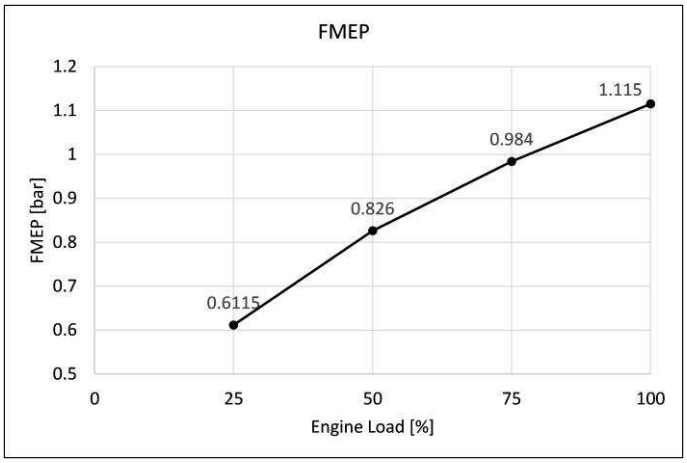

Fig. 76. FMEP data at different engine loads (case study 3)

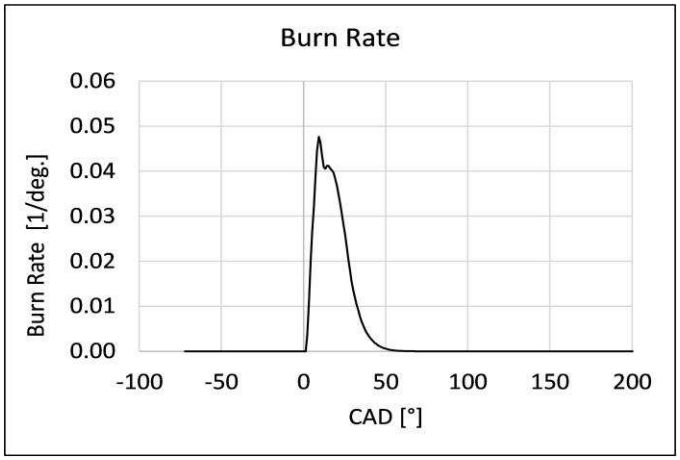

(a)

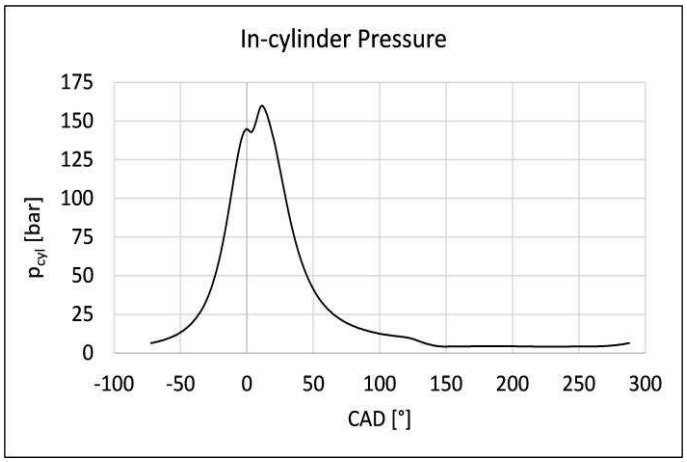

(b)

Fig. 77. Burning rate (a) and in-cylinder pressure (b) profiles for 100% load case (case study 3)

The peak cylinder pressure for the 100% load case is 160 bar.
The in-cylinder pressure profiles have been used as inputs for a profile-based combustion model in Ricardo WAVE, based on a heat release analysis using a secondary model setting in the software. The typical Start of Injection (SOI) and Start of Combustion (SOC) parameters have been setup from available experimental data for a comparable engine, supplied by the project partner National Technical University of Athens (NTUA).
Lambda (λ, air-fuel equivalence ratio, often used in WAVE as also AFR, Air-Fuel Ratio) data have been also provided by the project partner WinGD in order to validate the model concerning combustion requirements. Generally, in these types of engines, combustion is quite lean, with excess of air, in order to avoid soot formation. For all the considered operating points a lambda higher than 2.0 is considered (AFR higher than 28.5), depending on the data supplied by the project partner WinGD, which have not been reported in absolute numbers due to confidentiality reasons.
The fuel suggested by WinGD is Marine Diesel Oil (MDO) with a Lower Heating Value (LHV) of 42700 kJ/kg. A slightly modified diesel ($C_{15}H_{25}$) WAVE fuel file, in order to consider the proposed LHV, has been used in the simulations, and considered an acceptable approximation.

6.3.1.2 Assumptions and Methodology

First of all, a preliminary simulation campaign has been carried out simulating only a 1-cylinder engine model, considering supplied intake and exhaust boundary conditions, in order to perform a preliminary settings calibration.
Subsequently, considering that no specific data have been supplied for what concerns the engine manifolds, piping, Scavenge Air Cooler (SAC) and exhaust economizer dimensions, and, in general, the overall *engine geometry*, feasible dimensions for the lengths and volumes have been assumed based on information found in literature and after discussion with the project partners. Indeed, considering especially that the simulated engine is highly boosted, not much influence of detailed engine piping and manifolds geometry is expected. The model has then been calibrated and validated based on the performance and thermodynamic data (mass flows, temperatures and pressures) provided by WinGD. Having in mind the purpose of the study, which is not an engine performance optimization based on the engine real geometry, but rather an overall thermodynamic assessment concerning IMO Tier III operations with LP EGR and possible ORC based waste heat recovery systems, the accuracy of the model has been considered satisfactory.

Other assumptions have been used for the *scavenging profile curve*, which has not been supplied by WinGD and has not been estimated based on CFD calculations. In this case, the curve parameters have been used as calibration factors in the model, trying always to validate the model itself in the ±5% declared tolerance interval. A trial and error fitting procedure has been applied based on the supplied validation data and a scavenging efficiency in the range between 90 and 95% obtained, as agreed with WinGD and as reported in Ricardo WAVE:

$$\eta_{scav} = \frac{\left(m_{air,trapped} + m_{fuel,trapped}\right)}{m_{trapped}} = 1 - \frac{m_{residuals}}{m_{trapped}} \qquad (130)$$

In order to obtain another important validation parameter, which has not been provided, the in-cylinder pressure trace has been integrated over the engine cycle in order to obtain the Indicated Mean Effective Pressure (IMEP, bar). Subtracting the FMEP from the IMEP it has been possible to obtain the *BMEP (Brake mean Effective Pressure)*, which has been controlled, through the injected fuel mass flow in the model, in order to achieve the required engine performance for every simulated operating point.
For what concerns the *cylinders and engine block heat rejection*, no data have been provided by WinGD in order to calibrate the heat transfer model (Woschni), but some data are available for the same engine, with similar tuning configuration, from the online WinGD GTD online software [60]. A heat balance can be indeed estimated, for every of the operating conditions, from the data available. An example for the 100% load point is reported in Tab. 44 and Fig. 78. The fuel thermal power has been estimated from the fuel injected mass flow and the LHV, the economizer heat rejection from the SPP parameter (Steam Production Power, kW), while the exhaust gas term has been calculated as the difference between the fuel thermal power and the sum of all the other terms. All terms are considered at ISO conditions as also the simulations are (1 bar and 25°C).

100% Load - ISO	kW	%
Fuel Input Power	27021	100
Brake Power	13560	50.2
SAC LT	5209	19.3
Coolant Cylinders	1584	5.9
Lube Oil	904	3.3
Radiation	226	0.8
Economizer (SPP)	2410	8.9
Exhaust Gas	3128	11.6

Tab. 44. Tabulated heat balance for 100% load point (case study 3)

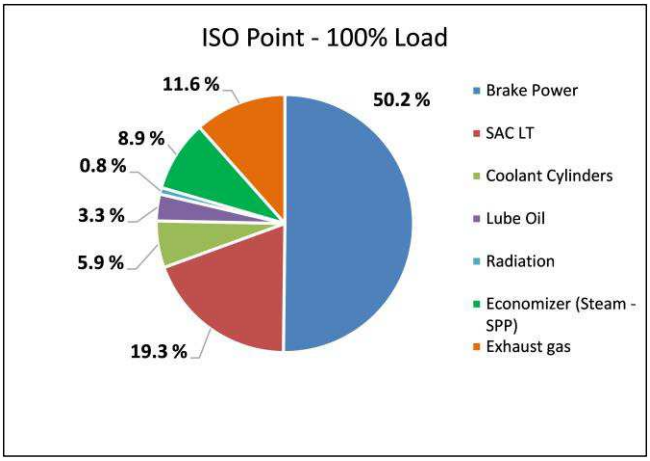

Fig. 78. Heat balance for 100% load point (case study 3)

The chart and the table report coolant, lubrication oil and radiation contributions, however, in Ricardo WAVE also the dissipated thermal power due to friction is considered as a separated contribution in the balance, even thought, in a real engine, part of the friction dissipated energy will be converted in heat and transferred to the coolant and oil loops, and to the environment as radiation as well.
For this reason, the friction dissipated power has been estimated from the following proportion:

$$\frac{BMEP}{\dot{W}_{brake}} = \frac{FMEP}{\dot{Q}_{frict}} \quad \rightarrow \quad \dot{Q}_{frict} = \frac{FMEP \cdot \dot{W}_{brake}}{BMEP} \qquad (131)$$

And subsequently, the cylinder heat transfer term (considering both lubrication oil and coolant contributions) has been estimated from the following formula, in order to be used as a comparison value for the calibration/validation of the model:

$$\dot{Q}_{cyl,HT} = \dot{Q}_{cool,cyl} + \dot{Q}_{oil} - \dot{Q}_{frict} - \dot{Q}_{rad} \quad (132)$$

This last term has been compared, in the validation procedure, with the value obtained, from Ricardo WAVE, using the Woschni heat transfer model, which has been calibrated using multiplying factors, following Ricardo guidelines for similar type of engines.
Both *Scavenge Air Cooler (SAC)* and *economizer* have been simulated, in Ricardo WAVE, using a single duct with multiple ducts count and two side junctions simulating volumes, in order to emulate the internal geometry of the heat exchangers considered. However, since no geometrical data were available about the components, the model has been calibrated using available friction and heat transfer multipliers in order to match the pressure and temperature data (and thus the heat rejection capabilities) provided by WinGD.
Concerning the turbocharger, an ABB A180-L model has been suggested by WinGD, and the steady-state performance maps have been obtained from ABB Turbo. Indeed, the model has been validated also with turbo-maps, however, considering the purpose of the study and the single operating points simulated, the final baseline model has been simulated imposing mapless turbine and compressor for the turbocharger with fixed efficiency values (in the range between 67 and 70%) obtained from the WinGD GTD software, in order to allow an easier model calibration and controllability.
An example of most of the data supplied for the validation of the baseline model has been reported, for the 100% load case, in Fig. 79, showing a conceptual scheme of the engine.

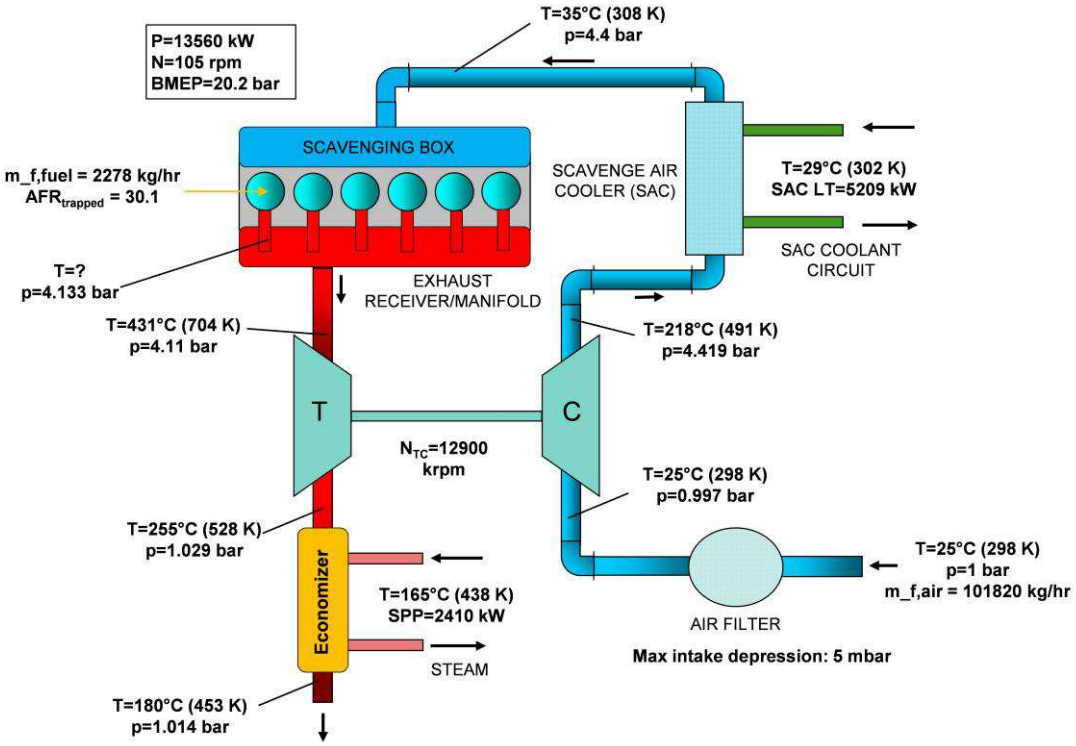

Fig. 79. Conceptual scheme of the engine with data supplied by WinGD for the model development and validation (100% load case) – (case study 3)

As already introduced previously, three different operating points have been evaluated: 100%, 75% and 50% load cases, which are reported in Fig. 80, giving an idea of the typical engine operations over a so-called “propeller curve”.

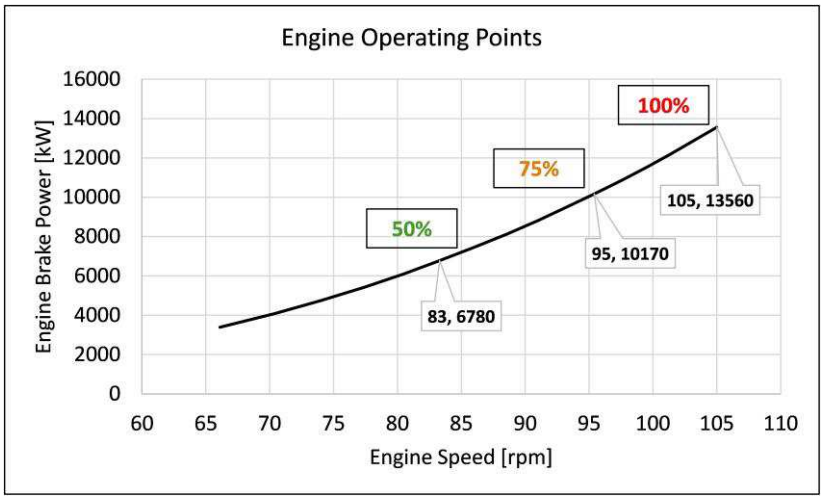

Fig. 80. Engine operating points ("propeller curve") – (case study 3)

The final baseline engine model developed in Ricardo WAVE has been reported in Fig. 81. A PID (Proportional-Integrative-Derivative) controller is visible in the scheme. It has been used to control the engine BMEP (and thus the brake power output) based on the injected fuel mass flow. The turbocharger has been calibrated in order to supply the right boost pressure, based on the data supplied by WinGD. All other parameters (heat transfer, pressure drops, etc) have been calibrated in the tolerance of ±5%. The validation results have been reported in section 6.3.5.1.

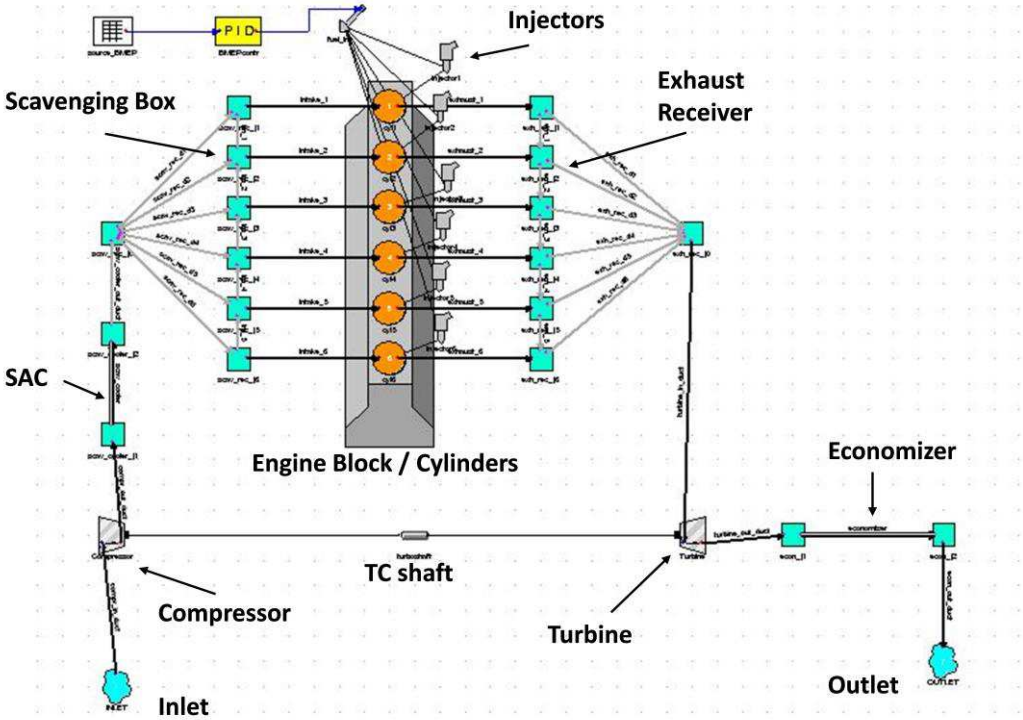

Fig. 81. Baseline engine model developed in Ricardo WAVE (case study 3)

6.3.1.3 LP EGR Model

As already stated in section 4.1.3.2, in a Low Pressure (LP) Exhaust Gas Recirculation (EGR) configuration, the exhaust gases are recirculated after the turbine and, in this case, after the economizer, to the intake of the engine, before the compressor, as reported in Fig. 82.

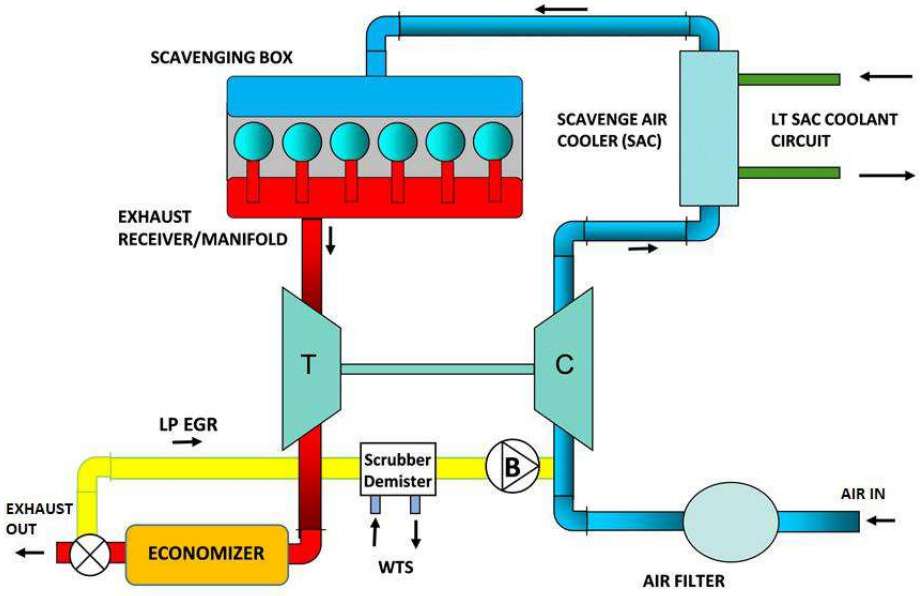

Fig. 82. LP EGR configuration scheme (case study 3)

The LP EGR architecture is used in order to meet IMO Tier III emissions regulations limits, recirculating some amount of exhaust gas in order to reduce, in particular, NO_x emissions.
The new engine layout introduces some new components, in particular: an on/off EGR valve, an EGR Scrubber/Demister with water injection, used to clean the exhaust gas from SO_x compounds, and an EGR blower, used to recirculate the exhaust gas to the intake in order to overcome the pressure drop between the exhaust and the intake lines. In Ricardo WAVE, the EGR valve has been modelled as an orifice, the Scrubber/Demister as a heat exchanger, as it has been done for SAC and economizer, while the blower as a mapless compressor with a low-pressure ratio.
No data were available from WinGD or the GTD software about a LP EGR configuration. For this reason, some assumptions and guidelines from WinGD experience have been considered and reported in Tab. 45.

Parameter	Value	Unit	Comments
Scrubber / Demister			
Pressure drop	100	mbar	75% load design point
Outlet temperature	60	°C	At all loads
EGR blower			
EGR blower isentropic efficiency	60 %	-	At all loads
EGR piping			
LP EGR piping pressure drop	20	mbar	Maximum suggested at all loads

Tab. 45. LP EGR circuit assumptions based on WinGD experience (case study 3)

As suggested by WinGD, in a real engine, saturated conditions (100% relative humidity) should be expected at the Scrubber/Demister outlet, due to the high amount of injected water which is used in order to clean the recirculated gas. Part of the water is condensed in the Demister and extracted from the gas line. From WinGD experience, a 3-4% (based on mass) of water in the exhaust line should already give saturation at the LP EGR line expected temperature and pressure conditions. A value of 2% has been estimated from the Ricardo WAVE simulations. However, due to the difficulty in the software to simulate water injection, and particularly ejection, from the gas line, and to the few information available about the possible LP EGR architecture, it has been decided, in first approximation, not to inject any water, but rather to keep the same gas composition obtained from the simulation in the exhaust line, accepting a small imprecision in the model.
Moreover, due to pressure, temperature and gas mixture composition interactions (in particular the water amount in the gas), condensation of water can happen, particularly in some locations in the gas line:

- *Scrubber/Demister outlet*: in the real engine, the demister is used to catch the condensate and eject it from the line;
- *EGR – intake air mixing manifold*: the drop in temperature, due to the mixing of EGR gas with a lower temperature intake air, can lead to formation of condensate, because, from psychrometry, a lower temperature gas can hold a lower amount of water at saturated conditions, thus condensing the water in excess;
- *SAC outlet:* due to the cooling effect of the Scavenge Air Cooler, in order to bring intake gas to the required temperature for the right combustion operations, formation of condensate can happen for the same considerations reported above. In this case, in a real engine, a mist catcher is used to catch the condensate and eject it from the line;

In the SAC, when condensation happens, an increased heat rejection to the cooling circuit can be expected due to the latent heat of condensation. This could have effects when considering a waste heat recovery system such an ORC.
However, due to the difficulty to simulate water injection (and ejection in particular) from the gas line, at the current state of the study, it has been decided not to consider this side of the analysis, in particular, for what concerns condensation issues. For this reason, the Scrubber/Demister has been simulated just as a normal heat exchanger without any water spray injection. A more accurate simulation model could be considered in future development stages.
The EGR recirculation rate targets (%) have been suggested by WinGD, and calculated based on the CO_2 volume fractions $[CO_2]$ in the intake ($[CO_2]_{in}$) and exhaust ($[CO_2]_{exh}$) lines of the engine, based on the following formula:

$$EGR\ rate\ (\%) = \frac{[CO_2]_{in} - [CO_2]_{air}}{[CO_2]_{exh}} = \frac{[CO_2]_{in}}{[CO_2]_{exh}} \quad (133)$$

$[CO_2]_{air}$ is the volumetric fraction of CO_2 at the engine inlet (ambient air), which has been considered 0, since the reference air has been assumed to be formed only by 21% oxygen and 79% nitrogen.
The volumetric fractions at the intake and exhaust are usually calculated as follows:

$$[CO_2]_{in} = \frac{\dot{V}_{(CO2)_{in}}}{\dot{V}_{in}} \qquad and \qquad [CO_2]_{exh} = \frac{\dot{V}_{(CO2)_{exh}}}{\dot{V}_{exh}} \quad (134)$$

The $\dot{V}$ terms are volumetric flows at the intake (*in*), at the exhaust (*exh*), of CO_2 at the intake ($CO_{2,\,in}$) and CO_2 at the exhaust ($CO_{2,\,exh}$).
Considering the Amagat's Law, which states that for a mixture of ideal gases, the volume fraction is equal to the mole fraction, the mole fractions of CO_2 at the compressor outlet ($y_{CO2,\,in}$) and the turbine

outlet ($y_{CO2,\,out}$) have been extracted from the WAVE model, and the EGR recirculation rate estimated as:

$$EGR_{RATE} = \frac{y_{CO2,in}}{y_{CO2,exh}} \qquad (135)$$

The EGR recirculation rates, reported in Tab. 46 as suggested by WinGD, have been targeted in the simulations.

EGR rate (%) - WinGD Target	
Load %	*EGR rate %*
100	20
75	40
50	40

Tab. 46. EGR recirculation rates (case study 3)

The engine model has been modified in WAVE in order to introduce the new LP EGR architecture. The model screenshot, with the LP EGR line highlighted, has been reported in Fig. 83.

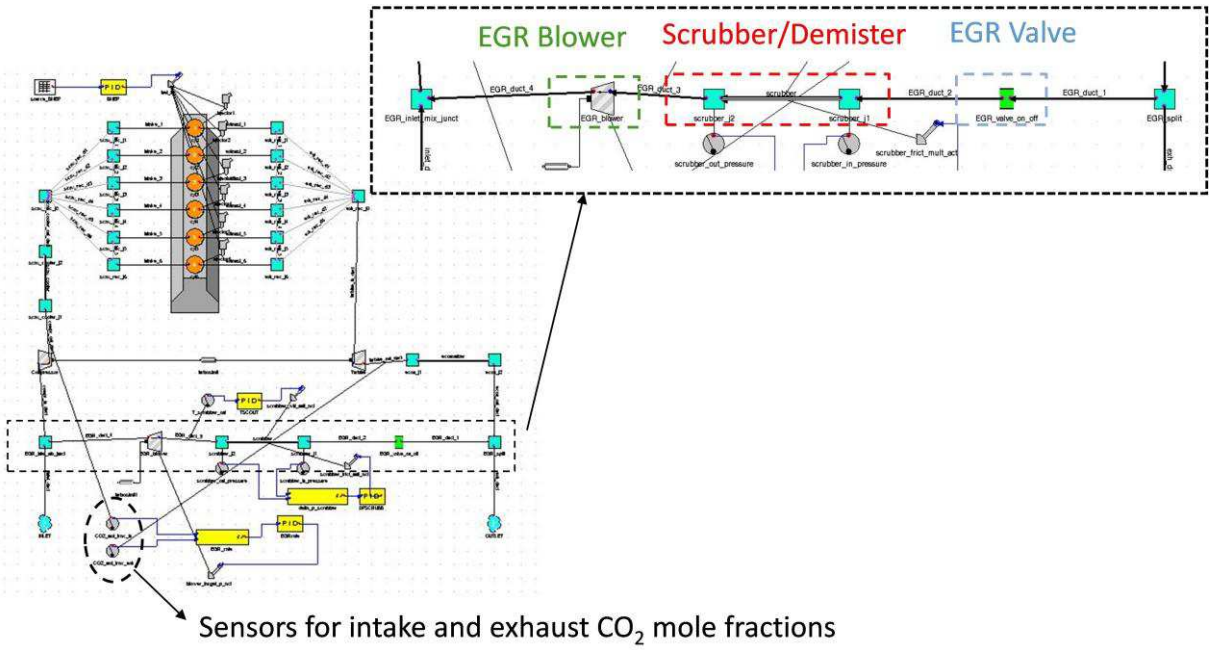

Fig. 83. LP EGR engine WAVE model (case study 3)

Additionally to the BMEP controller, used already in the baseline model without EGR, three other PID controllers have been used in the new model: 1) an EGR blower pressure ratio controller in order to achieve the required EGR rate, 2) a Scrubber/Demister heat transfer multiplier controller in order to achieve the required scrubber outlet temperature (333 K or 60°C), and 3) a Scrubber/Demister friction multiplier controller in order to control the component pressure drop (100 mbar at 40% EGR rate for 75% load design conditions). In this last case, the output settings of the PID have been kept fixed for the other operating points, in which the EGR mass flow is expected to be lower, in order to simulate a

scrubber designed for the maximum flow conditions. A tolerance value has been imposed on the convergence of the controllers in order to achieve the desired targets, and the PIDs have been constantly checked for convergence during the simulations.
Different operational strategies can be considered when introducing LP EGR. Indeed, the use of EGR will have effect on the other engine components and, in particular, on the turbocharger operations. When recirculating exhaust gas to the intake, the temperature of the intake gas mixture before the compressor rises of a certain ΔT, depending on the amount of gas recirculated. This will have impact on the compressor thermodynamic equilibrium, with a tendency to boost pressure and gas mass flow decrease, considering the same fixed turbocharger efficiency. At the same time, the different combustion will tend to decrease the performance of the turbine.
Two main operational strategies could be considered:

1) Improving the turbocharger efficiency in order to increase again the boost (in order to try to keep the same air-fuel ratio λ of the case without EGR). However, WinGD declared that the simulated turbocharger is already among the most efficient available on the market. This means, probably a two-stage turbocharger architecture could be needed in order to reach the required boost with EGR, thus increasing the system complexity;

2) The other possibility, which has been considered in this study, is the one having a lower impact on the engine architecture and turbocharger operations. Indeed, WinGD suggested to keep the same baseline turbocharger architecture (same fixed efficiency) and to allow a reduction in trapped air-fuel ratio. This will introduce a richer combustion, with higher exhaust gas temperature, increasing the gas enthalpy at turbine inlet, thus partially counterbalancing the decreased boost effect. However, combustion should be further evaluated with CFD techniques to avoid soot formation problems, and considering the impact of EGR on NO_x emissions;

As mentioned already, strategy 2) has been considered in this study. Emissions and soot have not been studied through CFD analysis, since the main objective of the study is the combined new architecture and waste heat recovery performance evaluation, rather than pollutants formation analysis. Calculation of emissions has been left, indeed, for a possible future work, and is going to be considered by the project partner NTUA in the frame of ECCO-MATE project.
For the same reasons reported above, and after an internal discussion in Ricardo and WinGD, in first approximation, for the 1-D WAVE simulations with LP EGR, the in-cylinder burning rate and pressure profiles, characterizing the combustion process, have been kept the same of the baseline case without EGR. The combustion profiles could be updated using CFD calculated data in a future analysis. For the actual analysis, the accuracy has been considered enough.
All engine geometry and model calibration parameters have been also kept constant as in the baseline model, in order to simulate just the implementation of the EGR line without any other engine modification.
The WAVE NO_x model has not been considered to estimate NO_x emissions, because no data for validation and calibration were available. For this reason, the emission model has not been considered reliable enough to supply accurate estimations.
The main goal of the 1-D WAVE analysis part of the work has been the estimation of the performance of the engine when introducing the LP EGR rates suggested by WinGD, and the extraction of the heat rejection boundary conditions for the ORC waste heat recovery study.
The results of this part of the work are reported, together with some model tuning studies suggested by WinGD, in section 6.3.5.1.

6.3.2 ORC Architectures

As already mentioned, the objective of the proposed work has been to evaluate the achievable BSFC improvement due to the installation of different steam Rankine Cycle (RC) and Organic Rankine Cycle (ORC) systems, in order to recover waste heat from different heat sources available from a two-stroke Diesel ship propulsion engine, operating both in Tier II (baseline model) and Tier III modes, employing, for this last case, a LP EGR architecture.
The scope of the work is to demonstrate how the use of waste heat recovery systems, such as RC and ORC, can be useful in order to mitigate the BSFC detrimental effect of the LP EGR in Tier III operation, allowing to achieve, at the same time, improved overall system performance when operating under Tier II limits.
Different thermodynamic process simulation models have been developed and used in order to assess the waste heat recovery achievable performance, while optimization algorithms have been used to achieve the best operating parameters leading to the highest power output obtainable, considering the calculated engine heat rejection boundary conditions. The modelling methodology has been already introduced in 5.2.

Four different Organic Rankine Cycle architectures have been evaluated in this study, with the main scope of recovering the possible waste heat sources from the topping engine: exhaust gas (economizer), Scavenge Air Cooler (SAC) and High Temperature (HT) jacket cooling water heat.
The concepts assessed are the following, and have been reported in the figures in the next pages:

1) Simple cycle architecture recovering exhaust gas heat from the economizer in a traditional tailpipe configuration, as the one proposed in common waste heat recovery systems;
2) Parallel cycle architecture recovering exhaust gas and SAC heat with a parallel evaporators configuration using the same evaporation pressure controlled by one pump;
3) Simple cycle architecture recovering heat from the HT jacket cooling water;
4) Simple cycle architecture recovering heat from the HT jacket cooling water and SAC heat;

In the concepts 2) and 4), an innovative two-stage SAC architecture is considered. In particular, in order to respect SAC gas outlet temperature requirements for cylinders' combustion (30-35°C as declared by WinGD), but at the same time recover part of the SAC heat to improve the ORC system performance, the SAC must be divided in two segments. The first segment is used to recover heat through the ORC circuit directly (concept 2) or through the HT jacket cooling water circuit (concept 4), which then is used to evaporate the ORC fluid. The second segment is used to cool the SAC gas to the required cylinders' inlet temperature, using the LT engine cooling circuit (around 29°C fresh water temperature).
All the architectures have been evaluated for both Tier II and Tier III operational modes, and for the three operating load points. The schemes of the ORC systems have been reported in Fig. 84 (1-2-3-4), in Tier II scenario, in order to slightly reduce sketches complexity.
In all the schemes, it is possible to observe the main ORC components: evaporator, condenser, expander (EXP) and pump (P).

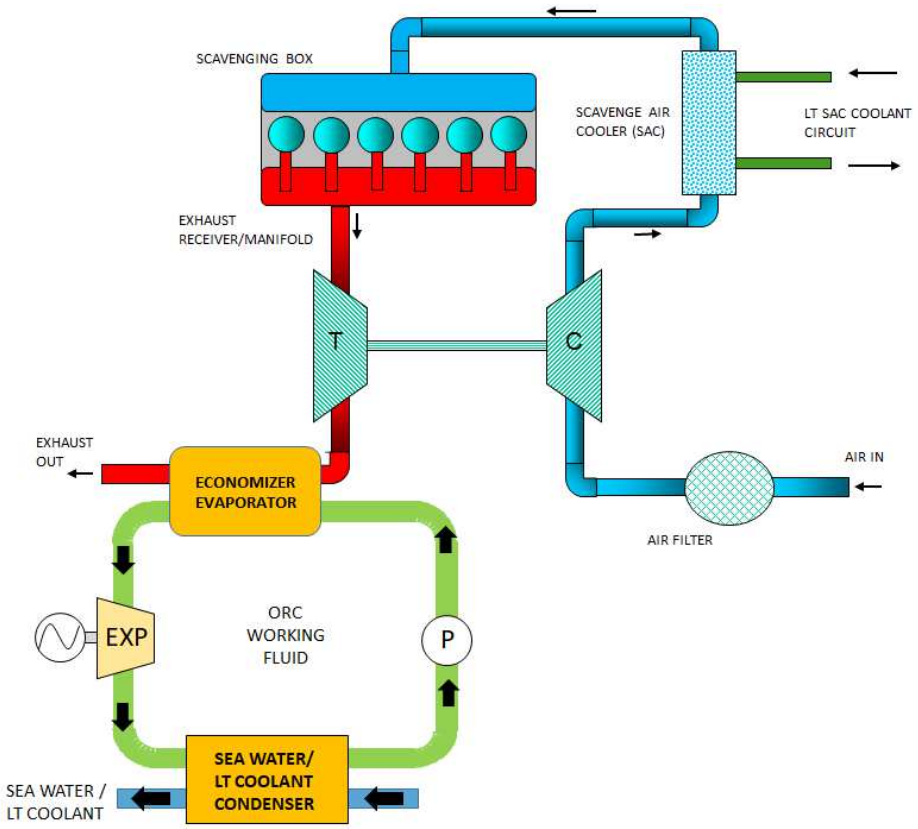
SCAVENGING BOX
SCAVENGE AIR COOLER (SAC)
LT SAC COOLANT CIRCUIT
EXHAUST RECEIVER/MANIFOLD
T
C
EXHAUST OUT
ECONOMIZER EVAPORATOR
AIR IN
AIR FILTER
EXP
ORC WORKING FLUID
P
SEA WATER/ LT COOLANT CONDENSER
SEA WATER / LT COOLANT

(1)

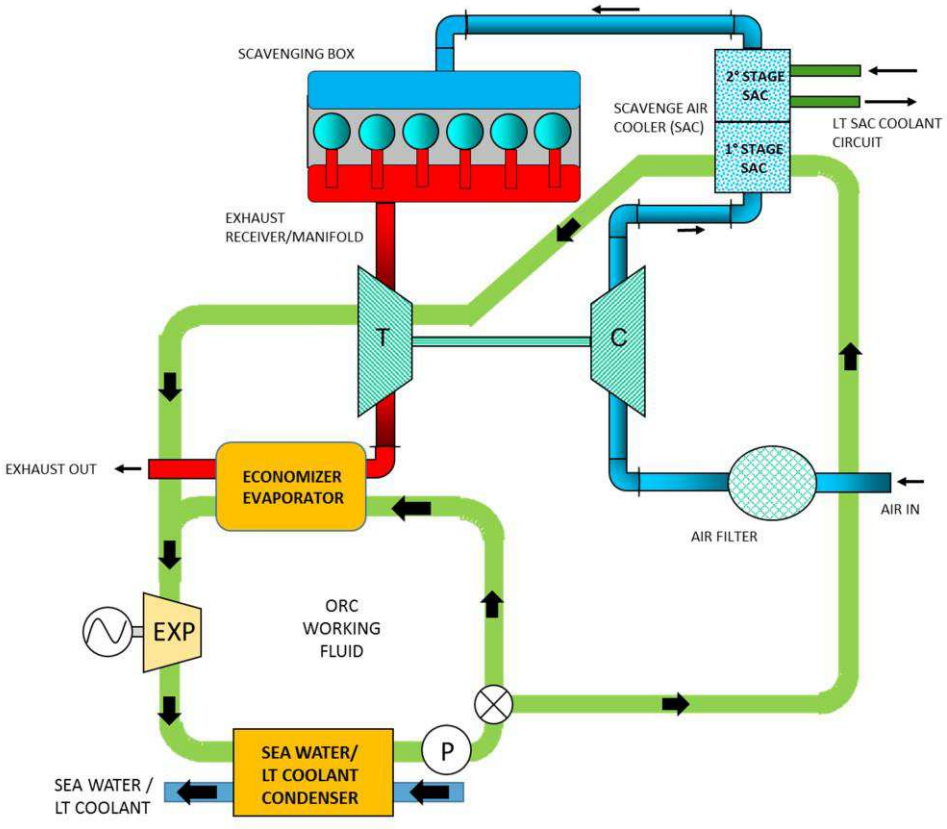
SCAVENGING BOX
2° STAGE SAC
SCAVENGE AIR COOLER (SAC)
1° STAGE SAC
LT SAC COOLANT CIRCUIT
EXHAUST RECEIVER/MANIFOLD
T
C
EXHAUST OUT
ECONOMIZER EVAPORATOR
AIR IN
AIR FILTER
EXP
ORC WORKING FLUID
P
SEA WATER/ LT COOLANT CONDENSER
SEA WATER / LT COOLANT

(2)

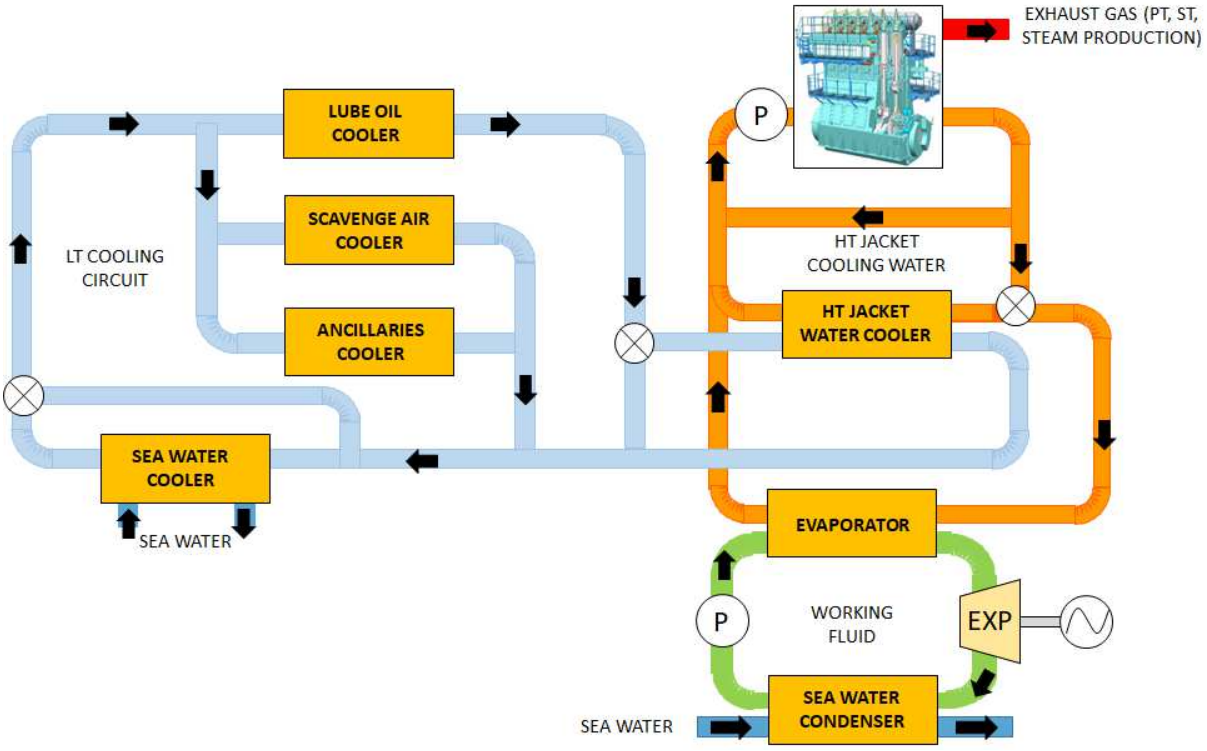

(3)

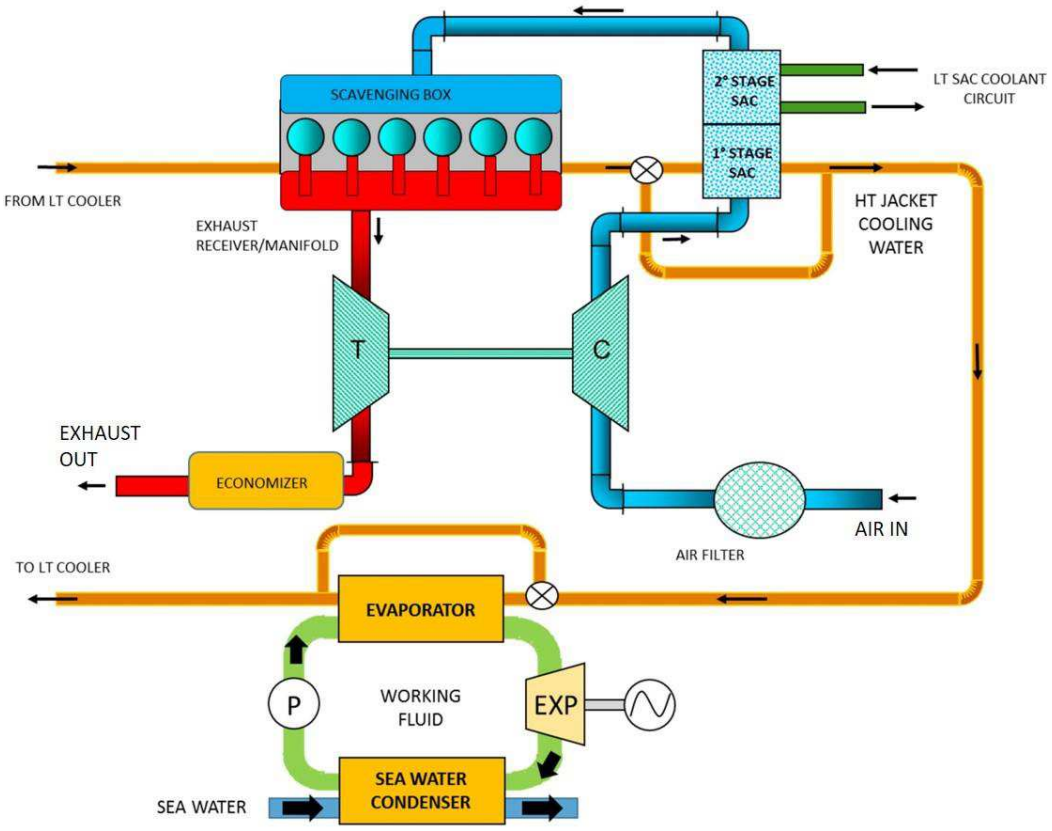

(4)

Fig. 84. ORC architectures considered in the study (case study 3)

The proposed concepts can be combined in order to obtain the maximum benefit in terms of possible engine BSFC improvement, trying to recover all the various heat sources available. In particular, two scenarios have been considered in the analysis:

1) *Concept 1 + Concept 4:* recovering exhaust gas (concept 1) and HT jacket cooling water with SAC (concept 4);
2) *Concept 2 + Concept 3:* recovering exhaust gas and SAC (concept 2) and HT jacket cooling water (concept 3);

6.3.3 Working Fluid Selection

Water-steam, as in a common Rankine cycle, is considered in this case study for the simple tailpipe (concept 1) and the parallel SAC/economizer (concept 2) systems. This has been done mostly because of the common use in ships, because of the safety in operations, and because no freezing issues are expected when the ORC system is installed on-board the ship in a climatized environment.
Other fluids have been evaluated for just one case (75% load, concept 1, Tier II operations without EGR) obtaining comparable performance to water-steam for the temperature levels considered, but resulting in more dangerous and unreliable operations, not giving a real improved benefit (the net power output achieved is very similar in absolute values). The fluids evaluated are ethanol, toluene, methanol, cyclohexane, cyclopentane and acetone.
R245fa, often used in ORC applications, is definitely not a suitable fluid for the temperature range considered. Indeed, very high cycle pressures are needed (even above critical) in order to match the heat source temperature profile and improve heat transfer, but at the same time, the cycle performance achievable with the other fluids cannot be matched.
However, when using fluids other than R245fa, it is necessary to achieve vacuum condensing pressures (below ambient pressure) in order to match the cooling fluid temperature profile (25°C, at condenser inlet), increase the pressure difference (and enthalpy drop) over the expander, thus increasing system performance. In this case radial turbines, even with multi-stage expansion could be needed.
Due to the higher latent heat of vaporization of water-steam, a lower amount of fluid is needed, compared to the other fluids, to achieve the same performance.
In case of water-steam, also, lower cycle operating pressures are also expected (around maximum 15 bar, from performed simulations) which, combined with the non-flammability, reactivity and safety, compared to the other fluids, lead to the choice of water as the most appropriate fluid.

For concepts (3) and concept (4), which are targeting lower temperature heat sources (80-120°C), other working fluids have been considered, more suitable for the required temperature levels than in the case of water-steam: R245fa, R1233zd(E), R123, R1234yf, R1234ze(E).
The fluids considered show a good compromise between environmental (GWP/ODP) and safety in-operations issues (health and low flammability). Concerning environmental issues, however, R245fa will be banned due to high GWP (100), but it has been considered due to the common use in literature studies and applications, as well as in available commercialized stationary systems.
R1233zd(E) is meant to be the replacement with low GWP of the R245fa refrigerant, showing, indeed, very similar T-s saturation curves shapes, as already reported in section 4.2.2.1.
R123, even if showing a good thermodynamic performance, will be also probably banned in the future due to its GWP level, and it shows some reactivity problems (R=1) compared to R1233zd(E).
Concerning R1234yf and R1234ze(E), especially for the first one, higher flammability issues (F=2) compared to R123 and R1233zd(E), disregard its utilization.

Moreover, for R1234ze(E) and R1234yf, in order to properly match the heat source temperature profile, it would be necessary to increase the evaporation pressure of the ORC system to a pressure next to the critical one. This is even more marked for concept (4), in which a higher heat source temperature is expected. In this case, it would be even necessary to go into the supercritical operational range, due to the fluids thermodynamic properties. Higher pressures, combined with possible flammability issues, can lead to problems in case of sealing failure, leading to leakage and ignition problems, discouraging the usage of these fluids.
From all the considerations reported above, it has been finally decided to assume R1233zd(E) as the best fluid for concepts (3) and (4). For this reason, results only for this particular fluid have been reported in this case study.
The main properties for all fluids mentioned can be observed in Tab. 11 and Tab. 12 in section 4.2.2.1.

6.3.4 Optimization Procedure and Assumptions

In this work, two thermodynamic process simulation models have been developed for a simple single evaporator configuration and a parallel evaporators configuration. The models have been developed in Engineering Equation Solver (EES) following what already reported in section 5.2.1.
In first approximation, not knowing exactly how the ORC power connections could be designed in the ship, a mechanical connection has been chosen in order to re-introduce the obtained net power from the waste heat recovery system into the main engine propeller shaft line (Fig. 85). A mechanical efficiency, η_{mech}, of a connecting gearbox has been assumed to be 0.98 [112,371]. The net power obtained from the ORC has then been calculated, in first approximation, as follows:

$$\dot{W}_{ORC,net,mech} = (\dot{W}_{EXP} - \dot{W}_P) \cdot \eta_{mech} \qquad (136)$$

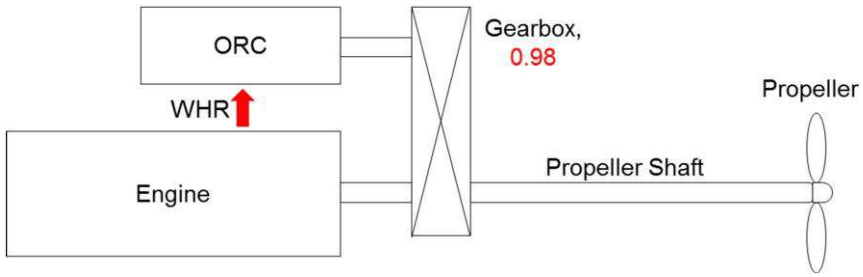

Fig. 85. ORC mechanical coupling to the main engine propeller shaft (case study 3)

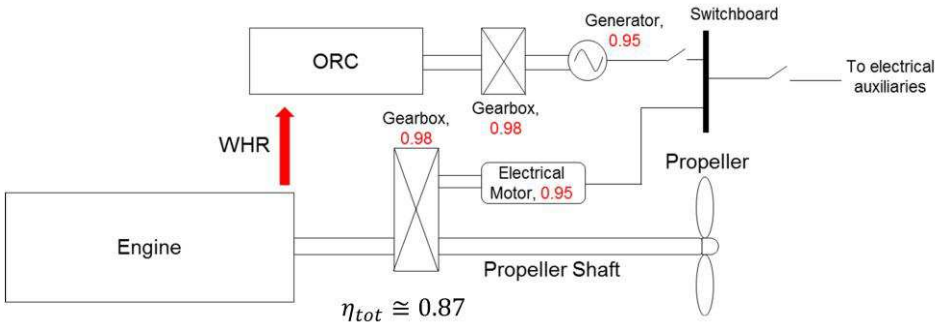

Fig. 86. ORC electric energy production for propulsive and auxiliaries ship applications (case study 3)

An electric power production configuration could be also possible, in order to generate electric power both for ship propulsion and auxiliaries. A possible scheme has been reported in Fig. 86. This configuration has not been considered in this study because of the more difficult estimation of BSFC improvement due to the waste heat recovery system use. However, the concept could be evaluated when a more flexible architecture is needed, able to supply on-demand both propulsive and electric power.
A rough estimation of the power consumption of the ORC sea cooling water pump has been performed, in order to understand how much the impact on the overall power balance could be. However, due to the preliminary character of the present analysis, the ORC sea water cooling circuit has not been sized and analysed. Moreover, variable speed pumps, adjusting the speed and the mas flow based on the cooling load required, could help in saving energy under different operating conditions, as reported by Theotokatos *et al.* [372].
Varying the sea water volume flow between 72 and 435 m^3/hr (around 20 to 120 kg/s mass flow), and the circuit head between 0 and 15 m_{H2O}, and considering a pump efficiency of 0.6, a power consumption between 0.5 and 30 kW can be expected. Data seems to be feasible considering what reported in [372]. However, due to the very variable conditions and to the preliminary character of the study, the sea water pump consumption has not been considered in the overall power balance, but this is an issue which must be evaluated when completely designing the system.
As already mentioned, an optimization procedure has been applied in order to obtain, as objective function, the highest possible ORC net power output, $\dot{W}_{ORC,net,mech}$, based on the boundary conditions for every case evaluated.
The optimization process has been carried out using the EES Optimization Toolbox, and the procedure developed in two steps, as done in the case study 1:

1) A *Genetic Algorithm (GA)* has been used to obtain a first global best solution, exploiting the characteristics of the GA of being robust to find a global optimum, but slow and not very accurate. This will guarantee to be close to the global optimal point;
2) A *Nelder-Mead Simplex Algorithm* is used as second step, starting from the GA solution, to find a more accurate best ORC power output, thus refining the search, exploiting the properties of this type of algorithm of being more accurate and fast converging to the solution, but being less robust in finding a global solution;

The constrained, assumptions and independent variables of the optimization procedure have been reported in Tab. 47, as a summary for all the ORC concepts analysed.
For the gas-gas heat exchangers, minimum pinch point values of 10°C have been imposed, as a trade-off between heat exchangers performance and size, and thus cost (concepts 1 and 2). While for the liquid-liquid or gas-liquid heat exchangers (and in particular in concepts 3 and 4), pinch points of 5°C have been considered, due to the higher overall heat transfer coefficient expected in these cases. Moreover, no boiling is expected in the HT jacket cooling water circuit, since at 4 bar circuit pressure levels, the boiling point of water is around 150°C, temperature which is not achieved even after SAC heat recovery in concept 4.
The maximum cycle evaporating pressure has been constrained to 30 bar and the maximum cycle temperature has been imposed lower than the critical one, due to safety reasons.
A sub-cooling temperature of 2°C has been also imposed in order to ensure the working fluid in liquid conditions at the pump inlet, thus also avoiding cavitation problems.
The vapour quality of the working fluid at the expander outlet has been constrained to be higher than 90% in order to avoid liquid droplets to form and damage the blades of a possible turbine expansion machine (most reasonable choice for applications of this size).
A limit on the discharged sea cooling water at the ORC condenser outlet of around 50°C has been imposed in the case legislative limitations are applied, while the mass flow of cooling medium is

imposed to realistic values, case per case. The sea water inlet temperature has been considered to be 25°C for average sea conditions.

Independent variables	
$\dot{m}_{wf}$ [kg/s]	ORC working fluid mass flow
p_{cond} [bar]	ORC condensing pressure
PR [-]	ORC pressure ratio (p_{evap}/p_{cond})
ΔT_{suph} [°C]	ORC degree of superheating
Constraints and Assumptions	
ΔT_{PP}	Minimum pinch-point temperature difference for the heat exchangers ▪ *Concepts 1-2*: 10°C ▪ *Concepts 3-4*: 5°C
$0.1\ °C \leq \Delta T_{suph} \leq 100\ °C$	Superheating degree (high superheating generally required for water systems and wet fluids to avoid high liquid fraction at expansion outlet)
$p_{evap} \leq 30\ bar$	Maximum constrained evaporation pressure
$p_{cond} \geq 0.1$ [bar]	Minimum condensation pressure. Vacuum accepted in order to increase the power output of the ORC (especially in case of water-driven RC in concepts 1 and 2)
$T_{exh,out} = T_{econ,,out}$	Minimum outlet temperature at the economizer outlet (from WAVE boundary conditions). Economizer heat rejection capabilities respected
$T_{cool,evap,out} = 75°C$	Minimum temperature of the coolant at the evaporator outlet (*concepts 3-4*). Temperature requirement for engine cooling jacket inlet respected
$x_{EXP,out} \geq 0.9$	Minimum expander outlet vapour quality to avoid high liquid fraction during the expansion process
$T_{max} \leq T_c$ [°C]	Cycle maximum temperature (expander inlet) lower than the fluid critical temperature (no-supercritical conditions evaluated)
$PR \leq 100$ [-]	Maximum pressure ratio
$\dot{m}_{cf}$ [kg/s]	Cooling fluid mass flow: ▪ *Concepts 1-2*: 20 kg/s of seawater ▪ *Concept 3*: 30 kg/s of seawater ▪ *Concept 4*: 120 kg/s of seawater
$T_{cf,cond,in} = 25$ [°C]	Condenser sea water inlet temperature
$T_{cf,cond,out} \leq 50$ [°C]	Condenser sea water outlet temperature
$\Delta T_{sub-cool} = 2°C$	Sub-cooling degree, in order to ensure liquid fluid at the pump inlet to avoid cavitation problems
$\eta_{EXP} = 0.7$	Expander isentropic efficiency (turbo-expander)
$\eta_P = 0.6$	Pump isentropic efficiency

Tab. 47. Independent variables and constraints for the four concepts optimized (case study 3)

The heat rejection capabilities of the economizer, modelled on the engine side in WAVE, have been respected imposing a limit on the exhaust economizer outlet temperature. The temperature limit, case per case, has been obtained from the 1-D engine calculations. If the economizer exhaust gas cooling limit (180-190°C) would have been decreased, for example, to 130°C (respecting sulphur deposition limits due to corrosion problems) an increased power output could be expected from the ORC, thus allowing an improvement in BSFC for the combined engine-ORC system.

The temperature of the HT jacket cooling water at the engine jacket inlet has been constrained always to be 75°C, in order to respect design engine cooling requirements from GTD data [60].
In the ORC model, the properties of sea water have been approximated with those of common water, while those of the exhaust and SAC gas have been approximated with those of normal air (considering the specific heat value will not differ too much). For the ORC working fluids, the properties have been directly retrieved from the EES internal database, through the use of appropriate functions.
In the proposed case study, a 60% isentropic efficiency for the pump and a 70% for the expander have been assumed. In the case of the expansion machine, if a turbo-expander is used, an efficiency up to 80-85% can be expected, as reported by Macchi *et al.* [112]. For this reason, if a high expansion efficiency can be ensured, the results proposed in this case study could be improved, leading to a better profitability of the ORC installation.
The results of the ORC calculations and the engine-ORC combined system BSFC benefits are reported in section 6.3.5.3. The approach used for the calculation of the boundary conditions for the ORC from the 1-D simulations is reported in section 6.3.5.2.

6.3.5 Results and Discussion

In this section, the results of the study have been reported divided by the engine 1-D simulations results, both for the baseline engine validation and the LP EGR model, the calculations of the boundary conditions for the ORC thermodynamic optimization and the combined engine-ORC systems performance. Finally, a preliminary economic analysis, based on some assumptions concerning typical ship operating profiles and fuel costs, has been carried out, with the scope of the demonstrating and estimating the possible benefits in terms of fuel operational costs, when recovering engine waste heat with ORC systems, as proposed in this case study.

6.3.5.1 Engine Simulations Results

In this section, the results regarding the engine 1-D analysis side of the work have been reported, focusing the attention on the validation of the baseline model (for Tier II operations) and the results of the model with the introduction of the LP EGR architecture (Tier III).
The data evaluated consider mostly the engine performance characteristics, gas lines temperatures and the heat rejection concerning the ORC suitable heat sources. The results are related to the three operating points considered: 100%, 75% and 50% load points.

Baseline Engine Model Validation

The final baseline engine validation has been carried out on the model with the BMEP controller reported in Fig. 81.
As discussed with WinGD, and as reported in the GTD software, the validation has been considered with a relative error tolerance of ±5%, which, considering the not extremely accurate geometrical information of the model, has been assumed enough, especially considering the purpose of this study. Several different parameters of the engine have been validated, but just some of them have been reported in Fig. 87(a-j), in order to keep the description as short as possible.
The Air-to-Fuel Ratio has been reported without a scale, due to confidentiality reasons requested by WinGD. The values for the baseline model are however in the lean combustion region, above 20.

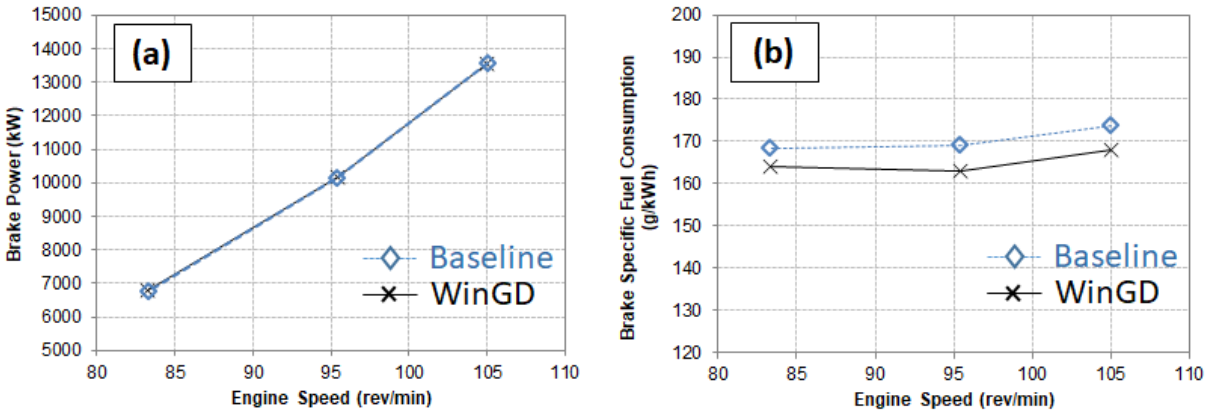

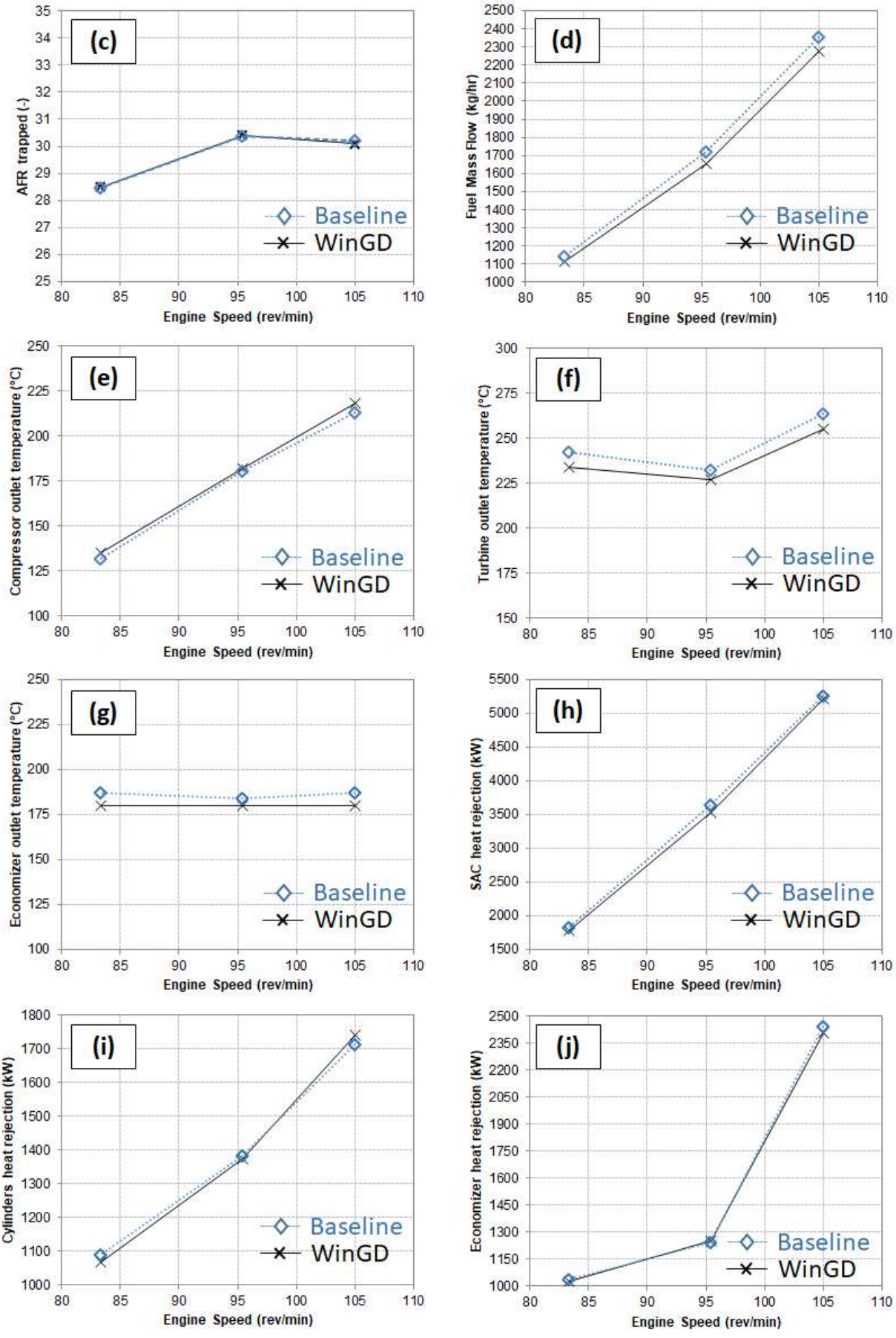

Fig. 87. Baseline engine model validation (case study 3)

The model developed shows a very good agreement (in the tolerance declared by WinGD) with the data supplied for validation. Also, heat transfer terms, of particular interest for the performed ORC analysis, and related to SAC, cylinders/engine-block and economizer heat rejection, have been also validated in the requested tolerance.
Exhaust gas turbine outlet temperature shows slightly higher values compared to those declared by WinGD, but still in the temperature tolerance range declared (±15°C) in the validated GTD software data.

LP EGR Model

The first simulation runs, when introducing the LP EGR circuit, have been performed not considering any tuning of the engine model, but just introducing the required EGR recirculation rate, and observing the impact on the performance of the engine and the main gas line parameters. The BMEP PID controller has still been kept in order to ensure the same BMEP, and thus brake power, of the baseline cases without EGR. Results for BSFC (a) and AFR (b) have been reported in Fig. 88, in order to carry out some observations. The AFR results have been reported in relative percentage form because of confidentiality reasons, requested by WinGD.

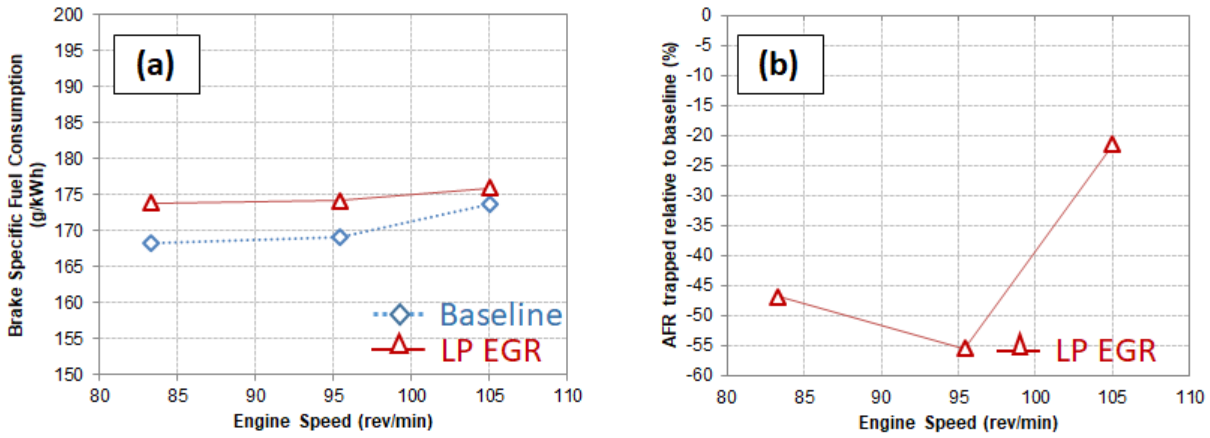

Fig. 88. LP EGR simulations preliminary results (without engine tuning) – (case study 3)

Observing what reported in Fig. 88(a) it is possible to see an increase in BSFC between 1.3 and 3.3% in case of LP EGR compared to the baseline model, as expected from available literature and experience with EGR systems. Concerning Fig. 88(b), it is possible to observe a marked decrease in AFR (and thus in λ), which in the case of 75% and 50% loads goes below 20 (or concerning λ below 1.4). This could lead to possible smoke and soot formation because of too rich combustion. The results, in particular for 75% and 50% loads, show λ values respectively of around 55% and 47% lower than the baseline case, declared too low compared to what expected by WinGD. For the 100% load point, the value of AFR (or λ) has been considered high enough.
For this reason, following the guidelines of WinGD, it has been decided to tune the engine model so to allow, for cases 75% and 50% load, an increase in λ, thus allowing some possible safety margin for smoke formation. Of course, a CFD validation of the assumptions should be carried out in further analysis steps, however, due to the purpose of the study, in this preliminary analysis the tuning has been considered enough in order to proceed with the waste heat recovery study, leaving the CFD analysis to the project partner NTUA, for further subsequent publications.

In particular, the EVC (Exhaust Valve Closure) event has been anticipated compared to the baseline model, in order to trap more scavenging fresh air, with the final goal of increasing the trapped λ. However, this solution tends at the same time to increase the cylinder pressure, and in particular the peak firing pressure of the engine, until possibly not acceptable values, due to operating, safety and material constraints. In order to decrease the firing pressure, the SOI (Start of Injection), and consequently the SOC (Start of Combustion), have been postponed. The combined tuning of these parameters, which in a real engine can be adjusted with a fully electronic valve actuation and injection system, leads to a compromise between acceptable peak firing pressure, acceptable λ values and fuel consumption.
Following WinGD guidelines, an acceptable value of the trapped λ has been considered, which should lead to a compromise with fuel consumption increase and peak firing pressure.
The exhaust valve lift profile for the case at 75% load has been reported in Fig. 89, as an example.

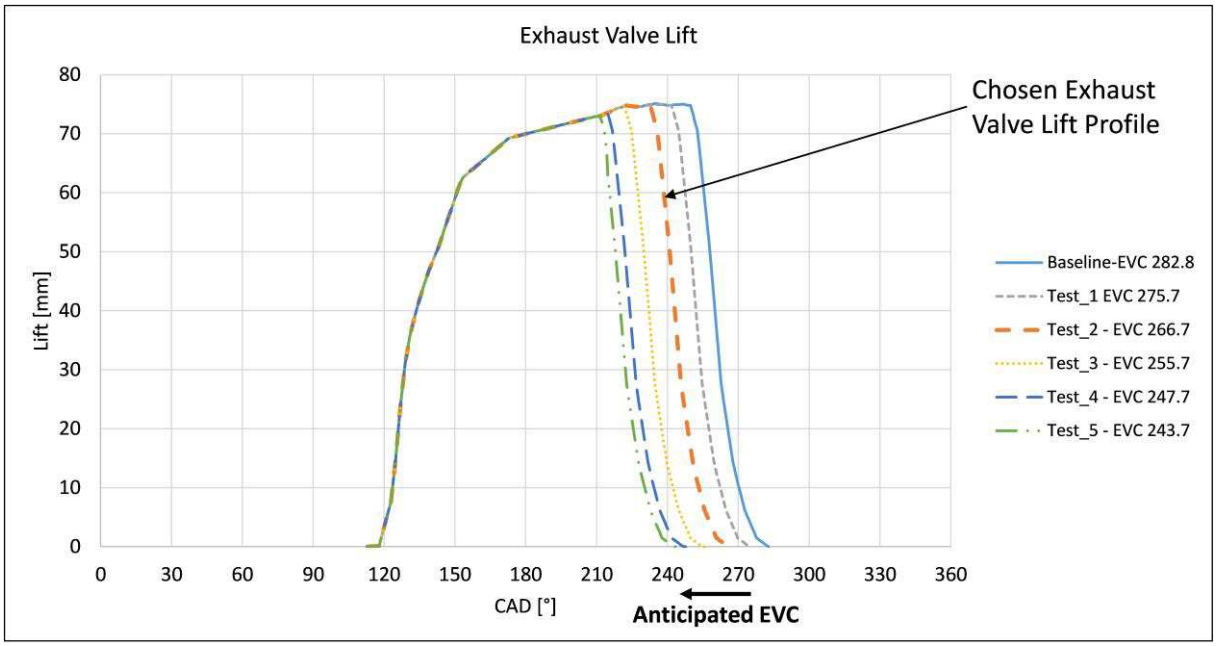

Fig. 89. Anticipation of EVC for the 75% load case (case study 3)

An increase of BSFC of around 3% compared to the model without tuning, and around 6% compared to the model without EGR has been achieved. The tuning resulted to be very sensitive in this case, with a small difference in SOI leading to quite high BSFC increase.
The exhaust valve lift profile for the case at 50% load has not been reported, but the same procedure used for the case at 75% load has been used, achieving around 0.1% increase BSFC compared to the model without tuning and 3.4% compared to the model without EGR. In this case, the tuning procedure was more efficient, regarding the compromise between fuel consumption and peak firing pressure. I higher AFR, compared to the 75% load case, could also be achieved.
An optimization of the proposed tuning parameters could be proposed for future studies, when considering a better trade-off with fuel consumption and firing pressures. For the purpose of the case study, the tuning campaign has been considered accurate enough.

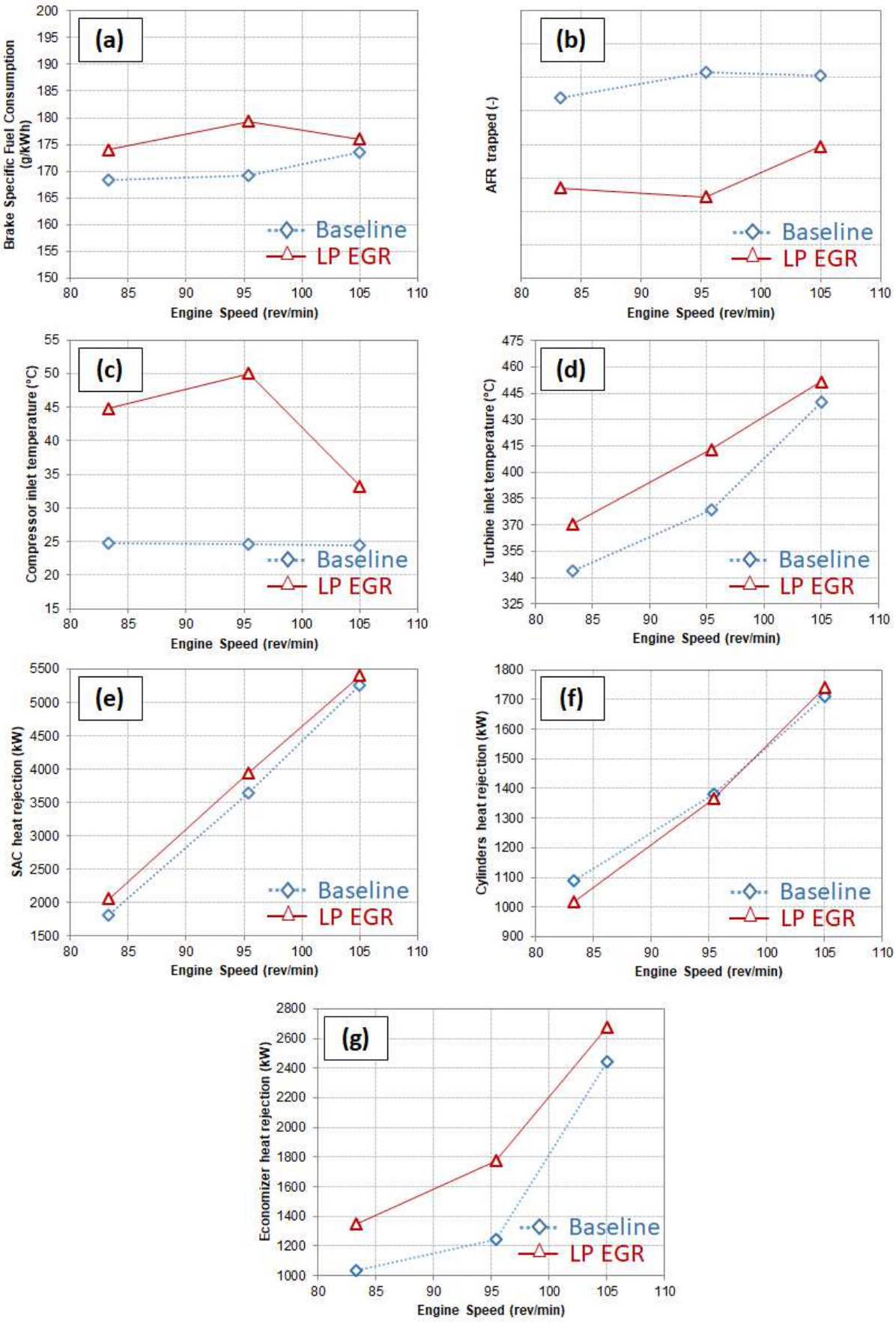

Fig. 90. Graphical comparison between baseline engine model and model with LP EGR (case study 3)

The results, concerning all main engine parameters have been reported in a graphical form in Fig. 90, for the engine model with no tuning, in case of the 100% load case, and with tuning for the cases with 75% and 50% loads. A comparison between baseline model and model with LP EGR after tuning has been proposed.
The BSFC increase due to the use of LP EGR, as observed in Fig. 90, is in the range between 1.3% (100% load) and 6.1% (75% load). In this last case, a quite high increase can be observed due to the model tuning compromise previously mentioned.
The results reported in the previous page also show that a LP EGR gas recirculation leads to an increase of compressor inlet (and outlet) temperature, depending on the amount of exhaust gas recirculated to the intake and, thus, on the operating point simulated (20 or 40% EGR rates used). An increase of compressor outlet temperature leads also to a subsequent increase of heat which must be rejected in the SAC in order to respect the same cylinders' intake temperatures for combustion requirements, as suggested by WinGD. This increased heat rejection could be exploited in an ORC bottoming cycle, in order to recover additional useful energy, using the concepts 2) and 4) reported in section 6.3.2.
At the same time, when adding EGR, an increased turbine inlet (and turbine outlet) temperature can be observed, with consequent increase also of heat that can be rejected in the economizer at all the three operating points simulated. This increased heat rejection could be also recovered through the use of a common steam Rankine cycle or an ORC on the exhaust line.
For what concerns the engine block or cylinders heat rejection, keeping the same heat transfer Woschni model settings of the baseline model, different trends can be observed from the histograms, sometimes obtaining an increased heat rejection, sometimes obtaining a decreased amount of heat rejected to coolant and oil circuits, but with not so marked variations compared to the other heat sources which could be considered for the heat recovery study, as it could be expected from similar data reported in Fig. 15 in section 4.1.3.2.
Regarding the scrubber, a sensible amount of heat is going to be rejected to the Water Treatment System (WTS), however, this heat will not be considered in this study because of the difficulty of designing an ORC system on the WTS loops, which contain different chemical compounds and slugs.
The EGR blower has also been modelled in this study, in order to push the EGR gas from the exhaust to the intake engine lines. The power consumption has been estimated imposing 60% efficiency and the data.
The data concerning the engine heat rejection, which have been further elaborated in order to extract the ORC analysis boundary conditions, have been reported in Fig. 91. A general increase in heat rejection can be observed, especially for Scavenge Air Cooler (SAC) and exhaust line economizer, in the cases with LP EGR. This can lead to a possible increase in the performance of the bottoming ORC system, due to the possibility to recover additional heat in order to produce additional useful energy.

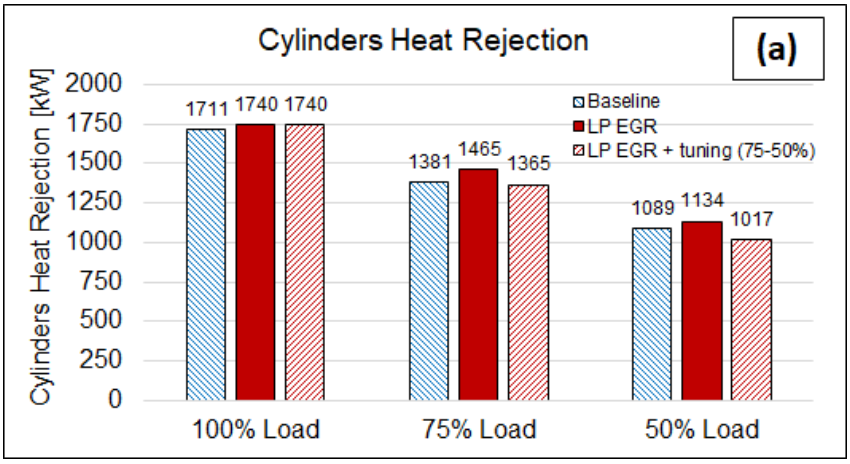

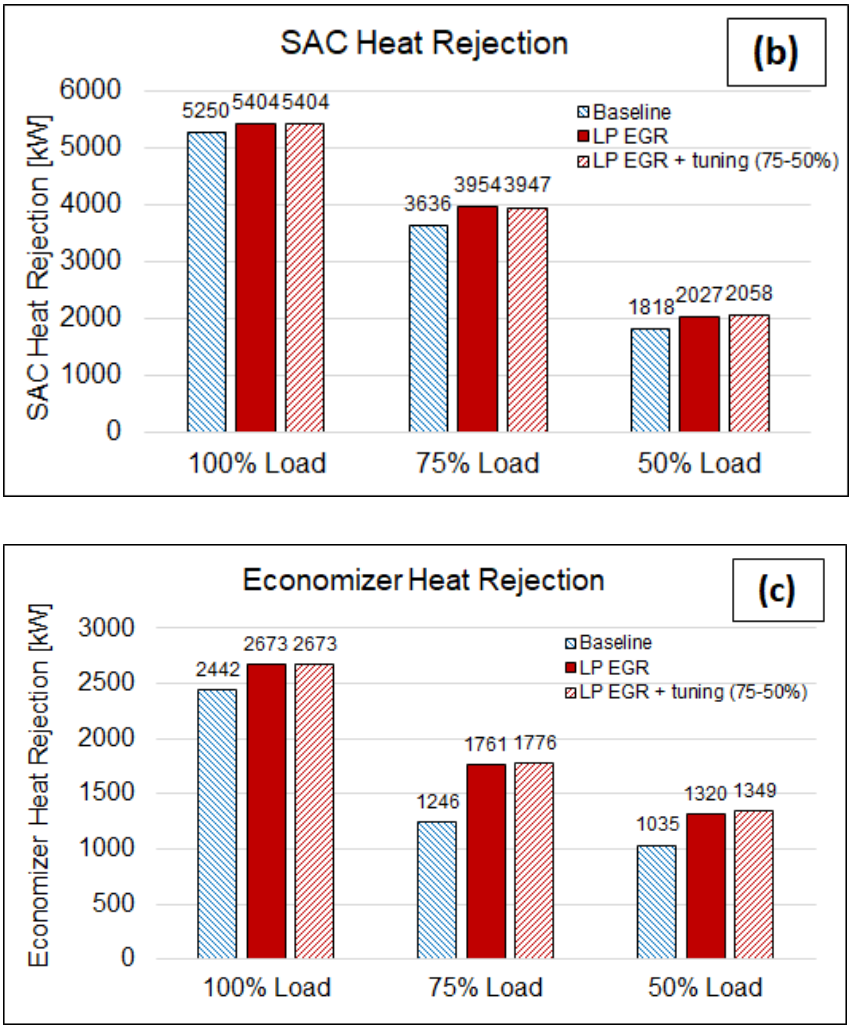

Fig. 91. Heat rejection comparison between baseline engine model and models with LP EGR (without and with engine tuning) – (case study 3)

6.3.5.2 ORC Boundary Conditions Calculations

The boundary conditions for the ORC analysis have been extracted from the 1-D model, as reported in Fig. 92, concerning SAC, economizer and cylinders/engine block heat rejection.
In Fig. 93, a conceptual scheme of the energy flows in the engine WAVE model has been reported, showing where boundary conditions have been evaluated.
Concerning economizer and SAC boundary conditions for the ORC analysis, the extraction of the parameters, needed for the simulations to be performed in EES, is quite simple, since they can be directly obtained from the WAVE model ducts components, at the left-hand side of each duct characterizing the component, in particular regarding mass flow and temperature of the gas lines.
Concerning the heat rejected to the HT jacket cooling water, as reported in Fig. 94, both friction and heat transfer rate have been considered. Indeed, these two energy fluxes are, in a real engine, contributing to the thermal power transferred to the cooling circuit, oil circuit, and some through radiation to the environment.

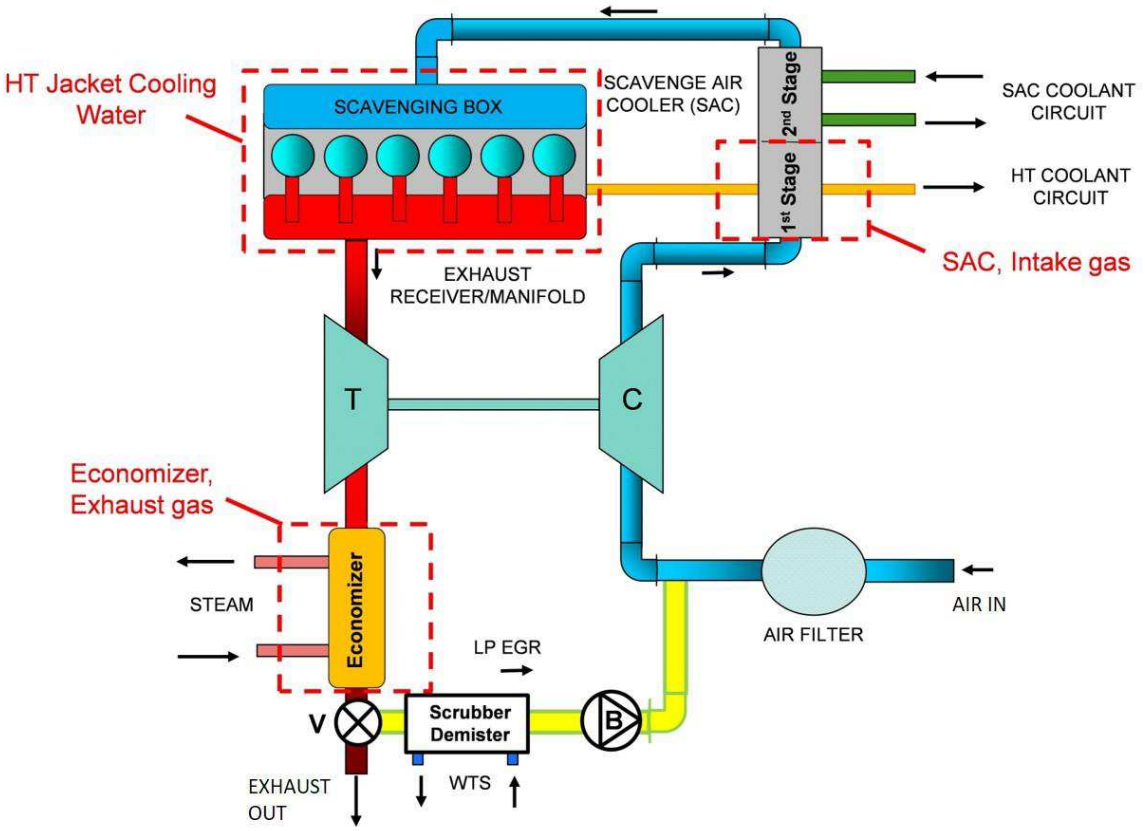

Fig. 92. Engine boundary conditions for the ORC analysis (case study 3)

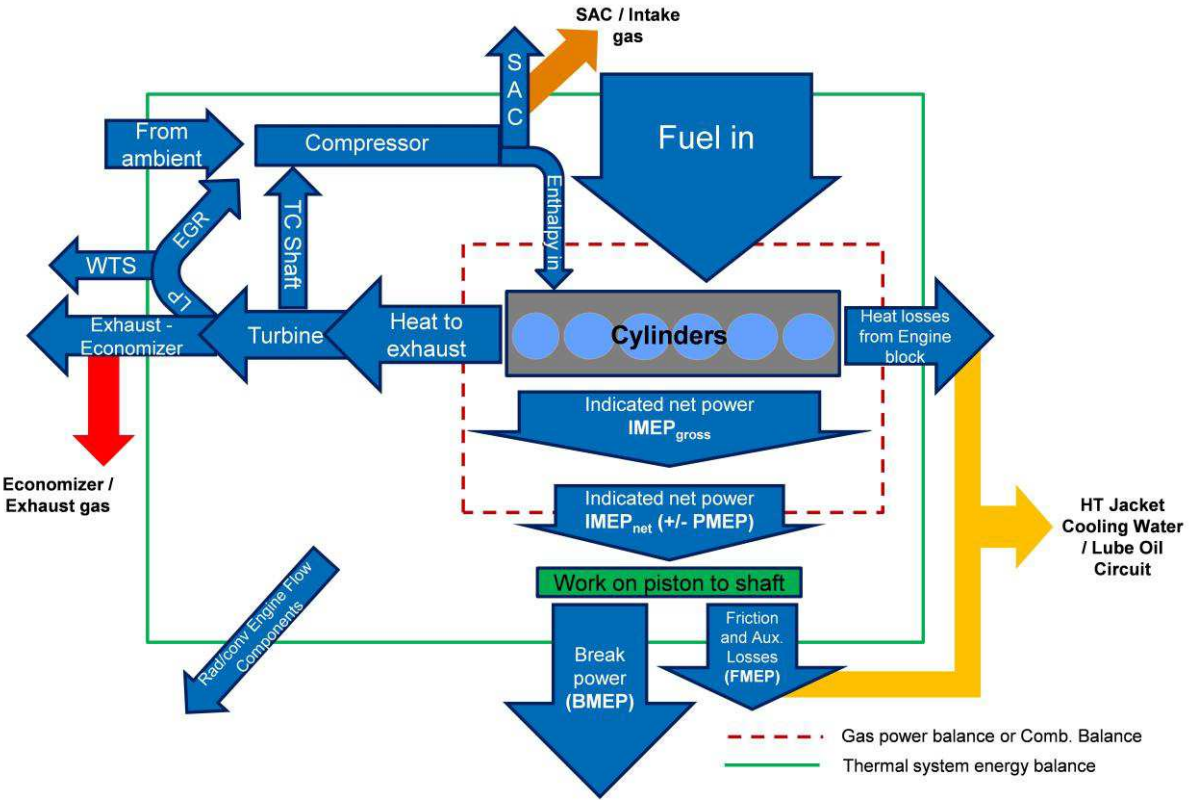

Fig. 93. Energy streams in the engine WAVE model with LP EGR (case study 3)

In this study, especially considering that the radiation term is usually not easy to be estimated, it has been decided to sum both friction losses and heat transfer losses and, following the guidelines of the WinGD GTD software, which gives some simplified heat balances for every operating point, a thermal power percentage split of the contributions to the HT jacket cooling water and to the oil circuit has been estimated.
From an analysis of the WinGD GTD heat balances results for the considered engine, the percentages reported in Tab. 48 have been assumed. The percentages have been estimated both considering and not considering the radiation term (rad.).

Heat Balance	**100% Load**		**75% Load**		**50% Load**	
	[kW]	**[%]**	**[kW]**	**[%]**	**[kW]**	**[%]**
Fuel Input Power	27021	100	19650	100	13205	100
Brake Power	13560	50	10170	52	6780	51
SAC LT	5209	19	3530	18	1774	13
Coolant Cylinders	1584	6	1224	6	888	7
Lube Oil	904	3	750	4	621	5
Radiation	226	1	226	1	226	2
Exhaust gas	5538	20	3750	19	2916	22
Coolant/Oil Balance	***Heat Rejection to Coolant and Oil Circuits (Baseline)***					
	100% Load		**75% Load**		**50% Load**	
	% with rad.	**% without rad.**	**% with rad.**	**% without rad.**	**% with rad.**	**% without rad.**
Coolant	67	64	66	62	64	59
Oil	33	36	34	38	36	41
Assumed Oil %	**35**		**37**		**39**	
Assumed Coolant %	**65**		**63**		**61**	

Tab. 48. HT jacket coolant and lubrication oil heat transfer percentage estimation (baseline engine) – (case study 3)

For the friction losses calculation, the injected fuel mass flow and the friction energy losses (as % of the injected fuel) have been extracted from WAVE, thus allowing to calculate the fuel thermal power lost due to friction as follows. The fuel injected thermal power has been calculated as:

$$\dot{Q}_{fuel,inj} = \dot{m}_{fuel} \cdot LHV \quad (137)$$

and the thermal power lost due to friction as (x_{frict} is the energy percentage loss due to friction and it is directly obtained from WAVE):

$$\dot{Q}_{frict} = \dot{Q}_{fuel,inj} \cdot x_{frict} \quad (138)$$

While the total rejected heat from the engine cylinders/block has been estimated as the sum of the heat transfer term (obtained from the Woschni model in WAVE) and the calculated friction term:

$$\dot{Q}_{tot,HT,cyl} = \dot{Q}_{cyl,HT} + \dot{Q}_{frict} \quad (139)$$

The $\dot{Q}_{tot,HT,cyl}$ term has been then divided in two separated terms, one related to the heat transfer to the HT jacket cooling water circuit, and one related to the lubrication oil circuit. The percentage split has been estimated for every operating point from the data obtained for the baseline engine from the WinGD GTD software, as reported in Tab. 48.
As it can be observed from Tab. 48, around 61-65% of the heat from the engine cylinders and block is transferred to the HT jacket cooling water circuit and the remaining to the lubrication oil circuit. This last one has not been considered between the possible ORC heat sources due to the expected very low temperatures but could be evaluated in future studies.
Once the heat rejected to the coolant has been estimated ($\dot{Q}_{cool,cyl}$), a short routine has been written in EES (Engineering Equations Solver), exploiting its database for different fluids, in order to estimate the HT jacket cooling water parameters at the engine jacket outlet, which are used as the boundary conditions for the ORC in concept (3), and as boundary conditions for the additional SAC heat recovery in concept (4). The following formula has been used in the EES script:

$$\dot{Q}_{cool,cyl} = \dot{m}_{cool} \cdot c_{p,cool} \cdot \left(T_{cool,ENG,out} - T_{cool,ENG,in}\right) \quad (140)$$

Two approaches can be considered:

1) The volumetric flow of coolant is assumed (108 m^3/h at design point in WinGD GTD) and the temperature of the fresh water at the engine outlet can be estimated, given an engine inlet temperature of 75°C (with a pressure of 4 bar for the circuit imposed);
2) The coolant engine outlet temperature is imposed (90°C as design point in WinGD GTD) and the volumetric flow of coolant can be estimated from the heat rejection $\dot{Q}_{cool,cyl}$ and an imposed inlet temperature of again 75°C;

The two approaches lead to slightly different (but quite similar) boundary conditions for the ORC, regarding temperature and volumetric (or mass) flow of coolant carrying the heat to the bottoming cycle. The approach number 1) has been chosen, keeping fixed the volumetric flow to the design one, proposed by the GTD WinGD software.
For what concerns the ORC concept 4), with recovery of 1st Stage SAC heat rejection using the HT jacket cooling water, the data of the HT coolant after the 1st Stage SAC need to be evaluated in order to obtain the boundary conditions for the ORC simulations.
Again, using EES, and knowing the previously calculated HT cooling water temperatures and mass flow at the engine outlet, for every case, and the SAC temperatures and mass flows from the WAVE simulations, it has been possible to estimate the increase in temperature of the HT coolant due to the recovery of 1st stage SAC heat.
In particular, for the calculation of the specific heats, the coolant has been approximated as fresh water, while the SAC gas has been approximated as air.
A heat balance equation has been implemented, with the only unknown being the 1st Stage SAC HT coolant outlet temperature ($T_{cool,SAC,out}$):

$$\dot{m}_{SAC,gas} \cdot c_{p,SAC,gas} \cdot \left(T_{gas,SAC,out} - T_{gas,SAC,in}\right) = \\ = \dot{m}_{cool,SAC,in} \cdot c_{p,cool} \cdot \left(T_{cool,SAC,out} - T_{cool,SAC,in}\right) \quad (141)$$

As gas outlet temperature of the 1st stage SAC ($T_{gas,SAC,out}$), a limit, considering 10°C higher than the coolant inlet temperature, has been imposed, as a trade-off for a good heat transfer process:

$$T_{gas,SAC,out} = T_{cool,SAC,in} + 10 \qquad (142)$$

All calculated data, regarding mass flows and temperatures, have been finally used as inputs for the ORC process simulation models. The results of the ORC and of the combined engine-ORC system, for the different cases and operating points, have been reported in the next section.

6.3.5.3 Combined Engine-ORC Simulations Results

As already mentioned before, for concepts (1) and (2), only *water-steam* has been considered as working fluid, while for concepts (3) and (4), three different fluids, with similar thermodynamic properties, have been evaluated: R123, R1233zd(E) and R245fa.
However, the results only for *R1233zd(E)* have been reported, since very similar in the range with the other fluids. Moreover, the *R1233zd(E)* is expected to be the replacement for R245fa in the very next future.
The results have been reported concept per concept (1 to 4), and about the two possible combined concepts scenario, regarding the ORC net power output, the engine-ORC combined power output and the BSFC improvement potential.
The EGR blower power consumption has been considered only in the BSFC charts for the sake of a shorter description, while regarding the power output, only the engine-ORC combined system has been considered, without EGR blower consumption in the power balance.

Concept (1): Exhaust Gas (Economizer)

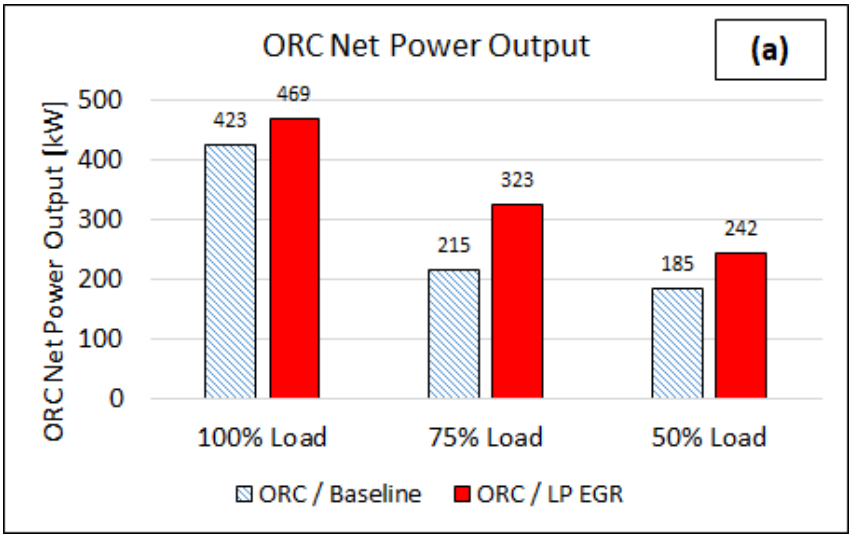

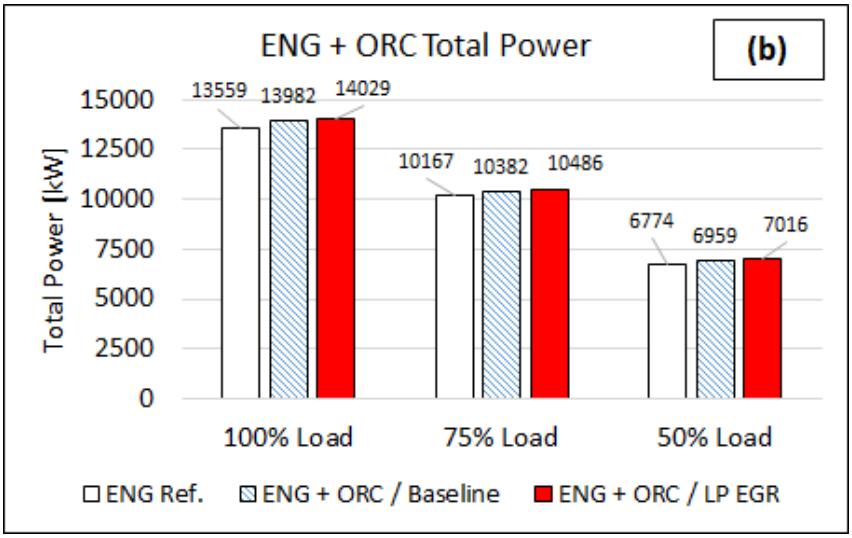

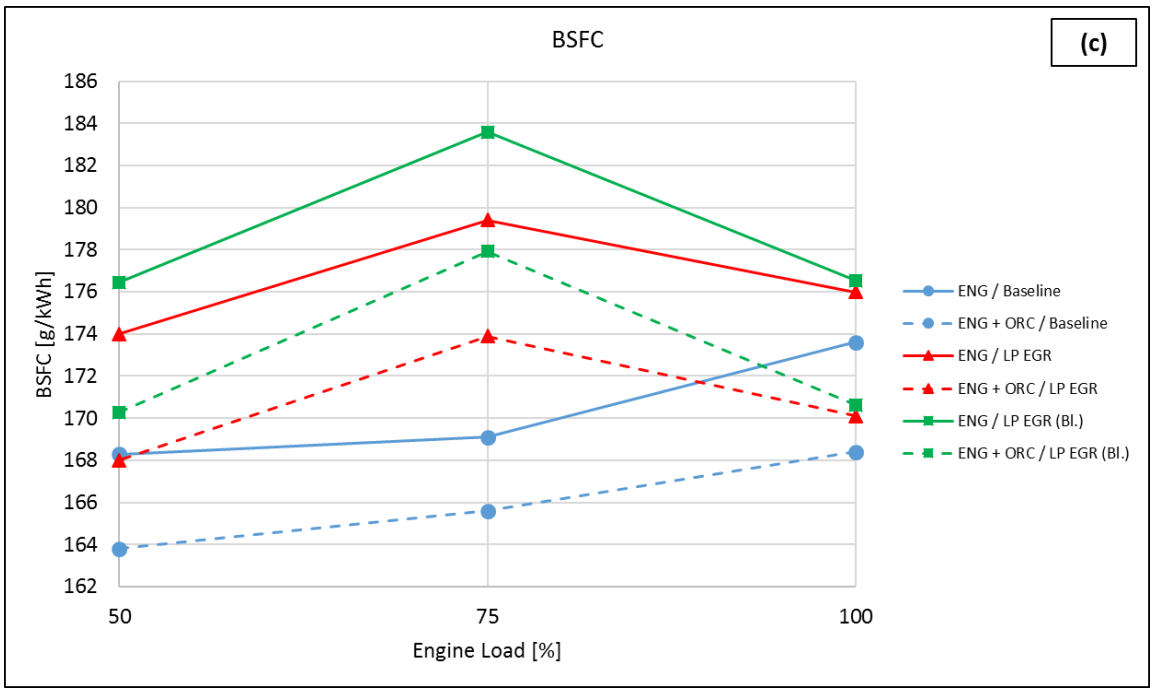

Fig. 94. Concept (1): ORC net power output (a), Engine + ORC total power output (b) and BSFC (c) – (case study 3)

ΔBSFC (%)			
	Engine Load		
Configuration	***100%***	***75%***	***50%***
ENG + ORC / Baseline (Tier II)	- 3.0	- 2.1	- 2.7
ENG + ORC / LP EGR (Tier III)	- 3.3	- 3.0	- 3.4

Tab. 49. Concept (1): BSFC improvement potential when fitting the ORC in Tier II and Tier III modes (case study 3)

In Fig. 94(a and b), the ORC net power output and the combined engine-ORC power output have been reported, while in Fig. 94(c) the BSFC values for the baseline engine (Tier II) and the LP EGR (Tier III) cases have been reported. The data in the graph (c) refer to the use or not of the ORC system, and

also to the presence in the power balance of the EGR blower consumption (Bl.). Segmented lines refer to the cases with ORC, while continuous lines to the cases with ORC.
In Tab. 49, the BSFC improvement in percentage when using the ORC system, compared to the case without ORC usage, is reported in case of Tier II and Tier III operations (comparison between, respectively, blue and red lines in graph (c)).
At 100% load case, it is not possible to recover all the heat available from the economizer, with an ORC system, imposing a cooling sea water mass flow of *20 kg/s* and a sea water cooling temperature at the condenser outlet of 40°C (as originally done), due to condenser heat rejection limitations. While, increasing the allowed sea water outlet temperature (up to 47-48°C in case of LP EGR, or +22/25°C compared to the inlet one), it is possible to reject the whole heat recovered, thus also increasing the ORC power output.
In the cases at 75% and 50% loads, with and without LP EGR, with 20 kg/s sea cooling water it is possible to achieve the full heat rejection (and heat recovery) capabilities of the ORC and economizer, at the same time respecting 40°C sea cooling water outlet limit.
The 20 kg/s sea water mass flow has been imposed in order to avoid too much water to be pumped into the circuit. Considering the high temperature drop available over the ORC, thus allowing a high-pressure ratio over the expander (high power output), the chosen amount of sea water seems to be reasonable as a trade-off between outlet cooling water temperature, ORC performance and possible sea water pump consumption (not considered in this step).
Considering water-steam as working fluid and with the imposed boundary conditions for the thermodynamic analysis, it is necessary to achieve vacuum condensation pressures to allow a good thermal match with the heat sink cooling fluid. This leads to the need of guaranteeing good sealing performance in order to avoid ambient air infiltration in the circuit.
A high-pressure ratio over the pump and expander is also needed to obtain high ORC power output performance. A turbine machine could be chosen (even multistage), considering the system size and performance.
A BSFC improvement is expected in Tier II operations, compared to the case without ORC, while in Tier III operations, some benefits, compared to Tier II, are expected only for the 100% load case when using the ORC (segmented red line is below the continuous blue one), but still allowing fuel savings compared to the Tier III case without waste heat recovery system, as reported in Fig. 94 and Tab. 49.

Concept (2): Exhaust Gas (Economizer) + SAC

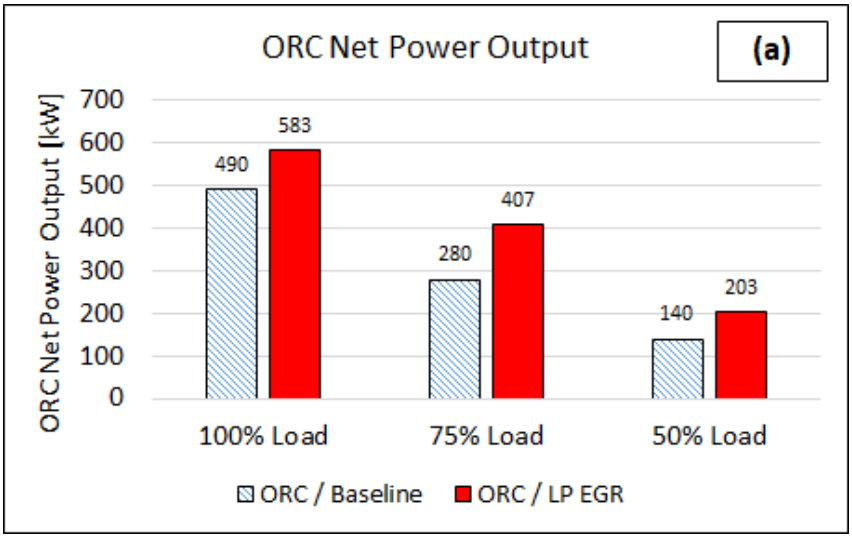

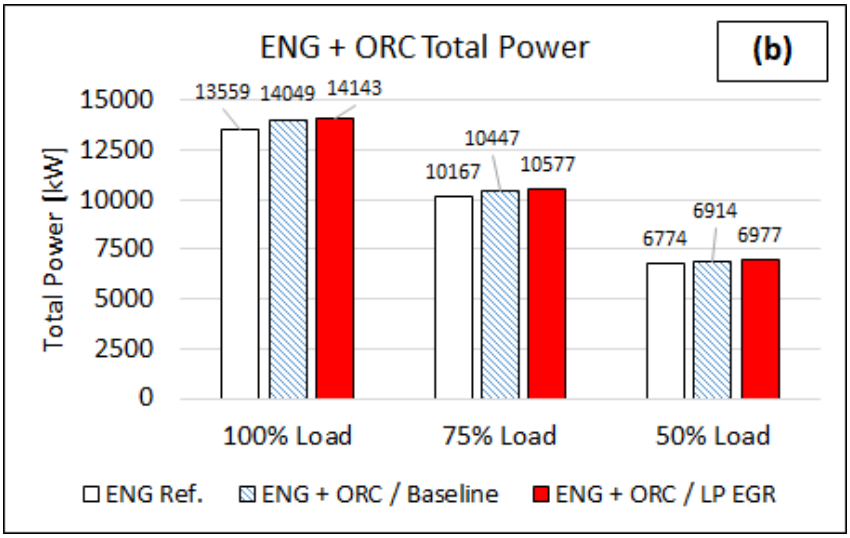

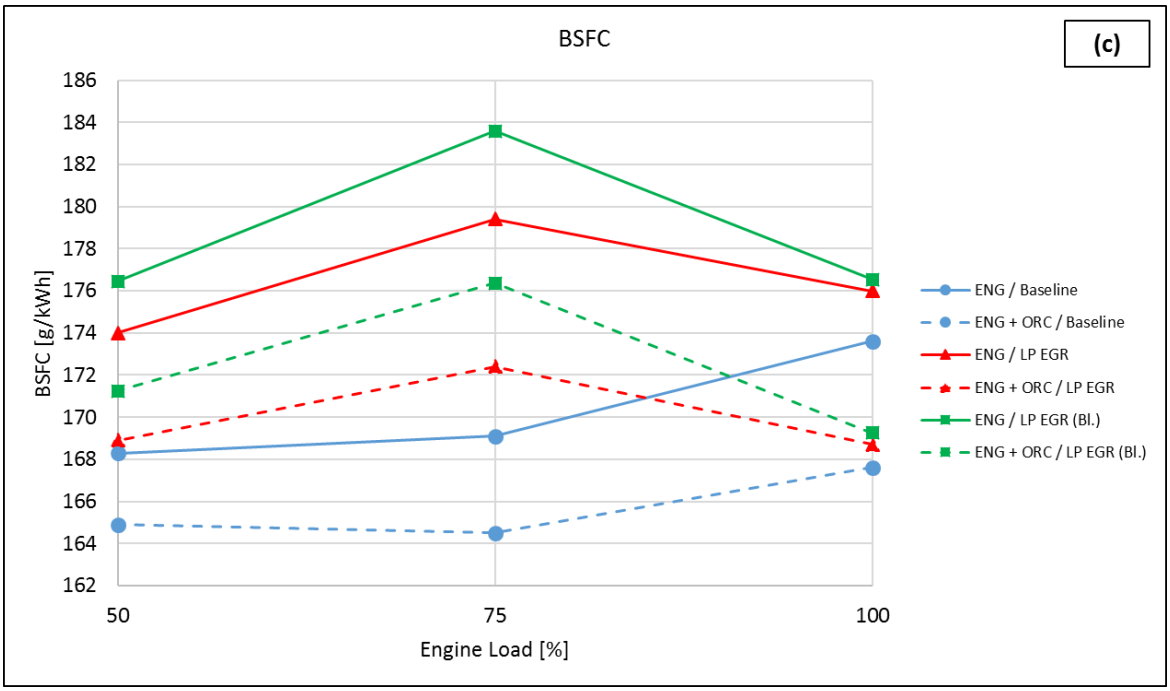

Fig. 95. Concept (2): ORC net power output (a), Engine + ORC total power output (b) and BSFC (c) – (case study 3)

ΔBSFC (%)			
	Engine Load		
Configuration	***100%***	***75%***	***50%***
ENG + ORC / Baseline (Tier II)	- 3.5	- 2.7	- 2.0
ENG + ORC / LP EGR (Tier III)	- 4.1	- 3.9	- 2.9

Tab. 50. Concept (2): BSFC improvement potential when fitting the ORC in Tier II and Tier III modes (case study 3)

The parallel cycle architecture (concept 2) leads to some advantages in terms of BSFC improvement, compared to the single exhaust evaporator architecture of concept (1).
In particular, this can be observed for the higher 100% and 75% load points, in which, the expected higher temperature of both exhaust gas and SAC gas, both with and without LP EGR, leads to a performance benefit when considering both heat sources recovery. Moreover, and this is more

important for this architecture, the temperature levels of the exhaust and SAC gas are in the same range, thus leading to the possibility of keeping the pressure ratio over the pump and expander, and thus the cycle evaporation pressure, at a reasonable high level, allowing a slight increase in ORC power output compared to the simple architecture.
However, the fact that the optimization procedure pushes towards the full recovery of the higher temperature heat source (in this case the exhaust gas) tends to limit the heat recovery from the lower temperature heat source (SAC). This is particularly affecting the cycle performance at 50% load, both with and without LP EGR, in which, the much lower temperature of SAC gas compared to the exhaust gas, limits the pressure ratio achievable over the expander and thus the power output. The model developed in this case is somehow limiting, because it does not allow to switch the SAC circuit off, thus imposing a maximum evaporation pressure constraint also to the exhaust gas side. In this case, or generally in a case with a heat source showing much lower temperature levels compared to the other one, it would be necessary to switch the lower temperature circuit off, basically returning to the simple single evaporator architecture performance (which are slightly higher at 50% load compared to the parallel one).
A dual loop system, or a system with two stage pressurization (two different staged pressurization levels as those reported in Fig. 25), could help, in this case, to achieve better performance, due to the full exploitation of the SAC heat.
The proposed parallel architecture could become interesting when considering a Tier III HP EGR configuration, in which the medium-high temperature EGR cooler heat could be recovered in parallel with the medium-high temperature exhaust gas (economizer) heat, thus allowing more comparable temperature levels, possibly achieving higher cycle performance.
With the proposed architecture, at 100% and 75% load, a slight improvement in performance has been achieved compared to concept (1), but probably not worth the system complication.
The usage of a lower boiling fluid, more suitable for lower temperatures, could slightly improve the performance of the system, especially at low 50% load, however, introducing complications mostly related to the use of a fluid which could be more dangerous or flammable.
A BSFC improvement has been achieved, using an ORC system both in Tier II and Tier III operations (Tab. 50). However, only at 100% load the BSFC of the LP EGR engine with ORC is lower than the one of the baseline in Tier II mode without EGR (Fig. 95-c).

Concept (3): HT Jacket Cooling Water

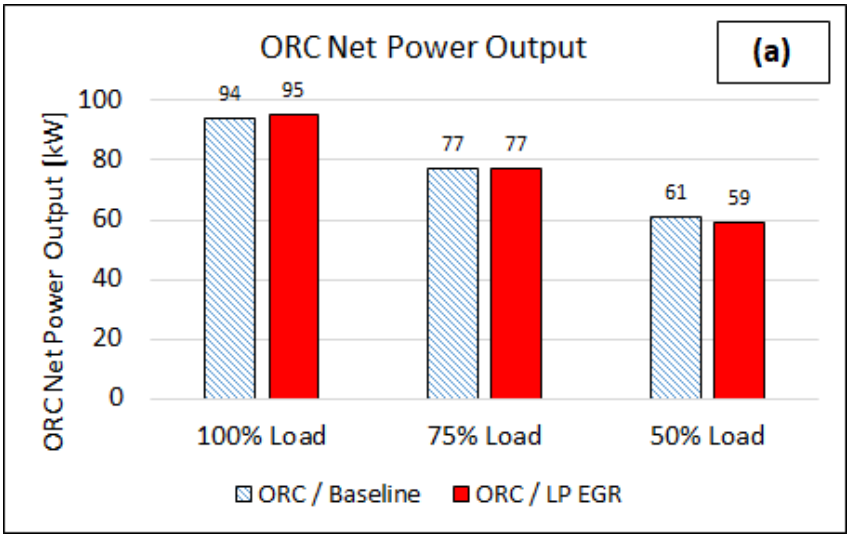

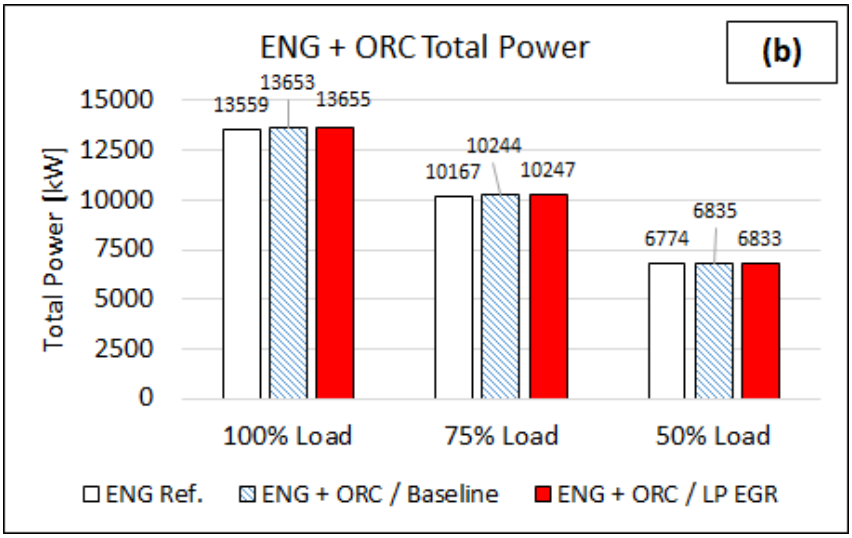

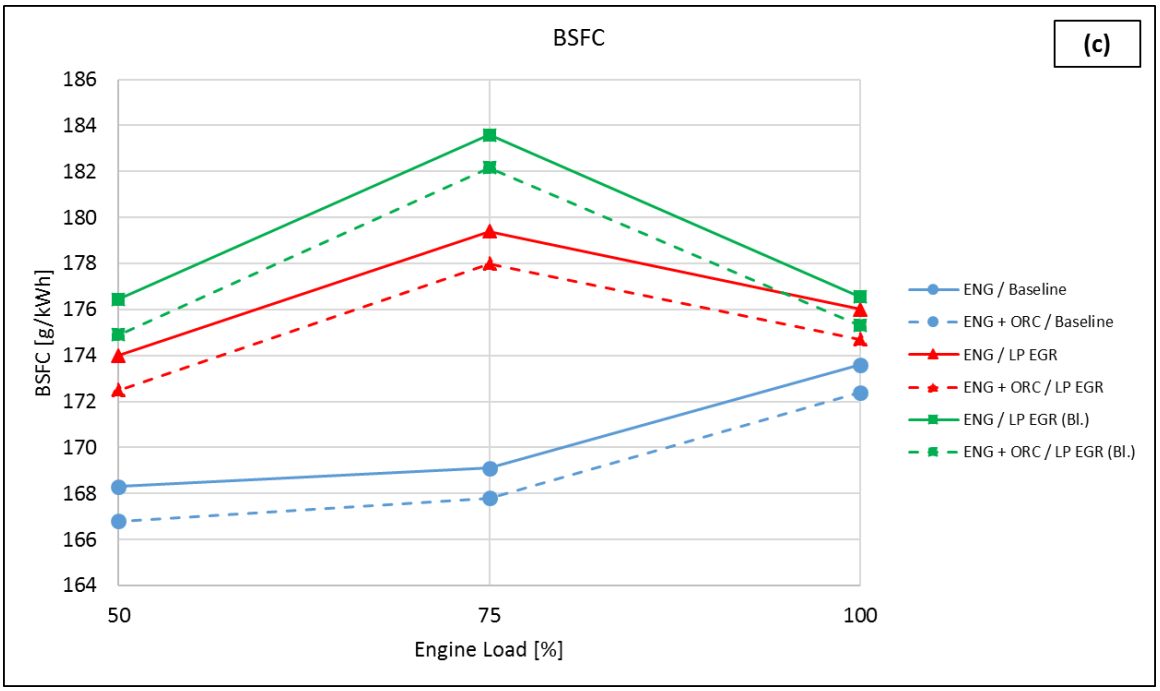

Fig. 96. Concept (3): ORC net power output (a), Engine + ORC total power output (b) and BSFC (c) – (case study 3)

ΔBSFC (%)			
	Engine Load		
Configuration	***100%***	***75%***	***50%***
ENG + ORC / Baseline (Tier II)	- 0.7	- 0.8	- 0.9
ENG + ORC / LP EGR (Tier III)	- 0.7	- 0.8	- 0.9

Tab. 51. Concept (3): BSFC improvement potential when fitting the ORC in Tier II and Tier III modes (case study 3)

Between the considered concepts, concept (3) is probably the simplest one, in terms of system complexity, easy installation and safety in operations. For example, no direct heat exchange between the working fluid and hot exhaust gas is needed, thus avoiding leakage and flammability problems.

However, this concept is also the one with lowest ORC net power production, due to the very low temperature levels expected at the engine HT jacket cooling water circuit outlet (between 80 and 88°C as estimated from the performed calculations), even if with high expected cooling water mass flow.
No real benefits are expected for the LP EGR cases, compared to the baseline, since no high variations for the heat transfer to the coolant have been observed and estimated during the engine 1-D simulation campaign.
A possible BSFC improvement in the range between 0.7 and 0.9% is expected for all cases with the proposed architecture, which leads to the consideration that a system as the one proposed should be used in synergy with another system recovering other heat sources in order to improve the achievable power output.

Concept (4): HT Jacket Cooling Water + SAC

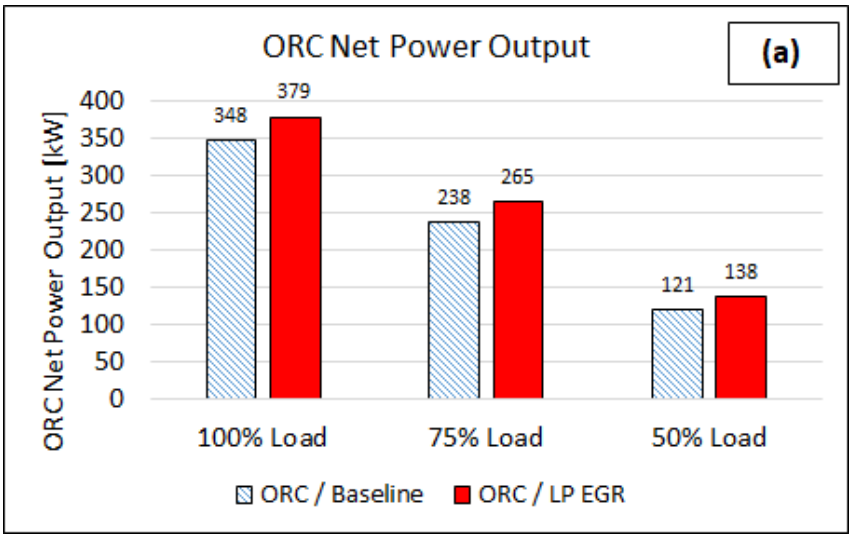

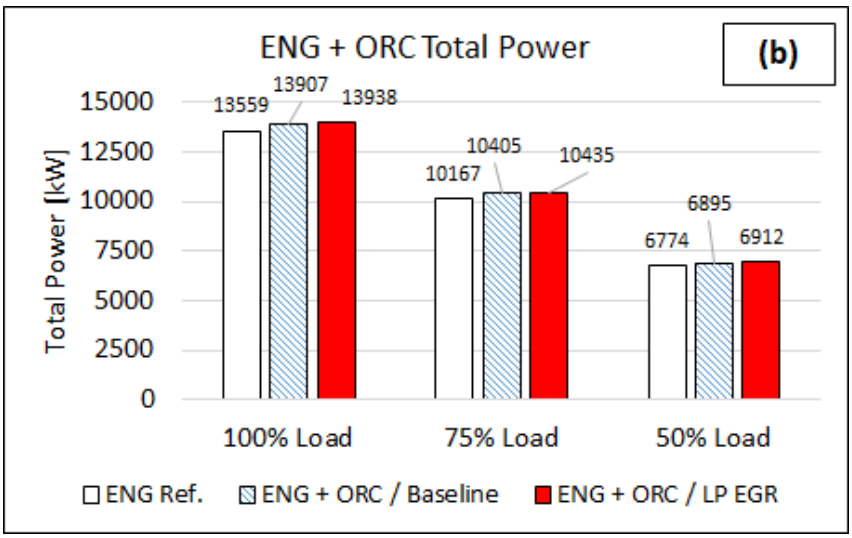

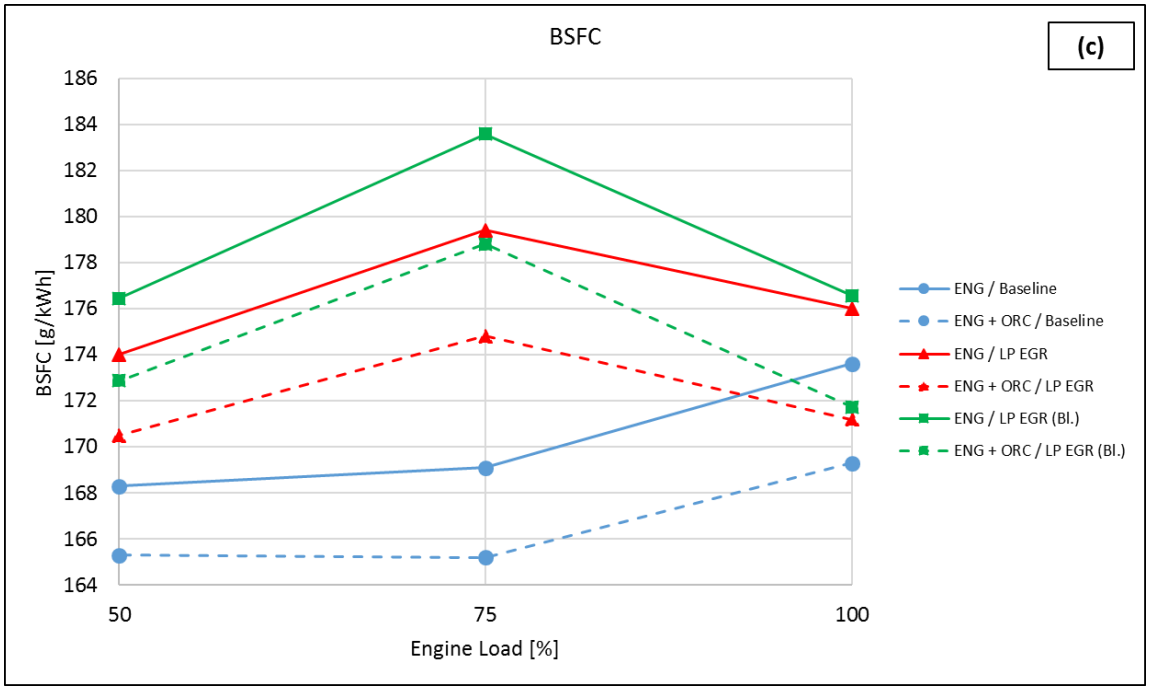

Fig. 97. Concept (4): ORC net power output (a), Engine + ORC total power output (b) and BSFC (c) – (case study 3)

ΔBSFC (%)			
	Engine Load		
Configuration	***100%***	***75%***	***50%***
ENG + ORC / Baseline (Tier II)	- 2.5	- 2.3	- 1.8
ENG + ORC / LP EGR (Tier III)	- 2.7	- 2.5	- 2.0

Tab. 52. Concept (4): BSFC improvement potential when fitting the ORC in Tier II and Tier III modes (case study 3)

The concept (4) is basically an evolution of concept (3), in which the temperature of the HT cooling water at the engine jacket outlet is increased due to the recovery of the heat from the 1st stage SAC (the SAC gas is cooled down to around 80-90°C to always ensure a ΔT of 10°C with the cooling water side). This is done to increase the thermal power available to be recovered from the coolant.
Increasing the coolant temperature allows also to increase the evaporation pressure of the ORC cycle and the pressure ratio over the expansion machine, thus improving the net generated power from the ORC system.
In this case, the operations with LP EGR allow also to even increase the ORC performance due to the higher expected temperatures of the SAC gas, which lead to increase heat rejection available to be recovered by the HT jacket cooling water.
At 100% load an increase in power output almost up to 3.5-4 times compared to the concept (3) is expected. Up to around 3.5 times for the 75% load case and 2 times for 50% load, due to the lower temperatures expected at these operating points.
Concept (4) seems to be very attractive considering both the thermodynamic performance point of view and the relative low complexity of installation, as well as safety and reliability in operations.
A combined utilization of a typical exhaust gas powered Rankine cycle can lead also to improved combined performance, as demonstrated further in the case study.
Generally, the concept (4) can be considered as a good compromise between low system complexity and achievable BSFC improvement.

Tier II vs. Tier III Operations. ORC Net Power Output

Generally, an increased power output is expected during Tier III operations due to the overall increase in temperature levels and heat rejection, especially for what concerns SAC and exhaust gas heat sources.
For the 75% load case, and during Tier II operations, the concept (4), with the considered boundary conditions is more effective compared to the typical tailpipe Rankine concept (1). Concept (2), as already stated, is slightly more effective than concept (1) at 100% and 75% load, but more complex and definitely not worth to be installed when considering 50% load operations, unless the SAC circuit can be switched off during these lower loads operations.
The concept (3) shows basically no improvements in Tier III operations compared to Tier II, due the similar HT jacket cooling water heat rejection, and a rather low power achieved compared to the other architectures considered.
In Fig. 98, the numbers refer to the various ORC concepts (1 to 4) as proposed in the case study.

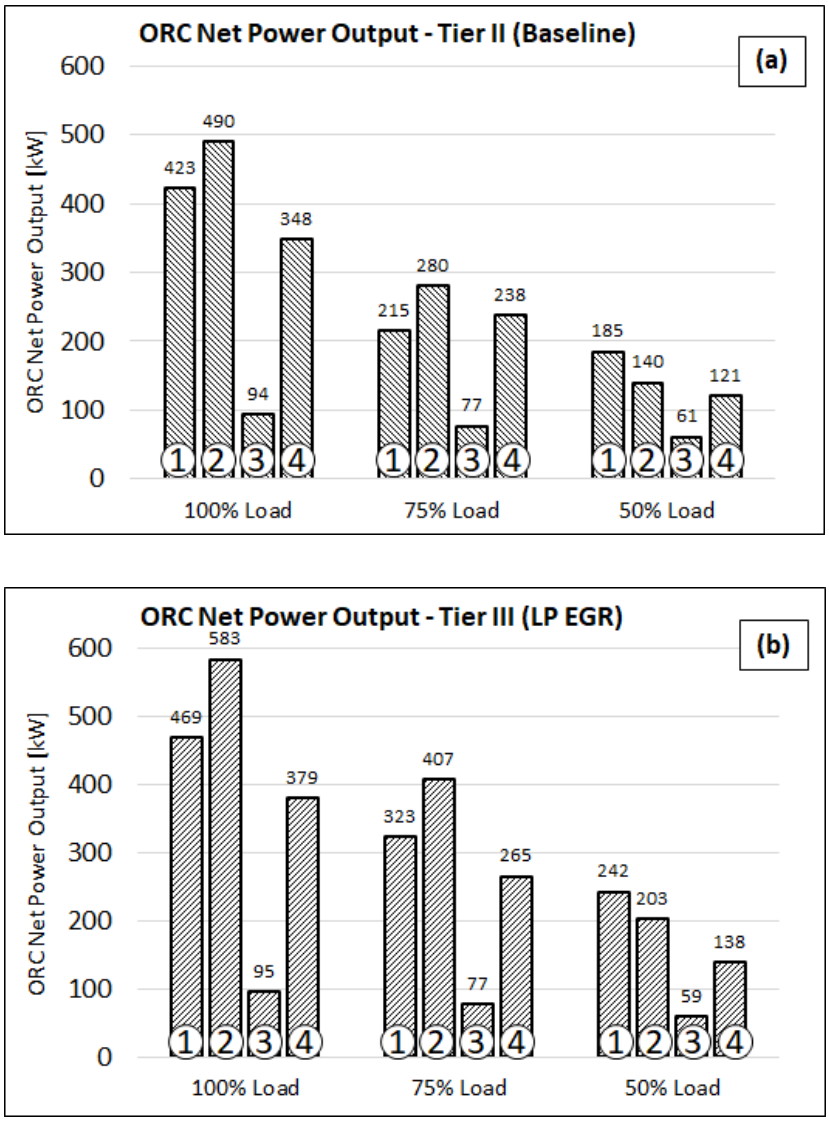

Fig. 98. ORC concepts (1 to 4) net power output: Tier II (baseline, a) and Tier III (LP EGR, b) – (case study 3)

Combined Concepts Scenarios

The various concepts have been combined in order to try to obtain the maximum benefit regarding BSFC improvement, allowing the full recovery of all heat sources. The two scenarios are:

1) *concept 1* + *concept 4:* exhaust gas (economizer) + HT jacket cooling water / SAC heat recovery;
2) *concept 2* + *concept 3:* exhaust gas (economizer) / SAC + HT jacket cooling water;

The results have been reported again for the total ORC net power output and for the BSFC improvement potential, in the same format of the single concepts for consistency reasons.

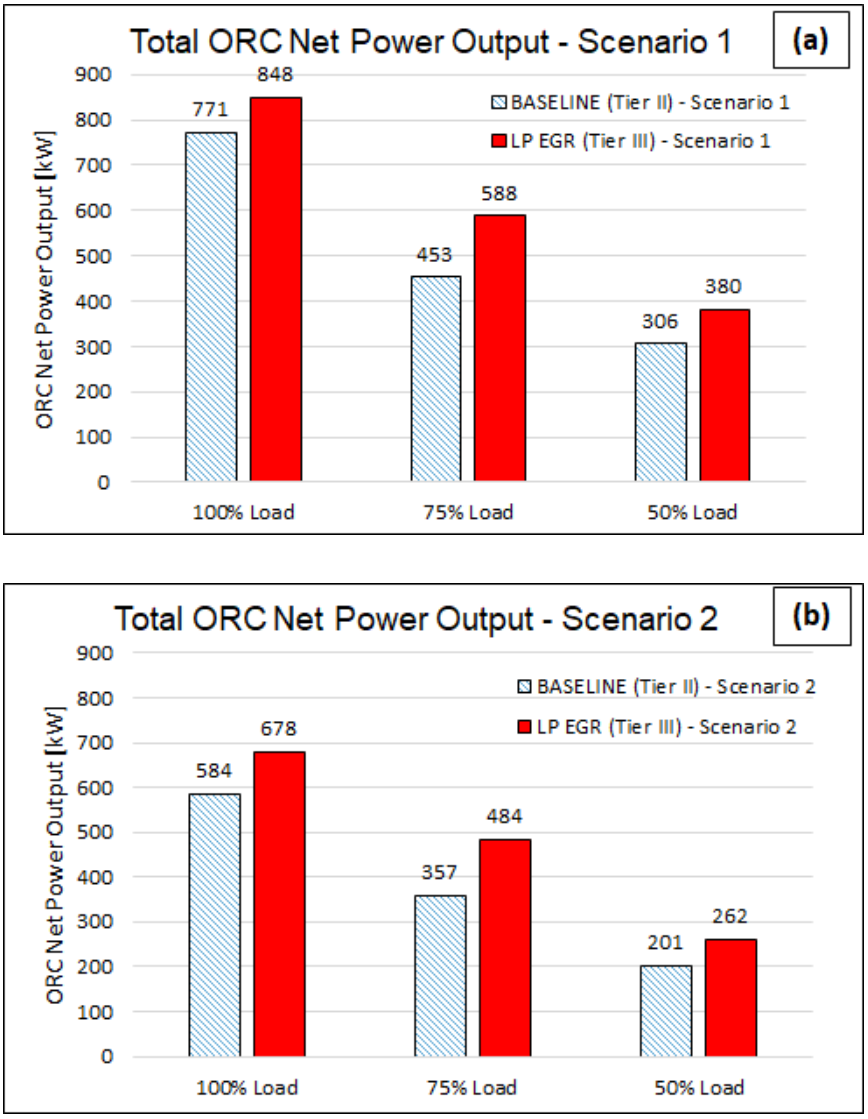

Fig. 99. Total ORC net power output in the two evaluated scenarios: 1 (a) and 2 (b) – (case study 3)

The results for the total ORC net power output have been reported in Fig. 99, for the two different scenarios and the Tier II and Tier III operations. Generally, scenario 1 allows a higher ORC net power output recovered, thus improving the BSFC of the combined engine-ORC system in a more marked way compared to scenario 2, at all three operating points evaluated.

The BSFC improvement graphs have been reported in Fig. 100.

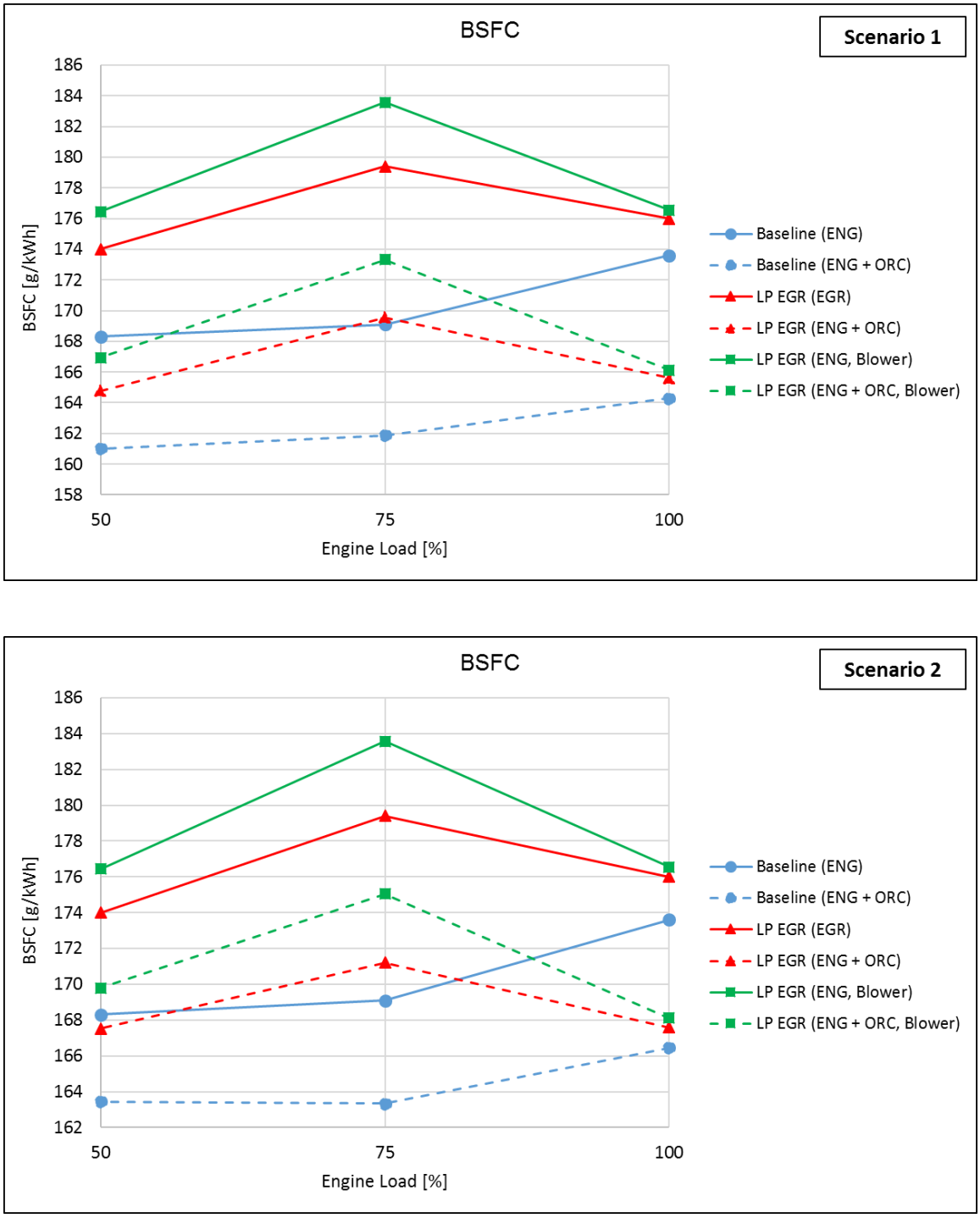

Fig. 100. BSFC for different operating points and Tier II / Tier III operations, with and without ORC. Scenarios 1 and 2 (case study 3)

The BSFC improvement potential when using the ORC systems for scenario (1) has been reported in Tab. 53, while for scenario (2) in Tab. 54. The second columns report the BSFC increase due to the LP EGR operations calculated from the 1-D engine simulations, for comparison reasons.

ΔBSFC (%)			
Engine Load	***Baseline*** vs ***LP EGR****	***Baseline*** vs ***Baseline + ORC***	***LP EGR*** vs ***LP EGR + ORC***
100%	+ 1.3	- 5.4	- 5.9
75%	+ 6.1	- 4.3	- 5.5
50%	+ 3.4	- 4.3	- 5.3

Tab. 53. BSFC improvement comparison when using the ORC systems in Tier II and Tier III operations. Scenario 1 (case study 3)

ΔBSFC (%)			
Engine Load	***Baseline*** vs ***LP EGR****	***Baseline*** vs ***Baseline + ORC***	***LP EGR*** vs ***LP EGR + ORC***
100%	+ 1.3	- 4.1	- 4.8
75%	+ 6.1	- 3.4	- 4.6
50%	+ 3.4	- 2.9	- 3.7

Tab. 54. BSFC improvement comparison when using the ORC systems in Tier II and Tier III operations. Scenario 2 (case study 3)

**Calculated from Ricardo WAVE 1-D simulations*

Scenario (1) allows a generally higher BSFC saving, up to 5.9% when comparing, for example, the LP EGR case, with and without heat recovery system installed.
Concerning the BSFC graph for scenario (1) in Fig. 100, it is possible to observe how, in absolute values, the use of waste heat recovery systems, with the layouts proposed, tends to almost completely mitigate the BSFC increase effect introduced with the use of LP EGR for Tier III operations (second columns in Tab. 53 and Tab. 54). In particular, for the load points 100% and 50%, the operation with LP EGR and ORC is even lower in terms of estimated BSFC compared to the normal Tier II operations (without ORC, comparison between the continuous blue line and the segmented red line), while for load point 75%, in which the proposed engine tuning leads to a more marked increase in BSFC with LP EGR, the use of ORC allows to reduce the BSFC to a level comparable to Tier II operations without EGR.
The same trends are visible in case of scenario (2), with the difference that the BSFC benefit introduced with the ORC is slightly lower compared to scenario (1) and, particularly for 75% load, the ORC systems are not able to completely withstand the increase of BSFC due to EGR operations.
When comparing only the Tier II operations, the use of ORCs allows to improve the overall BSFC in a quite marked way compared to the case without heat recovery system.
The green continuous and segmented lines refer to the cases in which the EGR blower power consumption has also been considered in the overall power balance, still showing the benefits of the ORC use, in particular for 100% and 50% load cases, but also for the 75% case, allowing consistent fuel savings.
Finally, it is possible to state how the scenario (1), with tailpipe exhaust ORC and HT jacket-SAC ORC, seems to be the most interesting in terms of overall performance. This scenario has been evaluated in a preliminary economic analysis reported in the next section.

6.3.5.4 Preliminary Economic Analysis – Scenario 1

A preliminary estimation of the economic benefit of using the ORC systems, as reported in Scenario (1), has been carried out in order to evaluate the fuel operational costs savings.
The estimation has been carried out on two simplified operating profiles: one representing typical full steaming operations [86], the other representing typical slow steaming operations [87], already reported in section 4.1.4.2.
Since just three operating points (100%, 75% and 50% loads) have been considered in the overall performed analysis, the operating profiles used have been reduced and simplified to be assessed based only on the available calculated data. This will introduce an error, since the BSFC will be different at the other operating points which have not been considered, but, at the same time, from the operating profiles analysis, it is possible, to observe how ships are sailing most of the time in the ranges of loads considered in the proposed study. A more detailed study would be required when considering all operating points, but at this stage of the analysis, and for the purpose of this estimation, the error can be considered as adequate.
The decreased BSFC due to the ORC installation has been considered as an input for the estimation, while the same brake power of the baseline cases, for every load, has been kept fixed for the sake of the analysis, in order to assess the possible reduced fuel mass flow consumed. This means that the additional ORC net produced power, re-introduced in the propeller line, is not considered, but just the estimated fuel savings derived from the use of the waste heat recovery systems are evaluated, even though the real effect would be the increase in power output, for the same engine injected fuel. This could basically lead to the choice of reducing the engine load slightly in order to save some fuel, however, changing the boundary conditions of the engine simulations.
In case of using the additional energy, produced from the ORC, to generate electricity, this could be more easily correlated to the savings in terms of fuel costs of on-board electric energy production through the main engine or auxiliary generators.
Since this is a preliminary estimation, the accuracy at this step of the analysis has been considered enough in order to demonstrate the possible economic benefits and the approach. Possible future studies should consider the economic side more in the details, with an overall ship energy management overview.
A vessel shipping time of 8144 hr/year (almost 340 days) has been assumed in the analysis as case study (from Burel *et al.* [57]), typical for a chemical tanker sailing 8 times/year from Dubai to Hamburg.
Cases with 100% time spent outside ECAs (Tier II operations), 100% time inside ECAs (Tier III operations) and for a typical ship ECAs percent resident time have been considered. The ECA residence time data has been obtained again from Burel *et al.* [57], and comes from a study carried out during a previous collaboration between University of Trieste, University of Udine, Cenergy, Wärtsilä, Navalprogetti, Rina Services, Area Science Park and Energy Automation, about the possibility of using LNG as a fuel for ship propulsion.
The fuel prices for Marine Diesel Oil (MDO) and Heavy Fuel Oil (HFO, IFO 380) have been assumed respectively to be 543 $/mt [373] and 339 $/mt [374].
The operating profiles assumed in the study have been reported in Fig. 101 [86,87], together with the simplified ones, obtained dividing the engine load steps in bigger intervals and summing up the contributions.
The percentage of time spent in ECAs for different types of ships has been reported in Fig. 102 [57]. The data have been elaborated, from the original source, in order to extract only the information for the types of ships which are generally powered by large low speed two-stroke Diesel propulsion units. In the analysis proposed, a Handysize tanker type has been chosen as a trade-off, showing an estimated 12.5% sailing time spent in ECAs, thus probably requiring the use of NO_x emission reduction technologies, such the LP EGR architecture investigated in this work.

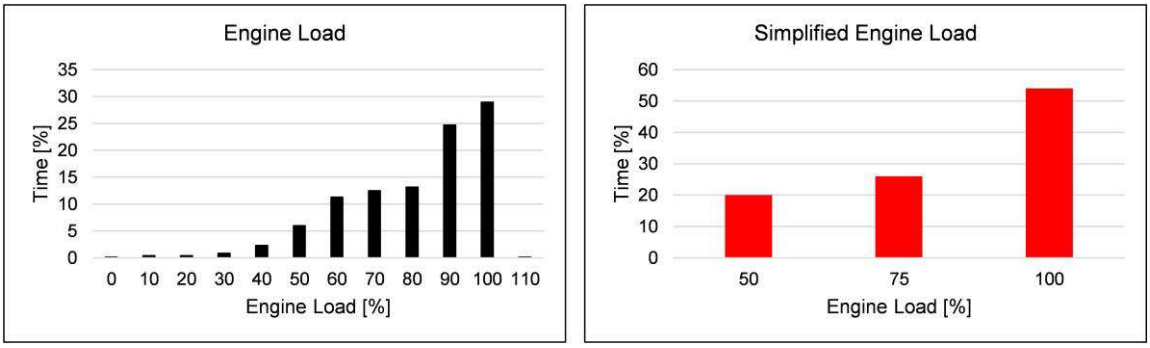

(a)

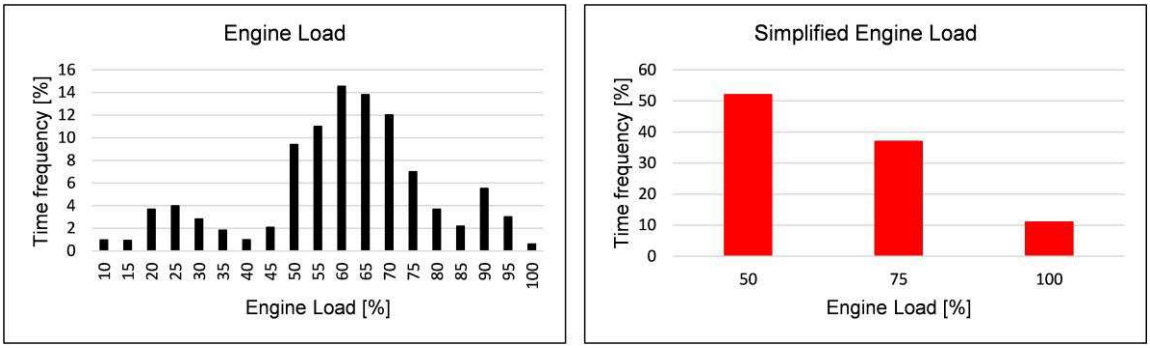

(b)

Fig. 101. (a) Full steaming and (b) slow steaming load operating profiles (case study 3)

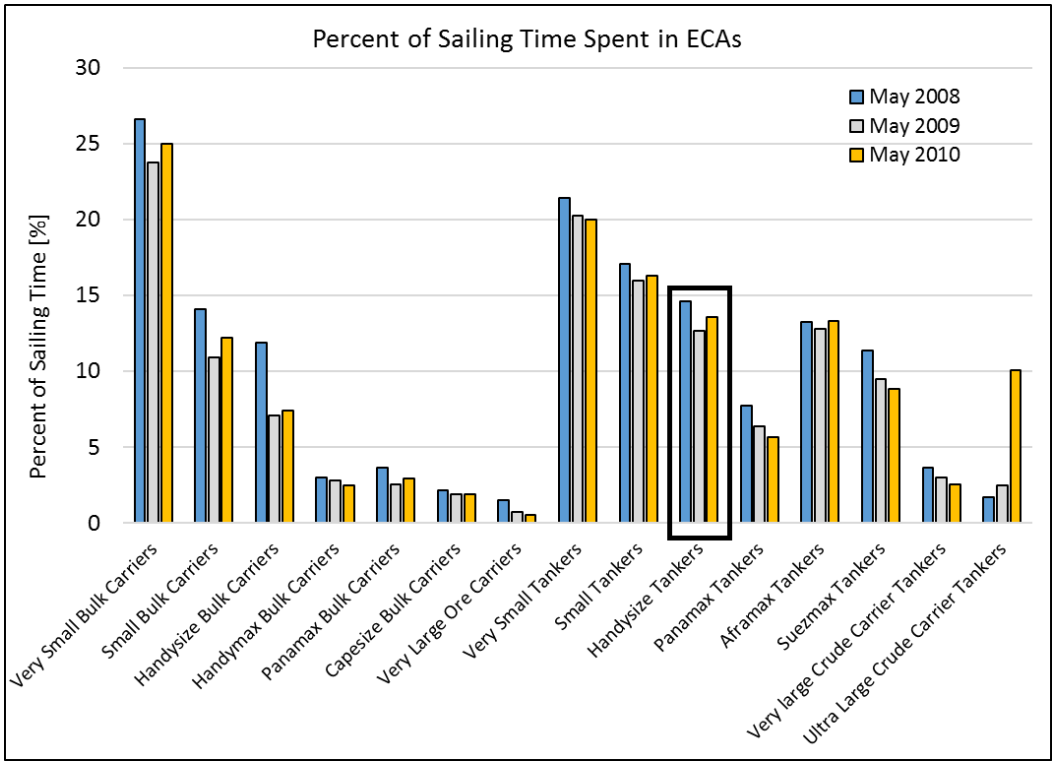

Fig. 102. Percent of time spent in ECAs for different types of ships generally powered by low speed two-stroke engines (case study 3)

From the fuel costs assumed, the BSFC savings estimated and the simplified operational profiles, it has been possible to estimate the annual operational fuel costs savings, which have been reported below for full steaming (Fig. 103) and slow steaming operations (Fig. 104), both considering only Tier II and Tier III single operations (completely outside or inside ECAs, a) or for an estimated 12.5% sailing time spent in ECAs (b). Data have been reported both for MDO and HFO, with and without using the ORC systems.

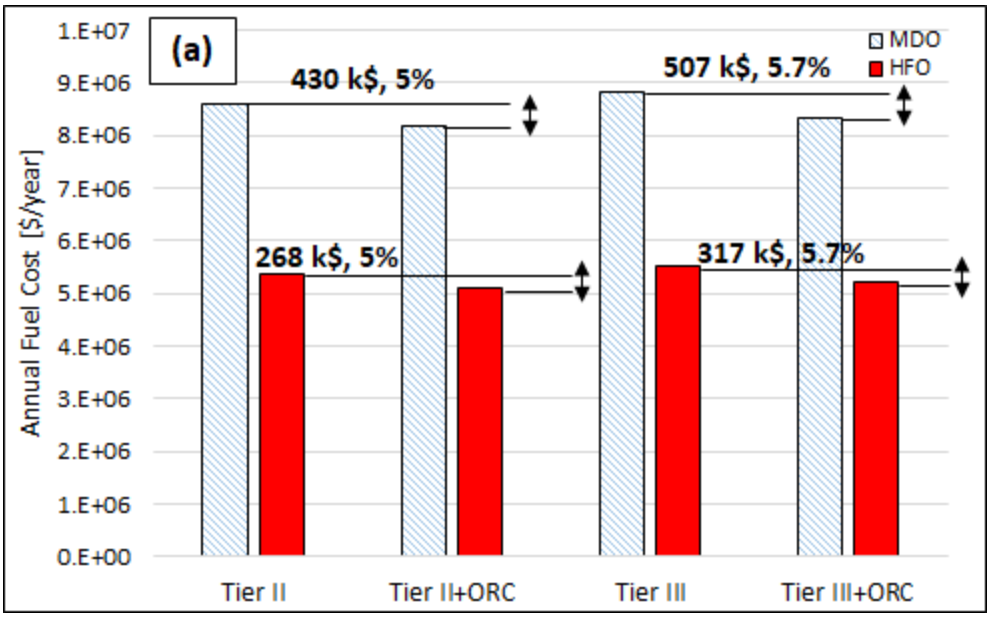

(a)

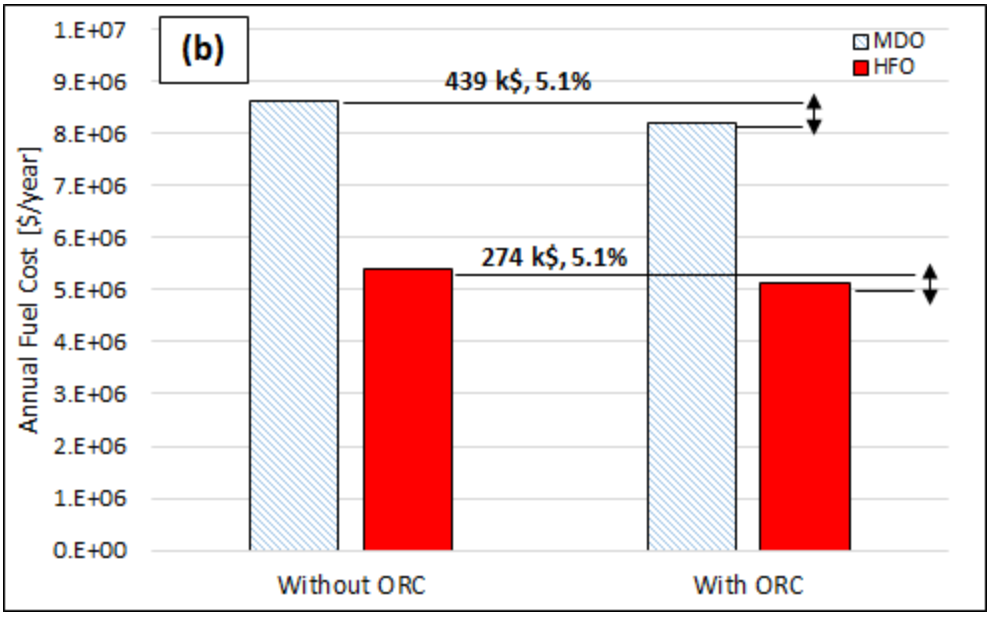

(b)

Fig. 103. Annual fuel costs savings for full steaming operations. (a) Tier II and Tier III operations, (b) 12.5% sailing time spent in ECAs (case study 3)

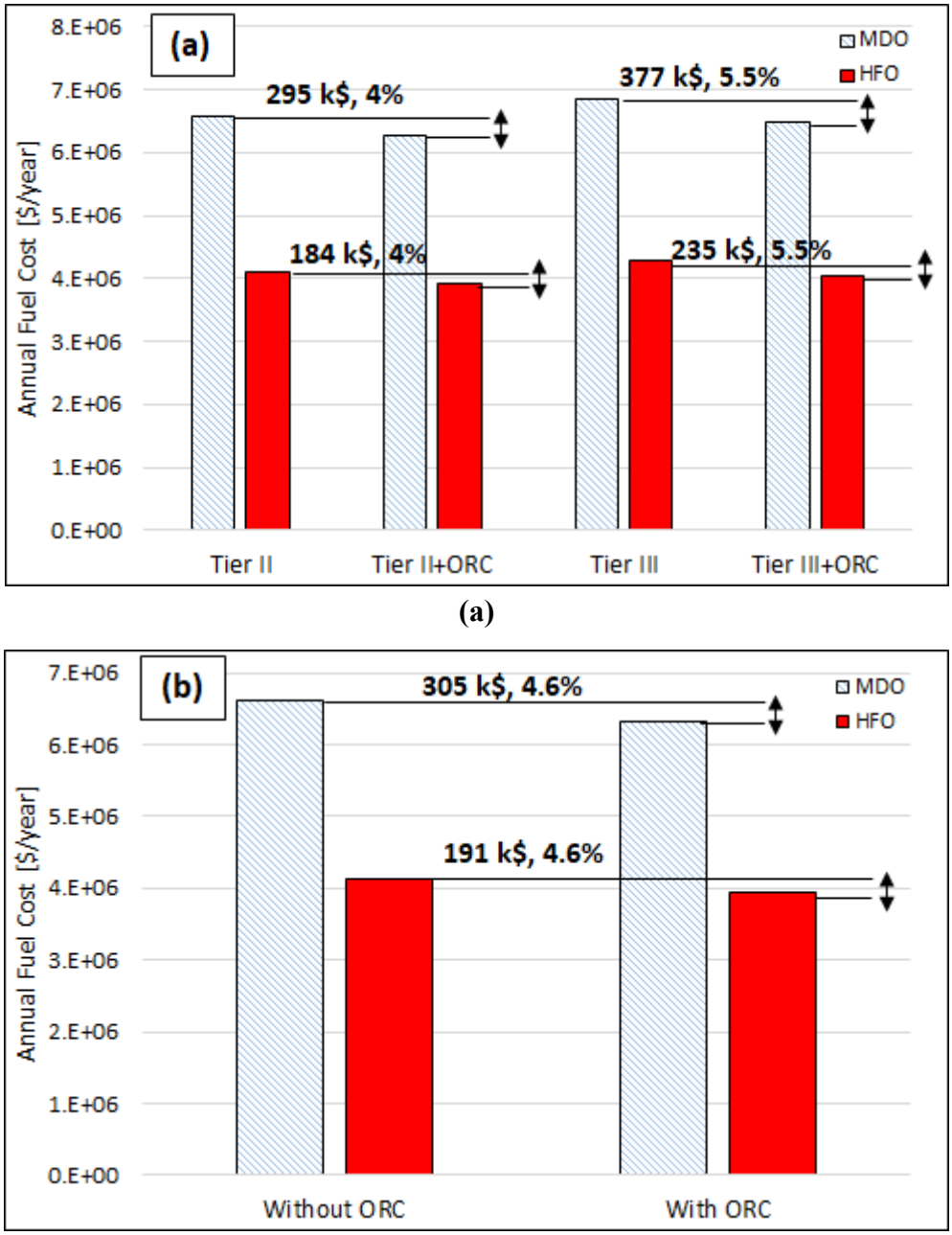

Fig. 104. Annual fuel costs savings for slow steaming operations. (a) Tier II and Tier III operations, (b) 12.5% sailing time spent in ECAs (case study 3)

From the reported charts, it is immediate to observe the difference in annual fuel costs between the use of MDO and HFO (MDO is a more refined fuel, thus more expensive), and between full steaming and slow steaming operations. This is anyway not very interesting because of the lower price of MDO compared to HFO, and the purpose of slow steaming, which is basically saving fuel, and thus costs.
What it is interesting to observe is the estimated reduction in annual fuel costs which can be obtained between operations with and without ORC waste heat recovery systems. In particular, higher savings (up to 5.7%) can be expected under full steaming conditions, while up to 5.5% under slow steaming conditions. Slightly higher benefits can be observed when operating in ECAs (Tier III), due to the better performance achievable for the ORCs, which are able to recover the increased heat rejection due to LP EGR operations. However, still between 4 and 5% annual fuel costs savings can be expected, in

slow and full steaming conditions, also when operating in Tier II mode, which is the most common operational mode, based on the data reported in the previous figures. Of course, the 12.5% ECAs sailing time shows a tendency to costs savings values more similar to Tier II operations.
The present preliminary economic analysis shows the potential for annual operational fuel costs savings due to the installation of ORC systems to recover heat from a typical two-stroke low speed ship propulsion unit. In a possible future study, however, more complete engine operational profiles should be considered, together with the estimation of the cost of development, installation and maintenance of the ORC system itself, which are going to affect the final choice of the fleet owners and manufactures. The right choice for the usage of the on-board ship produced additional energy must also be considered in a more detailed way when performing a more accurate study about the return of investment.

6.3.6 Conclusions

In the proposed case study, a complete 6 cylinders inline, 13.6 MW brake power, crosshead, two-stroke Diesel engine for main ship propulsion has been simulated using Ricardo WAVE.
The present model has been validated based on the data obtained from the project partner WinGD, showing a good agreement with the supplied performance results.
Once the baseline engine model has been validated for 100%, 75% and 50% load operating points, a LP EGR circuit concept architecture has been added in order to simulate possible IMO Tier III compatible operations. NO_x emissions have not been estimated, because real emissions data were not available to calibrate the model in WAVE, but, rather, EGR recirculation rates (based on CO_2 volumetric fractions) have been considered and realistic assumptions have been used regarding the LP EGR circuit implementation, based on the experience of WinGD.
The first objective of the work has been the assessment of the engine performance under LP EGR operations, and in particular, assessing the fuel consumption increase, which has been estimated, after adequate engine model tuning, to be in the range between 1.3 and 6.1% at the different considered operating points.
The second objective of the work has been assessing the heat rejection of the baseline and new LP EGR engine models, in order to extract the boundary conditions for the analysis of possible bottoming waste heat recovery architectures, using ORC systems, in order to improve the overall system fuel efficiency. An overall increase in heat rejection, due to LP EGR operations, can be observed from 1-D simulations, especially for the economizer and the SAC, thus leading to a higher potential for the waste heat recovery systems.
The mass flow and temperature data for the possible ORC suitable engine heat rejection sources (exhaust gas, SAC and HT jacket cooling water) have been used as inputs for the waste heat recovery study based on developed thermodynamic process simulation models.
Concerning the ORC systems, four different architectures have been assessed, with the goal of maximizing the net additional power output achievable, through the use of an optimization procedure, and based on the engine and environmental assumed boundary conditions.
Water-steam and R1233zd(E) have been considered as working fluids for the waste heat recovery systems. In the cases with lower temperature heat sources, and in particular recovering HT jacket cooling water, R245fa and R123 have also been assessed, but showing comparable thermodynamic performance to R1233zd(E) which, however, has lower environmental impact and is safer in operations. For these reasons, R1233zd(E) has been assumed the best choice for this application, together with common water-steam for higher temperature heat sources.
Single ORC architectures lead to fuel economy benefits in the range between 0.7% and 3.5%, depending on the heat sources recovered and the cycle layouts, in case of Tier II operations (outside

ECAs). While, in case of Tier III operations (inside ECAs), a fuel economy improvement in the range between 0.7% and 4.1% has been estimated but having in mind the increased engine fuel consumption due to EGR operations.
When combining the different ORC architectures, in order to try to fully exploit the engine waste heat available, a combined system (scenario 1) with a water-steam Rankine cycle on the exhaust gas side and an ORC recovering HT jacket cooling water and SAC heat, in an innovative two-stage SAC configuration, has been estimated to bring 5.4% fuel economy benefit in Tier II operation, and 5.9% in Tier III (at full load), while at the same time, keeping system complexity at a reasonable level. The results achieved show the possibility of mitigating the increase in fuel consumption effect of EGR operations through the use of waste heat recovery systems.
A preliminary economic feasibility analysis shows how, both under a full steaming or a slow steaming operating profile, and for a possible characteristic yearly shipping time, fuel cost savings in the order of 4% to 5.7% can be expected in Tier II, Tier III or in a combined Tier II – Tier III operations, when considering the use of waste heat recovery systems such as those evaluated in this study.
The proposed feasibility study shows how the combined use of emissions reduction technologies and strategies, such as in this case LP EGR, with waste heat recovery systems as ORCs, can help to achieve less polluting, but at the same time, still efficient ship propulsion engines.
Indeed, even though the LP EGR leads to an increase in fuel consumption, the waste heat recovery system can mitigate this drawback, allowing to recover engine waste heat which otherwise would be a loss for the system.
In the case of Tier II operations, which are the most common for the considered type of engines and ships, the waste heat recovery systems allow even a higher improvement in fuel economy, thus also in operational costs savings.
However, at the time in which this work has been carried out, the rather low cost of marine fuels tends to discourage the use of heat recovery systems, due to the additional costs of installation and maintenance, and the increased overall system complexity. If in the future, the cost of fuel is expected to increase again, waste heat recovery systems, as ORCs, could become very interesting in terms of return of investment and compromise between environmental pollution and economic benefits.
In particular, the use of Organic Rankine Cycles seems to be a feasible way, also for large two-stroke ship propulsion engines, to recover low-medium temperature waste heat and, in combination with traditional steam Rankine cycles, to increase overall system efficiency.
The approach proposed in this case study could be used to study possible other architectures combining the use of emission reduction strategies and waste heat recovery systems. An example is the study of a High Pressure (HP) EGR architecture, which could be a promising concept due to the medium-high temperature heat available from the EGR cooler, which could increase the power output achievable from the bottoming waste heat recovery system. In this case the trade-off with engine tuning should be assessed, and in particular the impact on the turbocharger operations.
Improved ORC layouts, for example considering dual loop and two-stage pressurization architectures, could be evaluated in order to recover heat sources, characterized by different temperature levels, in a combined more compact and efficient system.
A more detailed analysis about the overall system performance and economic benefits over a detailed ship operating profile should also be assessed.
Finally, during the collaboration with NTUA, in the frame of the ECCO-MATE project, the cylinders' boundary conditions, for the engine simulated with LP EGR configuration, have been supplied to the project partner, for further in-cyinder 3D-CFD emissions analysis and optimisation. A common publication is expected as output of the collaboration.

6.4 Case Study 4: Medium Duty Truck (Techno and Thermo-economic Approach)

The third proposed case study demonstrates the importance of introducing an economic analysis layer in the overall simulation process, in order to estimate the potential of the considered ORC technology to save operational costs. However, it is also very important to consider the investment costs and the overall cost formation process when developing a combined engine-waste heat recovery system. For this purpose, a techno and thermo-economic analysis, as already introduced in section 5.3, can help understanding which is the best trade-off between the benefit in terms of achievable power output, or fuel savings, and the possible cost impact of the system itself, which is a very important output of the developers' analysis when assessing the possible technology market penetration potential.
The purpose of what reported in this last case study is not to find the most efficient combined engine-ORC configuration, but rather to show the amount of information which can be extracted from a complete analysis approach, considering both energy, exergy and economic considerations. The methodology, if further developed in the direction of a user-friendly and powerful integrated co-simulation tool, could help the developers to go beyond the traditional engine and waste heat recovery systems' design approach, providing more complete insights about the behaviour of the overall system, the performance achievable and the costs expected to introduce the technology into the market.
Most of the theoretical background applied in this last case study has been already introduced in sections 5, considering engine, ORC, energy, exergy and economic analysis approaches. While for the previously reported case studies just some of the proposed analysis approaches have been used and implemented, in this last case study, developed as last in terms of chronological order, a full combined methodology has been applied, showing the potential of a synergic use of CAE industry-standard tools and process simulation techniques.
To the author's knowledge, no commercial software is able to provide the same simulation capabilities of what reported in this case study, and the proposed approach could be embedded in industry-standard powertrain simulation tools, in order to improve co-simulation capabilities, in the direction of an overall powertrain optimization approach, which seems to be one of the most important development trends in the marine and automotive industry.
The methodology has been applied to the case of a medium-duty Diesel engine for truck applications (below 10 tonnes). The engine has been simulated over a map of engine load and speed points typical of on-highway truck operations, considering in particular two main operating points: C100 (high load – high speed) and B50 (medium load – medium speed). The first point is representative of maximum heat rejection conditions expected during accelerations periods, while the second is more representative of a highway cruise condition.
The various ORC system concepts, both in terms of different working fluids and architectures, have been simulated and optimized at both operating points in order to show the differences in terms of performance and costs expected, when choosing different design points.
After an evaluation of the combined performance of the engine-ORC system when considering only the baseline engine, a strategy with insulation of the engine exhaust manifolds has been proposed, in order to show an example of combined synergic co-simulation approach. This scenario has been proposed also by Edwards *et al.* [292], but considering only the engine side and not the potential benefits for a combined engine-waste heat recovery system architecture and not even an economic analysis.
As a last step, just for one of the combined engine-ORC system configurations, a complete energy, exergy, techno and thermo-economic analysis has been reported, with the aim of showing the quantity and quality of information that can be extracted from a methodology as the one developed in this work. Some considerations and thoughts from the author's side have then been reported in order to show in for which purposes the methodology could be further developed.
The work reported in this case study has been introduced by the author in [375–377].

6.4.1 Reference Engine and Design Points

The reference engine model used for the fourth case study is the same reported in section 5.1.2 and section 5.1.3, and is typical of a EURO III medium-duty, direct injection Diesel engine suitable for small trucks applications. The WAVE model has been again reported in Fig. 105, and has a controller implemented in order to regulate the boost pressure of the compressor acting on the Waste-Gate (WG) rack of the turbine in order to ensure an adequate boost level for engine operations. The main engine data have been also reported in Tab. 55.

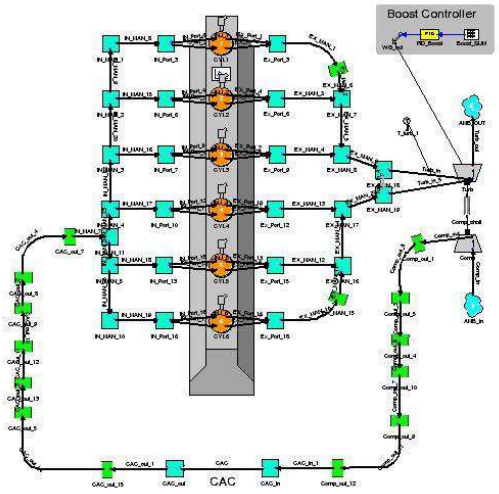

Fig. 105. WAVE engine model (case study 4)

Configuration	6 cylinders inline
Displacement [L]	5.9
Number of Valves / Cylinder	4
Turbocharging	1 Stage Turbocharger WG
Bore [mm]	102
Stroke [mm]	120
Clearance Height [mm]	0.7
Conrod Length [mm]	200
Geom. Compr. Ratio	17:1
Brake Power (full load) [kW]	200
Combustion Model	Multi Wiebe
Heat Transfer Model	Woschni

Tab. 55. Main engine model specifications (case study 4)

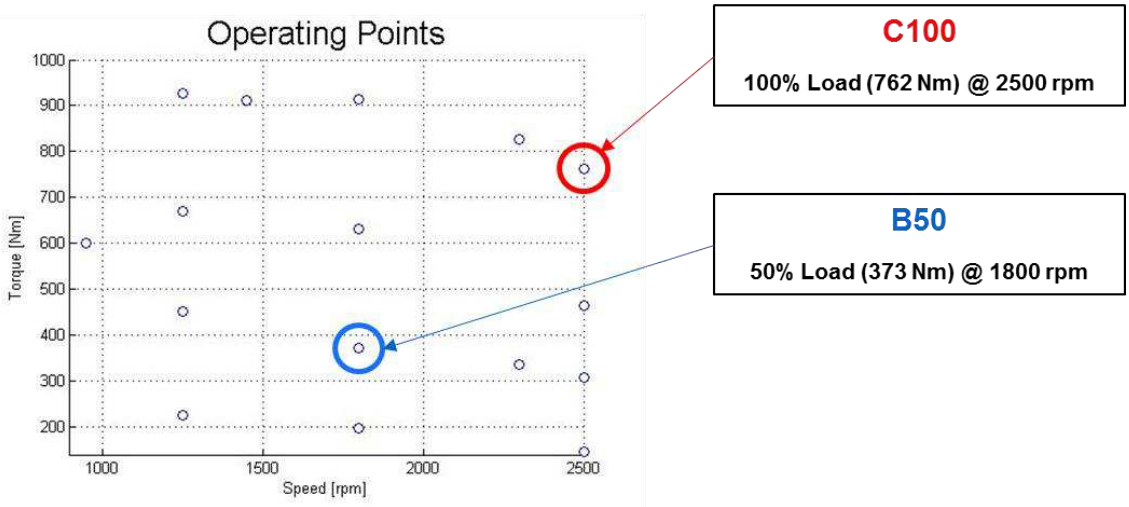

Fig. 106. Engine simulated and chosen design operating points (case study 4)

The engine has been simulated over an entire map of load and speed points (Fig. 106), in particular for 16 different operational conditions, both at full and part load conditions, with adequate validated settings concerning combustion, friction, heat transfer and all main engine operating parameters.

However, considering a possible truck highway-typical operational profile, as those reported in section 4.1.4.1, two main points have been mostly evaluated, focusing, as already introduced, on high-load / high-speed (C100) and medium-load / medium-speed operational ranges (B50):

- *C100*: representative of the engine main heat rejection conditions expected:
- *B50*: representative of the highway cruise conditions.

The nomenclature assumed refers to the ESC cycle reported in Fig. 10. The proposed operating points have been considered as design points for the ORC bottoming systems, representing the possible choices of designing the system at two different points depending on the developers' project constraints. The assumption is based on Ricardo's experience and internal discussions.

6.4.2 ORC Architectures and Working Fluids

For this case study, and in order to demonstrate the methodology, mainly three different simple ORC layouts have been proposed and simulated in MATLAB:

1) *Simple exhaust gas heat recovery (*Fig. 107 *a-b)*;
2) *Exhaust gas heat recovery with internal cycle recuperation (RECP,* Fig. 107 *c-d)*;
3) *Indirect Exhaust-to-Coolant heat recovery (*Fig. 107 *e)*;

The first two concepts have been simulated with two different heat sink configurations:

- *IC – Indirect Condensation*: the ORC working fluid is condensed using the high temperature engine coolant circuit (with a condenser inlet temperature of 95°C and a mass flow estimated from the engine heat rejection extracted from the WAVE simulations, assuming a $\Delta T = 95 - 85 = 10°C$ over the engine between inlet and outlet of the jacket). A similar configuration has been used in the case study 1, in section 6.1;
- *DC – Direct Condensation:* the ORC working fluids is condensed using directly the ambient air flowing into the vehicle cooling package. In this case, the cooling package performance has not been assessed, but rather an average inlet air temperature of 40°C and an average air mass flow of 8 kg/s have been imposed based on Ricardo experience and what reported by Panesar [306], just in order to show the approach;

The two heat sink configurations proposed are usually the two chosen by OEMs developing the systems for vehicles applications.
The third concept, recovering exhaust gas heat with a tailpipe heat exchanger transferring heat to the engine high temperature cooling circuit (without coolant phase change) in order to increase the coolant temperature, uses the DC heat sink configuration.
The indirect Exhaust-to-Coolant architecture is generally expected to be less efficient and performant compared to the cases with direct exhaust gas recovery due to the lower heat source temperature expected and the additional exhaust-coolant heat exchanger introducing high exergy losses. However, the interposed cooling circuit acts as a separation between the ORC working fluid and the exhaust gas, thus leading to safer operations (as often done with a thermal oil loop). The cooling circuit, however, acts also as a thermal buffer which dampens the exhaust gas temperature fluctuations, thus leading to, even if lower, a more constant expected ORC power output at different engine operating points, with decreased system controllability issues, compared to the more challenging direct exhaust-driven cycles.
Moreover, the proposed engine model has no Exhaust Gas Recirculation (EGR) circuit implemented. For this reason, a parallel architecture, with exhaust gas and EGR heat recovery, as the one proposed

in the case study 1 in section 6.1, cannot be used. The methodology, however, can be used to assess any kind of engine architecture that can be simulated in WAVE.
The combined engine-ORC concepts evaluated have been reported, in a schematic form, in the following figures, as done for the other case studies. A mechanical coupling between the ORC expander and the engine crankshaft, using a gearbox with fixed efficiency assumed (95%, [112]), has been proposed.

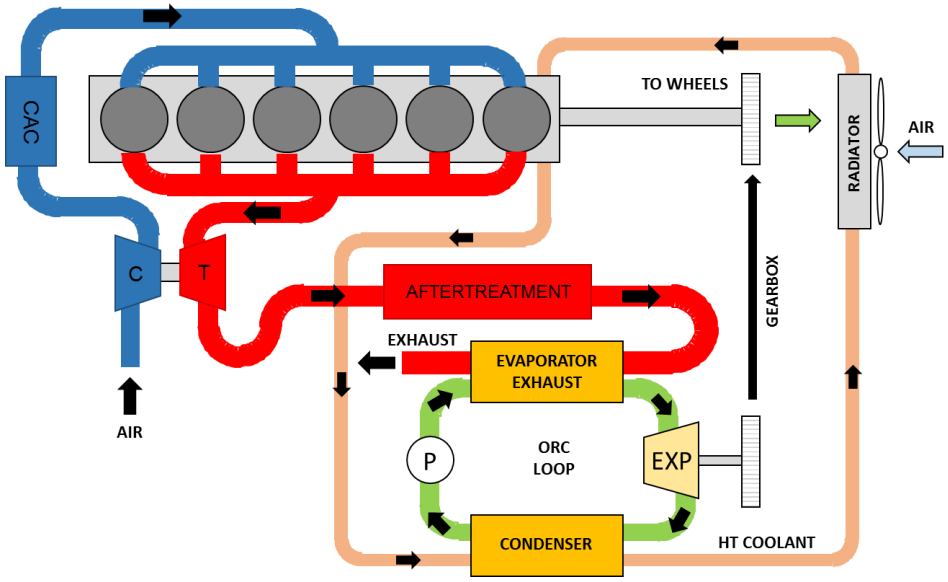

(a – Simple exhaust heat recovery with IC heat sink configuration)

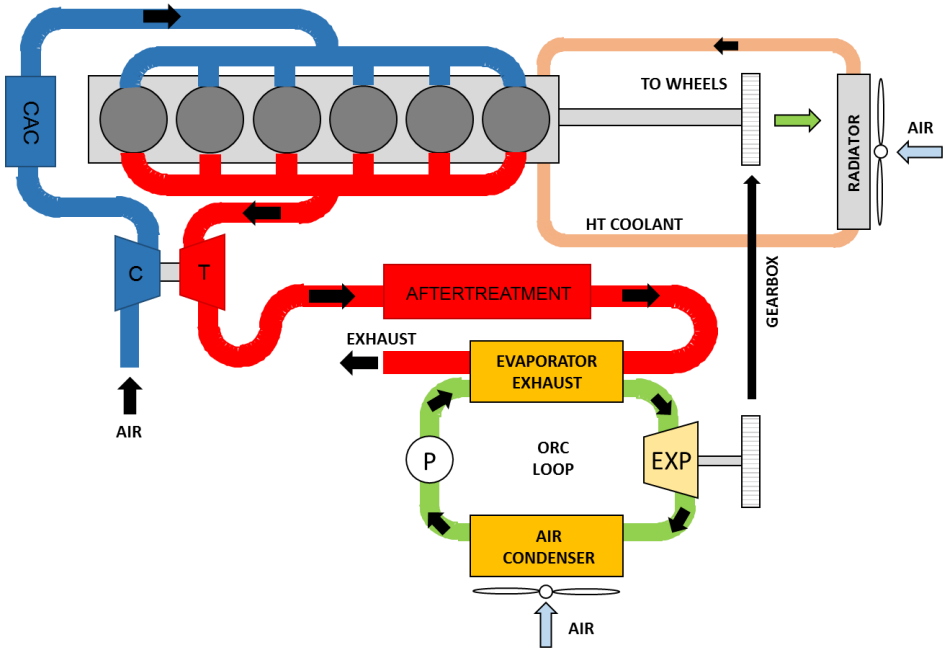

(b – Simple exhaust heat recovery with DC heat sink configuration)

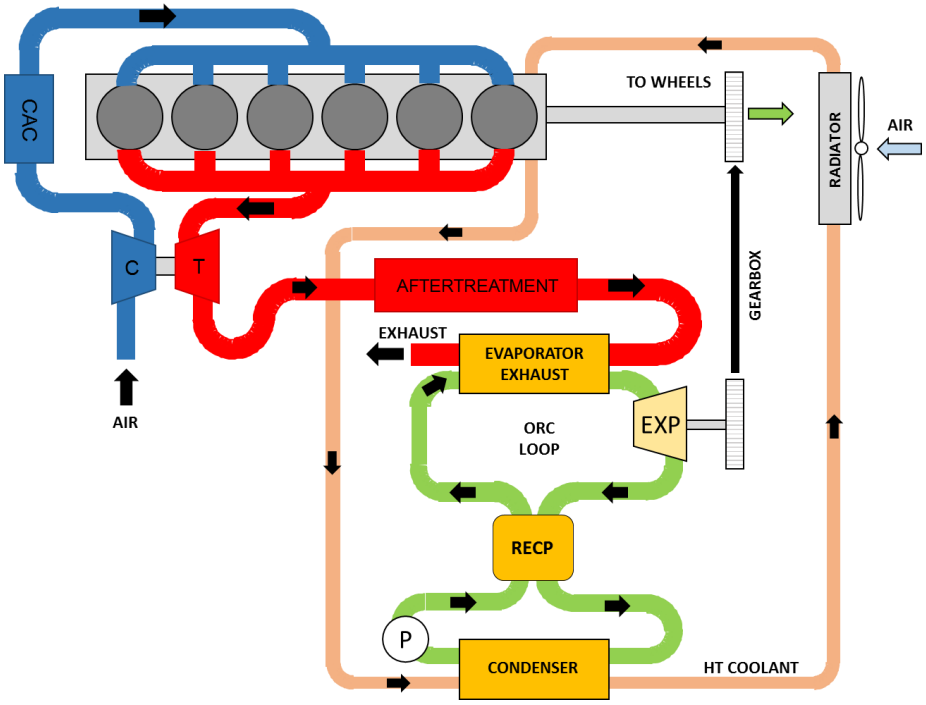

(c – Exhaust heat recovery with internal recuperation (RECP) and IC heat sink configuration)

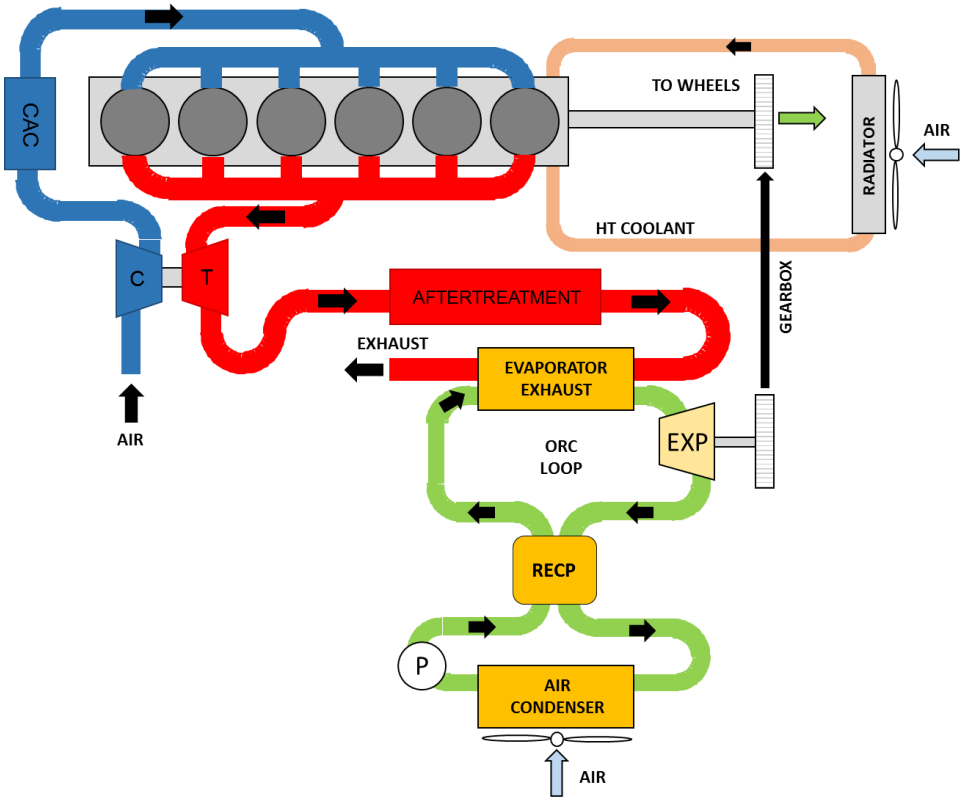

(d – Exhaust heat recovery with internal recuperation (RECP) and DC heat sink configuration)

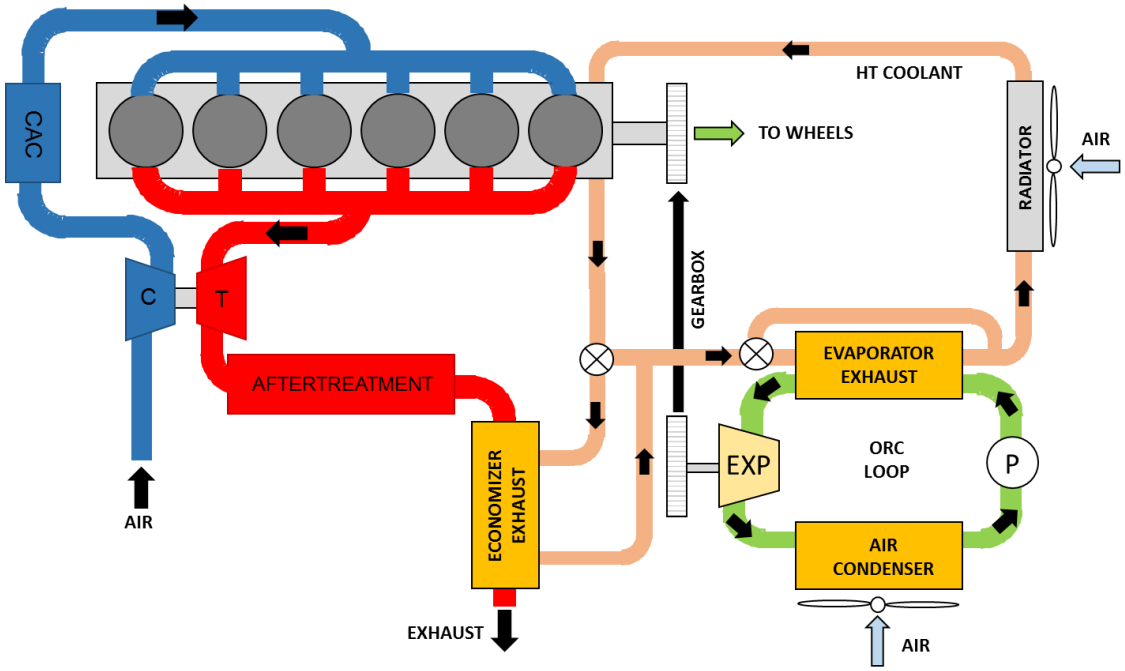

(e – Indirect Exhaust-to-Coolant heat recovery and DC heat sink configuration)

Fig. 107. Combined engine-ORC layouts (case study 4)

In the proposed schemes, the aftertreatment box has been reported. However, in the WAVE simulations, no aftertreatment has been simulated, thus assuming, for the ORC, the gas boundary conditions at the turbocharger's turbine (T in the schemes) outlet. Moreover, in this case study, in order to keep the models simpler, and considering that, for the ORC system a 0-D thermodynamic modelling approach has been used, no backpressure effect of the ORC evaporator has been considered on the engine performance side. Once more detailed models for the ORC evaporator would be available (geometry-based), the combined backpressure effect could be evaluated in a more accurate way. This is left for future developments, and it is not essential to demonstrate the methodology proposed.

Concerning the ORC working fluids evaluated, mainly four different fluids have been chosen, and are mostly those considered by OEMs and system developers in the field of automotive ORC applications. In particular, for the direct exhaust recovery architectures, the following fluids, suitable for high-temperature heat recovery, have been simulated:

- *toluene*
- *ethanol*
- *water*

For the indirect exhaust-to-coolant concept, the *R1233zd(E)*, suitable for lower temperature heat sources, has been analysed, also considering the fact that it is supposed to be the very next replacement for the well-known, but soon banned, R245fa.
The properties of the fluids considered can be observed in Tab. 11 and Tab. 12, in section 4.2.2.1.
Toluene and ethanol, in particular, are very flammable fluids, but due to their excellent thermodynamic properties in the range of exhaust gas temperatures simulated, they are still used by OEMs in ORC developments. Leakage-free and reliable components are then essential in order to avoid safety and flammability issues.

6.4.3 Optimization Procedure and Assumptions

In this case study, an example of parametric analysis, concerning the sweep of some important ORC operational parameters has been proposed in section 6.4.4.2. This has been done just for two of the concepts analysed (1 and 3 from Tab. 56): simple and recuperated direct exhaust gas recovery cycles running on toluene fluid (a dry fluid, thus being very suitable for internal recuperation), with IC heat sink.
However, due to the difficulty to compare different concepts, which may require different operating conditions to respect heat sources and heat sinks boundary conditions, an optimization procedure has been implemented in order to compare the performance and costs. The optimization has been proposed both for the baseline engine-ORC case and the case with the ORC bottoming the engine with exhaust manifolds insulation strategy.
The optimization has been carried out using ESTECO modeFrontier [378], a very versatile and powerful commercial software, able to perform constrained mono and multi-objective optimization, developed from a former spin-off of the University of Trieste. ModeFrontier can be easily interfaced to MATLAB.
The optimization has been carried out only on the ORC side, mostly due to the high computational time of the engine simulations at the actual state of the methodology development. If the WAVE post-processing routines could be embedded into a more user-friendly an efficient tool, the optimization could be applied to the overall combined engine-ORC powertrain, allowing for a synergic complete powertrain assessment.
All the 8 cases analysed in this part of the work have been reported in Tab. 56.

Case	**1**	**2**	**3**	**4**	**5**	**6**	**7**	**8**
Fluid	toluene	toluene	toluene	toluene	ethanol	ethanol	water	R1233zd(E)
Layout	Simple	Simple	RECP	RECP	Simple	Simple	Simple	Indirect Exhaust-to-Coolant
Heat Sink	IC	DC	IC	DC	IC	DC	IC	DC
Expansion Machine	piston	turbo	piston	turbo	piston	piston	turbo	scroll

Tab. 56. Cases simulated (case study 4)

As it can be observed, due to the need of choosing a suitable expansion machine technology, it has been decided to propose a piston expander for the cases with IC heat sink configuration, due to the expected lower expansion ratio (ratio between evaporation and condensation pressures) compared to the DC configuration. Indeed, with DC configuration, the lower ambient air temperature (40°C compared to the 95°C of the coolant temperature) could allow to decrease the condensing pressure, even below ambient (as done for cases 2 and 4), thus increasing the expansion ratio available. In these cases, a radial turbo-expander has been chosen, because able to provide, even if maybe with multiple-stages, a higher expansion ratio and higher efficiencies.
For case 6, however, due to the high condensing pressure of ethanol expected in DC configuration (well above ambient pressure), and thus lower expansion ratio available for similar maximum evaporation pressures, a piston expander has still been considered the best choice, due to the still good efficiency levels and the cheaper costs, compared to a turbo-expander. Moreover, a turbo-expander requires more complicated controlling strategies in order to avoid the presence of liquid phase during expansion, which could damage the turbine blades.

For case 7, due to the already high expansion ratios expected in case of water in a IC heat sink configuration, a DC configuration has not been simulated, because probably requiring too complicated multi-stages expansion machines.
Finally, for case 8, due to the low expansion ratio (and power output) expected for the proposed fluid (R1233zd(E)) and the heat source and sink boundary conditions, a cheap scroll expander, which could be developed as a retrofit of an AC-type compressor, has been considered the best trade-off between costs and performance.
In the optimization procedure, when a piston or scroll expander is chosen, an isentropic efficiency of 70% at design point has been assumed, while, for a turbo-expander, an efficiency of 80% has been fixed (Macchi *et al.* [112]). For scroll and piston expanders, these levels of efficiency can be reached, if the expander built-in expansion ratio is chosen in order to match the cycle required one. Some examples of data from experimental and modelling activities can be observed, to support the assumption, in the graphs reported in section 5.3.1.2. This leads to the observation that the right expansion machine must be designed based on the cycle expected pressure ratio requirements at the design point chosen, and it is not possible to choose the right expander without adequate cycle performance knowledge. Off-design evaluations are left to further steps of a project development but are not less important.
Of course, the proposed assumptions are suitable for a first phase of a project, in which the choice of the best ORC configuration is not clear. This will allow, at least, to compare different solutions in order to have an idea of which could be the most suitable considering the developers' requirements. Once the configuration has been chosen, a more detailed analysis is required in order to assess the components' performance with a higher level of accuracy.
For the same reasons, and in order to estimate the performance and costs of the heat exchangers, an approach considering a 0-D fixed-boundaries modelling and an estimation of the overall heat transfer coefficient from literature has been proposed. The overall heat transfer coefficients, for different heat transfer conditions (fluids, phases) and heat transfer equipment, have been kept fixed and assumed, as average values, as reported in Tab. 17 in section 5.3.1.1. Bejan *et al.* [303] and Panesar [306] declared the approach suitable, again, in a first phase of a project, in which a comparison between different architectures and concepts is the main purpose of the study. When choosing the configuration, a more detailed analysis is required, considering geometrical and detailed heat transfer considerations, using 1-D validated heat exchangers models. The proposed values of the overall heat transfer coefficients for the different heat exchangers in every case simulated have been reported in Tab. 57.

Case	**1**	**2**	**3**	**4**	**5**	**6**	**7**	**8**
Fluid	toluene	toluene	toluene	toluene	ethanol	ethanol	water	R1233zd(E)
Layout	Simple	Simple	RECP	RECP	Simple	Simple	Simple	Indirect Exhaust-to-Coolant
Heat Sink	IC	DC	IC	DC	IC	DC	IC	DC
Overall Heat Transfer Coefficients, U [W/m^{2}K]								
Evaporator	65	65	65	65	65	65	105	5500
Condenser	764	475	764	475	764	475	4000	700
Recuperator	/	/	200	200	/	/	/	/
Exhaust-to-Coolant	/	/	/	/	/	/	/	223

Tab. 57. Assumed average values for the Overall Heat Transfer coefficient (case study 4)

As done for the other case studies, also for the fourth case study, in order to carry out an optimization, the independent variables, the constraints and the assumptions must be identified, based on the simulations' requirements, and the heat source and heat sink boundary conditions.
A complete overview for all the cases analysed, has been reported in Tab. 58.

Independent variables	
$\dot{m}_{wf}$ [kg/s]	ORC working fluid mass flow
p_{cond} [bar]	ORC condensing pressure
PR [-]	ORC pressure ratio (p_{evap}/p_{cond})
ΔT_{suph} [°C]	ORC degree of superheating
$T_{exh,out}$ [°C]	Exhaust gas temperature at Exhaust-to-Coolant heat exchanger outlet (only for case 8)
Constraints	
$\Delta T_{PP} \geq 10\ °C$	Minimum pinch-point temperature difference for the heat exchangers
$0.1\ °C \leq \Delta T_{suph} \leq 100\ °C$	Superheating degree (high superheating generally required for water systems and wet fluids to avoid high liquid fraction at expansion outlet)
$p_{evap} \leq 35\ bar$	Maximum constrained evaporation pressure
p_{cond} [bar]	Minimum condensation pressure: ▪ *DC*: 0.5 bar (vacuum) in order to match better the lower temperature ambient air (adequate sealings required) ▪ *IC*: 1.2 bar (higher than ambient pressure)
$T_{exh,out} \geq 130\ °C$	Minimum exhaust gas evaporator (or exhaust-to-coolant heat exchanger) outlet temperature in order to avoid acid deposition problems
$x_{EXP,out} \geq 0.9$	Minimum expander outlet vapour quality to avoid high liquid fraction during the expansion process
$T_{max} \leq T_c$ [°C]	Cycle maximum temperature (expander inlet) lower than the fluid critical temperature (no-supercritical conditions evaluated)
$PR \leq 100$ [-]	Maximum pressure ratio
Assumptions	
$\dot{m}_{cf}$ [kg/s]	Cooling fluid mass flow: ▪ *DC*: 8 kg/s of air ▪ *IC*: estimated from WAVE simulations heat rejection data
$T_{cf,cond,in}$ [°C]	Condenser cooling fluid inlet temperature: ▪ *DC*: 40°C ▪ *IC*: 95°C
p_{cf} [bar]	Pressure of the cooling fluid: ▪ *DC*: 1.01325 bar (ambient air pressure) ▪ *IC*: 2.4 bar for the engine cooling circuit (typical value for HDDE applications, such as in case study 1)
$\Delta T_{sub-cool} = 2°C$	Sub-cooling degree, in order to ensure liquid fluid at the pump inlet to avoid cavitation problems
η_{EXP}	Expander isentropic efficiency: ▪ Piston, scroll: 0.7 ▪ Turbo-expander: 0.8
$\eta_P = 0.6$	Pump isentropic efficiency
$\varepsilon_{RECP} = 0.8$	Recuperator effectiveness
$\eta_{conv} = 0.95$	Energy conversion efficiency (mechanical crankshaft coupling)

Tab. 58. Table with independent variables, constraints and assumptions for the optimization procedure (case study 4)

The optimizations proposed in this case study are mostly of two types: mono-objective and multi-objective constrained optimization.
In case of a *mono-objective optimization*, the solution is unique and is the combination of the independent variables which leads to the best value for the objective function. In this work, in case of mono-objective optimization, it has been chosen to minimize the SIC (Specific Investment Cost, [$/kW]). The strategy leads to results very similar to the maximization of the ORC power output and the minimization of its total PEC (total Purchased Equipment Cost, [$]), as can be observed from the eq. (96). This type of optimization can be considered typical of a techno-economic analysis approach and is more familiar, in terms of comprehension, to the industry sector, in which the exergy concept is not well spread and understood.
Since the result is unique, the SIC minimization has been chosen to compare the effect of an insulated exhaust manifolds strategy compared to a baseline engine-ORC optimization.
In the case of a *multi-objective optimization*, a combined maximization of the ORC net mechanical power output, minimization of the ORC net power cost rate and minimization of the ORC total irreversibilities associated cost rate has been chosen, to demonstrate a possible thermo-economic optimization.
As observed, the main objective function is always the maximization of the ORC power output, which is reflected on the overall BSFC improvement compared to the engine without ORC. Indeed, no investment is worth if not enough power output is produced.
The other objectives are more related to the minimization of costs: investment costs for a techno-economic analysis, and operational streams-associated costs (cost rates) in case of a thermo-economic approach.
In case of a multi-objective optimization, the optimum is not anymore a unique solution, but rather a so-called Pareto front, in which different designs can lead to the best choice depending on the developer's requirements and needs. For this reason, the comparison of different cases with a multi-objective optimization is not always a simple task. For this purpose, an algorithm embedded in modeFrontier has been used in order to fix some criteria for the comparison of the different cases' best solution. The proposed approach is called Multi Criteria Decision Making (MCDM) and is briefly introduced in the results section.
The optimization runs have been carried out using a MOGA-II algorithm implemented in modeFrontier. The MOGA-II is an ESTECO proprietary Multi-Objective Genetic Algorithm declared to be reliable in finding the global optima of a constrained optimization problem.
An exemplification of the proposed optimization procedure has been proposed in Fig. 108.

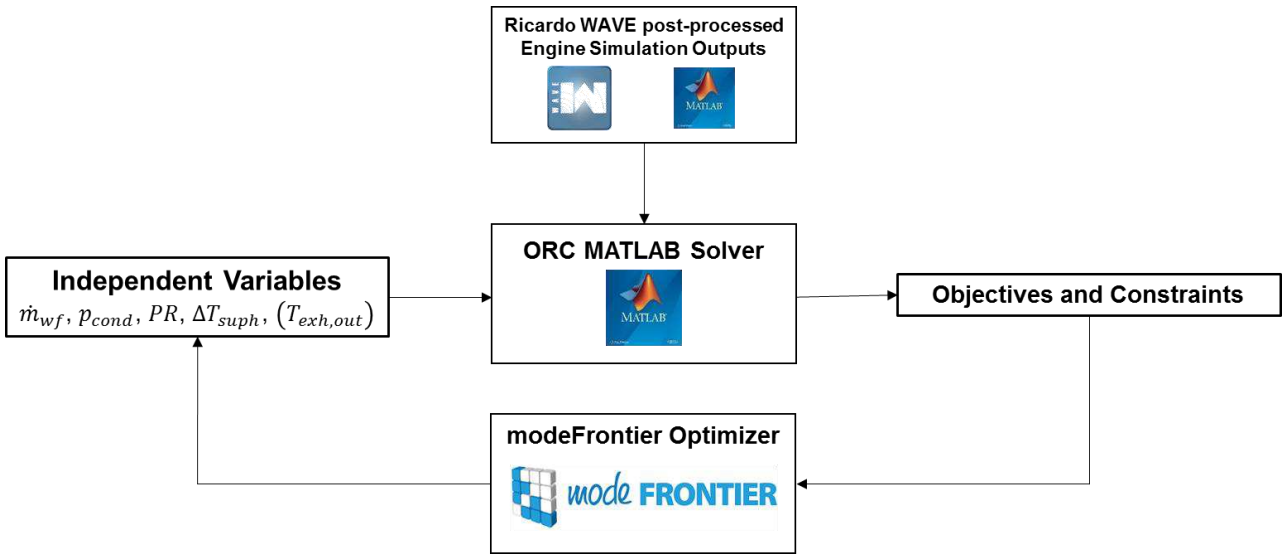

Fig. 108. Scheme of the optimization procedure (case study 4)

6.4.4 Results and Discussion

In this section, the results concerning the First Law, Second Law, techno and thermo-economic approaches have been reported, both for the baseline engine and ORC systems and the combined engine-ORC systems with engine exhaust manifolds insulation strategy.

6.4.4.1 Baseline Engine

As already mentioned, the theoretical background applied to the engine side calculations has been already introduced in section 5.1. The simulations have been carried out using Ricardo WAVE and the MATLAB-developed post-processing routines capable to calculate detailed First and Second Law cycle-averaged engine balances, based on every steady-state operating point simulated. The division of the control volumes proposed for the calculations of the engine energy and exergy balances contributions is the same reported in Fig. 39 in section 5.1.3.3.

First Law Analysis Results

The WAVE simulations results are generally just considering the gas-side balances. For this reason, the post-processing routines developed consider just the contributions in terms of heat transfer of the gas-mixtures to the cylinder walls, and in particular, the cylinder head, the cylinder liner and the piston crown, and the energy lost because of friction. These contributions are calculated with the already introduced Woschni model (section 5.1.1.2), for the heat transfer, and with the Chen-Flynn model (section 5.1.1.3) for the friction.
However, in a realistic engine, in first approximation, the heat transfer and friction contributions sum together, and the total energy is generally rejected as heat to the engine cooling jacket, to the oil circuit, and, a small amount, as radiation to the ambient.
For this reason, and following Ricardo WAVE guidelines, the energy streams to the cooling and the oil circuits have been estimated based on the results obtained from the heat transfer model and the friction model. This is very important in order to estimate the boundary conditions for the two circuits when using them as possible heat sources or heat sinks (as for the IC configuration with the coolant) for the ORC bottoming system.
What reported in this work is an estimation of the energy streams based on typical WAVE guidelines, associating the heat transfer through liner and cylinder head to the cooling circuit, and the heat transfer through the piston to the oil circuit. The same percentages are then estimated also for the friction energy. Of course, especially when a physical engine prototype is available, it is suggested to rely more on real test data for what concerns the temperatures and mass flows of the coolant and oil circuits.
However, the proposed approach, especially when in a feasibility study phase of an engine development project, can be used in order to estimate the requirements for the two circuits and assess some possible thermal management strategies for further developments.
In this case study, the estimated thermodynamic parameters, in particular for the cooling circuit, have been used as boundary conditions for the ORC analysis, which requires as inputs the mass flows and temperatures of the coolant, especially for the case 8 and for the cases in which the engine cooling circuit is used as heat sink for the ORC (IC).
After internal discussion with Ricardo thermal management experts, it has been decided to impose a $\Delta T_{cool} = 95 - 85 = 10°C$ over the engine cooling jacket circuit and, using the water fluid properties retrieved from EES (or REFPROP), the mass flow of coolant (in this case simple water has been

assumed) has been estimated for every engine simulated operating point, assuming a direct proportionality to the thermal power transferred to the cooling circuit. The oil boundary conditions are not calculated directly, but rather the thermal power transferred to the lubrication oil circuit has been estimated as difference between the overall heat and friction energy transfer and the coolant rejected heat, in order to draw the overall engine balance.
The energy balance has been calculated for all the 16 operating conditions, however, the full overview has been reported only for the considered C100 and B50 points.
The baseline engine energy breakdown analysis chart has been reported in Fig. 110.

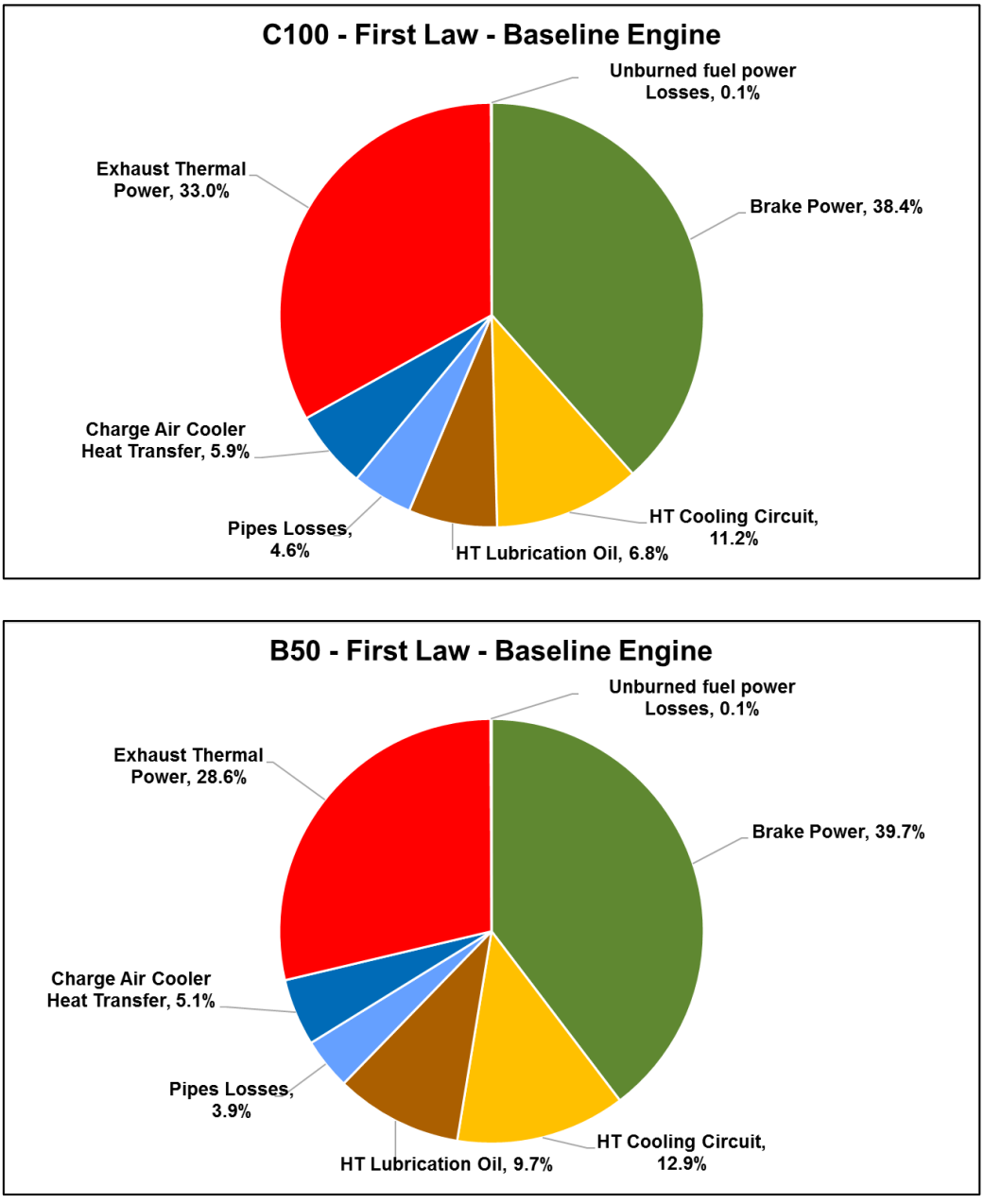

Fig. 109. Percentages distribution of the various energy streams of the baseline engine at C100 and B50 operating points (case study 4)

In Fig. 109 it is possible to observe how most of the energy introduced with the fuel is rejected as exhaust thermal power, CAC heat transfer, heat transfer (HT) to the lubrication oil circuit and the cooling circuit, while only around 38-40% is really converted into useful brake power. The energy

breakdown analysis ([kW]) can be also observed in Fig. 110. In Fig. 109, the term "pipe losses" refers to both intake / exhaust manifolds and pipes heat losses. These heat losses are generally mostly concentrating in the exhaust manifolds, due to the higher post-combustion temperatures compared to the intake line temperatures. Indeed, in Fig. 110, just the term "exhaust heat losses" has been reported, while the losses in the intake have been neglected because of much lower entity. Also the unburned gas energy contribution in the exhaust has not been reported, due to the very low value, as also reported by Rakopoulos *et al.* [290].

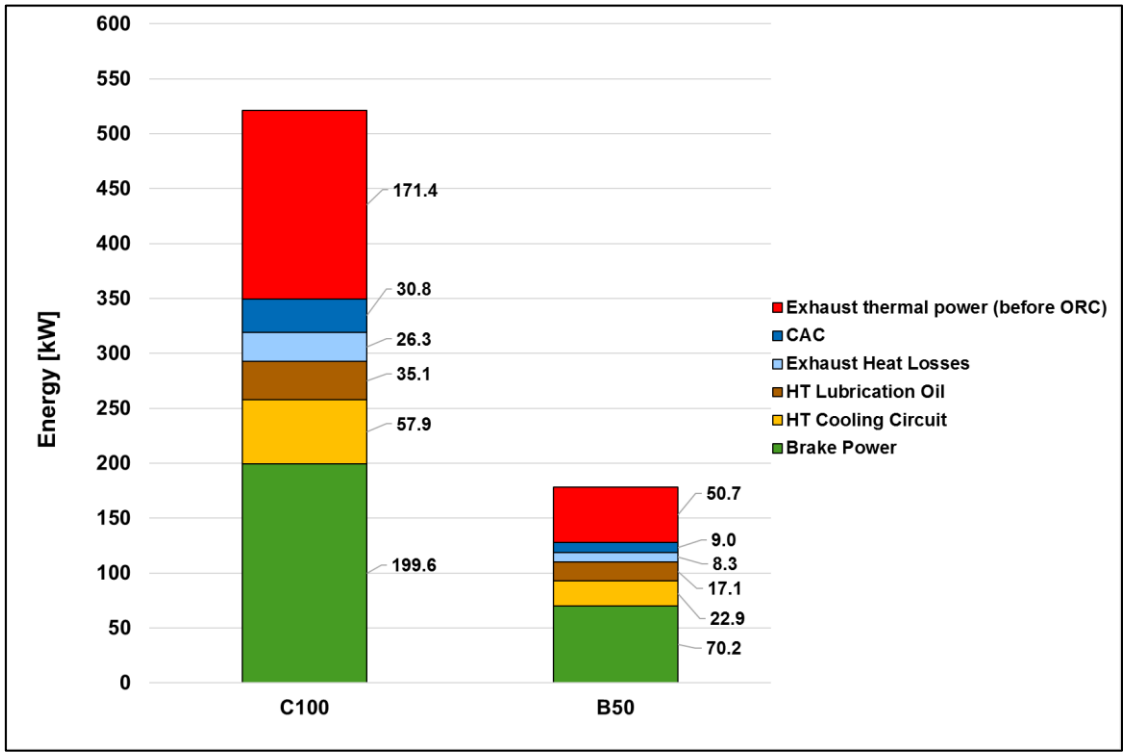

Fig. 110. Energy streams breakdown analysis for the baseline engine at C100 and B50 (case study 4)

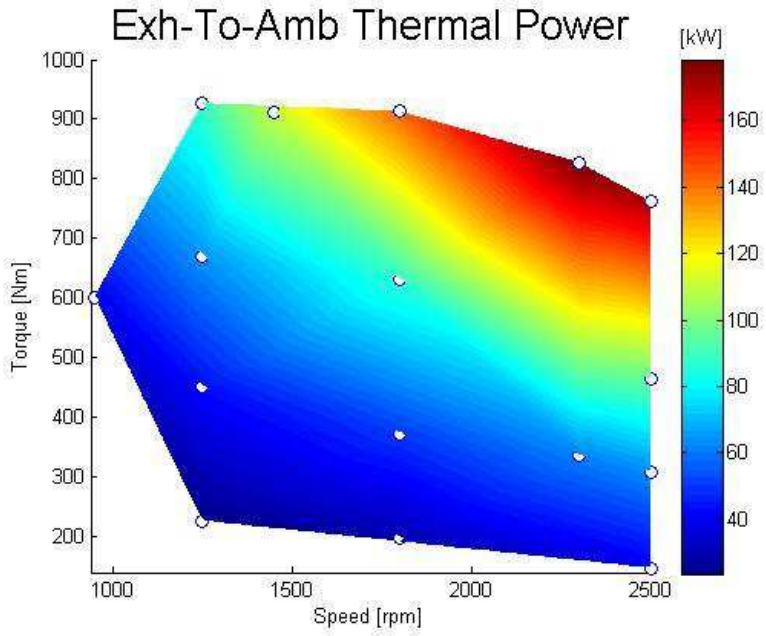

Fig. 111. Example of First Law analysis map. Exhaust gas thermal power (case study 4)

Some maps can also be drawn, about several First Law energy balance contributions, in order to show the trends over the entire engine load-speed map. One example for the exhaust gas thermal power has been reported in Fig. 111 (calculated assuming to cool down the gas to ambient temperature, 25°C). From the proposed map, as expected, it can be envisaged that a higher energy (or thermal power) is available in the exhaust gas, to be recovered with a possible ORC system, in the high-load / high-speed operational range (e.g. C100), due to higher exhaust mass flows and temperatures. At medium-load / medium-speed (e.g. B50) the energy rejected is sensibly lower.
Similar maps can be plotted for most of the engine sensible operational parameters and First Law balance contributions obtained from the WAVE simulations or post-processed.

Second Law Analysis Results

Even though a complete, detailed, First Law analysis of an engine model is not a feature which is usually implemented in performance simulation software such as Ricardo WAVE, its information can really help the engineers in order to develop effective thermal management strategies and sub-systems, allowing to calculate the energy flows for every operational point or scenario calculated in WAVE. This allows also to save time and costs associated to expensive testing campaigns on several different operational strategies. Nevertheless, the approach is quite common, with a lower level of details, in the industry.
What proposed in this section, and already introduced in its theoretical background in section 5.1.3, goes beyond the traditional energy formulations, proposing an entire and detailed Second Law analysis of the engine system. This allows to highlight in which engine sub-systems irreversibilities (exergy destruction and cycle inefficiencies) concentrate, and at the same time, to calculate all the exergy streams required for a thermo-economic analysis of a combined engine-ORC powertrain. As already introduced, to the author's knowledge, no commercial software is able to provide such a level of details in the analysis.
As done for the First Law analysis, the exergy balances have been calculated for all 16 operating points, however, the detailed charts have been reported only for the two analysed C100 and B50 points. The percentage charts have been reported in Fig. 112.

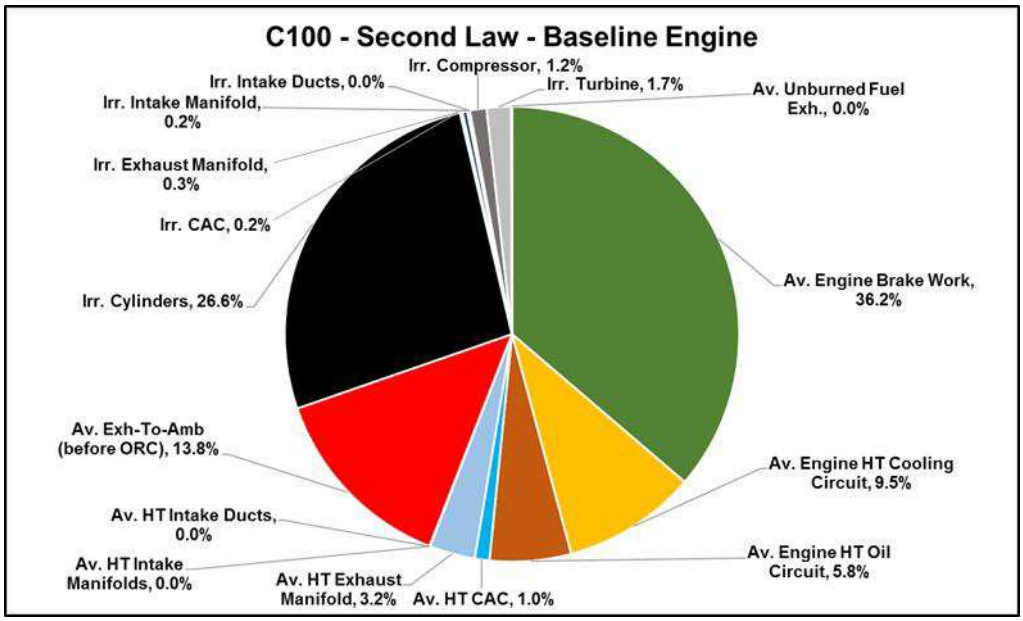

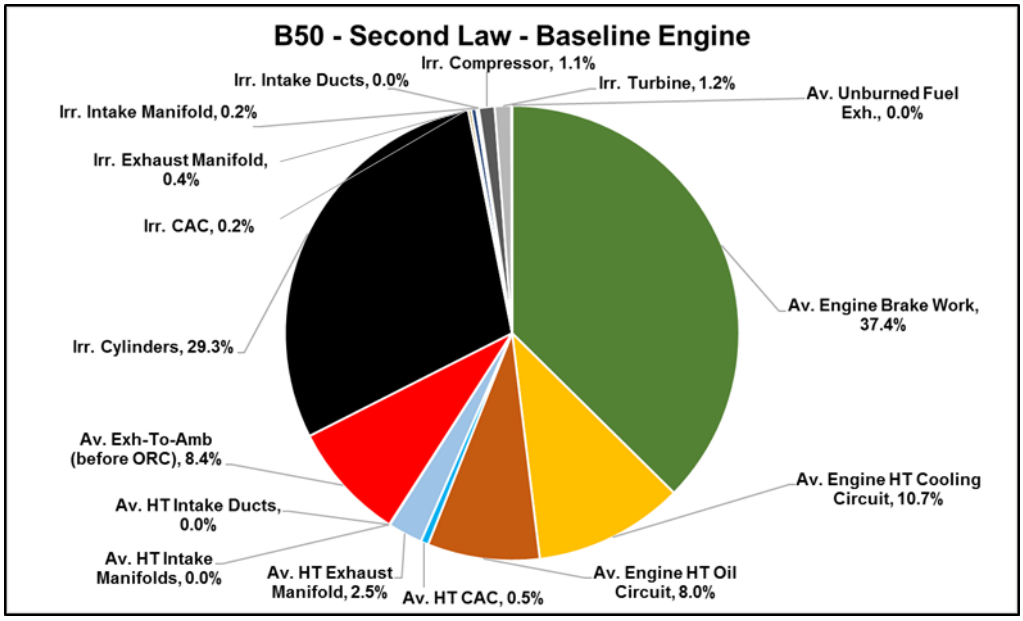

Fig. 112. Percentages distribution of the various exergy and irreversibilities contributions for the baseline engine at C100 and B50 operating points (case study 4)

Also for the Second Law Analysis, the breakdown exergy analysis, for C100 and B50 operating points, has been reported in Fig. 113.

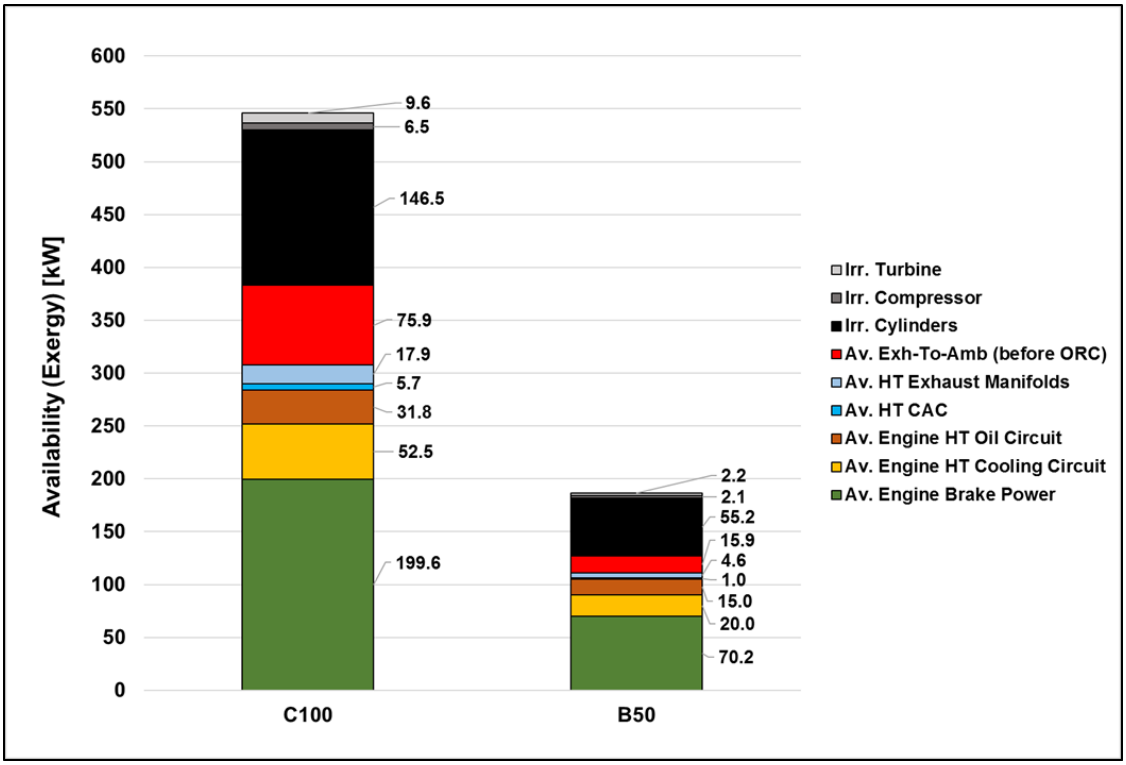

Fig. 113. Exergy streams breakdown analysis for the baseline engine at C100 and B50 operating points (case study 4)

As it can be observed from the proposed charts, the Second Law analysis is able to provide information which are not available through a common First Law analysis. It is possible to infer how not only

rejected streams are available, but rather 30 (C100) to 32.5% (B50) of the exergy introduced with the fuel is wasted in the production of irreversibilities (exergy destruction terms), being these inefficiencies for the engine system. The irreversibilities are mostly concentrated in the engine cylinders' control volume (26.6 to 29.3% of the fuel exergy) and are related to combustion inefficiencies and valves throttling. These results are perfectly in line with what reported by Rakopoulos *et al.* [290], for a similar type of engine, and demonstrate how, in order to develop a more efficient combined engine-ORC system, not only the ORC must be considered, but also an improvement considering combustion strategies is needed. In this case, a combined 1-D / 3-D CFD approach can help in the study of the in-cylinders processes, together with the thermodynamic impact on the overall engine gas line. For example, a high temperature combustion could improve the in-cylinder efficiency, decreasing the irreversibilities, at the same time increasing the exergy available in the exhaust gas, which can be recovered with an ORC. However, a trade-off with emissions must be considered, because a high temperature combustion is generally detrimental in terms of NO_x production.
Other sources of irreversibilities are concentrated mostly in the intake and exhaust manifolds, and, in a higher quantity, in the turbocharger, with the turbine generally being, from a Second Law analysis point of view, less efficient compared to the compressor.
Contributions related to exhaust gas released exergy, exergy transfer (related to heat transfer, "HT") to the coolant, oil circuit, CAC and heat losses in the exhaust manifolds are also not negligible terms. The recovery of these streams can be beneficial in order to produce additional useful power. Moreover, as presented in this study, the insulation of the exhaust manifolds can contribute to reduce the exergy losses towards the environment, at the same time directing an increased exergy (and energy) flow towards the exhaust for further heat recovery.
The analysis proposed is able also to provide in-cylinder information, as already reported in Fig. 40 and Fig. 41 in section 5.1.3.3.
As for the First Law analysis, also in case of a Second Law analysis, several maps can be produced for most of the analysis outputs and operating parameters. An example for the engine total irreversibilities percentage (calculated on the fuel injected exergy) has been reported in Fig. 114. The map shows how generally the engine is less efficient (dissipates more exergy) at high speed-low load points.

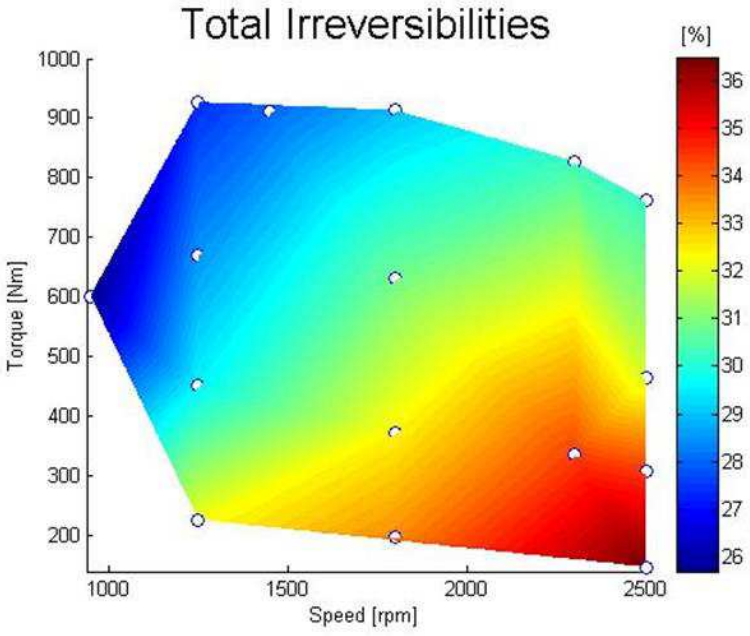

Fig. 114. Map of the percentage of irreversibilities calculated on the fuel injected availability (case study 4)

6.4.4.2 ORC Parametric Analysis Example (Baseline Engine, C100)

In this section, some examples of possible parametric analysis have been proposed just for the comparison of the cases 1 and 3: simple and recuperated ORC running on toluene, with IC heat sink configuration. This has been done in order to show some of the information that can be extracted from the detailed methodology developed.
From the baseline engine simulations and cooling circuit thermodynamic parameters estimation, the following boundary conditions for the ORC analysis have been extracted (Tab. 59). Additionally, all the engine exergy streams values, reported in Fig. 112 and Fig. 113 are necessary inputs for the ORC side calculations, especially when considering a thermo-economic approach as reported in section 5.3.4.
As already mentioned, in case of DC heat sink configuration, average values of 8 kg/s and 40°C ambient air mass flow and temperature have been assumed for the cooling package, for every operating point, in first approximation, following typical expected average conditions.

Parameter	Unit	C100	B50
Exhaust gas mass flow (after turbine), $\dot{m}_{exh}$	kg/s	0.309	0.162
Exhaust gas temperature (after turbine), T_{exh}	°C	501.4	315.8
Engine coolant mass flow (ORC cond. inlet), $\dot{m}_{cool}$	kg/s	1.38	0.545
Engine coolant temperature (ORC cond. inlet), $T_{cool,in}$	°C	95	95
Cooling circuit pressure, p_{cool}	bar	2.4	2.4

Tab. 59. Baseline engine boundary conditions for ORC analysis (IC heat sink) – (case study 4)

The parametric analysis examples have been reported just for the C100 case, in order to keep the report shorter, but can be proposed for every chosen design operating point.

Parametric Analysis – Pressure Ratio (Evaporation Pressure)

In the proposed parametric analysis study, the following conditions have been kept fixed, while the pump pressure ratio (thus the evaporation pressure, as reported in the figures) has been swept in order to show the sensitivity to the proposed parameter:

- ORC condensing pressure: 1.2 bar;
- ORC toluene mass flow: 0.18 kg/s;
- Superheating temperature difference: 5°C;
- Piston expander efficiency: 70%;

The effect of pressure ratio (or evaporation pressure) sweep on the ORC power output and the SIC can be observed in Fig. 115.
The typical ORC net mechanical power output trend with pressure ratio variation can be observed, with increased power output for increased pressure ratio (or evaporation pressure with fixed condensing pressure). The same power output is expected both for simple and recuperated system.

Indeed, the effect of the recuperator is to achieve the same power output with a lower heat recovery (and rejection), thus increasing the ORC thermal efficiency.
The system without recuperator (SIMPLE), with the proposed operating conditions, can reach SIC values of around 272 $/kW at high evaporation pressures (35 bar). The SIC value is compatible with Ricardo's analysis and it is starting to the enter the technology competitivity range. At low evaporation pressures (low pressure ratios), due to the low power output expected, the SIC values tend to become higher, showing the need of keeping higher evaporation pressures in order for the investment to be worth. The system with recuperator (RECP) shows higher SIC values (308 $/kW at 35 bar evaporation pressure), generally because of the additional cost of the recuperator, even though slightly cheaper evaporator and condenser are expected due to the lower heat recovery and rejection required, for the same power output. However, the benefit of the recuperated system, in case of vehicles applications, is a decreased heat rejection to the cooling package, with lower vehicle thermal management issues. The effects of an increase in weight should also be considered.

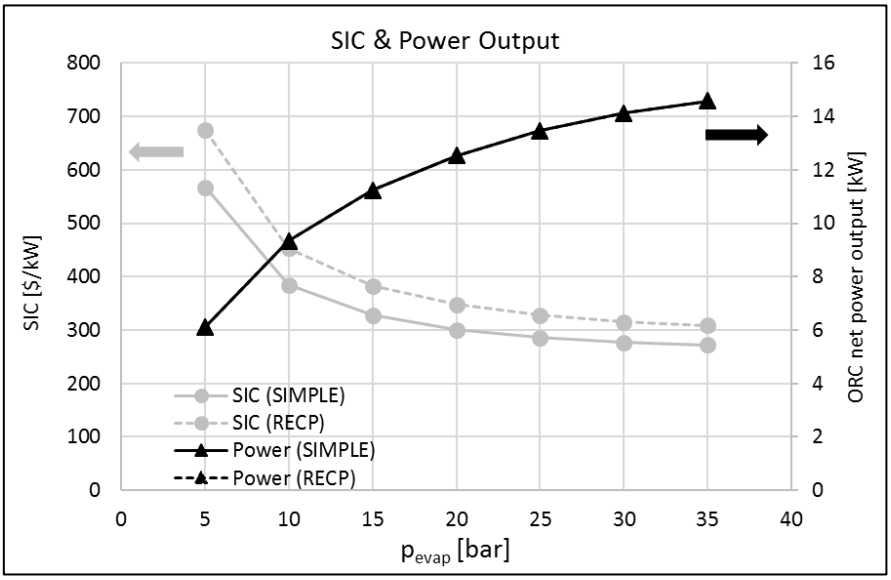

Fig. 115. Effect of pressure ratio (evaporation pressure) on ORC net power output and SIC (case study 4)

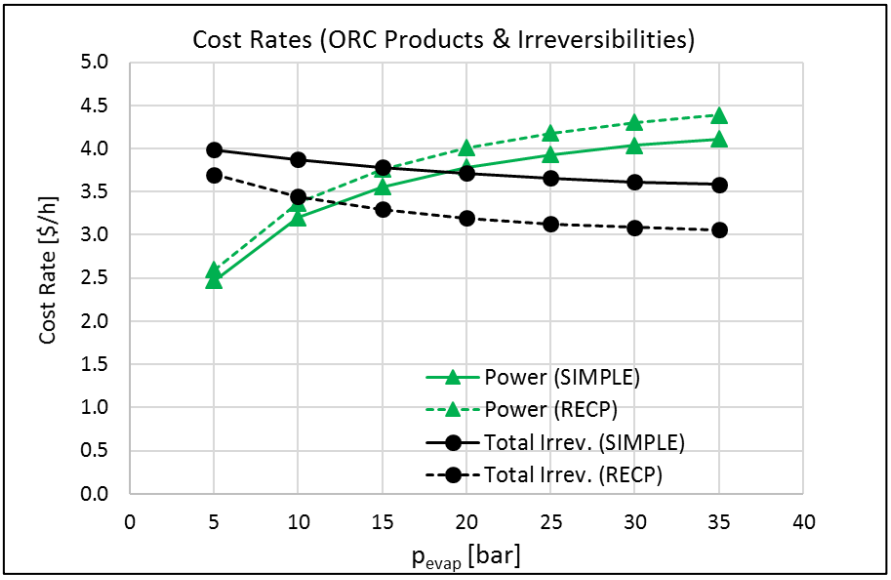

Fig. 116. Effect of pressure ratio (evaporation pressure) on ORC net power and total irreversibilities cost rates (case study 4)

The same parametric analysis has been also carried out considering some outputs of a thermo-economic approach: the cost rates of the ORC produced net mechanical power and "wasted" because of the overall ORC irreversibilities. The results have been reported in Fig. 116.
A parametric thermo-economic analysis shows how, at low evaporation pressures, more investment costs are "wasted" in the production of irreversibilities, rather than those really invested in the production of useful power. In particular, due to the lower irreversibilities produced using a recuperated (RECP) cycle, the trade-off between "useful" and "wasted" costs is better, with more costs invested in the production of power rather than irreversibilities, for an evaporation pressure above 10 bar (intersection of the segmented lines). In the case of the simple cycle, the positive trade-off starts from a higher evaporation pressure (20 bar, intersection of the continuous lines). A recuperated system however leads also to generally higher power production cost rates, due to the higher investment costs necessary to provide the same power output. The simple cycle wastes more costs in the production of irreversibilities.
The same type of information can be provided also for other streams, as reported in Fig. 117, in particular for the coolant (in the proposed configuration used as ORC heat sink) and the engine exhaust gas rejected to the environment after the ORC evaporator. These streams are not producing any real benefit for the overall system, unless they are further recovered in order to produce additional power, but requiring more complicated, un-reliable and expensive waste heat recovery layouts.

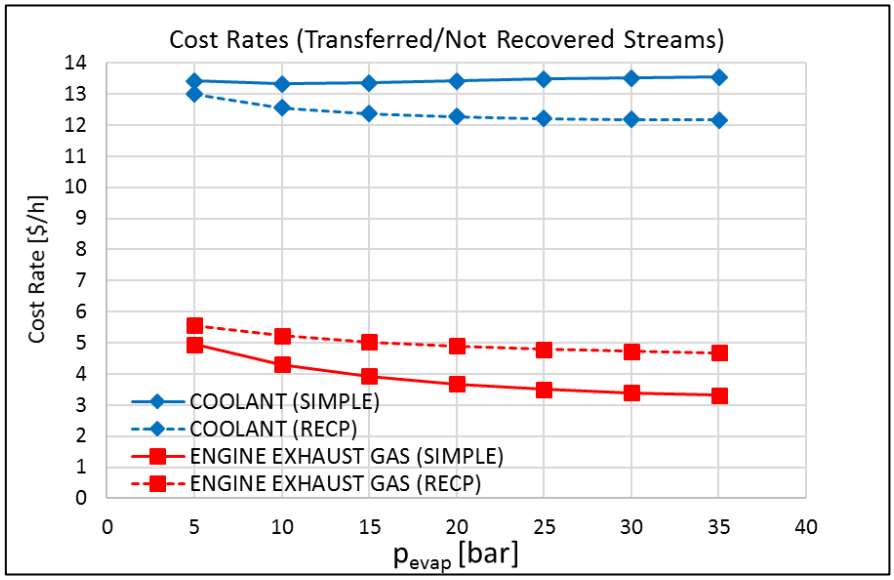

Fig. 117. Effect of pressure ratio (evaporation pressure) on coolant and exhaust gas associated cost rates (case study 4)

As it can be observed from Fig. 117, to a recuperated system are associated higher released exhaust gas cost rates and lower coolant cost rates, compared to a non-recuperated system. This because the recuperated system, even if more expensive, is able to recover and reject less heat, for the same useful power produced.
The proposed parametric analysis shows how, in order to achieve a good trade-off between "useful" and "wasted" costs, the pressure ratio and thus evaporation pressure must be kept high in order to generate less irreversibilities and more useful power output, even though costs generally increase with increased heat recovery and heat exchangers' dimensions.
Similar cost rates, in terms of absolute values [$/h] are associated to the production of power, irreversibilities and exhaust gas, while the cost rates associated to the coolant are higher, because the ORC system recovers heat, and due to its general low thermal efficiency, rejects most of the recovered heat to the heat sink, producing just a lower amount of power output.

It is important to remember in this case, that the costs calculated are coming from the overall combined engine-ORC analysis, considering all exergy streams and components costs of both engine and ORC. For this reason, the engine side analysis is essential.

Parametric Analysis – Superheating Degree

As done for the pressure ratio sweep, also the superheating degree has been swept, keeping all the other parameters with the proposed fixed values:

- ORC condensing pressure: 1.2 bar;
- ORC toluene mass flow: 0.18 kg/s;
- Pressure ratio: 25 (evaporation pressure 30 bar);
- Piston expander efficiency: 70%;

The influence of the superheating degree on the ORC power output and SIC has been reported in Fig. 118.

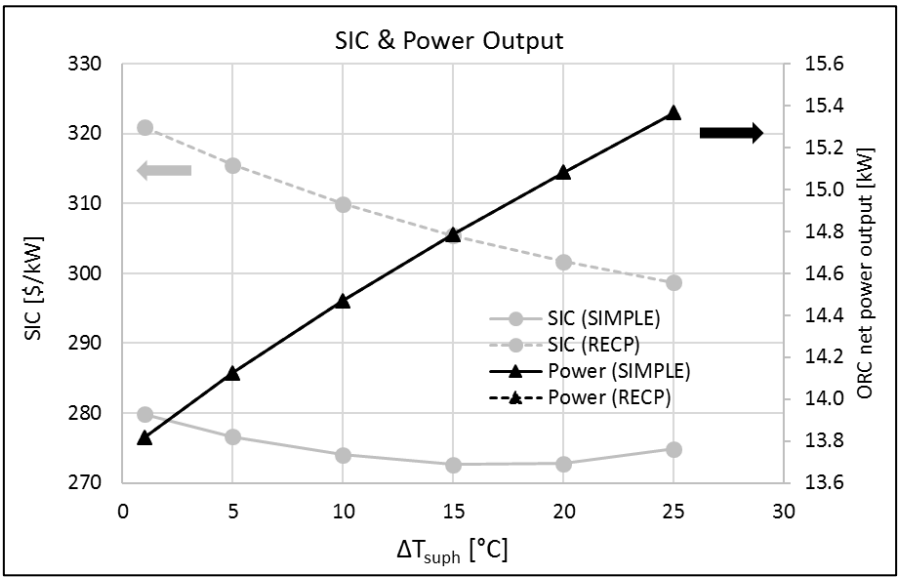

Fig. 118. Effect of superheating degree on ORC net power output and SIC (case study 4)

A slight superheating, considering the other variables fixed, can lead to around 1.6 kW improvement in terms of power output.
A decrease in SIC can be achieved with superheating in case of the recuperated system (RECP), mostly due to the increased power output and a parallel proportionally lower increase in investment costs (mostly related to the evaporator, which results in being bigger). A SIC slightly lower than 300 $/kW has been estimated for 25°C superheating.
In the case of the non-recuperated system, a trend with a minimum value (273 $/kW with 15°C superheating) can be envisaged. After the minimum value, an increase in superheating will just generate an increase in costs, rather than a real benefit in terms of power production, thus leading to an increase of SIC.

The effect of superheating on the cost rates is however generally less marked compared to the effect produced by the pressure ratio (or evaporation pressure), as can be observed from Fig. 119, reporting the cost rates for the ORC net generated power output and produced irreversibilities. It is possible to observe how the superheating degree influences slightly the power cost rate but has almost no impact on the irrevesibilities cost rate. This demonstrates some level of superheating can be beneficial.
The same trends happen for the other streams (coolant and exhaust gas), which are not reported in this case, for the sake of keeping the report shorter.

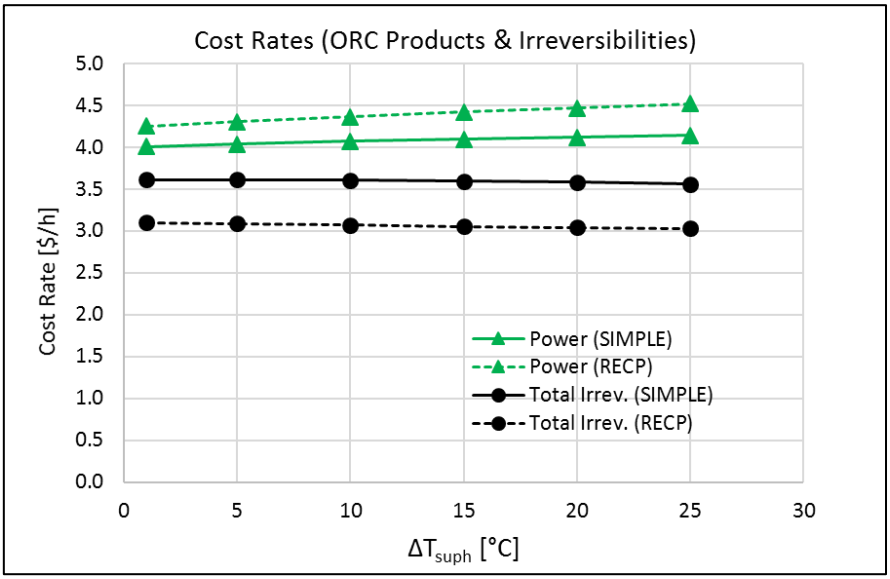

Fig. 119. Effect of superheating degree on ORC net power and total irreversibilities cost rates (case study 4)

Parametric Analysis – Expander Isentropic Efficiency

As done for the other parameters, also an expander isentropic efficiency parametric analysis has been carried out, in order to assess the impact of the expansion machine efficiency. The expander considered is a piston-type. The fixed parameters are:

- ORC condensing pressure: 1.2 bar;
- ORC toluene mass flow: 0.18 kg/s;
- Pressure ratio: 25 (evaporation pressure 30 bar);
- Superheating degree: 15°C;

The results of the expander isentropic efficiency parametric study on the ORC power output and SIC have been reported in Fig. 120.

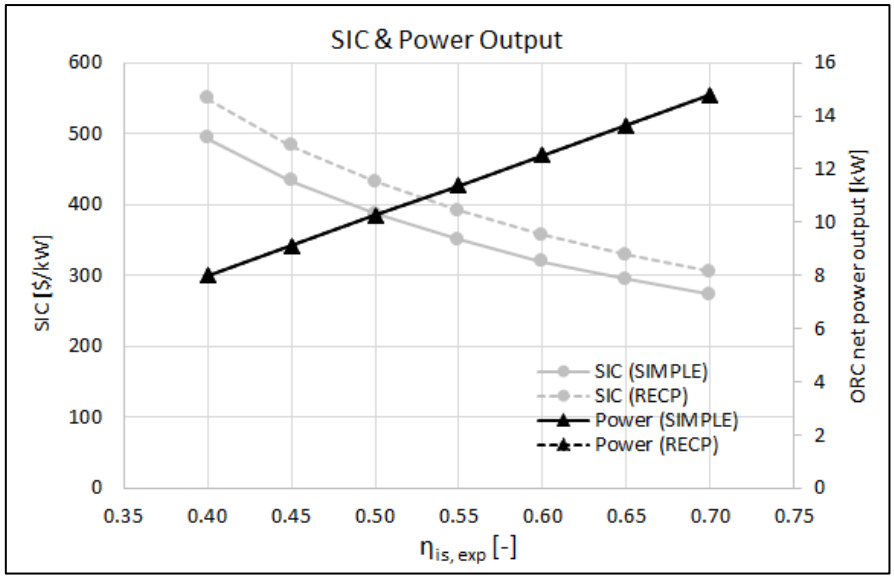

Fig. 120. Effect of expander isentropic efficiency on ORC net power output and SIC (case study 4)

What observed in the previous figure shows the importance of ensuring a high expansion machine isentropic efficiency in order to allow for high ORC power output and competitive SIC levels. For this reason, a cheap, but at the same time efficient, piston expander must be available or developed. The alternative is proposing a very efficient turbo-expander machine, which, however, is more expensive and requires improved control strategies.
The results of the expander isentropic efficiency study on the ORC power and irreversbilities cost rates can be observed in Fig. 121.

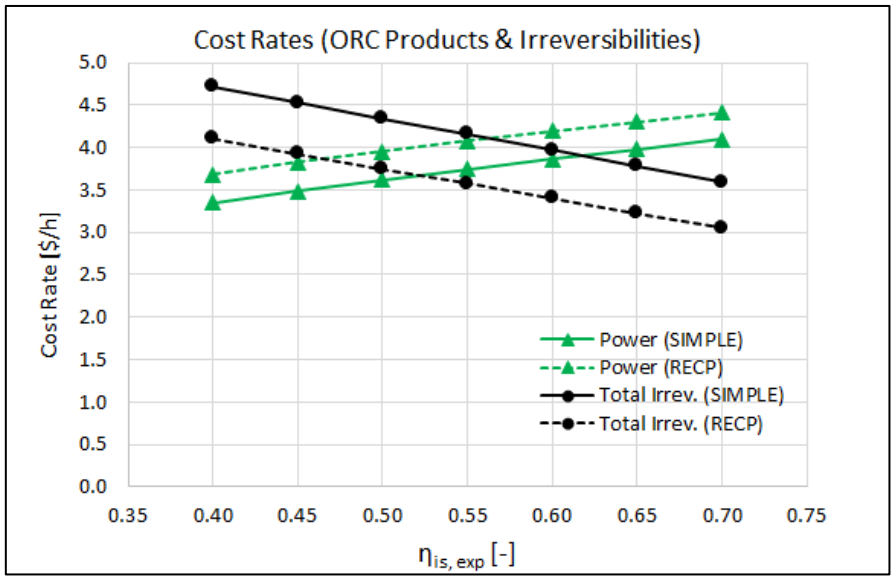

Fig. 121. Effect of expander isentropic efficiency on ORC net power and total irreversibilities cost rates (case study 4)

The trade-off between cost rates associated to "useful" power production and "wasted" irreversibilities becomes competitive after 45-50% expander efficiency levels for the recuperated system (REC), and even 60-65% for the simple non-recuperated system. Again, this demonstrates the higher efficiency and lower irreversibility of the recuperated cycle, which can also "accept" a less efficient expander when the design goal is ensuring that most of the invested costs are used to produce power, rather than dissipated in cycle inefficiencies.

6.4.4.3 ORC Optimization (Baseline Engine)

When comparing simple and recuperated systems running on toluene, the comparison can be considered easy and "fair", since the same cycle operating parameters can be kept fixed for both the configurations.
However, when deciding to compare the different cases with different working fluids, and even different architectures, the comparison becomes more complicated, due to required different operating conditions in order to respect heat sources and heat sinks constraints. For this reason, an optimization procedure has been proposed in order to compare the best operating conditions and configurations achieved for all the 8 cases considered in this case study.
As already introduced in section 6.4.3, two different, mono and multi-objective optimization examples have been proposed. However, the optimization choice depends always on the developers' requirements. Those selected in this case are just possible examples.

Techno-economic Mono-Objective Optimization

The goal of the proposed mono-objective techno-economic optimization is the minimization of the Specific Investment Cost (SIC, [$/kW]) of the different ORC concepts (1 to 8). The strategy is very similar to the combined maximization of the ORC net mechanical power output and minimization of the ORC total system Purchased Equipment Cost (PEC, [$]).
The results of the optimization lead to a unique best point for every of the cases analysed and have been reported both for the C100 and B50 engine operating points, considered as two different possible design points for the ORC (Fig. 122).

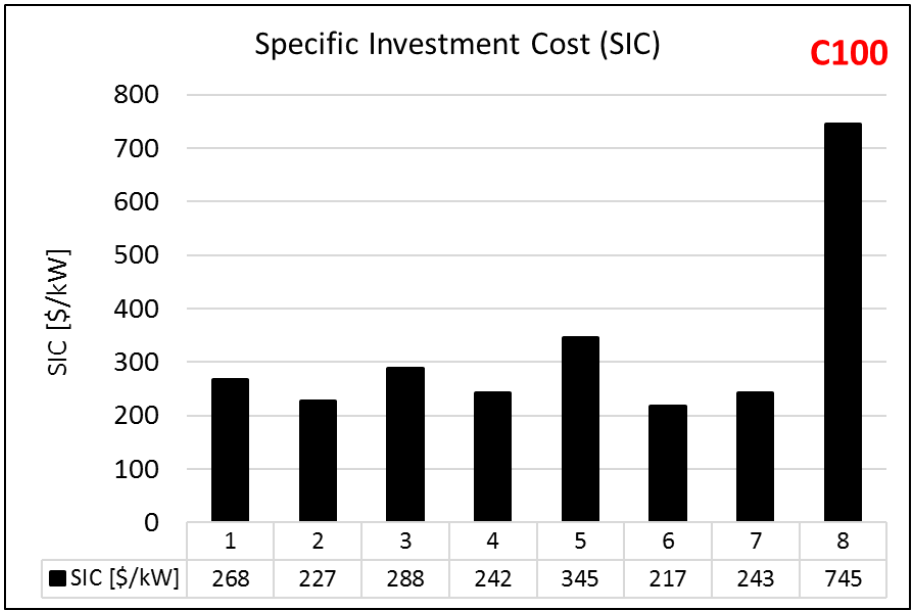

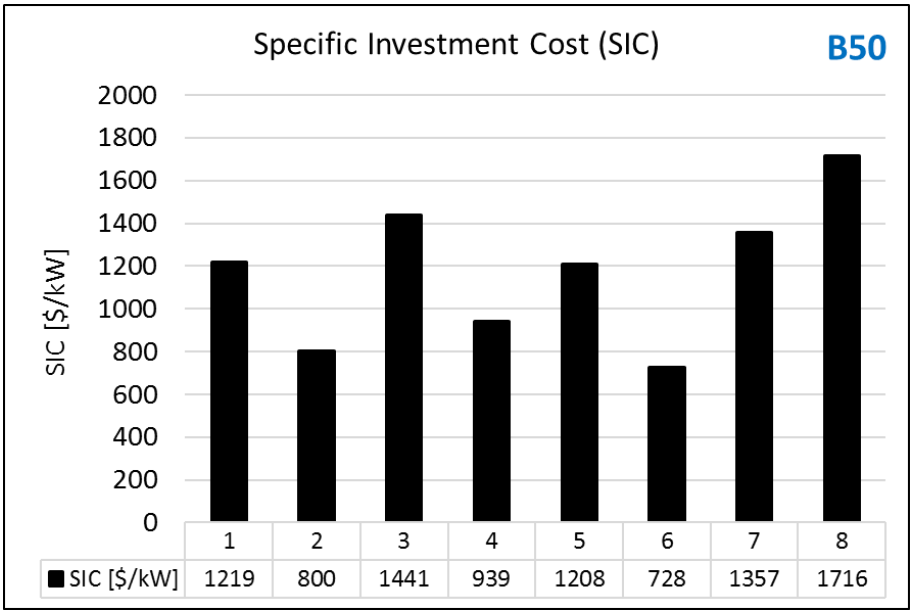

Fig. 122. ORC SIC minimization (baseline engine). C100 and B50 engine operating points – Techno-economic analysis (case study 4)

Other sensible results related to the optimization procedure have been also reported in Tab. 60, in particular considering achieved power output, combined engine-ORC BSFC improvement and ORC total PEC. The values for the main independent variables involved in the optimization have also been reported.

Case		**1**	**2**	**3**	**4**	**5**	**6**	**7**	**8**
Fluid		**toluene**	**toluene**	**toluene**	**toluene**	**ethanol**	**ethanol**	**water**	**R1233zd(E)**
Layout		**Simple**	**Simple**	**RECP**	**RECP**	**Simple**	**Simple**	**Simple**	**Indirect Exhaust-Coolant**
Heat Sink		**IC**	**DC**	**IC**	**DC**	**IC**	**DC**	**IC**	**DC**
Expansion Machine		***piston***	***turbo***	***piston***	***turbo***	***piston***	***piston***	***turbo***	***scroll***
C100									
$\dot{W}_{ORC,net,mech}$	[kW]	15.3	21.7	16.7	24.0	11.3	16.8	19.3	5.0
BSFC Impr.	[%]	7.1	9.8	7.7	10.8	5.4	7.8	8.8	2.4
PEC (ORC)	[$]	4111	4930	4815	5828	3915	3647	4696	3709
$\dot{m}_{wf}$	[kg/s]	0.19	0.19	0.20	0.20	0.12	0.11	0.04	0.53
p_{cond}	[bar]	1.20	0.50	1.23	0.50	4.47	1.20	1.97	4.07
PR	[-]	29.1	69.8	28.4	69.9	7.8	29.1	39.0	2.1
ΔT_{suph}	[°C]	7.17	1.01	10.81	7.31	33.13	32.99	74.00	13.32
$T_{exh,out}$	[°C]	/	/	/	/	/	/	/	130
B50									
$\dot{W}_{ORC,net,mech}$	[kW]	2.8	4.5	2.8	4.6	2.9	4.2	2.8	2.1
BSFC Impr.	[%]	3.8	6.1	3.8	6.1	3.9	5.7	3.8	2.8
PEC (ORC)	[$]	3408	3637	4026	4277	3436	3069	3741	3512
$\dot{m}_{wf}$	[kg/s]	0.051	0.055	0.051	0.058	0.035	0.031	0.008	0.23
p_{cond}	[bar]	1.20	0.50	1.20	0.50	3.83	1.20	1.53	3.40
PR	[-]	9.8	20.1	9.8	17.6	9.12	29.1	14.1	2.0
ΔT_{suph}	[°C]	0.1	0.1	0.1	0.2	1.1	17.1	37	14.5
$T_{exh,out}$	[°C]	/	/	/	/	/	/	/	130

Tab. 60. Mono-objective SIC minimization (baseline engine ORC). Cases results overview (case study 4)

Generally, from the reported data, it is possible to observe a higher SIC when designing all the systems at B50 rather than at C100 operating point. This mainly because of the lower achievable power output, compared to the still required investment costs (PEC), which are anyway higher at C100, due to the bigger components to recover and transform more heat into power.
With the proposed assumptions, the systems with a turbo-expander (cases 2-4-7) and DC heat sink (2-4) are showing lower SIC values, due to the higher pressure ratio (PR) achievable and thus higher expected expander efficiencies and power. Generally, however, they also require higher investment costs (PEC), mostly due to the more expensive turbo-expander compared to a piston one.
The system with ethanol, piston expander and DC heat sink (case 6) is able to achieve low SIC levels without the need of condensing below ambient pressures. This can be envisaged at both C100 and B50 operating points. However, a piston expander with high expansion ratios (PR=29.1) must be developed. Moreover, the heat exchanger performance when using ethanol, in terms of overall heat transfer coefficient, have been considered, in first approximation, the same of toluene, because of the scarse literature data available. Further investigations about the systems with ethanol are required, using more appropriate heat transfer correlations and accurate heat exchangers models, since the system seems to show, at least in this preliminary analysis, promising performance and cost trade-off.
In case of ethanol, piston expander and IC heat sink (case 5) the trade-off is not as good, but the lower pressure ratios achieved for both operating points seem to be more compatible with traditional piston expansion machines.
Generally, if a piston expander with high performance (70% isentropic efficiency) over a wide range of expansion ratios (7 to 30) is available, or can be developed, this could be the best choice, because of the cheaper expansion machine with lower controllability issues (wet expansion tolerated) compared to a turbo-expander.
In the case of the system with indirect exhaust-to-coolant strategy (case 8), higher SIC values are expected, compared to the concepts with direct exhaust gas recovery. Indeed, especially at C100, the net power output achievable is not comparable to the one that can be achieved with the other systems, even though the investment cost (PEC) is comparable or even lower (cheap scroll expander). At B50, however, the system becomes more interesting in terms of performance and cost trade-off, even if with still higher SIC values compared to the other concepts. Additionally, the indirect exhaust-to-coolant concept can be considered safer in operations, due to the cooling circuit interposed between the exhaust gas and the ORC working fluid. The R1233zd(E) shows also lower flammability issues compared to the alcohols or hydrocarbons used for direct exhaust gas recovery. The coolant circuit acts also as an energy “buffer” which dampens the fluctuations of the exhaust thermal power recovered (the exhaust temperature and mass flows levels are very dependent on the engine operating point which varies over the drive-cycle). This means a generally lower ORC power output expected, due to the lower heat source temperatures, but, at the same time, a stable expected performance during several engine operating conditions, with lower controllability problems.
All these considerations lead to the possible choice of the indirect exhaust-to-coolant concept when opting for a more conservative and precautionary design approach, which prefers a constant lower power output and safer operations, compared to higher performance, but flammability and controllability issues.
The water system (case 7) can be also safer in operations, and shows higher performance, however, due to the higher expansion ratios expected, even just with an IC heat sink configuration, a turbo-expander is probably required. A high level of superheating leads also to a bigger evaporator with packaging issues. At B50 however, more reasonable expansion ratios levels could lead to a piston-expander choice, thus decreasing the costs.
A multi-objective optimization, considering a combined maximization of net power output and minimization of PEC and SIC can also be proposed, generally leading to lower ORC net power output in order to contain the SIC and investment costs values. Decisional criteria, as an MCDM, are needed in this case in order to choose the best design fulfilling the developer’s requirements.

However, if a difference of around 1000 $ of systems' PEC values can be considered acceptable in the final choice, a simpler mono-objective optimization with SIC minimization is suggested.
An example of multi-objective optimization has been reported in the next sub-section, regarding a thermo-economic analysis approach.

Thermo-economic Multi-Objective Optimization

The goal of the proposed thermo-economic optimization example is to compare the various concepts trying to ensure a high level of power output but limiting the cost rates values related to the "useful" power production and those "wasted" in irreversibilities production, in order to obtain a performant but cheap-in-operation system.
Moreover, when average investment costs cannot be avoided, it is generally important, from an efficiency point of view, to try to have a positive trade-off between costs "invested" in the production of power and costs "wasted" in the production of irreversibilities (or un-useful streams).
In the proposed thermo-economic optimization, still the most important objective is to maintain a high power output level, otherwise the investment makes no sense. For this reason, when applying a MCDM (Multi-Criteria-Decision-Making) procedure, associating different decisional weights to the three main objectives, the power output has still been privileged over the other two objectives: minimum net power cost rate ($\dot{C}_{power}$) and minimum irreversibilities "wasted" cost rate ($\dot{C}_{irr}$). For this purpose, a linear MCDM algorithm has been applied in modeFrontier, considering as weighting factors *50%* for the power output and *25%* for each cost rate. This allows to fix a quantitative criterium in order to assess the various designs forming the Pareto front, in order to choose the best one and compare the different simulated cases. An example of Pareto front obtained from the modeFrontier optimization of case 1 (toluene, IC heat sink and piston expander at C100) has been reported in Fig. 123.
The criterium allows also to ensure a high power output, which otherwise would be too low when deciding to give more important to the minimization of the cost rates, which are, indeed, directly correlated to the amount of power and irreversibilities produced.

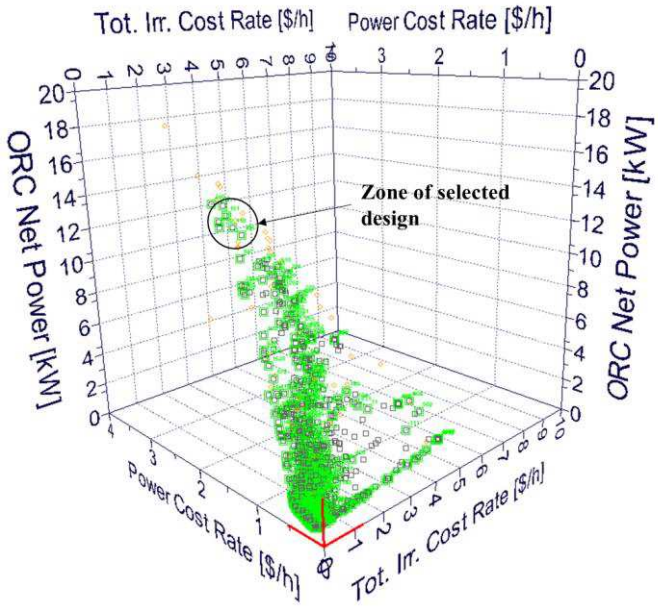

Fig. 123. Example of Pareto front output for case 1 at C100 (case study 4)

The results of the optimization and the MCDM weighted choice have been reported in Fig. 124.

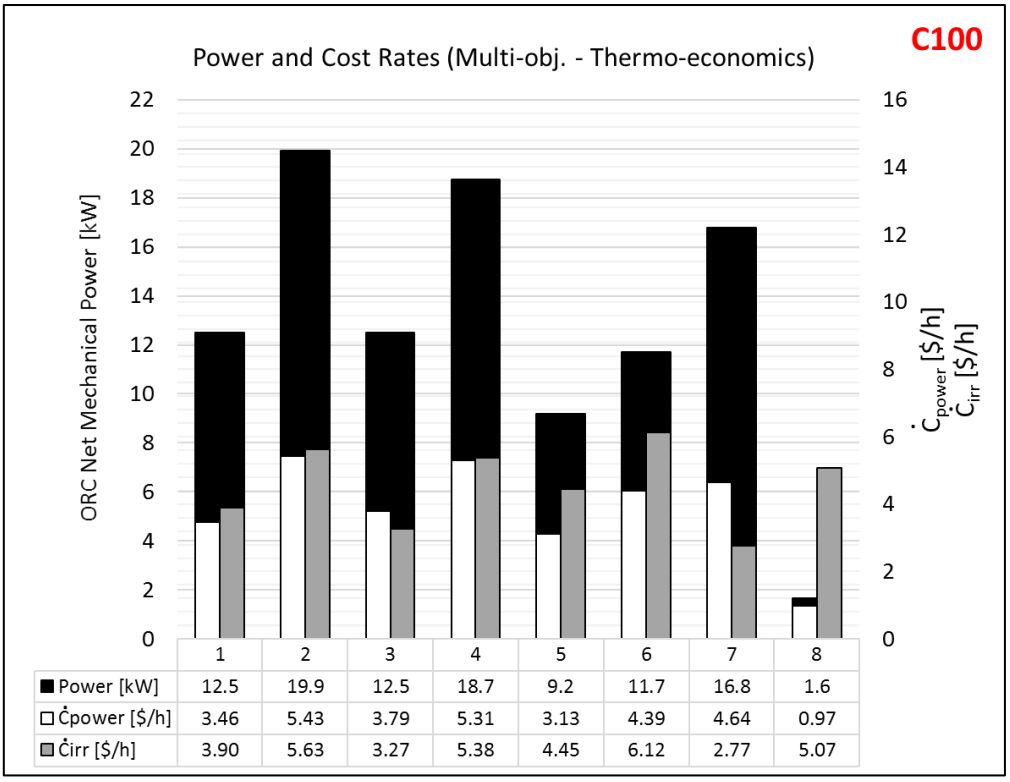

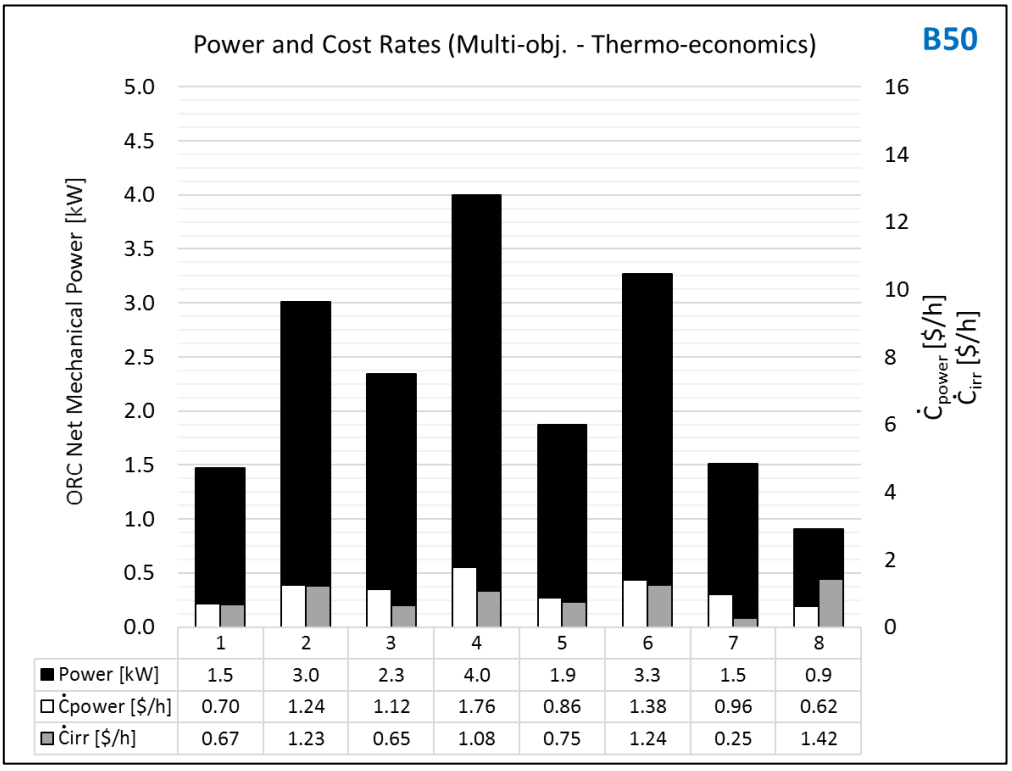

Fig. 124. ORC multi-objective thermo-economic optimization. C100 and B50 (case study 4)

As done for the case of SIC minimization (techno-economics) the overall results have been reported, also for the thermo-analysis in Tab. 61.

Case		1	2	3	4	5	6	7	8
Fluid		**toluene**	**toluene**	**toluene**	**toluene**	**ethanol**	**ethanol**	**water**	**R1233zd(E)**
Layout		**Simple**	**Simple**	**RECP**	**RECP**	**Simple**	**Simple**	**Simple**	**Indirect Exhaust-Coolant**
Heat Sink		**IC**	**DC**	**IC**	**DC**	**IC**	**DC**	**IC**	**DC**
Expansion Machine		***piston***	***turbo***	***piston***	***turbo***	***piston***	***piston***	***turbo***	***scroll***
C100									
BSFC Impr.	[%]	5.9	9.1	5.9	8.6	4.4	5.7	7.8	0.8
SIC	[$/kW]	318	240	355	298	424	279	270	2101
PEC (ORC)	[$]	3971	4773	4435	5584	3898	3268	4529	3465
$\dot{m}_{wf}$	[kg/s]	0.173	0.166	0.173	0.207	0.137	0.085	0.039	0.207
p_{cond}	[bar]	1.68	0.50	1.68	1.14	5.09	1.32	2.20	3.94
PR	[-]	14.2	41.4	14.2	19.7	5.1	19.4	23.4	1.9
ΔT_{suph}	[°C]	35.6	42.3	35.6	22.8	14.4	45.1	48.7	8.8
$T_{exh,out}$	[°C]	/	/	/	/	/	/	/	262
B50									
BSFC Impr.	[%]	2.1	4.1	3.2	5.4	2.6	4.4	2.1	1.3
SIC	[$/kW]	2280	1164	1695	1043	1766	900	2416	3731
PEC (ORC)	[$]	3360	3501	3974	4169	3299	2944	3644	3391
$\dot{m}_{wf}$	[kg/s]	0.031	0.042	0.048	0.046	0.03	0.025	0.004	0.143
p_{cond}	[bar]	2.41	1.11	1.34	0.50	5.16	1.20	1.35	4.03
PR	[-]	5.7	11.5	7.63	22.8	5.2	29	22.2	1.7
ΔT_{suph}	[°C]	47.2	18.2	1.9	1.4	0.1	9.5	44.5	9.1
$T_{exh,out}$	[°C]	/	/	/	/	/	/	/	228

Tab. 61. Multi-objective power and thermo-economic optimization. Cases results overview (case study 4)

When proposing this type of optimization, the ORC net power output results slightly reduced compared to the case with SIC minimization, in order to contain the cost rates associated to power production and irreversibilities.

The concepts with simple cycles and piston expander generally show lower, in terms of absolute values, power and irreversibilities cost rates, due, mostly, to the lower investment costs required, compared to recuperated cycles or the systems with a turbo-expander. Also, higher power output requires bigger components and higher investment costs and cost rates. An adequate combination of the main independent variables can, however, generate improved trade-offs.

At C100, most of the concepts, but the one running on water (7) and the one with toluene, recuperator and IC configuration (3), show higher cost rates "wasted" in irreversibilities than those invested in the production of power. This mostly because of the generally low First and Second Law efficiency of the ORC systems, which recover a high amount of energy (or exergy) to produce a low amount of useful mechanical power. Water and toluene (this last one in recuperated configuration), show better compromises because of their higher efficiencies when recovering high temperature heat sources.

The trade-off between power and irreversibilities cost rates is generally better (in favour of the power, or at least with similar cost rates) at B50. Investment costs and streams absolute values are also generally lower at B50 than at C100.

The recuperated cycles (3-4) show generally a better trade-off between the two cost rates, especially at B50, but also at C100. The recuperator, indeed, has the effect of improving the system efficiency and reducing the exergy destruction terms.

For the ethanol systems at C100, the cost rates "wasted" in irreversibilities are generally much higher than those invested in the generation of power. However, at B50, the situation reverses. Indeed, a fluid as ethanol is probably more suitable for B50 typical exhaust gas temperature levels (truck cruise conditions), while toluene and water are probably better for C100 levels (high loads operations). This is probably the reason why ethanol is one of the most considered fluids for ORC on-highway

applications, in which cruise operational points around B50 are expected, and toluene has more applications for stationary heat recovery.
The same considerations, in terms of safety and flammability, introduced in the previous optimization case, are still valid.
Finally, also from a thermo-economic (and Second Law) point of view, the indirect exhaust-to-coolant system (8), is very inefficient. The power production is, indeed, very low compared to the other concepts, especially at C100. The compromise between power and irreversibilities cost rates is also very negative, with most of the costs "wasted" in irreversibilities (or to rejected exergy streams not reported in the graphs, such as coolant and cooling air). The system is, indeed, very dissipative, recovering exhaust gas exergy just to transfer it to the coolant and the cooling air, or destroying it in the components (in particular the very dissipative exhaust-to-coolant heat exchanger, in which the bad thermal match between the fluids' streams is introducing a high amount of irreversibilities).
At B50, however, the compromise becomes more comparable to the other systems, leading to low cost rates and less negative trade-offs.
The indirect exhaust-to-coolant system has, however, cost rates in the absolute values ranges comparable to those of the other systems. This means that, even if generally the system is quite inefficient in terms of power production, the solution can still be rather cheap, or at least comparable, in terms of investments, to the others. This even more when considering the B50 point, in which the system's power output is more similar to those of the direct exhaust recovery systems. For this system, the positive considerations reported in the previous section, regarding safety, low flammability and expected stable power output at different engine operating points, are still valid.

6.4.4.4 Insulated Exhaust Manifolds Strategy – Engine Results

In order to show the benefits of a possible combined engine-ORC simulation approach, a new simulation campaign has been carried out considering a realistic level of insulation of the engine exhaust manifolds, between the engine exhaust ports and the turbocharger turbine.
The insulation strategy has been simulated imposing to "0" the wall heat transfer coefficient multiplier in the WAVE model for the pipes and junctions representing the exhaust control volume (Fig. 125). This reduces the heat transfer, but it is not representing a complete, and non-realistic, insulation because of the pipes conduction model still switched on.
The expected effect of this strategy is to decrease the heat losses (and their associated energy and exergy streams) in the exhaust manifolds, leading to an increased exhaust gas thermal power and exergy available to be recovered by a tailpipe ORC. An increase in exhaust gas temperature is indeed expected, allowing to increase the ORC performance.
From the performed simulations, no effect has been envisaged regarding the engine block heat rejection, thus not affecting the energy and exergy streams transferred to coolant and oil circuits. For this reason, the coolant boundary conditions for the ORC concepts with IC heat sink configurations and the case 8, have been kept the same.
Moreover, the turbine inlet temperature has been monitored, showing a peak of around 730°C at 100% Load and 1450 rpm, with all other simulated points showing lower temperature levels, this being generally compatible with safe turbocharger operations.

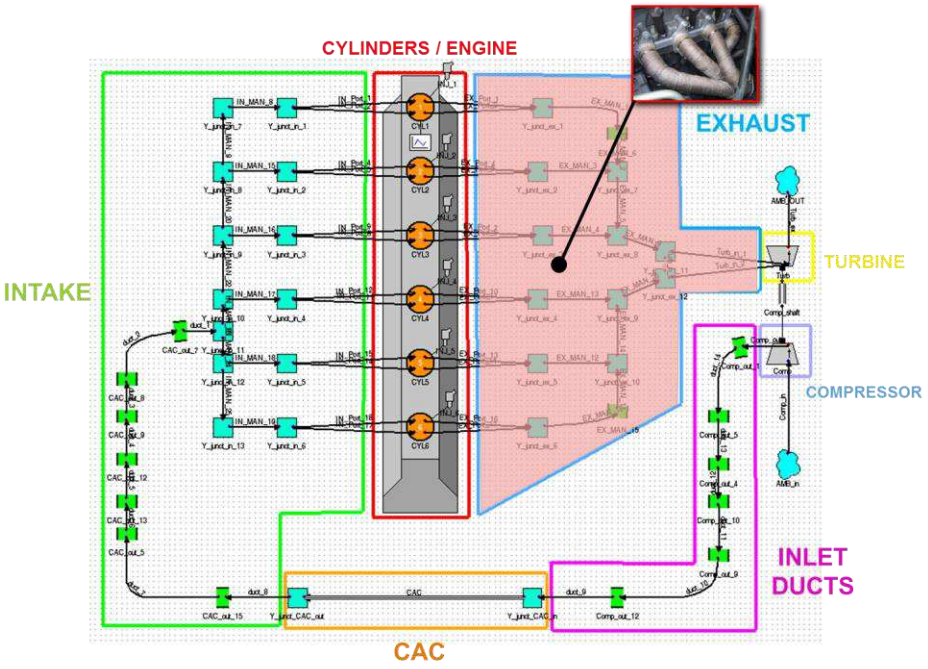

Fig. 125. Insulated engine exhaust manifolds strategy (case study 4)

The effects of the proposed strategy, on the engine side, have been reported in the next graphs.
In particular, considering a *First Law analysis* (Fig. 126 and Fig. 127) it is possible to observe that part of what in the baseline model was considered energy "Pipes Losses", mainly concentrated in the high temperature exhaust manifolds, are now becoming "Exhaust Thermal Power" available in the exhaust gas. Around 2.7% thermal power increase in the exhaust gas can be observed for the C100 operating point, while 2.5% for the B50. This is reflected in around 13.9 kW additional thermal power in the exhaust at C100 and 4.4 kW at B50. This is mostly due to an increase of around 35°C of the exhaust gas temperature after the turbine at C100, and 24°C at B50.

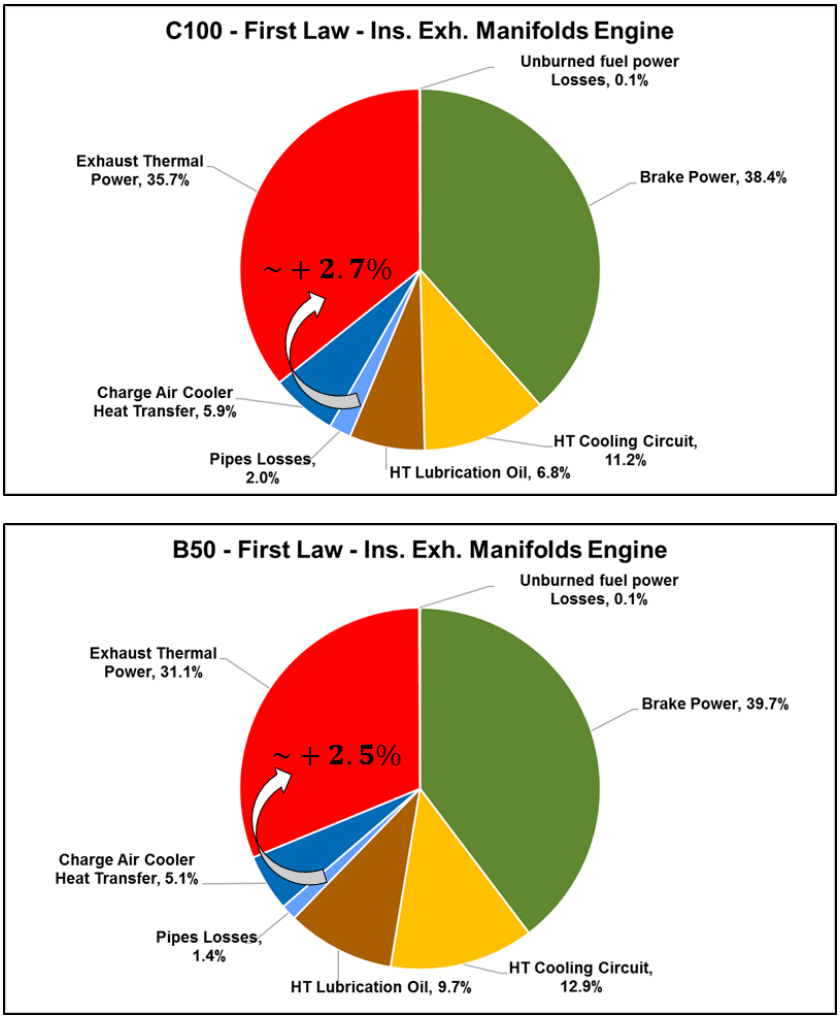

Fig. 126. Percentages distribution of the various energy streams of the engine with insulated exhaust manifolds strategy at C100 and B50 operating points (case study 4)

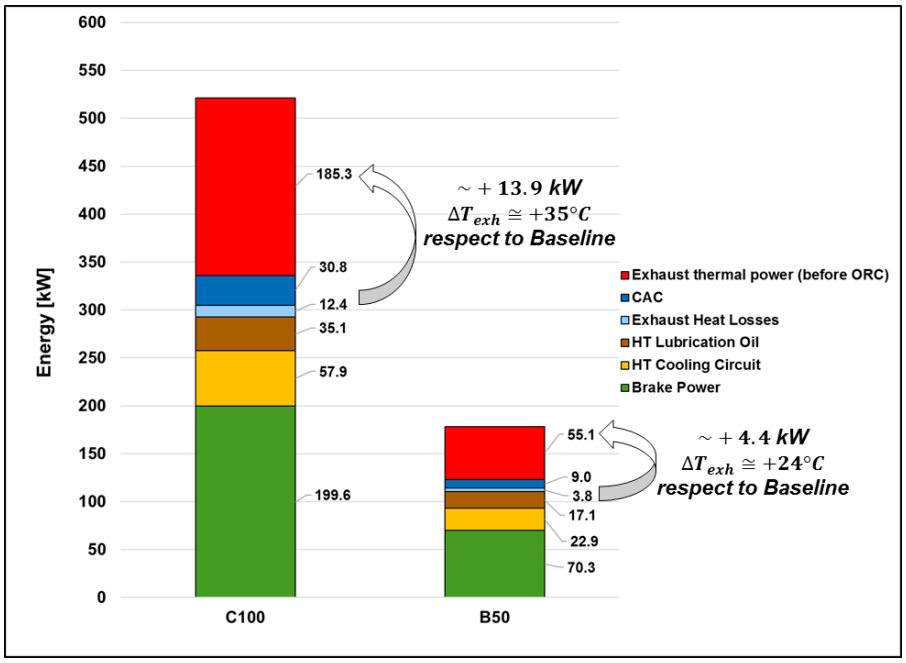

Fig. 127. Energy streams breakdown analysis for the engine with insulated exhaust manifolds strategy at C100 and B50 operating points (case study 4)

Similar results can be obtained also from a *Second Law analysis* point of view (Fig. 128). In this case, to keep the report shorter, only one chart, with the exergy breakdown analysis has been reported.
The effect of the insulated exhaust manifolds strategy is to decrease the availability losses in the exhaust pipes and junctions forming the engine exhaust control volume, and to increase the availability that can be recovered from the exhaust gas using an ORC.
Turbine and exhaust manifolds control volumes irreversibilities are also slightly increasing (+0.1% compared to the baseline engine case), even though the main effect is for sure the increase of the exhaust gas exergy (+1.6% for the C100 operating point and +1.2% for the B50).

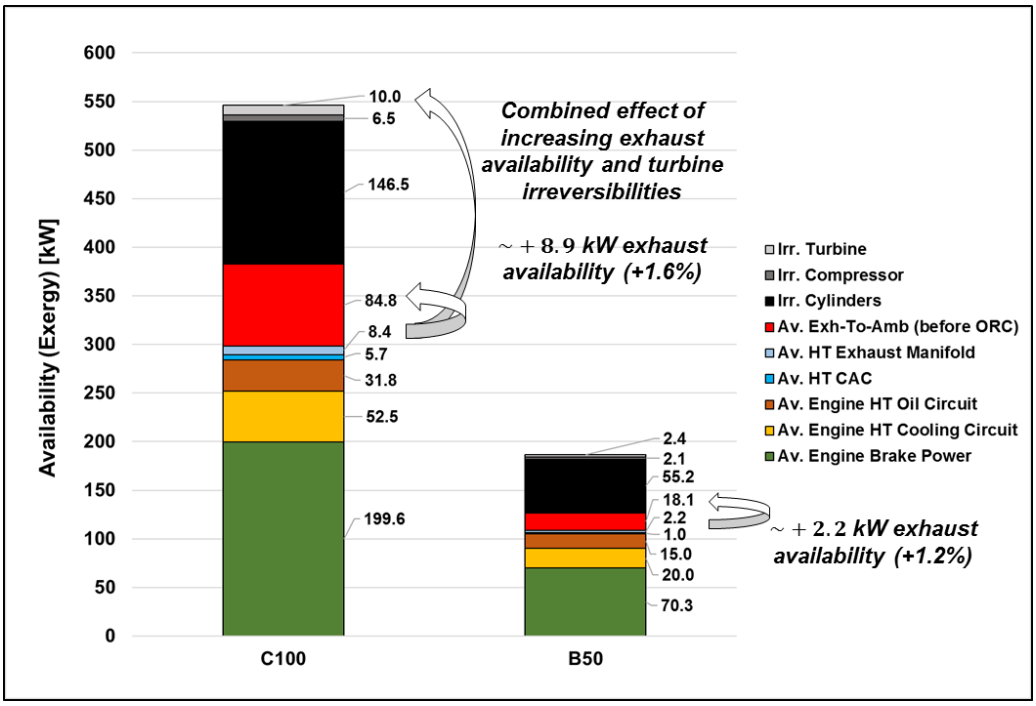

Fig. 128. Exergy [kW] streams overview for the engine with insulated exhaust manifolds strategy at C100 and B50 operating points (case study 4)

6.4.4.5 ORC Optimization (Insulated Exhaust Manifolds Engine)

A new optimization campaign has been carried out, in order to show the possible effect of insulating the engine exhaust manifolds together with the exhaust gas recovery using an ORC.
Considering that, as already mentioned, a multi-objective optimization with MCDM leads to the need of a choice from the developers' side to address the best configuration, which is not very often straight-forward, it has been decided to minimize the SIC, in order to have just one objective, which can be easily compared with the case with baseline engine without insulation.
The optimization has been again carried out for all the 8 ORC cases. Finally, just for the case 1 (simple cycle, toluene, IC heat sink and piston expander), the complete results of the overall methodology, considering energy, exergy, techno and thermo-economic considerations, have been reported as an example in section 6.4.4.6, in order to demonstrate the quality and quantity of information that can be extracted from the proposed combined approach.
The results of the new SIC minimization have been reported in Fig. 129, considering also a comparison with the cases with baseline engine, without insulation.

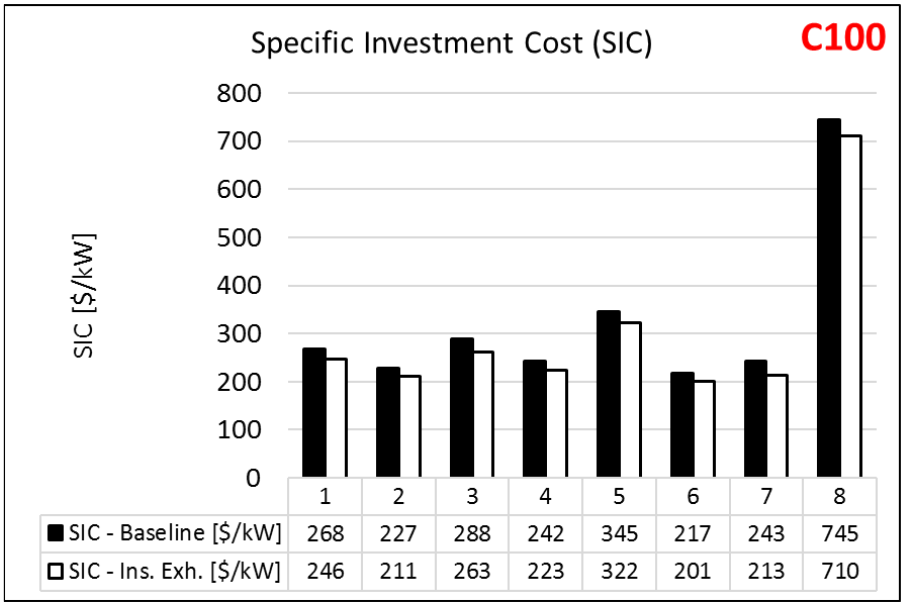

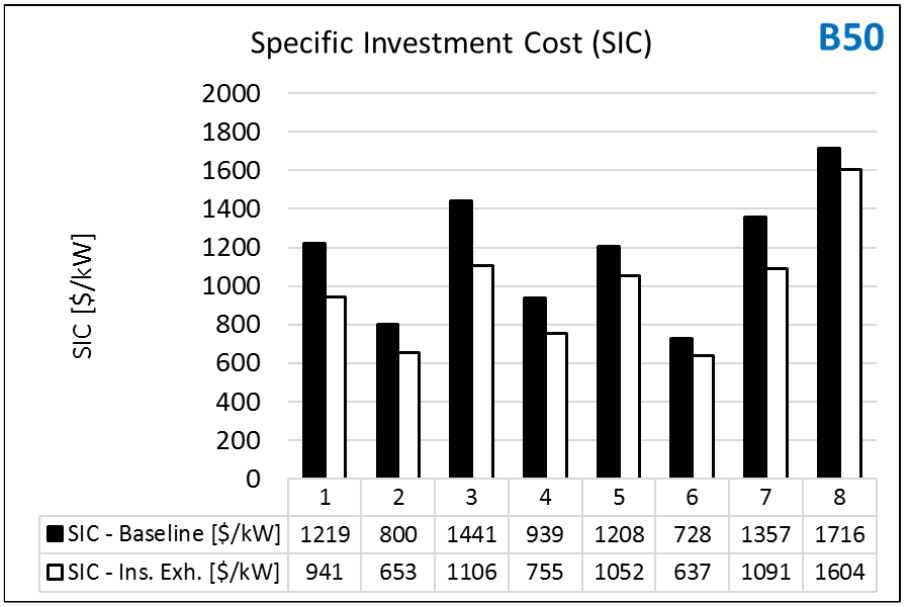

Fig. 129. ORC SIC minimization (engine with insulated exhaust manifolds). C100 and B50 engine operating points – Techno-economic analysis (case study 4)

All the main data related to the simulations carried out with SIC minimization and engine insulated exhaust manifolds strategy have been grouped in a unique format in Tab. 62. The data related to the baseline simulations can be observed in the previously reported Tab. 60.
In the proposed table, the comparisons in terms of relative percentage differences can be observed, showing the benefits of the insulation strategy both in terms of achievable power output and specific investment cost.
The insulated exhaust manifolds strategy leads also to a general increase of the heat which must be rejected from the ORC to the vehicle cooling package ($\Delta\dot{Q}_{out}$), because of the higher ORC heat recovery (and rejection). This issue must be assessed when analysing the overall vehicle performance. However, generally, at the B50 cruise operational point, the heat rejection is much lower than at C100. Active cooling packages systems, taking profit of the vehicle aerodynamics developments are also under research.

Case		1	2	3	4	5	6	7	8
Fluid		**toluene**	**toluene**	**toluene**	**toluene**	**ethanol**	**ethanol**	**water**	**R1233zd(E)**
Layout		**Simple**	**Simple**	**RECP**	**RECP**	**Simple**	**Simple**	**Simple**	**Indirect Exhaust-Coolant**
Heat Sink		**IC**	**DC**	**IC**	**DC**	**IC**	**DC**	**IC**	**DC**
Expansion Machine		***piston***	***turbo***	***piston***	***turbo***	***piston***	***piston***	***turbo***	***scroll***
C100 (Insulated Exhaust Manifolds)									
$\dot{W}_{ORC,net,mech}$	[kW]	16.8	23.9	18.4	26.6	12.2	18.4	23.0	5.3
BSFC Impr.	[%]	7.7	10.7	8.5	11.8	5.8	8.4	10.3	2.6
PEC (ORC)	[$]	4127	5041	4840	5949	3938	3690	4902	3738
$\dot{m}_{wf}$	[kg/s]	0.205	0.202	0.226	0.212	0.137	0.125	0.044	0.645
p_{cond}	[bar]	1.24	0.50	1.28	0.50	4.69	1.20	2.00	4.34
PR	[-]	28.3	69.9	27.3	69.9	7.4	29.1	41.8	1.9
ΔT_{suph}	[°C]	8.0	1.9	9.9	13.3	33.3	33.2	75.3	16.5
$T_{exh,out}$	[°C]	/	/	/	/	/	/	/	130
Comparisons with Baseline (C100) – Refer to Tab. 60									
ΔSIC	[%]	-8.1	-7.1	-8.9	-7.9	-6.6	-7.7	-12.3	-4.7
$\Delta\dot{W}_{ORC,net,mech}$	[%]	+8.4	+9.1	+9.4	+9.8	+7.2	+8.8	+16.0	+5.5
ΔPEC (ORC)	[%]	+0.4	+2.3	+0.5	+2.1	+0.6	+1.2	+4.4	+0.8
$\Delta\dot{Q}_{out}$	[%]	+9.1	+9.1	+10.7	+7.9	+9.1	+8.8	+14.2	+17.5
B50 (Insulated Exhaust Manifolds)									
$\dot{W}_{ORC,net,mech}$	[kW]	3.7	5.7	3.7	5.8	3.4	4.9	3.5	2.2
BSFC Impr.	[%]	5.0	7.6	5.0	7.7	4.6	6.5	4.7	3.0
PEC (ORC)	[$]	3504	3753	4115	4407	3538	3088	3813	3547
$\dot{m}_{wf}$	[kg/s]	0.061	0.059	0.060	0.063	0.041	0.034	0.009	0.263
p_{cond}	[bar]	1.20	0.50	1.20	0.50	4.10	1.20	1.60	3.47
PR	[-]	12.6	32.6	13.1	27.8	8.5	29.1	15.1	2.00
ΔT_{suph}	[°C]	0.1	0.1	0.1	0.1	7.5	27.6	81.5	7.1
$T_{exh,out}$	[°C]	/	/	/	/	/	/	/	
Comparisons with Baseline (B50) – Refer to Tab. 60									
ΔSIC	[%]	-22.8	-18.5	-23.2	-19.6	-12.9	-12.6	-19.6	-6.5
$\Delta\dot{W}_{ORC,net,mech}$	[%]	+33.2	+26.5	+33.1	+28.1	+18.2	+15.1	+26.7	+8.1
ΔPEC (ORC)	[%]	+2.8	+3.2	+2.2	+3.0	+3.0	+0.6	+1.9	+1.0
$\Delta\dot{Q}_{out}$	[%]	+19.0	+11.4	+15.9	+9.2	+16.6	+11.7	+16.4	+9.4

Tab. 62. Overall results for the ORC cases with engine insulated exhaust manifolds strategy. Comparisons with the baseline engine cases for C100 and B50 operating points (case study 4)

The case (6), with ethanol, piston expander and DC heat sink configuration, seems to have the best compromise in terms of SIC, at the same time allowing to still condense above ambient pressure (no need of effective sealing against air infiltration). The piston expander is also cheaper compared to a turbo-expander. However, as previously introduced, the heat exchangers performance have been estimated considering the same assumptions used for the systems with toluene (which is a hydrocarbon). More detailed investigations are needed, as already mentioned in the previous optimization campaign.

The case (7), with water, turbo-expander and IC heat sink configuration, leads also to good results, and in particular to a high SIC improvement when insulating the exhaust manifolds (especially at C100 with higher temperatures). Indeed, water is a fluid which is typically suitable for higher temperature heat recovery (as toluene is). Higher investment costs compared to most of the other systems are mostly due to the high turbo-expander machine cost and the bulkier evaporator.

Recuperated systems (3-4) are efficient in terms of power production, but generally more expensive in terms of investment. Systems with high power output (> 20 kW) tend also to recover and reject more

heat compared to other systems, thus probably creating issues for heat rejection in the cooling package. Ricardo's approach tends to limit the ORC power to 18-20 kW, by-passing the evaporator in case of higher expected heat recovery conditions. However, generally, recuperated systems are recovering (and rejecting) a proportionally lower amount of heat, for the same power production, compared to non-recuperated one, creating less problems to the vehicle cooling package, but introducing an additional heat exchanger, with weights and packaging issues.

After water systems, the systems showing better improvements in terms of SIC, using an insulated exhaust manifolds strategy, seem to be those with toluene and IC heat sink configuration, both simple and recuperated (1-3). Indeed, also toluene is a fluid showing benefits for high temperature heat sources recovery, and the insulation of the manifolds tends to increase the exhaust gas temperature, being this beneficial for these kinds of high-temperature suitable fluids.

As can be evinced from the percentage differences reported in Tab. 62, the best relative improvements in terms of SIC reduction, and generally increased power output, between the baseline case and the case with insulated exhaust manifolds can be observed for the B50 operating point (mid-load / mid-speed), in which an increase of around 24°C of the exhaust gas temperature is showing benefits in terms of higher ORC performance, allowing the ORC system to be more efficient, due to the higher temperature level of the heat source.

A decrease of around 23% of the SIC can be observed, for example, in the cases 1 and 3, with toluene, IC heat sink and piston expansion machine. The values of cycle pressure ratios, especially at B50, are also compatible with operations using a piston expander machine, which is cheaper than a turbo-expander.

For these reasons, an insulated exhaust manifolds strategy is beneficial for a truck application, mostly running at B50 at on-highway cruise conditions, in which an increase of the heat source temperature leads to better performance.

At C100 the improvement in these two cases is still good (8-9%) but assuming that a piston expander is able to withstand high cycle expansion ratios still ensuring a high isentropic efficiency. This leads to the consideration that an expansion machine able to provide high efficiencies at difference cycle expansion ratios should be developed, possibly also with variable built-in expansion ratio, or a control of the optimal expansion ratio (though valves operations, or variable-expansion-ratio systems) in order to match the cycle required values. Costs could be slightly higher in this case and further studies are necessary.

The indirect exhaust-coolant system (8) shows again more comparable performance/cost trade-off with the other systems only at B50, while at C100 the other systems are definitely more worth the investment. Moreover, an engine exhaust manifolds insulation strategy leads, in this case, to results improvements not comparable to those of the other systems. As already introduced in the previous optimization campaigns, the system can still be a good choice when more stable power output is desired over different cycle operating points, when a generally low investment cost is required and when safer operations can be preferred over higher performance.

The SIC values obtained from the simulations are in line, at list in the range of values, with those estimated from Ricardo's analysis and other few literature sources available (e.g. [340,341]). Data from literature are, however, generally scarse in number.

In the next section, some results for a complete analysis, with energy, exergy, techno and thermo-economic considerations, have been reported, in order to show the quality and quantity of the information which can be retrieved with an approach as the one proposed in this thesis.

The results have been proposed just for the case 1, due to the large amount of data: simple cycle, running on toluene, with IC heat sink configuration and a piston expander.

The charts are related to the engine with insulated exhaust manifolds, but comparison have been reported, in terms of values, with the case with baseline engine, for reference (reported in parenthesis in the proposed tables).

6.4.4.6 Example of Complete Engine-ORC Analysis Results

The results have been divided, in the next sub-sections, for energy (First Law), exergy (Second Law), techno and thermo-economic analysis approaches, showing the different levels of information, which can be retrieved from the proposed combined methodology.

First Law Analysis

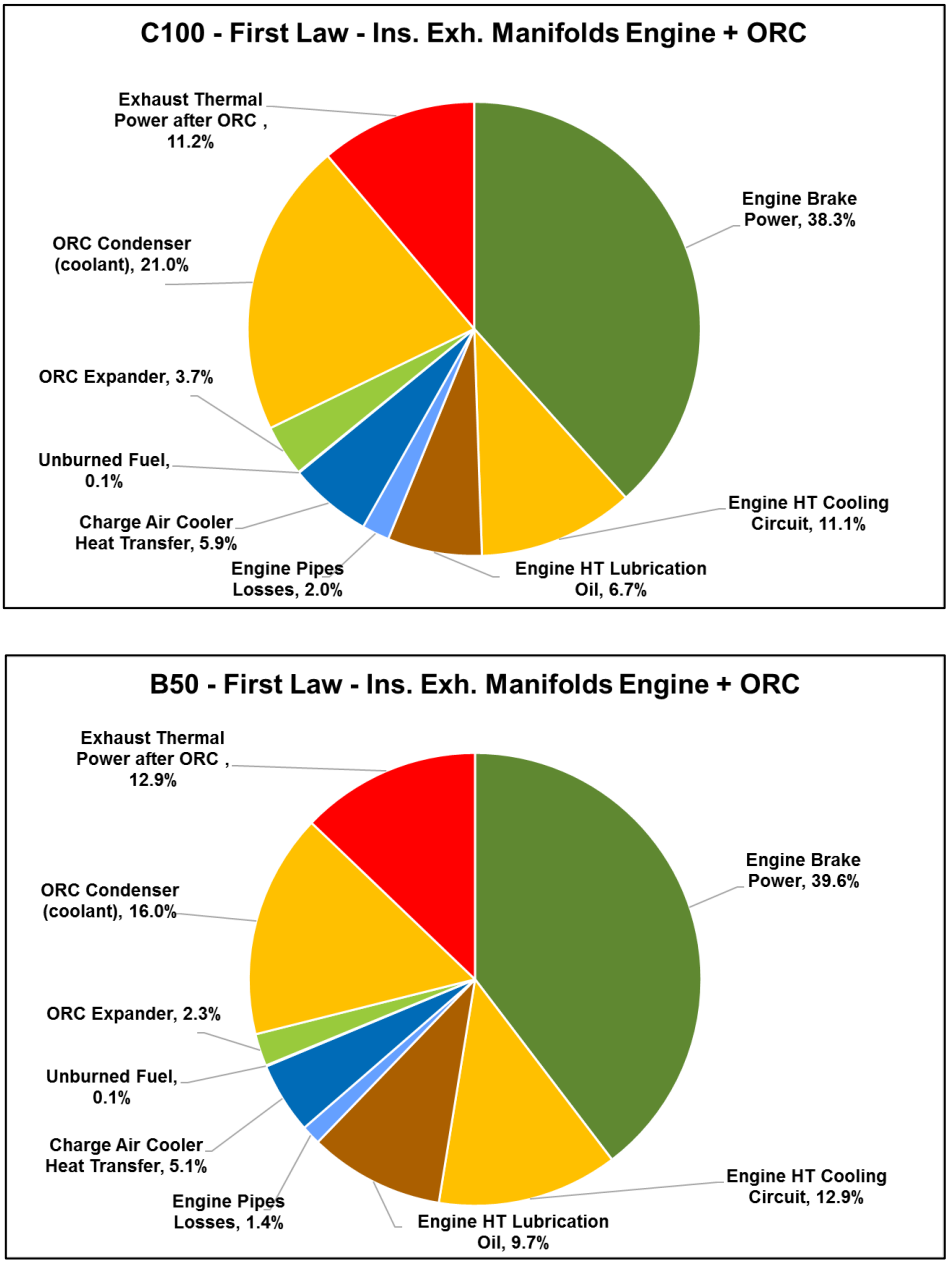

Fig. 130. Combined engine-ORC (insulated engine exhaust manifolds) First Law charts for ORC case 1 (case study 4)

As can be evinced from Fig. 130, the exhaust gas heat is recovered to produce additional power in the ORC system. In the case 1 proposed, with IC heat sink configuration, the heat recovered which in not converted in additional useful power in the ORC, is rejected to the engine coolant, which acts, in this case, as heat sink. This leads to an increase of the heat with must be rejected to the ambient from the

cooling circuit in the vehicle cooling package, leading to increased radiator dimensions required, or increased parasitic cooling fan consumption. In case of an ORC system with DC heat sink configuration, an additional condenser, of the AC-finned-tube type is needed in the vehicle cooling package.
Lower heat rejection issues are expected at B50, in which the heat recovered and rejected is lower.
A First Law analysis can be useful in order to assess all the energy flows in the combined powertrain and develop efficient thermal management strategies. A synergy with possible oil, cooling and AC circuits simulations could also be considered, when embedding the methodology in a complete, user-friendly and advanced-modelling capable platform.
The energy breakdown analysis for the main energy streams of the combined engine-ORC powertrain has been reported in Fig. 131, while in Tab. 63, the percentages of useful outputs (UPS, Useful Power Streams) and Rejected Streams (RS, energy streams not producing useful work) have been calculated. The values in parenthesis are referred to the baseline engine case. The data reported demonstrates a slight improvement in percentage in terms of power production using an insulated manifolds strategy. This means that more of the fuel chemical energy is converted in useful net power output, with increased overall system thermal efficiency.

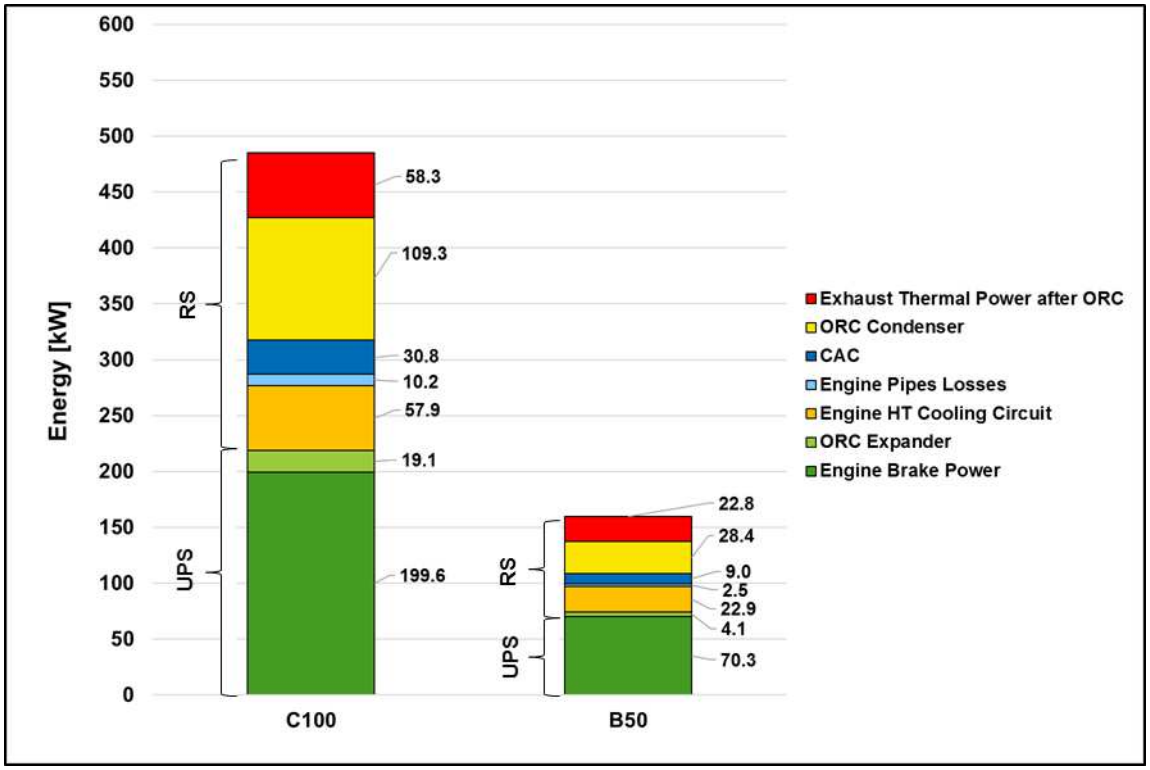

Fig. 131. Energy streams breakdown analysis for the combined engine-ORC system (insulated engine exhaust manifolds strategy) for the ORC case 1 (case study 4)

Operating Point	C100	B50
Useful Power Streams (UPS)	42% (41.7%)	42% (41.4%)
Rejected Streams (RS)	58% (58.3%)	58% (58.6%)

Tab. 63. Percentages split between useful and rejected energy streams of the combined engine-ORC system for ORC case 1 and insulated manifolds strategy (case study 4)

Second Law Analysis

The exergy percentage charts, for the combined engine-ORC system and C100 and B50 operating points, have been reported in Fig. 132.

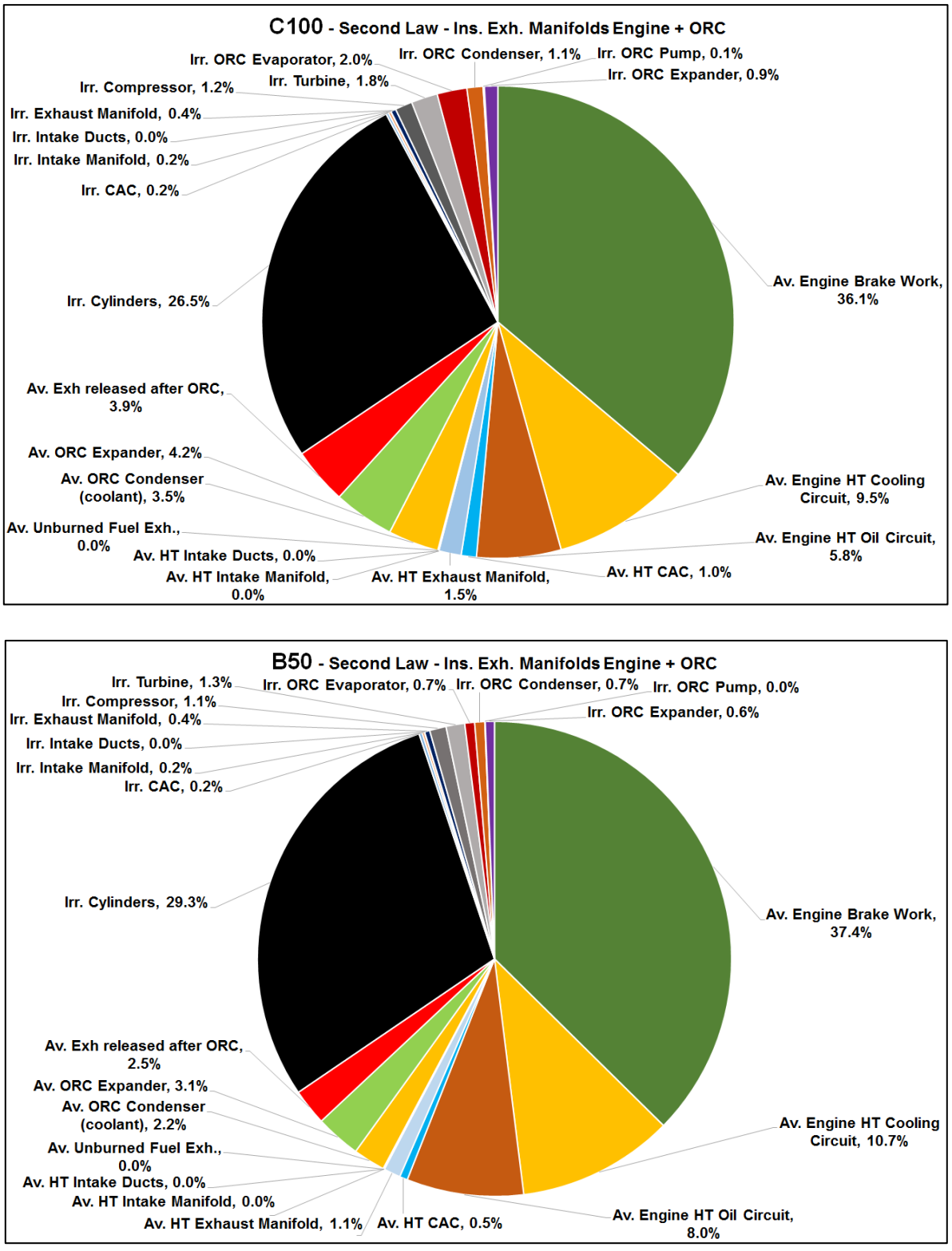

Fig. 132. Combined engine-ORC (insulated engine exhaust manifolds) Second Law charts for ORC case 1 (case study 4)

The Second Law analysis results demonstrate how not only useful power output and rejected streams can be allocated, but rather, part of the chemical exergy introduced with the fuel is destroyed due to the system's irreversibilities.
The irreversibilities, which can be thought as system inefficiencies, concentrate mostly in the engine cylinders, due to the combustion process and valves throttling, in the turbocharger, in the engine exhaust manifolds and, for the ORC side, in the evaporator, condenser and expander.
As can be evinced from the pie charts reported, the overall combined system irreversibilities account for almost the same amount of the useful net power output, demonstrating how, in order to develop an efficient combined system, not only the ORC must be improved, but rather a big effort in the improvement of combustion strategies must be considered.
A more efficient turbocharger could also allow to reach the same boost benefits of the actual one but saving additional energy and exergy which can be further recovered in the exhaust gas.
An improvement in the heat transfer in the ORC evaporator and condenser could also allow to improve the system efficiency. Super-critical or trans-critical cycles, as well as the use of zeotropic mixtures, can improve the ORC performance. However, the high pressures required for the cycles running above the critical pressure, could create safety problems, especially for the systems with direct exhaust gas recovery. While zeotropic mixtures, even though also promising in terms of heat transfer performance, could lead to issues when leakage or composition change could create different behaviours than what forecasted.
Other exergy streams, as coolant, oil and CAC could also be considered as heat sources for a possible bottoming cycle but are generally difficult to exploit due to the low temperature levels. More complicated, cascaded (dual loop) cycles, are required in this case, increasing costs, reliability, packaging and weight issues. These more advanced architectures are probably more suitable for large marine and stationary applications.
The complete system exergy breakdown analysis has been reported in Fig. 133, again for the engine with insulated exhaust manifolds, and the ORC case 1 as an example.

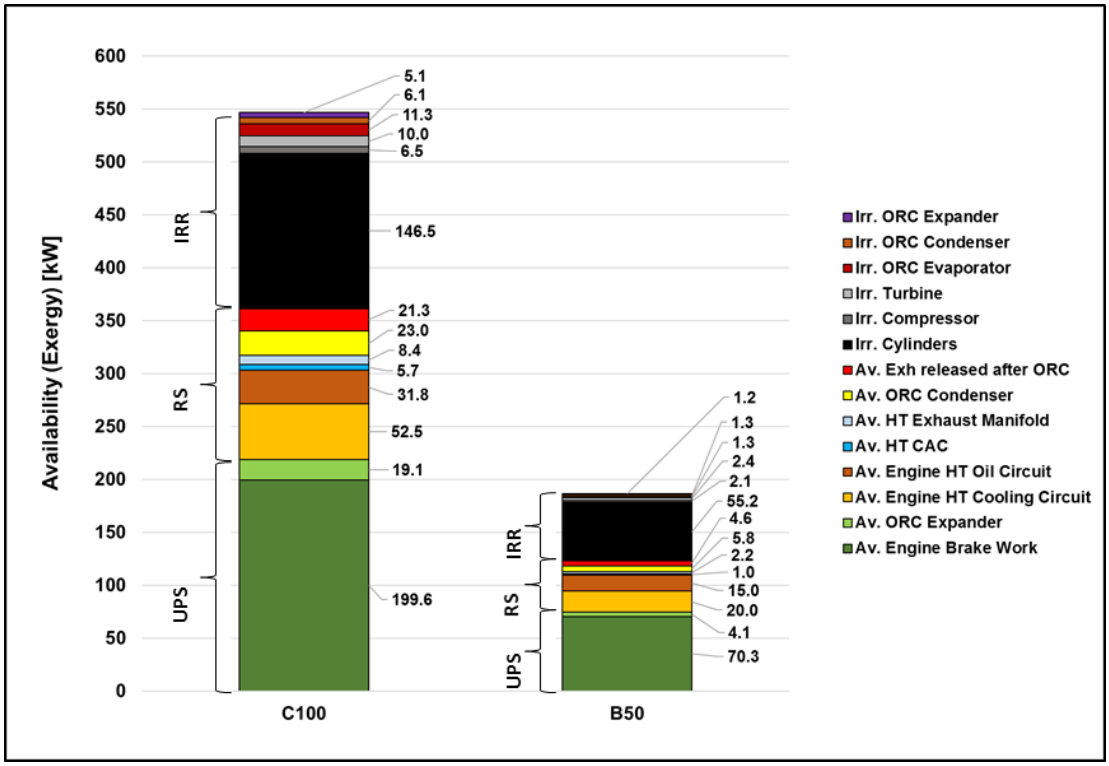

Fig. 133. Exergy streams breakdown analysis for the combined engine-ORC system (insulated engine exhaust manifolds strategy) for the ORC case 1 (case study 4)

In Tab. 64, the percentages of useful outputs (UPS, Useful Power Streams), Rejected Streams (RS, exergy streams not producing useful work) and irreversibilities (IRR) have been calculated. The values in parenthesis are referred to the baseline engine case.

Operating Point	C100	B50
Useful Power Streams (UPS)	39.7% (39.4%)	39.6% (39.0%)
Rejected Streams (RS)	25.9% (26.9%)	25.9% (26.9%)
Irreversibilities (IRR)	34.4% (33.7%)	34.5% (34.1%)

Tab. 64. Percentages split between useful, rejected exergy streams and irreversibilities of the combined engine-ORC system for ORC case 1 and insulated manifolds strategy (case study 4)

The values reported in the table show how the engine insulated exhaust manifolds strategy slightly improve the overall system performance compared to the baseline case (between parenthesis), in terms of higher power production and reduction of overall fuel chemical exergy percentage "wasted" in rejected streams. The strategy, however, increases also the percentage of exergy lost as irreversibilities, because of the higher irreversibilities produced.

Techno-economic Analysis

The Purchased Equipment Cost (PEC, [$]) breakdown analysis has been proposed in Tab. 65 and in Fig. 134, for the ORC systems (case 1) designed both at C100 and B50 operating points. In the tables, also the Specific Investment Cost (SIC, [$/kW]), and its improvement with the insulated exhaust manifolds, compared to the baseline engine case (between parenthesis), has been again reported.
The techno-economic analysis can give important information in order to design systems with a good compromise between performance and investment costs.
Due to the high heat recovery expected at C100, the evaporator leads to high investment costs when designing the system at this operating point. Moreover, valves, heat exchangers and expansion machine are generally the main voices of costs. In particular, as envisaged from Ricardo's analysis, valves are a non-negligible part of the system's costs.

Purchased Equipment Cost (PEC)		Operating Point	
		C100	***B50***
Fluid	[$]	102	102
Piping	[$]	230	230
Tank / Reservoir	[$]	290	290
Valves	[$]	750	750
Controls & Instrumentation + Additional Costs	[$]	230	230
Pump	[$]	133 (130)	78 (70)
Evaporator (Shell & Tube)	[$]	1017 (1026)	658 (586)
Condenser (Plate)	[$]	636 (634)	614 (612)
Expander + Mechanical Coupling (Piston)	[$]	739 (719)	551 (538)
Total PEC (ORC)	[$]	4127 (4111)	3504 (3408)
SIC (ORC)	**[$/kW]**	**246** (268)	**941 (**1219)

Tab. 65. PEC and SIC analysis for the ORC case 1, designed at C100 and B50 operating points with engine insulated exhaust manifolds (case study 4)

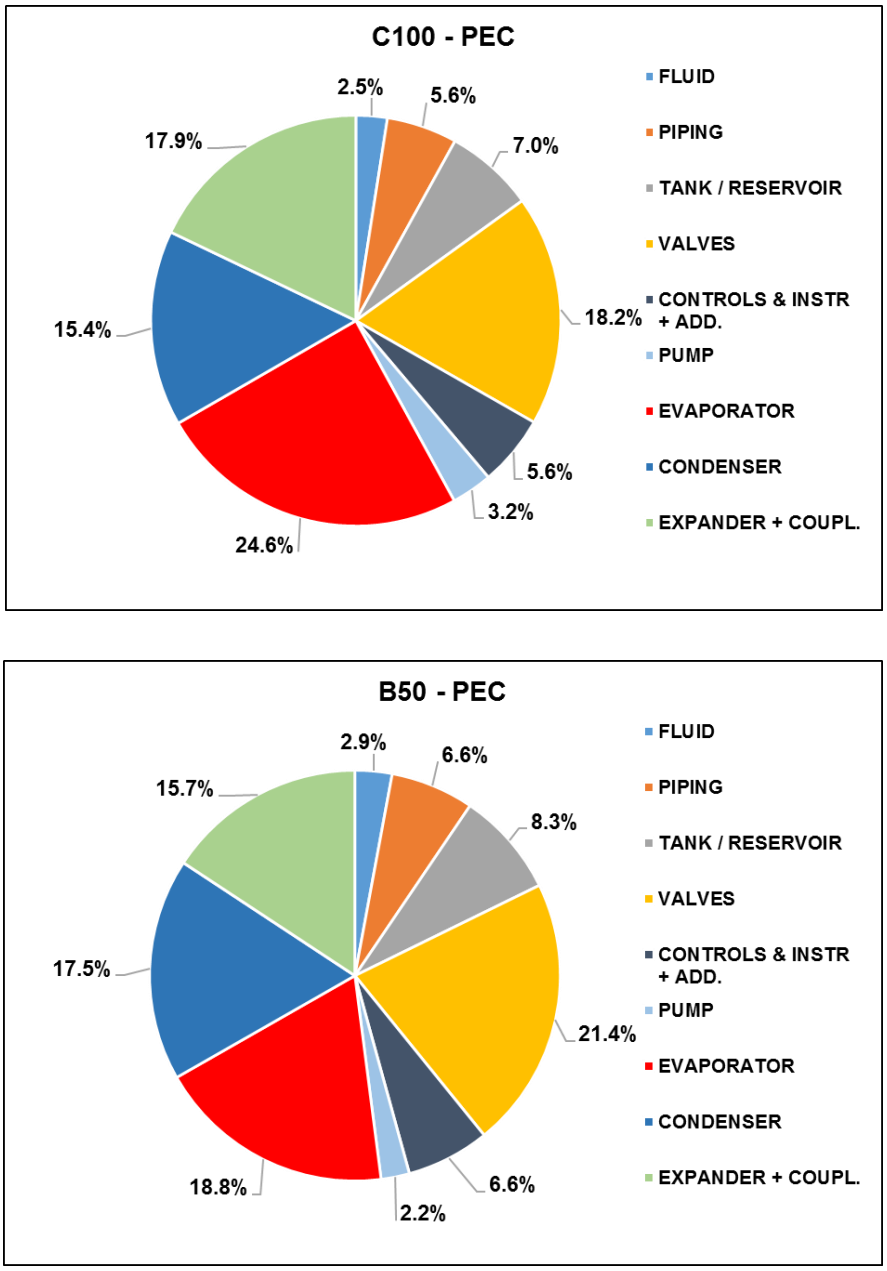

Fig. 134. PEC breakdown analysis for the ORC case 1, designed at C100 and B50 with engine insulated exhaust manifolds strategy (case study 4)

In the proposed work, as already mentioned previously, the topping engine has been evaluated as a "black box", considering just the entering and exiting streams, and an average PEC of 15000 € (17250 $ with the proposed 1.15 € to $ conversion rate). If adequate cost correlations would be available, also for all the engine main sub-components (e.g. engine block, turbocharger, CAC and so on), a similar approach, with a more detailed techno-economic analysis could be used, thus introducing another level of information in the common engine development approach.
Considering the engine fixed cost, and the results of the ORC analysis, the SIC values for the overall combined engine-ORC system can be estimated to be around 88 $/kW at C100 and 250 $/kW at B50.

Thermo-economic Analysis

As a last step, a thermo-economic analysis can be proposed, to understand the process of cost formation and the breakdown analysis of the cost rates for the several different exergy streams of the overall combined engine-ORC system.
It is important to reiterate that, in this case, levelized costs over a typical operational lifetime of the truck, have been calculated using the assumptions proposed in section 5.3.4.
The cost rates [$/h] breakdown analysis for the combined engine-ORC system has been reported in Fig. 135. In Tab. 66, the percentages split between cost rates invested for useful power production (UPS, Useful Power Streams), Rejected Streams (RS, as coolant, oil, heat losses, ORC cooling fluid, exhaust gas released) and irreversibilities (IRR) has been reported. Between parenthesis, again, the comparison with the baseline engine case without exhaust manifolds insulation. The insulation of the manifolds of the engine has been considered, in this case, a strategy which does not requires additional costs.
It is important also to state that, compared to a techno-economic analysis, which gives just an idea of the investment costs for the system, the thermo-economic analysis gives important hints to understand if the costs are really invested in the production of "useful" power or "wasted" in irreversibilities and unuseful streams, improving the information level which can be achieved.

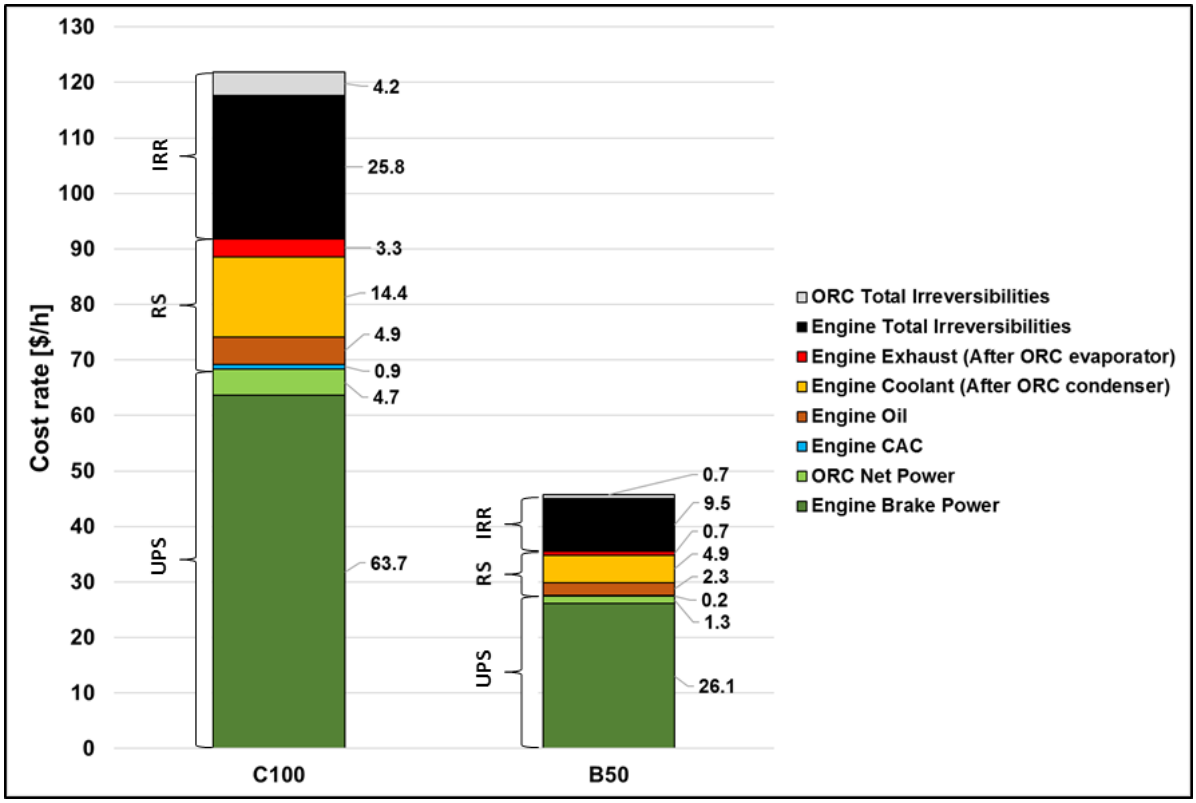

Fig. 135. Cost rates breakdown analysis for the combined engine-ORC system (insulated engine exhaust manifolds strategy) for the ORC case 1 (case study 4)

Operating Point	C100	B50
Useful Power Streams (UPS)	56.1% (57.2%)	60.0% (60.5%)
Rejected Streams (RS)	19.3% (18.6%)	17.7% (17.5%)
Irreversibilities (IRR)	24.6% (24.2%)	22.3% (22.0%)

Tab. 66. Percentages split between useful, rejected and irreversibilities related cost rates of the combined engine-ORC system for ORC case 1 and insulated manifolds strategy (case study 4)

The comparison with the baseline engine case shows a general slight increase of the cost rates in absolute values (not reported in the figure), mostly due to the slightly higher costs expected for the ORC using an insulated exhaust manifolds strategy and the higher exergy recovered, rejected and destroyed.
Also, a general worse distribution of the costs can be observed from Tab. 66 compared to the baseline case. Indeed, both at C100 and B50, it is possible to observe an increased percentage of costs "wasted" in irreversibilities and rejected streams, and decreased costs percentage invested in the production of power. This mostly due to the higher recovered exergy, and thus irreversibilities production, relatively to the generally low additional power production which is expected thanks to the proposed insulation strategy. However, an increase in power output achievable is still a positive output of the exhaust insulation strategy.
The percentage distribution is a bit better at B50, in which the exhaust temperatures are generally expected to be lower, thus improving the beneficial effect of an insulation strategy, which tends to increase the exhaust temperature.
However, both for the baseline engine case, and the case with engine exhaust manifolds insulation, the cost rates distribution is still in favour of the power production, meaning that the combined engine-ORC system is still leading to more costs invested in power production than those "wasted" in the production of irreversibilities, or unused, rejected streams.

6.4.5 Conclusions

The scope of the work proposed in this fourth case study is not to address the best possible combined engine-ORC configuration, but rather to show some examples of how the proposed methodology can help in designing more efficient and cost-competitive systems, using the principles of energy (industry-standard), but also of exergy, techno and thermo-economics.
From the proposed case study, some additional considerations can be drawn, for example:

- it is important to use, or develop, a cheap piston expander which, however, should be able to provide high efficiency at high expansion ratios up to around 30 (expected at C100 peak cycle operational points, where exhaust gas temperatures are higher). A piston expansion machine with a variable built-in expansion ratio (achievable with valves operations or variable expansion ratios systems) could also allow to instantaneously match the cycle expected expansion ratio, thus allowing an improved cycle efficiency. In this case, the machine could become more expensive and adequate controlling strategies, over the drive cycle, should be developed;
- turbo-expanders are generally more expensive but can theoretically achieve higher efficiencies and higher expansion ratios. They present, however, also more controllability issues, in order to avoid wet expansions with possible blade damages;
- the availability of efficient components, and in particular heat transfer equipment, but at acceptable costs, is essential for a competitive technology. This is true in particular for evaporators (finned-tubes and shell and tubes) and expansion machines;
- simple ORC layouts, such as exhaust gas recovery only (or parallel exhaust/EGR architectures when EGR is available) are still a cheap and reliable solution with lower controllability, packaging and weight issues, especially for vehicles applications;
- with an appropriate optimization of the engine and ORC operational conditions, and some strategies, as insulations of expected high temperature and high heat losses sub-components, it is possible to reach competitive SIC values for the combined engine-ORC system. In particular, the strategy with insulation of the engine exhausts manifolds is more beneficial at B50 (medium load, medium speed), rather than at C100 (high load, high speed), because of the expected lower temperatures of the exhaust gas. In this case, an increase of the exhaust gas temperature leads to a proportionally better improvement in the ORC performance compared to the C100 point, in which the temperatures are expected already high enough;
- an indirect exhaust-to-coolant configuration (case 8 of the proposed case study) can still be a good choice in terms of constant, even if lower, expected power output, at different operating conditions, safer operations and contained investment costs;

Finally, some considerations must be reported about the overall engine-ORC architecture, considering both emissions and performance, in possible combination with waste heat recovery systems.
When an engine emission reduction strategy without EGR is chosen by the engine developer and manufacturer, it could be useful to target some solutions in order to increase the exhaust gas temperatures to improve the ORC system performance. For example, the adoption of a so called Low Heat Rejection engine concept (LHR), with ceramic combustion chamber insulation inserts, could allow a higher temperature combustion with reduction of in-cylinders irreversibilities and associated wasted costs. A compromise with expected increased NO_x emissions and material resistance issues should, however, be considered. An engine exhaust manifolds insulation strategy could contribute to a further decrease of heat losses and increase of exhaust temperature, thus being beneficial for waste heat recovery. In both cases, safe turbocharger operations, in term of maximum allowed temperatures must be considered, as well as impact on the vehicle cooling package performance.

When no EGR is used, a very efficient SCR must be available for NO_x emissions abatement, together with a full aftertreament chain for other emissions reduction. The scenario has been proposed in Fig. 136-a.
In case of an engine with EGR strategy, the same methodology proposed in this thesis, can be used to assess if the recovery of EGR heat, with parallel or series ORC configurations, coupled with a low temperature combustion strategy, typical of EGR operations, could be beneficial, in terms of performance and cost. A comparison with the simple tailpipe architecture can be proposed. The engine-ORC architecture with EGR can be observed in Fig. 136-b.
A compromise between performance, emissions and cost must always be considered in the final choice, and the proposed methodology can support the developers' final decision in the choice of the best layout and operational strategy.

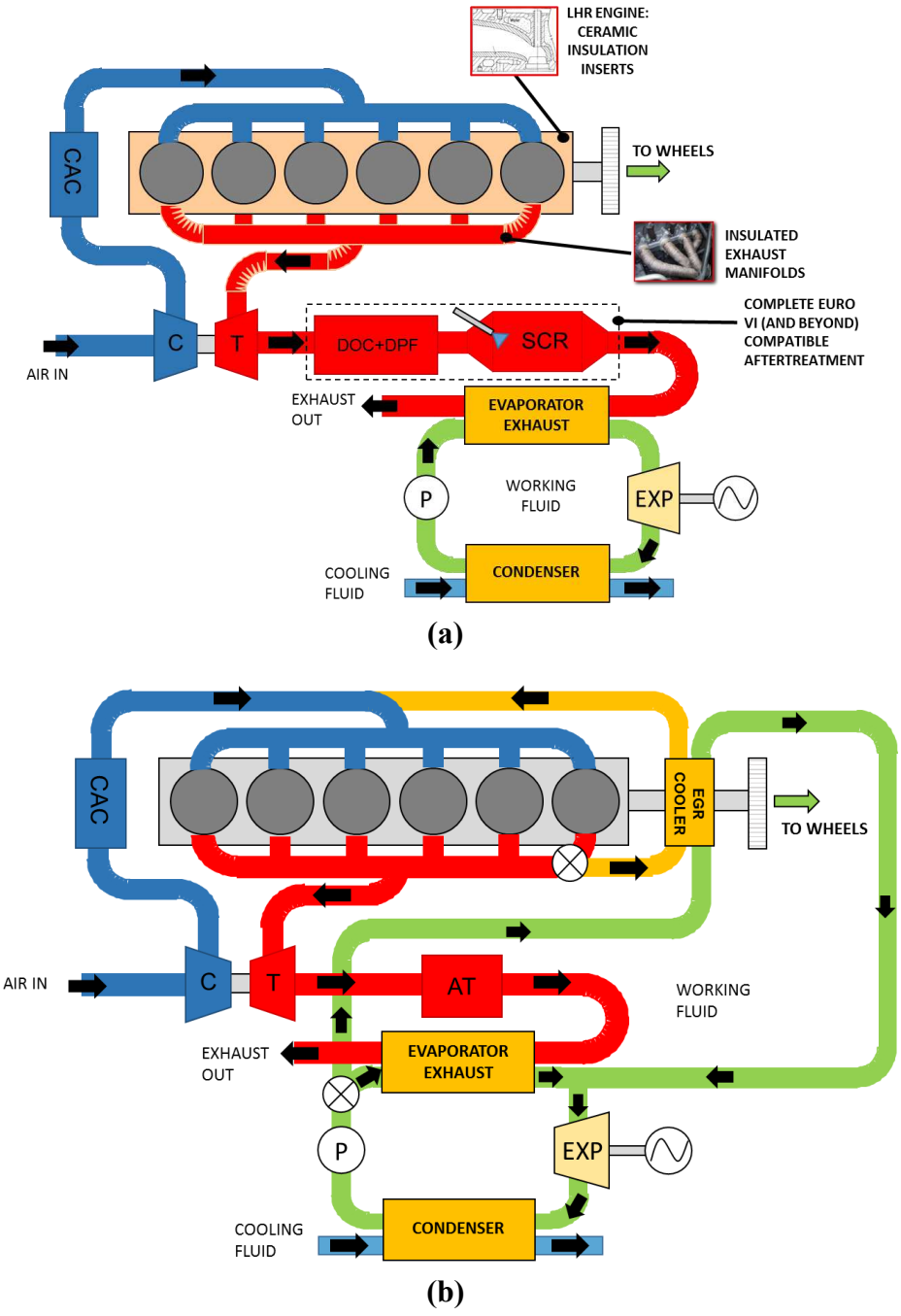

Fig. 136. (a) Low Heat Rejection, high temperature combustion, engine concept with ORC tailpipe exhaust gas heat recovery. (b) Engine with EGR and parallel exhaust / EGR ORC heat recovery (case study 4)

7 Conclusions

The research question investigated in this Ph.D. is related to the possibility of developing clean Diesel internal combustion engine powertrains, for marine and commercial vehicle applications, which at the same time should be efficient and at a reasonable cost, recovering the engine wasted heat by means of waste heat recovery systems, such as, in particular, ORC and water-steam Rankine cycles.
The work proposed in this thesis focuses on the first stages of a development project, in which accurate feasibility studies are required to choose the best powertrain configuration, in terms of expected performance and costs. In particular, the combined engine-ORC system has been evaluated, but the methodology proposed can be extended to other powertrain sub-systems (e.g. cooling and oil circuits, hybrid architectures, AC systems). For this reason, the research proposed in this work is not only focusing on the waste heat recovery system itself, as often proposed in literature, but rather on the combined complete system formed by the synergic engine and ORC interactions, with the scope to understand if it is possible to increase the powertrain efficiency.
Indeed, in the common ORC system development approach available in literature, the engine and waste heat recovery systems are generally considered as two separated systems, with the engine developed apart and just supplying the thermodynamic boundary conditions for the bottoming cycle development. On the contrary, the scope of the proposed work is to open the way to a more synergic approach for the development of the powertrain, thought as a unique system, which operating conditions and architecture can influence the overall performance and costs.
For this purpose, the use, and further development, of industry standard 1-D engine gas dynamic simulation codes and thermodynamic process simulation techniques, can help the developers to save time and costs, as well to optimize the overall system, in the direction of a total combined powertrain co-simulation, which is, to the author's acquired experience, the actual trend followed both by the marine and automotive industries.
The work carried out in the frame of the ECCO-MATE project collaboration allowed the author to investigate different topics related to both engine and ORC systems, and their relative issues. The most interesting and innovative conclusions, related to different aspects of the system's development and achieved through the proposed case studies and methodology, can be summarized as follows:

- *engine architectures*: today's heavy and medium duty Diesel engines, for marine and commercial vehicles applications, are very complex systems, developed in the last decades in order to reach the maximum possible efficiency. Several advanced turbocharging strategies are currently proposed in order to improve engine performance, such as Waste-Gate (WG), Variable Geometry Turbines (VGT), multiple-stages turbochargers. Advanced combustion strategies are still under development in order to improve efficiency and reduce emissions, as demonstrated by the work carried out by many project partners in the ECCO-MATE project. Moreover, emission reduction strategies, such as effective Selective Catalytic Reduction (SCR) or different Exhaust Gas Recirculation (EGR) architectures, as those proposed in this work, are also the focus of engine developers. These technologies directly affect the engine performance, as well as the energy and exergy streams in the overall powertrain, influencing, in particular, the combined synergy with possible waste heat recovery systems, such as ORC. In particular, EGR and variable geometry turbochargers (VGT) are technologies which could allow to propose new heat sources for heat recovery systems, such as ORC, and to mitigate the drawbacks of a combined engine-ORC system installation (backpressure), as evaluated in the proposed case studies, allowing, at the same time, lower pollutants emissions levels;
- *ORC architectures and heat sources*: as already introduced, the ORC layouts are directly influenced by the engine architecture and emission reduction strategies chosen: in particular the availability of different heat sources, at different temperature levels, to be recovered with a waste heat recovery system. Higher temperature sources, such as exhaust gas and EGR, are

generally preferred because of the higher exergy available, and the expected improved performance and compact ORC system achievable. Simple, parallel or series recovery architectures, exploiting these high temperature sources, are to be preferred for vehicles applications, where a compromise between performance, cost, weight and packaging must be considered. However, mostly in vehicles applications, if the recovery of EGR is beneficial in terms of additional power production with lower cooling demands, the recovery of exhaust gas increases the power production, but also the heat that must be rejected to the vehicle cooling package. More advanced and complicated architectures, recovering also lower temperature heat sources, can be proposed, mostly for marine applications, in which higher performance could be achieved even if with more expensive and bulkier systems. For example, for large two-stroke marine Diesel engines, as those analysed, lower temperature heat sources, such as Scavenge Air Cooling (SAC) and engine coolant, can become very interesting to be recovered, because of the high amount of energy available, even if at lower temperatures, and the possibility of using simple and reliable architectures. Fuel consumption improvements between 5 and 10 % can be expected, depending on the application, the engine-ORC configuration, the heat sources recovered, the working fluid and the design point chosen;

- *ORC working fluid choice*: as often reported in this work, the choice of the most suitable working fluid is directly related to the performance of the system and the temperatures of the recovered heat sources and of the heat sink. In particular, water, alcohols and hydrocarbons are generally showing higher performance for higher temperature heat sources, such as exhaust gas and EGR, while refrigerants are mostly suitable for lower temperature heat recovery, such as the heat available in the engine coolant. However, the choice of the most suitable fluid is not only a matter of performance, but also of safety, flammability and health issues, with alcohols and hydrocarbons generally more dangerous. For this purpose, the use of the NFPA classification can help the developer to understand which fluids must be treated more carefully, or even avoided, depending on the application and its constraints;
- *ORC heat sink choice*: while for marine and stationary applications, the availability of sea and fresh water (or enough required space for air-cooled units) for ORC cooling purposes leads to decreased issues in the choice of the right heat sink and cooling fluid layout, in vehicle applications the problem becomes more important. Indeed, the need of rejecting a high amount of heat to the ambient, in order to condense the ORC fluids, leads to a high thermal load on the vehicle cooling package. This generally results in a bulkier cooling package with possible higher parasitic fan power consumption (especially in off-highway applications where the ram air effect is almost negligible) and, as well, heat exchangers' packaging issues. As already stated, when EGR is available, it is recommended to recover as much heat as possible from the EGR cooler, which otherwise should be rejected to the cooling circuit. This will decrease the thermal load on the vehicle cooling package and allow to obtain additional useful power output;
- *ORC produced energy usage*: another issue is how to use the additional power produced by the waste heat recovery system. In particular, mechanical coupling with the engine crankshaft seems to be the cheapest and most efficient solution, due to the expected higher energy conversion efficiencies. However, especially when hybrid vehicles architectures, or marine hybrid Diesel-electric propulsion systems are considered, electricity generation can be proposed, allowing more flexible energy utilization configurations, even if with expected higher costs and system complications;
- *economic considerations*: even if very often not considered in literature studies, economic considerations are the final leading forces when addressing the possible technology competitiveness and market penetration potential. For this reason, an economic analysis is generally the final requisite of a complete, effective feasibility study, and must be always considered in the development process and fully embedded in the analysis approach proposed. As examples from the proposed case studies, in large two-stroke marine propulsion

applications, as those examined, an operational fuel cost saving between 184 and 507 k$/year can be expected, when using ORC, depending on the operational behaviour adopted. While, in medium-duty truck applications, a competitive Specific Investment Cost (SIC) between 200 and 300 $/kW can be achieved with relatively simple configurations and strategies.

The activity carried out in this research project led to the development of the combined engine-ORC analysis methodology proposed, step-by-step, through different case studies in this work, which potential can be highlighted in the below-reported main considerations and analysis steps:

- a *Fist Law analysis* allows to retrieve the required boundary conditions information for a detailed thermal management assessment of the overall powertrain, addressing all energy streams related to the engine and the waste heat recovery system. This could be useful as a starting point for the development of the powertrain, but also of the cooling and oil circuits, as well as other powertrain thermal sub-systems;
- a detailed *Second Law analysis* can guide the developer in the direction of understanding where system inefficiencies concentrate (irreversibilities) and which components or sub-systems to target in order to propose improvement strategies. A combined use of a detailed exergy analysis coupled with in-cylinder 3D-CFD techniques, as those proposed by the project partners in the frame of the ECCO-MATE project, could also allow to study new combustion strategies to improve the combustion efficiency, but also to assess the effects of the various combustion parameters on the overall powertrain architecture, including potential waste heat recovery and other sub-systems;
- as demonstrated mostly in the last case study, it is important also to add economic considerations to the overall analysis. Indeed, most of the time, it is not only the most performing system which has the highest penetration into the market, but rather the system with the best compromise between performance and costs. For these reasons:
    - a *techno-economic analysis* can be used to assess the expected trade-off between costs and performance, in order to address, for every technology, the expected competitivity in terms of a fruitful investment;
    - a detailed *thermo-economic analysis* can be also a very powerful instrument to understand the process of cost formation and the expected economic efficiency of the combined powertrain over its expected operational lifetime. Indeed, only through a thermo-economic analysis it is possible to understand how much of the investment and operational costs is really invested for “useful” power production, and how much is “wasted” in the production of exergy or materials streams which are not used, or just discharged to the environment without a real positive effect for the powertrain. Moreover, being a thermo-economic analysis directly linked to the exergy concept, it is able to provide an insight on the costs which are invested just for the production of irreversibilties. These costs are just “wasted” because of system internal inefficiencies. This is something which cannot be envisaged from a traditional analysis approach.

The proposed methodology, if implemented and developed in a user-friendly and flexible analysis tool, can contribute to the development of a performant and cost effective new generation of powertrains, composed of synergic and fully integrated different sub-systems, with the main purpose of improving the overall efficiency but, at the same time, reduce pollutants emissions, at affordable and reasonable costs, saving development time and optimizing system performance.

8 Future Developments

In this work, the methodology has been applied to combined engine-ORC systems, in order to evaluate the performance of the overall powertrain, allowing a better understanding of the thermodynamic processes involved.
To the best of the author's knowledge, at the current status of development, there is no commercially-available software performing this kind of complete analysis for automotive and marine internal combustion engine-based powertrains, and generally used 1-D gas dynamic engine simulations tools are not programmed and developed to perform a complete and detailed First and Second Law analysis.
As already introduced, the proposed approach, if further developed in the direction of a more user-friendly and integrated tool, could help the developers in designing the next generation of waste heat recovery systems, which would not be any longer just a retrofitting of the combustion engine, but rather a synergic unique system, in which the most important components, sub-systems, the architecture and operating parameters, could be optimized in order to lead to the highest performance and lowest costs and emissions.
On the engine side, different strategies, technologies and approaches, could be studied and developed, such as:

- *Low Heat Rejection (LHR) engines*: the combustion chamber could be insulated with ceramic inserts in order to decrease the heat losses and improve combustion efficiency, decreasing irreversibilities formation (a compromise with emissions, engine materials resistance and costs should be also considered);
- *advanced EGR architectures*: in order to reduce NO_x emissions, but at the same time an additional heat source for a possible waste heat recovery system;
- *turbocharging and turbo-compounding strategies*: two-stage turbocharging, WG and VGT turbochargers and their possible interaction with ORC and waste heat recovery systems. Turbo-compounded engines could be also evaluated;
- *combustion strategies*: development of combustion strategies with an adequate synergy between 1-D overall engine and 3-D in-cylinder CFD simulations, assessing the impact of combustion settings and strategies on the entire powertrain and its subsystems, such as also waste heat recovery technologies. Emissions could be quantified in a more reliable way;
- *aftertreatment models' development*: a combined reliable emission modelling approach, based on detailed chemistry, could be considered in order to assess the trade-off between performance, costs and emission formation;
- *transient studies and operating cycle analysis*: with an efficient development of the energy and exergy post-processing routines, possibly embedded in a user-friendly tool, also the engine transient operations, and their impact on the energetic, exergetic and economic performance could be assessed. Drive cycles analysis could then be possible, when using transient capable models.

On the waste heat recovery side, some further developments and studies are also needed, for example:

- *development of more advanced ORC components' models*: this could allow to get rid of some of the assumptions proposed in this work, such as the absence of heat and pressure losses for the ORC components, the fixed expansion machines efficiencies and the average overall heat transfer coefficients assumed. However, as for example in the case of physically-based expanders and heat exchangers models, the need of referencing to suitable geometrical configurations will increase the number of the independent variables involved in the optimization process. The complexity of the models will also sensibly increase the computational time required for the calculations, leading to a more complex optimization

procedure. In the preliminary phase of a project, as the one targeted in this work, a compromise between accuracy and time must be considered, especially in the industrial sector and when the main goal is to choose the best technology and configuration for further, more detailed, developments;

- *simulation of more complex ORC architectures*: the availability of modular and computationally stable ORC components' models could allow to simulate and assess different ORC concepts, with more complicated architectures, such as dual loop and two-stage pressurization. Super-critical and trans-critical cycles operational conditions could also be proposed;
- *simulation of working fluids mixtures*: the methodology could be extended to the evaluation of mixtures. Zeotropic mixtures could be considered as a possible solution in order to reduce the irreversibilities in the ORC evaporator and condenser with a better thermal match between the fluids streams. This could allow also to reduce the costs wasted in irreversibilities, through a detailed thermo-economic analysis;
- *simulation of other waste heat recovery cycles*: with the same approach proposed for the ORC systems in this work, several other waste heat recovery technologies could be assessed, such as: turbo-compounding, Brayton cycles, absorption and adsorption cycles, Goswami cycles, Kalina cycles, six-stroke concepts and many more, depending on the application and industrial requirements;
- *off-design and transient operating cycles analysis*: more advanced components' models can allow to evaluate the combined powertrain performance at different operating points, expected during the specific application's duty cycle, addressing the benefits in terms of performance and cost over the overall detailed operational regime;
- *co-simulation*: other powertrain sub-systems could be also evaluated, when a powerful co-simulation environment is developed (e.g. AC systems, cooling and oil circuits, hybrid architectures). In particular, when considering waste heat recovery systems in automotive applications, an adequate assessment of the performance of the vehicle cooling circuit and cooling package capabilities should be considered in the details. To fulfil the proposed requirements, Ricardo is developing IGNITE, a tool for full powertrain co-simulation, in which the proposed routines could be fully embedded;
- *optimization techniques:* the development of an overall embedded optimization procedure, or the use of powerful optimization tools should be considered, in order to address the best powertrain configurations, based on the applications' and developers' requirements and constraints.

All the observations proposed could lead to the development of a powerful computational tool for overall powertrain design and optimization, able to go beyond the traditional engineering approach, in order to develop the next generation of clean and efficient combined powertrains.

References

[1] US EPA. Global Greenhouse Gas Emissions Data n.d. http://www3.epa.gov/climatechange/ghgemissions/global.html (accessed February 4, 2016).

[2] Third IMO Greenhouse Gas Study 2014 - Executive Summary and Final Report - International Maritime Organization (IMO). 2014.

[3] Ricardo. EMLEG - Emissions Legislation Database n.d. http://www.emleg.com/ (accessed September 1, 2015).

[4] IMO, International Maritime Organization - Prevention of Air Pollution from Ships n.d. http://www.imo.org/en/OurWork/environment/pollutionprevention/airpollution/pages/air-pollution.aspx (accessed October 19, 2016).

[5] International: IMO Marine Regulations - DieselNet n.d. https://www.dieselnet.com/standards/inter/imo.php (accessed December 1, 2016).

[6] MARPOL Annex VI - EEDI & SEEMP n.d. http://www.marpol-annex-vi.com/eedi-seemp/ (accessed December 1, 2016).

[7] Heywood JB. Internal Combustion Engine Fundamentals. MCGraw-Hill; 1988.

[8] Ferguson CR, Kirkpatrick AT. Internal Combustion Engines Applied Thermosciences. 2nd ed. John Wiley & Sons, Inc.; 2001.

[9] Benson RS. The Thermodynamics and Gas Dynamics of Internal Combustion Engines - Volume I. Clarendon Press - Oxford; 1982.

[10] Caton JA. An Introduction to Thermodynamic Cycle Simulations for Internal Combustion Engines. Wiley & Sons; 2016.

[11] Ricardo Software. Ricardo WAVE n.d. http://www.ricardo.com/en-GB/What-we-do/Software/Products/WAVE/ (accessed February 4, 2016).

[12] EnginLink - Power Systems Research n.d. https://www.powersys.com/enginlink (accessed March 1, 2016).

[13] Zhang Q, Pennycott A, Brace CJ. A review of parallel and series turbocharging for the diesel engine. Proc Inst Mech Eng , Part D J Automob Eng 2013;227:1723–33. doi:10.1177/0954407013492108.

[14] Neukirchner H, Semper T, Lüdeitz D, Dingel O. Symbiosis of Energy Recovery and Downsizing. MTZ Worldw 2014;75:4–9.

[15] Squaiella LLF, Martins CA, Lacava PT. Strategies for emission control in diesel engine to meet Euro VI. Fuel 2013;104:183–93. doi:10.1016/j.fuel.2012.07.027.

[16] Codan E, Vlaskos I. ABB Turbocharging - Turbocharging medium speed diesel engines with extreme Miller timing Contents Turbocharging medium speed diesel engines with extreme Miller timing n.d.

[17] Dec JE. Advanced compression-ignition engines - Understanding the in-cylinder processes. Proc Combust Inst 2009;32 II:2727–42. doi:10.1016/j.proci.2008.08.008.

[18] Holmberg K, Andersson P, Nylund NO, Mäkelä K, Erdemir A. Global energy consumption due to friction in trucks and buses. Tribol Int 2014;78:94–114. doi:10.1016/j.triboint.2014.05.004.

[19] Johnson T V. Review of Vehicular Emissions Trends. SAE Int J Engines 2015;8:1152–67. doi:10.4271/2015-01-0993.

[20] Lecompte S, Huisseune H, Van Den Broek M, Vanslambrouck B, De Paepe M. Review of organic Rankine cycle (ORC) architectures for waste heat recovery. Renew Sustain Energy Rev 2015;47:448–61. doi:10.1016/j.rser.2015.03.089.

[21] Quoilin S, Van Den Broek M, Declaye S, Dewallef P, Lemort V. Techno-economic survey of organic rankine cycle (ORC) systems. Renew Sustain Energy Rev 2013;22:168–86. doi:10.1016/j.rser.2013.01.028.

[22] Aghaali H, Ångström H-E. A review of turbocompounding as a waste heat recovery system for internal combustion engines. Renew Sustain Energy Rev 2015;49:813–24. doi:10.1016/j.rser.2015.04.144.

[23] Hamid Elsheikh M, Shnawah DA, Sabri MFM, Said SBM, Haji Hassan M, Ali Bashir MB, et al. A review on thermoelectric renewable energy: Principle parameters that affect their performance. Renew Sustain Energy Rev 2014;30:337–55. doi:10.1016/j.rser.2013.10.027.

[24] Orr B, Akbarzadeh A, Mochizuki M, Singh R. A review of car waste heat recovery systems utilising thermoelectric generators and heat pipes. Appl Therm Eng 2016;101:490–5. doi:10.1016/j.applthermaleng.2015.10.081.

[25] Hannan MA, Azidin FA, Mohamed A. Hybrid electric vehicles and their challenges: A review. Renew Sustain Energy Rev 2014;29:135–50. doi:10.1016/j.rser.2013.08.097.

[26] M. Sabri MF, Danapalasingam KA, Rahmat MF. A review on hybrid electric vehicles architecture and energy management strategies. Renew Sustain Energy Rev 2016;53:1433–42. doi:10.1016/j.rser.2015.09.036.

[27] Sulaiman N, Hannan MA, Mohamed A, Majlan EH, Wan Daud WR. A review on energy management system for fuel cell hybrid electric vehicle: Issues and challenges. Renew Sustain Energy Rev 2015;52:802–14. doi:10.1016/j.rser.2015.07.132.

[28] Hao H, Liu Z, Zhao F, Li W. Natural gas as vehicle fuel in China: A review. Renew Sustain Energy Rev 2016;62:521–33. doi:10.1016/j.rser.2016.05.015.

[29] Imran M, Yasmeen T, Ijaz M, Farooq M, Wakeel M. Research progress in the development of natural gas as fuel for road vehicles : A bibliographic review (1991 – 2016). Renew Sustain Energy Rev 2016;66:702–41. doi:10.1016/j.rser.2016.08.041.
[30] Chauhan BS, Singh RK, Cho HM, Lim HC. Practice of diesel fuel blends using alternative fuels: A review. Renew Sustain Energy Rev 2016;59:1358–68. doi:10.1016/j.rser.2016.01.062.
[31] Gürü M, Karakaya U, Altıparmak D, Alıcılar A. Improvement of Diesel fuel properties by using additives. Energy Convers Manag 2002;43:1021–5. doi:10.1016/S0196-8904(01)00094-2.
[32] Keskin A, Gürü M, Altıparmak D. Influence of tall oil biodiesel with Mg and Mo based fuel additives on diesel engine performance and emission. Bioresour Technol 2008;99:6434–8. doi:10.1016/j.biortech.2007.11.051.
[33] Mussatto SI. A closer look at the developments and impact of biofuels in transport and environment; what are the next steps? Biofuel Res J 2016;3:331–331. doi:10.18331/BRJ2016.3.1.2.
[34] Shahir VK, Jawahar CP, Suresh PR. Comparative study of diesel and biodiesel on CI engine with emphasis to emissions - A review. Renew Sustain Energy Rev 2015;45:686–97. doi:10.1016/j.rser.2015.02.042.
[35] Tabatabaei M, Karimi K, Sárvári Horváth I, Kumar R. Recent trends in biodiesel production. Biofuel Res J 2015;2:258–67. doi:10.18331/BRJ2015.2.3.4.
[36] Mousavi G SM, Faraji F, Majazi A, Al-Haddad K. A comprehensive review of Flywheel Energy Storage System technology. Renew Sustain Energy Rev 2017;67:477–90. doi:10.1016/j.rser.2016.09.060.
[37] DieselNet. European Stationary Cycle (ESC) n.d. https://www.dieselnet.com/standards/cycles/esc.php (accessed October 2, 2015).
[38] MAN Diesel & Turbo - Tier III Compliance Low Speed Engines. 2010.
[39] Exhaust gas emission control today and tomorrow - Application on MAN B&W Two-stroke Marine Diesel Engines - Man Diesel & Turbo. n.d.
[40] Emission Project Guide - MAN Diesel & Turbo. 2015.
[41] Waste Heat Recovery System (WHRS) for Reduction of Fuel Consumption, Emission and EEDI - MAN Diesel & Turbo. 2012.
[42] Tier III Two-Stroke Technology - MAN Diesel & Turbo. n.d.
[43] ME-GI Gas-ready Ship - MAN Diesel & Turbo. n.d.
[44] Ollus R. Imo Tier 3 Regulation - How To Deal With the Present Situation. Cimac, 2014.
[45] Tremuli P. Developments and Perspectives of Marine Engines. Clean Combust. Greenh. Gases, Brussel: 2008.
[46] Troberg M, Delneri D. Tier III Emission Roadmap for Marine Engine Application. MTZ Worldw 2010;71:12–7.
[47] Schneiter D. Tier III Programme: Technical Position, Status and Outlook. Licens. Conf., Interlaken: WinGD; 2015, p. 1–18.
[48] US EPA - Technical Bulletin - Nitrogen oxides (NOx), why and how they are controlled. 1999.
[49] US EPA - Costs of Emission Reduction Technologies for Category 3 Marine Engines. 2009.
[50] ICCT - Reducing Greenhouse Gas Emissions from Ships - Cost Effectiveness of Available Options - White Paper. 2011.
[51] Geist MA, Holtbecker R, Chung SY. Marine Diesel NOx Reduction Technique - A New Sulzer Diesel Ltd Approach. SAE Int. Congr. Expo., Detroit, Michigan, USA: 1997. doi:10.4271/970321.
[52] Lamas MI, Rodrìguez CG. Emissions from marine engines and NOx reduction methods. J Marit Res 2012;9:77–82.
[53] Yang ZL, Zhang D, Caglayan O, Jenkinson ID, Bonsall S, Wang J, et al. Selection of techniques for reducing shipping NOx and SOx emissions. Transp Res Part D Transp Environ 2012;17:478–86. doi:10.1016/j.trd.2012.05.010.
[54] Wik C, Niemi S. Low emission engine technologies for future Tier 3 legislations- Options and case studies. J Shipp Trade 2016:1–34. doi:10.1186/s41072-016-0009-z.
[55] Yfantis EA, Zannis TC, Pariotis EG, Katsanis JS, Roumeliotis I. NOx Reduction Technologies for Marine Diesel Engines - Operational, Environmental and Economical Aspects. Green Trasp., Athens, Greece: 2016.
[56] Feng L, Tian J, Long W, Gong W, Du B, Li D, et al. Decreasing NOx of a Low-Speed Two-Stroke Marine Diesel Engine by Using In-Cylinder Emission Control Measures. Energies 2016. doi:10.3390/en9040304.
[57] Burel F, Taccani R, Zuliani N. Improving sustainability of maritime transport through utilization of Liquefied Natural Gas (LNG) for propulsion. Energy 2013;57:412–20. doi:10.1016/j.energy.2013.05.002.
[58] Hiraoka N, Miyanagi A, Kuroda K, Ito K, Nakagawa T, Ueda T. The World's First Onboard Verification Test of UE Engine with Low Pressure EGR complied with IMO's NOx Tier III Regulations. Mitsubishi Heavy Ind Tech Rev 2016;53:40–7.
[59] Raptotasios SI, Sakellaridis NF, Papagiannakis RG, Hountalas DT. Application of a multi-zone combustion model to investigate the NOx reduction potential of two-stroke marine diesel engines using EGR. Appl Energy 2015;157:814–23. doi:10.1016/j.apenergy.2014.12.041.
[60] Winterthur Gas & Diesel (WinGD) - General Technical Data (GTD) n.d. https://www.wingd.com/en/media/general-technical-data/ (accessed December 3, 2016).
[61] Wärtsilä 20 Product Guide - Wärtsilä. 2013.

[62] Woodyard D. Pounders - Marine Diesel Engines and Gas Turbines. 9th Ed. 2009.
[63] Vlaskos I. An analysis of the market and technology review for marine engines and auxiliary equipment over the next 12 months. Asian Mar. Eng. Conf., Singapore: 2015.
[64] Heim K. Existing and future demands on the turbocharging of modern large two-stroke diesel engines. 8-th Supercharging Conf. Dresden, 2002, p. 1–18.
[65] Variable Turbine Area - MAN Diesel & Turbo Brochure. n.d.
[66] Yoshihisa O, Keiichi S, Yukio Y. Application of a Large Hybrid Turbocharger for Marine Electric-power Generation. Mitsubishi Heavy Ind Tech Rev 2012;49:29–33.
[67] Keiichi S, Ono Y, Yukio Y, Sakamoto M. Energy Savings through Electric-assist Turbocharger for Marine Diesel Engines. Mitsubishi Heavy Ind Tech Rev Heavy Ind Tech Rev 2015;52:36–41.
[68] Yfantis EA, Zannis TC, Katsanis I, Papagiannakis RG, Siritoglou P, Lamprou A. Miller Cycle Application in Marine Diesel Engines for NOx Reduction : A Review. ASHRAE Int. Conf. Energy Environ. Ships, Athens, Greece: 2015.
[69] Codan E, Huber T. Application of two stage turbocharging systems on large engines. 10th Int Conf Turbochargers Turbocharging 2012:55–69.
[70] He S, Du B, Feng L, Fu Y, Cui J, Long W. A Numerical Study on Combustion and Emission Characteristics of a Medium-Speed Diesel Engine Using In-Cylinder Cleaning Technologies 2015:4118–37. doi:10.3390/en8054118.
[71] Codan E, Wüthrich J. Turbocharging solutions for EGR on large diesel engines. Aufladetechnische Konf 2013 2013.
[72] Katsanos C, Hountalas DT, Zannis TC, Yfantis EA. Potentiality for Optimizing Operational Performance and Thermal Management of Diesel Truck Engine Rankine Cycle by Recovering Heat in EGR Cooler. SAE 2010 World Congr. Exhib., Detroit, Michigan, USA: 2010. doi:10.4271/2010-01-0315.
[73] Hountalas DT, Mavropoulos GC, Katsanos C, Knecht W. Improvement of bottoming cycle efficiency and heat rejection for HD truck applications by utilization of EGR and CAC heat. Energy Convers Manag 2012;53:19–32. doi:10.1016/j.enconman.2011.08.002.
[74] Latz G, Erlandsson O, Skåre T, Contet A, Andersson S, Munch K. Performance Analysis of a Reciprocating Piston Expander and a Plate Type Exhaust Gas Recirculation Boiler in a Water-Based Rankine Cycle for Heat Recovery from a Heavy Duty Diesel Engine. Energies 2016;9:495. doi:10.3390/en9070495.
[75] Lion S, Michos CN, Vlaskos I, Taccani R. A thermodynamic feasibility study of an Organic Rankine Cycle (ORC) for Heavy Duty Diesel Engine (HDDE) waste heat recovery in off- highway applications. ECOS 2016, Portoroz, Slovenia: 2016.
[76] Hansen JP, Kaltoft J, Bak F, Gørtz J, Pedersen M, Underwood C. Reduction of SO2 , NOx and Particulate Matter from Ships with Diesel Engines. 2014.
[77] Lahtinen JM. Closed-loop Exhaust Gas Scrubber Onboard a Merchant Ship - Technical, Economical, Environmental and Operational Viewpoints. University of Vaasa. Acta Wasaensia 342. Energy Technology 1. 2016.
[78] CEAS Engine Calculations - MAN n.d. http://marine.man.eu/two-stroke/ceas (accessed January 7, 2017).
[79] Okabe M, Sakaguchi K, Sugihara M, Miyanagi A, Hiraoka N, Murata S. World's Largest Marine 2-Stroke Diesel Test Engine , the 4UE-X3 - Development in Compliance with the Next Version of Environmental Regulations and Gas Engine Technology -. Mitsubishi Heavy Ind Tech Rev 2013;50:55–62.
[80] Ueda T. Development of Low Pressure Exhaust Gas Recirculation System for Mitsubishi UE. J JIME 2015;50:1–12.
[81] Lion S, Vlaskos I, Rouaud C, Taccani R. A review of waste heat recovery and Organic Rankine Cycles (ORC) in on-off highway vehicle heavy duty diesel engine applications. Renew Sustain Energy Rev 2017;79:691–708. doi:10.1016/j.rser.2017.05.082.
[82] US EPA. Nonregulatory Nonroad Duty Cycles n.d. http://www.epa.gov/otaq/regs/nonroad/nrcycles.htm (accessed September 29, 2015).
[83] Bialystocki N, Konovessis D. On the estimation of ship's fuel consumption and speed curve : A statistical approach. J Ocean Eng Sci 2016;1:157–66. doi:10.1016/j.joes.2016.02.001.
[84] Lee CY, Lee HL, Zhang J. The impact of slow ocean steaming on delivery reliability and fuel consumption. Transp Res Part E Logist Transp Rev 2015;76:176–90. doi:10.1016/j.tre.2015.02.004.
[85] Slow Steaming Practices in the Global Shipping Industry - MAN. 2012.
[86] Cerup-Simonsen B, de Kat JO, Jakobsen OG, Pedersen LR, Petersen JB, Posborg T. An integrated approach towards cost-effective operation of ships with reduced GHG emission. Soc Nav Archit Mar Eng Trans 2010;2:1–18.
[87] Baldi F, Bengtsson S, Andersson K. The influence of propulsion system design on the carbon footprint of different marine fuels. Low Carbon Shipp. Conf., 2013, p. 1–12.
[88] Saidur R, Rezaei M, Muzammil WK, Hassan MH, Paria S, Hasanuzzaman M. Technologies to recover exhaust heat from internal combustion engines. Renew Sustain Energy Rev 2012;16:5649–59. doi:10.1016/j.rser.2012.05.018.

[89] Jadhao JS, Thombare DG. Review on Exhaust Gas Heat Recovery for I . C . Engine. Int J Eng Innov Technol 2013;2:93–100.
[90] Mohd Noor A, Che Puteh R, Rajoo S. Waste Heat Recovery Technologies In Turbocharged Automotive Engine – A Review. J Mod Sci Technol 2014;2:108–19.
[91] Gabriel-Buenaventura A, Azzopardi B. Energy recovery systems for retrofitting in internal combustion engine vehicles: A review of techniques. Renew Sustain Energy Rev 2015;41:955–64. doi:10.1016/j.rser.2014.08.083.
[92] Karvonen M, Kapoor R, Uusitalo A, Ojanen V. Technology competition in the internal combustion engine waste heat recovery: A patent landscape analysis. J Clean Prod 2016;112:3735–43. doi:10.1016/j.jclepro.2015.06.031.
[93] Shu G, Liang Y, Wei H, Tian H, Zhao J, Liu L. A review of waste heat recovery on two-stroke IC engine aboard ships. Renew Sustain Energy Rev 2013;19:385–401. doi:10.1016/j.rser.2012.11.034.
[94] Ichiki Y, Shiraishi K, Kanaboshi T, Ono Y, Ohta Y. Development of Super Waste-Heat Recovery System for Marine Diesel Engines. Mitsubishi Heavy Ind Tech Rev 2011;48:17–21.
[95] Choi BC, Kim YM. Thermodynamic analysis of a dual loop heat recovery system with trilateral cycle applied to exhaust gases of internal combustion engine for propulsion of the 6800 TEU container ship. Energy 2013;58:404–16. doi:10.1016/j.energy.2013.05.017.
[96] Ma Z, Yang D, Guo Q. Conceptual Design and Performance Analysis of an Exhaust Gas Waste Heat Recovery System for a 10000TEU Container Ship. Polish Marit Res 2012;19:31–8. doi:10.2478/v10012-012-0012-8.
[97] Dimopoulos GG, Georgopoulou CA, Kakalis NMP. Modelling and optimisation of an integrated marine combined cycle system. Proc. 24th Int. Conf. Effic. Cost, Optim. Simul. Energy Convers. Syst. Process. ECOS 2011, 2011.
[98] Dimopoulos GG, Georgopoulou CA, Kakalis NMP. The introduction of exergy analysis to the thermo-economic modelling and optimisation of a marine combined cycle system. Proc. 25th Int. Conf. Effic. Cost, Optim. Simul. Energy Convers. Syst. Process. ECOS 2012, 2012.
[99] Dimopoulos GG, Georgopoulou CA, Stefanatos IC, Zymaris AS, Kakalis NMP. A general-purpose process modelling framework for marine energy systems. Energy Convers Manag 2014;86:325–39. doi:10.1016/j.enconman.2014.04.046.
[100] MAN B&W S60ME-C8.5 - IMO Tier II - Project Guide - MAN Diesel & Turbo. 2016.
[101] Larsen U, Sigthorsson O, Haglind F. A comparison of advanced heat recovery power cycles in a combined cycle for large ships. Energy 2014;74:260–8. doi:10.1016/j.energy.2014.06.096.
[102] Singh DV, Pedersen E. A review of waste heat recovery technologies for maritime applications. Energy Convers Manag 2016;111:315–28. doi:10.1016/j.enconman.2015.12.073.
[103] Srikhirin P, Aphornratana S, Chungpaibulpatana S. A review of absorption refrigeration tehnologies. Renew Sustain Energy Rev 2001;5:343–72.
[104] Zhang X, He M, Zhang Y. A review of research on the Kalina cycle. Renew Sustain Energy Rev 2012;16:5309–18. doi:10.1016/j.rser.2012.05.040.
[105] Modi A, Haglind F. Perfomance analysis of a Kalina cycle for a central receiver solar thermal power plant with direct steam generation. n.d.
[106] Bombarda P, Invernizzi CM, Pietra C. Heat recovery from Diesel engines: A thermodynamic comparison between Kalina and ORC cycles. Appl Therm Eng 2010;30:212–9. doi:10.1016/j.applthermaleng.2009.08.006.
[107] Ayou DS, Bruno JC, Saravanan R, Coronas A. An overview of combined absorption power and cooling cycles. Renew Sustain Energy Rev 2013;21:728–48. doi:10.1016/j.rser.2012.12.068.
[108] Demirkaya G. Theoretical and Experimental Analysis of Power and Cooling Cogeneration Utilizing Low Temperature Heat Sources. PhD Thesis, University of South Florida, 2011.
[109] Xu F, Goswami DY, Bhagwat SS. A combined power/cooling cycle. Energy 2000;25:233–46. doi:10.1016/S0360-5442(99)00071-7.
[110] Jackson N. Split Cycle Recuperated Combustion Engines. Ricardo plc Internal Report. Ricardo Plc 2014.
[111] Scuderi Group. Scuderi Power Group n.d. http://www.scuderigroup.com/ (accessed February 5, 2016).
[112] Macchi E, Astolfi M. Organic Rankine Cycle (ORC) Power Systems - Technologies and Applications. 1st Ed. Woodhead Publishing; 2016.
[113] Briggs I, McCullough G, Spence S, Douglas R, O'Shaughnessy R, Hanna A, et al. Waste Heat Recovery on a Diesel-Electric Hybrid Bus Using a Turbogenerator. SAE 2012 Commer. Veh. Eng. Congr., 2012. doi:10.4271/2012-01-1945.
[114] Briggs I, McCullough G, Spence S, Douglas R, O'Shaughnessy R, Hanna A, et al. A parametric study of a turbogenerator on a Diesel-electric hybrid bus. ASME 2013 TurboEXPO, 2013.
[115] Liu X, Deng YD, Li Z, Su CQ. Performance analysis of a waste heat recovery thermoelectric generation system for automotive application. Energy Convers Manag 2015;90:121–7. doi:10.1016/j.enconman.2014.11.015.
[116] Twaha S, Zhu J, Yan Y, Li B. A comprehensive review of thermoelectric technology: Materials, applications, modelling and performance improvement. Renew Sustain Energy Rev 2016;65:698–726. doi:10.1016/j.rser.2016.07.034.
[117] Lan S, Rouaud C, Stobart R, Chen R, Yang Z. The Potential of Thermoelectric Generator in Parallel Hybrid Vehicle Applications Potential for TEG in Hybrid Vehicle. SAE Tech Pap 2017. doi:10.4271/2017-01-0189.Copyright.

[118] Thombare DG, Verma SK. Technological development in the Stirling cycle engines. Renew Sustain Energy Rev 2008;12:1–38. doi:10.1016/j.rser.2006.07.001.
[119] Alizadeh A, Vlaskos I, Feulner P. Exhaust gas heat recovery on large engines, potential, opportunities, limitations. Ricardo Deutschl GmbH, CIMAC 2010.
[120] Mehta V, Gohil RK, Bavarva JP, Saradava BJ. Waste heat recovery using stirling engine. Int J Adv Eng Technol 2012;III:305–10.
[121] Bailey M. Waste Heat Recovery from Adiabatic Diesel Engines by Exhaust-Driven Brayton Cycles. vol. 168257. 1983.
[122] Bailey M. Comparative Evaluation of Three Alternative Power Cycles for Waste Heat Recovery from the Exhaust of Adiabatic Diesel Engines. vol. 86953. 1985.
[123] Liu JP, Fu JQ, Ren C, Wang LJ, Xu ZX, Deng BL. Comparison and analysis of engine exhaust gas energy recovery potential through various bottom cycles. Appl Therm Eng 2013;50:1219–34. doi:10.1016/j.applthermaleng.2012.05.031.
[124] Song B, Zhuge W, Zhao R, Zheng X, Zhang Y, Yin Y, et al. An investigation on the performance of a Brayton cycle waste heat recovery system for turbocharged diesel engines. J Mech Sci Technol 2013;27:1721–9. doi:10.1007/s12206-013-0422-2.
[125] Galindo J, Serrano J, Dolz V, Kleut P. Brayton cycle for internal combustion engine exhaust gas waste heat recovery. Adv Mech Eng 2015;7:168781401559031. doi:10.1177/1687814015590314.
[126] Touré A, Stouffs P. Modeling of the Ericsson engine. Energy 2014;76:445–52. doi:10.1016/j.energy.2014.08.030.
[127] Benajes J, Serrano JR, Molina S, Novella R. Potential of Atkinson cycle combined with EGR for pollutant control in a HD diesel engine. Energy Convers Manag 2009;50:174–83. doi:10.1016/j.enconman.2008.08.034.
[128] Crosby I, Akbari P. Thermodynamic analysis of the Atkinson cycle. Sci. Coop. Int. Work. Eng. Branches, vol. c, 2014, p. 297–304.
[129] Arai M, Amagai K, Ida Y. New Concept for Six-Stroke Diesel Engine. SAE Tech Pap Ser 1994. doi:10.4271/941922.
[130] Conklin JC, Szybist JP. A highly efficient six-stroke internal combustion engine cycle with water injection for in-cylinder exhaust heat recovery. Energy 2010;35:1658–64. doi:10.1016/j.energy.2009.12.012.
[131] Ailloud C, Delaporte B, Schmitz G, Keromnes A, Le Moyne L. Development and Validation of a Five Stroke Engine. SAE Tech Pap 2013. doi:doi:10.4271/2013-24-0095.
[132] Williams DR, Koci C, Fiveland S. Compression Ignition 6-Stroke Cycle Investigations. SAE Int J Engines 2014;7:2014-01–1246. doi:10.4271/2014-01-1246.
[133] Kéromnès A, Delaporte B, Schmitz G, Le Moyne L. Development and validation of a 5 stroke engine for range extenders application. Energy Convers Manag 2014;82:259–67. doi:10.1016/j.enconman.2014.03.025.
[134] Hayasaki T, Okamoto Y. A Six-Stroke DI Diesel Engine Under Dual Fuel Operation. SAE Tech Pap Ser 2014.
[135] Arabaci E, Içingür Y, Solmaz H, Uyumaz A, Yilmaz E. Experimental investigation of the effects of direct water injection parameters on engine performance in a six-stroke engine. Energy Convers Manag 2015;98:89–97. doi:10.1016/j.enconman.2015.03.045.
[136] Arabaci E, İçingür Y. Thermodynamic investigation of experimental performance parameters of a water injection with exhaust heat recovery six-stroke engine. J Energy Inst 2016;89:569–77. doi:10.1016/j.joei.2015.06.006.
[137] Stuart K, Yan T, Mathias J. Thermodynamic Analysis of a Five-Stroke Engine with Heat Transfer and Mass Loss. SAE Tech Pap 2017. doi:10.4271/2017-01-0633.
[138] Tsolakis A, Theinnoi K, Wyszynski ML, Xu HM. Exhaust gas fuel reforming for IC Engines using diesel type fuels. SAE Int Fuels Lubr Meet 2007:1289–94. doi:10.4271/2007-01-2044.
[139] Pratapas JM, Kozlov A, Lyford-Pike E, LaPointe L, Moh D. 331 kW high-efficiency, low-emission engine using thermochemical fuel reforming. Energy Research and Development Division, California Energy Commission, 2013.
[140] Phillips F, Gilbert I, Pirault J-P, Megel M. Scuderi Split Cycle Research Engine: Overview, Architecture and Operation. SAE Int J Engines 2011;4:2011-01–0403. doi:10.4271/2011-01-0403.
[141] Meldolesi R, Badain N. Scuderi Split Cycle Engine: Air Hybrid Vehicle Powertrain Simulation Study. SAE Tech 2012. doi:10.4271/2012-01-1013.
[142] Dong G, Morgan RE, Heikal MR. A novel split cycle internal combustion engine with integral waste heat recovery. Appl Energy 2015. doi:10.1016/j.apenergy.2015.02.024.
[143] Dong G, Morgan RE, Heikal MR. Thermodynamic analysis and system design of a novel split cycle engine concept. Energy 2016;102:576–85. doi:10.1016/j.energy.2016.02.102.
[144] Tartière T. ORC Market : A World Overview. ORC World Map n.d. http://orc-world-map.org/analysis.html (accessed June 29, 2017).
[145] NFPA (National Fire Protection Association). NFPA 704 Standard n.d. www.nfpa.org (accessed October 10, 2015).
[146] Northeaster University. Northeastern University - NFPA Hazard Rating System n.d. www.ehs.neu.edu/laboratory_safety/general_information/nfpa_hazard_rating (accessed October 10, 2015).

[147] Lemmon EW, Huber ML, McLinden MO. NIST Standard Reference Database 23: Reference Fluid Thermodynamic and Transport Properties-REFPROP,2013 n.d.
[148] The Montreal Protocol on Substances that Deplete the Ozone Layer - UNEP, Ozone Secretariat United Nations Environment Programme. 2000.
[149] Saleh B, Koglbauer G, Wendland M, Fischer J. Working fluids for low-temperature organic Rankine cycles. Energy 2007;32:1210–21. doi:10.1016/j.energy.2006.07.001.
[150] Abadi GB, Kim KC. Investigation of organic Rankine cycles with zeotropic mixtures as a working fl uid : Advantages and issues. Renew Sustain Energy Rev 2017;73:1000–13. doi:10.1016/j.rser.2017.02.020.
[151] Bao J, Zhao L. A review of working fluid and expander selections for organic Rankine cycle. Renew Sustain Energy Rev 2013;24:325–42. doi:10.1016/j.rser.2013.03.040.
[152] Panesar AS, Morgan RE, Miché NDD, Heikal MR. Working fluid selection for a subcritical bottoming cycle applied to a high exhaust gas recirculation engine. Energy 2013;60:388–400. doi:10.1016/j.energy.2013.08.015.
[153] Lai NA, Wendland M, Fischer J. Working fluids for high-temperature organic Rankine cycles. Energy 2011;36:199–211. doi:10.1016/j.energy.2010.10.051.
[154] Dong B, Xu G, Cai Y, Li H. Analysis of zeotropic mixtures used in high-temperature Organic Rankine cycle. Energy Convers Manag 2014;84:253–60. doi:10.1016/j.enconman.2014.04.026.
[155] Shu G, Gao Y, Tian H, Wei H, Liang X. Study of mixtures based on hydrocarbons used in ORC (Organic Rankine Cycle) for engine waste heat recovery. Energy 2014;74:428–38. doi:10.1016/j.energy.2014.07.007.
[156] Eyerer S, Wieland C, Vandersickel A, Spliethoff H. Experimental study of an ORC (Organic Rankine Cycle) and analysis of R1233zd-E as a drop-in replacement for R245fa for low temperature heat utilization. Energy 2016;103:660–71. doi:10.1016/j.energy.2016.03.034.
[157] Edwards S, Eitel J, Pantow E, Geskes P, Lutz R, Tepas J. Waste Heat Recovery: The Next Challenge for Commercial Vehicle Thermomanagement. SAE Int J Commer Veh 2012:395–406. doi:10.4271/2012-01-1205.
[158] Maybin B, Hanna A, Rouaud C, Porteous S, Baxter J, Douglas R, et al. The Energy and Thermal Management of A Hybrid Double Deck Bus. 23rd Aachen Colloq. Automob. Engine Technol., 2014.
[159] Tian H, Liu L, Shu G, Wei H, Liang X. Theoretical research on working fluid selection for a high-temperature regenerative transcritical dual-loop engine organic Rankine cycle. Energy Convers Manag 2014;86:764–73. doi:10.1016/j.enconman.2014.05.081.
[160] Oomori H, Ogino S. Waste heat reocvery of passenger car using a combination of Rankine bottoming cycle and evaporative engine cooling system. SAE Tech Pap 1993. doi:10.4271/930880.
[161] Panesar AS. An innovative Organic Rankine Cycle system for integrated cooling and heat recovery. Appl Energy 2017;186:396–407. doi:10.1016/j.apenergy.2016.03.011.
[162] Panesar AS, Heikal MR, Morgan RE. A Novel Organic Rankine Cycle System for Heavy Duty Diesel Engines. Sustain. Therm. Energy Manag., Newcastle, United Kingdom: 2015.
[163] Tian H, Liu L, Shu G, Wei H, Liang X. Theoretical research on working fluid selection for a high-temperature regenerative transcritical dual-loop engine organic Rankine cycle. Energy Convers Manag 2014;86:764–73. doi:10.1016/j.enconman.2014.05.081.
[164] Shu G, Liu L, Tian H, Wei H, Xu X. Performance comparison and working fluid analysis of subcritical and transcritical dual-loop organic Rankine cycle (DORC) used in engine waste heat recovery. Energy Convers Manag 2013;74:35–43. doi:10.1016/j.enconman.2013.04.037.
[165] Wang EH, Zhang HG, Fan BY, Ouyang MG, Yang FY, Yang K, et al. Parametric analysis of a dual-loop ORC system for waste heat recovery of a diesel engine. Appl Therm Eng 2014;67:168–78. doi:10.1016/j.applthermaleng.2014.03.023.
[166] Yang F, Dong X, Zhang H, Wang Z, Yang K, Zhang J, et al. Performance analysis of waste heat recovery with a dual loop organic Rankine cycle (ORC) system for diesel engine under various operating conditions. Energy Convers Manag 2014;80:243–55. doi:10.1016/j.enconman.2014.01.036.
[167] Shu G, Liu L, Tian H, Wei H, Liang Y. Analysis of regenerative dual-loop organic Rankine cycles (DORCs) used in engine waste heat recovery. Energy Convers Manag 2013;76:234–43. doi:10.1016/j.enconman.2013.07.036.
[168] Wang EH, Zhang HG, Zhao Y, Fan BY, Wu YT, Mu QH. Performance analysis of a novel system combining a dual loop organic Rankine cycle (ORC) with a gasoline engine. Energy 2012;43:385–95. doi:10.1016/j.energy.2012.04.006.
[169] Zhang HG, Wang EH, Fan BY. A performance analysis of a novel system of a dual loop bottoming organic Rankine cycle (ORC) with a light-duty diesel engine. Appl Energy 2013;102:1504–13. doi:10.1016/j.apenergy.2012.09.018.
[170] Meinel D, Wieland C, Spliethoff H. Effect and comparison of different working fluids on a two-stage organic rankine cycle (ORC) concept. Appl Therm Eng 2014;63:246–53. doi:10.1016/j.applthermaleng.2013.11.016.
[171] Smolen S. Simulation and Thermodynamic Analysis of a Two-Stage Organic Rankine Cycle for Utilisation of Waste Heat at Medium and Low Temperature Levels. Energy Sci Technol 2011;1:64–78.
[172] Li X, Zhao C, Hu X. Thermodynamic analysis of Organic Rankine Cycle with Ejector. Energy 2012;42:342–9. doi:10.1016/j.energy.2012.03.047.

[173] Li X, Li X, Zhang Q. The first and second law analysis on an organic Rankine cycle with ejector. Sol Energy 2013;93:100–8. doi:10.1016/j.solener.2013.04.003.
[174] Li X, Huang H, Zhao W. A supercritical or transcritical Rankine cycle with ejector using low-grade heat. Energy Convers Manag 2014;78:551–8. doi:10.1016/j.enconman.2013.11.020.
[175] Fu J, Liu J, Deng B, Feng R, Yang J, Zhou F, et al. An approach for exhaust gas energy recovery of internal combustion engine : Steam-assisted turbocharging. Energy Convers Manag 2014;85:234–44. doi:10.1016/j.enconman.2014.05.067.
[176] Fu J, Liu J, Yang Y, Ren C, Zhu G. A new approach for exhaust energy recovery of internal combustion engine: Steam turbocharging. Appl Therm Eng 2013;52:150–9. doi:10.1016/j.applthermaleng.2012.11.035.
[177] Fu J, Liu J, Ren C, Wang L, Deng B, Xu Z. An open steam power cycle used for IC engine exhaust gas energy recovery. Energy 2012;44:544–54. doi:10.1016/j.energy.2012.05.047.
[178] Larsen U, Wronski J, Graa J, Baldi F, Pierobon L. Expansion of organic Rankine cycle working fluid in a cylinder of a low-speed two-stroke ship engine. Energy 2016. doi:10.1016/j.energy.2016.11.069.
[179] Xu J, Liu C. Effect of the critical temperature of organic fluids on supercritical pressure Organic Rankine Cycles. Energy 2013;63:109–22. doi:10.1016/j.energy.2013.09.068.
[180] Schuster A, Karellas S, Aumann R. Efficiency optimization potential in supercritical Organic Rankine Cycles. Energy 2010;35:1033–9. doi:10.1016/j.energy.2009.06.019.
[181] Le VL, Feidt M, Kheiri A, Pelloux-Prayer S. Performance optimization of low-temperature power generation by supercritical ORCs (organic Rankine cycles) using low GWP (global warming potential) working fluids. Energy 2014;67:513–26. doi:10.1016/j.energy.2013.12.027.
[182] Chen H, Goswami DY, Rahman MM, Stefanakos EK. A supercritical Rankine cycle using zeotropic mixture working fluids for the conversion of low-grade heat into power. Energy 2011;36:549–55. doi:10.1016/j.energy.2010.10.006.
[183] Persichilli M, Kacludis A, Zdankiewicz E, Held T. Supercritical CO2 Power Cycle Developments and Commercialization: Why sCO2 can Displace Steam. Power-Gen India Cent. Asia, Pragati Maidan, New Delhi, India: 2012.
[184] Smith IK. Development of the Trilater Flash Cycle System. Part 1: Fundamental Considerations. J Power Energy 1993;207:179–94.
[185] Zamfirescu C, Dincer I. Thermodynamic analysis of a novel ammonia-water trilateral Rankine cycle. Thermochim Acta 2008;477:7–15. doi:10.1016/j.tca.2008.08.002.
[186] Fischer J. Comparison of trilateral cycles and organic Rankine cycles. Energy 2011;36:6208–19. doi:10.1016/j.energy.2011.07.041.
[187] Yari M, Mehr AS, Zare V, Mahmoudi SMS, Rosen MA. Exergoeconomic comparison of TLC (trilateral Rankine cycle), ORC (organic Rankine cycle) and Kalina cycle using a low grade heat source. Energy 2015;83:712–22. doi:10.1016/j.energy.2015.02.080.
[188] Ho T, Mao SS, Greif R. Increased power production through enhancements to the Organic Flash Cycle (OFC). Energy 2012;45:686–95. doi:10.1016/j.energy.2012.07.023.
[189] Lopes J, Douglas R, McCullough G, O'Shaughnessy R, Hanna A, Rouaud C, et al. Review of Rankine Cycle Systems Components for Hybrid Engines Waste Heat Recovery. SAE 2012 Commer. Veh. Eng. Congr., Rosemont, Illinois, USA: 2012. doi:10.4271/2012-01-1942.
[190] Lin W, Yuan J, Sundén B. Review on graphite foam as thermal material for heat exchangers. World Renew. Energy Congr. 2011 - Sweden, Linköping, Sweden: 2011, p. 748–55. doi:10.3384/ecp11057748.
[191] Mavridou S, Mavropoulos GC, Bouris D, Hountalas DT, Bergeles G. Comparative design study of a diesel exhaust gas heat exchanger for truck applications with conventional and state of the art heat transfer enhancements. Appl Therm Eng 2010;30:935–47. doi:10.1016/j.applthermaleng.2010.01.003.
[192] Olofsson A. Investigation of Materials for Use in Exhaust Gas Condensate Environment with Focus on EGR Systems. Umeå University, 2012.
[193] Hatami M, Ganji DD, Gorji-Bandpy M. A review of different heat exchangers designs for increasing the diesel exhaust waste heat recovery. Renew Sustain Energy Rev 2014;37:168–81. doi:10.1016/j.rser.2014.05.004.
[194] Landelle A, Tauveron N, Haberschill P, Revellin R, Colasson S. Organic Rankine cycle design and performance comparison based on experimental database. Appl Energy 2017. doi:10.1016/j.apenergy.2017.04.012.
[195] Lemort V, Quoilin S. Advances in ORC expander design. Int. Symp. Adv. Waste Heat Valoris. Technol., Kortrijk, Belgium: 2012.
[196] Clemente S, Micheli D, Reini M, Taccani R. Performance Analysis and Modeling of Different Volumetric Expanders for Small-Scale Organic Rankine Cycles. ASME 2011 5th Int. Conf. Energy Sustain., Washington, DC, USA: 2011, p. 375–84. doi:10.1115/ES2011-54302.
[197] Libertine n.d. http://www.libertine.co.uk/ (accessed June 30, 2017).
[198] Endo T, Kawajiri S, Kojima Y, Takahashi K, Baba T, Ibaraki S, et al. Study on Maximizing Exergy in Automotive Engines. SAE 2007 World Congr., Detroit, Michigan, USA: 2007.
[199] Bredel E, Nickl J, Bartosch S. Waste Heat Recovery in Drive Systems of Today and Tomorrrow. MTZ Worldw

2011;72:52–6.
[200] Song P, Wei M, Shi L, Danish SN, Ma C. A review of scroll expanders for organic Rankine cycle systems. Appl Therm Eng 2015;75:54–64. doi:10.1016/j.applthermaleng.2014.05.094.
[201] Clemente S, Micheli D, Reini M, Taccani R. Energy efficiency analysis of Organic Rankine Cycles with scroll expanders for cogenerative applications. Appl Energy 2012;97:792–801. doi:10.1016/j.apenergy.2012.01.029.
[202] Micheli D, Reini M, Taccani R. Multiple expansion ORC for small scale – low temperature heat recovery. Proc ECOS 2016 2016.
[203] Qiu G, Liu H, Riffat S. Expanders for micro-CHP systems with organic Rankine cycle. Appl Therm Eng 2011;31:3301–7. doi:10.1016/j.applthermaleng.2011.06.008.
[204] Subramanian SN. 2013 DOE Vehicle Technologies Program Review - Heavy Duty Roots Expander Heat Energy Recovery (HD-REHER) - Presentation, EATON 2013.
[205] SteamDrive Piston Expander n.d. http://www.steamdrive.de/web/index.php?id=4 (accessed November 21, 2016).
[206] Barber-Nichols. Turbines n.d. http://www.barber-nichols.com/products/turbines/turbine-alternators (accessed February 5, 2016).
[207] Air Squared. Scroll Expanders n.d. https://airsquared.com/products/scroll-expanders/e15h022a-sh/ (accessed November 21, 2016).
[208] Electratherm - Twi Screw Expander n.d. https://electratherm.com/orc-knowledge-center-2/frequently-asked-questions/ (accessed February 5, 2016).
[209] Doyle EF, DiNanno LR, Saunders K. Installation of a Diesel Organic Rankine Compound Engine in a Class 8 Truck for a Single-Vehicle Test. SAE Tech Pap Ser 1979.
[210] Schmiederer K, Edwards S, Pantow E, Geskes P, Lutz R, Mohr M, et al. The Potential Fuel Consumption of a Truck Engine plus Rankine Cycle System , derived from Performance Measurements over Steady State and Transient Test Cycles at Constant Emissions Levels. 33. Int. Wiener Mot., 2012, p. 1–26.
[211] Organic Rankine Cycle Expander: solar thermal, engine exhaust, bio-gas, industrial heat, geothermal. Brochure, Verdicorp Environmental Technologies n.d.
[212] Fuller RL. Phase I Final Report - Conversion of Low Temperature Waste Heat Utilizing Hermetic Organic Rankine Cycle - Barber-Nichols, Report. n.d.
[213] Green Turbine 15 kW, Brochure, Green Turbine n.d.
[214] Nelson CR. Exhaust Energy Recovery, Cummins, DEER Conference 2006.
[215] Infinity Turbine n.d. http://www.infinityturbine.com/ (accessed February 5, 2016).
[216] Enogia n.d. http://www.enogia.com/ (accessed June 30, 2017).
[217] Seher D, Lengenfelder T, Gerhardt J, Eisenmenger N, Hackner M, Krinn I. Waste Heat Recovery for Commercial Vehicles with a Rankine Process. 21 St Aachen Colloq Automob Engine Technol 2012 2012.
[218] Anschel P. A System-Level Approach to the Development of Optimized ORC Waste Heat Recovery Components for Heavy Duty Truck - Borg Warner Inc. Engine ORC Consort. EORCC 2016, Belfast, United Kingdom: 2016.
[219] Electratherm n.d. https://electratherm.com (accessed February 5, 2016).
[220] Air Squared. E22H038A-SH, semi hermetic 5 kW scroll expander for lubricated or oil-free operation with gases other than air n.d. http://airsquared.com/products/scroll-expanders/e22h038a-sh/ (accessed February 5, 2016).
[221] Cretegny D, Kane M, Favrat D. Project HT Scroll - Nouveau Système de Cogénération à Turbine Spirale Haute Température - Rapport Annuel. 2008.
[222] Bouzid S, Schlager G. United States Patent Application Publication. Rotary Vane Expander, Liebherr-Machines Bulle SA, 2012.
[223] EXOES. EVE , Energy Via Exhaust : Waste heat recovery through Rankine Cycle on heavy duty vehicle - Exoès company. 15e cycle confèrences Util. Ration. l'ènergie Environ., 2014.
[224] Viking Development Group. CraftEngine n.d. http://www.vdg.no/?menuid=16 (accessed February 18, 2016).
[225] Patel PS, Doyle EF. Compounding the truck diesel engine with an organic Rankine-cycle system. SAE Automot. Eng. Congr. Expo., Detroit, Michigan, USA: 1976. doi:10.4271/760343.
[226] DiBella FA, DiNanno LR, Koplow MD. Laboratory and On-Highway Testing of Diesel Organic Rankine Compound Long-Haul Vehicle Engine. SAE Tech Pap Ser 1983:29–38.
[227] Chammas R El, Clodic D. Combined Cycle for Hybrid Vehicles. SAE 2005 World Congr. Exhib., Warrendale, Pennsylvania, USA: 2005.
[228] Nelson CR. Exhaust Energy Recovery. Cummins 2009.
[229] Arias DA, Shedd TA, Jester RK. Theoretical Analysis of Waste Heat Recovery from an Internal Combustion Engine in a Hybrid Vehicle. SAE 2006 World Congr. Exhib., Detroit, Michigan, USA: 2006.
[230] Kadota M, Yamamoto K. Advanced Transient Simulation on Hybrid Vehicle Using Rankine Cycle System. SAE Int J Engines 2008;1:240–7.
[231] Freymann R, Strobl W, Obieglo A. The Turbosteamer: A system Introducing the Principle of Cogeneration in Automotive Applications. MTZ Worldw 2008;69:20–7. doi:10.1007/BF03226909.
[232] Ringler J, Seifert M, Guyotot V, Hübner W. Rankine Cycle for Waste heat Recovery of IC Engines. SAE Int J Engines 2009.

[233] Briggs T, Wagner RM, Edwards KD, Curran S, Nafziger E. A Waste Heat Recovery System for Light Duty Diesel Engines. SAE 2010 Powertrain Fuels Lubr. Meet., 2010. doi:10.4271/2010-01-2205.
[234] Aneja R, Singh S, Sisken K, Dold R, Oelschlegel H. Exhaust Heat Driven Rankine Cycle for a Heavy Duty Diesel Engine (DAIMLER Presentation). DEER 2011, Detroit, Michigan, USA: 2011.
[235] BOSCH. Diesel Systems - Waste Heat Recovery System for commercial vehicles - Brochure, Robert BOSCH GmbH, 2014.
[236] Furukawa T, Nakamura M, Machida K, Shimokawa K. A Study of the Rankine Cycle Generating System for Heavy Duty HV Trucks. SAE 2014 World Congr. Exhib., Detroit, Michigan, USA: 2014. doi:10.4271/2014-01-0678.
[237] Howell T, Gibble J, Tun C. Development of an ORC system to improve HD truck fuel efficiency - Ricardo. Deer Conf., vol. 1, 2011, p. 1–21.
[238] Nolan C, Douglas R, O'Shaughnessy R, Rouaud C, Foley A. Improving Fuel Economy Application of the Organic Rankine Cycle on a Hybrid Bus. 5th ATA Eur Work Mob Air Cond Veh Therm Syst 2014.
[239] Nolan C, O'Shaughnessy R, Douglas R, Rouaud C. Waste heat recovery utilising engine coolant on a hybrid bus. Veh. Therm. Manag. Syst. Conf. Proc., Coventry, UK: 2013.
[240] Nolan C, O'Shaughnessy R, Douglas R, Rouaud C, Hanna A, Seaman R. Waste heat recovery to improve fuel economy on a hybrid bus. MTZ Heavy Duty Off Highw. Mot. 2013, 2013.
[241] Katsanos C, Hountalas DT, Pariotis EG. Thermodynamic analysis of a Rankine cycle applied on a diesel truck engine using steam and organic medium. Energy Convers Manag 2012;60:68–76. doi:10.1016/j.enconman.2011.12.026.
[242] Latz G, Andersson S, Munch K. Comparison of Working Fluids in Both Subcritical and Supercritical Rankine Cycles for Waste-Heat Recovery Systems in Heavy-Duty Vehicles. SAE 2012 World Congr. Exhib., Detroit, Michigan, USA: 2012. doi:10.4271/2012-01-1200.
[243] Serrano JR, Dolz V, Novella R, García A. HD Diesel engine equipped with a bottoming Rankine cycle as a waste heat recovery system. Part 2: Evaluation of alternative solutions. Appl Therm Eng 2012;36:279–87. doi:10.1016/j.applthermaleng.2011.10.024.
[244] Macián V, Serrano JR, Dolz V, Sánchez J. Methodology to design a bottoming Rankine cycle, as a waste energy recovering system in vehicles. Study in a HDD engine. Appl Energy 2013;104:758–71. doi:10.1016/j.apenergy.2012.11.075.
[245] Yang C, Xie H, Zhou S. Efficiency Analysis of the Rankine Cycle System Used for Engine Exhaust Energy Recovery under Driving Cycle. SAE 2014 World Congr. Exhib., 2014. doi:10.4271/2014-01-0671.
[246] Amicabile S, Lee J-I, Kum D. A comprehensive design methodology of organic Rankine cycles for the waste heat recovery of automotive heavy-duty diesel engines. Appl Therm Eng 2015;87:574–85. doi:10.1016/j.applthermaleng.2015.04.034.
[247] Di Battista D, Mauriello M, Cipollone R. Waste heat recovery of an ORC-based power unit in a turbocharged diesel engine propelling a light duty vehicle. Appl Energy 2015;152:109–20. doi:10.1016/j.apenergy.2015.04.088.
[248] Di Battista D, Mauriello M, Cipollone R. Effects of an ORC Based Heat Recovery System on the Performances of a Diesel Engine. SAE Int 2015;1608:1–11. doi:10.4271/2015-01-1608.
[249] Allouache A, Leggett S, Hall MJ, Tu M, Baker C, Fateh H. Simulation of Organic Rankine Cycle Power Generation with Exhaust Heat Recovery from a 15 liter Diesel Engine. SAE Int J Mater Manuf 2015;8:2015-01–0339. doi:10.4271/2015-01-0339.
[250] Yamaguchi T, Aoyagi Y, Uchida N, Fukunaga A, Kobayashi M, Adachi T, et al. Fundamental Study of Waste Heat Recovery in the High Boosted 6-cylinder Heavy Duty Diesel Engine. SAE Int J Mater Manuf 2015;8. doi:10.4271/2015-01-0326.
[251] Latz G, Erlandsson O, Skåre T, Contet A. Water-based Rankine-cycle waste heat recovery systems for engines: challenges and opportunities. ASME ORC 2015, 2015, p. 1–10.
[252] Glover S, Douglas R, De Rosa M, Zhang X, Glover L. Simulation of a multiple heat source supercritical ORC (Organic Rankine Cycle) for vehicle waste heat recovery. Energy 2015;93:1568–80. doi:10.1016/j.energy.2015.10.004.
[253] Pradhan S, Thiruvengadam A, Thiruvengadam P, Besch MC. Investigating the Potential of Waste Heat Recovery as a Pathway for Heavy-Duty Exhaust Aftertreatment Thermal Management. SAE Tech Pap 2015. doi:10.4271/2015-01-1606.Copyright.
[254] Grelet V, Dufour P, Nadri M, Reiche T, Lemort V. Modeling and control of Rankine based waste heat recovery systems for heavy duty trucks. IFAC Proc. Vol., vol. 48, Elsevier Ltd.; 2015, p. 568–73. doi:10.1016/j.ifacol.2015.09.028.
[255] Grelet V, Reiche T, Lemort V, Nadri M, Dufour P. Transient performance evaluation of waste heat recovery rankine cycle based system for heavy duty trucks. Appl Energy 2016;165:878–92. doi:10.1016/j.apenergy.2015.11.004.
[256] Feru E, Murgovski N, de Jager B, Willems F. Supervisory control of a heavy-duty diesel engine with an electrified waste heat recovery system. Control Eng Pract 2016;54:190–201. doi:10.1016/j.conengprac.2016.06.001.
[257] Torregrosa A, Galindo J, Dolz V, Royo-Pascual L, Haller R, Melis J. Dynamic tests and adaptive control of a

bottoming organic Rankine cycle of IC engine using swash-plate expander. Energy Convers Manag 2016;126:168–76. doi:10.1016/j.enconman.2016.07.078.
[258] Usman M, Imran M, Yang Y, Park BS. Impact of organic Rankine cycle system installation on light duty vehicle considering both positive and negative aspects. Energy Convers Manag 2016;112:382–94. doi:10.1016/j.enconman.2016.01.044.
[259] Nelson CR. Heavy Duty Truck Engine - Achieving High Engine Efficiency at 2010 Emissions, Cummins, DEER Conference 2006.
[260] Wright MW, Hodges S, Chambers J, Kolar T, Kanoczova B. Volvo ORC Final Report And Calibration Guidelines, Ricardo-VOLVO Internal Report,. 2012.
[261] Öhman H, Lundqvist P. Comparison and analysis of performance using Low Temperature Power Cycles. Appl Therm Eng 2013;52:160–9. doi:10.1016/j.applthermaleng.2012.11.024.
[262] OPCON Marine n.d. http://opconenergysystem.com/en/opcon-marine-3/ (accessed May 7, 2016).
[263] Larsen U, Pierobon L, Haglind F, Gabrielii C. Design and optimisation of organic Rankine cycles for waste heat recovery in marine applications using the principles of natural selection. Energy 2013;55:803–12. doi:10.1016/j.energy.2013.03.021.
[264] Bonafin J, Pinamonti P, Reini M, Tremuli P. Performance Improving of an Internal Combustion Engine for Ship Propulsion with a Bottom ORC. ECOS 2010, Lausanne, Switzerland: 2010.
[265] Baldi F, Gabrielii C. A feasibility analysis of waste heat recovery systems for marine applications. Energy 2015;80:654–65. doi:10.1016/j.energy.2014.12.020.
[266] Baldi F, Larsen U, Gabrielii C. Comparison of different procedures for the optimisation of a combined Diesel engine and organic Rankine cycle system based on ship operational profile. Ocean Eng 2015;110:85–93. doi:10.1016/j.oceaneng.2015.09.037.
[267] Song J, Yin S, Gu C. Thermodynamic analysis and performance optimization of an ORC (Organic Rankine Cycle) waste heat recovery system for marine diesel engines. Energy 2015;82:976–85. doi:10.1016/j.energy.2014.05.014.
[268] Yun E, Park H, Yoon SY, Kim KC. Dual parallel organic Rankine cycle (ORC) system for high efficiency waste heat recovery in marine application. J Mech Sci Technol 2015;29:2509–15. doi:10.1007/s12206-015-0548-5.
[269] Yfantis EA, Katsanis JS, Pariotis EG, Zannis TC, Papagiannakis RG. First-Law and Second-Law Waste Heat Recovery Analysis of a Four-Stroke Marine Diesel Engine Equipped with a Regenerative Organic Rankine Cycle System. 5th Int Symp Sh Oper Manag 2015:1–11.
[270] Soffiato M, Frangopoulos CA, Manente G, Rech S, Lazzaretto A. Design optimization of ORC systems for waste heat recovery on board a LNG carrier. Energy Convers Manag 2015;92:523–34. doi:10.1016/j.enconman.2014.12.085.
[271] Sciubba E, Tocci L, Toro C. Thermodynamic analysis of a Rankine dual loop waste thermal energy recovery system. Energy Convers Manag 2016;122:109–18. doi:10.1016/j.enconman.2016.05.066.
[272] Beyene A, Sciubba E, Tocci L, Toro C. Modelling and simulation of waste heat recovery systems for marine applications. ECOS 2015, 2015.
[273] Michos CN, Lion S, Vlaskos I, Taccani R. Analysis of the backpressure effect of an Organic Rankine Cycle (ORC) evaporator on the exhaust line of a turbocharged heavy duty diesel power generator for marine applications. Energy Convers Manag 2017;132:347–60. doi:10.1016/j.enconman.2016.11.025.
[274] Hountalas DT, Katsanos C, Mavropoulos GC. Efficiency Improvement of Large Scale 2-Stroke Diesel Engines Through the Recovery of Exhaust Gas Using a Rankine Cycle. Procedia - Soc Behav Sci 2012;48:1444–53. doi:10.1016/j.sbspro.2012.06.1120.
[275] Yang M-H, Yeh R-H. Analyzing the optimization of an organic Rankine cycle system for recovering waste heat from a large marine engine containing a cooling water system. Energy Convers Manag 2014;88:999–1010. doi:10.1016/j.enconman.2014.09.044.
[276] Wang X, Shu G-Q, Tian H, Liang Y, Wang X. Simulation and Analysis of an ORC-Desalination Combined System Driven by the Waste Heat of Charge Air at Variable Operation Conditions. SAE Tech Pap 2014. doi:10.4271/2014-01-1949.Copyright.
[277] Grljušić M, Medica V, Radica G. Thermodynamic Analysis of a Ship Power Plant Operating with Waste Heat Recovery through Combined Heat and Power Production. Energies 2014;8:4273–99. doi:10.3390/en8054273.
[278] Grljušić M, Medica V, Radica G. Calculation of efficiencies of a ship power plant operating with waste heat recovery through combined heat and power production. Energies 2015;8:4273–99. doi:10.3390/en8054273.
[279] Yuksek EL, Mirmobin P. Waste heat utilization of main propulsion engine jacket water in marine application. ASME ORC 2015 Proc 3rd Int Semin ORC Power Syst 2015.
[280] Yang M-H. Optimizations of the waste heat recovery system for a large marine diesel engine based on transcritical Rankine cycle. Energy 2016;113:1109–24. doi:10.1016/j.energy.2016.07.152.
[281] Andreasen JG, Meroni A, Haglind F. Comparison of organic and steam Rankine cycle power systems for waste heat recovery on large ships. Energies 2017:1–23. doi:10.3390/en10040547.
[282] Calnetix - Hydrocurrent Organic Rankine Cycle Systems n.d. http://www.calnetix.com/calnetix-hydrocurrent-marine-orc-shipboard-heat-recovery (accessed May 7, 2016).

[283] Hydrocurrent TM Organic Rankine Cycle Module 125EJW - Compact and High-performance Waste Heat Recovery System Utilizing Low Temperature Heat Source. Mitsubishi Heavy Ind Tech Rev Heavy Ind Tech Rev 2015;52:53–5.
[284] Climeon AG n.d. http://climeon.com/ (accessed January 14, 2017).
[285] Chen SK, Flynn PF. Development of a Single Cylinder Compession Ignition Research Engine. SAE Pap 1965.
[286] Chase MW, Curnutt JL, Downey JR, McDonald RA, Syverud AN, Valenzuela EA. JANAF Thermochemical Tables, 1982 Supplement. Midland, Michigan: 1982.
[287] McBride BJ, Zehe MJ, Gordon S. NASA Glenn Coefficients for Calculating Thermodynamic Properties of Individual Species. Tech Rep NASA 2002;211556:291. doi:NASA/TP—2002-211556.
[288] NIST WebBook n.d. http://webbook.nist.gov/chemistry/ (accessed June 16, 2016).
[289] Payri F, Olmeda P, Martín J, Carreño R. Experimental analysis of the global energy balance in a DI diesel engine. Appl Therm Eng 2015;89:545–57. doi:10.1016/j.applthermaleng.2015.06.005.
[290] Rakopoulos CD, Giakoumis EG. Second-law analyses applied to internal combustion engines operation. Prog Energy Combust Sci 2006;32:2–47. doi:10.1016/j.pecs.2005.10.001.
[291] Rakopoulos CD, Giakoumis EG. Speed and Load Effects on the availability balances and irreversibilities production in a multi-cylinder turbocharged diesel engine. Appl Therm Eng 1997;17:299–313. doi:10.1016/S1359-4311(96)00014-2.
[292] Edwards KD, Wagner RM, Graves RL. Identification of Potential Efficiency Opportunities in Internal Combustion Engines Using a Detailed Thermodynamic Analysis of Engine Simulation Results. SAE 2008 World Congr., Detro: 2008.
[293] Flynn PF, Hoag KL, Kamel MM, Primus RJ. A New Perspective on Diesel Engine Evaluation Based on Second Law Analysis. SAE Pap 1984:840032.
[294] Moran MJ. Availability analysis: A guide to efficient energy use. Prentice Hall; 1982.
[295] Ricardo IGNITE - Ricardo Software n.d. https://software.ricardo.com/products/ignite (accessed August 24, 2017).
[296] Ziviani D, Beyene A, Venturini M. Advances and challenges in ORC systems modeling for low grade thermal energy recovery. Appl Energy 2014;121:79–95. doi:10.1016/j.apenergy.2014.01.074.
[297] Klein SA. EES (Engineering Equation Solver) - Professional Version V9.710-3D. F-Chart Software n.d. http://www.fchart.com/ (accessed January 20, 2016).
[298] MATLAB 2011b - Mathworks n.d.
[299] Diesel Exhaust Gas - DieselNet n.d. https://www.dieselnet.com/tech/diesel_exh.php (accessed April 27, 2015).
[300] Moran MJ, Shapiro HN, Boettner D, Bailey M. Fundamentals of Engineering Thermodynamics. 7th ed. 2011.
[301] Yang K, Zhang H, Song S, Zhang J, Wu Y, Zhang Y, et al. Performance analysis of the vehicle diesel Engine-ORC combined system based on a screw expander. Energies 2014;7:3400–19. doi:10.3390/en7053400.
[302] Branchini L, De Pascale A, Peretto A. Systematic comparison of ORC configurations by means of comprehensive performance indexes. Appl Therm Eng 2013;61:129–40. doi:10.1016/j.applthermaleng.2013.07.039.
[303] Bejan A, Tsatsaronis G, Moran MJ. Thermal Design and Optimization. John Wiley & Sons, Inc.; 1996.
[304] Valero A, Torres C. Thermoeconomic Analysis. Exergy, Energy Syst Anal Optim - Encycl Life Support Syst 1994:1–32.
[305] Rosen M a, Dincer I. Exergy as the confluence of energy, environment and sustainable development. Exergy, An Int J 2001;1:3–13. doi:10.1016/S1164-0235(01)00004-8.
[306] Panesar AS. An innovative organic Rankine cycle approach for high temperature applications. Energy 2016;115:1436–50. doi:10.1016/j.energy.2016.05.135.
[307] Incropera FP, DeWitt DP, Bergman TL, Lavine A. Fundamentals of heat and mass transfer. 6th ed. Wiley; 2007.
[308] Shah RK, Sekulic DP. Fundamentals of Heat Exchanger Design. Wiley; 2003.
[309] Astolfi M. An innovative approach for the techno-economic optimization of organic rankine cycles. Politecnico di Milano, 2014.
[310] Towler G, Sinnott R. Chemical Engineering Design. Principles, Practice and Economics of Plant and Process Design. Elsevier; 2008.
[311] Hu K, Zhu J, Li T, Zhang W. R245fa Evaporation Heat Transfer and Pressure Drop in a Brazed Plate Heat Exchanger for Organic Rankine Cycle (ORC). Proc World Geotherm Congr 2015 2015:19–25.
[312] Fu B-R. A Flow Rate Control Approach on Off-Design Analysis of an Organic Rankine Cycle System. Energies 2016;9:759. doi:10.3390/en9090759.
[313] Suárez S, Fuente D, Roberge D, Greig AR. Safety and CO2 emissions : Implications of using organic fl uids in a ship ' s waste heat recovery system. Mar Policy 2016:1–13. doi:10.1016/j.marpol.2016.02.008.
[314] Sinnott R. Chemical Engineering Design. Elsevier; 2005.
[315] VDI. VDI Heat Atlas. Second Edi. 2010.
[316] Perry R, Green D, Maloney JO. Perry's Chemical Engineers' Handbook. MCGraw-Hill; 1999.
[317] Peters MS, Timmerhaus KD. Plant Design and Economics for Chemical Engineers. 4th ed. McGraw-Hill Chemical Engineering series; 1991.
[318] Yoo SY, Lee DW, Yoo S-Y, Lee D-W. An Experimental Study on Performance of Automotive Condenser and

Evaporator. Int Refrig Air Cond Conf 2004;July 12-15:1–7.
[319] Lemort V, Guillaume L, Legros A, Declaye S, Quoilin S. A comparison of piston, screw and scroll expanders for small scale Rankine cycle systems. 3rd Int. Conf. microgeneration Relat. Technol., 2013.
[320] Glavatskaya Y, Podevin P, Lemort V, Shonda O, Descombes G. Reciprocating Expander for an Exhaust Heat Recovery Rankine Cycle for a Passenger Car Application. Energies 2012;5:1751–65. doi:10.3390/en5061751.
[321] Winandy E, Saavedra O C, Lebrun J. Simplified modelling of an open-type reciprocating compressor. Int J Therm Sci 2002;41:183–92. doi:10.1016/S1290-0729(01)01296-0.
[322] Kim YM, Shin DG, Kim CG. Optimization of design pressure ratio of positive displacement expander for vehicle engine waste heat recovery. Energies 2014;7:6105–17. doi:10.3390/en7096105.
[323] Oudkerk J-F, Dickes R, Dumont O, Lemort V. Experimental performance of a piston expander in a small- scale organic Rankine cycle. 9th Intrenational Conf Compressors Their Syst 2015;90:12066. doi:10.1088/1757-899X/90/1/012066.
[324] Oudkerk J-F. Contribution to the Characterization of Piston Expanders for their Use in Small-Scale Power Production Systems. University of Liege, 2016.
[325] Winandy E, Saavedra O CS, Lebrun J. Experimental analysis and simplified modelling of a hermetic scroll refrigeration compressor. Appl Therm Eng 2002;22:107–20. doi:10.1016/S1359-4311(01)00083-7.
[326] Lemort V, Quoilin S, Cuevas C, Lebrun J. Testing and modeling a scroll expander integrated into an Organic Rankine Cycle. Appl Therm Eng 2009;29:3094–102. doi:10.1016/j.applthermaleng.2009.04.013.
[327] Quoilin S, Lemort V, Lebrun J. Experimental study and modeling of an Organic Rankine Cycle using scroll expander. Appl Energy 2010;87:1260–8. doi:10.1016/j.apenergy.2009.06.026.
[328] Declaye S, Quoilin S, Guillaume L, Lemort V. Experimental study on an open-drive scroll expander integrated into an ORC (Organic Rankine Cycle) system with R245fa as working fluid. Energy 2013;55:173–83. doi:10.1016/j.energy.2013.04.003.
[329] Mendoza LC, Navarro-Esbrí J, Bruno JC, Lemort V, Coronas A. Characterization and modeling of a scroll expander with air and ammonia as working fluid. Appl Therm Eng 2014;70:630–40. doi:10.1016/j.applthermaleng.2014.05.069.
[330] Giuffrida A. Modelling the performance of a scroll expander for small organic Rankine cycles when changing the working fluid. Appl Therm Eng 2014;70:1040–9. doi:10.1016/j.applthermaleng.2014.06.004.
[331] Muhammad U, Imran M, Lee DH, Park BS. Design and experimental investigation of a 1kW organic Rankine cycle system using R245fa as working fluid for low-grade waste heat recovery from steam. Energy Convers Manag 2015;103:1089–100. doi:10.1016/j.enconman.2015.07.045.
[332] Yun E, Kim D, Yoon SY, Kim KC. Experimental investigation of an organic Rankine cycle with multiple expanders used in parallel. Appl Energy 2015;145:246–54. doi:10.1016/j.apenergy.2015.02.022.
[333] Taccani R, Obi JB, De Lucia M, Micheli D, Toniato G. Development and Experimental Characterization of a Small Scale Solar Powered Organic Rankine Cycle (ORC). Energy Procedia 2016;101:504–11. doi:10.1016/j.egypro.2016.11.064.
[334] Braimakis K, Karellas S. Integrated thermoeconomic optimization of standard and regenerative ORC for different heat source types and capacities. Energy 2017;121:570–98. doi:10.1016/j.energy.2017.01.042.
[335] Turton R, Bailie RC, Whiting WB, Shaeiwitz JA. Analysis, Synthesis, and Design of Chemical Processes. vol. 53. 3rd ed. Pearson Education, Inc.; 2009. doi:10.1017/CBO9781107415324.004.
[336] Lemmens S. A Perspective on Costs and Cost Estimation Techniques for Organic Rankine Cycle Systems. 3rd Int Semin ORC Power Syst 2015:1–10.
[337] Lemmens S. Cost engineering techniques and their applicability for cost estimation of organic rankine cycle systems. Energies 2016;9. doi:10.3390/en9070485.
[338] Quoilin S, Declaye S, Tchanche BF, Lemort V. Thermo-economic optimization of waste heat recovery Organic Rankine Cycles. Appl Therm Eng 2011;31:2885–93. doi:10.1016/j.applthermaleng.2011.05.014.
[339] Baxter J, Porteous S, Rouaud C. TERS - Thermal Energy Recovery System. Ricardo 2014.
[340] Park T, Teng H, Hunter GL, van der Velde B, Klaver J. A Rankine Cycle System for Recovering Waste Heat from HD Diesel Engines - Experimental Results. SAE Int 2011. doi:10.4271/2011-01-1337.
[341] Walter L. Definition , design and thermal integration of a WHR system. AVL IPCP, Graz, Austria: 2013, p. 130–7.
[342] European Environment Agency. Transport fuel prices and taxes n.d. https://www.eea.europa.eu/data-and-maps/indicators/fuel-prices-and-taxes/assessment-6/#generic-metadata (accessed May 5, 2017).
[343] Georges E, Declaye S, Dumont O, Quoilin S, Lemort V. Design of a small-scale organic Rankine cycle engine used in a solar power plant. Int J Low-Carbon Technol 2013;8:134–41. doi:10.1093/ijlct/ctt030.
[344] Tsatsaronis G. Application of Thermo-economics to the Design and Synthesis of Energy Plants. Exergy, Energy Syst Anal Optim - Encycl Life Support Syst 1994:13.
[345] Tsatsaronis G. Thermoeconomic analysis and optimization of energy systems. Prog Energy Combust Sci 1993;19:227 257. doi:10.1016/0360-1285(93)90016-8.
[346] Abusoglu A, Kanoglu M. Exergoeconomic analysis and optimization of combined heat and power production: A

review. Renew Sustain Energy Rev 2009;13:2295–308. doi:10.1016/j.rser.2009.05.004.
[347] Lazzaretto A, Tsatsaronis G. SPECO: A systematic and general methodology for calculating efficiencies and costs in thermal systems. Energy 2006;31:1257–89. doi:10.1016/j.energy.2005.03.011.
[348] Abusoglu A, Kanoglu M. Exergetic and thermoeconomic analyses of diesel engine powered cogeneration: Part 2 - Application. Appl Therm Eng 2009;29:234–41. doi:10.1016/j.applthermaleng.2008.02.025.
[349] Abusoglu A, Kanoglu M. Exergetic and thermoeconomic analyses of diesel engine powered cogeneration: Part 1 - Formulations. Appl Therm Eng 2009;29:234–41. doi:10.1016/j.applthermaleng.2008.02.025.
[350] Seyyedvalilu MH, Mohammadkhani F. A Parametric Study on Exergy and Exergoeconomic Analysis of a Diesel Engine based Combined Heat and Power System. Int J Eng 2015;28:608–17.
[351] Khaljani M, Saray RK, Bahlouli K. Evaluation of a combined cycle based on an HCCI (Homogenous Charge Compression Ignition) engine heat recovery employing two organic Rankine cycles. Energy 2016;107:748–60. doi:10.1016/j.energy.2016.03.142.
[352] Xia J, Wang J, Lou J, Zhao P, Dai Y. Thermo-economic analysis and optimization of a combined cooling and power (CCP) system for engine waste heat recovery. Energy Convers Manag 2016;128:303–16. doi:10.1016/j.enconman.2016.09.086.
[353] Guillaume L, Legros A, Dickes R, Lemort V. Thermo-Economic Optimization of Organic Rankine Cycle Systems for Waste Heat Recovery From Exhaust and Recirculated Gases of Heavy Duty. VTMS 13 - Veh. Therm. Manag. Syst. Conf., London, UK: 2017, p. 109–25.
[354] F-Chart Software. EES - Genetic Method n.d. http://www.fchart.com/ees/eeshelp/genetic_method.htm (accessed February 5, 2016).
[355] F-Chart Software. EES - Nelder Mead Simplex Method n.d. http://www.fchart.com/ees/eeshelp/nelder_mead_simplex_method.htm (accessed February 5, 2016).
[356] Lion S, Michos CN, Vlaskos I, Taccani R. A thermodynamic feasibility study of an Organic Rankine Cycle (ORC) for Heavy Duty Diesel Engine (HDDE) waste heat recovery in off- highway applications. Int J Energy Environ Eng 2017:1–18. doi:10.1007/s40095-017-0234-8.
[357] Qiu T, Li X, Liang H, Liu X, Lei Y. A method for estimating the temperature downstream of the SCR (selective catalytic reduction) catalyst in diesel engines. Energy 2014;68:311–7. doi:10.1016/j.energy.2014.02.101.
[358] Cowell T. The Performance of Engine Cooling Heat Exchangers (Internal Ricardo Resources). University of brighton, VTS Consult Ltd., 2008.
[359] Nellis GF, Klein SA. Heat Transfer. 2009.
[360] F-Chart Software. EES help - Heat Transfer Library - Internal Flow - DuctFlow 2016. http://fchart.com/ees/heat_transfer_library/internal_flow/hs1110.htm (accessed January 1, 2016).
[361] Multi-Wing. Optimiser 2016. http://www.multi-wing.com/Downloads/Optimiser (accessed February 5, 2016).
[362] Ružić D, Časnji F. Agricultural tractor cab characteristics relevant for microclimatic conditions. J Appl Eng Sci 2011;9:323–30.
[363] Kyoto Protocol To the United Nations Framework Convention on Climate Change. United Nations, 1998.
[364] NIST. NIST Reference Fluid Thermodynamic and Transport Properties Database (REFPROP) n.d. http://www.nist.gov/srd/nist23.cfm (accessed February 5, 2016).
[365] F-Chart Software. Engineering Equation Solver (EES) n.d. http://www.fchart.com/ees/ (accessed February 5, 2016).
[366] Saidur R, Rezaei M, Muzammil WK, Hassan MH, Paria S, Hasanuzzaman M. Technologies to recover exhaust heat from internal combustion engines. Renew Sustain Energy Rev 2012;16:5649–59. doi:10.1016/j.rser.2012.05.018.
[367] DOWNTHERM Q - Heat Transfer Fluid. Product Technical Data. The Dow Chemical Company, n.d.
[368] NFPA 704: Standard System for the Identification of the Hazards of Materials for Emergency Response, 2017 Edition. National Fire Protection Association. 2017.
[369] Frangopoulos CA, Keramioti DE. Multi-Criteria evaluation of energy systems with sustainability considerations. Entropy 2010;12:1006–20. doi:10.3390/e12051006.
[370] Lion S, Vlaskos I, Taccani R. Preliminary thermodynamic analysis of waste heat recovery in marine diesel engines using Organic Rankine Cycles. ECOS 2017, San Diego, US: 2017.
[371] Benvenuto G, Campora U, Trucco A. Comparison of ship plants layouts for power propulsion systems with energy recovery. J Mar Eng Technol 2014;4177:329–40. doi:10.1080/20464177.2014.11658117.
[372] Theotokatos G, Sfakianakis K, Vassalos D. Investigation of ship cooling system operation for improving energy efficiency. J Mar Sci Technol 2016;22:38–50. doi:10.1007/s00773-016-0395-9.
[373] Bunker Index n.d. www.bunkerindex.com (accessed March 3, 2017).
[374] Insee - Institut national de la statistique et des études économiques n.d. www.bdm.insee.fr (accessed January 12, 2016).
[375] Lion S, Vlaskos I, Rouaud C, Taccani R. First and Second Law Analysis of Internal Combustion Engines and Waste Heat Recovery with Organic Rankine Cycle (ORC). ECCO-MATE Conf. I Combust. Process. Mar. Automot. Engines, Lund, Sweden: 2016.

[376] Lion S, Vlaskos I, Rouaud C, Taccani R. First and Second Law Analysis Approach for the Study of Internal Combustion Engine Waste Heat Recovery with Organic rankine Cycles (ORC). 3rd Annu. Engine ORC Consort. Work. Automot. Station. Engine Ind., Belfast, United Kingdom: 2016.
[377] Lion S, Vlaskos I, Rouaud C, Thelen W, Taccani R. Optimisation of Internal Combustion Engine Coupled with Organic Rankine Cycle with Exergo-Economic Approach. 4th Annu. Engine ORC Consort. Work. Automot. Station. Engine Ind., Detroit, Michigan, USA: 2017.
[378] ESTECO - modeFrontier n.d. http://www.esteco.com/modefrontier (accessed October 10, 2017).